Ciona intestinalis in the spotlight of metabolomics and microbiomics: New insights into its invasiveness and the biotechnological potential of its associated microbiota

Dissertation

in fulfilment of the requirements for the degree of Dr. rer. nat.

of the Faculty of Mathematics and Natural Sciences

at Kiel University

conducted at the Research Unit Marine Natural Products Chemistry,

GEOMAR Helmholtz-Centre for Ocean Research Kiel

submitted by

Caroline Utermann

Kiel, 2021

First examiner: Prof. Dr. Deniz Tasdemir

Second examiner: Prof. Dr. Antje Labes

Date of the oral examination: 05/03/2021

Acknowledgements

Table of Contents

Publications and author contributions

The results presented in this dissertation have been published in the form of research articles as indicated below.

Utermann, C., Blümel, M., Busch, K., Buedenbender, L., Lin, Y., Haltli, B.A., Kerr, R.G., Briski, E., Hentschel, U., and Tasdemir, D., 2020. Comparative microbiome and metabolome analyses of the marine tunicate *Ciona intestinalis* from native and invaded habitats. *Microorganisms*, 8, 2022, DOI: 10.3390/microorganisms8122022.

Contribution	Author(s) (abbreviated)
Conceptualization	**C.U.**, M.B., and D.T.
Sampling	**C.U.**, B.A.H.
Experiments and data curation	**C.U.**, K.B., L.B., and Y.L.
Data analysis	**C.U.**, K.B., L.B., and Y.L.
Resources	R.G.K., E.B., U.H., and D.T.
Writing, original manuscript	**C.U.**
Writing, review and editing	**C.U.**, M.B., and D.T.

Utermann, C., Echelmeyer, V.A., Blümel, M., and Tasdemir, D., 2020. Culture-dependent microbiome of the *Ciona intestinalis* tunic: Isolation, bioactivity profiling and untargeted metabolomics. *Microorganisms,* 8, 1732; DOI: 10.3390/microorganisms8111732.

Contribution	Author(s) (abbreviated)
Conceptualization	**C.U.**, M.B., and D.T.
Sampling	**C.U.**
Experiments and data curation	**C.U.** and V.A.E.
Data analysis	**C.U.**
Writing, original manuscript	**C.U.**
Writing, review and editing	**C.U.**, M.B., and D.T.

Utermann, C., Echelmeyer, V.A., Oppong-Danquah, E., Blümel, M., and Tasdemir, D., 2021. Diversity, bioactivity profiling and untargeted metabolomics of the cultivable gut microbiota of *Ciona intestinalis. Marine Drugs,* 19, 6; DOI: 10.3390/md19010006.

Contribution	Author(s) (abbreviated)
Conceptualization	**C.U.**, M.B., and D.T.
Sampling	**C.U.**
Experiments and data curation	**C.U.**, V.A.E., and E.O.D.
Data analysis	**C.U.**, E.O.D.
Writing, original manuscript	**C.U.**
Writing, review and editing	**C.U.**, M.B., and D.T.

Abbreviations

Abbreviation	Definition
A375	Human malignant melanoma cell line
A549	Human lung cancer cell line
Ab	*Acinetobacter baumannii*
AMP(s)	Antimicrobial peptides
ANOSIM	Analysis of similarities
ANOVA	Analysis of variance
ARB	Antibiotic-resistant bacteria
BGC(s)	Biosynthetic gene cluster(s)
BLAST	Basic Local Alignment Search Tool
BWH	Biological weapon hypothesis
CAG	Casamino-acids-glucose medium
Ca	*Candida albicans*
CB	*Ciona intestinalis* medium adjusted to Baltic Sea salinity
CFM-ID	Competitive Fragmentation Modeling for Metabolite Identification
Cn	*Cryptococcus neoformans*
CN	*C. intestinalis* medium adjusted to North Sea salinity
COX3-ND1	Cytochrome c oxidase subunit 3-NADH dehydrogenase subunit 1
DMSO	Dimethyl sulfoxide
DNA	Desoxyribonucleic acid
DNP	Dictionary of Natural Products
Ec	*Escherichia coli*
Efm	*Enterococcus faecium*
EICA	Evolution of increased competitive ability hypothesis
ERH	Enemy release hypothesis
EtOAc	Ethyl acetate
FDA	U.S. Food and Drug Administration
FBMN	Feature-based molecular networking/network
G	Gut of *C. intestinalis*
GNPS	Global Natural Products Social Molecular Networking
GYM	Glucose-yeast-malt medium
H	Helgoland
HCT116	Human colon cancer cell line
IB	Inner body of *C. intestinalis*
IC_{50}	Half maximal inhibitory concentration
ISDB-UNPD	*In-silico* MS/MS database-based workflow of the Universal Natural Product Database
ITS	Internal transcribed spacer
K	Kiel

Abbreviation	Definition
Kp	*Klebsiella pneumoniae*
LC	Liquid chromatography
MB	Marine Broth
MB231	Human breast cancer cell line
MeOH	Methanol
MIC	Minimum inhibitory concentration
MNP(s)	Marine natural product(s)
MRSA	Methicillin-resistant *Staphylococcus aureus*
MS	Mass spectrometry
MS/MS	Tandem mass spectrometry
NADH	Nicotinamide adenine dinucleotide hydride
NCBI	National Center for Biotechnology Information
NGS	Next generation sequencing
NIS	Non-indigenous species (= non-native species)
nMDS	Non-metric multidimensional scaling
NP(s)	Natural product(s)
NP Atlas	The Natural Products Atlas
NWH	Novel weapon hypothesis
OSMAC	One strain - many compounds
OTU(s)	Operational taxonomic unit(s)
PCoA	Principal coordinates analysis
PDA	Potato dextrose agar
PEI	Prince Edward Island
Psa	*Pseudomonas aeruginosa*
psu	Practical salinity unit
QToF	Quadrupole time-of-flight
RDP	Ribosomal Database Project
rRNA	Ribosomal RNA
SM(s)	Secondary metabolite(s)
T	Tunic of *C. intestinalis*
TRBA	Technical rules for biological agents
TSB	Trypticase soy broth
W	Seawater reference sample
WSP	Wickerham medium
UPLC	Ultra-high performance liquid chromatography

Abstract

The tunicate *Ciona intestinalis* is one of the most notorious invasive ascidian species. In Prince Edward Island (PEI, Canada), *C. intestinalis* causes heavy fouling on farmed mussels leading to significant economic losses. Except for general beneficial eco-physiological characteristics of invasive ascidians, reasons underlying *C. intestinalis'* invasiveness remain obscure. This study aimed to shed light on two additional factors potentially promoting its invasion success, i.e., bioactive secondary metabolites and associated microbiota, which reportedly contribute to the invasiveness of other marine species. Therefore, microbiomes and metabolomes of invasive (PEI) and native (Helgoland and Kiel, Germany) *C. intestinalis* populations were comparatively studied, a novelty in invasive ascidian research.

Apart from being problematic invasive species, ascidians and their associated microbiota are a rich source for bioactive marine natural products (MNPs) relevant for human health. However, the biodiscovery potential of *C. intestinalis*-associated microorganisms remains largely unknown. Accordingly, this doctoral research project targeted to explore bioactivities and the chemical repertoire of culturable bacteria and fungi associated with *C. intestinalis.*

Amplicon sequencing-based bacterial community analysis of gut, tunic, and seawater (control) samples revealed species-specificity and a diverse microbiota (39 phyla). The UPLC-MS/MS-based untargeted metabolomics approach revealed a diverse chemical inventory dominated by alkaloids and lipids. In addition to core bacteria and metabolites present in all samples, also tissue- and location-specific bacteria and metabolites were observed. Notably, highest microbial and chemical diversity were detected in the invasive *C. intestinalis* population (PEI). In combination, these results suggest a high adaptive capacity of *C. intestinalis*. In addition, several detected bacteria and secondary metabolites reportedly have antimicrobial, antifouling, and other relevant bioactivities, potentially promoting its overall health, fitness, and competitiveness. In conjunction with microbiome data, this first global metabolome study on *C. intestinalis* indicated microbial associates and chemical weapons as additional relevant factors promoting its invasion success. Therefore, this work contributes important basic knowledge for future projects scrutinizing the invasiveness of *C. intestinalis*.

To investigate the potential of microorganisms associated with *C. intestinalis* in marine biodiscovery, isolates were obtained from tunics (T) and guts (G) due to their pivotal functions for the ascidian's defense against, e.g., pathogens, and their reportedly different bacterial communities. In total, 89 (T) and 61 (G) bacteria as well as 22 (T) and 40 (G) fungi were isolated and identified from Helgoland and Kiel specimens. Many extracts showed antibacterial (T: 42%, G: 64%), antifungal (T: 10%, G: 11%), and/or anticancer (T: 6%, G: 22%) activities. A 2-step selection procedure considering bioactivity and metabolite profiles was applied to prioritize the most promising MNPs producers. This led to the selection of seven tunic- and nine gut-derived microbial extracts affiliated to the fungal group of ascomycetes (69%) and the bacterial taxa Actinobacteria (25%) and *Bacillus* sp. (6%). Through an UPLC-MS/MS-based dereplication workflow including molecular networking, *in-silico* approaches and manual database comparison, 170 compounds belonging to >40 different chemical families were putatively annotated, displaying a vast chemical diversity. Although this represents a significant increase in annotation rates compared to previous studies, still many compounds even from well-studied organisms (e.g., *Penicillium* and *Streptomyces* spp.) remained unknown. In summary, this study demonstrated a huge pharmaceutical potential of the culturable microbiota associated with *C. intestinalis*, including discovery of various putatively novel compounds. Application of novel selection and integrated dereplication procedures proved successful for strain prioritization and compound annotation. Furthermore, this strategy highlighted particularly fungi as so far uncharted and exceptionally promising resource for putatively novel anticancer and antimicrobial lead compounds of high interest.

Zusammenfassung

Das Manteltier *Ciona intestinalis* ist eine der problematischsten invasiven Seescheidenarten. In der kanadischen Provinz Prince Edward Island (PEI) führt massiver Bewuchs von Zucht-Muscheln durch *C. intestinalis* zu erheblichen wirtschaftlichen Einbußen. Die ökophysiologischen Eigenschaften invasiver Seescheiden liefern lediglich eine unvollständige Erklärung für die Invasivität von *C. intestinalis* und es ist unklar, ob weitere Aspekte eine Rolle spielen. Ziel dieser Arbeit war es daher, mögliche zusätzliche Faktoren aufzuzeigen, die zu einer erfolgreichen Ansiedlung von *C. intestinalis* in neuen Habitaten beitragen könnten. Hierzu wurden sowohl bioaktive Sekundärmetabolite als auch assoziierte Mikroorganismen von *C. intestinalis* untersucht, welche beide in der Literatur bereits als wichtige Faktoren für die Invasivität mariner Arten identifiziert wurden. Erstmals wurden in dieser Arbeit vergleichende Untersuchungen des Mikrobioms und des Metaboloms invasiver (PEI) und einheimischer (Helgoland und Kiel, Deutschland) *C. intestinalis* Populationen durchgeführt.

Neben ihrer hohen Invasivität sind Seescheiden und ihre assoziierten Mikroorganismen als ergiebige Quelle für bioaktive marine Naturstoffe mit hohem Anwendungspotenzial für die medizinische Forschung bekannt. Allerdings ist das Potenzial der mit *C. intestinalis* assoziierten Mikroorganismen diesbezüglich weitgehend unbekannt. Demzufolge war ein weiteres Ziel dieses Promotionsprojekts, die mit *C. intestinalis* assoziierten, kultivierbaren Bakterien und Pilze hinsichtlich ihrer Bioaktivität und ihres Repertoires an Sekundärmetaboliten zu erforschen.

Für die Analyse hinsichtlich zusätzlicher Invasivitätsfaktoren wurde die bakterielle Diversität des Darms und der Tunica von *C. intestinalis* sowie von Meerwasserproben (Kontrolle) mittels Amplikon-Sequenzierung vergleichend untersucht. Diese Analysen resultierten in einer diversen (39 Phyla) und *C. intestinalis*-spezifischen Bakteriengemeinschaft. Darüber hinaus wurde mittels vergleichender, ungerichteter UPLC-MS/MS-basierter Metabolomanalysen ein vielfältiges, von Alkaloiden und Lipiden dominiertes Sekundärmetabolitspektrum gefunden. Interessanterweise wurden neben Seescheiden-spezifischen Bakterien-Sequenzen und ubiquitär vorkommenden Metaboliten auch solche mit gewebe- und standortspezifischem Vorkommen detektiert. Besonders hervorzuheben ist hier die erhöhte mikrobielle und chemische Diversität in der invasiven *C. intestinalis* Population (PEI). Zusammengenommen deuten diese Ergebnisse auf eine hohe Anpassungsfähigkeit von *C. intestinalis* hin. Darüber hinaus sind für einige der *C. intestinalis*-assoziierten Bakterien und Sekundärmetabolite bereits antimikrobielle, antifouling sowie andere relevante Bioaktivitäten beschrieben worden, welche potenziell zu einer Erhöhung der Gesundheit, Fitness und Konkurrenzfähigkeit der Seescheide beitragen. Diese erste globale Metabolomstudie von *C. intestinalis* weist in Verbindung mit dem erhobenen Mikrobiomdatensatz darauf hin, dass assoziierte Mikroorganismen und Sekundärmetabolite möglicherweise zusätzliche, für den Invasionserfolg von *C. intestinalis* relevante Faktoren darstellen. Daher liefert die vorliegende Arbeit wichtige Basisdaten für zukünftige Projekte rund um die Invasivität von *C. intestinalis*.

Um das Potenzial der *C. intestinalis*-assoziierten Mikroorganismen für die Wirkstoffforschung zu untersuchen, wurden Mikroorganismen von Tunica (T) und Darm (G) einheimischer *C. intestinalis* (Helgoland und Kiel) isoliert. Diese Gewebe wurden aufgrund ihrer zentralen Rolle z.B. in der Abwehr von Pathogenen sowie ihrer bekanntermaßen unterschiedlichen Bakteriengemeinschaften ausgewählt. Insgesamt wurden 89 (T) bzw. 61 (G) Bakterien sowie 22 (T) bzw. 40 (G) Pilze isoliert und identifiziert. Viele Extrakte zeigten antibakterielle (T: 42%, G: 64%), fungizide (T: 10%, G: 11%) und/oder krebszellhemmende (T: 6%, G: 22%) Aktivitäten. Ein zweistufiges Selektionsverfahren, welches die Bioaktivitäts-

und Metabolitprofile der Isolate berücksichtigte, wurde zur Priorisierung der vielversprechendsten Naturstoffproduzenten-Stämme angewendet. So wurden sieben (T) bzw. neun (G) mikrobielle Extrakte ausgewählt, die den Schlauchpilzen (69%), den Actinobakterien (25%) und *Bacillus* sp. (6%) zugeordnet wurden. Im Folgenden wurde ein UPLC-MS/MS-basierter Dereplikationsprozess genutzt, der molekulare Netzwerke, *in-silico* Verfahren und manuelle Datenbanksuchen beinhaltete. Mit 170 mutmaßlich identifizierten Substanzen aus über 40 verschiedenen chemischen Familien konnte so eine immense chemische Vielfalt ermittelt werden. Auch wenn diese Ergebnisse eine signifikante Steigerung erfolgreich identifizierter Substanzen im Vergleich zu Literaturdaten darstellen, blieben viele Metabolite auch von bereits sehr gut erforschten Mikroorganismen (z.B. *Penicillium* und *Streptomyces* spp.) unannotiert.

Zusammengefasst zeigt diese Arbeit, dass die mit *C. intestinalis* assoziierte, kultivierbare mikrobielle Gemeinschaft ein enormes Potenzial für die Wirkstoffentwicklung hat. Dies beinhaltet auch die Entdeckung vieler neuartiger Substanzen. Eine neue Selektionsmethode und ein integriertes Dereplikationsverfahren wurden erfolgreich zur Priorisierung von mikrobiellen Extrakten und zur Substanzidentifikation angewendet. Außerdem hebt diese Studie insbesondere die bisher völlig unerforschte *C. intestinalis*-assoziierte Pilzgemeinschaft als äußerst vielversprechende Quelle für möglicherweise neuartige krebshemmende und antimikrobielle Wirkstoffe hervor.

Introduction

1   Marine natural products to combat infectious diseases and cancer

Cancer is after cardiac diseases the most life-threatening non-infectious disease today. More than nine million cancer-related deaths worldwide were projected for 2018 (Bray et al. 2018, WHO 2018). Cancer incidences continuously rise, mainly due to an aging society, and will probably exceed 20 million per annuum by 2025 (DePinho 2000, Ferlay et al. 2015). Despite remarkable advances in terms of efficacy and cure rates, most available chemotherapies still cause severe (long-term) side effects (Nurgali et al. 2018). Another serious risk for human health is imposed by the globally rising number of antibiotic-resistant bacteria (ARB). ARB-related deaths are estimated to reach 10 million within the next decades and currently >3 million new ARB infections are registered yearly in Europe and the USA (Luepke and Mohr 2017, Cassini et al. 2019). Mainly driven by excessive and often inappropriate use of antibiotics especially in medicine and agriculture, many human pathogenic bacteria have developed resistance to antibiotics. As a consequence, >70% of clinically relevant human pathogens nowadays show resistance towards at least one antimicrobial agent (Watkins and Bonomo 2016). Hence, novel drugs to combat infectious diseases and cancer are urgently needed (Khalifa et al. 2019, Hifnawy et al. 2020).

Natural products (NPs) are used since millennia to cure all kinds of diseases and represent the most rewarding resource for drug development (Harvey 2008, Martins et al. 2014). The term NPs usually refers to small molecules (<1500 Da) not directly related to growth and propagation of an organism. Being mostly classified as secondary metabolites (SMs), they offer competitive advantages and thus fulfill important functions for the producing organism such as defense, competition, and communication (Wishart 2008, Stuart et al. 2020).

In contrast to long-standing research on terrestrial NPs (TNPs) that led to the discovery of >150,000 compounds, the exploration of the marine realm started only in the 1950s. Isolation of the nucleosides spongothymidine and spongosine from the Caribbean demosponge *Tectitethya crypta* (formerly known as *Cryptotethya crypta*) marks the beginning of marine NPs (MNPs) research (Bergmann and Burke 1955, Molinski et al. 2009, Shang et al. 2018). Their discovery inspired the development of the first marine-derived drug, the anticancer agent cytarabine. Cytarabine (marketed as Cytosar-U®) was approved for treatment of leukemia by the U.S. Food and Drug Administration (FDA) in 1969 (Molinski et al. 2009, Romano et al. 2017). Since then, >30,000 MNPs have been discovered (Carroll et al. 2020). Marine-sourced molecules presumably serve as basis for more than half of the drugs FDA-approved between 1981 and 2002, highlighting their enormous biodiscovery potential (Blockley et al. 2017). Evidence suggests that marine organisms are much more prolific producers of bioactive molecules than terrestrials. The proportion of MNPs with anticancer properties (1%) is 100-fold higher than for TNPs (Palanisamy et al. 2017, Shang et al. 2018) and marine drug discovery has a ~4-fold higher success rate when compared to TNPs research (Sigwart et al. 2021). So far, 14 MNPs entered the market as drugs, of which the majority (9 MNPs) was approved as therapeutic agents against cancer[1]. However, no marine-derived compound has yet been approved or entered clinical trials for treatment of microbial infections.

---

[1] According to the Marine Pharmacology Clinical Pipeline, last updated in October 2020. Available at https://www.midwestern.edu/departments/marinepharmacology/clinical-pipeline.xml (accessed on 04.01.2021)

1.1 Drug discovery potential of ascidians

Marine sedentary invertebrates such as sponges and tunicates[2] are among the most talented producers of MNPs. This is mainly attributed to their sedentary lifestyle that triggered evolution of various defense mechanisms, such as chemical defense, alternative to escape in order to protect themselves against fouling organisms, predators, and pathogens (Proksch et al. 2002, Schmidt and Donia 2010, Leal et al. 2012; more details in Section 2.1).

Biodiscovery studies on the chordate subphylum Tunicata delivered already more than 1300 MNPs (Miyako et al. 2020) that are mainly classified as alkaloids (79%; Figure 1a). All tunicate-derived MNPs have been isolated from the class Ascidiacea. Among them, the most diverse order Aplousobranchia (including, e.g., the genera *Aplidium* and *Didemnum* spp.; see also Section 2) contributed to 75% of the isolated MNPs between 1994 and 2014 (Figure 1b). Most ascidian-derived MNPs show bioactivities, with anticancer (64%) and antimicrobial (17%) activities being the most frequently reported (Figure 1c). The fact that three out of nine approved marine anticancer drugs are tunicate-derived (Figure 1d) underlines the high potential of ascidians to deliver novel compounds with anticancer activities (Menna 2009).
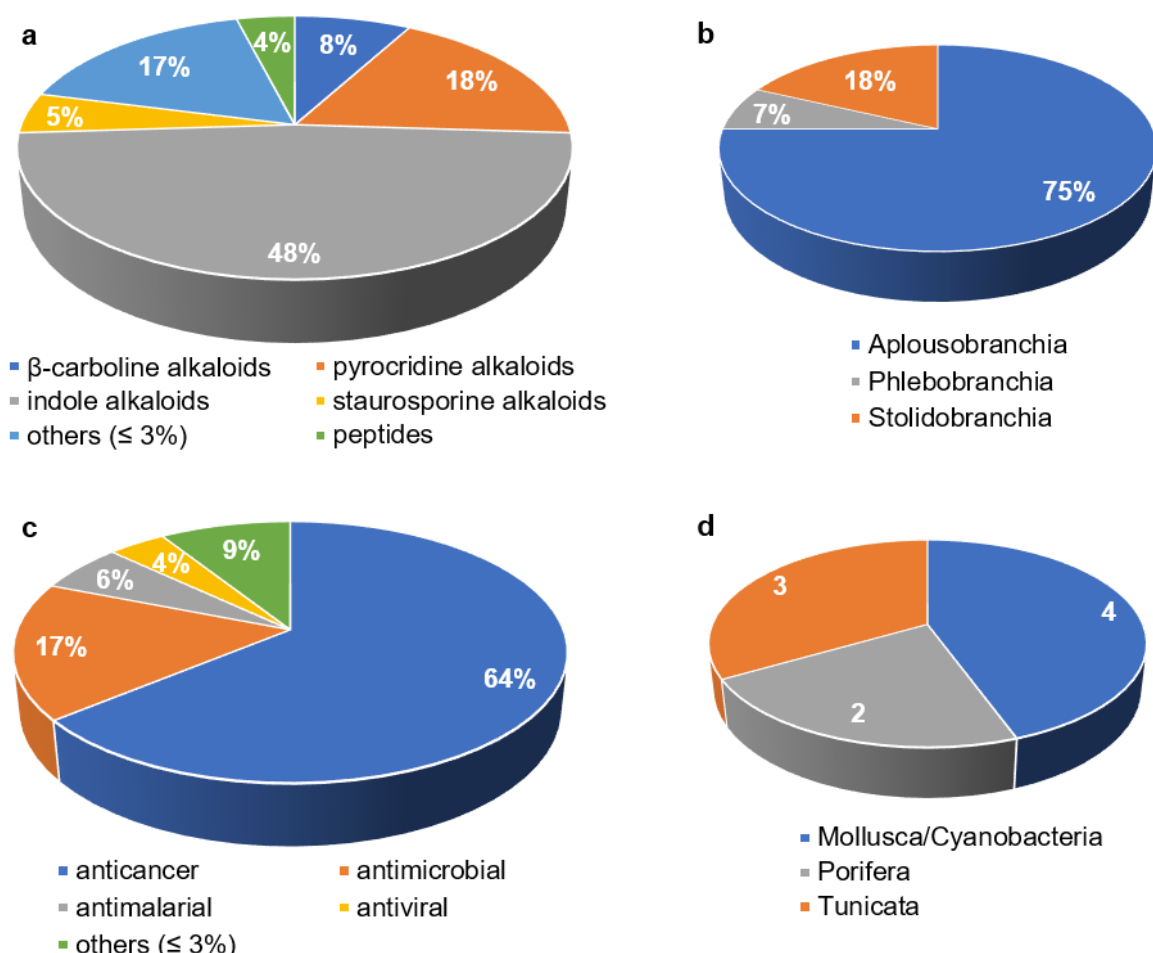
Figure 1. Characteristics and MNP discovery potential of ascidian-derived compounds. Ascidian-derived MNPs published between 1994 and 2014 (modified after Palanisamy et al. 2017). The chemical family of the isolated compounds (**a**), the taxonomic classification of the producing ascidian at order level (**b**), and reported bioactivities (**c**) are given. Figure 1d displays the origin of nine clinically approved marine anticancer drugs according to the Marine Pharmacology Clinical Pipeline[1].

---

[2] The presence of a notochord and dorsal nerve cord during the larval stage places tunicates unambiguously in the phylum Chordata, but still most studies include tunicates to the informal group invertebrates (Leal et al. 2012). Accordingly, in this study, the subphylum Tunicata is included in the group of marine invertebrates.

After 40 years of research, the anticancer agent Yondelis® (trabectedin/ecteinascidin-743; Figure 2) was the first ascidian-sourced drug that entered the market in 2007. Extracts of the colonial tunicate *Ecteinascidia turbinata* were already reported in 1969 to show antitumor properties, but structure elucidation of the complex tetrahydroisoquinoline alkaloid trabectedin was only completed in 1990 (Molinski et al. 2009, Gerwick and Moore 2012). Another 10 years were needed for the development of an appropriate semi-synthetic production process for trabectedin to solve the supply issue, i.e., ~1 t of *E. turbinata* were needed to gain 1 g of trabectedin (Cuevas and Francesch 2009, Martins et al. 2014).

didemnin B
Trididemnum solidum

plitidepsin (Aplidin ®)
Aplidium albicans

lurbinectedin (Zepzelca®)
synthetic analog of trabectedin

trabectedin (Yondelis®)
Ecteinascidia turbinata

lissoclinotoxin A
Lissoclinum perforatum
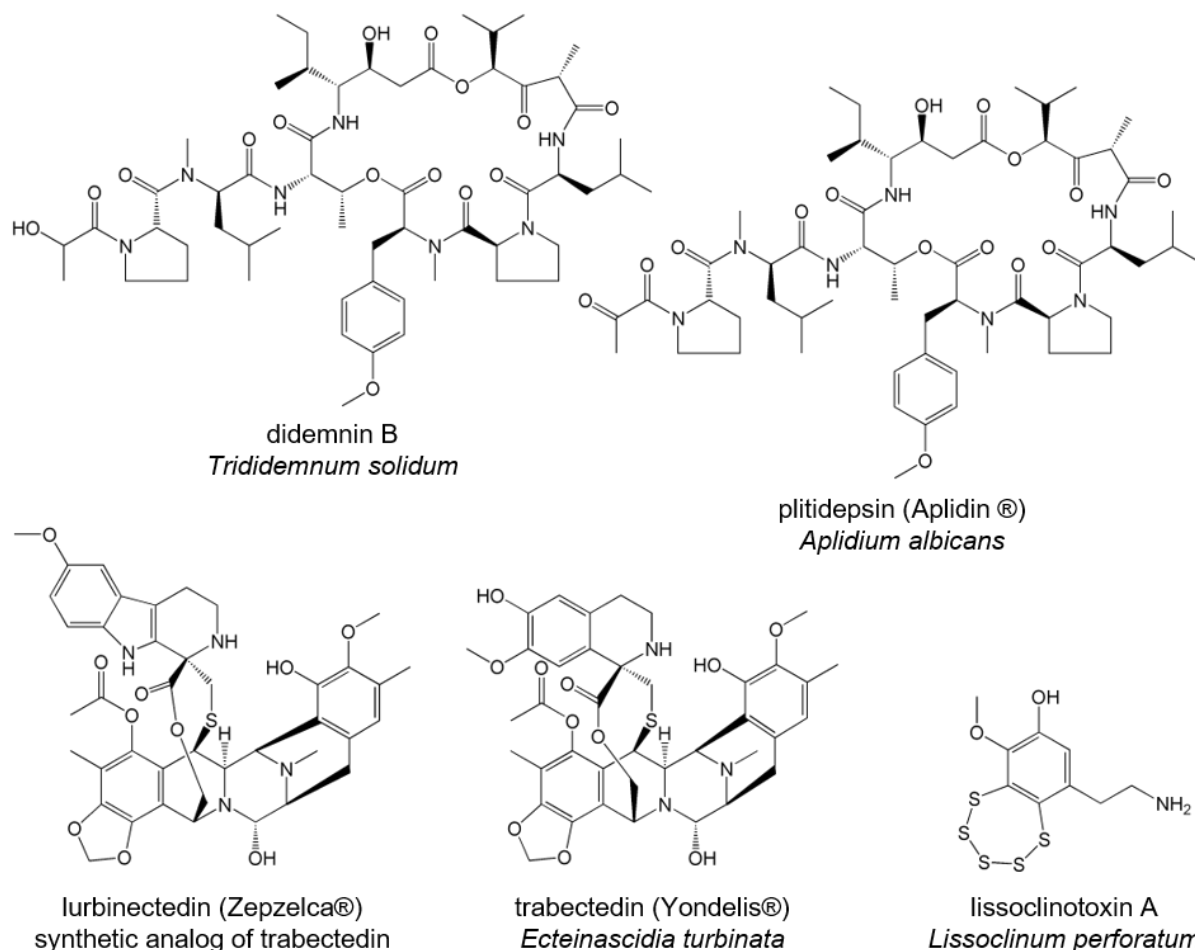
Figure 2. Anticancer and antimicrobial lead compounds isolated from ascidians. Compound names, trade names (if approved as drug) and the source of isolation are displayed for each structure.

Didemnin B represents another prominent example of an ascidian-derived MNP (Figure 2). It was isolated in the 1980s along with other cytotoxic cyclic depsipeptides from the Caribbean tunicate *Trididemnum solidum* (Rinehart et al. 1981). Although didemnin B showed potent *in vitro* and *in vivo* antiproliferative activity (Rinehart et al. 1981), clinical trials had to be stopped in phase II due to several negative side effects such as neuromuscular toxicity. Notably, the structurally similar compound plitidepsin (dehydrodidemnin B, Aplidin®; Figure 2) originally isolated from the Mediterranean tunicate *Aplidium albicans* showed comparable antitumor properties, but lower cytotoxicity (Molinski et al. 2009, Xu et al. 2012). Aplidin® combined with the corticosteroid dexamethasone was approved in 2018 by the Australian Regulatory Agency as 3rd/4th line anticancer agent for treatment of multiple myeloma

(Dyshlovoy and Honecker 2020)[3]. Most recently, lurbinectedin (Zepzelca®; Figure 2), a synthetic analog of trabectedin, was FDA-approved as treatment against small cell lung cancer. In addition, lurbinectedin is currently in clinical trials (phase III[1]) for treatment of, e.g., ovarian and breast cancer (Markham 2020).

Although no antimicrobial marine lead compound entered clinical trials so far, a current review presented 159 ascidian-derived compounds showing antibacterial activity, often in conjunction with other activities, e.g., antifungal (Casertano et al. 2020). For example, the polysulfide lissoclinotoxin A isolated from the colonial ascidian *Lissoclinum perforatum* shows a broad spectrum of activities against bacteria, fungi, and cancer cell lines (Figure 2). Most excitingly, it exhibited higher potency against the human pathogen *Staphylococcus aureus* (MIC 0.08 to 0.15 µg/mL) than the commercial antibiotic cefotaxime (MIC 1.2 to 10 µg/mL; Litaudon et al. 1994, Casertano et al. 2020). Moreover, antimicrobial peptides isolated from the solitary tunicate *Styela clava* included the polypeptide clavanin A, which showed promising antimicrobial properties when encapsulated with nanoparticles. *In vivo* bacterial sepsis assays, in which mice were infected with a polymicrobial mixture of human pathogens such as *Staphylococcus aureus*, showed increased survival rates to up to 100% when nanoformulated clavanin A was applied (Saude et al. 2014, Casertano et al. 2020).

1.2 Marine-derived microorganisms as resource for bioactive marine natural products

Recent evidence suggests that at least 8% of ascidian-derived metabolites are of microbial origin and several compounds originally isolated from ascidians have been shown to be actually produced by bacterial associates (Schmidt 2015, Bauermeister et al. 2018). Among them, didemnin B and trabectedin (ET-743) represent the most prominent examples. According to recent meta-omics studies, didemnin B is produced by marine-derived Alphaproteobacteria of the genus *Tistrella* (Xu et al. 2012) and trabectedin synthesis was demonstrated in the yet unculturable gammaproteobacterial *E. turbinata*-symbiont *Candidatus* Endoecteinascidia frumentensis (Rath et al. 2011). Another example is provided by the tambjamines, which were isolated from taxonomically very different marine invertebrate groups such as ascidians and bryozoans. This alkaloid family harbors many bioactive metabolites, inhibiting growth of bacteria, fungi, and cancer cells (Picott et al. 2019). In 2007, Burke and co-workers showed that tambjamine YP1 (Figure 3) is actually biosynthesized by the Gammaproteobacterium *Pseudoalteromonas tunicata*, which has been isolated from various marine surfaces including the solitary tunicate *Ciona intestinalis* (Burke et al. 2007). Similarly, patellamides, cytotoxic cyclic peptides, are frequently isolated from didemnid ascidians such as *Lissoclinum* species. Genome sequencing and heterologous expression evinced the production of patellamide A and C (Figure 3) by the cyanobacterial symbiont *Prochloron didemni* (Schmidt et al. 2005).

Over 150 MNPs have been isolated from ascidian-associated microbes in the past two decades (Chen et al. 2018). One example is the novel polyketide forazoline A that was obtained from the *E. turbinata*-associated actinobacterium *Actinomadura* sp. (Figure 3). This halogenated polyketide is a promising antifungal lead, since it showed *in vivo* activity against the human pathogen *Candida albicans* (MIC 16 µg/mL) and no toxicity (Wyche et al. 2014). This is in accordance with a general trend increasingly revealing symbiotic and free living marine-derived microorganisms as major source for the drug discovery pipeline,

---

[3] According to the oncology pipeline of PharmaMar. Available at https://pharmamar.com/science-and-innovation/oncology-pipeline/?lang=en (accessed on 18.01.2021)

outperforming marine invertebrates, algae, and mangroves (Figure 4; Bhatnagar and Kim 2010, Carroll et al. 2020). In 2019, the majority of reported marine compounds were of microbial origin (66%), with fungi (47%) taking the lead position as source for novel MNPs. While ten years ago only ~1000 MNPs were known from marine-derived fungi (Rateb and Ebel 2011), today >5000 are published (Carroll et al. 2020). The importance of marine microorganisms for drug discovery is highlighted by the microbial origin of two out of three MNPs currently in phase III clinical anticancer trials[1]. These are the cyclic dipeptide plinabulin (Figure 3), which was inspired by the fungal diketopiperazine halimide (Giddings and Newman 2019), and salinosporamide A (marizomib; Figure 3) produced by the actinobacterium *Salinispora tropica* (Feling et al. 2003, Wang et al. 2020).

forazoline A
Actinomadura sp.

patellamide A
Prochloron didemni

patellamide C
Prochloron didemni

tambjamine YP1
Pseudoalteromonas tunicata

plinabulin
Aspergillus sp.

salinosporamide A
Salinispora tropica

Phase III clinical trial
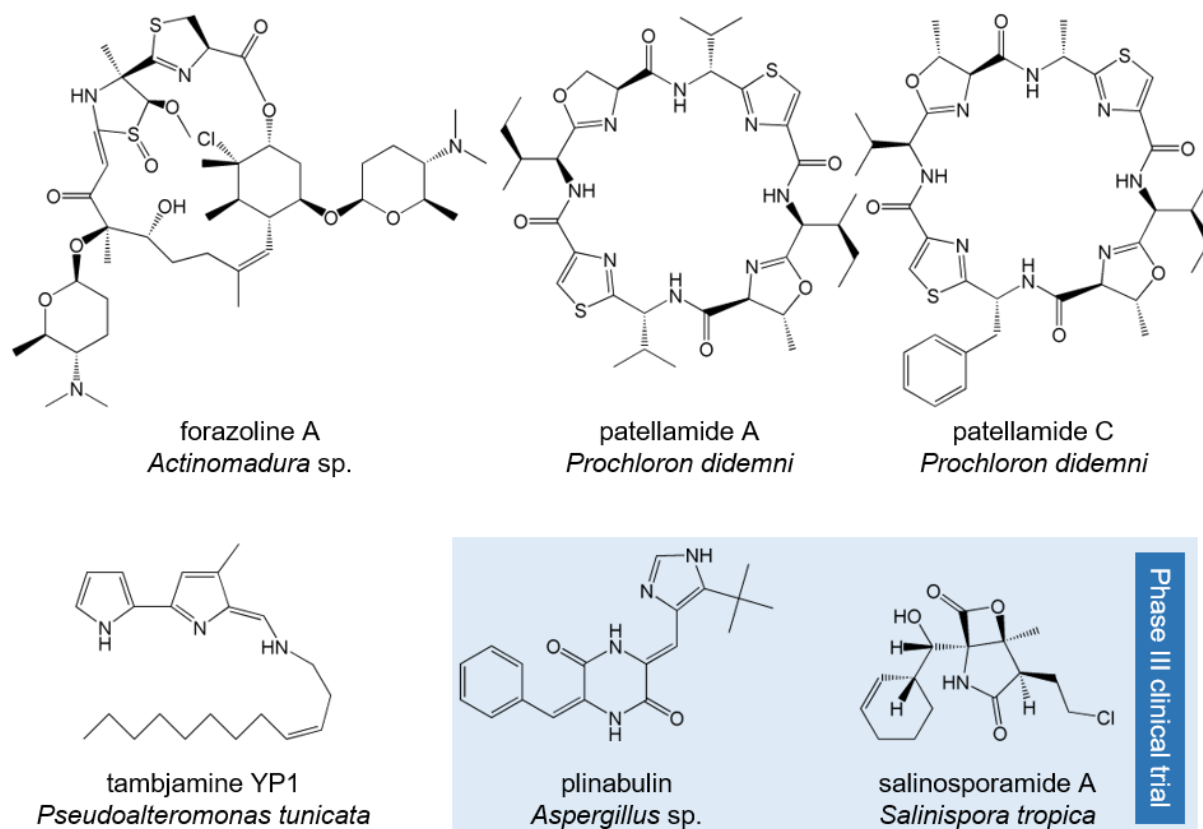
Figure 3. Bioactive secondary metabolites isolated from marine microorganisms. Chemical structures are displayed with their compound name and the bacterial or fungal producer.
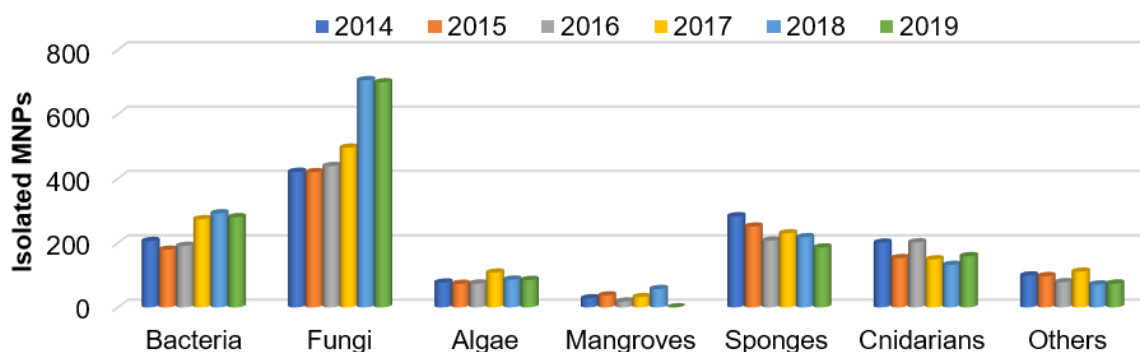
Figure 4. Original source of isolated MNPs published between 2014 and 2019. This graph was based on the annual MNPs report (Carroll et al. 2020). Data for 2019, which will be part of the 2021 MNPs report, are provided courtesy of Prof. Dr. Anthony Carroll (personal communication). Others: Bryozoans, echinoderms, mollusks, and tunicates.

2   The tunicate class Ascidiacea

Ascidians (sea squirts) are a fully marine class within the chordate subphylum Tunicata, the closest relatives of the vertebrates. Tunicate phylogeny has been challenging, mainly due to the low resolving power of previously used marker genes. Phylogenomic studies revealed that tunicates include the classes Appendicularia, Ascidiacea, and Thaliacea (Figure 5a). The class Ascidiacea can be further divided into the orders Aplousobranchia, Phlebobranchia, and Stolidobranchia, and is with ~3000 described species by far the largest tunicate class (Shenkar et al. 2017, Delsuc et al. 2018, Kocot et al. 2018).

Earliest geological records of tunicates date back to the early Cambrian period (~542 mya; Chen et al. 2003). Nowadays, ascidians are found all over the globe, from Alaska to Antarctica. Sea squirts colonize diverse habitats ranging from shallow waters to the deep sea, including soft and hard substrates as well as artificial structures (Shenkar and Swalla 2011). Species diversity is highest in the epi- and mesopelagic zone (Lambert 2005), but deep-sea ascidian species have been collected from below 8000 m (Sanamyan and Sanamyan 2006). Many ascidian species show broad environmental tolerances, with reported temperature limits from approximately -2 °C to +35 °C. Most ascidians can survive salinities between 25 ‰ and 40 ‰, but there are few reported species with much lower (12 ‰) or higher (>44 ‰) salinity tolerance limits (Shenkar and Swalla 2011, Zhan et al. 2015).

Although showing different lifestyles (colonial vs. solitary organisms) and diverse colors and shapes (Figure 5b), ascidians share general characteristics and body plan features (Figure 5c; Zeng et al. 2006, Holland 2016). Ascidians have a sessile lifestyle and a tough protective outer coating, the tunic. The tunic is a dense matrix mainly consisting of the cellulose-like polysaccharide tunicin and complex proteins such as collagen and elastin (Holland 2016, Franchi and Ballarin 2017). With few exceptions, ascidians are filter-feeders: Seawater enters the body via an oral (inhaling) siphon, is filtered through the branchial basket, where food particles are trapped by mucus, and exits via the atrial (exhaling) siphon (Lemaire 2011, Holland 2016). The alimentary tract is compartmentalized (i.e., esophagus, stomach, gut) and challenged by the constant exposure to microorganisms entering the sea squirt during water filtration. In that respect, the gut plays a pivotal role for the animal's immunity, exemplified by variable region-containing chitin-binding proteins (VCBPs). VCBPs are mainly expressed in the gut epithelium and modulate its microbial colonization and immune defense (Dishaw et al. 2016, Franchi and Ballarin 2017). Finally, sea squirts are broadcast-spawning hermaphrodites, i.e., they reproduce sexually by ejecting both eggs and sperms simultaneously. The embryo rapidly develops to a tadpole larva that exhibits basic chordate characteristics such as a notochord and a dorsal nerve cord (Lemaire et al. 2008, Holland 2016). Colonial ascidians also reproduce asexually via budding (Holland 2016).
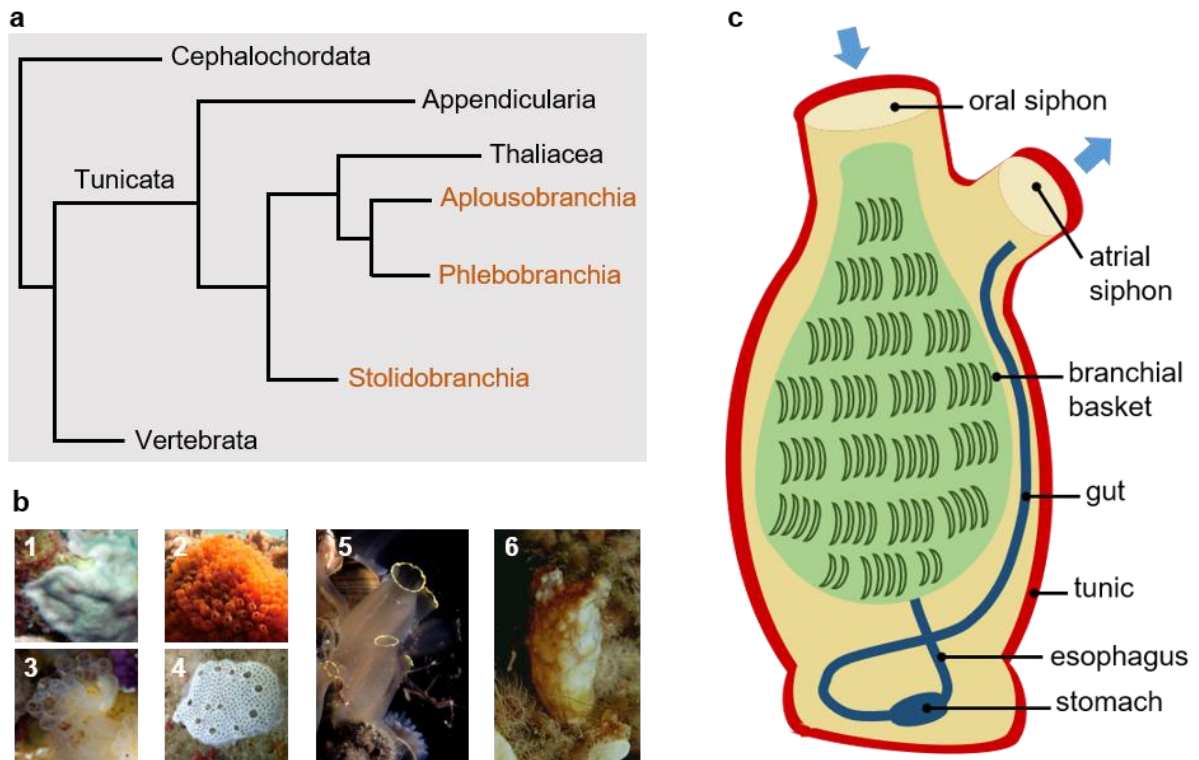
Figure 5. The tunicate class Ascidiacea. (**a**) Phylogenetic tree of tunicates and their closest relatives based on Delsuc et al. 2018. Orange names: Orders of the class Ascidiacea. (**b**) Prominent MNPs producers (1-4) and invasive species (5-6): *Trididemnum solidum* (1), *Ecteinascidia turbinata* (2), *Aplidium albicans* (3), *Lissoclinum perforatum* (4), *Ciona intestinalis* (5), and *Styela clava* (6). Pictures 1-3 were obtained under the terms and conditions of the CC BY 4.0 license (https://creativecommons.org/licenses/by/4.0/) from Hoeksema et al. 2020 (1) and Dou and Dong 2019 (2, 3). Pictures 4-6 were obtained from The Dutch Ascidians Homepage (www.ascidians.com) with permission from Dr. Arjan Gittenberger (GiMaRIS). (**c**) Simplified and generalized body plan of ascidians.

2.1 Key strategies of ascidians to escape predation, fouling, and infection

Sedentary and soft-bodied animals such as ascidians are continuously exposed to fouling and pathogens, are unable to escape from predation, and are in direct competition with other benthic species for resources such as food and space. To survive in this hostile environment, ascidians have developed multifold physical and chemical defense strategies. Physical defenses include tunic toughness and in some species accumulation of spicules within the tunic. Major chemical defense strategies involve highly acidic tunics (pH ≤2), accumulation of toxic heavy metals such as vanadium, and defensive chemicals, of which the latter appear most crucial for survival and performance (Stoecker 1980, Pisut and Pawlik 2002, López-Legentil et al. 2006, Erwin et al. 2013). Antimicrobial peptides (AMPs) are important for the ascidian's immune response towards invading microorganisms. For instance, two AMPs (Ci-MAM-A24 and Ci-PAP-A22) originating from hemocytes of *C. intestinalis* exerted potent antimicrobial activities, e.g., Ci-MAM-A24 inhibited growth of marine bacteria (MIC 0.1-3.1 µM; Fedders et al. 2008, Di Bella et al. 2011, Sperstad et al. 2011). In addition to AMPs, chemical defense is provided by predator deterring SMs. This was first demonstrated in 1990 for *Atapozoa* sp. (later identified as *Sigillina signifera*). Crude extracts and tambjamine alkaloids from this ascidian repelled, e.g., carnivorous fish (Paul et al. 1990, López-Legentil et al. 2006). Similarly, ascididemin obtained from *Cystodytes* spp. significantly reduced predation by the puffer fish *Canthigaster solandri* (López-Legentil et al. 2006). Despite these intriguing examples, for most SMs, the ecological function remains unclear (Lopanik and Clay 2014).

2.2   Microbial associates of ascidians: Friends or foes?

Today's consensus is that macroorganisms are not regarded as single organisms, but as a complex host-microbiota entity, named holobiont (Zilber-Rosenberg and Rosenberg 2008) or metaorganism (Bosch and McFall-Ngai 2011). Many ascidian species have been demonstrated to harbor diverse host-specific bacterial communities that vary with geographic location and environmental parameters (Tianero et al. 2015). In addition, species-specific bacterial symbionts are essential for survival and fitness of the host, mainly by providing bioactive metabolites with various ecological functions and by assisting nutrient supply (Franzenburg et al. 2013, Tianero et al. 2015). The cyanobacterium *Prochloron* spp. associated with the colonial ascidians *Lissoclinum patella* and *Didemnum molle* provides UV-shielding compounds such as mycosporine-like amino acids (Hirose et al. 2006, Morita and Schmidt 2018). The above-mentioned didemnins, ecteinascidins, and tambjamines are excellent examples of symbiont-mediated chemical defense for deterrence of predators (Florez et al. 2015, Morita and Schmidt 2018). Cyanobacterial associates such as *Prochloron* or *Synechocystis* spp. complement the diet of their heterotrophic filter-feeding hosts by providing photosynthetically fixed carbon (up to 100%) and by nitrogen recycling (Donia et al. 2011, Morita and Schmidt 2018). In contrast to numerous examples of beneficial bacteria-ascidian partnerships, the ascidian mycobiome remains largely unexplored. First studies on ascidian-associated fungi are solely based on cultivation and therefore, host-specificity and their ecological roles remain to be proven (Yarden 2014, López-Legentil et al. 2015). Interestingly, no microbial pathogens are – to our knowledge – known from sea squirts, giving further evidence for a well-working defense system against microbial infections.

2.3   The sea vase tunicate *Ciona intestinalis*

Ciona intestinalis, commonly known as sea vase tunicate, is a solitary sea squirt belonging to the family Cionidae (order Phlebobranchia; Figure 6a) that consists of 18 different species (Carver et al. 2006, Shenkar and Swalla 2011, Mastrototaro et al. 2020). In 1767, *C. intestinalis* was first described by Carl von Linné (latin: *Carolus Linnaeus*) under the name *Ascidia intestinalis* (Linnaeus 1767, Brunetti et al. 2015). It follows a typical ascidian body plan, including the tunic, two siphons, and the digestive organs. The sea vase tunicate has a cylindrical and translucent body of pale greenish to orange color and the siphons show yellowish pigmentation at the margins (Figure 6b-f; Millar 1953, Carver et al. 2006). With a long reproductive season in temperate regions (spring to autumn) and ~500-1000 produced eggs per individual per day, *C. intestinalis* shows a high reproductive capacity. Moreover, it grows rapidly (~2 cm/month) and reaches maturity already after ca. 2 months (Dybern 1965, Carver et al. 2006, Harris et al. 2017). Adults reach up to 15 cm in length and 3 cm in diameter (Carver et al. 2006). The total life-span of *C. intestinalis* varies from months to years, with cold-water-adapted animals showing longer lifespans, e.g., in Northern European waters individuals live 12-18 months (Dybern 1965, Carver et al. 2003). *C. intestinalis* is characterized by broad environmental tolerance: it can survive water temperatures from -1 °C to +35 °C (eurytherm) and salinities from 12 ‰ to 40 ‰ (euryhaline), which is the highest salinity tolerance reported for ascidians (Zhan et al. 2015). Some generalist ascidian predators such as fish (e.g., combtooth blenny *Scartichthys viridis*), crustaceans (e.g., rock shrimp *Rhyncocinetes typus* and shore crab *Carcinus maenas*), and the common sea star *Asterias rubens* reportedly prey upon adult *C. intestinalis* (Carver et al. 2006, Dumont et al. 2011).
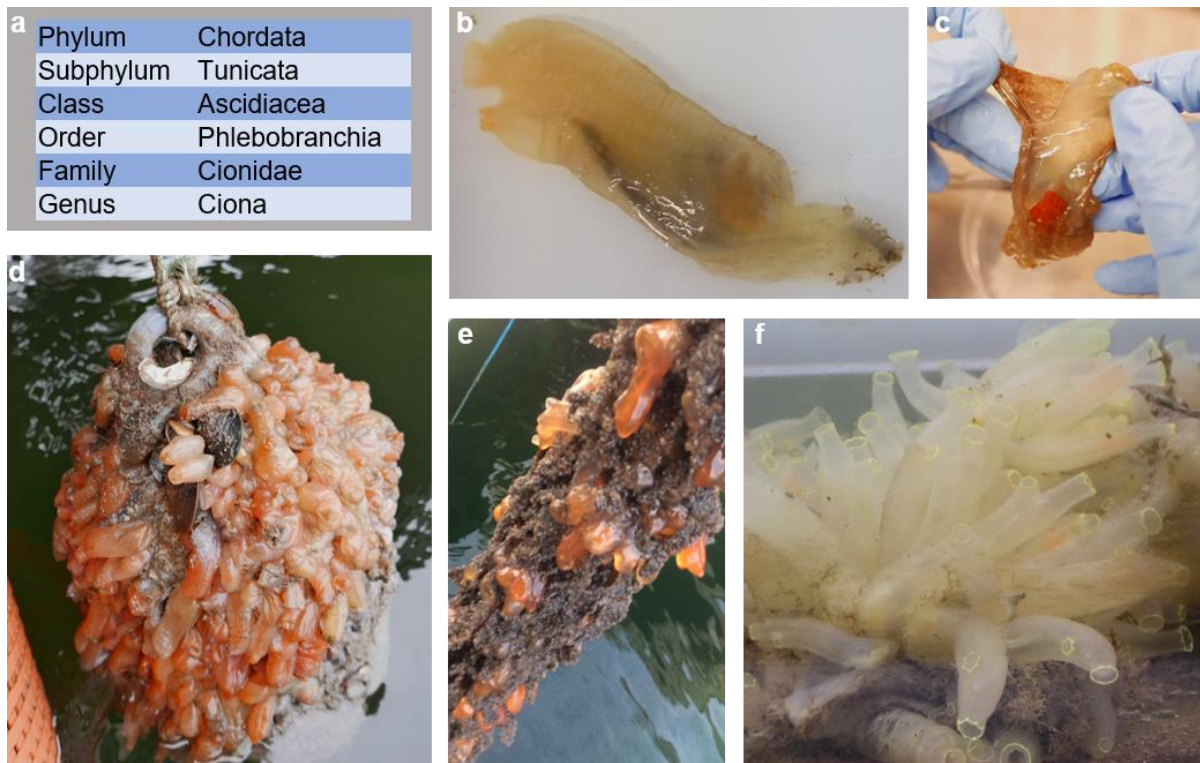
Figure 6. The sea vase tunicate *Ciona intestinalis*. The taxonomic classification of *C. intestinalis* is displayed in **a**. Pictures b-f show *C. intestinalis* in the laboratory and in natural habitats: A specimen sampled in Helgoland (**b**), the opened tunic of a specimen from Prince Edward Island (**c**), *C. intestinalis* growing on a buoy (**d**) or on farmed *Laminaria saccharina* in Kiel Fjord (**e**), and an underwater *C. intestinalis* population (**f**). Pictures 6b-e were taken by Caroline Utermann, picture 6f was retrieved under CC BY-NC-SA 4.0 license (https://creativecommons.org/licenses/by-nc-sa/4.0/) from the World Register of Marine Species (http://www.marinespecies.org/index.php; author: Perezoso).

Ascidians are due their close relation to the vertebrates (including the tadpole larvae) and their fast reproduction perfect model organisms for animal evolution and development (Kumano and Nishida 2007, Delsuc et al. 2018). *Ciona* spp. are particularly favorable model species due to their rapid embryogenesis, easy cultivation and propagation in the laboratory, and their translucent body that allows non-invasive observation of all internal organs (Corbo et al. 2001, Satoh et al. 2003, Dishaw et al. 2012). Research on *Ciona* spp. was further spurred by the release of the *C. intestinalis*[4] and *C. savignyi* genomes in 2002 (Dehal et al. 2002) and 2005 (Vinson et al. 2005), respectively. Genome sequencing of *C. intestinalis*[4] was an important milestone, since it was the first published genome of an invertebrate chordate. Its comparably small genome size (~160 Mb) is another aspect rendering *C. intestinalis*[4] an attractive model species (Satoh and Levine 2005, Satou et al. 2019). *Ciona* spp. were also recently proposed as suitable model organisms for ecotoxicity (Gallo and Tosti 2015, Eliso et al. 2020) and host-microbe interaction studies (Leigh et al. 2016).

2.4 Taxonomic revision and global distribution of the *C. intestinalis* species complex

The precise taxonomic placement of species is crucial for many research fields, including the developmental and evolutionary research conducted with the model organism *C. intestinalis* (Caputi et al. 2007). However, the phylogenetic relationship of *C. intestinalis* and its closely related species *C. robusta* was the subject of long scientific debate (Brunetti et

---

[4] Previously re-assigned to *C. robusta* (see Section 2.4)

al. 2015, Pennati et al. 2015). In 2007, it was demonstrated that *C. intestinalis* consists of two cryptic species, termed *C. intestinalis* spA and spB (Caputi et al. 2007). Only five years later researchers presented compelling genetic and morphological evidence that *C. intestinalis* spA was misidentified and must be assigned to the distinct species *C. robusta* described by Hoshino and Tokioka in 1967. *Ciona intestinalis* spB is correctly assigned as *C. intestinalis* Linnaeus 1767 *sensu* Millar 1953 (Brunetti et al. 2015, Pennati et al. 2015, Mastrototaro et al. 2020)[5]. Since *C. intestinalis* and *C. robusta* show high morphological similarity, the above presented studies used mitochondrial and nuclear gene markers to corroborate their findings. The only reliable morphology-based discrimination criterion (i.e., *C. robusta* shows 'small raised regions' on the tunic surface close to the siphons) requires sophisticated knowledge and equipment. Hence, identification of *C. intestinalis* and *C. robusta* should always be based on molecular marker genes (Brunetti et al. 2015).

Ciona intestinalis* and *C. robusta* are both denoted as shallow water species and show a cosmopolitan distribution (Figure 7). *Ciona intestinalis* is more common in cold waters and has its origin in the NE Atlantic (including Baltic and North Seas). Nowadays, it is also found in the NW Atlantic (US and Canadian coast) as well as Bohai and Yellow Seas (China). *Ciona robusta*, which is native to the NW Pacific (Japan and Korea), is more adapted to warmer regions. This species has colonized several other geographic areas, i.e., the NE Pacific, the Mediterranean Sea, and additional regions in the Southern hemisphere. Moreover, co-occurrence of both species has been reported from the English Channel as well as the French and Spanish Atlantic coast (Caputi et al. 2007, Procaccini et al. 2011, Brunetti et al. 2015, Bouchemousse et al. 2016).
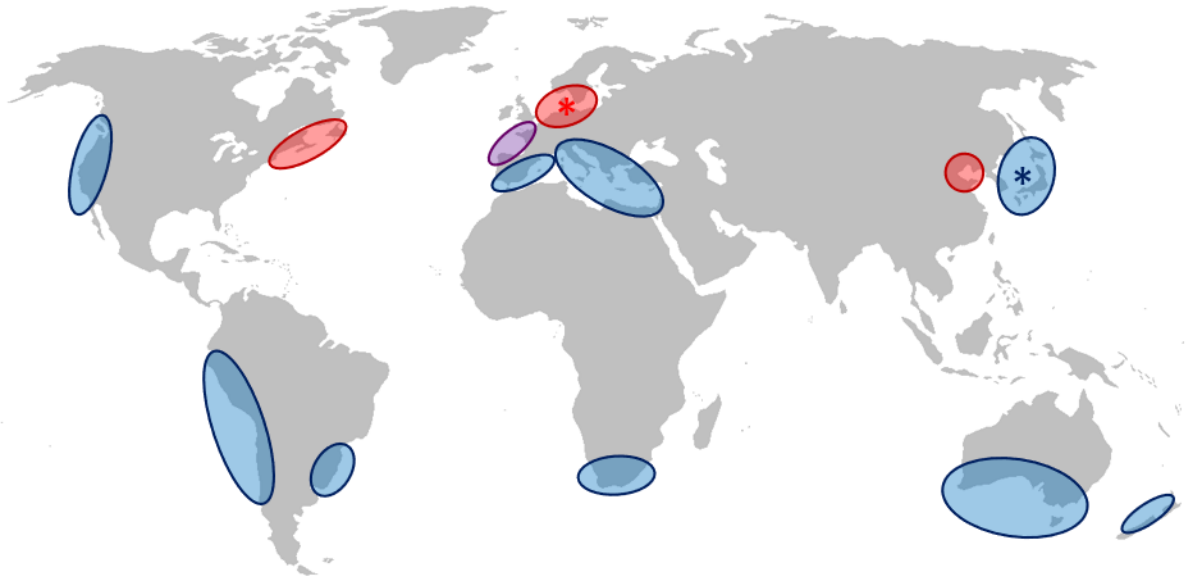
Figure 7. Global distribution of *C. intestinalis* and *C. robusta*. The gene marker-based distribution of *C. intestinalis* (red) and *C. robusta* (blue) is displayed. The contact zone of *C. intestinalis* and *C. robusta* is highlighted in purple. Native habitats are marked by an asterisk. This illustration was inspired by Caputi et al. 2007 and is based on the molecular studies of Zhan et al. 2010 and Bouchemousse et al. 2016. The map was retrieved from https://de.wikipedia.org/wiki/Datei:World_map_blank_without_borders.svg, where it was published by user Crates under the CC BY-SA 4.0 license (https://creativecommons.org/licenses/by-sa/4.0/).

---

[5] Whenever hereinafter referencing studies published before the taxonomic revision in 2015, the new taxonomy will be applied, i.e., *C. intestinalis* type A is changed to *C. robusta*.

2.5 Current state of play: Chemical and microbiome research on *Ciona* species

Although ascidians and their microbial associates are versatile producers of bioactive SMs, research on *Ciona* spp. is comparably low, i.e., Cionidae contributed only to 4% of MNPs isolated from ascidians between 1994 and 2014 (Palanisamy et al. 2017). Chemical investigations on European *C. intestinalis* delivered the above presented AMPs Ci-MAM-A24 and Ci-PAP-A22 (Helgoland, Germany), promising antibiotic lead compounds against antibiotic-resistant bacteria (Fedders et al. 2010, Di Bella et al. 2011), as well as the octapeptide cionin purified from Swedish specimens (Figure 8; Johnson and Rehfeld 1990). The polypeptides CS5931 and Cs-mChM-1, which were isolated from *C. savignyi* collected in China (Yellow Sea), are promising anticancer agents (Cheng et al. 2012, Dou et al. 2018). For instance, CS5931 inhibited the proliferation of six cancer cell lines and showed *in vitro* and *in vivo* anti-angiogenic activity rendering it a good anticancer drug candidate (Cheng et al. 2012, Liu et al. 2014). The bromophysostigmine alkaloids urochordamine A and B (Figure 8), both purified from Japanese *C. savignyi*, are potential metamorphosis inducers as they reportedly promote settlement and metamorphosis of the tadpole larvae (Tsukamoto et al. 1993). Furthermore, they show antibacterial activity against *Bacillus marinus*. Due to the detection of urochordamines and structurally related compounds in various marine invertebrates, a microbial origin was suggested (Tsukamoto et al. 1993). Two halogenated tyrosine-derived alkaloids, iodo- and bromocionin (Figure 8), were purified from *C. edwardsii* (Naples, Italy). Iodocionin showed selective *in vitro* activity against cell line L5178Y (mouse lymphoma; IC_{50} of 7.75 µg/mL; Aiello et al. 2010). A novel alkyl sulfate (Figure 8) from the same species also collected in Naples did not exert any cytotoxic effects (Imperatore et al. 2012). Chemical analyses of *C. robusta* led to the isolation of many sterols, including the ubiquitous cytotoxic sterol 24-hydroperoxy-24-vinylcholesterol isolated from *C. robusta* sampled in the Mediterranean Sea (Corsica, France; Figure 8; Guyot and Davoust 1982). Finally, the sperm-activating and -attracting factor 3,4,7,26-tetrahydroxycholestane-3,26-disulfate (Figure 8) was isolated from *C. robusta* and *C. savignyi* collected in Japan (Yoshida et al. 2002).

Two studies exploring the chemical composition of Norwegian *C. intestinalis* evinced differential lipid composition of tunic and inner body tissues as well as higher amounts of carbohydrates in the tunic, while inner body tissues were comparably richer in proteins (Zhao et al. 2015, Zhao and Li 2016). Nevertheless, no metabolomics study assessing the SM composition of *Ciona* spp. was conducted so far.

Three culture-independent studies revealed a diverse and rich bacterial community associated with the gut and tunic of *Ciona* species. *Ciona intestinalis* collected in the North Atlantic (Massachusetts, USA) harbored ascidian-specific microbiomes different from the ambient seawater, with few dominating strains mainly affiliated to Alphaproteobacteria and Bacteroidetes (Blasiak et al. 2014). A comparative analysis of the tunic microbiome of *C. robusta, C. savignyi* and two Stolidobranch ascidians sampled at different locations in New Zealand showed geographically conserved and species-specific microbiomes (Cahill et al. 2016). *Ciona intestinalis* and *C. robusta* sampled at three different sites (San Diego and Woods Hole, USA; Naples, Italy) showed large overlap of their gut microbiomes and, in contrast to the tunic, the gut microbiota was dominated by Gammaproteobacteria and Verrucomicrobia (Dishaw et al. 2014). The mycobiota of *Ciona* spp. has not been assessed by culture-independent methods yet, but recently few Ascomycete fungi such as *Acremonium*, *Penicillium*, and *Trichoderma* were isolated from the gut of *C. robusta* (Liberti et al. 2019). However, to the best of our knowledge no records exist on culturable fungi associated with *C. intestinalis*. Moreover, the biotechnological potential of microorganisms associated with *Ciona* spp. has only been investigated once: *Pseudoalteromonas tunicata*, a tunic-associated

bacterium isolated from *C. intestinalis* collected in the Gullmarsfjorden (Swedish west coast), exhibits antibacterial, antifouling, and antilarval activity and therefore, may contribute to the chemical defense of its host (Holmström et al. 1998). Accordingly, the potential of *C. intestinalis* associated microbiota in marine biodiscovery remains largely untapped.

urochordamine A

urochordamine B

iodocionin

bromocionin

24-hydroperoxy-24-vinylcholesterol

cionin

sodium 10-(hydroxymethyl)-
2,6,14-trimethylpentadecyl sulfate

3,4,7,26-tetrahydroxycholestane-3,26-disulfate
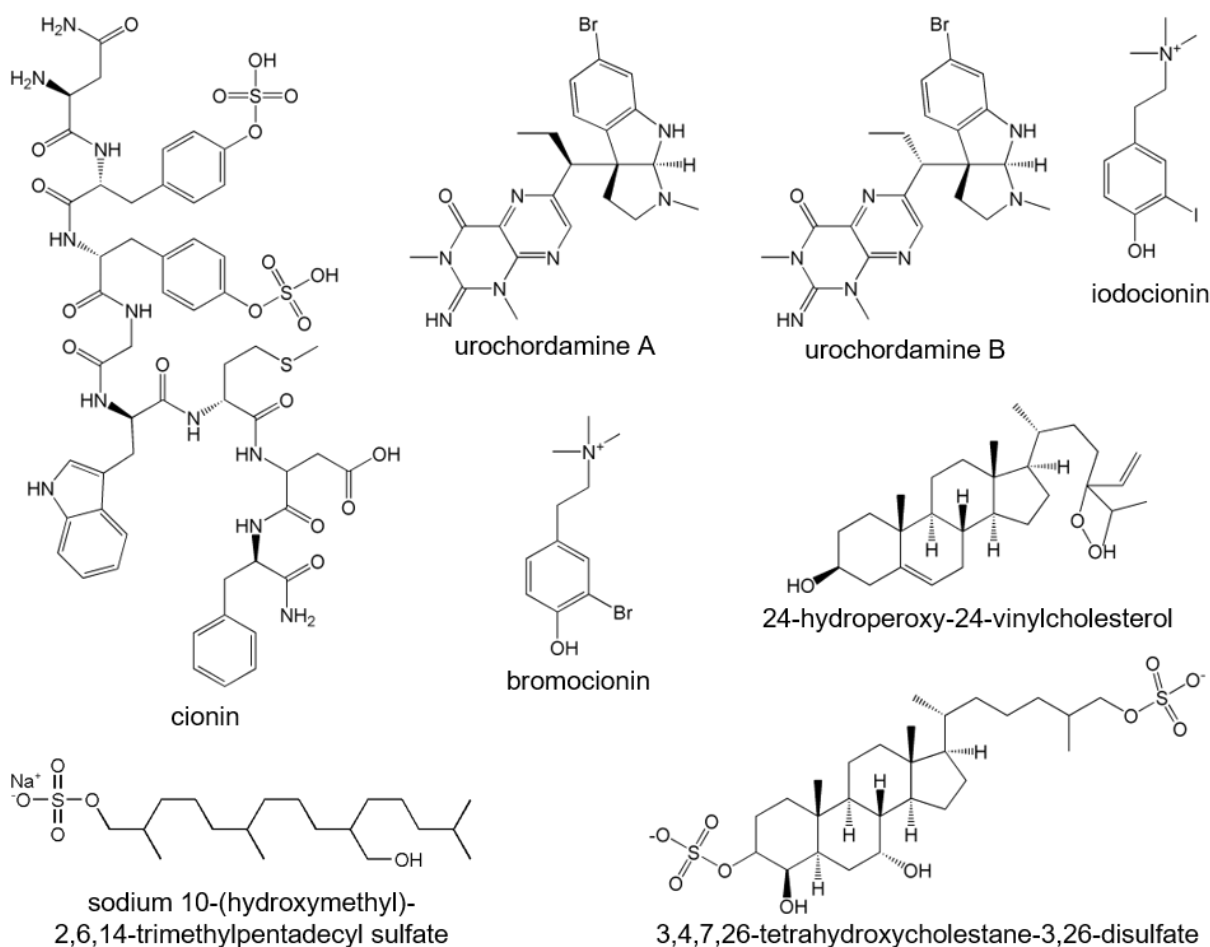
Figure 8. Examples of natural products isolated from *Ciona* species. Chemical structures of four discussed peptides are not shown, since the structure was not given in the respective publication.

3 Biological invasions

In invasion biology, terminology for species that spread beyond their natural habitat has not been used consistently (Kolar and Lodge 2001, Colautti and MacIsaac 2004). Following Kolar and Lodge, species successfully introduced outside their native habitat are termed non-indigenous (or non-native) species (NIS). When NIS become highly abundant and expand their range in the non-native habitat, they are defined as invasive species (Kolar and Lodge 2001, Falk-Petersen et al. 2006). Invasive species with tremendous ecological or economic impact are often referred to as nuisance or pest species (Falk-Petersen et al. 2006). They are a major threat to our planet's biodiversity ranking second among the causes for global diversity loss (Kolar and Lodge 2001, Molnar et al. 2008, Simberloff et al. 2013). For instance, pest species can reduce local species richness, lead to decline or extinction of native species, alter food webs and nutrient cycles, and thereby disrupt key ecological processes (Simberloff et al. 2013, Chan and Briski 2017). Invasive species also cause serious economic damages. For instance, the US shipping industry estimates that fouling on ship hulls costs $120 billion per

year, mainly due to increased water resistance leading to raised fuel consumption (Susick et al. 2019).

The major steps during the invasion process are (1) the transport to a new location, (2) the release and survival in the new habitat, (3) the successful population establishment, and (4) the range expansion going beyond the original arrival point (Kolar and Lodge 2001, Lockwood et al. 2005). Nowadays, anthropogenic activities are the main vector for species spread surpassing capabilities of natural species dispersal (Zhan et al. 2015). In marine realm, human-driven species transport occurs mainly via shipping (hull fouling, transport in ballast water) and aquaculture activities such as movement of fouled gear (Molnar et al. 2008, Zhan et al. 2015). According to the "Tens Rule", 10% of introduced species successfully establish in the new habitat and 10% thereof turn into invasive species with significant ecological and economic impact (Williamson and Fitter 1996). However, there is increasing evidence that this rate is largely underestimated, e.g., ~25% of transported invertebrates are currently believed to establish in newly colonized habitats (Jaric and Cvijanovic 2012, Jeschke and Pyšek 2018).

3.1 Concepts of invasion in the marine realm

Why certain species turn into notorious invaders when colonizing new habitats, has puzzled scientists since decades and at least 30 invasion hypotheses have been developed to date (Catford et al. 2009). An important finding across several studies is that invasion success is usually not explained by a single concept but rather the interplay of several factors (Lau and Schultheis 2015). In contrast to various proofs for terrestrial invasions, only few invasion concepts have been tested for marine NIS so far (Chan and Briski 2017). The 'enemy release hypothesis' (ERH), which assumes that NIS successfully establish in new habitats due to absence of specialized predators and pathogens, has been suggested as relevant factor for propagation of several marine NIS (Keane and Crawley 2002, Joshi and Vrieling 2005). For example, the crab *Carcinus maenas* and the gastropod *Littorina littorea* are significantly less parasitized in invaded habitats compared to their native habitats (Torchin et al. 2002). Due to release from specialized predators, NIS can decrease chemical defenses and invest left-over resources into biomass production and propagation, which is predicted by the 'evolution of increased competitive ability hypothesis' (EICA; Blossey and Notzold 1995, Doorduin and Vrieling 2011). This potential resource shift has been suggested for the brown alga *Sargassum muticum*, which is native in the Pacific (Japan, China), but has spread along the European Atlantic and North Sea coast. Feeding assays showed grazing preference of common North Sea herbivores towards non-native specimens (North Sea) compared to native *S. muticum* (Japan). This suggests a lowered chemical defense of *S. muticum* in its invaded habitat (Schwartz et al. 2016, Chan and Briski 2017). The 'novel weapon hypothesis' (NWH) implies that allelopathic compounds such as defensive SMs produced by newly arrived species impose negative effects on native species, due to the lack of adaptation to the newly introduced molecules (Callaway and Ridenour 2004, Svensson et al. 2013). This theory has been proven for the invasive red alga *Bonnemaisonia hamifera*, since its invasion success could be linked to the halogenated SM 1,1,3,3-tetrabromo-2-heptanone. This novel chemical weapon produced by *B. hamifera* inhibits settlement of propagules from native algal species and significantly deters native herbivores (Enge et al. 2012, Svensson et al. 2013). According to the 'biological weapons hypothesis' (BWH), NIS transport pathogens or parasites to new habitats that harm native species (Strauss et al. 2012, Vilcinskas 2015). This concept applies for the North American crayfish *Pacifastacus leniusculus* when introduced to the North Sea. The invasive crayfish served as vector for the fungus *Aphanomyces astaci*, the causal agent of crayfish plague, which led to significant losses in native crayfish populations (Holdich et al.

2009, Vilcinskas 2015). The 'generalist host hypothesis' claims that non-native specimens are more flexible with regard to their associated microbiota and are thereby lesser disturbed when specialized microbial symbionts were lost during the invasion of new habitats (Klock et al. 2015). So-called "host promiscuity" was recently suggested for the invasive red seaweed *Agarophyton vermiculophyllum* by applying controlled microbial disturbance in native and invasive specimens in a common garden experiment. Higher growth rates combined with lower bacterial beta-diversity in non-native macroalga specimens indicated high microbial flexibility as a potential benefit during invasion (Bonthond et al. 2021).

3.2   Ascidians as invasive species

The class Ascidiacea includes many species with non-native distribution and among them, several are notorious invasive species causing worldwide severe ecological and economic problems (Zhan et al. 2015, Kocot et al. 2018). A review by Shenkar and Swalla (2011) lists 64 ascidian species with non-native distribution, most of which belonged to the order Stolidobranchia (Shenkar and Swalla 2011, Lins et al. 2018). Invasive ascidians cause drastic changes in the benthic macrobiota, such as lowering species diversity. Economic losses are mainly reported from aquaculture sites, since ascidians often overgrow mussels cultivated on long lines (Zhan et al. 2015). When fouling on mussels, ascidians are in direct competition for food and space with them and hence, overgrowth leads to significantly reduced mussel production (Davidson et al. 2017, Palanisamy et al. 2018, Lins and Rocha 2020). Additionally, the time-consuming removal of ascidians from aquaculture gear leads to an increase of operational costs of up to 30% (Carman et al. 2010). The successful invasion of ascidians is probably promoted by several favorable characteristics such as their broad environmental tolerance, rapid growth, and high fertility (Sargent et al. 2013, Caputi et al. 2019). Moreover, anthropogenic activities facilitate establishment in new habitats: Invasive ascidians are more tolerant towards pollution and eutrophication compared to native species and preferably settle on man-made substrates such as aquaculture facilities and docks (Shenkar and Swalla 2011, Caputi et al. 2019). Growing on such submersed artificial substrates leads to lower predation pressure by benthic predators, which was shown to be a key factor for predominance of, e.g., *Ascidiella aspersa* and *C. robusta* on artificial structures such as mussel farms (Atalah et al. 2020, Giachetti et al. 2020). Due to the generally low natural dispersal capacity of ascidian larvae, transport to new habitats is mainly achieved via hitch-hiking on artificial structures such as vessels and aquaculture gear (Lambert 2005, Lins et al. 2018, Atalah et al. 2020). Projected future climate conditions will also affect the distribution of invasive ascidians, leading to a habitat range increase for some species and a decrease for others. The largest spread was predicted for *C. savignyi*, with up to 82% habitat expansion within this century (Zhang et al. 2020). *Ciona intestinalis* will presumably – due to a prolonged reproductive season as response to raising water temperatures – also expand its geographic range (Harris et al. 2017).

3.3   The case study: *C. intestinalis* as notorious invader in Prince Edward Island

The tunicate *C. intestinalis* is one of the most harmful fouling organisms in the NW Atlantic (Fitridge et al. 2012). It has spread more than 1000 km within 15 years: from Nova Scotia over Prince Edward Island (PEI) to Newfoundland (Carman et al. 2019). The first record of *C. intestinalis* in PEI, the smallest Canadian province located in the Gulf of Saint Lawrence, was in 2004 in a saline estuary, the Montague River (Ramsay et al. 2009). Only two years later, *C. intestinalis* had already colonized large parts of PEI's coastline and evolved into the

predominant fouling species (Figure 9a-b; Ramsay et al. 2008). During this short time period, *C. intestinalis* nearly completely replaced the invasive clubbed tunicate *Styela clava*, which was until then the dominant fouling ascidian in PEI (Ramsay et al. 2008). With abundances of up to five individuals per cm^2, *C. intestinalis* poses a great threat to PEI's mussel industry (Ramsay et al. 2008, Davidson et al. 2017). It causes severe economic damages on aquaculture operations harvesting the blue mussel *Mytilus edulis*. Heavy fouling raises mussel mortality rates up to 50% (Daigle and Herbinger 2009) and removal activities significantly increase maintenance costs (Davidson et al. 2017). This is particularly detrimental for PEI, since it is the largest Canadian mussel producer. In 2018, PEI's aquaculture sites produced >80% of all mussels harvested in Canada equaling Can $29.1 million[6] (Patanasatienkul et al. 2019). Furthermore, invasive *C. robusta* can decrease species richness and alter sessile invertebrate communities (Blum et al. 2007).

Due to these negative impacts, it is of high academic and economic interest to elucidate why *C. intestinalis* is transforming into a pest species in new habitats while showing moderate abundance in its native habitats (Rius et al. 2011). Compared to eurythermal *C. intestinalis*, its competitor *S. clava* has a narrower temperature tolerance limit ranging from +2 to +23 °C (Clarke and Therriault 2007). However, a recent study indicates that neither temperature nor salinity can explain the high abundance and rapid growth of *C. intestinalis*, but that these abiotic parameters rather determine whether the ascidian can survive in its new habitat or not (Murphy et al. 2019). Notably, *C. intestinalis* starts spawning when seawater temperature reaches 8 °C, while its competitor *S. clava* needs water temperatures above 12 °C. This so-called "4 °C gap" means in fact that recruitment of *C. intestinalis* starts ca. one month earlier, which is a significant advantage for settlement on (artificial) substrates. (Ramsay et al. 2008). Furthermore, it is assumed that PEI is particularly susceptible to invasive ascidians. Such highly industrial areas are characterized by nutrient loaded waters and plenty of artificial substrate, which are – as outlined above – beneficial factors for the establishment of non-native ascidians (Locke et al. 2007, Ramsay et al. 2008). Nevertheless, none of these factors alone sufficiently explains the invasiveness of *C. intestinalis* (Figure 9c). Moreover, none of the above presented invasion hypotheses have been tested for this invasive ascidian; hence, it is indispensable to continue research on additional factors promoting the rapid propagation of *C. intestinalis* in PEI and other invaded habitats (Murphy et al. 2019).

---

[6] Statistics Canada, Table 32-10-0107-01 Aquaculture, production and value. Available at
https://www150.statcan.gc.ca/t1/tbl1/en/tv.action?pid=3210010701 (accessed on 21.12.2020)
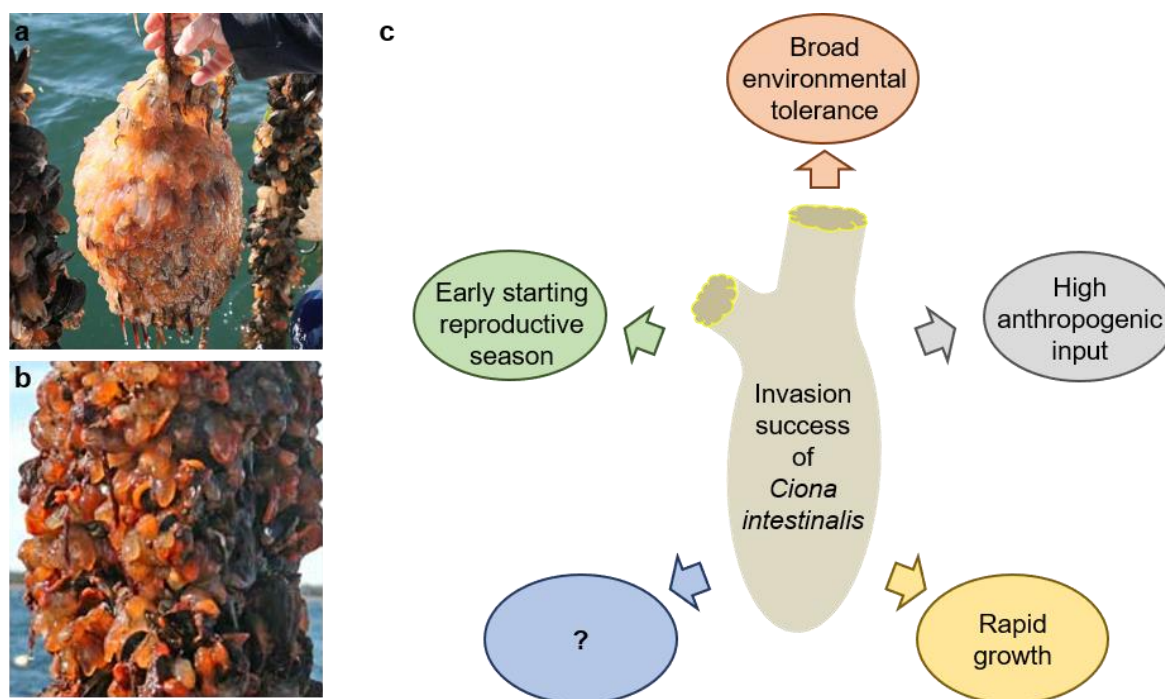
Figure 9. The invasion success of *C. intestinalis* in PEI. Photographs of *C. intestinalis* fouling on farmed mussels in PEI (**a**, **b**) and potential underlying reasons for its invasion success (**c**) are displayed. Pictures (a, b) were obtained from The Dutch Ascidians Homepage (www.ascidians.com) with permission from Dr. Arjan Gittenberger (GiMaRIS).

4 Recent advances in metabolome and microbiome research

During the past decades, technological innovations accelerated the development of multiple 'omic approaches' such as (meta)genomics, transcriptomics, proteomics, and metabolomics. The omics toolbox enables analysis of biological systems at different levels, e.g., genes, proteins, and metabolites (Horgan and Kenny 2011, Misra et al. 2018). Common approaches and application fields of metabolomics and microbiomics, the two omics techniques applied in this doctoral research project, are outlined below.

4.1 Untargeted metabolomics

Metabolomics studies aim to perform a global analysis of all small metabolites (usually <1500 Da) present in any organism or biological system at a certain time point (Wishart 2008, Chaleckis et al. 2019). Liquid chromatography-mass spectrometry (LC-MS) has emerged as the standard analytical technique used in metabolomics, due to its high sensitivity, sample throughput, and resolution (Grim et al. 2019, Stuart et al. 2020). LC-MS-based metabolomics allows rapid metabolome analysis of minute amounts of crude extracts containing thousands of different metabolites (Figure 10; Patti et al. 2012). To gain a global picture of the chemical inventory of an organism, tissue or cell, untargeted metabolomics approaches using tandem mass spectrometry (MS/MS) are applied to analyze all detectable metabolites (Chaleckis et al. 2019). Accordingly, untargeted metabolomics experiments gather a huge amount of data requiring thorough pre-processing. The most common automatic pre-processing tools XCMS and MZmine 2 aid for instance the removal of contaminant peaks (Myers et al. 2017). Pre-processed data can be subjected to statistical analyses, manual dereplication, i.e., search in classical NP databases, and automated dereplication tools. Among the computational tools, molecular networking (MN), which is freely provided at the GNPS platform (Wang et al. 2016), has revolutionized untargeted metabolomics studies. MN is an algorithm-based visualization

17

approach that automatically calculates the structural relatedness (i.e., cosine score) of all detected ions based on their MS/MS spectra. Since each compound, displayed as nodes in the MN, has a specific fragmentation pattern resembling its core structural features, similar compounds will be connected in the MN and form one molecular cluster (Duncan et al. 2015, Quinn et al. 2017). Last year, feature-based MN (FBMN) was introduced. FBMN shows improved clustering and annotation by incorporating additional features such as the isotopic pattern, retention time, and quantitative information (Nothias et al. 2020). During the past years, additional MS/MS-based dereplication tools have been developed (e.g., Allard et al. 2016, Mohimani et al. 2018). Among them, *in-silico* fragmentation tools such as the *in-silico* MS/MS database (ISDB) dereplication workflow, which compares *in-silico* generated MS/MS spectra of >170,000 known NPs to experimentally acquired MS/MS spectra (Allard et al. 2016), currently provide the best annotation rates (Chaleckis et al. 2019, Grim et al. 2019).
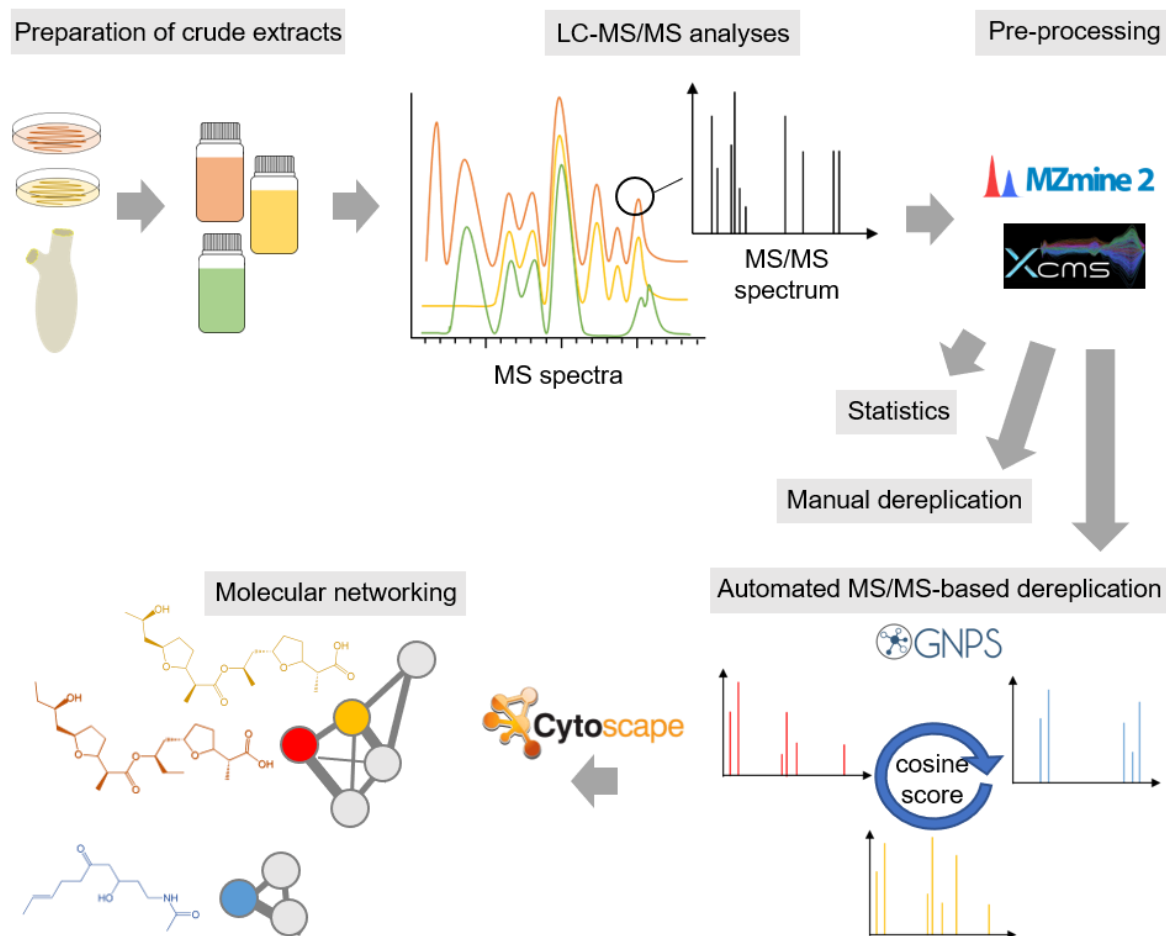
Figure 10. Generalized workflow of an untargeted LC-MS/MS-based metabolomics experiment.

Such automated dereplication tools have become invaluable for compound annotation in order to avoid re-isolation of known NPs, one major obstacle of the classical NP discovery pipeline (Culp et al. 2019). For instance, MN-based studies demonstrated efficient dereplication and comparative analysis of hundreds of microbial extracts (Crüsemann et al. 2016, Fan et al. 2019) or the targeted isolation of novel bioactive compounds from marine invertebrates (Bracegirdle et al. 2020, Li et al. 2020). Nevertheless, dereplication is still a challenging task, since the vast majority of compounds detected in untargeted metabolomics experiments remain unknown (da Silva et al. 2015). Metabolomics has also been successfully applied to investigate the invasiveness of, e.g., terrestrial plants. UPLC-QToF-MS-based

profiling of *Bunias orientalis* (Brassicaceae) revealed distinct chemistry for most analyzed native and invasive populations with enhanced production of defensive indole glucosinolates in invasive populations (Tewes et al. 2018). The MN-guided analyses of 61 plant species allowed the comparative investigation of 36,561 unique compounds, an unmanageable task if to be done manually. Their analysis gave evidence for the 'enemy release hypothesis' and 'novel weapon hypothesis', since invasive species were chemically more distinct when compared to the native flora and invasive plants with the largest chemical novelty were lesser preferred by native herbivores (Sedio et al. 2020). Chemical investigations on invasive macroalgae revealed similar trends such as lowered palatability and rapid chemical defense adaptation contributing to the invasive character of red seaweed *Gracilaria vermiculophylla* (Hammann et al. 2013, Saha et al. 2016). However, metabolomics has not been applied to study the invasiveness of ascidians.

4.2 Sequencing-based microbial community analyses

Microbial communities have attracted scientists since decades due to key functions of microorganisms in the health and fitness of the hosts (Franzenburg et al. 2013) and due to provision of other essential ecosystem services (Martiny et al. 2015). The microbial diversity of any environmental sample is nowadays assessed by high-throughput culture-independent methods, so-called next generation sequencing (NGS) technologies. Their development and continuous improvement allow simultaneous comparative analysis of several hundreds of samples with steadily decreasing costs (Martiny et al. 2015, Goodwin et al. 2016). Culture-independent analysis of environmental samples can be achieved via two different approaches, i.e., amplicon sequencing of a target gene (most often the 16S rRNA gene; Figure 11) and metagenomics, which aims to sequence the full genomic repertoire of a given sample (Hamady and Knight 2009, Quince et al. 2017). Both approaches have their pros and cons, e.g., comparatively expensive and time-consuming metagenomic analyses allow in-depth microbial community analysis at a functional level, while amplicon sequencing is more sensitive and lesser time intense, but limited to one gene and prone to PCR errors (Sekse et al. 2017). Similar to metabolome analysis, amplicon sequencing, which has been applied in this study, requires several bioinformatic steps to pre-process raw sequencing data. For example, sequence reads are quality-filtered and taxonomically classified, which is often based on operational taxonomic units (OTUs) clustered at a 97% similarity threshold. The open-source software tools mothur and QIIME2 are the most commonly applied pre-processing tools (Christensen et al. 2018, Knight et al. 2018, Pollock et al. 2018). Various tools are nowadays available for visualization and statistical analyses of high-throughput sequencing data, e.g., several packages integrated in the R software environment (R Core Team 2017) or the web-based tool MicrobiomeAnalyst (Dhariwal et al. 2017).

In terms of microbial diversity analysis, NGS approaches are superior to classical culture-dependent studies, since the latter usually target microorganisms easily growing under standard laboratory conditions, which represents only 0.001-1% of the actual microbiota (Alain and Querellou 2009, Garza and Dutilh 2015, Gutleben et al. 2018). Amplicon sequencing studies have been established as invaluable tool to characterize microbial communities, such as the sponge microbiome, probably the most intensely studied marine invertebrate phylum (e.g., Hentschel et al. 2012, Thomas et al. 2016). Furthermore, metagenomics significantly contributed to our knowledge of NPs and their producers. It became apparent that there is a discrepancy between biosynthetic gene clusters (BGCs) detected in microbial genomes and the number of actually detected SMs, because most BGCs remain silent in artificial laboratory environments (Duncan et al. 2015, van Bergeijk et al. 2020). Nevertheless, classical cultivation

of NP producers is still highly efficient for MNP discovery and therefore, remains a popular tool among NP chemists (Chen et al. 2017). This is mainly attributed to the fact that this well-established and straightforward workflow does not rely on a priori knowledge of BGCs and does not involve external expression of the target compound(s) in heterologous host, which is often a challenging and tedious task.
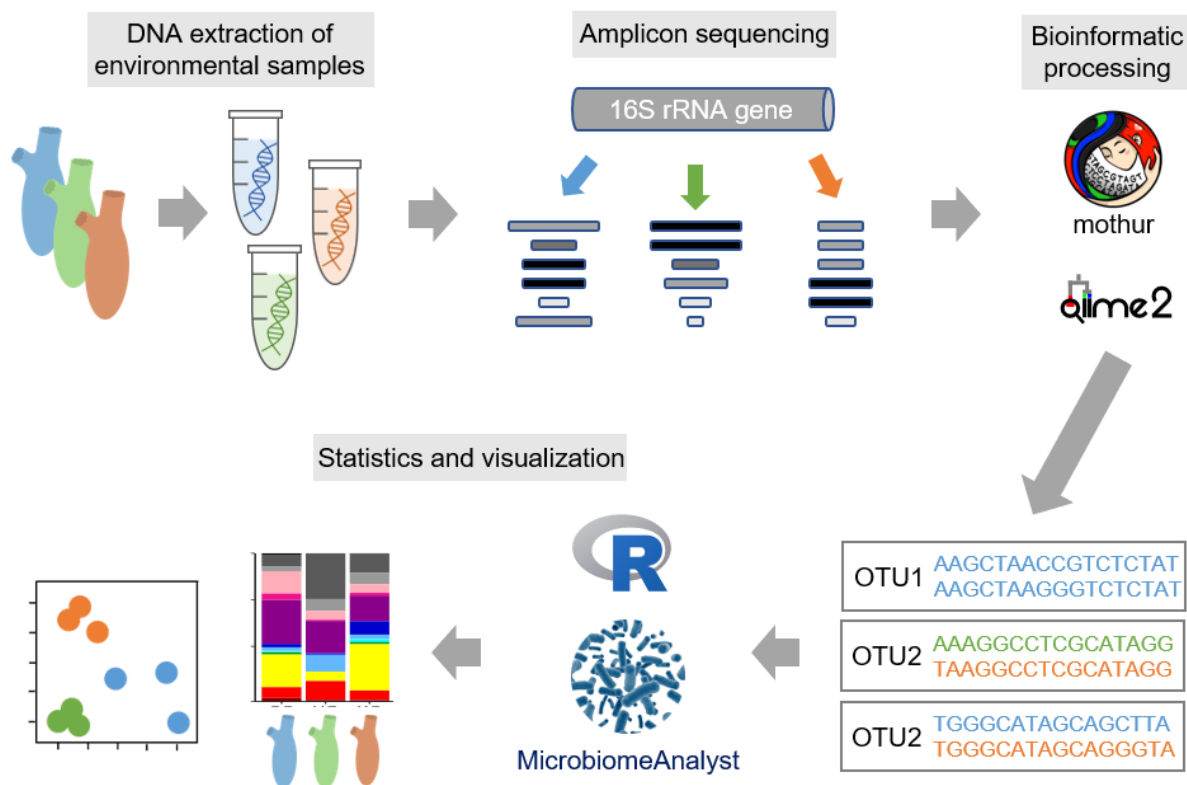
Figure 11. Generalized workflow of microbiome analysis via 16S rRNA gene amplicon sequencing.

Microbiome studies also aid deciphering host-microbe interactions, such as their significance for the invasiveness of certain species. Recent studies comparatively inspecting microbiomes of native and invasive ascidian populations evinced a correlation of microbial and genetic diversity (Casso et al. 2020, Goddard-Dwyer et al. 2020), distinct microbiomes of native and non-native populations (Dror et al. 2019, Goddard-Dwyer et al. 2020), high microbial variability (Casso et al. 2020, Goddard-Dwyer et al. 2020), and a combination of horizontal and vertical symbiont transmission (Evans et al. 2018, Goddard-Dwyer et al. 2020), of which the latter two suggest high flexibility when adapting to new environments. Whether native and invasive *C. intestinalis* host variable and differential microbial communities remains to be tested.

5   Research objectives

Ascidians and their associated microbiota are on the one hand a treasure trove for bioactive MNPs, while being on the other hand notorious invaders significantly threatening aquaculture industry and biodiversity at a global scale. Nevertheless, these intriguing research areas have only been poorly studied in the prominent model organism *C. intestinalis*. Despite its broad environmental tolerance, research on additional factors promoting the invasion success of *C. intestinalis* in PEI is lacking, e.g., the role of beneficial microbial associates and bioactive SMs for the ascidian's invasiveness has not been studied yet. Hence, the first objective of this thesis (Chapter 1) was to investigate for the first time the potential contribution of (bioactive) SMs and the host-specific microbiota to the devastating invasive nature of *C. intestinalis* in PEI. Therefore, the associated bacterial community and the metabolome of native (Helgoland, North Sea, Germany; Kiel Fjord, Baltic Sea, Germany) and invasive (PEI) *C. intestinalis* populations were comparatively analyzed to address the following research questions:

a) What are the core microbes and the global metabolome of *C. intestinalis*?
b) What is the impact of the analyzed tissue on the associated bacterial community (gut vs. tunic) and on the metabolite production (inner body vs. tunic)?
c) What is the influence of (i) biogeography and (ii) invasiveness on the microbial community composition and metabolite profiles?
d) Do the associated bacteria and SMs contribute to the invasion success of *C. intestinalis* in PEI, including specific metabolites and bacteria potentially conveying beneficial effects for *C. intestinalis*?

The culturable microbial fraction of *C. intestinalis* remains largely unstudied (bacteria) or even unknown (fungi). Moreover, apart from one single study, their biotechnological potential has not been investigated so far. To fill this knowledge gap and potentially provide the MNP discovery pipeline with promising candidate strains for urgently needed novel antimicrobial and anticancer lead compounds, the second part of this thesis (Chapters 2 and 3) aimed to explore the diversity and biodiscovery potential of the culturable microbial community associated with the sea vase tunicate. Since the culturable microbiota of ascidians reportedly differs between different tissues (Chen et al. 2018) and environmental conditions impact the culture-dependent microbial diversity (Alain and Querellou 2009), tunic- (Chapter 2) and gut-associated (Chapter 3) bacterial and fungal specimens sampled at two different geographic locations (Helgoland and Kiel) were analyzed. The specific objectives of these studies were:

a) Identify the culturable bacterial and fungal diversity of the tunic (Chapter 2) and the gut (Chapter 3) of *C. intestinalis*
b) Investigate the biotechnological potential of bacterial and fungal isolates with regard to anticancer or antimicrobial activities
c) Select the most promising microbial crude extracts for future discovery of novel bioactive MNPs
d) Explore the metabolomes of promising bioactive crude extracts to identify putatively novel and bioactive metabolites/molecular clusters

Associated microbial communities were either characterized via amplicon sequencing of the 16S rRNA gene (culture-independent; Chapter 1) or by isolating the culturable fraction (culture-dependent; Chapters 2 and 3). Metabolome analyses performed in Chapters 1 to 3 were based on UPLC-QToF-MS/MS measurements. MZmine 2-pre-processed data were subjected to an integrated dereplication workflow combining state-of-the-art automated tools (FBMN, ISDB) with classical (M)NP databases.

6 References

Aiello, A.; Fattorusso, E.; Imperatore, C.; Menna, M.; Muller, W.E. Iodocionin, a cytotoxic iodinated metabolite from the Mediterranean ascidian *Ciona edwardsii*. *Mar. Drugs* 2010, 8, 285-291, doi:10.3390/md8020285.

Alain, K.; Querellou, J. Cultivating the uncultured: Limits, advances and future challenges. *Extremophiles* 2009, 13, 583-594, doi:10.1007/s00792-009-0261-3.

Allard, P.M.; Peresse, T.; Bisson, J.; Gindro, K.; Marcourt, L.; Pham, V.C.; Roussi, F.; Litaudon, M.; Wolfender, J.L. Integration of molecular networking and *in-silico* MS/MS fragmentation for natural products dereplication. *Anal. Chem.* 2016, 88, 3317-3323, doi:10.1021/acs.analchem.5b04804.

Atalah, J.; Fletcher, L.M.; Davidson, I.C.; South, P.M.; Forrest, B.M. Artificial habitat and biofouling species distributions in an aquaculture seascape. *Aquac. Environ. Interact.* 2020, 12, 495-509, doi:10.3354/aei00380.

Bauermeister, A.; Branco, P.C.; Furtado, L.C.; Jimenez, P.C.; Costa-Lotufo, L.V.; da Cruz Lotufo, T.M. Tunicates: A model organism to investigate the effects of associated-microbiota on the production of pharmaceuticals. *Drug Discov. Today Dis. Models* 2018, 28, 13-20, doi:10.1016/j.ddmod.2019.08.008.

Bergmann, W.; Burke, D.C. Contributions to the study of marine products. XXXIX. The nucleosides of sponges. *J. Org. Chem.* 1955, 20, 1501-1507, doi:10.1021/jo01128a007.

Bhatnagar, I.; Kim, S.K. Immense essence of excellence: Marine microbial bioactive compounds. *Mar. Drugs* 2010, 8, 2673-2701, doi:10.3390/md8102673.

Blasiak, L.C.; Zinder, S.H.; Buckley, D.H.; Hill, R.T. Bacterial diversity associated with the tunic of the model chordate *Ciona intestinalis*. *ISME J.* 2014, 8, 309-320, doi:10.1038/ismej.2013.156.

Blockley, A.; Elliott, D.R.; Roberts, A.P.; Sweet, M. Symbiotic microbes from marine invertebrates: Driving a new era of natural product drug discovery. *Diversity* 2017, 9, 49, doi:10.3390/d9040049.

Blossey, B.; Notzold, R. Evolution of increased competitive ability in invasive nonindigenous plants: A hypothesis. *J. Ecol.* 1995, 83, 887, doi:10.2307/2261425.

Blum, J.C.; Chang, A.L.; Liljesthrom, M.; Schenk, M.E.; Steinberg, M.K.; Ruiz, G.M. The non-native solitary ascidian *Ciona intestinalis* (L.) depresses species richness. *J. Exp. Mar. Biol. Ecol.* 2007, 342, 5-14, doi:10.1016/j.jembe.2006.10.010.

Bonthond, G.; Bayer, T.; Krueger-Hadfield, S.A.; Starck, N.; Wang, G.; Nakaoka, M.; Kunzel, S.; Weinberger, F. The role of host promiscuity in the invasion process of a seaweed holobiont. *ISME J.* 2021, doi:10.1038/s41396-020-00878-7.

Bosch, T.C.; McFall-Ngai, M.J. Metaorganisms as the new frontier. *Zoology* 2011, 114, 185-190, doi:10.1016/j.zool.2011.04.001.

Bouchemousse, S.; Bishop, J.D.; Viard, F. Contrasting global genetic patterns in two biologically similar, widespread and invasive *Ciona* species (Tunicata, Ascidiacea). *Sci. Rep.* 2016, 6, 24875, doi:10.1038/srep24875.

Bracegirdle, J.; Stevenson, L.J.; Page, M.J.; Owen, J.G.; Keyzers, R.A. Targeted isolation of rubrolides from the New Zealand marine tunicate *Synoicum kuranui*. *Mar. Drugs* 2020, 18, 337, doi:10.3390/md18070337.

Bray, F.; Ferlay, J.; Soerjomataram, I.; Siegel, R.L.; Torre, L.A.; Jemal, A. Global cancer statistics 2018: GLOBOCAN estimates of incidence and mortality worldwide for 36 cancers in 185 countries. *CA Cancer J. Clin.* 2018, 68, 394-424, doi:10.3322/caac.21492.

Brunetti, R.; Gissi, C.; Pennati, R.; Caicci, F.; Gasparini, F.; Manni, L. Morphological evidence that the molecularly determined *Ciona intestinalis* type A and type B are different species: *Ciona robusta* and *Ciona intestinalis*. *J. Zoolog. Syst. Evol. Res.* 2015, 53, 186-193, doi:10.1111/jzs.12101.

Burke, C.; Thomas, T.; Egan, S.; Kjelleberg, S. The use of functional genomics for the identification of a gene cluster encoding for the biosynthesis of an antifungal tambjamine in the marine bacterium *Pseudoalteromonas tunicata*. *Environ. Microbiol.* 2007, 9, 814-818, doi:10.1111/j.1462-2920.2006.01177.x.

Cahill, P.L.; Fidler, A.E.; Hopkins, G.A.; Wood, S.A. Geographically conserved microbiomes of four temperate water tunicates. *Environ. Microbiol. Rep.* 2016, 8, 470-478, doi:10.1111/1758-2229.12391.

Callaway, R.M.; Ridenour, W.M. Novel weapons: Invasive success and the evolution of increased competitive ability. *Front. Ecol. Environ.* 2004, 2, 436-443, doi:10.1890/1540-9295(2004)002[0436:Nwisat]2.0.Co;2.

Caputi, L.; Andreakis, N.; Mastrototaro, F.; Cirino, P.; Vassillo, M.; Sordino, P. Cryptic speciation in a model invertebrate chordate. *Proc. Natl. Acad. Sci. USA* 2007, 104, 9364-9369, doi:10.1073/pnas.0610158104.

Caputi, L.; Toscano, F.; Arienzo, M.; Ferrara, L.; Procaccini, G.; Sordino, P. Temporal correlation of population composition and environmental variables in the marine invader *Ciona robusta*. *Mar. Ecol.* 2019, 40, e12543, doi:10.1111/maec.12543.

Carman, M.R.; Colarusso, P.D.; Neckles, H.A.; Bologna, P.; Caines, S.; Davidson, J.D.; Evans, N.T.; Fox, S.E.; Grunden, D.W.; Hoffman, S.; et al. Biogeographical patterns of tunicates utilizing eelgrass as substrate in the western North Atlantic between 39° and 47° north latitude (New Jersey to Newfoundland). *Manag. Biol. Invasions* 2019, 10, 602-616, doi:10.3391/mbi.2019.10.4.02.

Carman, M.R.; Morris, J.A.; Karney, R.C.; Grunden, D.W. An initial assessment of native and invasive tunicates in shellfish aquaculture of the North American east coast. *J. Appl. Ichthyol.* 2010, 26, 8-11, doi:10.1111/j.1439-0426.2010.01495.x.

Carroll, A.R.; Copp, B.R.; Davis, R.A.; Keyzers, R.A.; Prinsep, M.R. Marine natural products. *Nat. Prod. Rep.* 2020, 37, 175-223, doi:10.1039/c9np00069k.

Carver, C.E.; Chisholm, A.; Mallet, A.L. Strategies to mitigate the impact of *Ciona intestinalis* (L.) biofouling on shellfish production. *J. Shellfish Res.* 2003, 22, 621-631.

Carver, C.E.; Mallet, A.L.; Vercaemer, B. Biological synopsis of the solitary tunicate *Ciona intestinalis*. *Can. Man. Rep. Fish. Aquat. Sci.* 2006, 2746, 1-55.

Casertano, M.; Menna, M.; Imperatore, C. The ascidian-derived metabolites with antimicrobial properties. *Antibiotics* 2020, 9, 510, doi:10.3390/antibiotics9080510.

Cassini, A.; Högberg, L.D.; Plachouras, D.; Quattrocchi, A.; Hoxha, A.; Simonsen, G.S.; Colomb-Cotinat, M.; Kretzschmar, M.E.; Devleesschauwer, B.; Cecchini, M.; et al. Attributable deaths and disability-adjusted life-years caused by infections with antibiotic-resistant bacteria in the EU and the European Economic Area in 2015: A population-level modelling analysis. *Lancet Infect. Dis.* 2019, 19, 56-66, doi:10.1016/s1473-3099(18)30605-4.

Casso, M.; Turon, M.; Marco, N.; Pascual, M.; Turon, X. The microbiome of the worldwide invasive ascidian *Didemnum vexillum*. *Front. Mar. Sci.* 2020, 7, 201, doi:10.3389/fmars.2020.00201.

Catford, J.A.; Jansson, R.; Nilsson, C. Reducing redundancy in invasion ecology by integrating hypotheses into a single theoretical framework. *Divers. Distrib.* 2009, 15, 22-40, doi:10.1111/j.1472-4642.2008.00521.x.

Chaleckis, R.; Meister, I.; Zhang, P.; Wheelock, C.E. Challenges, progress and promises of metabolite annotation for LC-MS-based metabolomics. *Curr. Opin. Biotechnol.* 2019, 55, 44-50, doi:10.1016/j.copbio.2018.07.010.

Chan, F.T.; Briski, E. An overview of recent research in marine biological invasions. *Mar. Biol.* 2017, 164, 121, doi:10.1007/s00227-017-3155-4.

Chen, J.Y.; Huang, D.Y.; Peng, Q.Q.; Chi, H.M.; Wang, X.Q.; Feng, M. The first tunicate from the Early Cambrian of South China. *Proc. Natl. Acad. Sci. USA* 2003, 100, 8314-8318, doi:10.1073/pnas.1431177100.

Chen, L.; Fu, C.; Wang, G. Microbial diversity associated with ascidians: A review of research methods and application. *Symbiosis* 2017, 71, 19-26, doi:10.1007/s13199-016-0398-7.

Chen, L.; Hu, J.S.; Xu, J.L.; Shao, C.L.; Wang, G.Y. Biological and chemical diversity of ascidian-associated microorganisms. *Mar. Drugs* 2018, 16, 362, doi:10.3390/md16100362.

Cheng, L.; Wang, C.; Liu, H.; Wang, F.; Zheng, L.; Zhao, J.; Chu, E.; Lin, X. A novel polypeptide extracted from *Ciona savignyi* induces apoptosis through a mitochondrial-mediated pathway in human colorectal carcinoma cells. *Clin. Colorectal Cancer* 2012, 11, 207-214, doi:10.1016/j.clcc.2012.01.002.

Christensen, H.; Andersson, A.J.; Jørgensen, S.L.; Vogt, J.K. 16S rRNA amplicon sequencing for metagenomics. In *Introduction to Bioinformatics in Microbiology*, Christensen, H., Ed. Springer International Publishing: Cham, Switzerland, 2018; p. 135-161.

Clarke, C.L.; Therriault, T.W. Biological synopsis of the invasive tunicate *Styela clava* (Herdman 1881). *Can. Man. Rep. Fish. Aquat. Sci.* 2007, 2807, 23.

Colautti, R.I.; MacIsaac, H.J. A neutral terminology to define 'invasive' species. *Divers. Distrib.* 2004, 10, 135-141, doi:10.1111/j.1366-9516.2004.00061.x.

Corbo, J.C.; Di Gregorio, A.; Levine, M. The ascidian as a model organism in developmental and evolutionary biology. *Cell* 2001, 106, 535-538, doi:10.1016/s0092-8674(01)00481-0.

Crüsemann, M.; O'Neill, E.C.; Larson, C.B.; Melnik, A.V.; Floros, D.J.; da Silva, R.R.; Jensen, P.R.; Dorrestein, P.C.; Moore, B.S. Prioritizing natural product diversity in a collection of 146 bacterial strains based on growth and extraction protocols. *J. Nat. Prod.* 2016, 80, 588-597, doi:10.1021/acs.jnatprod.6b00722.

Cuevas, C.; Francesch, A. Development of Yondelis (trabectedin, ET-743). A semisynthetic process solves the supply problem. *Nat. Prod. Rep.* 2009, 26, 322-337, doi:10.1039/b808331m.

Culp, E.J.; Yim, G.; Waglechner, N.; Wang, W.; Pawlowski, A.C.; Wright, G.D. Hidden antibiotics in actinomycetes can be identified by inactivation of gene clusters for common antibiotics. *Nat. Biotechnol.* 2019, 37, 1149–1154, doi:10.1038/s41587-019-0241-9.

da Silva, R.R.; Dorrestein, P.C.; Quinn, R.A. Illuminating the dark matter in metabolomics. *Proc. Natl. Acad. Sci. USA* 2015, 112, 12549-12550, doi:10.1073/pnas.1516878112.

Daigle, R.M.; Herbinger, C.M. Ecological interactions between the vase tunicate (*Ciona intestinalis*) and the farmed blue mussel (*Mytilus edulis*) in Nova Scotia, Canada. *Aquat. Invasions* 2009, 4, 177-187, doi:10.3391/ai.2009.4.1.18.

Davidson, J.; Landry, T.; Johnson, G.; Quijón, P. A cost-benefit analysis of four treatment regimes for the invasive tunicate *Ciona intestinalis* on mussel farms. *Manag. Biol. Invasions* 2017, 8, 163-170, doi:10.3391/mbi.2017.8.2.04.

Dehal, P.; Satou, Y.; Campbell, R.K.; Chapman, J.; Degnan, B.; De Tomaso, A.; Davidson, B.; Di Gregorio, A.; Gelpke, M.; Goodstein, D.M.; et al. The draft genome of *Ciona intestinalis*: Insights into chordate and vertebrate origins. *Science* 2002, 298, 2157-2167, doi:10.1126/science.1080049.

Delsuc, F.; Philippe, H.; Tsagkogeorga, G.; Simion, P.; Tilak, M.K.; Turon, X.; Lopez-Legentil, S.; Piette, J.; Lemaire, P.; Douzery, E.J.P. A phylogenomic framework and timescale for comparative studies of tunicates. *BMC Biol.* 2018, 16, 39, doi:10.1186/s12915-018-0499-2.

DePinho, R.A. The age of cancer. *Nature* 2000, 408, 248-254, doi:10.1038/35041694.

Dhariwal, A.; Chong, J.; Habib, S.; King, I.L.; Agellon, L.B.; Xia, J. MicrobiomeAnalyst: A web-based tool for comprehensive statistical, visual and meta-analysis of microbiome data. *Nucleic Acids Res.* 2017, 45, 180-188, doi:10.1093/nar/gkx295.

Di Bella, M.A.; Fedders, H.; De Leo, G.; Leippe, M. Localization of antimicrobial peptides in the tunic of *Ciona intestinalis* (Ascidiacea, Tunicata) and their involvement in local inflammatory-like reactions. *Results Immunol.* 2011, 1, 70-75, doi:10.1016/j.rinim.2011.09.001.

Dishaw, L.J.; Flores-Torres, J.; Lax, S.; Gemayel, K.; Leigh, B.; Melillo, D.; Mueller, M.G.; Natale, L.; Zucchetti, I.; De Santis, R.; et al. The gut of geographically disparate *Ciona intestinalis* harbors a core microbiota. *PLoS ONE* 2014, 9, e93386, doi:10.1371/journal.pone.0093386.

Dishaw, L.J.; Flores-Torres, J.A.; Mueller, M.G.; Karrer, C.R.; Skapura, D.P.; Melillo, D.; Zucchetti, I.; De Santis, R.; Pinto, M.R.; Litman, G.W. A Basal chordate model for studies of gut microbial immune interactions. *Front. Immunol.* 2012, 3, 96, doi:10.3389/fimmu.2012.00096.

Dishaw, L.J.; Leigh, B.; Cannon, J.P.; Liberti, A.; Mueller, M.G.; Skapura, D.P.; Karrer, C.R.; Pinto, M.R.; De Santis, R.; Litman, G.W. Gut immunity in a protochordate involves a secreted immunoglobulin-type mediator binding host chitin and bacteria. *Nat. Commun.* 2016, 7, 10617, doi:10.1038/ncomms10617.

Donia, M.S.; Fricke, W.F.; Partensky, F.; Cox, J.; Elshahawi, S.I.; White, J.R.; Phillippy, A.M.; Schatz, M.C.; Piel, J.; Haygood, M.G.; et al. Complex microbiome underlying secondary and primary metabolism in the tunicate-*Prochloron* symbiosis. *Proc. Natl. Acad. Sci. USA* 2011, 108, 1423-1432, doi:10.1073/pnas.1111712108.

Doorduin, L.J.; Vrieling, K. A review of the phytochemical support for the shifting defence hypothesis. *Phytochem. Rev.* 2011, 10, 99-106, doi:10.1007/s11101-010-9195-8.

Dou, X.; Dong, B. Origins and bioactivities of natural compounds derived from marine ascidians and their symbionts. *Mar. Drugs* 2019, 17, 670, doi:10.3390/md17120670.

Dou, X.; Li, X.; Yu, H.; Dong, B. Dual roles of ascidian chondromodulin-1: Promoting cell proliferation whilst suppressing the growth of tumor cells. *Mar. Drugs* 2018, 16, 59, doi:10.3390/md16020059.

Dror, H.; Novak, L.; Evans, J.S.; Lopez-Legentil, S.; Shenkar, N. Core and dynamic microbial communities of two invasive ascidians: Can host-symbiont dynamics plasticity affect invasion capacity? *Microb. Ecol.* 2019, 78, 170-184, doi:10.1007/s00248-018-1276-z.

Dumont, C.P.; Gaymer, C.F.; Thiel, M. Predation contributes to invasion resistance of benthic communities against the non-indigenous tunicate *Ciona intestinalis*. *Biol. Invasions* 2011, 13, 2023-2034, doi:10.1007/s10530-011-0018-7.

Duncan, K.R.; Crusemann, M.; Lechner, A.; Sarkar, A.; Li, J.; Ziemert, N.; Wang, M.; Bandeira, N.; Moore, B.S.; Dorrestein, P.C.; et al. Molecular networking and pattern-based genome mining

improves discovery of biosynthetic gene clusters and their products from *Salinispora* species. *Chem. Biol.* 2015, 22, 460-471, doi:10.1016/j.chembiol.2015.03.010.

Dybern, B.I. The life cycle of *Ciona intestinalis* (L.) f. typica in relation to the environmental temperature. *Oikos* 1965, 16, 109, doi:10.2307/3564870.

Dyshlovoy, S.A.; Honecker, F. Marine compounds and cancer: Updates 2020. *Mar. Drugs* 2020, 18, 643, doi:10.3390/md18120643.

Eliso, M.C.; Manfra, L.; Savorelli, F.; Tornambe, A.; Spagnuolo, A. New approaches on the use of tunicates (*Ciona robusta*) for toxicity assessments. *Environ. Sci. Pollut. Res. Int.* 2020, 27, 32132–32138, doi:10.1007/s11356-020-09781-2.

Enge, S.; Nylund, G.M.; Harder, T.; Pavia, H. An exotic chemical weapon explains low herbivore damage in an invasive alga. *Ecology* 2012, 93, 2736-2745, doi:10.1890/12-0143.1.

Erwin, P.M.; Pineda, M.C.; Webster, N.; Turon, X.; Lopez-Legentil, S. Down under the tunic: Bacterial biodiversity hotspots and widespread ammonia-oxidizing archaea in coral reef ascidians. *ISME J.* 2013, 8, 575-588, doi:10.1038/ismej.2013.188.

Evans, J.S.; Erwin, P.M.; Shenkar, N.; Lopez-Legentil, S. A comparison of prokaryotic symbiont communities in nonnative and native ascidians from reef and harbor habitats. *FEMS Microbiol. Ecol.* 2018, 94, fiy139, doi:10.1093/femsec/fiy139.

Falk-Petersen, J.; Bøhn, T.; Sandlund, O.T. On the numerous concepts in invasion biology. *Biol. Invasions* 2006, 8, 1409-1424, doi:10.1007/s10530-005-0710-6.

Fan, B.; Parrot, D.; Blümel, M.; Labes, A.; Tasdemir, D. Influence of OSMAC-based cultivation in metabolome and anticancer activity of fungi associated with the brown alga *Fucus vesiculosus*. *Mar. Drugs* 2019, 17, 67, doi:10.3390/md17010067.

Fedders, H.; Michalek, M.; Grotzinger, J.; Leippe, M. An exceptional salt-tolerant antimicrobial peptide derived from a novel gene family of haemocytes of the marine invertebrate *Ciona intestinalis*. *Biochem. J.* 2008, 416, 65-75, doi:10.1042/BJ20080398.

Fedders, H.; Podschun, R.; Leippe, M. The antimicrobial peptide Ci-MAM-A24 is highly active against multidrug-resistant and anaerobic bacteria pathogenic for humans. *Int. J. Antimicrob. Agents* 2010, 36, 264-266, doi:10.1016/j.ijantimicag.2010.04.008.

Feling, R.H.; Buchanan, G.O.; Mincer, T.J.; Kauffman, C.A.; Jensen, P.R.; Fenical, W. Salinosporamide A: A highly cytotoxic proteasome inhibitor from a novel microbial source, a marine bacterium of the new genus *Salinospora*. *Angew. Chem. Int. Ed. Engl.* 2003, 42, 355-357, doi:10.1002/anie.200390115.

Ferlay, J.; Soerjomataram, I.; Dikshit, R.; Eser, S.; Mathers, C.; Rebelo, M.; Parkin, D.M.; Forman, D.; Bray, F. Cancer incidence and mortality worldwide: Sources, methods and major patterns in GLOBOCAN 2012. *Int. J. Cancer* 2015, 136, E359-386, doi:10.1002/ijc.29210.

Fitridge, I.; Dempster, T.; Guenther, J.; de Nys, R. The impact and control of biofouling in marine aquaculture: A review. *Biofouling* 2012, 28, 649-669, doi:10.1080/08927014.2012.700478.

Florez, L.V.; Biedermann, P.H.; Engl, T.; Kaltenpoth, M. Defensive symbioses of animals with prokaryotic and eukaryotic microorganisms. *Nat. Prod. Rep.* 2015, 32, 904-936, doi:10.1039/c5np00010f.

Franchi, N.; Ballarin, L. Immunity in Protochordates: The tunicate perspective. *Front. Immunol.* 2017, 8, 674, doi:10.3389/fimmu.2017.00674.

Franzenburg, S.; Walter, J.; Kunzel, S.; Wang, J.; Baines, J.F.; Bosch, T.C.; Fraune, S. Distinct antimicrobial peptide expression determines host species-specific bacterial associations. *Proc. Natl. Acad. Sci. USA* 2013, 110, E3730-3738, doi:10.1073/pnas.1304960110.

Gallo, A.; Tosti, E. The ascidian *Ciona intestinalis* as model organism for ecotoxicological bioassays. *J. Mar. Sci. Res. Dev.* 2015, 05, 1000e1138, doi:10.4172/2155-9910.1000e138.

Garza, D.R.; Dutilh, B.E. From cultured to uncultured genome sequences: Metagenomics and modeling microbial ecosystems. *Cell. Mol. Life Sci.* 2015, 72, 4287-4308, doi:10.1007/s00018-015-2004-1.

Gerwick, W.H.; Moore, B.S. Lessons from the past and charting the future of marine natural products drug discovery and chemical biology. *Chem. Biol.* 2012, 19, 85-98, doi:10.1016/j.chembiol.2011.12.014.

Giachetti, C.B.; Battini, N.; Castro, K.L.; Schwindt, E. Invasive ascidians: How predators reduce their dominance in artificial structures in cold temperate areas. *J. Exp. Mar. Biol. Ecol.* 2020, 533, 151459, doi:10.1016/j.jembe.2020.151459.

Giddings, L.-A.; Newman, D.J. Bioactive compounds from extremophilic marine fungi. In *Fungi in Extreme Environments: Ecological Role and Biotechnological Significance*, Tiquia-Arashiro, S.M.; Grube, M., Eds. Springer International Publishing: Cham, Switzerland, 2019; p. 349-382.

Goddard-Dwyer, M.; Lopez-Legentil, S.; Erwin, P.M. Microbiome variability across the native and invasive range of the ascidian *Clavelina oblonga*. *Appl. Environ. Microbiol.* 2020, 87, e02233-02220, doi:10.1128/AEM.02233-20.

Goodwin, S.; McPherson, J.D.; McCombie, W.R. Coming of age: Ten years of next-generation sequencing technologies. *Nat. Rev. Genet.* 2016, 17, 333-351, doi:10.1038/nrg.2016.49.

Grim, C.M.; Luu, G.T.; Sanchez, L.M. Staring into the void: Demystifying microbial metabolomics. *FEMS Microbiol. Lett.* 2019, 366, fnz135, doi:10.1093/femsle/fnz135.

Gutleben, J.; Chaib De Mares, M.; van Elsas, J.D.; Smidt, H.; Overmann, J.; Sipkema, D. The multi-omics promise in context: From sequence to microbial isolate. *Crit. Rev. Microbiol.* 2018, 44, 212-229, doi:10.1080/1040841X.2017.1332003.

Guyot, M.; Davoust, D. Hydroperoxy-24 vinyl-24 cholesterol, nouvel hydroperoxyde naturel isolé de deux tuniciers: *Phallusia mamillata* et *Ciona intestinalis*. *Tetrahedron Lett.* 1982, 23, 1905-1906, doi:10.1016/S0040-4039(00)87217-2.

Hamady, M.; Knight, R. Microbial community profiling for human microbiome projects: Tools, techniques, and challenges. *Genome Res.* 2009, 19, 1141-1152, doi:10.1101/gr.085464.108.

Hammann, M.; Wang, G.; Rickert, E.; Boo, S.M.; Weinberger, F. Invasion success of the seaweed *Gracilaria vermiculophylla* correlates with low palatibility. *Mar. Ecol. Prog. Ser.* 2013, 486, 93-103, doi:10.3354/meps10361.

Harris, A.M.; Moore, A.M.; Lowen, J.B.; DiBacco, C. Seasonal reproduction of the non-native vase tunicate *Ciona intestinalis* (Linnaeus, 1767) in Nova Scotia, Canada, in relation to water temperature. *Aquat. Invasions* 2017, 12, 33-41, doi:10.3391/ai.2017.12.1.04.

Harvey, A.L. Natural products in drug discovery. *Drug Discov. Today* 2008, 13, 894-901, doi:10.1016/j.drudis.2008.07.004.

Hentschel, U.; Piel, J.; Degnan, S.M.; Taylor, M.W. Genomic insights into the marine sponge microbiome. *Nat. Rev. Microbiol.* 2012, 10, 641-654, doi:10.1038/nrmicro2839.

Hifnawy, M.S.; Fouda, M.M.; Sayed, A.M.; Mohammed, R.; Hassan, H.M.; AbouZid, S.F.; Rateb, M.E.; Keller, A.; Adamek, M.; Ziemert, N.; et al. The genus *Micromonospora* as a model microorganism for bioactive natural product discovery. *RSC Adv.* 2020, 10, 20939-20959, doi:10.1039/d0ra04025h.

Hirose, E.; Hirabayashi, S.; Hori, K.; Kasai, F.; Watanabe, M.M. UV protection in the photosymbiotic ascidian *Didemnum molle* inhabiting different depths. *Zoolog. Sci.* 2006, 23, 57-63, doi:10.2108/zsj.23.57.

Hoeksema, B.W.; García-Hernández, J.E.; van Moorsel, G.W.N.M.; Olthof, G.; ten Hove, H.A. Extension of the recorded host range of Caribbean Christmas tree worms (*Spirobranchus* spp.) with two scleractinians, a zoantharian, and an ascidian. *Diversity* 2020, 12, 115, doi:10.3390/d12030115.

Holdich, D.M.; Reynolds, J.D.; Souty-Grosset, C.; Sibley, P.J. A review of the ever increasing threat to European crayfish from non-indigenous crayfish species. *Knowl. Manag. Aquatic Ecosyst.* 2009, 394-395, 11p1–46, doi:10.1051/kmae/2009025.

Holland, L.Z. Tunicates. *Curr. Biol.* 2016, 26, 146-152, doi:10.1016/j.cub.2015.12.024.

Holmström, C.; James, S.; Neilan, B.A.; White, D.C.; Kjelleberg, S. *Pseudoalteromonas tunicata* sp. nov., a bacterium that produces antifouling agents. *Int. J. Syst. Bacteriol.* 1998, 48, 1205-1212, doi:10.1099/00207713-48-4-1205

Horgan, R.P.; Kenny, L.C. 'Omic' technologies: Genomics, transcriptomics, proteomics and metabolomics. *Obstet. Gynaecol.* 2011, 13, 189-195, doi:10.1576/toag.13.3.189.27672.

Imperatore, C.; Aiello, A.; D'Aniello, F.; Luciano, P.; Vitalone, R.; Meli, R.; Raso, G.M.; Menna, M. New bioactive alkyl sulfates from Mediterranean tunicates. *Molecules* 2012, 17, 12642-12650, doi:10.3390/molecules171112642.

Jaric, I.; Cvijanovic, G. The Tens Rule in invasion biology: Measure of a true impact or our lack of knowledge and understanding? *Environ. Manag.* 2012, 50, 979-981, doi:10.1007/s00267-012-9951-1.

Jeschke, J.M.; Pyšek, P. Tens rule. In *Invasion Biology: Hypotheses and Evidence*, Jeschke, J.M.; Heger, T., Eds. CAB International: Wallingford, UK, 2018; p. 124-132.

Johnson, A.H.; Rehfeld, J. Cionin: A disulfotyrosyl hybrid of cholecystokinin and gastrin from neutral ganglion of the protochordate *Ciona intestinalis*. *J. Biol. Chem.* 1990, 265, 3054-3058, doi:10.1016/S0021-9258(19)39732-7.

Joshi, J.; Vrieling, K. The enemy release and EICA hypothesis revisited: Incorporating the fundamental difference between specialist and generalist herbivores. *Ecol. Lett.* 2005, 8, 704-714, doi:10.1111/j.1461-0248.2005.00769.x.

Keane, R.M.; Crawley, M.J. Exotic plant invasions and the enemy release hypothesis. *Trends Ecol. Evol.* 2002, 17, 164-170, doi:10.1016/S0169-5347(02)02499-0.

Khalifa, S.A.M.; Elias, N.; Farag, M.A.; Chen, L.; Saeed, A.; Hegazy, M.F.; Moustafa, M.S.; Abd El-Wahed, A.; Al-Mousawi, S.M.; Musharraf, S.G.; et al. Marine natural products: A source of novel anticancer drugs. *Mar. Drugs* 2019, 17, 491, doi:10.3390/md17090491.

Klock, M.M.; Barrett, L.G.; Thrall, P.H.; Harms, K.E.; van Kleunen, M. Host promiscuity in symbiont associations can influence exotic legume establishment and colonization of novel ranges. *Divers. Distrib.* 2015, 21, 1193-1203, doi:10.1111/ddi.12363.

Knight, R.; Vrbanac, A.; Taylor, B.C.; Aksenov, A.; Callewaert, C.; Debelius, J.; Gonzalez, A.; Kosciolek, T.; McCall, L.I.; McDonald, D.; et al. Best practices for analysing microbiomes. *Nat. Rev. Microbiol.* 2018, 16, 410-422, doi:10.1038/s41579-018-0029-9.

Kocot, K.M.; Tassia, M.G.; Halanych, K.M.; Swalla, B.J. Phylogenomics offers resolution of major tunicate relationships. *Mol. Phylogenet. Evol.* 2018, 121, 166-173, doi:10.1016/j.ympev.2018.01.005.

Kolar, C.S.; Lodge, D.M. Progress in invasion biology: Predicting invaders. *Trends Ecol. Evol.* 2001, 16, 199-204, doi:10.1016/s0169-5347(01)02101-2.

Kumano, G.; Nishida, H. Ascidian embryonic development: An emerging model system for the study of cell fate specification in chordates. *Dev. Dyn.* 2007, 236, 1732-1747, doi:10.1002/dvdy.21108.

Lambert, G. Ecology and natural history of the protochordates. *Can. J. Zool.* 2005, 83, 34-50, doi:10.1139/z04-156.

Lau, J.A.; Schultheis, E.H. When two invasion hypotheses are better than one. *New Phytol.* 2015, 205, 958-960, doi:10.1111/nph.13260.

Leal, M.C.; Puga, J.; Serodio, J.; Gomes, N.C.; Calado, R. Trends in the discovery of new marine natural products from invertebrates over the last two decades - where and what are we bioprospecting? *PLoS ONE* 2012, 7, e30580, doi:10.1371/journal.pone.0030580.

Leigh, B.A.; Liberti, A.; Dishaw, L.J. Generation of germ-free *Ciona intestinalis* for studies of gut-microbe interactions. *Front. Microbiol.* 2016, 7, 2092, doi:10.3389/fmicb.2016.02092.

Lemaire, P. Evolutionary crossroads in developmental biology: The tunicates. *Development* 2011, 138, 2143-2152, doi:10.1242/dev.048975.

Lemaire, P.; Smith, W.C.; Nishida, H. Ascidians and the plasticity of the chordate developmental program. *Curr. Biol.* 2008, 18, R620-631, doi:10.1016/j.cub.2008.05.039.

Li, F.; Pandey, P.; Janussen, D.; Chittiboyina, A.G.; Ferreira, D.; Tasdemir, D. Tridiscorhabdin and didiscorhabdin, the first discorhabdin oligomers linked with a direct C-N bridge from the sponge *Latrunculia biformis* collected from the deep sea in Antarctica. *J. Nat. Prod.* 2020, 83, 706-713, doi:10.1021/acs.jnatprod.0c00023.

Liberti, A.; Cannon, J.P.; Litman, G.W.; Dishaw, L.J. A soluble immune effector binds both fungi and bacteria via separate functional domains. *Front. Immunol.* 2019, 10, 369, doi:10.3389/fimmu.2019.00369.

Linnaeus, C. *Systema naturae. Editio duodecima reformata.* Holmiae, Stockholm, 1767.

Lins, D.; Rocha, R. Cultivated brown mussel (*Perna perna*) size is reduced through the impact of three invasive fouling species in southern Brazil. *Aquat. Invasions* 2020, 15, 114-126, doi:10.3391/ai.2020.15.1.08.

Lins, D.M.; de Marco, P.; Andrade, A.F.A.; Rocha, R.M.; MacIsaac, H. Predicting global ascidian invasions. *Divers. Distrib.* 2018, 24, 692-704, doi:10.1111/ddi.12711.

Litaudon, M.; Trigalo, F.; Martin, M.-T.; Frappier, F.; Guyot, M. Lissoclinotoxins: Antibiotic polysulfur derivatives from the tunicate *Lissoclinum perforatum*. Revised structure of lissoclinotoxin A. *Tetrahedron* 1994, 50, 5323-5334, doi:10.1016/s0040-4020(01)80690-6.

Liu, G.; Liu, M.; Wei, J.; Huang, H.; Zhang, Y.; Zhao, J.; Xiao, L.; Wu, N.; Zheng, L.; Lin, X. CS5931, a novel polypeptide in *Ciona savignyi*, represses angiogenesis via inhibiting vascular endothelial growth factor (VEGF) and matrix metalloproteinases (MMPs). *Mar. Drugs* 2014, 12, 1530-1544, doi:10.3390/md12031530.

Locke, A.; Hanson, J.M.; Ellis, K.M.; Thompson, J.; Rochette, R. Invasion of the southern Gulf of St. Lawrence by the clubbed tunicate (*Styela clava* Herdman): Potential mechanisms for invasions of Prince Edward Island estuaries. *J. Exp. Mar. Biol. Ecol.* 2007, 342, 69-77, doi:10.1016/j.jembe.2006.10.016.

Lockwood, J.L.; Cassey, P.; Blackburn, T. The role of propagule pressure in explaining species invasions. *Trends Ecol. Evol.* 2005, 20, 223-228, doi:10.1016/j.tree.2005.02.004.

Lopanik, N.B.; Clay, K. Chemical defensive symbioses in the marine environment. *Funct. Ecol.* 2014, 28, 328-340, doi:10.1111/1365-2435.12160.

López-Legentil, S.; Erwin, P.M.; Turon, M.; Yarden, O. Diversity of fungi isolated from three temperate ascidians. *Symbiosis* 2015, 66, 99-106, doi:10.1007/s13199-015-0339-x.

López-Legentil, S.; Turon, X.; Schupp, P. Chemical and physical defenses against predators in *Cystodytes* (Ascidiacea). *J. Exp. Mar. Biol. Ecol.* 2006, 332, 27-36, doi:10.1016/j.jembe.2005.11.002.

Luepke, K.H.; Mohr, J.F., 3rd. The antibiotic pipeline: Reviving research and development and speeding drugs to market. *Expert Rev. Anti-Infect. Ther.* 2017, 15, 425-433, doi:10.1080/14787210.2017.1308251.

Markham, A. Lurbinectedin: First Approval. *Drugs* 2020, 80, 1345-1353, doi:10.1007/s40265-020-01374-0.

Martins, A.; Vieira, H.; Gaspar, H.; Santos, S. Marketed marine natural products in the pharmaceutical and cosmeceutical industries: Tips for success. *Mar. Drugs* 2014, 12, 1066-1101, doi:10.3390/md12021066.

Martiny, J.B.; Jones, S.E.; Lennon, J.T.; Martiny, A.C. Microbiomes in light of traits: A phylogenetic perspective. *Science* 2015, 350, aac9323, doi:10.1126/science.aac9323.

Mastrototaro, F.; Montesanto, F.; Salonna, M.; Viard, F.; Chimienti, G.; Trainito, E.; Gissi, C. An integrative taxonomic framework for the study of the genus *Ciona* (Ascidiacea) and description of a new species, *Ciona intermedia. Zool. J. Linn. Soc.* 2020, doi:10.1093/zoolinnean/zlaa042.

Menna, M. Antitumor potential of natural products from Mediterranean ascidians. *Phytochem. Rev.* 2009, 8, 461-472, doi:10.1007/s11101-009-9131-y.

Millar, R.H. *Ciona*. In *L.M.B.C. Memoirs on Typical British Marine Plants and Animals, XXXV*, Colman, J.S., Ed. The University Press of Liverpool: Liverpool, UK, 1953; p. 1-123.

Misra, B.B.; Langefeld, C.D.; Olivier, M.; Cox, L.A. Integrated omics: Tools, advances, and future approaches. *J. Mol. Endocrinol.* 2018, 62, R21-R45, doi:10.1530/JME-18-0055.

Miyako, K.; Yasuno, Y.; Shinada, T.; Fujita, M.J.; Sakai, R. Diverse aromatic metabolites in the solitary tunicate *Cnemidocarpa irene*. *J. Nat. Prod.* 2020, 83, 3156-3165, doi:10.1021/acs.jnatprod.0c00789.

Mohimani, H.; Gurevich, A.; Shlemov, A.; Mikheenko, A.; Korobeynikov, A.; Cao, L.; Shcherbin, E.; Nothias, L.F.; Dorrestein, P.C.; Pevzner, P.A. Dereplication of microbial metabolites through database search of mass spectra. *Nat. Commun.* 2018, 9, 4035, doi:10.1038/s41467-018-06082-8.

Molinski, T.F.; Dalisay, D.S.; Lievens, S.L.; Saludes, J.P. Drug development from marine natural products. *Nat. Rev. Drug Discov.* 2009, 8, 69-85, doi:10.1038/nrd2487.

Molnar, J.L.; Gamboa, R.L.; Revenga, C.; Spalding, M.D. Assessing the global threat of invasive species to marine biodiversity. *Front. Ecol. Environ.* 2008, 6, 485-492, doi:10.1890/070064.

Morita, M.; Schmidt, E.W. Parallel lives of symbionts and hosts: Chemical mutualism in marine animals. *Nat. Prod. Rep.* 2018, 35, 357-378, doi:10.1039/c7np00053g.

Murphy, K.J.; Sephton, D.; Klein, K.; Bishop, C.D.; Wyeth, R.C. Abiotic conditions are not sufficient to predict spatial and interannual variation in abundance of *Ciona intestinalis* in Nova Scotia, Canada. *Mar. Ecol. Prog. Ser.* 2019, 628, 105-123, doi:10.3354/meps13076.

Myers, O.D.; Sumner, S.J.; Li, S.; Barnes, S.; Du, X. Detailed investigation and comparison of the XCMS and MZmine 2 chromatogram construction and chromatographic peak detection methods for preprocessing mass spectrometry metabolomics data. *Anal. Chem.* 2017, 89, 8689-8695, doi:10.1021/acs.analchem.7b01069.

Nothias, L.F.; Petras, D.; Schmid, R.; Dührkop, K.; Rainer, J.; Sarvepalli, A.; Protsyuk, I.; Ernst, M.; Tsugawa, H.; Fleischauer, M.; et al. Feature-based molecular networking in the GNPS analysis environment. *Nat. Methods* 2020, 17, 905-908, doi:10.1038/s41592-020-0933-6.

Nurgali, K.; Jagoe, R.T.; Abalo, R. Editorial: Adverse effects of cancer chemotherapy: Anything new to improve tolerance and reduce sequelae? *Front. Pharmacol.* 2018, 9, 245, doi:10.3389/fphar.2018.00245.

Palanisamy, S.K.; Rajendran, N.M.; Marino, A. Natural products diversity of marine ascidians (tunicates; Ascidiacea) and successful drugs in clinical development. *Nat. Prod. Bioprospect.* 2017, 7, 1-111, doi:10.1007/s13659-016-0115-5.

Palanisamy, S.K.; Thomas, O.P.; G, P.M. Bio-invasive ascidians in Ireland: A threat for the shellfish industry but also a source of high added value products. *Bioengineered* 2018, 9, 55-60, doi:10.1080/21655979.2017.1392421.

Patanasatienkul, T.; Sanchez, J.; Davidson, J.; Revie, C.W. The application of a mathematical model to evaluate the effectiveness of control strategies against *Ciona intestinalis* in mussel production. *Front. Vet. Sci.* 2019, 6, 271, doi:10.3389/fvets.2019.00271.

Patti, G.J.; Yanes, O.; Siuzdak, G. Metabolomics: The apogee of the omics trilogy. *Nat. Rev. Mol. Cell Biol.* 2012, 13, 263-269, doi:10.1038/nrm3314.

Paul, V.J.; Lindquist, N.; Fenical, W. Chemical defenses of the tropical ascidian *Atapozoa* sp. and its nudibranch predators *Nembrotha* spp. *Mar. Ecol. Prog. Ser.* 1990, 59, 109-118, doi:10.3354/meps059109.

Pennati, R.; Ficetola, G.F.; Brunetti, R.; Caicci, F.; Gasparini, F.; Griggio, F.; Sato, A.; Stach, T.; Kaul-Strehlow, S.; Gissi, C.; et al. Morphological differences between larvae of the *Ciona intestinalis* species complex: Hints for a valid taxonomic definition of distinct species. *PLoS ONE* 2015, 10, e0122879, doi:10.1371/journal.pone.0122879.

Picott, K.J.; Deichert, J.A.; deKemp, E.M.; Schatte, G.; Sauriol, F.; Ross, A.C. Isolation and characterization of tambjamine MYP1, a macrocyclic tambjamine analogue from marine bacterium *Pseudoalteromonas citrea*. *MedChemComm* 2019, 10, 478-483, doi:10.1039/c9md00061e.

Pisut, D.P.; Pawlik, J.R. Anti-predatory chemical defenses of ascidians: Secondary metabolites or inorganic acids? *J. Exp. Mar. Biol. Ecol.* 2002, 270, 203-214, doi:10.1016/S0022-0981(02)00023-0.

Pollock, J.; Glendinning, L.; Wisedchanwet, T.; Watson, M. The madness of microbiome: Attempting to find consensus "best practice" for 16S microbiome studies. *Appl. Environ. Microbiol.* 2018, doi:10.1128/AEM.02627-17.

Procaccini, G.; Affinito, O.; Toscano, F.; Sordino, P. A new animal model for merging ecology and evolution. In *Evolutionary Biology–Concepts, Biodiversity, Macroevolution and Genome Evolution*, Pontarotti, P., Ed. Springer: Berlin/Heidelberg, Germany, 2011; p. 91-106.

Proksch, P.; Edrada, R.A.; Ebel, R. Drugs from the seas - current status and microbiological implications. *Appl. Microbiol. Biotechnol.* 2002, 59, 125-134, doi:10.1007/s00253-002-1006-8.

Quince, C.; Walker, A.W.; Simpson, J.T.; Loman, N.J.; Segata, N. Shotgun metagenomics, from sampling to analysis. *Nat. Biotechnol.* 2017, 35, 833-844, doi:10.1038/nbt.3935.

Quinn, R.A.; Nothias, L.F.; Vining, O.; Meehan, M.; Esquenazi, E.; Dorrestein, P.C. Molecular networking as a drug discovery, drug metabolism, and precision medicine strategy. *Trends Pharmacol. Sci.* 2017, 38, 143-154, doi:10.1016/j.tips.2016.10.011.

Ramsay, A.; Davidson, J.; Bourque, D.; Stryhn, H. Recruitment patterns and population development of the invasive ascidian *Ciona intestinalis* in Prince Edward Island, Canada. *Aquat. Invasions* 2009, 4, 169-176, doi:10.3391/ai.2009.4.1.17.

Ramsay, A.; Davidson, J.; Landry, T.; Arsenault, G. Process of invasiveness among exotic tunicates in Prince Edward Island, Canada. *Biol. Invasions* 2008, 10, 1311-1316, doi:10.1007/s10530-007-9205-y.

Rateb, M.E.; Ebel, R. Secondary metabolites of fungi from marine habitats. *Nat. Prod. Rep.* 2011, 28, 290-344, doi:10.1039/c0np00061b.

Rath, C.M.; Janto, B.; Earl, J.; Ahmed, A.; Hu, F.Z.; Hiller, L.; Dahlgren, M.; Kreft, R.; Yu, F.; Wolff, J.J.; et al. Meta-omic characterization of the marine invertebrate microbial consortium that produces the chemotherapeutic natural product ET-743. *ACS Chem. Biol.* 2011, 6, 1244-1256, doi:10.1021/cb200244t.

Rinehart, K.L., Jr.; Gloer, J.B.; Hughes, R.G., Jr.; Renis, H.E.; McGovren, J.P.; Swynenberg, E.B.; Stringfellow, D.A.; Kuentzel, S.L.; Li, L.H. Didemnins: Antiviral and antitumor depsipeptides from a Caribbean tunicate. *Science* 1981, 212, 933-935, doi:10.1126/science.7233187.

Rius, M.; Heasman, K.G.; McQuaid, C.D. Long-term coexistence of non-indigenous species in aquaculture facilities. *Mar. Pollut. Bull.* 2011, 62, 2395-2403, doi:10.1016/j.marpolbul.2011.08.030.

Romano, G.; Costantini, M.; Sansone, C.; Lauritano, C.; Ruocco, N.; Ianora, A. Marine microorganisms as a promising and sustainable source of bioactive molecules. *Mar. Environ. Res.* 2017, 128, 58-69, doi:10.1016/j.marenvres.2016.05.002.

Saha, M.; Wiese, J.; Weinberger, F.; Wahl, M.; Thornber, C. Rapid adaptation to controlling new microbial epibionts in the invaded range promotes invasiveness of an exotic seaweed. *J. Ecol.* 2016, 104, 969-978, doi:10.1111/1365-2745.12590.

Sanamyan, K.E.; Sanamyan, N.P. Deep-water ascidians (Tunicata: Ascidiacea) from the northern and western Pacific. *J. Nat. Hist.* 2006, 40, 307-344, doi:10.1080/00222930600628416.

Sargent, P.; Wells, T.; Matheson, K.; McKenzie, C.; Deibel, D. First record of vase tunicate, *Ciona intestinalis* (Linnaeus, 1767) in coastal Newfoundland waters. *BioInvasions Rec.* 2013, 2, 89-98, doi:10.3391/bir.2013.2.2.01.

Satoh, N.; Levine, M. Surfing with the tunicates into the post-genome era. *Genes Dev.* 2005, 19, 2407-2411, doi:10.1101/gad.1365805.

Satoh, N.; Satou, Y.; Davidson, B.; Levine, M. *Ciona intestinalis*: An emerging model for whole-genome analyses. *Trends Genet.* 2003, 19, 376-381, doi:10.1016/S0168-9525(03)00144-6.

Satou, Y.; Nakmura, R.; Deli, Y.; Yoshida, R.; Hamada, M.; Fujie, M.; Hisata, K.; Takeda, H.; Satoh, N. A nearly-complete genome of *Ciona intestinalis* type A (*C. robusta*) reveals the contribution of inversion to chromosomal evolution in the genus *Ciona*. *Genome Biol. Evol.* 2019, 11, 3144-3157, doi:10.1093/gbe/evz228.

Saude, A.C.; Ombredane, A.S.; Silva, O.N.; Barbosa, J.A.; Moreno, S.E.; Araujo, A.C.; Falcao, R.; Silva, L.P.; Dias, S.C.; Franco, O.L. Clavanin bacterial sepsis control using a novel methacrylate nanocarrier. *Int. J. Nanomedicine* 2014, 9, 5055-5069, doi:10.2147/IJN.S66300.

Schmidt, E.W. The secret to a successful relationship: Lasting chemistry between ascidians and their symbiotic bacteria. *Invertebr. Biol.* 2015, 134, 88-102, doi:10.1111/ivb.12071.

Schmidt, E.W.; Donia, M.S. Life in cellulose houses: Symbiotic bacterial biosynthesis of ascidian drugs and drug leads. *Curr. Opin. Biotechnol.* 2010, 21, 827-833, doi:10.1016/j.copbio.2010.10.006.

Schmidt, E.W.; Nelson, J.T.; Rasko, D.A.; Sudek, S.; Eisen, J.A.; Haygood, M.G.; Ravel, J. Patellamide A and C biosynthesis by a microcin-like pathway in *Prochloron didemni*, the cyanobacterial symbiont of *Lissoclinum patella*. *Proc. Natl. Acad. Sci. USA* 2005, 102, 7315-7320, doi:10.1073/pnas.0501424102.

Schwartz, N.; Rohde, S.; Hiromori, S.; Schupp, P.J. Understanding the invasion success of *Sargassum muticum*: Herbivore preferences for native and invasive *Sargassum* spp. *Mar. Biol.* 2016, 163, 181, doi:10.1007/s00227-016-2953-4.

Sedio, B.E.; Devaney, J.L.; Pullen, J.; Parker, G.G.; Wright, S.J.; Parker, J.D. Chemical novelty facilitates herbivore resistance and biological invasions in some introduced plant species. *Ecol. Evol.* 2020, 10, 8770-8792, doi:10.1002/ece3.6575.

Sekse, C.; Holst-Jensen, A.; Dobrindt, U.; Johannessen, G.S.; Li, W.; Spilsberg, B.; Shi, J. High throughput sequencing for detection of foodborne pathogens. *Front. Microbiol.* 2017, 8, 2029, doi:10.3389/fmicb.2017.02029.

Shang, J.; Hu, B.; Wang, J.; Zhu, F.; Kang, Y.; Li, D.; Sun, H.; Kong, D.X.; Hou, T. Cheminformatic insight into the differences between terrestrial and marine originated natural products. *J. Chem. Inf. Model.* 2018, 58, 1182-1193, doi:10.1021/acs.jcim.8b00125.

Shenkar, N.; Shmuel, Y.; Huchon, D. The invasive ascidian *Ciona robusta* recorded from a Red Sea marina. *Mar. Biodiv.* 2017, 48, 2211–2214, doi:10.1007/s12526-017-0699-y.

Shenkar, N.; Swalla, B.J. Global diversity of Ascidiacea. *PLoS ONE* 2011, 6, e20657, doi:10.1371/journal.pone.0020657.

Sigwart, J.D.; Blasiak, R.; Jaspars, M.; Jouffray, J.-B.; Tasdemir, D. Unlocking the potential of marine biodiscovery. *Nat. Prod. Rep.* 2021, doi:10.1039/d0np00067a.

Simberloff, D.; Martin, J.L.; Genovesi, P.; Maris, V.; Wardle, D.A.; Aronson, J.; Courchamp, F.; Galil, B.; Garcia-Berthou, E.; Pascal, M.; et al. Impacts of biological invasions: What's what and the way forward. *Trends Ecol. Evol.* 2013, 28, 58-66, doi:10.1016/j.tree.2012.07.013.

Sperstad, S.V.; Haug, T.; Blencke, H.M.; Styrvold, O.B.; Li, C.; Stensvag, K. Antimicrobial peptides from marine invertebrates: Challenges and perspectives in marine antimicrobial peptide discovery. *Biotechnol. Adv.* 2011, 29, 519-530, doi:10.1016/j.biotechadv.2011.05.021.

Stoecker, D. Chemical defenses of ascidians against predators. *Ecology* 1980, 61, 1327-1334, doi:10.2307/1939041.

Strauss, A.; White, A.; Boots, M. Invading with biological weapons: The importance of disease-mediated invasions. *Funct. Ecol.* 2012, 26, 1249-1261, doi:10.1111/1365-2435.12011.

Stuart, K.A.; Welsh, K.; Walker, M.C.; Edrada-Ebel, R. Metabolomic tools used in marine natural product drug discovery. *Expert Opin. Drug Discov.* 2020, 15, 499-522, doi:10.1080/17460441.2020.1722636.

Susick, K.; Scianni, C.; Mackie, J.A. Artificial structure density predicts fouling community diversity on settlement panels. *Biol. Invasions* 2019, 22, 271–292, doi:10.1007/s10530-019-02088-5.

Svensson, J.R.; Nylund, G.M.; Cervin, G.; Toth, G.B.; Pavia, H.; Callaway, R. Novel chemical weapon of an exotic macroalga inhibits recruitment of native competitors in the invaded range. *J. Ecol.* 2013, 101, 140-148, doi:10.1111/1365-2745.12028.

R Core Team. *R: A language and enviroment for statistical computing*, R Foundation for Statistical Computing: Vienna, Austria, 2017.

Tewes, L.J.; Michling, F.; Koch, M.A.; Müller, C.; Lau, J. Intracontinental plant invader shows matching genetic and chemical profiles and might benefit from high defence variation within populations. *J. Ecol.* 2018, 106, 714-726, doi:10.1111/1365-2745.12869.

Thomas, T.; Moitinho-Silva, L.; Lurgi, M.; Bjork, J.R.; Easson, C.; Astudillo-Garcia, C.; Olson, J.B.; Erwin, P.M.; Lopez-Legentil, S.; Luter, H.; et al. Diversity, structure and convergent evolution of the global sponge microbiome. *Nat. Commun.* 2016, 7, 11870, doi:10.1038/ncomms11870.

Tianero, M.D.; Kwan, J.C.; Wyche, T.P.; Presson, A.P.; Koch, M.; Barrows, L.R.; Bugni, T.S.; Schmidt, E.W. Species specificity of symbiosis and secondary metabolism in ascidians. *ISME J.* 2015, 9, 615-628, doi:10.1038/ismej.2014.152.

Torchin, M.E.; Lafferty, K.D.; Kuris, A.M. Parasites and marine invasions. *Parasitology* 2002, 124, 137-151, doi:10.1017/s0031182002001506.

Tsukamoto, S.; Hirota, H.; Kato, H.; Fusetani, N. Urochordamines A and B: Larval settlement/metamorphosis-promoting, pteridine-containing physostigmine alkaloids from the tunicate *Ciona savignyi*. *Tetrahedron Lett.* 1993, 34, 4819-4822, doi:10.1016/S0040-4039(00)74097-4.

van Bergeijk, D.A.; Terlouw, B.R.; Medema, M.H.; van Wezel, G.P. Ecology and genomics of Actinobacteria: New concepts for natural product discovery. *Nat. Rev. Microbiol.* 2020, 18, 546–558, doi:10.1038/s41579-020-0379-y.

Vilcinskas, A. Pathogens as biological weapons of invasive species. *PLoS Pathog.* 2015, 11, e1004714, doi:10.1371/journal.ppat.1004714.

Vinson, J.P.; Jaffe, D.B.; O'Neill, K.; Karlsson, E.K.; Stange-Thomann, N.; Anderson, S.; Mesirov, J.P.; Satoh, N.; Satou, Y.; Nusbaum, C.; et al. Assembly of polymorphic genomes: Algorithms and application to *Ciona savignyi*. *Genome Res.* 2005, 15, 1127-1135, doi:10.1101/gr.3722605.

Wang, E.; Sorolla, M.A.; Krishnan, P.D.G.; Sorolla, A. From seabed to bedside: A review on promising marine anticancer compounds. *Biomolecules* 2020, 10, 248, doi:10.3390/biom10020248.

Wang, M.; Carver, J.J.; Phelan, V.V.; Sanchez, L.M.; Garg, N.; Peng, Y.; Nguyen, D.D.; Watrous, J.; Kapono, C.A.; Luzzatto-Knaan, T.; et al. Sharing and community curation of mass spectrometry data with Global Natural Products Social Molecular Networking. *Nat. Biotechnol.* 2016, 34, 828-837, doi:10.1038/nbt.3597.

Watkins, R.R.; Bonomo, R.A. Overview: Global and local impact of antibiotic resistance. *Infect. Dis. Clin. North Am.* 2016, 30, 313-322, doi:10.1016/j.idc.2016.02.001.

WHO 2018.Global health estimates 2016: Deaths by cause, age, sex, by country and by region, 2000–2016. World Health Organization, Geneva, Switzerland. Available online: https://www.who.int/news-room/fact-sheets/detail/the-top-10-causes-of-death (accessed on 12.11.2020).

Williamson, M.; Fitter, A. The varying success of invaders. *Ecology* 1996, 77, 1661-1666, doi:10.2307/2265769.

Wishart, D.S. Applications of metabolomics in drug discovery and development. *Drugs R D* 2008, 9, 307-322, doi:10.2165/00126839-200809050-00002.

Wyche, T.P.; Piotrowski, J.S.; Hou, Y.; Braun, D.; Deshpande, R.; McIlwain, S.; Ong, I.M.; Myers, C.L.; Guzei, I.A.; Westler, W.M.; et al. Forazoline A: Marine-derived polyketide with antifungal *in vivo* efficacy. *Angew. Chem.* 2014, 53, 11583-11586, doi:10.1002/anie.201405990.

Xu, Y.; Kersten, R.D.; Nam, S.J.; Lu, L.; Al-Suwailem, A.M.; Zheng, H.; Fenical, W.; Dorrestein, P.C.; Moore, B.S.; Qian, P.Y. Bacterial biosynthesis and maturation of the didemnin anti-cancer agents. *J. Am. Chem. Soc.* 2012, 134, 8625-8632, doi:10.1021/ja301735a.

Yarden, O. Fungal association with sessile marine invertebrates. *Front. Microbiol.* 2014, 5, 228, doi:10.3389/fmicb.2014.00228.

Yoshida, M.; Murata, M.; Inaba, K.; Morisawa, M. A chemoattractant for ascidian spermatozoa is a sulfated steroid. *Proc. Natl. Acad. Sci. USA* 2002, 99, 14831-14836, doi:10.1073/pnas.242470599.

Zeng, L.; Jacobs, M.W.; Swalla, B.J. Coloniality has evolved once in Stolidobranch ascidians. *Integr. Comp. Biol.* 2006, 46, 255-268, doi:10.1093/icb/icj035.

Zhan, A.; Briski, E.; Bock, D.G.; Ghabooli, S.; MacIsaac, H.J. Ascidians as models for studying invasion success. *Mar. Biol.* 2015, 162, 2449-2470, doi:10.1007/s00227-015-2734-5.

Zhang, Z.; Capinha, C.; Karger, D.N.; Turon, X.; MacIsaac, H.J.; Zhan, A. Impacts of climate change on geographical distributions of invasive ascidians. *Mar. Environ. Res.* 2020, 159, 104993, doi:10.1016/j.marenvres.2020.104993.

Zhao, Y.; Li, J. Ascidian bioresources: Common and variant chemical compositions and exploitation strategy - examples of *Halocynthia roretzi, Styela plicata, Ascidia* sp. and *Ciona intestinalis*. *Z. Naturforsch. C* 2016, 71, 165-180, doi:10.1515/znc-2016-0012.

Zhao, Y.; Wang, M.; Lindstrom, M.E.; Li, J. Fatty acid and lipid profiles with emphasis on n-3 fatty acids and phospholipids from *Ciona intestinalis*. *Lipids* 2015, 50, 1009-1027, doi:10.1007/s11745-015-4049-1.

Zilber-Rosenberg, I.; Rosenberg, E. Role of microorganisms in the evolution of animals and plants: The hologenome theory of evolution. *FEMS Microbiol. Rev.* 2008, 32, 723-735, doi:10.1111/j.1574-6976.2008.00123.x.

Results

Chapter 1

Comparative microbiome and metabolome analyses of the marine tunicate *Ciona intestinalis* from native and invaded habitats

Utermann, C., Blümel, M., Busch, K., Buedenbender, L., Lin, Y., Haltli, B.A., Kerr, R.G., Briski, E., Hentschel, U., and Tasdemir, D., 2020, *Microorganisms,* 8, 2022; DOI: 10.3390/microorganisms8122022.
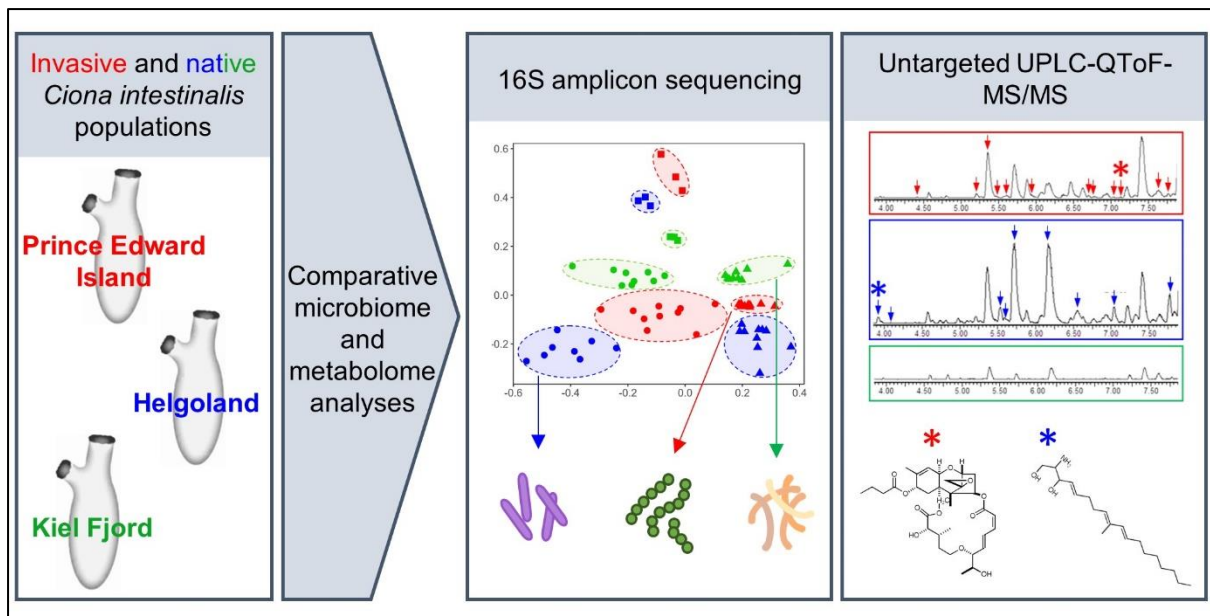
Article

Comparative Microbiome and Metabolome Analyses of the Marine Tunicate *Ciona intestinalis* from Native and Invaded Habitats

Caroline Utermann [1], Martina Blümel [1], Kathrin Busch [2], Larissa Buedenbender [1], Yaping Lin [3,4], Bradley A. Haltli [5], Russell G. Kerr [5], Elizabeta Briski [3], Ute Hentschel [2,6] and Deniz Tasdemir [1,6,*]

[1] GEOMAR Centre for Marine Biotechnology (GEOMAR-Biotech), Research Unit Marine Natural Products Chemistry, GEOMAR Helmholtz Centre for Ocean Research Kiel, Am Kiel-Kanal 44, 24106 Kiel, Germany; cutermann@geomar.de (C.U.); mbluemel@geomar.de (M.B.); larissa.buedenbender@alumni.griffithuni.edu.au (L.B.)

[2] Research Unit Marine Symbioses, GEOMAR Helmholtz Centre for Ocean Research Kiel, Duesternbrooker Weg 20, 24105 Kiel, Germany; kbusch@geomar.de (K.B.); uhentschel@geomar.de (U.H.)

[3] Research Group Invasion Ecology, Research Unit Experimental Ecology, GEOMAR Helmholtz Centre for Ocean Research Kiel, Duesternbrooker Weg 20, 24105 Kiel, Germany; linyaping2012@hotmail.com (Y.L.); ebriski@geomar.de (E.B.)

[4] Chinese Academy of Sciences, Research Center for Eco-Environmental Sciences, 18 Shuangqing Rd., Haidian District, Beijing 100085, China

[5] Department of Chemistry, University of Prince Edward Island, 550 University Avenue, Charlottetown, PE C1A 4P3, Canada; bhaltli@upei.ca (B.A.H.); rkerr@upei.ca (R.G.K.)

[6] Faculty of Mathematics and Natural Sciences, Kiel University, Christian-Albrechts-Platz 4, 24118 Kiel, Germany

* Correspondence: dtasdemir@geomar.de; Tel.: +49-431-6004430

Abstract: Massive fouling by the invasive ascidian *Ciona intestinalis* in Prince Edward Island (PEI, Canada) has been causing devastating losses to the local blue mussel farms. In order to gain first insights into so far unexplored factors that may contribute to the invasiveness of *C. intestinalis* in PEI, we undertook comparative microbiome and metabolome studies on specific tissues from *C. intestinalis* populations collected in invaded (PEI) and native regions (Helgoland and Kiel, Germany). Microbial community analyses and untargeted metabolomics revealed clear location- and tissue-specific patterns showing that biogeography and the sampled tissue shape the microbiome and metabolome of *C. intestinalis*. Moreover, we observed higher microbial and chemical diversity in *C. intestinalis* from PEI than in the native populations. Bacterial OTUs specific to *C. intestinalis* from PEI included Cyanobacteria (e.g., *Leptolyngbya* sp.) and Rhodobacteraceae (e.g., *Roseobacter* sp.), while populations from native sampling sites showed higher abundances of e.g., Firmicutes (Helgoland) and Epsilonproteobacteria (Kiel). Altogether 121 abundant metabolites were putatively annotated in the global ascidian metabolome, of which 18 were only detected in the invasive PEI population (e.g., polyketides and terpenoids), while six (e.g., sphingolipids) or none were exclusive to the native specimens from Helgoland and Kiel, respectively. Some identified bacteria and metabolites reportedly possess bioactive properties (e.g., antifouling and antibiotic) that may contribute to the overall fitness of *C. intestinalis*. Hence, this first study provides a basis for future studies on factors underlying the global invasiveness of *Ciona* species.

Keywords: biological invasion; ascidian; *Ciona intestinalis*; Prince Edward Island; microbiome; symbionts; untargeted metabolomics; bioactive secondary metabolites

1. Introduction

Biological invasions represent the second largest cause of biodiversity loss and is only surpassed by anthropogenic species extinction [1–3]. The marine coastal environment is one of the most invaded ecosystems globally, with at least 84% of coastal habitats affected by invasive species [4,5]. Shipping and aquaculture are considered as main vectors for the spread of marine invasive species (MIS) [4,5]. Characteristic features of MIS include high phenotypic plasticity, high fertility, and rapid growth [4,6]. MIS are often responsible for dramatic ecosystem changes, e.g., lowering species diversity, alteration of food webs and nutrient cycling [3,5], and cause drastic economic losses in various industrial sectors [5,7]. Several common invasion hypotheses have been applied to understand mechanisms allowing certain marine organisms to become invasive [7]. The prominent "enemy release hypothesis" states that invasive species thrive in their newly colonized habitats by escaping from specialized predators [1]. The "evolution of increased competitive ability hypothesis" assumes that due to lowered predation-pressure, invasive species reduce expensive specialized chemical defenses and reallocate these vacant resources towards growth and reproduction [7,8]. In the marine realm, re-distribution of resources has been suggested for the brown alga *Sargassum* spp., since herbivores preferably graze on seaweeds from the invaded population [7,9]. According to the "novel weapon hypothesis", invasive species produce defensive metabolites conferring a competitive advantage to the invader and a potentially negative impact to native congeners [10]. 1,1,3,3-tetrabromo-2-heptanone, a secondary metabolite produced by the invasive red alga *Bonnemaisonia hamifera,* inhibits the settlement of indigenous algae [11] and is therefore an impressive example for this hypothesis. Chemical defense is often provided or aided by microbial symbionts, highlighting the importance of microbiome in invasion [12]. The "biological weapon hypothesis" postulates a transport of potential microbial pathogens and parasites by the invasive species to new habitats [13]. For instance, the crayfish *Pacifastacus leniusculus* transported the fungal pathogen *Aphanomyces astaci* to Europe, which significantly reduced native North Sea crayfish populations [13,14].

Tunicates are sessile filter-feeders with a protective outer coating, the tunic [15,16]. The fully marine tunicate class Ascidiacea is one of the most invasive marine taxa worldwide and therein *Ciona intestinalis* and its sister species *C. robusta* are among the most notorious invasive ascidians [4,17]. The sea vase *C. intestinalis* is native to the NE Atlantic and its adjacent seas (North and Baltic Seas), where it occurs in moderate abundances [17,18]. In recent years, *C. intestinalis* has spread globally and is generally regarded as a pest in invaded habitats in the NW Atlantic and Bohai and Yellow Seas (China) [17,18]. *Ciona intestinalis* reportedly reduces species richness of the sessile macrobiota in invaded habitats [19]. It is also a successful macrofouler on mussels cultivated on long lines and directly competes for food and space [17,20]. Fouling by *C. intestinalis* causes high mussel mortalities (up to 50%), leading to significant economic losses for the aquaculture industry [16,21]. Its substantial economic impact is well demonstrated in Prince Edward Island (PEI, Canada). Here, the tunicate was first observed in 2004 and rapidly became the most problematic fouling species [20]. PEI's aquaculture economy is particularly compromised by invasive ascidians, since it produces >80% of all Canadian farmed mussels, accounting for an economic value of approx. Can $28 million per annum [22]. Together with the above outlined characteristics of MIS, *C. intestinalis*' adaptive capacity (eurytherm, −1–35 °C, and euryhaline, 12–40‰) is considered as a major factor for its invasiveness [4]. Genetic admixture and epigenetic modifications are also regarded as promotive factors for rapid acclimation and the trans-Atlantic spread of *C. intestinalis* [23,24]. However, factors promoting the invasiveness of *C. intestinalis* are still not fully understood.

Current evidence suggests a prominent role for defensive secondary metabolites and associated (potentially pathogenic) microbiota in globally successful MIS [10,13,25]. Herein, we aimed at gaining first insights into their potential roles for the invasiveness of *C. intestinalis*. Therefore, integrated metabolome and microbiome studies on *C. intestinalis* specimens from native (Helgoland, Germany, North Sea and Kiel, Germany, Baltic Sea) and invaded (PEI,

Canada, Gulf of Saint Lawrence) habitats were performed. The microbiome of the tunic and the gut was characterized, comparatively, by amplicon sequencing of the V3-V4 hypervariable region of the 16S rRNA gene. Likewise, the tunic and inner body of individual *C. intestinalis* specimens were comparatively profiled by a UPLC-MS/MS-based (ultra-performance liquid chromatography-tandem mass spectrometry) untargeted metabolomics approach. Furthermore, the global metabolome of the three ascidian populations was investigated by untargeted metabolomics using state-of-the-art tools (global natural products social molecular networking (GNPS) dereplication workflow [26], in-silico prediction [27], molecular networking (MN) [26]).

2. Materials and Methods

2.1. Sampling

Sampling of native *C. intestinalis* specimens was conducted in September 2017 in Helgoland (Germany, North Sea; 54°10'37.6" N 7°53'35.0" E; <1 m depth) and Kiel Fjord (Germany, Baltic Sea; 54°22'55.4" N, 10°94'3.4" E; ca. 3 m depth). Invasive specimens were sampled in PEI (Canada, Atlantic Ocean; 46°10'12.8" N 62°33'52.1" W; ca. 2 m depth) in October 2017. Seawater samples (1 L each) were collected aseptically in triplicate. Ascidian and water samples were immediately transported to the laboratory and processed at the same day. For individual genetic and chemical analyses of *C. intestinalis*, 10 intact individuals were chosen per sampling location, transferred into sterile 50 mL reaction tubes and promptly frozen at −80 °C. For chemical extractions at population level, approximately 0.5 kg of ascidian material were collected per sampling site in plastic bags and directly frozen at −80 °C. Seawater samples were sterile filtered as described in Parrot et al. 2019 [28] and filters were stored until further processing at −80 °C. For genotyping and microbiome analysis, individual animals were briefly thawed and dissected under sterile conditions. To ensure reproducibility, all dissections were done by the same person. First, the tunic was separated from the mantle and the remaining body. An approximately 4 cm^2 piece of the tunic was cut for extraction of microbial DNA. Subsequently, the gut was removed from the inner body and the gut content was removed by flushing it with sterile ultrapure water (sterile filtered and UV-treated) by using an injection needle attached to a syringe. A subsample of the gut (0.04 cm^2), which was stored at −20 °C until further processing, was taken for genotyping the *C. intestinalis* individuals. From individuals with a very short gut (individuals CT4, KT3-5), a small part of the tunic was frozen for genotyping instead. Another ca. 2 cm of gut tissue was immediately subjected to microbial DNA extraction. For individual metabolomics analysis, the remaining gut, mantle, and inner body tissues (hereinafter referred to as "inner body") were placed into a sterile 50 mL reaction tube and the remaining tunic into a sterile 15 mL reaction tube. Samples were stored at −80 °C until metabolomic analysis.

2.2. Genotyping

To validate the taxonomic identification of *C. intestinalis* for all three sampling locations, 30 individuals (10 per sampling site) were genotyped with the mitochondrial marker fragment COX3-ND1 [29]. Genomic DNA was extracted from gut or tunic tissue using the proteinase K method [30]. Amplification of the target DNA fragment was performed with the primers TX3F and TN1R [29] in 25 µL reactions containing approximately 100 ng template DNA, 1 U TaKaRa Ex Taq (Takara, Dalian, China), 2.5 µL of 10X Ex Taq buffer and 200 µM dNTP mixture. Besides an increased elongation time of 45 s, PCR conditions were applied as previously described by Zhan et al. 2010 [31]. The target band (ca. 600 bp) was purified from a 1% TBE gel by using purification beads (iCloning Beijing Biotech, Beijing, China). Subsequent Sanger sequencing was performed with the primer TX3F on an ABI 3130*xl* capillary sequencer. Sequences were aligned in BioEdit [32] using the ClustalW [33] multiple alignment tool. Phylogeny was inferred by constructing a Maximum Likelihood tree based on the General

Time Reversible model [34] in MEGA7 [35]. All collected specimens were identified as *C. intestinalis* (Figure S1).

2.3. Microbiome Analysis

2.3.1. DNA Extraction, Library Preparation, and Sequencing

For microbial community composition analyses, genomic DNA was extracted from tunic ($n = 30$), gut ($n = 30$), and seawater samples ($n = 9$; Table S1) using the DNeasy PowerSoil Kit (Qiagen, Hilden, Germany). A piece of the respective tissue (gut: approximately 1 cm in length, tunic: approximately 2.5 × 1.5 cm) or a piece of the filter equivalent to 250 mL seawater reference sample was transferred into a provided PowerBead Tube containing 60 µL of solution C1. The tubes were shaken for 20 min at a frequency of 30/s in a mixer mill MM 200 (Retsch, Hahn, Germany). All subsequent steps were performed according to the manufacturers' instructions besides the final step. In order to increase the DNA concentration, 30 µL instead of 100 µL of solution C6 were added to the column. The quantity of the extracted DNA was checked with a NanoDrop. The V3-V4 hypervariable region of the 16S rRNA gene was amplified with the primer pair 341F/806R [36] using the following thermal cycling conditions: 30 s 98 °C; 30 cycles of 9 s 98 °C, 30 s 55 °C, 30 s 72 °C; 10 min 72 °C. Amplified DNA fragments were separated by agarose gel (1%) electrophoresis and amplicons of the expected size (ca. 465 bp) were excised from the gel, and the DNA purified via gel elution (QIAquick Gel Extraction Kit, Qiagen), normalized, and pooled. Sequencing was performed on an Illumina MiSeq platform (MiSeqFGx) using the Illumina MiSeq Reagent Kit v. 3 (2 × 300 bp). Demultiplexing was performed based on 0 mismatches in the barcode sequences. Raw amplicon sequences were deposited in the Sequence Read Archive of NCBI (BioProject: PRJNA635604).

2.3.2. Bioinformatic Processing and Statistical Analysis

Primer and adapter trimming of demultiplexed raw sequences was done with Cutadapt v. 2.3 [37]. This was followed by quality filtering using BBDuk [38]. Trimmed and quality filtered raw sequence reads were further processed with mothur v. 1.42.0 [39] by applying a modified version of the established MiSeq SOP [40]. Briefly, contigs containing ambiguous bases or homopolymers >8 bp were removed. Filtered contigs were aligned to the SILVA database (release 132; [41]). Subsequent filtering steps removed unaligned contigs, gap-only columns, and singletons. Contigs were preclustered as suggested by Huse and co-workers [42] and non-bacterial sequences were removed by taxonomic sequence classification using the Wang et al. method [43] at a bootstrap threshold of 80%. After eliminating chimeric sequences with the UCHIME algorithm [44], contigs were binned at a 97% similarity level into operational taxonomic units (OTUs). OTUs were classified with the 16S rRNA gene SILVA reference alignment file. Two replicates from Helgoland (HG6, HG8) and two replicates from Kiel (KG10, KT6) were removed from the dataset since the number of sequence reads was extremely low (3–118 reads).

Subsequent data analysis was done with R v. 3.5.2 [45] using the packages *phyloseq* [46], *vegan* [47], and *picante* [48]. The OTU abundance table was rarefied based on the maximum number of 3647 sequences common to all samples. Alpha diversity was estimated by calculating OTU richness, Chao1, Faith's phylogenetic diversity (Faith's PD), Simpson, and Shannon indices. Alpha diversity indices were statistically compared across sampling locations and sample types via one-way ANOVA and Tukey's honest significance difference (HSD) test by using the *aov()* and *TukeyHSD()* functions in R. In order to compare the microbial diversity among sample types, non-metric multidimensional scaling (nMDS) was performed on OTU counts, which were rarefied and square root transformed for standardization (Bray-Curtis similarity index). In order to consider phylogenetic relatedness of OTUs, an additional nMDS plot based on weighted UniFrac distances [49] was calculated. Statistical testing was done by analysis of similarity (ANOSIM) calculations executed in Past

v. 3.12 [50]. The Marker Data Profiling workflow offered by the platform MicrobiomeAnalyst [51] was used for detection of bacterial taxa that differed significantly between the sample types and sampling locations. Briefly, the original OTU abundance table was rarefied to the minimum library size. Significantly different bacterial taxa were statistically identified via the Kruskal-Wallis-Test (comparison of multiple groups). P values were adjusted for multiple testing using the false discovery rate (FDR) method as suggested by Benjamini and Hochberg [52].

2.4. Metabolome Analysis

2.4.1. Solvent Extraction

For individual metabolome analyses, single ascidian specimens were dissected into inner body and tunic ($n = 60$, i.e., 10 replicates per sampling site and tissue; Table S2). Freeze-dried inner bodies and tunics were separately ground. Solvent extractions were performed by maceration in a 1:20 (solid:liquid) ratio in 3 cycles over 24 h (2 × 4 h, 1 × overnight) in the dark at 120 rpm and 22 °C. First, samples were extracted with ultrapure water in order to remove sea salts. Between the cycles and after the last extraction step, the water was separated from the cell material via centrifugation (4500 rpm, 7 min, Beckmann J2-21M centrifuge, Beckman Coulter, Brea, CA, USA). Prior to solvent extraction, the leftover cell material was again freeze-dried. Subsequent solvent extraction was done with methanol (MeOH) and dichloromethane (DCM; both purchased at AppliChem, Darmstadt, Germany). The extraction procedure was similar to the water extraction described above; the solvent was however removed by decantation instead of centrifugation. MeOH and DCM extracts were combined, filtered through a 0.2 µM PTFE syringe filter (Carl Roth, Karlsruhe, Germany), and evaporated to dryness on a rotary evaporator. Two blank extractions processed in the same manner served as control samples for UPLC-MS analysis. Organic extracts were combined and evaporated to dryness. The pooled ascidian bulk samples (i.e., approximately 500 g of fresh whole ascidians per sampling site) for population analyses were extracted similarly, using 13.0 g of freeze-dried samples ($n = 3$ per sampling site).

2.4.2. LC-MS/MS Analysis and Data Pre-Processing

All solvents used for the LC-MS analyses were ULC-MS grade from Biosolve Chimie (Dieuze, France) and ultra-purified water was prepared with an Arium Lab water system (Sartorius, Goettingen, Germany). Prior to UPLC-QToF-MS/MS measurements, extracts were diluted with MeOH to a final concentration of 0.1 mg/mL and blank MeOH samples were used as solvent controls. Analyses were performed with an Acquity UPLC I-Class System coupled to a Xevo G2-XS QTof Mass Spectrometer (Waters, Milford, MA, USA), which was equipped with an Acquity UPLC HSS T3 column (High Strength Silica C18, 1.8 µm, 2.1 × 100 mm, Waters) operating at 40 °C. The injection volume was 5.0 µL. A binary mobile phase system (A: 0.1% formic acid in ultra-purified water, B: 0.1% formic acid in acetonitrile) was pumped at a flow rate of 0.6 mL/min by applying the following gradient (% of A given): initial, 99%; 2.5 min, 50%; 12.5 min, 0%; followed by washing and reconditioning of the column. The total run time was 16 min. The MS and MS/MS spectra were recorded in positive mode as previously described by Parrot et al. [28].

Recorded data were converted with msconvert [53] to mzXML format. Data pre-processing was conducted with MZmine v. 2.38 [54] by applying the following parameters. The mass list was compiled with a noise level of 500. Using this mass list, chromatograms were built with the following thresholds: minimum time span: 0.01 min, minimum peak height: 500, m/z tolerance: 0.01 (or 10 ppm). Chromatogram deconvolution was done with the baseline cut-off algorithm at a baseline level of 500, a minimum peak height of 1000 and a peak duration range of 0 to 0.5 min. Grouping of isotopic peaks was performed by applying the isotopic peaks grouper algorithm with the following parameters: m/z tolerance: 0.01 (or 10 ppm), retention time (R_t) tolerance: 1.0 min, maximum charge: 3. In a final step, all samples

were combined into one peak list by using the join aligner algorithm (m/z tolerance: 0.01 (or 10 ppm), R_t tolerance: 0.5 min, weight m/z:R_t: 75:25). Compounds detected in MeOH or extraction blanks were removed from this list. The resulting data were saved in the GNPS compatible data format MGF and the comprehensive peak list was exported to Microsoft Excel 2010 for further analysis. The peak area of population level extracts was used to investigate whether a peak was homogenously distributed across all sampling locations or showed an enhanced (at least 10-fold increase compared to other sampling sites) or exclusive production at one sampling site.

2.4.3. Molecular Networking and Dereplication

Pre-processed MS/MS data were submitted to the Feature-Based Molecular Networking (FBMN) workflow available at the online platform GNPS [26]. Briefly, consensus spectra were constructed with a parent mass and MS/MS fragment ion tolerance of 0.02 Da. FBMN were created with edges filtered to have a cosine score above 0.5 and more than 6 matched peaks (4 for individual metabolomes). The remaining parameters were set as previously described by Parrot et al. [28]. The FBMN was visualized with Cytoscape v. 3.7.1 [55] and nodes were color-coded by a presence-absence matrix. For automated dereplication, files were subjected to the dereplication workflow of GNPS, which was combined with the in-silico MS/MS database-based workflow of the Universal Natural Product Database (ISDB-UNPD) [27]. In addition, MS chromatograms were manually inspected and putative molecular formulae were predicted by MassLynx v. 4.1 (Waters). Putative molecular formulae were searched for known chemical entities in common natural products databases (Dictionary of Natural Products (DNP): http://dnp.chemnetbase.com, MarinLit: http://pubs.rsc.org/marinlit/ and Reaxys: https://www.reaxys.com). Putative hits were validated by biological origin. The detected fragmentation pattern was verified with the in-silico fragmentation tool CFM-ID [56] for putatively identified compounds.

2.4.4. Statistical Analysis

The average yields of population level extracts were statistically compared across the three different sampling locations via one-way ANOVA and a subsequent Tukey's HSD test as described above. For statistical comparison of the metabolite profiles at individual ($n = 10$ per sampling site and tissue) and population extract level ($n = 3$ per sampling site), nMDS plots were compiled (Bray-Curtis similarity index). Peak areas of individual level extracts were normalized by dry weight (Table S3). Significance of observed clusters (location and tissue) was tested with ANOSIM (Bray-Curtis similarity index). Finally, a Mantel test was performed using the R package *vegan* in order to test correlation of individual tunic microbiomes and metabolomes (Bray-Curtis similarity matrices).

3. Results

3.1. Comparative Microbiome Analysis of Tunic and Gut From Invasive and Native C. intestinalis

The microbiome of *C. intestinalis* and seawater reference samples from three locations was explored by amplicon sequencing of the V3-V4 hypervariable region of the bacterial 16S rRNA gene. Sampling was conducted at an invaded (PEI, Canada, C) and two native habitats of *C. intestinalis*, i.e., Helgoland (H) and Kiel (K). From each location, three different sample types (tunic: T, gut: G, seawater samples: W) were analyzed (Table S1). Quality filtering reduced the total number of read pairs from 2443581 to 1292969 (Figure S2). Binning of raw read pairs into OTUs at a similarity level of 97% and subsequent rarefying yielded 5211 OTUs.

Across all samples, considerable proportions of singletons (26.1%) and rare OTUs (99.8% with <1% relative abundance) were detected. According to the distribution of singletons, rarefaction curves indicated sufficient coverage of gut and not yet completely saturated curves

for tunic and seawater samples (Figure S3). Average OTU richness was higher in tunic (413) than in gut (247) samples (ANOVA: df: 2, F: 9.1, $p < 0.001$, Tukey's HSD: $p = 0.0012$; Table S4). Similarly, tunic samples showed higher phylogenetic diversity (20.5) than gut samples (14.7; ANOVA: df: 2, F: 6.1, $p = 0.003$, Tukey's HSD: $p = 0.02$). The Shannon and Simpson diversity indices were similar for both tissues (Shannon: 3.9 (G), 3.7 (T); Simpson: 0.89 (G), 0.88 (T)). Location-wise, all alpha diversity measures were on average highest for Canadian *C. intestinalis* specimens. For instance, the diversity measures were on average higher in the Canadian population (PD: 21.9, Shannon: 4.3, Simpson: 0.93) when comparing to Helgoland (PD: 12.1, Shannon: 3.4, Simpson: 0.90) and Kiel Fjord populations (PD: 18.6, Shannon: 3.7, Simpson: 0.84). One-way ANOVA verified significantly different OTU richness and PD when comparing all samples (ANOVA PD: df: 8, F: 9.3, $p < 0.001$; ANOVA OTU count and Chao1: df: 8, F: 10.0–18.6, $p < 0.001$), but was insignificant for the Shannon and Simpson diversity indices (ANOVA: df: 8, F: 1.3–2.1, $p > 0.05$). The subsequently calculated Tukey's HSD test revealed for some compared groups significant differences, e.g., the number of detected OTUs and the PD was significantly higher in Canadian tunics compared to that of Helgoland ($p < 0.01$), while comparison to Kiel tunics was insignificant ($p > 0.05$; Table S5).

Phylogenetic analysis assigned OTUs to 39 different bacterial phyla. Although differential abundances across the different samples were observed, the phyla Proteobacteria (53.8%), Bacteroidetes (16.6%), Cyanobacteria (8.5%), and Actinobacteria (5.1%) were the most abundant across all sample types (Figure 1). Multivariate ordination showed different clusters matching the nine different sample groups (i.e., three locations and three sample types; Figure 2). Hence, microbiome profiling revealed clustering by both sample type and location (Figure 2 and Figure S4). Ascidian microbiomes from all three sampling sites differed significantly from seawater reference samples (R: 0.73–0.96, $p = 0.001$), but also tunic and gut tissues had different microbiome profiles (R: 0.70, $p = 0.001$; Table S6). ANOSIM also confirmed the observed clustering by sampling site statistically (R: 0.73–0.98, $p = 0.001$). In order to verify the robustness of the beta-diversity results, we applied an additional ordination based on weighted UniFrac distances. In accordance with the nMDS plot based on the Bray-Curtis similarity index, the UniFrac-based ordination plot showed clustering by sample type and sampling location while being less apparent (Figure S5). ANOSIM on weighted UniFrac distances confirmed distinct clustering of the nine sample groups (R: 0.86, $p < 0.001$) and revealed stronger impact of the sample type (R: 0.73, $p < 0.001$) compared to the sampling locations (R: 0.24, $p < 0.001$).
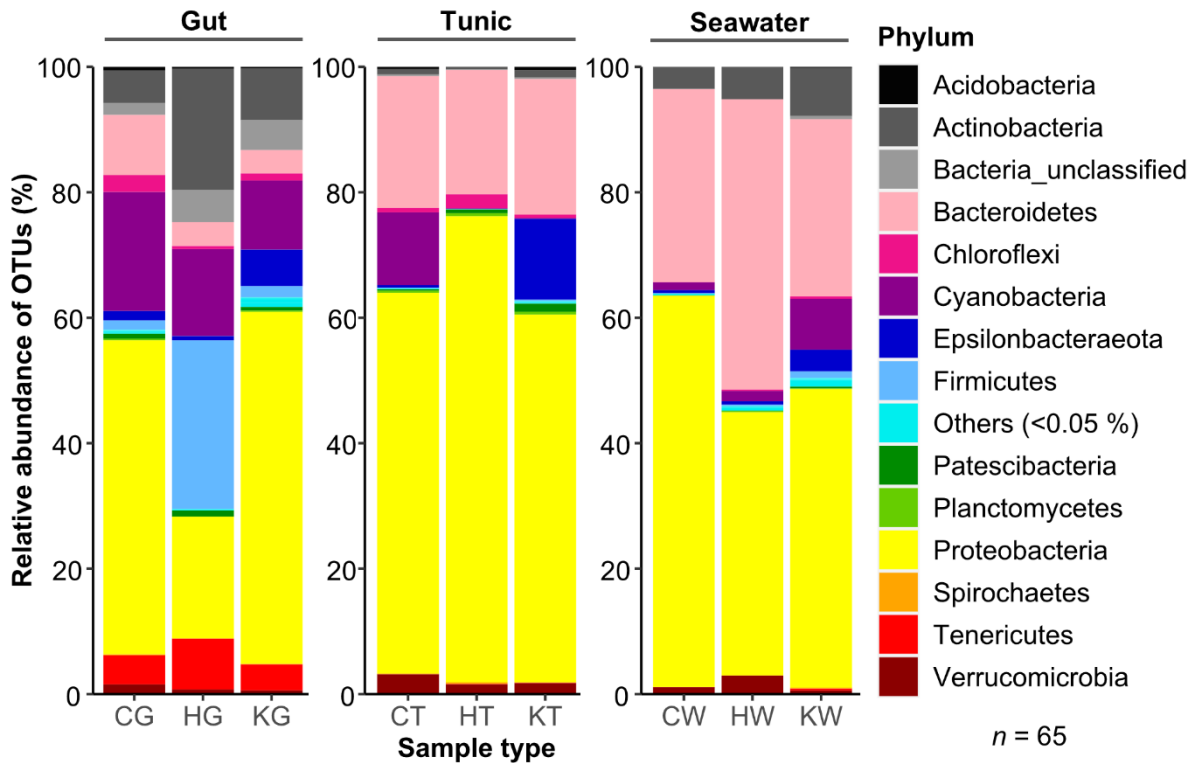
Figure 1. Comparative microbiome analysis of three *C. intestinalis* populations. The taxonomic assignment was conducted with SILVA (release 132) and is shown on the phylum level. Replicates were combined by calculating the median relative abundance for each phylum. Samples were abbreviated with a letter for the respective sampling site (Canada, C; Helgoland, H; Kiel, K) and sample type (gut, G; tunic, T; seawater, W).
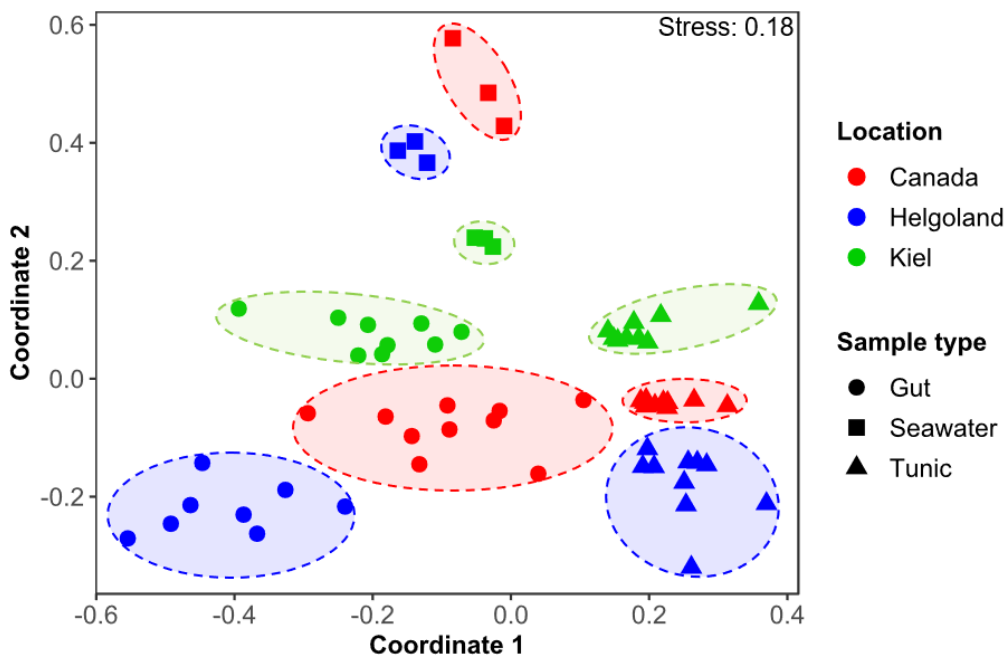
Figure 2. Across sample type and geographic origin comparison of the *C. intestinalis*-associated microbiome. The 2D nMDS plot was calculated using the full set of detected OTUs (5211) and is based on a Bray-Curtis similarity matrix.

In-depth analyses elucidated the main bacterial taxa with significantly differential abundance (Tables S7–S10). Gut microbiomes were dominated by Cyanobacteria,

Proteobacteria, and Firmicutes (the latter only in Helgoland samples; Figure 1, Table S7). Among the most abundant OTUs, four were highly abundant in all gut samples (OTUs 6, 8, 10, 16), and some were specifically prevalent in guts from one sampling location, i.e., OTU4 (K), OTU13 (H) and OTU15 (C; Table S9). Tunic tissues from all three sampling locations were mainly colonized by Proteobacteria (mainly Alphaproteobacteria) and Bacteroidetes (Figure 1, Tables S7 and S8), which matches the dominant OTUs in tunic samples (OTUs 1, 2, 7: Alphaproteobacteria, OTU3: Bacteroidetes; Table 1, Tables S9 and S10). Comparison of the tissue-specific microbiotas showed that the gut was enriched with Actinobacteria, Cyanobacteria, Firmicutes, and Tenericutes, whereas the tunic had a higher abundance of Bacteroidetes, Proteobacteria, and Verrucomicrobia (Table S7). Tissue-specific bacterial associations were corroborated by several OTUs, showing tissue-specificity towards gut (OTUs 6, 8, 10, 16) or tunic (OTUs 1–3, 7), irrespective of the geographical origin (Table 1, Table S9). Finally, OTU2 (unclassified Rhizobiales) and OTU6 (*Synechococcus* sp.) were present in all tunic and gut samples and are hence regarded as core OTUs (Table 1, Table S9 and S10). Notably, among the abundant bacterial OTUs (≥1%) that showed significantly different abundances, six OTUs were previously isolated from the gut (OTUs 7, 10, 16) or tunic (OTUs 1–3) of *C. intestinalis*, which matches with the dominant sample type determined in this study for the abundant OTUs.

With regard to the geographic location, the phylum Epsilonbacteraeota was specifically associated with all Kiel samples (e.g., OTUs 5, 20, 24 assigned to *Arcobacter* sp.), while Helgoland specimens showed a higher proportion of Actinobacteria (e.g., *Bifidobacterium* OTU13) and various Firmicutes (e.g., OTUs 36, 39 47, 50, 68) in their gut (Tables S7–S9). Cyanobacteria (e.g., *Leptolyngbya* sp. OTU14 (*Acrophormium* is the heterotypic synonym of *Leptolyngbya*) and unclassified Oxyphotobacteria OTU80) and Alphaproteobacteria (e.g., *Roseobacter* sp. OTU15, *Ruegeria* sp. OTU106, and unclassified Rhodobacteraceae OTUs 59 and 74) were elevated in tunics or guts from Canadian specimens, respectively. Interestingly, the cyanobacterial genus *Leptolyngbya* (e.g., OTU 14) was only detected in ascidians from PEI, while the actinobacterial genus *Bifidobacterium* was exclusive to guts of ascidians from Helgoland specimens and *Pseudomonas* sp. were only identified in Kiel Fjord samples.

Table 1. Frequent bacterial OTUs (≥1%) with significantly different abundance across nine different sample groups (sample type and sampling location). The predominant sample type and (if applicable) sampling location (in brackets) in this study are indicated for each OTU. OTUs were classified with BLAST down to the lowest possible taxonomic rank and are given with the accession number and isolation source. Relative abundances, statistics, and full BLAST results are given in Tables S9 and S10. Ubc: Uncultured bacterium clone.

OTU	Lowest Classification (BLAST)	Accession Number (BLAST)	Isolation Source According To BLAST	Dominant Sample Type (Location) This Study
OTU1	*Kordiimonas* sp.	KF494349.1	*Ciona intestinalis* (tunic)	Tunic
OTU2	Rhizobiales	MN006421.1	Various, e.g., *Ciona intestinalis* (tunic)	Tunic
OTU3	*Arenibacter* sp.	KF494352.1	*Ciona intestinalis* (tunic)	Tunic
OTU4	*Pseudomonas* sp.	MH244157.1	Sediment	Gut (Kiel)
OTU6	*Synechococcus* sp.	MH358353.1	Marine environment	Gut
OTU7	Uncultured alphaproteobacterium_1-21	FJ659126.1	Ascidian (*Aplidium conicum*; tunic)	Tunic
OTU8	*Synechococcus* sp.	KU867940.1	Seawater	Gut
OTU10	Ubc Woods-Hole_a5143	KF798938.1	*Ciona intestinalis* (gut)	Gut
OTU11	Rhodobacteraceae	KU173743.1	Seawater	Seawater
OTU13	*Bifidobacterium dentium*	LR134349.1	Human	Gut (Helgoland)
OTU15	*Roseobacter* sp.	MK224709.1	Red algae	Gut (Canada)
OTU16	Ubc Woods-Hole_a5449	KF799049.1	*Ciona intestinalis* (gut)	Gut
OTU17	*Litoreibacter* sp.	KJ513684.1	Seawater	Several

Seawater samples from all three sampling sites were dominated by Proteobacteria and Bacteroidetes (Figure 1, Table S7). High abundance of Bacteroidetes contributed to the differences observed with ascidian microbiomes. Moreover, most of the OTUs abundant in the ascidian samples (Table 1 and Table S9) were much less abundant or absent from seawater samples. For example, higher abundances of Cyanobacteria in the Canadian population and of Firmicutes in Helgoland samples were not observed in the seawater references from the same sites (Figure 1, Tables S7–S9).

Consequently, the microbiome of *C. intestinalis* clearly correlates with sampling location (C, H, K) and sample type (G, T, W) and differed from the surrounding seawater.

3.2. Comparative Metabolomics of C. intestinalis Extracts

UPLC-QToF-MS/MS was used to mine the metabolome of organic extracts of the three different *C. intestinalis* populations. Ascidian samples were extracted at (i) population level (pooled samples of 13 g freeze-dried whole ascidian specimens per sampling site and replicate) to examine the ascidians' global chemical profile at different locations and at (ii) individual level for comparing tunic and inner body tissues (see Table S2). Instead of the gut, we extracted the full inner body, since gut tissues did not yield enough extract for metabolomics.

Population extracts from Canadian samples yielded significantly lower quantity of extracts (0.3 g ± 0.01) compared to those from Helgoland (0.4 g ± 0.02) and Kiel Fjord (0.5 g ± 0.01; Figure S6; ANOVA: df: 2, F: 61.73, $p < 0.0001$, Tukey's HSD for all comparisons $p < 0.01$). Manual peak picking yielded 121 abundant metabolites, which were annotated by manual and automated dereplication tools, i.e., DNP, MarinLit, GNPS [26], and ISDB-UNPD [27]. The MN, which contained 44 clusters, further aided the putative annotation and verification of known compounds (Figure 3). This combined approach led to the putative annotation of 41 compounds to known natural products (NPs) or chemical families, which translates into a high annotation rate of 34% (Figure S7, Table S11). Putatively annotated compounds showed a broad chemical diversity, such as alkaloids (**5**, **35**, **41**, **43**, **49**, **53**, **58**, **87**, **89**, **90**, **96**, **103**, **105**, **108**, **117**), lipids (**6**, **12**, **14**, **15**, **25**, **26**, **50**, **59**, **64**, **73**, **79**, **88**, **95**, **101**, **104**, **107**, **111**), peptides (**55**), polyketides (**75**, **100**), and terpenoids (**24**, **56**, **60**, **69**, **99**, **120**). The high abundance of lipids and terpenoids was confirmed by MN, since the three largest clusters were assigned to

lipids and tetrapyrrole-type pigments (Figure 3). The majority of the putatively annotated NPs derived from ascidians or marine invertebrates (58%), but a considerably high portion of metabolites was of microbial origin (32%; Table S11). Nevertheless, two thirds of the detected peaks and many clusters in the MN remained unknown and may represent potentially new compounds.
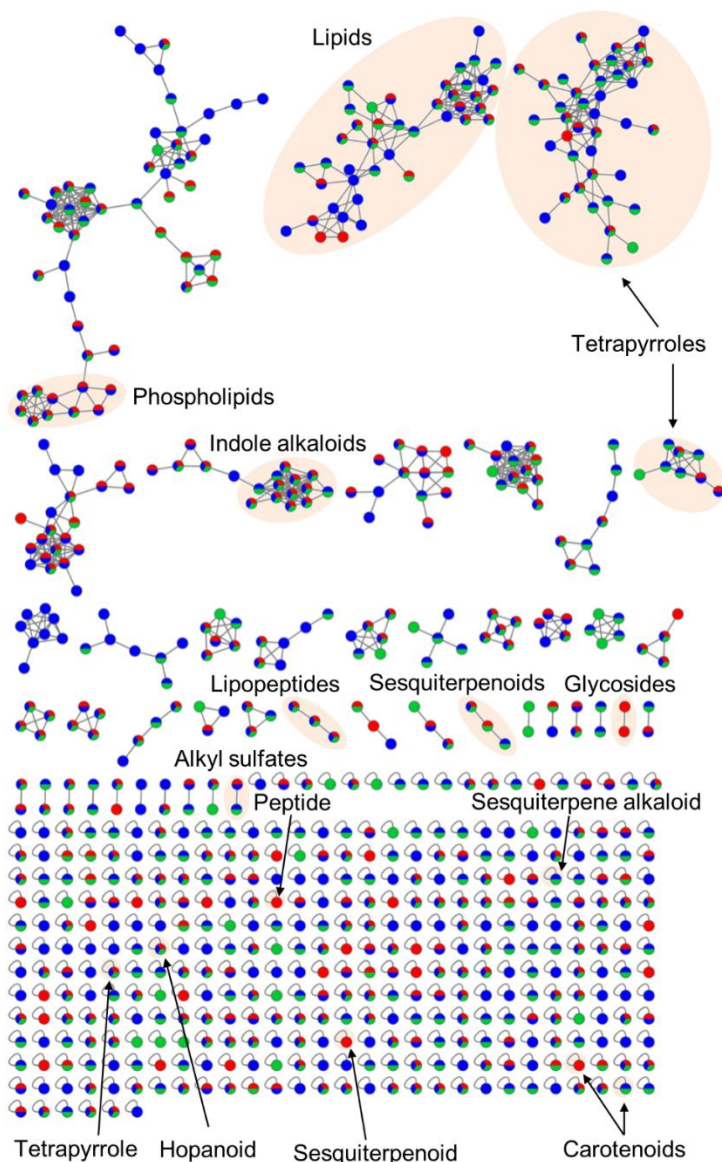
Figure 3. Global molecular network (MN) of three different *C. intestinalis* populations. The MN was constructed via the online platform GNPS [26] by using pre-filtered MS/MS-data of the population level metabolome study. Nodes are color-coded and reflect their sampling site: red: Canada, blue: Helgoland, green: Kiel. Putatively annotated clusters or nodes are highlighted.

With 1156 abundant peaks, the individual inner body and tunic metabolomes also exhibited a high chemical diversity (Figure S8). Several clusters in the MN were predominantly associated with either inner body or tunic and notably, 195 nodes were exclusively detected in tunic tissues, but only 98 in inner body samples. For instance, the tetrapyrrole purpurin 18 (**108**) was only present in the inner body of *C. intestinalis* and two carotenoids (**56**, **99**) were exclusively detected in its tunic (Table S11). Several metabolites were highly abundant in one tissue, e.g., several lipids were more often detected in either inner body (**12**, **14**, **50**) or tunic samples (**64**, **104**). Most of the putatively identified compounds, e.g., unsaturated fatty acids

(**95**, **104**, **111**), indole alkaloids (**43**, **49**, **53**), and polyunsaturated amino alcohols (**12**, **14**, **64**), were detected in both tissues. Comparative metabolome analysis of individual ascidian samples proved tissue-specific metabolite profiles (R: 0.68, p = 0.0001; Figure S9, Table S12). Individuals from one sampling site showed variability and hence, geography-based chemotypes were much less apparent than in the population level analysis, i.e., samples did not cluster clearly with respect to the three sampling locations. Statistical testing confirmed little separation by sampling site (R: 0.23–0.45, p = 0.0025–0.0001; Table S12). Finally, individual tunic metabolite profiles were statistically tested for correlation with the respective individual microbial community compositions. In line with the lesser apparent geography-based clustering of individual metabolomes, no clear correlation was detected (R: 0.26, p = 0.002; Figure S10, Table S12).

Comparison of the metabolomes at population level (pooled whole ascidian samples) showed distinct clustering relating to the three different sampling locations (Figure 4a). However, two replicates (H3, K1) deviated from their respective sample group. The main reason for these two outliers is the detection of a few peaks that were specifically enhanced or unique to these replicates (Table S11). When only core metabolites (i.e., detected in all samples) were compared, samples clearly clustered by their geographic origin (Figure 4b). Statistical comparison confirmed the observed clustering by sampling sites (R: 0.6–1), although ANOSIM results were insignificant (p > 0.05; Table S12).
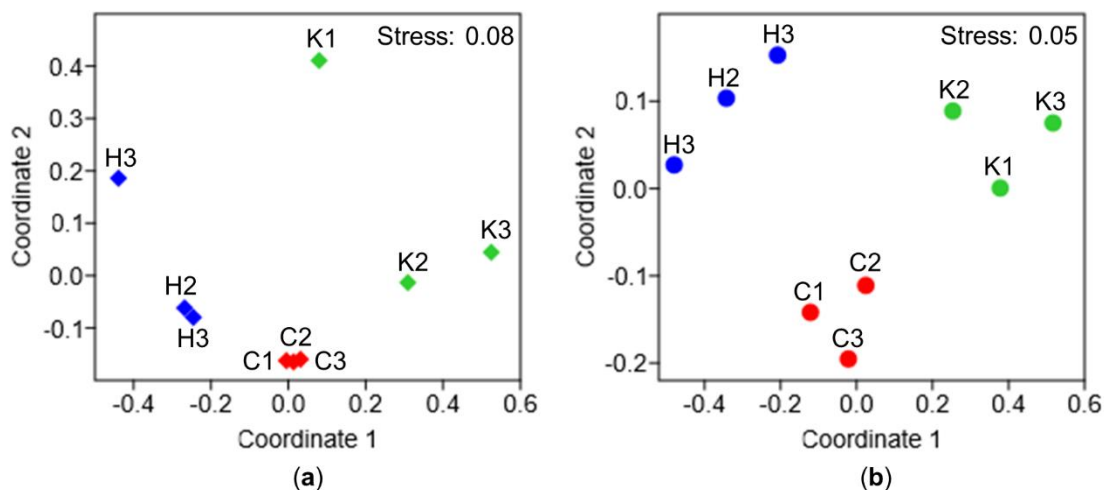
Figure 4. Comparative chemical profiling of geographically distinct *C. intestinalis* populations. Chemical profiling was performed with population level extracts. The 2D nMDS plot was constructed using (**a**) the full set of detected metabolites or (**b**) a restricted dataset containing only core metabolites detected in all samples. Similarity matrices were calculated with the Bray-Curtis similarity index based on the peak area. Sampling locations are color-coded: red: Canada (replicate C1–C3), blue: Helgoland (replicate H1–H3), green: Kiel (replicate K1–K3).

In-depth chemical investigations of *C. intestinalis* from different locations revealed that most compounds (80%) were common to all population level extracts. However, 24 metabolites appeared to be unique to one sampling location while 19 metabolites had higher quantities in one sampling site (Table S11, Figure 5). Canadian and Helgoland samples were chemically the most diverse and contained the highest number of location-specific metabolites. Eighteen metabolites were exclusive and another eleven showed enhanced production (at least 10-fold higher abundance) in Canadian samples compared to extracts of Helgoland and Kiel specimens (Figure 5, Table S11). Only six compounds were exclusive to Helgoland population extracts and none were identified from Kiel samples. Eight compounds showed enhanced production in Helgoland samples, while only two compounds were enhanced in Kiel samples.
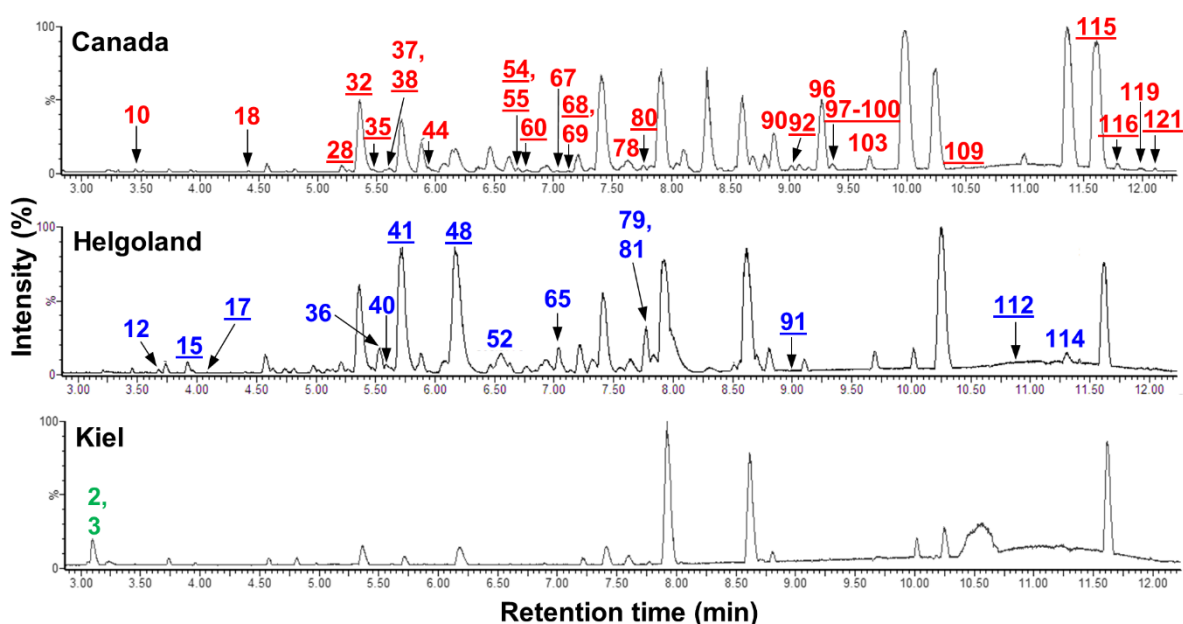
Figure 5. UPLC-MS chromatograms of *C. intestinalis* extracts from different sampling sites. For each sampling site, one representative extract was selected (Canada: C1, Helgoland: H2, Kiel: K2). Metabolites with enhanced or exclusive (underlined numbers) production in one of the three sampling locations are labelled with the respective peak number. Peak annotation is in accordance with Table S11 and annotated peaks were color-coded reflecting their sampling location (red: Canada, blue: Helgoland, green: Kiel).

Of the 29 compounds that showed enhanced or exclusive production in Canadian extracts, nine were putatively identified as the peptide MIP-A3 (**55**), the sesquiterpenoid antibiotic YM 47525 (**60**), and the anthracycline polyketide rubomycin M (**100**), plus six pigments belonging to carotenoid (**69**, **99**) and tetrapyrrole (**35**, **90**, **96**, **103**) classes (Figure 6). Four metabolites specific to Helgoland samples were putatively annotated to the sphingolipids crucigasterin 277 (**12**) and D-erythro-4,8,10-sphingatrienine (**15**), the alkyl sulfate sodium 10-(hydroxymethyl)-2,6,14-trimethylpentadecyl sulfate (**79**), and the chemical family of tetrapyrroles (**41**). The two compounds with enhanced production in *C. intestinalis* from Kiel Fjord could not be linked to any known NP and remain therefore unknown.

The crude extracts were visually different, i.e., the Canadian *C. intestinalis* extracts had a strong green color, whereas Helgoland and Kiel Fjord samples appeared orange (Figure S11). This color difference may (partly) be explained by the presence of four Canada-specific tetrapyrrole-type pigments (**35**, **90**, **96**, **103**; Figures 5 and 6, Table S11).

47
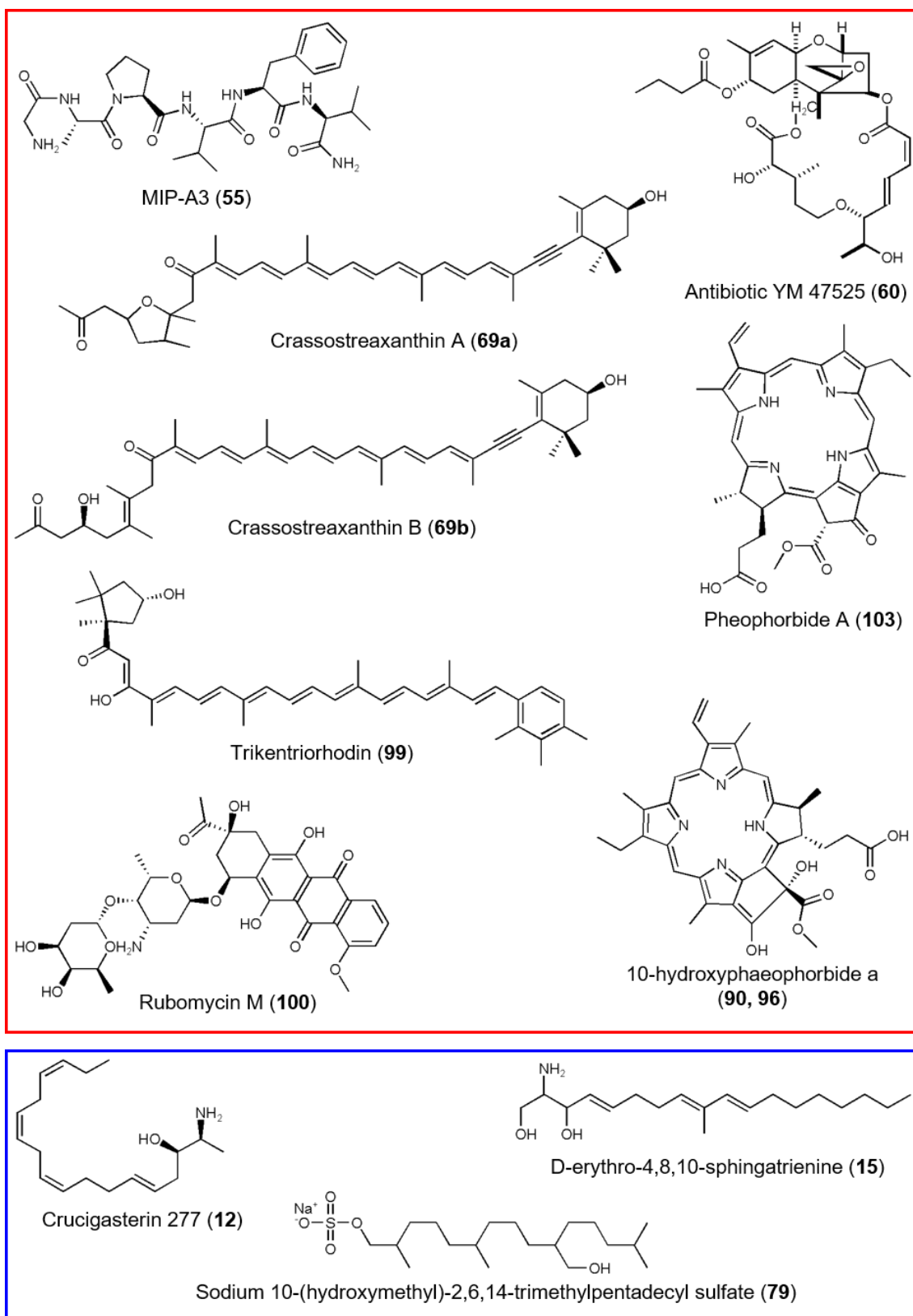
Figure 6. Metabolites with enhanced or exclusive production in *C. intestinalis* specimens from Canada (red) and Helgoland (blue). Peak annotation of putatively identified compounds from Canadian and Helgoland population extracts is in accordance with Table S11.

4. Discussion

In order to gain first insights on potential factors contributing to the invasiveness of *C. intestinalis,* we comparatively profiled the microbiome and metabolome of different tissues of native and invasive specimens. The overall bacterial diversity of the tunic of specimens from all three locations was comparable to that of *C. robusta*, but higher than previously reported for *C. intestinalis* and *C. savignyi* [57,58] (Table S4). Dominance of Alphaproteobacteria and Bacteroidetes in the tunic (Figure 1, Tables S7 and S8) is in line with previous results for *C. intestinalis* from the North Atlantic coast [57]. Additionally, the composition of the ascidian's gut microbiome is largely consistent with a previous study [59], although we found higher abundances of Actinobacteria, Tenericutes, and Verrucomicrobia. Our results showed a higher alpha diversity for specimens from the invasive population (Canada) compared to the native populations from Kiel and Helgoland (Tables S4 and S5). Further studies including several invasive populations are necessary to confirm this finding and shed light into the impact of invasiveness vs. population variation on alpha diversity.

Species-specific microbial assemblages are well-known for ascidians [60–62], including *C. intestinalis* [58]. Accordingly, ascidian microbiomes analyzed in this study differed significantly from the surrounding seawater (Figures 1 and 2, Tables S4, S6–S9). For instance, while some bacterial taxa such as Cyanobacteria (Canada) and Firmicutes (Helgoland guts) were highly abundant in the ascidian microbiome, these taxa showed extremely low abundance in the ambient seawater samples. We detected several abundant ascidian-specific OTUs accounting for 20% of the total sequence reads (OTUs 1–3, 7, 10, 16), which were previously reported for *C. intestinalis* from e.g., the NW Atlantic US-coast [57,59] (Table 1, Table S9 and S10). This corroborates that some abundant bacteria are stably associated with *C. intestinalis* across different geographic scales and seasons [58,59]. We further demonstrated tissue-specific associations of bacteria (Figure 2 and Figure S4, Tables S6–S9), which represents to our knowledge the first comparative study of the gut and tunic microbiome. Location-specific microbial patterns were more prevalent than tissue-specificity contrasting a previous study showing a geographically conserved microbiome of *Ciona* spp. [58]. This may be explained by different sampling strategies; we sampled from different regions (Atlantic Ocean, North and Baltic Seas), while the previous study had comparably low levels of geographic separation (<300 km distance; [58]). Geography-based microbial variation is a well-known phenomenon that was previously described for e.g., the invasive ascidian *Herdmania momus* [61]. Site-specific microbial patterns can be attributed to different environmental conditions, such as salinity, i.e., oceanic (Helgoland, Canada) versus brackish (Kiel), and different levels of anthropogenic input (high: Kiel, Canada; low: offshore-island Helgoland). For example, the high abundance of *Arcobacter* sp. (Epsilonproteobacterium; Tables S8 and S9) in Kiel samples may point to fecal pollution at this location, since *Arcobacter* sp. correlates with fecal pollution but not salinity [63]. Firmicutes dominated the gut of Helgoland ascidians, including *Clostridium* sp. (Figure 1, Tables 1, S7–S9) that is known as a common gut symbiont of marine fish supplying them with e.g., fatty acids [64]. Nevertheless, reasons for this specific association of Firmicutes with the gut of Helgoland *C. intestinalis* remain obscure.

In addition to environmental factors shaping the microbiome of the three different populations, haplotype-diversity of the host may also have impacted the microbial diversity of *C. intestinalis.* A recent study on the microbiome of colonial ascidian *Clavelina oblonga* revealed lower haplotype-diversity in the invasive populations, suggesting that lower genetic diversity correlates with the decreased microbial diversity detected in the invasive specimens [65]. However, the investigation of the impact of genetic diversity on microbial diversity is beyond the scope of the present study.

To investigate the contribution of the microbiome to the overall fitness of *C. intestinalis*, we focused on bacterial taxa conveying potential beneficial effects for *C. intestinalis* (Tables S7–S10). Cyanobacteria, which were abundant in the gut and tunic (only Canadian specimens) of *C. intestinalis*, are known to produce a variety of toxins against e.g., marine

invertebrates and fishes [66]. For instance, cytotoxic and antibacterial compounds were already isolated from *Leptolyngbya* spp. [67,68], a cyanobacterial genus detected only in Canadian *C. intestinalis* samples. The Alphaproteobacteria *Roseobacter* sp. (mainly Canada), *Ruegeria* sp. (mainly Canada and Helgoland), and *Kiloniella* sp. (mainly Helgoland and Kiel) and the Cyanobacterium *Synechococcus* sp. (all sites) are known producers of bioactive compounds such as antimicrobial and antifouling agents [69–72]. Moreover, several bacteria such as *Arcobacter* sp. (mainly Kiel), *Roseobacter* sp. (mainly Canada), and *Ruegeria* sp. (mainly Canada and Helgoland) play a role in nitrogen cycling [65,72] and hence, may thrive in eutrophic habitats such as PEI and Kiel Fjord [60,61]. Additionally, symbiosis with heavy metal resistant bacteria (known from some Alteromonadales and *Vibrio* spp., observed at all three sampling sites) may be beneficial for *C. intestinalis*, especially in marine areas with high anthropogenic activity [60,61]. Specific associations of bacterial taxa with capacity to provide ecologically relevant functions (e.g., chemical defense, heavy metal resistance) may enhance the overall performance of *C. intestinalis*. Further investigations analyzing several invasive populations are needed to verify the role of these microbes, in particular those specific to Canadian ascidians, for the global expansion of *C. intestinalis*.

Previous studies suggested that both symbiont recruitment strategies, vertical and horizontal transmission, play crucial, complementary roles for survival, but also establishment of invasive ascidians in new ecosystems [25,60,61,73]. Vertical symbiont transmission (intergenerational transfer of core microbes) ensures stability of core microbiota and their functions in host health, but is considered to lower the adaptability of the macrobiont [25,61]. Horizontal transmission (active recruitment of beneficial microorganisms from the surrounding seawater) plays an important role for invasive species by enabling rapid acclimation to the new habitat [25,61,74]. In this study, we also observed a combination of location-independent core and site-specific microbial signatures in all three sampled populations, i.e., several abundant OTUs were detected either across broad geographical ranges (in this and previous studies; core microbes) or were exclusive to one sampling site (site-specific microbes). Hence, these results corroborate previous findings indicating a combination of vertical and horizontal symbiont transmission [25,60,61,73].

The integrated metabolomics approach combining automated and manual dereplication tools clearly outperformed classical dereplication techniques [75] by significantly increasing annotation rates (this study: combined 34%, max. 12% for single methods, Table S11). Similar to previous studies on ascidians [62,76], we detected a high abundance of lipids (41%; Figure 3 and Figure S7, Table S11). Alkaloids were also abundant (37%), which was expected since ascidians are prolific producers of alkaloids [77,78]. Being the sister group of vertebrates, ascidians have a rich repertoire of secondary metabolites [78,79] and with 19 putatively annotated molecular families, *C. intestinalis* showed a diverse metabolome. Many putatively annotated metabolites were previously isolated from other marine invertebrates indicating a microbial/microalgal origin, as reported for 10-hydroxyphaeophorbide a (**90**, **96**) [80]. We putatively identified a comparably high share of microbial metabolites (32%), providing support for higher abundance of microbial metabolites in ascidians than previously estimated [78,81]. Furthermore, we detected the bacterial producers (e.g., *Moorea* sp. and *Bacillus* sp.) of several putatively identified compounds (**26**, **43**, **59**, **88**, **117**) in the tunicate microbiome. However, we did not observe a clear correlation between the individual tunic microbiomes and metabolomes (Figure S10), which may be due to multiple drivers, such as diet, age, stress, abiotic environmental parameters, phenotypic plasticity, and inter-individual genetic variations, influencing the microbial community and metabolite production on individual level [82–84].

Remarkable location- and tissue-specific patterns were also observed in the metabolome of individual and population samples (Figures 4 and 5, Figure S9, Tables S11 and S12). Location-specific metabolites are commonly reported, also from ascidians [62]. The individual metabolomes revealed lesser pronounced site-specific signatures possibly due to high inter-individual variability [82,85]. Moreover, the tissue type (inner body vs. tunic) had a significant impact on individual metabolomes. This is in line with a study reporting differential lipid

composition of inner body and tunic extracts of *C. intestinalis* [76]. Notably, the native population from Kiel Fjord showed the lowest chemical diversity. In the brackish Kiel Fjord salinities go down to approximately 12 psu (average salinity 18 psu), which is at the lower tolerance limit of *C. intestinalis* [4]. Salinity can influence the metabolite production of e.g., the clam *Ruditapes philippinarum* [86] and therefore, the comparably low salinity in Kiel Fjord may have contributed to the lower chemical diversity.

Similar to the microbiome, we inspected putatively annotated compounds with regard to their known bioactivities. Several putatively annotated metabolites are reportedly cytotoxic (**43**, **87**, **89**, **103**, **105**) or have antimicrobial activities (**14**, **60**, **87**, **89**, **100**). Notably, while most bioactive compounds were present in all three populations (**14**, **43**, **87**, **89**, **103**, **105**), two metabolites (**60**, **100**) were only detected in the invasive population from Canada. The putatively identified antibiotic YM 47525 (**60)** has been shown to be fungicidal against *Candida albicans* [87], thus may provide *C. intestinalis* with protection against pathogenic fungi. Likewise, the anthracycline polyketide rubomycin M (**100**) that was putatively annotated in the Canadian population is a potent antibiotic [88]. The detected bioactive secondary metabolites may contribute to the chemical defense of *C. intestinalis*, a finding previously reported from various other ascidians [62,83].

Evidence from the terrestrial biosphere suggests that the invasion success of plants is promoted via a richer and more specific chemical repertoire [89,90]. This may also account for *C. intestinalis*, since we observed higher chemical diversity in invasive specimens (Figures 5 and 6, Table S11). Furthermore, we observed significantly lower extract yields with invasive *C. intestinalis* specimens (Figure S6). As outlined above, this phenomenon, a shifted metabolism towards growth and reproduction, is known as the "evolution of increased competitive ability hypothesis" [8], which may be one explanation for the lower quantity of the Canadian ascidian extracts. These two interesting findings require further studies on additional invasive populations to identify the impact of invasiveness, population variation, and environmental variation.

In this study, we simultaneously examined for the first time the metabolome and microbiome of native and invasive specimens of *C. intestinalis*. Both the geographical location and the tissue type (either gut or tunic) significantly impacted the microbial community composition and metabolite profiles of different *C. intestinalis* populations. Stable core OTUs and tissue- or location-specific bacterial taxa and metabolites suggest a high degree of flexibility when adapting to new environmental conditions. While additional sampling is needed to verify the role of microbes and metabolites during invasion, our results give first evidence that invasive *C. intestinalis* contain a richer microbiome and metabolome that may enhance its adaptive capacity in the new environment. Several ascidian-associated microbes have reported bioactivities (e.g., antimicrobial) or other ecologically relevant functions (e.g., nitrogen metabolization, antifouling), potentially contributing to the health and fitness of *C. intestinalis*. Some putatively annotated metabolites may provide beneficial bioactivities (e.g., antimicrobial) supporting the ascidian's chemical defense. Hence, beneficial microbiota and chemical weapons may be relevant factors in addition to other reported characteristics (e.g., broad tolerance of abiotic environmental parameters, fast accumulation of biomass, high fertility) regarding the global expansion of *Ciona* species. Additional studies on several invasive and native populations across broad geographical scales will be necessary to understand the contribution of the microbiota and metabolome to its global invasion success.

Supplementary Materials: The following are available online at http://www.mdpi.com/2076-2607/8/12/2022/s1, Figure S1: Genotyping of *C. intestinalis* with the mitochondrial marker gene COX3-ND1, Figure S2: Influence of the quality filtering steps on the total number of observed read pairs from amplicon sequencing, Figure S3: Rarefaction curves of OTU abundances for *C. intestinalis* and seawater samples, Figure S4: Multivariate ordination plots of the bacterial community associated with *C. intestinalis*, Figure S5: Across sample type and geographic origin comparison of the *C. intestinalis* associated microbiome, Figure S6: Extraction yields of crude extracts from population level extractions, Figure S7: Chemical structures of putatively identified compounds in crude extracts of *C. intestinalis* by

UPLC-MS/MS analysis, Figure S8: Molecular network (MN) of individual *C. intestinalis* metabolomes, Figure S9: Multivariate ordination plots of UPLC-MS profiles of *C. intestinalis* extracts, Figure S10: Statistical correlation of individual tunic microbiomes and metabolomes, Figure S11: Solvent extracts of different *C. intestinalis* samples, Table S1: Metadata for microbiome samples analyzed in this study, Table S2: Metadata for metabolome samples analyzed in this study, Table S3: Parameters of the individual extractions, Table S4: Alpha diversity measures of amplicon sequences, Table S5: Tukey's HSD test comparing observed (OTU count), estimated (Chao1) OTUs, and phylogenetic diversity (PD) detected in ascidian samples at three different sampling sites, Table S6: ANOSIM comparison of amplicon sequencing results, Table S7: Significantly different abundant bacterial phyla, Table S8: Significantly different abundant bacterial classes, families and genera, Table S9: Significantly different abundant OTUs, Table S10: Classification of abundant OTUs detected in this study, Table S11: Putative annotation of metabolites detected in *C. intestinalis* bulk extracts (population level), Table S12: ANOSIM comparison of UPLC-MS/MS profiles of *C. intestinalis* extracts.

Conflicts of Interest: The authors declare no conflict of interest.

References

1. Keane, R.M.; Crawley, M.J. Exotic plant invasions and the enemy release hypothesis. *Trends Ecol. Evol.* **2002**, *17*, 164–170, doi:10.1016/S0169-5347(02)02499-0.
2. Blackburn, T.M.; Bellard, C.; Ricciardi, A. Alien versus native species as drivers of recent extinctions. *Front. Ecol. Environ.* **2019**, *17*, 203–207, doi:10.1002/fee.2020.
3. Simberloff, D.; Martin, J.L.; Genovesi, P.; Maris, V.; Wardle, D.A.; Aronson, J.; Courchamp, F.; Galil, B.; Garcia-Berthou, E.; Pascal, M.; et al. Impacts of biological invasions: What's what and the way forward. *Trends Ecol. Evol.* **2013**, *28*, 58–66, doi:10.1016/j.tree.2012.07.013.
4. Zhan, A.; Briski, E.; Bock, D.G.; Ghabooli, S.; MacIsaac, H.J. Ascidians as models for studying invasion success. *Mar. Biol.* **2015**, *162*, 2449–2470, doi:10.1007/s00227-015-2734-5.
5. Molnar, J.L.; Gamboa, R.L.; Revenga, C.; Spalding, M.D. Assessing the global threat of invasive species to marine biodiversity. *Front. Ecol. Environ.* **2008**, *6*, 485–492, doi:10.1890/070064.
6. Astudillo, J.C.; Leung, K.M.; Bonebrake, T.C. Seasonal heterogeneity provides a niche opportunity for ascidian invasion in subtropical marine communities. *Mar. Environ. Res.* **2016**, *122*, 1–10, doi:10.1016/j.marenvres.2016.09.001.
7. Chan, F.T.; Briski, E. An overview of recent research in marine biological invasions. *Mar. Biol.* **2017**, *164*, 121, doi:10.1007/s00227-017-3155-4.
8. Doorduin, L.J.; Vrieling, K. A review of the phytochemical support for the shifting defence hypothesis. *Phytochem. Rev.* **2011**, *10*, 99–106, doi:10.1007/s11101-010-9195-8.
9. Schwartz, N.; Rohde, S.; Hiromori, S.; Schupp, P.J. Understanding the invasion success of *Sargassum muticum*: Herbivore preferences for native and invasive *Sargassum* spp. *Mar. Biol.* **2016**, *163*, 181, doi:10.1007/s00227-016-2953-4.
10. Callaway, R.M.; Ridenour, W.M. Novel weapons: Invasive success and the evolution of increased competitive ability. *Front. Ecol. Environ.* **2004**, *2*, 436–443, doi:10.1890/1540-9295(2004)002[0436:Nwisat]2.0.Co;2.

11. Svensson, J.R.; Nylund, G.M.; Cervin, G.; Toth, G.B.; Pavia, H.; Callaway, R. Novel chemical weapon of an exotic macroalga inhibits recruitment of native competitors in the invaded range. *J. Ecol.* **2013**, *101*, 140–148, doi:10.1111/1365-2745.12028.

12. Kowalski, K.P.; Bacon, C.; Bickford, W.; Braun, H.; Clay, K.; Leduc-Lapierre, M.; Lillard, E.; McCormick, M.K.; Nelson, E.; Torres, M.; et al. Advancing the science of microbial symbiosis to support invasive species management: A case study on *Phragmites* in the Great Lakes. *Front. Microbiol.* **2015**, *6*, 95, doi:10.3389/fmicb.2015.00095.

13. Vilcinskas, A. Pathogens as biological weapons of invasive species. *PLoS Pathog.* **2015**, *11*, e1004714, doi:10.1371/journal.ppat.1004714.

14. Capinha, C.; Larson, E.R.; Tricarico, E.; Olden, J.D.; Gherardi, F. Effects of climate change, invasive species, and disease on the distribution of native European crayfishes. *Conserv. Biol.* **2013**, *27*, 731–740, doi:10.1111/cobi.12043.

15. Holland, L.Z. Tunicates. *Curr. Biol.* **2016**, *26*, 146–152, doi:10.1016/j.cub.2015.12.024.

16. Carver, C.E.; Mallet, A.L.; Vercaemer, B. Biological synopsis of the solitary tunicate *Ciona intestinalis*. *Can. Man. Rep. Fish. Aquat. Sci.* **2006**, *2746*, 1–55.

17. Rius, M.; Heasman, K.G.; McQuaid, C.D. Long-term coexistence of non-indigenous species in aquaculture facilities. *Mar. Pollut. Bull.* **2011**, *62*, 2395–2403, doi:10.1016/j.marpolbul.2011.08.030.

18. Bouchemousse, S.; Bishop, J.D.; Viard, F. Contrasting global genetic patterns in two biologically similar, widespread and invasive *Ciona* species (Tunicata, Ascidiacea). *Sci. Rep.* **2016**, *6*, 24875, doi:10.1038/srep24875.

19. Blum, J.C.; Chang, A.L.; Liljesthrom, M.; Schenk, M.E.; Steinberg, M.K.; Ruiz, G.M. The non-native solitary ascidian *Ciona intestinalis* (L.) depresses species richness. *J. Exp. Mar. Biol. Ecol.* **2007**, *342*, 5–14, doi:10.1016/j.jembe.2006.10.010.

20. Ramsay, A.; Davidson, J.; Landry, T.; Arsenault, G. Process of invasiveness among exotic tunicates in Prince Edward Island, Canada. *Biol. Invasions* **2008**, *10*, 1311–1316, doi:10.1007/s10530-007-9205-y.

21. Daigle, R.M.; Herbinger, C.M. Ecological interactions between the vase tunicate (*Ciona intestinalis*) and the farmed blue mussel (*Mytilus edulis*) in Nova Scotia, Canada. *Aust. J. Chem.* **2009**, *4*, 177–187, doi:10.3391/ai.2009.4.1.18.

22. Patanasatienkul, T.; Sanchez, J.; Davidson, J.; Revie, C.W. The application of a mathematical model to evaluate the effectiveness of control strategies against *Ciona intestinalis* in mussel production. *Front. Vet. Sci.* **2019**, *6*, 271, doi:10.3389/fvets.2019.00271.

23. Hudson, J.; Johannesson, K.; McQuaid, C.D.; Rius, M. Secondary contacts and genetic admixture shape colonization by an amphiatlantic epibenthic invertebrate. *Evol. Appl.* **2019**, *13*, 600–612, doi:10.1111/eva.12893.

24. Ni, P.; Murphy, K.J.; Wyeth, R.C.; Bishop, C.D.; Li, S.; Zhan, A. Significant population methylation divergence and local environmental influence in an invasive ascidian *Ciona intestinalis* at fine geographical scales. *Mar. Biol.* **2019**, *166*, 143, doi:10.1007/s00227-019-3592-3.

25. Evans, J.S.; Erwin, P.M.; Shenkar, N.; Lopez-Legentil, S. A comparison of prokaryotic symbiont communities in nonnative and native ascidians from reef and harbor habitats. *FEMS Microbiol. Ecol.* **2018**, *94*, fiy139, doi:10.1093/femsec/fiy139.

26. Wang, M.; Carver, J.J.; Phelan, V.V.; Sanchez, L.M.; Garg, N.; Peng, Y.; Nguyen, D.D.; Watrous, J.; Kapono, C.A.; Luzzatto-Knaan, T.; et al. Sharing and community curation of mass spectrometry data with Global Natural Products Social Molecular Networking. *Nat. Biotechnol.* **2016**, *34*, 828–837, doi:10.1038/nbt.3597.

27. Allard, P.M.; Peresse, T.; Bisson, J.; Gindro, K.; Marcourt, L.; Pham, V.C.; Roussi, F.; Litaudon, M.; Wolfender, J.L. Integration of molecular networking and *in-silico* MS/MS fragmentation for natural products dereplication. *Anal. Chem.* **2016**, *88*, 3317–3323, doi:10.1021/acs.analchem.5b04804.

28. Parrot, D.; Blümel, M.; Utermann, C.; Chianese, G.; Krause, S.; Kovalev, A.; Gorb, S.N.; Tasdemir, D. Mapping the surface microbiome and metabolome of brown seaweed *Fucus vesiculosus* by

amplicon sequencing, integrated metabolomics and imaging techniques. *Sci. Rep.* **2019**, *9*, 1061, doi:10.1038/s41598-018-37914-8.

29. Iannelli, F.; Pesole, G.; Sordino, P.; Gissi, C. Mitogenomics reveals two cryptic species in *Ciona intestinalis. Trends Genet.* **2007**, *23*, 419–422, doi:10.1016/j.tig.2007.07.001.

30. Waters, J.M.; Dijkstra, L.H.; Wallis, G.P. Biogeography of a southern hemisphere freshwater fish: How important is marine dispersal? *Mol. Ecol.* **2000**, *9*, 1815–1821, doi:10.1046/j.1365-294x.2000.01082.x.

31. Zhan, A.; Macisaac, H.J.; Cristescu, M.E. Invasion genetics of the *Ciona intestinalis* species complex: From regional endemism to global homogeneity. *Mol. Ecol.* **2010**, *19*, 4678–4694, doi:10.1111/j.1365-294X.2010.04837.x.

32. Hall, T.A. BioEdit: A user-friendly biological sequence alignment editor and analysis program for Windows 95/98/NT. *Nucleic Acids Symp. Ser.* **1999**, *41*, 95–98, doi:10.14601/Phytopathol_Mediterr-14998u1.29.

33. Thompson, J.D.; Higgins, D.G.; Gibson, T.J. Clustal-W: Improving the sensitivity of progressive multiple sequence alignment through sequence weighting, position-specific gap penalties and weight matrix choice. *Nucleic Acids Res.* **1994**, *22*, 4673–4680, doi:10.1093/nar/22.22.4673.

34. Nei, M.; Kumar, S. *Molecular Evolution and Phylogenetics*; Oxford University Press: Oxford, UK, 2000.

35. Kumar, S.; Stecher, G.; Tamura, K. MEGA7: Molecular evolutionary genetics analysis version 7.0 for bigger datasets. *Mol. Biol. Evol.* **2016**, *33*, 1870–1874, doi:10.1093/molbev/msw054.

36. Yu, Y.; Lee, C.; Kim, J.; Hwang, S. Group-specific primer and probe sets to detect methanogenic communities using quantitative real-time polymerase chain reaction. *Biotechnol. Bioeng.* **2005**, *89*, 670–679, doi:10.1002/bit.20347.

37. Martin, M. Cutadapt removes adapter sequences from high-throughput sequencing reads. *EMBnet J.* **2011**, *17*, 10–12, doi:10.14806/ej.17.1.200.

38. Bushnell, B. BBTools Software Package. 2019. Available online: http://sourceforge.net/projects/bbmap (accessed on 30 June 2019).

39. Schloss, P.D.; Westcott, S.L.; Ryabin, T.; Hall, J.R.; Hartmann, M.; Hollister, E.B.; Lesniewski, R.A.; Oakley, B.B.; Parks, D.H.; Robinson, C.J.; et al. Introducing mothur: Open-source, platform-independent, community-supported software for describing and comparing microbial communities. *Appl. Environ. Microbiol.* **2009**, *75*, 7537–7541, doi:10.1128/AEM.01541-09.

40. Kozich, J.J.; Westcott, S.L.; Baxter, N.T.; Highlander, S.K.; Schloss, P.D. Development of a dual-index sequencing strategy and curation pipeline for analyzing amplicon sequence data on the MiSeq Illumina sequencing platform. *Appl. Environ. Microbiol.* **2013**, *79*, 5112–5120, doi:10.1128/AEM.01043-13.

41. Quast, C.; Pruesse, E.; Yilmaz, P.; Gerken, J.; Schweer, T.; Yarza, P.; Peplies, J.; Glockner, F.O. The SILVA ribosomal RNA gene database project: Improved data processing and web-based tools. *Nucleic Acids Res.* **2013**, *41*, 590–596, doi:10.1093/nar/gks1219.

42. Huse, S.M.; Welch, D.M.; Morrison, H.G.; Sogin, M.L. Ironing out the wrinkles in the rare biosphere through improved OTU clustering. *Environ. Microbiol.* **2010**, *12*, 1889–1898, doi:10.1111/j.1462-2920.2010.02193.x.

43. Wang, Q.; Garrity, G.M.; Tiedje, J.M.; Cole, J.R. Naive Bayesian classifier for rapid assignment of rRNA sequences into the new bacterial taxonomy. *Appl. Environ. Microbiol.* **2007**, *73*, 5261–5267, doi:10.1128/AEM.00062-07.

44. Edgar, R.C.; Haas, B.J.; Clemente, J.C.; Quince, C.; Knight, R. UCHIME improves sensitivity and speed of chimera detection. *Bioinformatics* **2011**, *27*, 2194–2200, doi:10.1093/bioinformatics/btr381.

45. R Core Team. *R: A Language and Enviroment for Statistical Computing*; R Foundation for Statistical Computing: Vienna, Austria, 2017.

46. McMurdie, P.J.; Holmes, S. Phyloseq: An R package for reproducible interactive analysis and graphics of microbiome census data. *PLoS ONE* **2013**, *8*, e61217, doi:10.1371/journal.pone.0061217.

47. Oksanen, J.; Blanchet, F.G.; Friendly, M.; Kindt, R.; Legendre, P.; McGlinn, D.; Minchin, P.R.; O'Hara, R.B.; Simpson, G.L.; Solymos, P.; et al. Package vegan v. 2.5-6: Community ecology package. 2019. Available online: https://cran.r-project.org/src/contrib/Archive/vegan/ (accessed on 14 January 2020).

48. Kembel, S.W.; Cowan, P.D.; Helmus, M.R.; Cornwell, W.K.; Morlon, H.; Ackerly, D.D.; Blomberg, S.P.; Webb, C.O. Picante: R tools for integrating phylogenies and ecology. *Bioinformatics* **2010**, *26*, 1463–1464, doi:10.1093/bioinformatics/btq166.

49. Lozupone, C.; Knight, R. UniFrac: A new phylogenetic method for comparing microbial communities. *Appl. Environ. Microbiol.* **2005**, *71*, 8228–8235, doi:10.1128/AEM.71.12.8228-8235.2005.

50. Hammer, Ø.; Harper, D.A.T.; Ryan, P.D. PAST: Paleontological statistics software package for education and data analysis. *Palaeontol. Electron.* **2001**, *4*, 1–9.

51. Dhariwal, A.; Chong, J.; Habib, S.; King, I.L.; Agellon, L.B.; Xia, J. MicrobiomeAnalyst: A web-based tool for comprehensive statistical, visual and meta-analysis of microbiome data. *Nucleic Acids Res.* **2017**, *45*, 180–188, doi:10.1093/nar/gkx295.

52. Benjamini, Y.; Hochberg, Y. Controlling the false discovery rate: A practical and powerful approach to multiple testing. *J. R. Stat. Soc. Ser. B Stat. Methodol.* **1995**, *57*, 289–300, doi:10.1111/j.2517-6161.1995.tb02031.x.

53. Chambers, M.C.; Maclean, B.; Burke, R.; Amodei, D.; Ruderman, D.L.; Neumann, S.; Gatto, L.; Fischer, B.; Pratt, B.; Egertson, J.; et al. A cross-platform toolkit for mass spectrometry and proteomics. *Nat. Biotechnol.* **2012**, *30*, 918–920, doi:10.1038/nbt.2377.

54. Pluskal, T.; Castillo, S.; Villar-Briones, A.; Oresic, M. MZmine 2: Modular framework for processing, visualizing, and analyzing mass spectrometry-based molecular profile data. *BMC Bioinform.* **2010**, *11*, 395, doi:10.1186/1471-2105-11-395.

55. Shannon, P.; Markiel, A.; Ozier, O.; Baliga, N.S.; Wang, J.T.; Ramage, D.; Amin, N.; Schwikowski, B.; Ideker, T. Cytoscape: A software environment for integrated models of biomolecular interaction networks. *Genome Res.* **2003**, *13*, 2498–2504, doi:10.1101/gr.1239303.

56. Allen, F.; Pon, A.; Wilson, M.; Greiner, R.; Wishart, D. CFM-ID: A web server for annotation, spectrum prediction and metabolite identification from tandem mass spectra. *Nucleic Acids Res.* **2014**, *42*, 94–99, doi:10.1093/nar/gku436.

57. Blasiak, L.C.; Zinder, S.H.; Buckley, D.H.; Hill, R.T. Bacterial diversity associated with the tunic of the model chordate *Ciona intestinalis*. *ISME J.* **2014**, *8*, 309–320, doi:10.1038/ismej.2013.156.

58. Cahill, P.L.; Fidler, A.E.; Hopkins, G.A.; Wood, S.A. Geographically conserved microbiomes of four temperate water tunicates. *Environ. Microbiol. Rep.* **2016**, *8*, 470–478, doi:10.1111/1758-2229.12391.

59. Dishaw, L.J.; Flores-Torres, J.; Lax, S.; Gemayel, K.; Leigh, B.; Melillo, D.; Mueller, M.G.; Natale, L.; Zucchetti, I.; De Santis, R.; et al. The gut of geographically disparate *Ciona intestinalis* harbors a core microbiota. *PLoS ONE* **2014**, *9*, e93386, doi:10.1371/journal.pone.0093386.

60. Evans, J.S.; Erwin, P.M.; Shenkar, N.; Lopez-Legentil, S. Introduced ascidians harbor highly diverse and host-specific symbiotic microbial assemblages. *Sci. Rep.* **2017**, *7*, 11033, doi:10.1038/s41598-017-11441-4.

61. Dror, H.; Novak, L.; Evans, J.S.; Lopez-Legentil, S.; Shenkar, N. Core and dynamic microbial communities of two invasive ascidians: Can host-symbiont dynamics plasticity affect invasion capacity? *Microb. Ecol.* **2019**, *78*, 170–184, doi:10.1007/s00248-018-1276-z.

62. Tianero, M.D.; Kwan, J.C.; Wyche, T.P.; Presson, A.P.; Koch, M.; Barrows, L.R.; Bugni, T.S.; Schmidt, E.W. Species specificity of symbiosis and secondary metabolism in ascidians. *ISME J.* **2015**, *9*, 615–628, doi:10.1038/ismej.2014.152.

63. Collado, L.; Inza, I.; Guarro, J.; Figueras, M.J. Presence of *Arcobacter* spp. in environmental waters correlates with high levels of fecal pollution. *Environ. Microbiol.* **2008**, *10*, 1635–1640, doi:10.1111/j.1462-2920.2007.01555.x.

64. Egerton, S.; Culloty, S.; Whooley, J.; Stanton, C.; Ross, R.P. The gut microbiota of marine fish. *Front. Microbiol.* **2018**, *9*, 873, doi:10.3389/fmicb.2018.00873.

65. Goddard-Dwyer, M.; Lopez-Legentil, S.; Erwin, P.M. Microbiome variability across the native and invasive range of the ascidian *Clavelina oblonga*. *Appl. Environ. Microbiol.* **2020**, doi:10.1128/AEM.02233-20.

66. Martins, R.; Fernandez, N.; Beiras, R.; Vasconcelos, V. Toxicity assessment of crude and partially purified extracts of marine *Synechocystis* and *Synechococcus* cyanobacterial strains in marine invertebrates. *Toxicon* **2007**, *50*, 791–799, doi:10.1016/j.toxicon.2007.06.020.

67. Medina, R.A.; Goeger, D.E.; Hills, P.; Mooberry, S.L.; Huang, N.; Romero, L.I.; Ortega-Barria, E.; Gerwick, W.H.; McPhail, K.L. Coibamide A, a potent antiproliferative cyclic depsipeptide from the Panamanian marine cyanobacterium *Leptolyngbya* sp. *J. Am. Chem. Soc.* **2008**, *130*, 6324–6325, doi:10.1021/ja801383f.

68. Choi, H.; Engene, N.; Smith, J.E.; Preskitt, L.B.; Gerwick, W.H. Crossbyanols A−D, toxic brominated polyphenyl ethers from the Hawai'ian bloom-forming cyanobacterium *Leptolyngbya crossbyana*. *J. Nat. Prod.* **2010**, *73*, 517–522, doi:10.1021/np900661g.

69. Brinkhoff, T.; Bach, G.; Heidorn, T.; Liang, L.; Schlingloff, A.; Simon, M. Antibiotic production by a *Roseobacter* clade-affiliated species from the German Wadden Sea and its antagonistic effects on indigenous isolates. *Appl. Environ. Microbiol.* **2004**, *70*, 2560–2565, doi:10.1128/aem.70.4.2560-2565.2003.

70. Wiese, J.; Thiel, V.; Nagel, K.; Staufenberger, T.; Imhoff, J.F. Diversity of antibiotic-active bacteria associated with the brown alga *Laminaria saccharina* from the Baltic Sea. *Mar. Biotechnol.* **2009**, *11*, 287–300, doi:10.1007/s10126-008-9143-4.

71. Brilisauer, K.; Rapp, J.; Rath, P.; Schollhorn, A.; Bleul, L.; Weiss, E.; Stahl, M.; Grond, S.; Forchhammer, K. Cyanobacterial antimetabolite 7-deoxy-sedoheptulose blocks the shikimate pathway to inhibit the growth of prototrophic organisms. *Nat. Commun.* **2019**, *10*, 545, doi:10.1038/s41467-019-08476-8.

72. Pujalte, M.J.; Lucena, T.; Ruvira, M.A.; Arahal, D.R.; Macián, M.C. *The Family Rhodobacteraceae*; Springer: Berlin/Heidelberg, Germany, 2014; pp. 439–512.

73. Casso, M.; Turon, M.; Marco, N.; Pascual, M.; Turon, X. The microbiome of the worldwide invasive ascidian *Didemnum vexillum*. *Front. Mar. Sci.* **2020**, *7*, 201, doi:10.3389/fmars.2020.00201.

74. Rosenberg, E.; Zilber-Rosenberg, I. The hologenome concept of evolution after 10 years. *Microbiome* **2018**, *6*, 78, doi:10.1186/s40168-018-0457-9.

75. da Silva, R.R.; Dorrestein, P.C.; Quinn, R.A. Illuminating the dark matter in metabolomics. *Proc. Natl. Acad. Sci. USA* **2015**, *112*, 12549–12550, doi:10.1073/pnas.1516878112.

76. Zhao, Y.; Wang, M.; Lindstrom, M.E.; Li, J. Fatty acid and lipid profiles with emphasis on n-3 fatty acids and phospholipids from *Ciona intestinalis. Lipids* **2015**, *50*, 1009–1027, doi:10.1007/s11745-015-4049-1.

77. Menna, M. Important classes of bioactive alkaloids from marine ascidians: Structures, isolation and bioactivity. *Curr. Top. Med. Chem.* **2014**, *14*, 207–223, doi:10.2174/1568026613666131213155813.

78. Bauermeister, A.; Branco, P.C.; Furtado, L.C.; Jimenez, P.C.; Costa-Lotufo, L.V.; da Cruz Lotufo, T.M. Tunicates: A model organism to investigate the effects of associated-microbiota on the production of pharmaceuticals. *Drug Discov. Today Dis. Models* **2018**, *28*, 13–20, doi:10.1016/j.ddmod.2019.08.008.

79. Palanisamy, S.K.; Rajendran, N.M.; Marino, A. Natural products diversity of marine ascidians (Tunicates; Ascidiacea) and successful drugs in clinical development. *Nat. Prod. Bioprospect.* **2017**, *7*, 1–111, doi:10.1007/s13659-016-0115-5.

80. Endo, H.; Hosoya, H.; Koyama, T.; Ichioka, M. Isolation of 10-hydroxypheophorbide a as a photosensitizing pigment from alcohol-treated *Chlorella* cells. *Agric. Biol. Chem.* **1982**, *46*, 2183–2193, doi:10.1080/00021369.1982.10865422.

81. Schmidt, E.W.; Donia, M.S. Life in cellulose houses: Symbiotic bacterial biosynthesis of ascidian drugs and drug leads. *Curr. Opin. Biotechnol.* **2010**, *21*, 827–833, doi:10.1016/j.copbio.2010.10.006.

82. Utermann, C.; Parrot, D.; Breusing, C.; Stuckas, H.; Staufenberger, T.; Blümel, M.; Labes, A.; Tasdemir, D. Combined genotyping, microbial diversity and metabolite profiling studies on farmed *Mytilus* spp. from Kiel Fjord. *Sci. Rep.* **2018**, *8*, 7983, doi:10.1038/s41598-018-26177-y.

83. Erwin, P.M.; Carmen Pineda, M.; Webster, N.; Turon, X.; López-Legentil, S. Small core communities and high variability in bacteria associated with the introduced ascidian *Styela plicata*. *Symbiosis* **2012**, *59*, 35–46, doi:10.1007/s13199-012-0204-0.

84. Johnson, C.H.; Patterson, A.D.; Idle, J.R.; Gonzalez, F.J. Xenobiotic metabolomics: Major impact on the metabolome. *Annu. Rev. Pharmacol. Toxicol.* **2012**, *52*, 37–56, doi:10.1146/annurev-pharmtox-010611-134748.

85. Rochfort, S.J.; Ezernieks, V.; Maher, A.D.; Ingram, B.A.; Olsen, L. Mussel metabolomics—Species discrimination and provenance determination. *Food Res. Int.* **2013**, *54*, 1302–1312, doi:10.1016/j.foodres.2013.03.004.

86. Wu, H.; Liu, X.; Zhang, X.; Ji, C.; Zhao, J.; Yu, J. Proteomic and metabolomic responses of clam *Ruditapes philippinarum* to arsenic exposure under different salinities. *Aquat. Toxicol.* **2013**, *136–137*, 91–100, doi:10.1016/j.aquatox.2013.03.020.

87. Sugawara, T.; Tanaka, A.; Nagai, K.; Suzuki, K.; Okada, G. New members of the trichothecene family. *J. Antibiot.* **1997**, *50*, 778–780, doi:10.7164/antibiotics.50.778.

88. Zbarskiĭ, V.B.; Lazhko, E.I.; Pomanova, N.P.; Fomicheva, E.V.; Saburova, T.P. Rubomycins M and N-new anthracycline antibiotics. *Russ. J. Bioorg. Chem.* **1991**, *17*, 1698–1701.

89. Macel, M.; de Vos, R.C.; Jansen, J.J.; van der Putten, W.H.; van Dam, N.M. Novel chemistry of invasive plants: Exotic species have more unique metabolomic profiles than native congeners. *Ecol. Evol.* **2014**, *4*, 2777–2786, doi:10.1002/ece3.1132.

90. Wolf, V.C.; Berger, U.; Gassmann, A.; Müller, C. High chemical diversity of a plant species is accompanied by increased chemical defence in invasive populations. *Biol. Invasions* **2011**, *13*, 2091–2102, doi:10.1007/s10530-011-0028-5.

Publisher's Note: MDPI stays neutral with regard to jurisdictional claims in published maps and institutional affiliations.

Chapter 2

Culture-dependent microbiome of the *Ciona intestinalis* tunic: Isolation, bioactivity profiling and untargeted metabolomics

Utermann, C., Echelmeyer, V.A., Blümel, M., and Tasdemir, D. 2020, *Microorganisms,* 8, 1732; DOI: 10.3390/microorganisms8111732
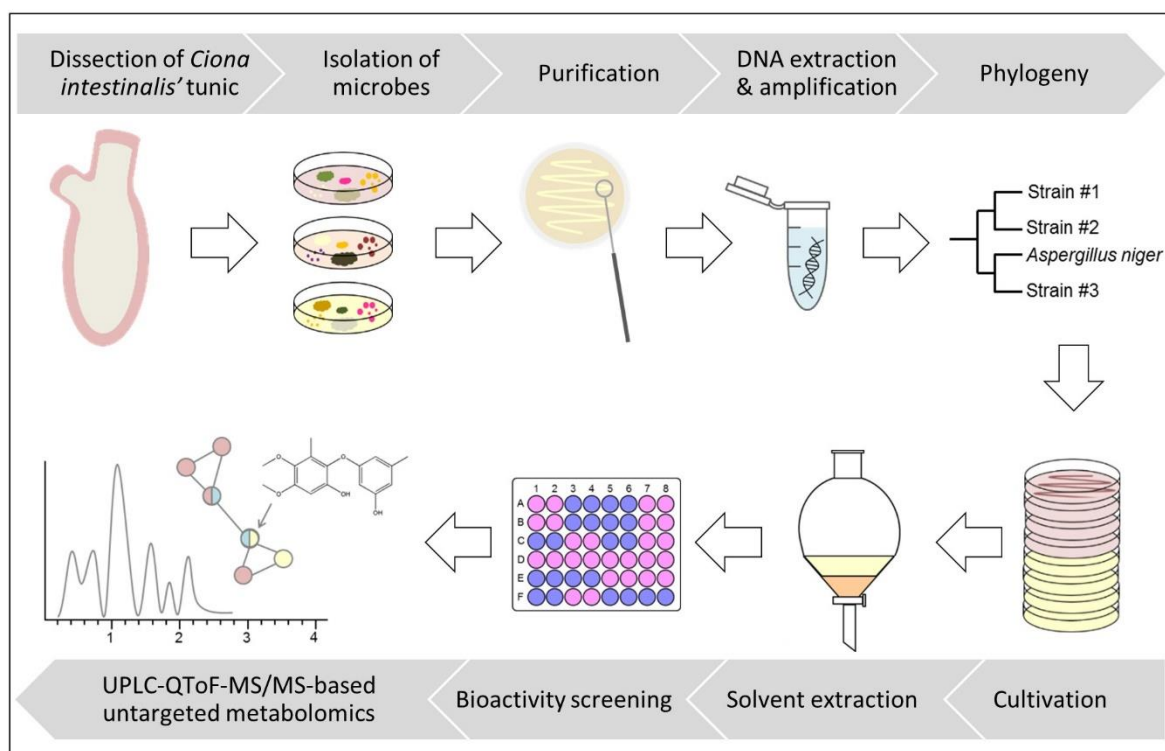
Culture-Dependent Microbiome of the *Ciona intestinalis* Tunic: Isolation, Bioactivity Profiling and Untargeted Metabolomics

Caroline Utermann [1], Vivien A. Echelmeyer [1], Martina Blümel [1] and Deniz Tasdemir [1,2,*]

[1] GEOMAR Centre for Marine Biotechnology (GEOMAR-Biotech), Research Unit Marine Natural Products Chemistry, GEOMAR Helmholtz Centre for Ocean Research Kiel, Am Kiel-Kanal 44, 24106 Kiel, Germany; cutermann@geomar.de (C.U.); vivienechelmeyer@web.de (V.A.E.); mbluemel@geomar.de (M.B.)

[2] Kiel University, Christian-Albrechts-Platz 4, 24118 Kiel, Germany

[*] Correspondence: dtasdemir@geomar.de; Tel.: +49-431-600-4430

Abstract: Ascidians and their associated microbiota are prolific producers of bioactive marine natural products. Recent culture-independent studies have revealed that the tunic of the solitary ascidian *Ciona intestinalis* (sea vase) is colonized by a diverse bacterial community, however, the biotechnological potential of this community has remained largely unexplored. In this study, we aimed at isolating the culturable microbiota associated with the tunic of *C. intestinalis* collected from the North and Baltic Seas, to investigate their antimicrobial and anticancer activities, and to gain first insights into their metabolite repertoire. The tunic of the sea vase was found to harbor a rich microbial community, from which 89 bacterial and 22 fungal strains were isolated. The diversity of the tunic-associated microbiota differed from that of the ambient seawater samples, but also between sampling sites. Fungi were isolated for the first time from the tunic of *Ciona*. The proportion of bioactive extracts was high, since 45% of the microbial extracts inhibited the growth of human pathogenic bacteria, fungi or cancer cell lines. In a subsequent bioactivity- and metabolite profiling-based approach, seven microbial extracts were prioritized for in-depth chemical investigations. Untargeted metabolomics analyses of the selected extracts by a UPLC-MS/MS-based molecular networking approach revealed a vast chemical diversity with compounds assigned to 22 natural product families, plus many metabolites that remained unidentified. This initial study indicates that bacteria and fungi associated with the tunic of *C. intestinalis* represent an untapped source of putatively new marine natural products with pharmacological relevance.

1. Introduction

Marine organisms are highly valuable sources for bioactive natural products (NPs) [1,2] and have yielded about 30,000 compounds so far [3]. With over 1000 described marine natural products (MNPs), ascidians (phylum Chordata, subphylum Tunicata) range among the most prolific producers of MNPs [4–6]. Being soft-bodied, sessile organisms, ascidians rely on chemical defense strategies that involve secondary metabolites for repelling predators, pathogens, and fouling organisms [6–8]. The tunic, the outermost tissue of ascidians, represents the initial defense barrier [9,10]. Similar to other marine living surfaces, the tunic is the site of various chemical communications and of particular interest for discovery of bioactive MNPs [11,12]. Ascidians are holobionts [6,13] that are hosts to a diverse, stable and species-specific microbial community [14,15]. Accordingly, many secondary metabolites originally isolated from ascidians are nowadays believed to be produced by symbiotic microorganisms [4,6,7]. Strikingly, the majority of MNPs derived from ascidian-associated microbes show potent bioactivities, in particular cytotoxicity and antimicrobial activities [6,16]. The most

prominent examples of anticancer MNPs of bacterial origin include the alkaloid trabectedin, the source of the approved anticancer drug Yondelis®, and the cyclic peptide didemnin B that once progressed to phase II clinical trial as anticancer drug candidate [1,16–18]. Trabectedin is produced by the *Ecteinascidia turbinata* symbiont *Candidatus* Endoecteinascidia frumentensis [1,16,17] and didemnin B was suggested to originate from culturable bacteria affiliated to *Tistrella* spp. rather than from its original source, the ascidian *Trididemnum solidum* [16,18]. Moreover, the polyketide arenimycin that inhibits multidrug-resistant *Staphylococcus aureus* [19] is only one out of several antibiotics produced by actinobacteria associated with *E. turbinata* [16,20,21]. Another example is trichodermamide B, an antimicrobial and cytotoxic dipeptide that was isolated from the *Didemnum molle*–associated fungus *Trichoderma virens* [22].

Ciona intestinalis (family Cionidae; formerly *C. intestinalis* type B), also known as sea vase, is a solitary tunicate distributed in the North Atlantic Ocean as well as Baltic, North, Bohai and Yellow Seas [23–25]. The sea vase is one of the most notorious invasive species with cross-continental expansion in the northern hemisphere causing significant ecological and economic problems [23,25,26]. Due to its vertebrate-like larvae, rapid embryogenesis, translucent body, short life cycle, and its fully sequenced genome, it is also a popular model organism for developmental biology [23,27]. Little is known about the chemical inventory of *Ciona* spp. [5], but a few compounds with promising biological activities have been reported, such as the cytotoxic metabolite iodocionin [28] and the antimicrobial peptide Ci-MAM-A24 [29]. Previous culture-independent microbiome studies have demonstrated a broad bacterial diversity associated with the tunic of *Ciona* spp. [9,30], however, only a few reports are available on the isolation of bacterial strains from the tunic of *Ciona* spp. [9,16,31]. Indeed, the gammaproteobacterium *Pseudoalteromonas tunicata* represents the only example of a tunic-associated bacterial isolate from *C. intestinalis* producing metabolites with antibacterial and antifouling activities [31,32].

In order to fill this gap, this study investigated the culture-dependent microbial diversity associated with the tunic of the solitary ascidian *C. intestinalis* and gained first insights into the biotechnological potential of the culturable tunic-associated microbiota. Taking the large adaptive capacity of *C. intestinalis* and its microbiome to a broad range of environmental conditions into account, we selected two collection sites: a location in the North Sea (Helgoland) with marine salinity (~30 psu) and another collection site in the Baltic Sea (Kiel Fjord) characterized as brackish (~18 psu). A culture-dependent approach yielded overall 111 tunic-associated isolates, of which 89 were bacterial and 22 were fungal strains. In addition, microbes were isolated from seawater samples (bacteria: 92 isolates, fungi: 9 isolates), which served as reference for comparison of the microbial diversity of the ascidian's tunic. As ascidian-associated microbes have previously yielded novel metabolites with promising antibiotic and anticancer activities, the organic extracts of tunic-derived strains were tested against a panel of human pathogens (bacteria and fungi) and cancer cell lines. The most bioactive and promising extracts were selected and subjected to an UPLC-MS/MS-based untargeted metabolomics study. The putative annotation of known MNPs was aided by automated dereplication tools such as feature-based molecular networking (FBMN; [33]) and the *in-silico* MS/MS database-based (ISDB) dereplication pipeline [34]. By employing the bioactivity and chemical diversity as main filters, several promising extracts were prioritized for in-depth chemical studies in future.

2. Materials and Methods

2.1. Sampling

Specimens of *C. intestinalis* were sampled in September 2017 in Helgoland (Germany, North Sea; 54.177102, 7.893053) and Kiel Fjord (Germany, Baltic Sea; 54.382062, 10.162059). In Helgoland, samples were collected from below a pontoon by scuba diving (<1 m) and in Kiel from an overgrown mussel-cultivation basket at approximately 3 m depth.

Seawater reference samples were collected aseptically at the same sites. Ascidian and water samples were immediately transported to the local laboratory and processed on the same day.

2.2. Isolation of Microorganisms

To isolate a broad diversity of bacteria and fungi from *C. intestinalis*, we used six different agar media (1.8% agar each). Two of the media were designed to mimic the original habitat of the microorganisms, namely *C. intestinalis* media adjusted to Baltic (CB) or North Sea (CN) salinity. Therefore, *C. intestinalis* was freeze-dried (Alpha 2-4 LSC, Martin Christ Gefriertrocknungsanlagen, Osterode, Germany) at 0.52 mbar and − 80 °C. The freeze-dried material was processed into a semi-coarse powder using a pulverisette (Pulverisette 14, sieve ring p-14, 1 mm pore size, trapezoidal perforation; Fritsch, Idar-Oberstein, Germany). 1.5% of *C. intestinalis* powder was added and the salt concentration was adjusted to the salinity of the Baltic Sea (1.8% Instant Ocean (Blacksburg, VA, USA)) or of the North Sea (3% Instant Ocean).

The other four solid media used were MB (3.74% Marine Broth 2216), PDA (potato dextrose agar) [35], TSB (0.3% trypticase soy broth, 1% sodium chloride) and modified WSP (Wickerham medium) [36]. Ingredients were purchased from AppliChem (Darmstadt, Germany; agar bacteriology grade, sodium chloride), Becton Dickinson (Sparks, MD, USA; Marine Broth 2216, malt extract, trypticase soy broth), Merck (Darmstadt, Germany; D (+)-glucose monohydrate, peptone from soymeal, yeast extract granulated) and Sigma Aldrich (Steinheim, Germany; potato infusion powder). In order to remove planktonic bacteria loosely attached to the tunic, the tunic was thoroughly rinsed with sterile artificial seawater (3% and 1.8% Instant Ocean for Helgoland and Kiel samples, respectively) prior to dissection. Four individuals per sampling site were selected and their tunic was removed using sterilized scissors. Two different strategies, i.e., tissue homogenization and imprinting, were applied for isolation of tunic-associated microbes. For homogenization, the tunic tissue was placed into a sterile 15 mL reaction tube, which was filled to a final ratio of 1:1:1 with glass beads (0.5–2 mm diameter) and sterile artificial seawater ($n = 2$). The mixture was homogenized for 2 min at 2000 rpm on a Vortex mixer (HS120212, Heathrow Scientific, IL, USA). Homogenates (original concentration) and their 1:10 and 1:100 dilutions were plated as 100 µL aliquots onto the different agar media. For imprinting, tunic samples were imprinted on the respective agar plates ($n = 2$). Additionally, 100 µL and 500 µL aliquots of seawater reference samples were plated in duplicate. Inoculated petri dishes were kept for three weeks in the dark at 22 °C. After one week and after three weeks, all plates were evaluated and different colony morphotypes were selected for purification. The selected isolates were transferred to fresh medium until pure cultures were obtained. Purified strains were cryopreserved at − 80 °C until further analyses by using the ready-to-use Microbank™ system (Pro Lab Diagnostics, Richmond Hill, ON, Canada).

2.3. Identification of Bacterial and Fungal Strains

DNA extraction of bacteria and fungi was performed as described previously [37]. A slight modification in the respective protocols was applied by repeating the centrifugation step. When the DNA extraction was not successful, the extraction process was repeated by using the DNeasy Plant Mini Kit (Qiagen, Hilden, Germany). For this, bacterial strains were cultivated for 2 days in liquid MB medium and fungal strains for 5 days in liquid PDA. A 2 mL subsample of the culture was centrifuged for 10 min at 5000 g and the supernatant was discarded. The cell pellet was incubated with 400 µL AP1 buffer, 4 µL RNase A, and 4 µL Proteinase K (20 mg/mL, Analytik Jena, Jena, Germany) for approximately 2 h at 65 °C and rotation at 700 rpm (TMix 220, Analytik Jena). Afterwards, DNA extraction was performed according to the manufacturer's instructions from step 9 onwards. DNA was eluted using 50 µL AE buffer and step 19 was skipped. PCR amplification of bacterial and fungal DNA was realized by using universal primers amplifying the 16S rRNA gene or the ITS1-5.8S-ITS2 region as described

before [37]. Those fungal specimens, for which ITS1-2 sequencing did not allow identification at genus level, were additionally amplified with primers spanning the small (18S) and large (28S) subunit of the rRNA gene [38,39]. The protocol for amplification of the 28S rRNA gene [39] was modified as follows: initial denaturation at 94 °C for 3 min, 35 cycles of denaturation (94 °C, 1 min), annealing (55 °C, 30 s), and elongation (72 °C, 2 min), as well as a final elongation step at 72 °C for 5 min. PCR products were Sanger sequenced [40] at LGC Genomics GmbH (Berlin, Germany). Sequences were trimmed and transformed to FASTA format with ChromasPro V1.33 (Technelysium Pty. Ltd., South Brisbane, Australia). FASTA files were submitted to BLAST (Basic Local Alignment Search Tool, [41]) at NCBI (National Center for Biotechnology Information). Whenever BLAST comparison did not allow identification of bacteria to genus level, FASTA sequences were additionally submitted to the Naive Bayesian rRNA Classifier v2.11 of the Ribosomal Database Project (RDP, [42]). The taxonomical hierarchy was inferred at a 95% confidence threshold with the RDP 16S rRNA training set. DNA sequences of all microbial isolates are available in GenBank under the accession numbers MW012283-371 (tunic-associated bacteria), MW012374-78 (tunic-associated fungi, 18S), MW012380-87 (seawater-derived fungi, ITS), MW013337-428 (seawater-derived bacteria), MW014884-87 (seawater-derived fungi, 18S), MW017476-94 (tunic-associated fungi, ITS), MW017496-97 (tunic-associated fungi, 28S), and MW017498-99 (seawater-derived fungi, 28S).

2.4. Cultivation of Tunic-Associated Microbial Strains

In total, 111 microbial strains were isolated from the tunic of *C. intestinalis*. Safety level determination in accordance with the German safety guidelines TRBA 460 (Technical Rules for Biological Agents, July 2016) and TRBA 466 (August 2015) excluded 19 strains from further analyses. When ≥2 strains belonged to the same species, only one representative strain was selected, leading to the exclusion of another 23 strains. Hence, 69 tunic-associated strains were cultivated on 2 different media: bacteria were grown on glucose-yeast-malt (GYM) [43] and MB media while the fungal isolates were grown on casamino-acids-glucose (CAG) [44] and PDA media. If not stated otherwise, ingredients for CAG and GYM were purchased at Carl Roth (Karlsruhe, Germany). CAG, GYM, and PDA media were selected as culture media, since they proved in previous studies as particularly suitable for production of a variety of novel bioactive compounds (e.g., [35,36,45]). The commonly used MB medium was selected in addition to ensure sufficient growth of all bacterial isolates for chemical investigations. Precultures were inoculated by streaking a bead from the cryo-preservation tube onto the respective solid agar media, which was then grown in the dark at 22 °C until the agar was completely covered by microbial colonies. For main cultures, 5 (fungi) or 10 (bacteria) agar plates per strain were inoculated on each medium in duplicate (i.e., 20 or 40 plates per strain) by gentle streaking with an inoculation loop. For colonies that could not be transferred by an inoculation loop, a small piece of overgrown agar was cut and streaked onto the main culture plates. Main cultures were incubated in the dark at 22 °C for 7 (bacteria) or 21 days (fungi). Notably, 61% of the bacterial strains did not grow on GYM and were hence only cultivated on MB.

2.5. Solvent Extraction

The agar was cut into pieces with a flat spatula and transferred into a glass bottle. Following the addition of ethyl acetate (EtOAc; VWR International, Leuven, Belgium) to fungal (200 mL) and bacterial cultures (400 mL), the mixture was homogenized for 30 s at 13,000 rpm (T25 basic Ultra Turrax IKA-Werke, Staufen, Germany). Homogenization was followed by maceration overnight in the dark at 120 rpm and 22 °C. EtOAc was decanted into a separatory funnel and partitioned against the equal volume of ultra-purified water (Arium Lab water systems, Sartorius, Goettingen, Germany) to remove mainly salts and water-soluble media ingredients. The aqueous phase was discarded and the EtOAc phase was collected in a round

bottom flask. Another 200 or 400 mL EtOAc was added to the agar and after 15 min sonication, a second round of extraction was performed. The EtOAc extracts were combined and evaporated to dryness using a rotary evaporator. Dried extracts were resuspended in 4 mL methanol (MeOH; ULC-MS grade, Biosolve Chimie, Dieuze, France), filtered into pre-weighed vials through a 0.2 µm PTFE filter (VWR International, Darmstadt, Germany) and re-dried under nitrogen blow. Vials were stored at − 20 °C until further processing. Extracts were coded as follows: *C. intestinalis* (C), location (Helgoland = H or Kiel = K), tissue (tunic = T), strain number and medium (CAG, GYM, MB, PDA), e.g., CHT56-CAG refers to the extract of strain 56 isolated from the tunic of *C. intestinalis* sampled in Helgoland cultured on medium CAG. As a control, the four different cultivation media were extracted using the same protocol.

2.6. Bioactivity Screening

Crude extracts were screened for antimicrobial and anticancer activities. For this aim, dried organic crude extracts were re-dissolved in dimethyl sulfoxide (DMSO; Carl Roth) at a concentration of 20 mg/mL. The antimicrobial test panel comprised the pathogenic yeast *Candida albicans* (Ca, DSM 1386), the yeast-like fungus *Cryptococcus neoformans* (Cn, DSM 6973), and the bacterial ESKAPE panel (*Enterococcus faecium*, Efm, DSM 20477; methicillin-resistant *Staphylococcus aureus*, MRSA, DSM 18827; *Klebsiella pneumoniae*, Kp, DSM 30104; *Acinetobacter baumannii*, Ab, DSM 30007; *Pseudomonas aeruginosa*, Psa, DSM 1128; *Escherichia coli*, Ec, DSM 1576). Since none of the tested crude extracts showed inhibition of the Gram-negative pathogens (Kp, Ab, Psa, Ec), only results from bioassays against Gram-positive test strains (MRSA, Efm) are described herein. Anticancer activities were assessed by testing inhibition of proliferation of the following cell lines: A375 (malignant melanoma cell line), A549 (lung carcinoma cell line), HCT116 (colon cancer cell line), and MB231 (human breast cancer line MDA-MB231). Test organisms and cell lines were ordered either at Leibniz Institute DSMZ-German Collection of Microorganisms and Cell Cultures (Braunschweig, Germany) or at CLS-Cell Lines Service (Eppelheim, Germany). All bioassays were performed in 96-well microplates at a final extract concentration of 100 µg/mL, as described previously [46]. The following chemicals were used as positive controls: chloramphenicol (MRSA), ampicillin (Efm), nystatin (Ca), amphotericin (Cn), and doxorubicin (cancer cell lines). The half maximal inhibitory concentration (IC_{50}) was determined as previously described [46] for extracts selected for in-depth metabolomic analyses (for selection see results Section 3.3.).

2.7. UPLC–QToF–MS/MS Analyses

Chemical diversity of the selected bioactive crude extracts was explored via an untargeted UPLC-QToF-MS/MS-based metabolomics approach. ULC-MS grade solvents were purchased from Biosolve Chimie or from LGC Standards (Wesel, Germany). LC-MS/MS analyses were performed on an Acquity UPLC I-Class system coupled to a Xevo G2-XS QToF mass spectrometer (Waters, Milford, MA, USA), equipped with an Acquity UPLC HSS T3 column (High Strength Silica C18, 1.8 µm, 2.1 × 100 mm, Waters) operating at 40 °C. Crude extracts were dissolved in MeOH at a concentration of 1.0 mg/mL and the injection volume was 0.3 µL. A binary mobile phase system (A: 0.1% formic acid in ultra-purified water, B: 0.1% formic acid in acetonitrile) was pumped at a flow rate of 0.6 mL/min by applying a linear gradient (% of A given): initial, 99%; 11.5 min, 1%; 14.5 min, 1%; washing and reconditioning of the column until 16 min. Acquisition of MS and MS/MS spectra was performed as previously described [47], despite the following modifications: spectra were recorded in positive mode and the acquisition range was set to *m/z* 50–1200. The capillary voltage was kept at 3 kV. Solvent (MeOH) and media controls (CAG, GYM, MB, PDA) were analyzed using the same conditions.

2.8. Bioinformatic Processing and Dereplication Workflow

Acquired LC-MS/MS data were converted to the mzXML format using the ProteoWizard tool msconvert 3.0.20010 [48]. The publicly available software MZmine 2 [49] was used to denoise data and for automatic generation of peak lists (for parameters see Table S1). Compounds also detected in MeOH or media blanks were removed from the peak lists. Comparative analysis of the metabolite profiles based on generated peak lists was performed by PCoA plotting (Euclidean distance) in Past v3.12 [50] and sample clustering was statistically tested using ANOSIM (Euclidean distance).

Metabolite profiling led to selection of seven crude extracts for in-depth dereplication (CHT56-CAG, CHT58-PDA, CKT35-PDA, CKT43-GYM and -MB, CKT91-CAG and -PDA; for selection see results Section 3.3.). Pre-processed MS/MS data were exported in MGF format, uploaded to the Global Natural Products Social Molecular Networking (GNPS) online platform [51] and submitted to the FBMN workflow [33]. Consensus spectra were constructed with a parent mass tolerance and a MS/MS fragment ion tolerance of 0.02 Da. Edges of the MN were filtered to have a cosine score >0.7 (CHT58: 0.8) and more than 6 matched peaks. Cytoscape v3.7.1 [52] was used for visualization of the computed FBMN.

For identification of known chemical scaffolds, LC-MS/MS chromatograms were inspected manually and putative molecular formulae were predicted by MassLynx v4.1 (Waters). The obtained molecular formulae were compared against common natural products databases (Dictionary of Natural Products (DNP): http://dnp.chemnetbase.com, MarinLit: http://pubs.rsc.org/marinlit/, The Natural Products Atlas (NP Atlas) [53] and Reaxys: https://www.reaxys.com). In addition, automated dereplication of detected metabolites was realized via the GNPS dereplication workflow and the ISDB dereplication pipeline [34]. Putative hits were validated based on the criteria biological origin, retention time and -if detected- their fragmentation pattern, which was aided by the *in-silico* fragmentation prediction tool CFM-ID [54].

3. Results

3.1. The Culture-Dependent Microbial Diversity of C. intestinalis

In total, 111 bacterial and fungal isolates were obtained from the tunic of *C. intestinalis* and 101 from seawater references sampled at two sites (Figure 1a, Table S2). Bacteria clearly dominated the strain collection (85%). Both tunic and seawater samples collected in the Baltic Sea (Kiel Fjord) yielded a higher number of isolates (tunic: 53 bacteria and 14 fungi; seawater: 63 bacteria and 4 fungi) than the Helgoland samples (tunic: 36 bacteria and 8 fungi, seawater: 29 bacteria and 5 fungi; Figure S1). Application of different isolation media revealed considerable differences with respect to the number of isolates obtained (Figure 1b). Most strains were isolated on WSP (24%) and MB (23%) media, whereas PDA medium yielded the least number of isolates (4%). One third of isolates was derived from the *C. intestinalis* media adjusted to Baltic Sea (CB) and North Sea salinity (CN). Moreover, 19 strains, e.g., the tunic-associated microbes *Kiloniella laminariae* (CKT60, Alphaproteobacteria) and *Pithomyces chartarum* (CKT81, Dothideomycetes*;* Table S2) were only retrieved from the isolation media CB and CN. Hence, the in-house designed *C. intestinalis* media CB and CN proved successful, highlighting the importance of mimicking the environmental conditions for isolation of a diverse microbial community [55,56].
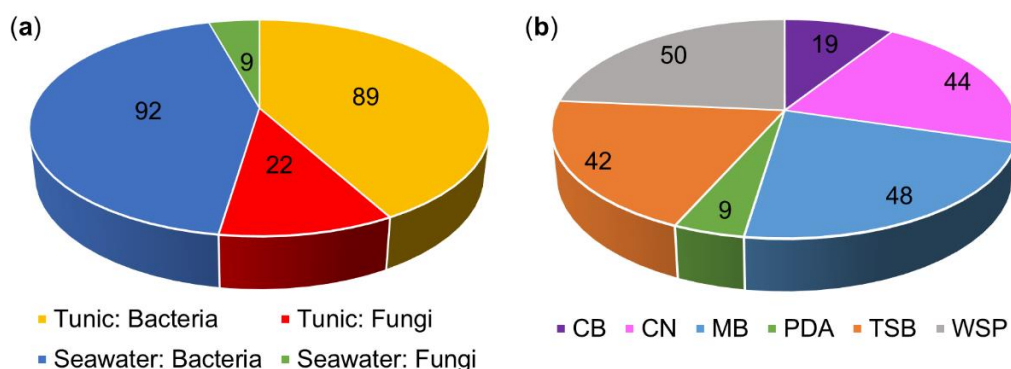
Figure 1. Number of microbial strains isolated from the tunic of *C. intestinalis* and seawater reference. Numbers are given separately for bacteria and fungi from tunic and seawater samples (**a**) and for the six different cultivation media (**b**). CB: *C. intestinalis* medium adjusted to the salinity of the Baltic Sea, CN: *C. intestinalis* medium adjusted to the salinity of the North Sea, MB: marine broth, PDA: potato dextrose agar, TSB: trypticase soy broth and WSP: modified Wickerham medium.

Phylogenetic analyses assigned the tunic- and seawater-derived isolates to six different microbial phyla (bacteria: Actinobacteria, Bacteroidetes, Firmicutes, Proteobacteria; fungi: Ascomycota, Basidiomycota), which can be further split up into 30 orders and 82 genera (Table S2). Seven isolates were identified only to a higher taxonomic rank (family or order level).

Seven bacterial orders (Alteromonadales, Bacillales, Corynebacteriales, Flavobacteriales, Micrococcales, Rhodobacterales, Vibrionales) were detected in all samples (Figure 2a, Figures S2 and S3). Vibrionales was the most abundant order across the four different samples. The tunics of *C. intestinalis* sampled in Kiel showed by far the highest microbial diversity with isolates being affiliated to 22 different microbial orders, of which eight were exclusive to this sample type (bacteria: Burkholderiales, Enterobacterales, Kiloniellales, Xanthomonadales, Streptomycetales; fungi: Glomerellales, Helotiales, Microascales). Tunic samples from Helgoland specimens contained only two exclusive orders, i.e., Caulobacterales and Leotiomycetes *incertae sedis*. Tunic samples from Helgoland and Kiel Fjord yielded a higher microbial diversity than seawater reference samples, where microbial orders exclusive to the tunic (HT = 2, KT = 8, shared = 1) exceeded those exclusive to seawater samples (HW = 1, KW = 2, shared = 1; Figure 2a). The exclusive microbial orders of the ambient seawater samples were affiliated to the fungal orders Chaetosphaeriales (KW), Filobasidiales (HW), Sakaguchiales (KW), and the bacterial order Sphingomonadales (HW and KW; Figures S2 and S3).

At genus level, only little overlap of tunic and seawater samples was observed (Figure 2b), since *Vibrio* was the only microbial genus that was identified in all samples (Figure 3). Tunic isolates showed 41 specific microbial genera (Figure 2b), among them the abundant bacterial genera *Arenibacter* (Flavobacteria; 3 isolates), *Ruegeria* (Alphaproteobacteria; 5 isolates), *Streptomyces* (Actinobacteria; 4 isolates), and the Sordariomycete fungus *Fusarium* sp. (4 isolates; Figure 3). Most bacterial tunic isolates were affiliated to the genera *Bacillus* (9 isolates), *Pseudomonas* (13 isolates; only detected in Kiel samples), and *Vibrio* (19 isolates; Figure 3a). *Vibrio* sp. was the predominant genus in seawater samples (15 isolates) along with the genera *Pseudoalteromonas* (14 isolates) and *Psychrobacter* (6 isolates). Seawater samples yielded also several exclusive bacterial genera, such as *Erythrobacter* (Alphaproteobacteria; 4 isolates), the gammaproteobacterial genera *Pseudoalteromonas* (14 isolates) and *Psychrobacter* (6 isolates) as well as the actinobacterial genus *Rhodococcus* (4 isolates). Fungi were much lesser abundant (22 isolates) in the tunic than bacteria (89 isolates). The isolated tunic-associated fungal community was dominated by *Fusarium* sp. (4 isolates) and *Penicillium* sp. (4 isolates; Figure 3b). Seawater samples yielded only nine fungal

isolates of which five (*Candida* sp., *Cryptococcus* sp., *Dendrophoma* sp., *Purpureocillium* sp., and *Sakaguchia* sp.) were exclusive to the seawater samples.
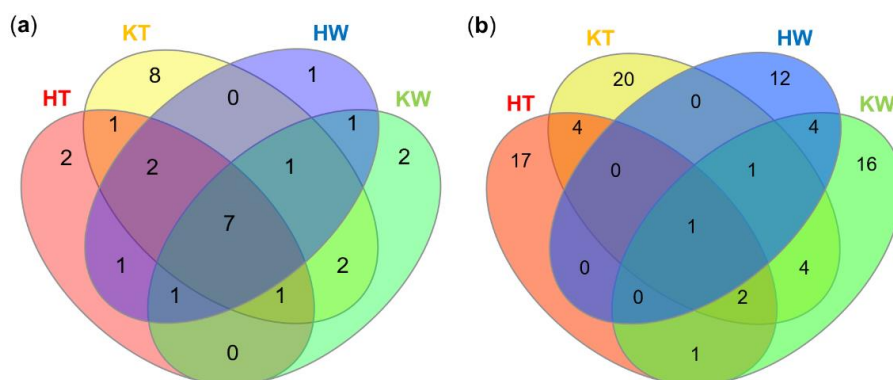
Figure 2. Venn diagrams showing the number of shared and exclusive microbial taxa across sample types and sampling locations. The distribution of taxa is given for microbial orders (**a**) and genera (**b**). H, Helgoland; K, Kiel; T, Tunic; W, Seawater.
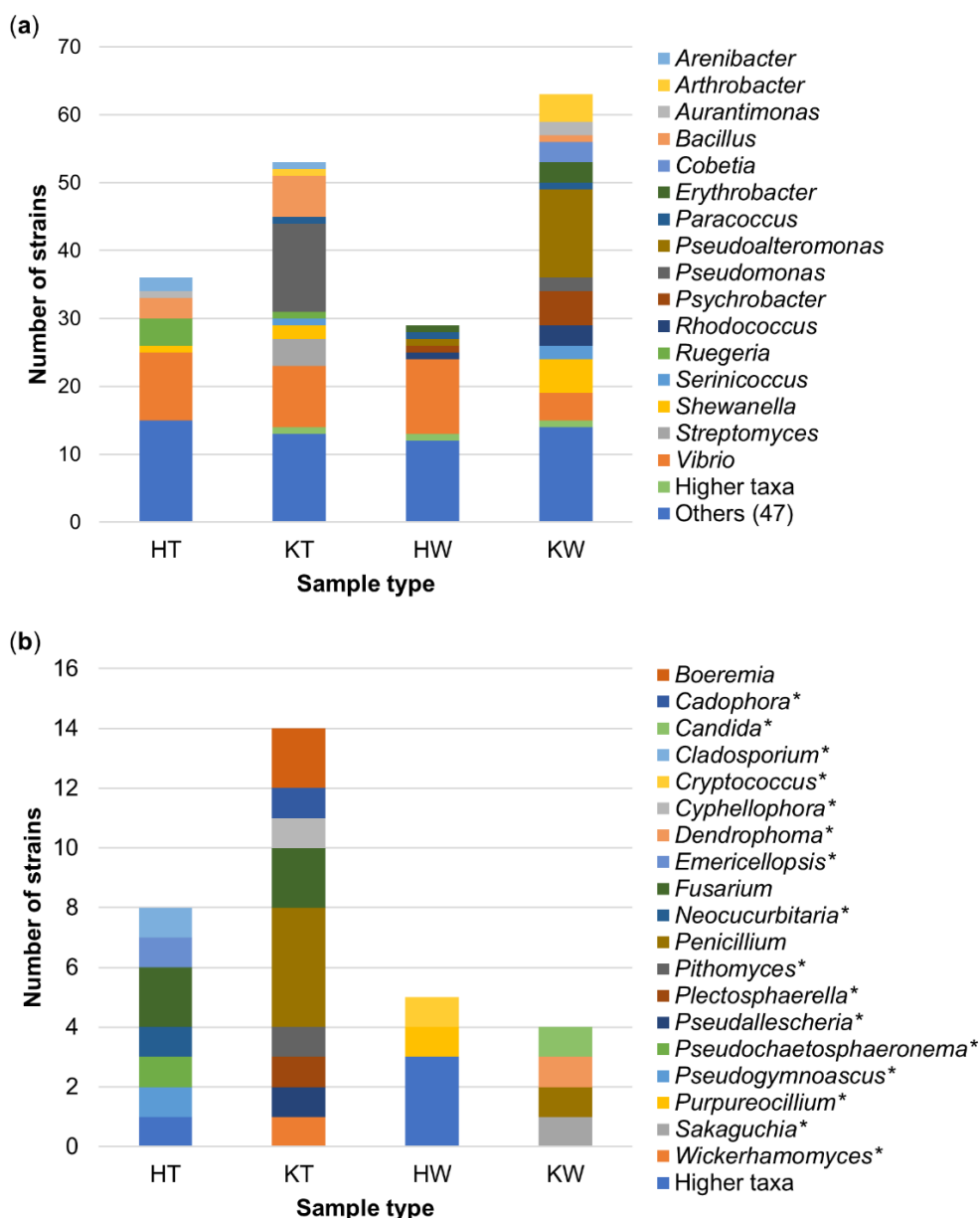
Figure 3. Taxonomic distribution of microorganism genera associated with the tunic of *C. intestinalis* and in seawater samples. Abundances of bacterial (**a**) and fungal (**b**) genera are given. Higher taxa: strain was not identified to a genus but to family or order level. Others: bacterial genera comprising ≤2 strains. * = fungal genera that were exclusive to one sample group. H, Helgoland; K, Kiel; T, Tunic; W, Seawater.

3.2. Anticancer and Antimicrobial Activities of Bacterial and Fungal Extracts

In total, 105 microbial extracts from tunic-derived isolates were screened for their in vitro antimicrobial and anticancer activities. Nearly half of these extracts (45%) exhibited considerable bioactivity (≥80% inhibition at 100 µg/mL test concentration) in at least one bioassay (Table S3). Most of the microbial crude extracts showed antimicrobial activity (44%; Figure 4). None of the tested extracts had an inhibitory effect towards Gram-negative pathogens but many extracts were active against the Gram-positive bacteria methicillin-resistant *S. aureus* (MRSA) (n = 44) and *E. faecium* (n = 29). Of these, only nine extracts inhibited additionally the growth of *C. albicans* (inhibition between 88 and 100% at 100 µg/mL test concentration), i.e., crude extracts of the fungi *Fusarium* sp. (CKT84-CAG and CKT84-PDA), *Penicillium* sp. (CKT35-CAG and CKT35-PDA), *Penicillium brasilianum* (CKT49-PDA),

the crude extract of the *Pithomyces chartarum* (CKT81-CAG and CKT81-PDA), and *Pyrenochaeta* sp. (CHT58-PDA) as well as the extract from the bacterium *Streptomyces* sp. (CKT43-GYM). Antifungal activity against *C. neoformans* was only detected in the *Pyrenochaeta* sp. extract CHT58-PDA and in the extracts of *Streptomyces* sp. strain CKT43 (CKT43-GYM and CKT43-MB; inhibition between 87 and 100% at 100 µg/mL test concentration). Only six extracts inhibited the proliferation of cancer cell lines (inhibition between 81 and 98% at 100 µg/mL test concentration). They belonged to *Boeremia exigua* (CKT91-CAG and CKT91-PDA), *Cadophora luteo-olivacea* (CKT85-CAG), *Emericellopsis maritima* (CHT37-PDA), *Pseudogymnoascus destructans* (CHT56-CAG), and *Streptomyces* sp. (CKT43-GYM). Notably, the fungal extract CHT56-CAG (*P. destructans*) showed selective activity against the breast cancer cell line MB231 (81% inhibition at 100 µg/mL test concentration; other tested cancer cell lines ≤20% inhibition at 100 µg/mL test concentration).
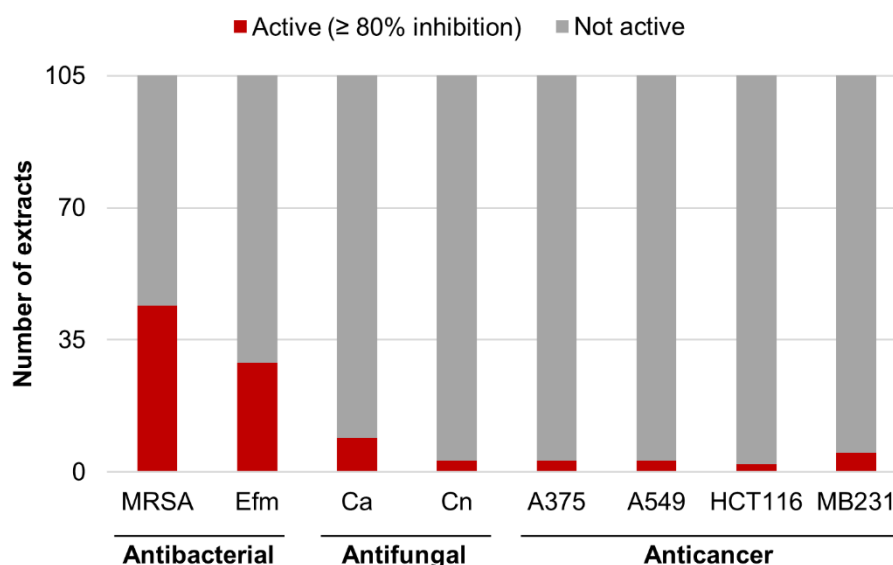
Figure 4. Bioactivities of microbial extracts (*n* = 105). Number of active extracts (≥80% inhibition at 100 µg/mL test concentration) in the categories antibacterial (MRSA: Methicillin-resistant *Staphylococcus aureus*, Efm: *Enterococcus faecium*), antifungal (Ca: *Candida albicans*, Cn: *Cryptococcus neoformans*) or anticancer activity (A375: Malignant melanoma cell line, A549: Lung carcinoma cell line, HCT116: Colon cancer cell line, MB231: Human breast cancer cell line).

3.3. Extract Selection for Metabolomic Analyses and IC$_{50}$ Determinations

Due to the high number of extracts with bioactivity (*n* = 47), further prioritization steps were necessary to select the most promising candidates for in-depth chemical analyses. The first criterion we applied was a high bioactivity threshold (≥80% inhibitory activity at 100 µg/mL) selecting extracts with (1) antimicrobial (combined antibacterial and antifungal) or (2) anticancer or (3) both antimicrobial (antibacterial plus antifungal) and anticancer activity (Table S4). Hence, extracts showing (1) high antibacterial activity against the human pathogens MRSA and *E. faecium* plus high antifungal activity against at least one of the pathogenic yeasts (*C. albicans, C. neoformans*) or (2) high activity against at least one of the cancer cell lines (A375, A549, HCT116, MB231) or (3) a combination of both high antimicrobial and anticancer activity, were selected (Tables S3 and S4). This approach led to the selection of 12 extracts deriving from the fungi *E. maritima* (CHT37-PDA), *P. destructans* (CHT56-CAG), *Pyrenochaeta* sp. (CHT58-PDA), *Penicillium* sp. (CKT35-PDA), *P. brasilianum* (CKT49-PDA), *P. chartarum* (CKT81-CAG and CKT81-PDA), *Fusarium* sp. (CKT84-CAG and CKT84-PDA), *C. luteo-olivacea* (CKT85-CAG), *B. exigua* (CKT91-CAG and CKT91-PDA), and two bacterial extracts from *Streptomyces* sp. (CKT43-GYM and CKT43-MB).

The second criterion for prioritization relied on the chemical distinctiveness of the fungal extracts, which was judged by a comparative LC-MS/MS-based metabolite profiling strategy. UPLC-MS/MS data of the 12 fungal extracts were pre-processed with MZmine 2. The automatically generated peak lists were statistically compared with regard to chemical diversity (number and intensity of peaks, *m/z* value and retention time of detected compounds) resulting in a PCoA plot (Figure 5). Four extracts, deriving from *Pyrenochaeta* sp. strain CHT58 (PDA medium), *Penicillium* sp. strain CKT35 (PDA medium), and the *B. exigua* isolate CKT91 (CAG and PDA media), showed a statistically different clustering from the remaining samples, indicating considerable chemical differences in their metabolomes (Figure 5; R: 0.78, *p*: 0.0001; Table S5). Notably, the crude extract of the fungus *Pyrenochaeta* sp. CHT58 (PDA medium) had the most different metabolome (R: 0.98, *p*: 0.007), reflected by the exceptionally high number of detected peaks (284 peaks, compared to 74–187 peaks in all other extracts; Table S1). These four extracts were prioritized and subjected to in-depth chemical investigations.
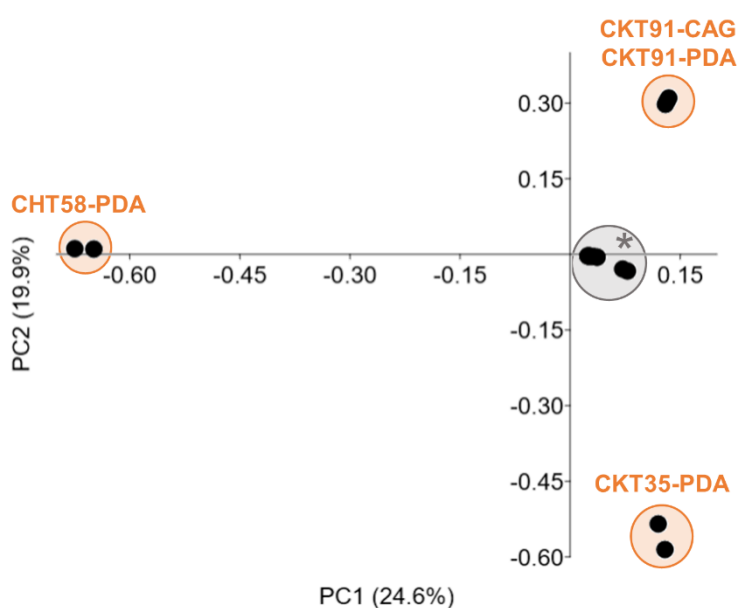
Figure 5. UPLC-MS/MS-based metabolite profiling of 12 pre-selected bioactive tunic-derived fungal extracts. The PCoA plot (Euclidean distance) was calculated using a pre-processed peak list based on UPLC-MS/MS data. *: cluster comprises the following extracts: CHT37-PDA, CHT56-CAG, CKT49-PDA, CKT81-CAG, CKT81-PDA, CKT84-CAG, CKT84-PDA, CKT85-CAG.

Since *Streptomyces* sp. strain CKG43 (GYM and MB media) was the only bacterial extract showing considerable bioactivities (Table S3), it was also selected for in-depth metabolomic analyses. In addition, the extract of the ascomycete-type fungus *P. destructans* CHT56 grown on CAG medium was chosen for chemical analyses due to its selective anticancer activity against breast cancer cell line MB231 (Table S3). In summary, the bioactivity- and chemical diversity-based selection approach led to the prioritization of five fungal and two bacterial extracts for in-depth untargeted metabolomics analyses.

Half maximal inhibitory concentrations (IC$_{50}$) against the tested microbial pathogens and cancer cell lines were determined for all seven prioritized extracts (Table 1). *B. exigua* strain CKT91 grown on media CAG and PDA showed the lowest IC$_{50}$ values against the tested cancer cell lines, e.g., lung cancer cell line A549 was inhibited with IC$_{50}$ values of 4.3 and 5.4 µg/mL. Considerable antimicrobial activity was detected in all extracts (IC$_{50}$ values between 1.4 and 74.8 µg/mL), except for the extract *B. exigua* CKT91-CAG. In particular, the *P. destructans* extract CHT56-CAG and the *Streptomyces* sp. extracts CKT43-GYM and CKT43-

MB showed remarkable activity against MRSA with IC_{50} values between 6.1 µg/mL and 12 µg/mL. Moreover, *Streptomyces* sp. extract CKT43-GYM showed the strongest activity against *E. faecium* with an IC_{50} value of 5.1 µg/mL. The lowest IC_{50} values against the tested pathogenic yeasts *C. albicans* and *C. neoformans* were exhibited by the *Streptomyces* extracts CKT43-GYM and CKT43-MB, respectively, and the fungal extract CHT58-PDA (*Pyrenochaeta* sp.).

Table 1. Antimicrobial and anticancer activities of selected extracts. IC_{50} values are expressed in µg/mL. MRSA: Methicillin-resistant *Staphylococcus aureus*, Efm: *Enterococcus faecium*, Ca: *Candida albicans*, Cn: *Cryptococcus neoformans*, A375: Malignant melanoma, A549: Lung carcinoma, HCT116: Colon cancer, MB231: Breast cancer. Positive controls: Chloramphenicol (MRSA), ampicillin (Efm), nystatin (Ca), amphotericin (Cn), doxorubicin (A375, A549, HCT116, MB231).

Extract Code	Taxonomic Classification	MRSA	Efm	Ca	Cn	A375	A549	HCT116	MB231
CHT56-CAG	*P. destructans*	6.1	16.7	>100	>100	>100	>100	>100	51.2
CHT58-PDA	*Pyrenochaeta* sp.	35.4	17	12	14	>100	>100	>100	>100
CKT35-PDA	*Penicillium* sp.	74.8	38	21	51	>100	>100	>100	>100
CKT91-CAG	*B. exigua*	>100	>100	>100	>100	42.4	4.3	29.8	8.3
CKT91-PDA	*B. exigua*	19.8	67	>100	>100	37.6	5.4	23.0	7.8
CKT43-GYM	*Streptomyces* sp.	12	5.1	7.1	6.8	26.1	31.9	30.9	40.9
CKT43-MB	*Streptomyces* sp.	9.3	20	12	1.4	>100	>100	>100	>100
Positive control		1.2	2.4	7.2	0.1	0.4	16.3	33.1	7.9

3.4. Metabolomic Analyses of Bioactive Tunic-Associated Microbial Strains

The metabolome of the seven prioritized crude extracts of *P. destructans* (CHT56-CAG), *Pyrenochaeta* sp. (CHT58-PDA), *Penicillium* sp. (CKT35-PDA), *Streptomyces* sp. (CKT43-GYM and CKT43-MB), and *B. exigua* (CKT91-CAG and CKT91-PDA) was investigated by state-of-the-art automated dereplication tools (FBMN, ISDB) combined with multiple databases (DNP, MarinLit, NP Atlas, Reaxys). Putative annotations of abundant compounds (i.e., compounds showing distinct peaks in the LC-MS chromatograms above the set minimum peak height) are shown in Supplementary Tables S6–S10 and in Figure S4. The respective annotated FBMNs are depicted in Supplementary Figures S5–S8. The analyzed chemical space of the seven selected microbial extracts comprised in total 22 different chemical families. Overall annotation rates varied between 24% (*Streptomyces* sp. strain CKT43) and 73% (*Penicillium* sp. strain CKT35). This highlights the strength of the dereplication strategy applied herein, as the annotation rates in untargeted metabolomics experiments are approximately 1.8% [57].

The global FBMN of the five selected fungal extracts consisted of 817 nodes, of which 394 fell into 36 clusters containing at least three nodes (Figure 6). Many clusters (70%) were putatively annotated to various NP classes, such as alkaloids (cytochalasans and phenylalanine derivatives), polyketides (benzofuran, hydropyranoindeno, napthoquinone and phthalide derivatives), and terpenoids (di- and meroterpenoids). Most molecular clusters were produced by only one fungal extract, but two clusters, putatively identified as terpenoids, were represented by several nodes from all five fungal extracts.
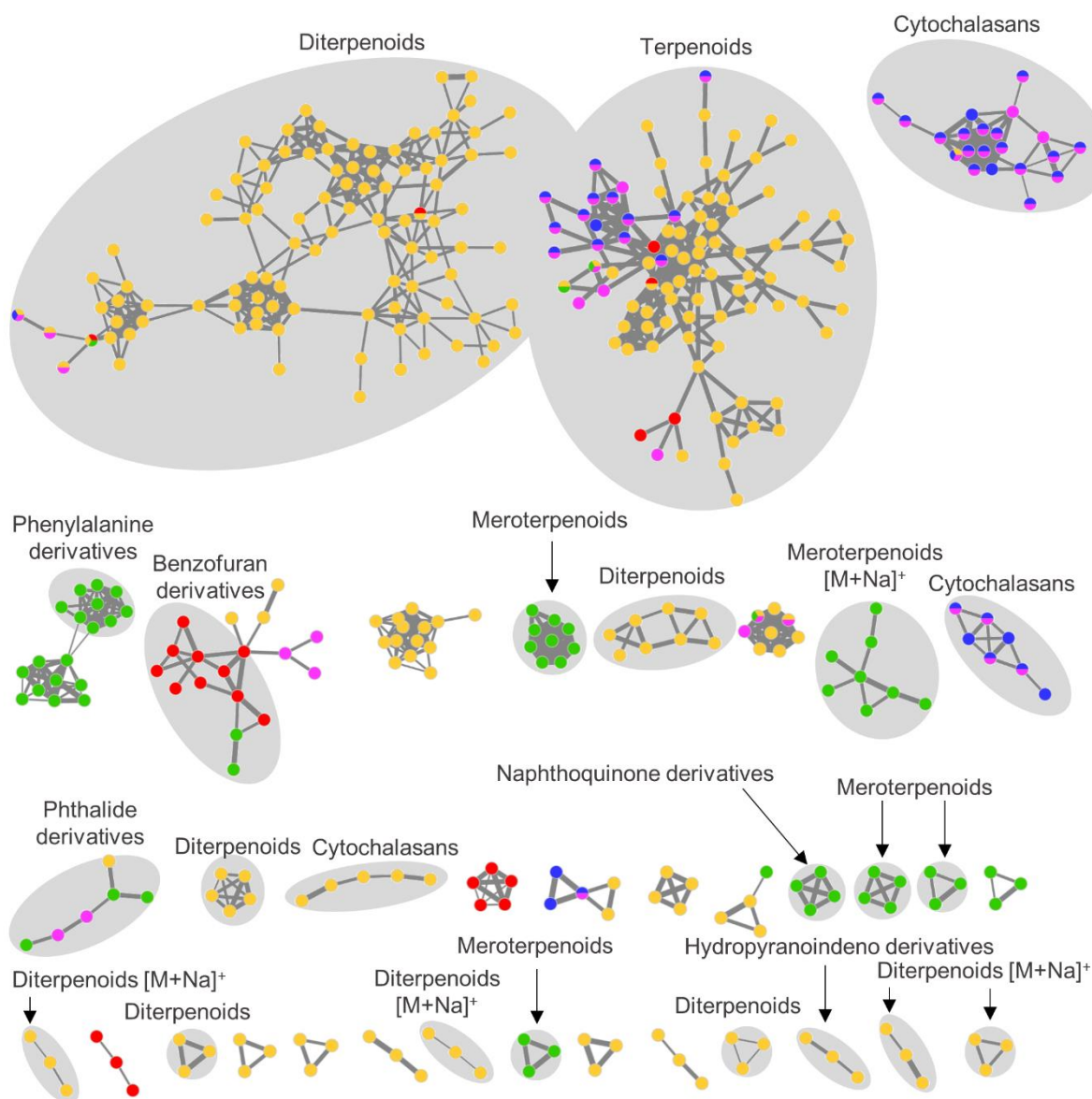
Figure 6. Global FBMN of five bioactive fungal extracts. The FBMN was constructed in Global Natural Products Social Molecular Networking (GNPS) with pre-processed MS/MS data. Molecular clusters containing at least three nodes are displayed and the width of edges corresponds to the respective cosine score. Putatively annotated clusters are highlighted in grey. Fungal extracts are color-coded as follows: red = *P. destructans* extract CHT56-CAG, yellow = *Pyrenochaeta* sp. extract CHT58-PDA, green = *Penicillium* sp. extract CKT35-PDA, blue = *B. exigua* extract CKT91-CAG, pink = CKT91-PDA. Putatively annotated compounds are listed in Tables S6–S9 in the Supplementary Materials.

The *Pyrenochaeta* sp. strain CHT58 (PDA medium) showed an extraordinarily high chemical diversity (284 nodes; Figure 6 and Figure S5, Table S6). Most compounds were putatively identified as diterpenoids, such as the aphidicolins (**5**,**7–10**,**12–14**,**16–18**,**20**,**24**,**27**,**29**,**32**,**34**,**41**,**46**). Furthermore, the macrolide talarodilactone B (**28**), the cytochalasan alkaloid periconiasin I (**23**), a pyrrolizidine alkaloid (**30**) and some polyketides (**2**,**6**,**47**) were putatively annotated. No match to any known compound was found for 18 abundant compounds (**1**,**3**,**4**,**11**,**21**,**22**,**25**,**33**,**35–40**,**43**,**44**,**48**,**49**; Table S6) in any of the databases used, hence they may represent compounds not described in the literature.

The *P. destructans* isolate cultivated on medium CAG (CHT56-CAG) produced compounds of polyketide (**55**,**60–62**) and terpenoid (**56**,**65**,**67**,**70**) origin (Figure 6 and Figure

S6, Table S7). Accordingly, the two largest clusters in the FBMN, which consisted in total of 78 nodes, were putatively assigned to benzofuran-type polyketides and sesquiterpenoids. Dereplicated terpenoids belonged to the chemical families of di-(**70**), mero- (**65**,**67**) and sesquiterpenoids (**56**), isolated from marine-derived fungi from the orders of Eurotiales, Hypocreales, and Pleosporales. Sixteen abundant compounds (**52–54**,**57–59**,**63**,**64**,**66**,**68**,**69**,**71–75**) and two clusters in the MN could not be annotated to any known metabolite and may therefore represent new compounds.

The antimicrobial extract of *Penicillium* sp. (CKT35-PDA) contained a broad chemical diversity with six different putatively identified chemical families (Figure 6 and Figure S7, Table S8). Its FBMN profile was dominated by one large cluster, which contained the benzofuran derivatives penibenzone C (**77**), penicifuran C (**79**), and D (**82**) as well as mycophenolic acid and its methyl ester derivative (**85**, **90**). In addition, the naphthoquinone derivative flaviolin (**76**), the phenylalanine derivative asperphenamate (**96**) and its analog B (**89**), the quinolone alkaloid quinolactacin A (**81**), and several meroterpenoids (**83**,**84**,**86**,**87**,**92**,**93**) were putatively identified from extract CKT35-PDA. However, six abundant compounds (**78**,**88**,**91**,**94**,**95**,**97**) and three molecular clusters in the FBMN could not be annotated to any known NP classes.

The metabolome of the tunic-associated fungus *B. exigua* strain CKT91 (former scientific name: *Phoma exigua*) cultivated on the media CAG and PDA was dominated by the PKS-NRPS hybrid family of cytochalasans (**100–107**,**110**; Figure 6 and Figure S8, Table S9), which were detected in crude extracts from both culture media. The three largest clusters in the FBMN were putatively annotated to this chemical family, which is well known from *Phoma* spp. For instance, deoxaphomin C (**107**) and proxiphomin (**110**) were putatively identified compounds in this family. Moderate to weak antibacterial activity was observed in extract CKT91-PDA and interestingly, this extract contained more specific nodes ($n = 25$) in the FBMN than CKT91-CAG ($n = 16$). Two compounds specific to medium PDA were putatively identified as cytochalasin Z_{11} (**105**) and the ergosterol-type steroid dankasterone B (**109**).

The extracts from *Streptomyces* sp. strain CKT43, CKT43-GYM, and CKT43-MB, showed a diverse metabolome, with 187 nodes in the FBMN and two different NP classes (Figure 7, Table S10). The alkylphenol anaephene A (**141**), the deformylated antimycin derivative A1a (**146**), the butenolide MKN-003A (**123**), and surugamides (**126–129**) were detected in extracts derived from both cultivation media (GYM, MB). The *Streptomyces* sp. crude extract CKT43-MB accounted for the majority of nodes in the FBMN and contained 15 unique compounds (**112**,**116**,**117**,**119**,**122**,**124**,**125**,**130–133**,**135–137**,**145**) whereas the fermentation of this strain on medium GYM yielded only seven unique compounds (**118**,**121**,**134**,**142**,**144**,**147**,**148**; Table S10). Notably, only extract CKT43-GYM showed anticancer activities, but none of its unique compounds was annotated to a known NP. Moreover, several unknown clusters in the FBMN were not assigned to any known compound and remain potentially new.
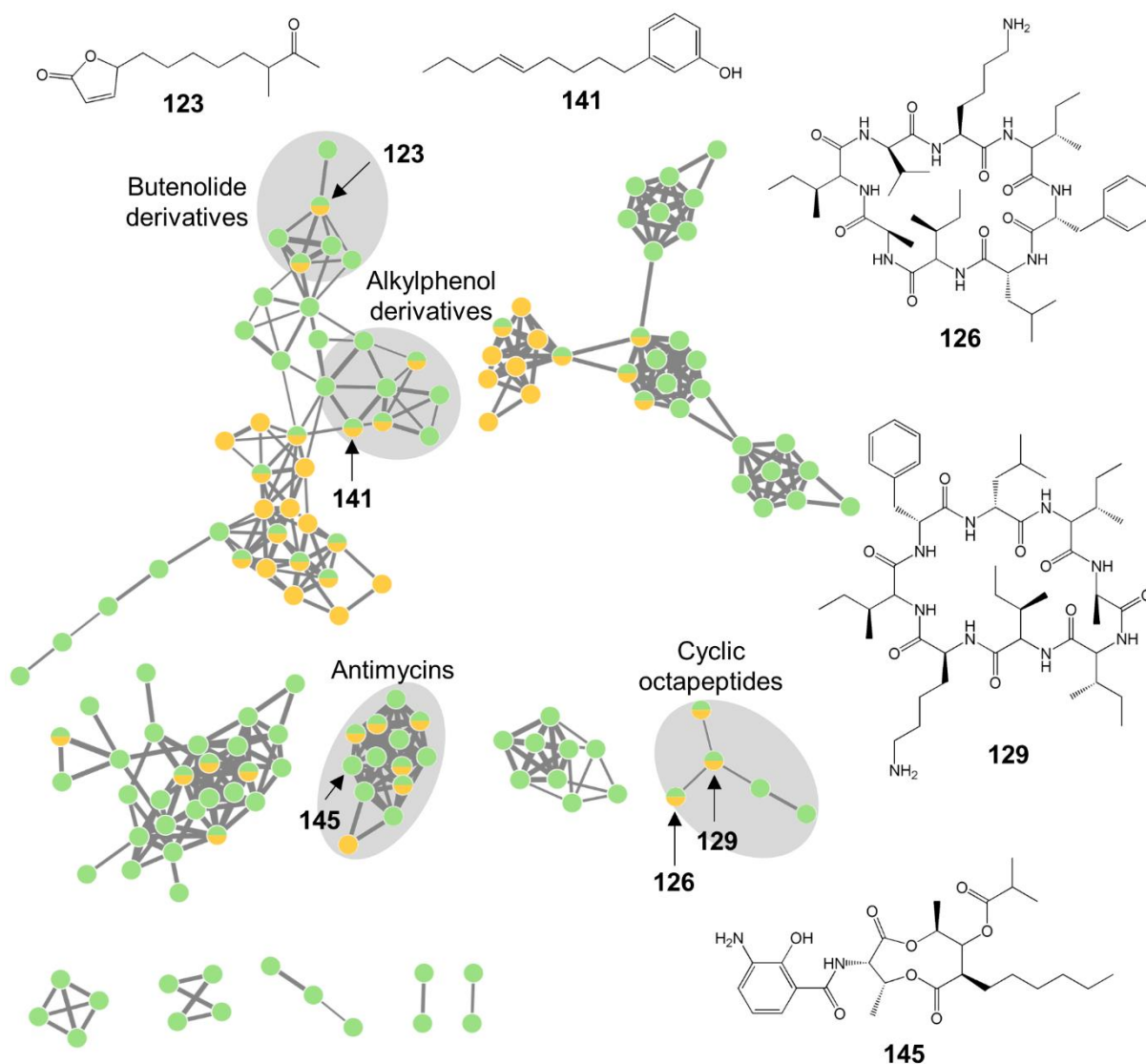
Figure 7. The global metabolome of *Streptomyces* sp. strain CKT43. The annotated global FBMN was constructed in GNPS with pre-processed MS/MS data. Single nodes are not displayed and the width of edges corresponds to the respective cosine score. Putatively annotated clusters are highlighted in grey and putatively identified compounds are annotated in the MN (for identification see Table S10). Nodes are color-coded by the respective cultivation medium: yellow = GYM, green = MB.

In summary, the prioritized extracts derived from diverse microorganisms showed differential and diverse metabolomes. Two to seven chemical families were putatively annotated in the seven extracts from five microbial strains. In particular, *P. destructans* strain CHT56 and *Pyrenochaeta* sp. strain CHT58 promise to be versatile MNPs producing strains, due to the high diversity of putatively annotated chemical families (Tables S6 and S7).

4. Discussion

This study aimed to assess the biotechnological potential of the culturable microbial community associated with the tunic of the solitary ascidian *C. intestinalis.* Therefore, ascidians were sampled at two collection sites with different salinity levels. Isolation efforts yielded 89 bacterial and 22 fungal tunic-associated strains affiliated to 51 microbial genera (Figure 1, Figure 3 and Figure S1, Table S2). As expected [9,30], tunic-derived isolates differed from the surrounding seawater (Figures 1–3, Figures S2 and S3). The comparably higher abundance of tunic-associated Alphaproteobacteria, such as the tunic-specific

Rhodobacteraceae *Ruegeria, Leisingera* and *Litoreibacter*, Flavobacteria (e.g., *Arenibacter*) and Firmicutes (mainly *Bacillus*) is in accordance with reports on the culture-dependent [58,59] or -independent [9,30,60] microbiome of *C. intestinalis* and other ascidian species. In particular, Rhodobacteraceae and the ubiquitous *Bacillus* sp. are common associates of marine invertebrates [60,61]. Notably, several bacterial taxa isolated from the tunic, e.g., *Bacillus* sp., are mobile. Although mobility is not necessary when being associated with the ascidian's tunic, one way of active movement described from *Bacillus* sp. is swarming on solid surfaces as a response to various environmental cues [62,63]. Moreover, it is likely that several tunic-associated bacteria were recruited from the seawater [60,64], where flagella enable their movement in the water column [62,63]. Tunic- and seawater-derived isolates also differed between the sampling sites. This finding can be attributed to the different environmental conditions of the Baltic and North Sea, as Kiel Fjord in the Baltic is characterized by brackish water (~18 psu), whereas seawater around Helgoland island (which is in ca. 50 km distance to mainland Germany) in the North Sea has oceanic salinity (~30 psu). The high abundance of some bacterial genera such as *Pseudomonas* in Baltic samples may be attributed to the lower salt tolerance described for some strains affiliated to these genera (e.g., [65]). In addition, the higher microbial diversity of Kiel Fjord samples may be attributed to the fact that Kiel Fjord is an area with high anthropogenic impact featuring several harbors, the highly frequented Kiel Canal (ship traffic) and industry, while Helgoland is an offshore island with substantially lower anthropogenic input. Despite the observed differences between the sampling sites and sample types, culture-dependent studies usually capture only 0.001–1% of the actual microbial diversity of a habitat, a phenomenon well-known as the "great plate count anomaly" [66,67]. Moreover, isolation of microorganisms is usually biased towards easily culturable, fast growing microorganisms and therefore, does not necessarily reflect the complete microbial diversity of the explored environmental sample [66,67]. Out of 37 bacterial genera isolated from the tunic of *C. intestinalis*, only *Arenibacter* and *Kiloniella* were previously isolated from the same source [9]. Previous culture-independent studies [9,30] on the bacterial diversity of the tunic of *C. intestinalis* identified sequences affiliated to the four bacterial phyla that were also detected in this study (Actinobacteria, Bacteroidetes, Firmicutes, Proteobacteria). Although fungi were reported from other ascidians [68], we provide here the first evidence for fungi associated with the tunic of *C. intestinalis*. In combination, these results indicate that *C. intestinalis* hosts a diverse and specific culture-dependent microbiota associated with its tunic. This is in line with previous results presenting a further evidence that ascidians are a rich source of microorganisms [6,16,68].

The in vitro screening effort performed in this study revealed a high number of bioactive crude extracts (45%), pointing out the exceptional potential of the tunic-associated microbiota of *C. intestinalis* for pharmaceutical applications (Figure 4, Table S3,). Most of the active extracts inhibited the Gram-positive pathogens MRSA (94%) and *E. faecium* (62%), but only few showed anticancer activity (13%). This contrasts with a recent review that analyzed bioactive ascidian-derived microbial compounds that showed higher rates of cytotoxicity (47%) than antimicrobial activity (31%) [16]. However, the vast potential of marine-derived microorganisms for discovery of novel antibiotics from ascidians and other marine invertebrates is known [69–71]. The fact that pathogenic Gram-negative bacteria were not inhibited by any of our tunic-associated microorganisms is in line with their general lesser susceptibility towards antibiotics due to their additional outer membrane [70,72].

The only microorganism isolated from the tunic of European *C. intestinalis* so far, *Pseudoalteromonas tunicata*, shows a variety of bioactivities such as antibacterial and larval toxicity preventing micro- and macrofouling on the ascidian's tunic [32,73]. For *C. intestinalis,* the allocation of defensive compounds on the tunic is crucial, since the tunic lacks other physical defense strategies, such as spicules or accumulation of acid or vanadium [74,75]. Although potential chemical defense functions of the screened tunic-associated microbiota cannot be clarified within the scope of this study, the high number of bioactive extracts

detected in this study is in line with numerous reports of ascidian-derived microorganisms producing novel MNPs with various pharmaceutical properties [1,6,16].

In order to prioritize the most promising extracts for in-depth metabolomic analyses out of the 47 bioactive extracts in total, two selection criteria were applied, i) an 80% bioactivity threshold (at 100 µg/mL test concentration) for anticancer or antimicrobial (antibacterial and antifungal) activity, and ii) chemical distinctiveness based on a statistical comparison of metabolite profiles. Application of these selection criteria resulted in the prioritization of four extracts derived from three tunic-associated fungal strains (*Pyrenochaeta* sp. extract CHT58-PDA, *Penicillium* sp. extract CKT35-PDA, *B. exigua* extracts CKT91-CAG and -PDA), and two extracts from a *Streptomyces* sp. bacterium (CKT43-GYM and -MB). Additionally, one fungal extract (*P. destructans* extract CHT56-CAG) was selected for further chemical investigations because of its selective anticancer activity.

The fungal genera *Pseudogymnoascus* and *Pyrenochaeta* are relatively rare in marine habitats but were previously isolated from a few marine invertebrates [76,77]. Diterpenoids dominated the metabolome of the crude extract of *Pyrenochaeta* sp. (CHT58-PDA) with two big molecular clusters in the FBMN (Figure S5, Table S6). Diterpenoids frequently form sodium adducts during ionization (e.g., [78]) explaining the appearance of a large cluster of sodiated diterpenoids in the network (Figure S5). These diterpenoids were previously reported from other members of the fungal class Dothideomycetes (*Pyrenochaeta* is affiliated to this class) but also from various other fungal taxa (Eurotiomycetes, Leotiomycetes, Sordariomycetes) underlining their ubiquitous distribution in terrestrial and marine fungi [79]. Surprisingly, the PDA extract of the underexplored *Pyrenochaeta* sp. showed by far the most diverse metabolome (Figure 6 and Figure S5, Tables S1 and S7) reflected by the highest number of detected metabolites. None of the putatively annotated compounds in this extract has reported activities against *C. albicans* or *C. neoformans*, although the extract showed strong antifungal activity (Table 1). This may suggest that one or several of the putatively novel metabolites (**1,3,4,11,21,22,25,33,35–40,43,44,48,49**; Table S6) are responsible for the detected antifungal activity. The moderate antibacterial activity of this extract may be due to the putatively identified anthraquinone derivative 10-deoxybostrycin (**6**) as well as the pyrrolizidine alkaloid CJ-16,264 (**30**), both of which have been reported to display antibacterial activities against *S. aureus* [20,80].

Among the putatively identified compounds detected in the CAG extract of *P. destructans* strain CHT56, the polyketides phialofurone (**60**) and 3,4-dihydro-6-methoxy-8-hydroxy-3,4,5-trimethyl-isocoumarin-7-carboxylic acid methyl ester (**61**) and the diterpenoid (9ξ,13α)-6,9-dihydroxypimara-5,8(14),15-trien-7-one (**70**) are reportedly cytotoxic against several human cancer cell lines [81–83]. Hence, these putatively identified compounds may be responsible for the detected moderate anticancer activity, which is being observed for the first time in a *Pseudogymnoascus* sp. extract. However, none of the putatively identified compounds of the CHT56-CGA extract is known for activity against MRSA, *E. faecium* or the cancer cell line MB231.

The largely unexplored fungal strains CHT56 (*P. destructans*) and CHT58 (*Pyrenochaeta* sp.) thus emerge as a promising source for the discovery of (novel) bioactive MNPs. Observed antibacterial or antifungal activities of extracts from both strains were not explained by the putatively identified compounds. Finally, both extracts contained several compounds and molecular clusters that could not be linked to any known compounds neither by automated nor manual dereplication using multiple pipelines and databases. These extracts deserve attention in future chemical isolation studies, as the unidentified metabolites may represent new bioactive MNPs.

The remaining five selected bioactive extracts were derived from strains affiliated to extensively studied microbial taxa, *B. exigua* (formerly *P. exigua*, strain CKT91), *Penicillium* (strain CKT35) and *Streptomyces* (strain CKT43), all of which are prolific producers of MNPs [79,84–86] with hundreds (*Phoma*: 378) to thousands of described NPs (*Penicillium*: 2634, *Streptomyces*: 8769; number of isolated NPs retrieved from DNP on 04.09.2020). *Penicillium,*

Phoma (former taxonomic classification of strain CKT91, *B. exigua*) and *Streptomyces* spp. are facultative marine microorganisms frequently isolated from various marine environments [16,85,87], including Kiel Fjord habitats [88,89].

Penicillium is among the best studied and richest fungal genera with enormous metabolic capacity to produce diverse types of pharmaceutically relevant metabolites with antibiotic, anticancer and anti-inflammatory activities (e.g., [90,91]). Interestingly, the selected *Penicillium* sp. extract CKT35-PDA showed a completely different chemical profile compared to that of strain *Penicillium brasilianum* CKT49 grown in the same medium (Figure 5). Species- and even strain-specific metabolomes have been demonstrated for *Penicillium* spp. For example, the putatively identified compounds andrastin A (**92**) and 4′-hydroxy-mycophenolic acid (**83**) were previously described as chemotaxonomic markers for *Penicillium* spp. or strains [92,93]. Notably, one third of the putatively identified compounds from the *Penicillium* sp. CKT35-PDA extract were also detected in three sea foam-derived *Penicillium* spp. strains analyzed in our previous study [93]. The dereplicated polyketides penicifuran C and D (**77,79**), the meroterpenoid mycophenolic acid (**85**), and the phenylalanine derivative asperphenamate (**96**) reportedly inhibit the growth of *Staphylococcus* spp. [94–96]. Antifungal activity against *C. albicans* and *C. neoformans* has never been reported for any putatively annotated compound in this extract. Moreover, six compounds (**78,88,91,94,95,97**; Table S8) and some clusters in the *Penicillium* sp. CKT35 FBMN (Figure S7) remain unannotated and may represent novel metabolites.

The *B. exigua* (formerly *P. exigua*) extracts CKT91-CAG and -PDA were clearly dominated by cytochalasans, hybrids of polyketides and amino acids (Figure 6 and Figure S8, Table S9). Cytochalasans are a large chemical family produced by several fungal taxa with various bioactivities such as antimicrobial, antiparasitic, antiviral, and cytotoxic activities [97,98]. Several of the putatively identified cytochalasans (**100**,**102–104**,**106**,**107**,**110**) have been reported to inhibit the proliferation of lung carcinoma cell line A549, which may underlie the strong anticancer bioactivities observed in both *B. exigua* extracts [97,99]. However, neither the putatively annotated cytochalasans nor the sterol dankasterone B (**110**) have reported antimicrobial activities.

Dereplication of the GYM and MB extracts of *Streptomyces* sp. (CKT43) generated the lowest annotation rate (24%; Figure 7, Table S10) suggesting a highly unexplored chemical space. *Streptomyces* spp. are a very prolific source of novel bacterial MNPs (for example marine-derived *Streptomyces* spp. yielded 167 novel metabolites in 2018 [79]), and they still remain a treasure trove for biodiscovery of new MNPs. According to our literature survey, no antimicrobial activity has been reported from the putatively annotated compounds. Notably, anticancer activity was only detected in CKT43-CAG extract but none of the specific compounds for this extract could be annotated to a known NP. Only the putatively identified deformylated antimycins (**160,161**), detected in both extracts, inhibit the proliferation of HeLa cells [100]. It remains to be proven whether the putatively novel compounds detected in CKT43-CAG (**118**,**121**,**134**,**142**,**144**,**147**,**148**; Table S10) are responsible for the anticancer activities of this extract.

The five prioritized strains isolated from the tunic of *C. intestinalis* appear to produce unknown chemical scaffolds with potential bioactivities for the discovery of novel anticancer or antimicrobial lead compounds. All extracts deserve further scientific attention with regard to isolation and characterization of their putatively novel and bioactive constituents. Particularly the *Streptomyces* sp. isolate CKT43 is promising for in-depth chemical studies, since the majority of compounds could not be matched to any known compound in multiple databases and *Streptomyces* spp. are some of the most prolific producers of antibiotics and anticancer drugs [3,79,84].

In summary, the present study identified a diverse culturable microbiome associated with the tunic of *C. intestinalis* that differed from the ambient seawater, but also between the two sampling sites. To our knowledge, this is the first report of fungi being associated with the tunic of *C. intestinalis*. The isolated tunic microbiota appeared as a highly rich reservoir of MNPs

with antimicrobial and cytotoxic activities. Untargeted metabolomics studies on seven selected extracts indicated a high chemical diversity with compounds putatively assigned to alkaloids, lipids, peptides, polyketides, and terpenoids. However, many detected metabolites could not be annotated to any known NP and may therefore be new. Their chemical structure and bioactivity profiles need to be verified in future scale-up studies following their purification and structure elucidation. Hence, this study suggests that the so far unexplored tunic-associated microbiota of *C. intestinalis* from Helgoland and Kiel Fjord may be an excellent resource for replenishing the MNPs discovery pipeline with novel bioactive compounds.

Supplementary Materials: The following are available online at http://www.mdpi.com/2076-2607/8/11/1732/s1, Figure S1: Number of microbial strains isolated from the tunic of *C. intestinalis* and seawater reference, Figure S2**:** Distribution of bacterial orders across the sample types and their geographic locations, Figure S3: Distribution of fungal orders across the sample types and their geographic locations, Figure S4: Chemical structures of putatively identified compounds in crude extracts of five selected candidate strains isolated from the tunic of *C. intestinalis*, Figure S5: FBMN of the crude extract of *Pyrenochaeta* sp. strain CHT58 cultivated on PDA medium, Figure S6: FBMN of the crude extract of *Pseudogymnoascus destructans* strain CHT56 cultivated on CAG medium, Figure S7: FBMN of the crude extract of *Penicillium* sp. strain CKT35 cultivated on PDA medium, Figure S8: FBMN of the crude extracts of *Boeremia exigua* strain CKT91 cultivated on CAG (blue nodes) and PDA (red nodes) media, Table S1: Parameters for MZmine-processing of UPLC-MS/MS data, Table S2: Identification of microbial strains isolated from *C. intestinalis* and seawater reference in Helgoland and Kiel Fjord, Table S3: Bioactivity (%) of crude extracts derived from tunic-associated microbial strains at a test concentration of 100 µg/mL, Table S4: Bioactivity-based selection criterion for the prioritization of extracts for in-depth chemical analyses, Table S5: ANOSIM comparison of chemically different extracts, Table S6: Putative annotation of metabolites detected in the crude extract of *Pyrenochaeta* sp. strain CHT58 cultivated on PDA medium, Table S7: Putative annotation of metabolites detected in the crude extract of *Pseudogymnoascus destructans* strain CHT56 cultivated on CAG medium, Table S8: Putative annotation of metabolites detected in the crude extract of *Penicillium* sp. strain CKT35 cultivated on PDA medium, Table S9: Putative annotation of metabolites detected in the crude extracts of *Boeremia exigua* strain CKT91 cultivated on CAG and PDA media, Table S10: Putative annotation of metabolites detected in the crude extracts of *Streptomyces* sp. strain CKT43 cultivated on GYM and MB media.

References

1. Blockley, A.; Elliott, D.R.; Roberts, A.P.; Sweet, M. Symbiotic microbes from marine invertebrates: Driving a new era of natural product drug discovery. *Diversity* **2017**, *9*, 49, doi:10.3390/d9040049.
2. Ambrosino, L.; Tangherlini, M.; Colantuono, C.; Esposito, A.; Sangiovanni, M.; Miralto, M.; Sansone, C.; Chiusano, M.L. Bioinformatics for marine products: An overview of resources, bottlenecks, and perspectives. *Mar. Drugs* **2019**, *17*, 576, doi:10.3390/md17100576.
3. Carroll, A.R.; Copp, B.R.; Davis, R.A.; Keyzers, R.A.; Prinsep, M.R. Marine natural products. *Nat. Prod. Rep.* **2019**, *36*, 122–173, doi:10.1039/c8np00092a.

4. Schmidt, E.W.; Donia, M.S. Life in cellulose houses: Symbiotic bacterial biosynthesis of ascidian drugs and drug leads. *Curr. Opin. Biotechnol.* **2010**, *21*, 827–833, doi:10.1016/j.copbio.2010.10.006.

5. Palanisamy, S.K.; Rajendran, N.M.; Marino, A. Natural products diversity of marine ascidians (Tunicates; Ascidiacea) and successful drugs in clinical development. *Nat. Prod. Bioprospect.* **2017**, *7*, 1–111, doi:10.1007/s13659-016-0115-5.

6. Bauermeister, A.; Branco, P.C.; Furtado, L.C.; Jimenez, P.C.; Costa-Lotufo, L.V.; da Cruz Lotufo, T.M. Tunicates: A model organism to investigate the effects of associated-microbiota on the production of pharmaceuticals. *Drug Discov. Today Dis. Models* **2018**, *28*, 13–20, doi:10.1016/j.ddmod.2019.08.008.

7. Schmidt, E.W. The secret to a successful relationship: Lasting chemistry between ascidians and their symbiotic bacteria. *Invertebr. Biol.* **2015**, *134*, 88–102, doi:10.1111/ivb.12071.

8. Florez, L.V.; Biedermann, P.H.; Engl, T.; Kaltenpoth, M. Defensive symbioses of animals with prokaryotic and eukaryotic microorganisms. *Nat. Prod. Rep.* **2015**, *32*, 904–936, doi:10.1039/c5np00010f.

9. Blasiak, L.C.; Zinder, S.H.; Buckley, D.H.; Hill, R.T. Bacterial diversity associated with the tunic of the model chordate *Ciona intestinalis. ISME J.* **2014**, *8*, 309–320, doi:10.1038/ismej.2013.156.

10. Franchi, N.; Ballarin, L. Immunity in Protochordates: The tunicate perspective. *Front. Immunol.* **2017**, *8*, 674, doi:10.3389/fimmu.2017.00674.

11. Armstrong, E.; Yan, L.; Boyd, K.G.; Wright, P.C.; Burgess, J.G. The symbiotic role of marine microbes on living surfaces. *Hydrobiologia* **2001**, *461*, 37–40, doi:10.1023/A:1012756913566.

12. Egan, S.; Thomas, T.; Kjelleberg, S. Unlocking the diversity and biotechnological potential of marine surface associated microbial communities. *Curr. Opin. Microbiol.* **2008**, *11*, 219–225, doi:10.1016/j.mib.2008.04.001.

13. Steinert, G.; Taylor, M.W.; Schupp, P.J. Diversity of actinobacteria associated with the marine ascidian *Eudistoma toealensis. Mar. Biotechnol.* **2015**, *17*, 377–385, doi:10.1007/s10126-015-9622-3.

14. Tianero, M.D.; Kwan, J.C.; Wyche, T.P.; Presson, A.P.; Koch, M.; Barrows, L.R.; Bugni, T.S.; Schmidt, E.W. Species specificity of symbiosis and secondary metabolism in ascidians. *ISME J.* **2015**, *9*, 615–628, doi:10.1038/ismej.2014.152.

15. Lopez-Legentil, S.; Turon, X.; Espluga, R.; Erwin, P.M. Temporal stability of bacterial symbionts in a temperate ascidian. *Front. Microbiol.* **2015**, *6*, 1022, doi:10.3389/fmicb.2015.01022.

16. Chen, L.; Hu, J.S.; Xu, J.L.; Shao, C.L.; Wang, G.Y. Biological and chemical diversity of ascidian-associated microorganisms. *Mar. Drugs* **2018**, *16*, 362, doi:10.3390/md16100362.

17. Rath, C.M.; Janto, B.; Earl, J.; Ahmed, A.; Hu, F.Z.; Hiller, L.; Dahlgren, M.; Kreft, R.; Yu, F.; Wolff, J.J.; et al. Meta-omic characterization of the marine invertebrate microbial consortium that produces the chemotherapeutic natural product ET-743. *ACS Chem. Biol.* **2011**, *6*, 1244–1256, doi:10.1021/cb200244t.

18. Xu, Y.; Kersten, R.D.; Nam, S.J.; Lu, L.; Al-Suwailem, A.M.; Zheng, H.; Fenical, W.; Dorrestein, P.C.; Moore, B.S.; Qian, P.Y. Bacterial biosynthesis and maturation of the didemnin anti-cancer agents. *J. Am. Chem. Soc.* **2012**, *134*, 8625–8632, doi:10.1021/ja301735a.

19. Asolkar, R.N.; Kirkland, T.N.; Jensen, P.R.; Fenical, W. Arenimycin, an antibiotic effective against rifampin- and methicillin-resistant *Staphylococcus aureus* from the marine actinomycete *Salinispora arenicola. J. Antibiot.* **2010**, *63*, 37–39, doi:10.1038/ja.2009.114.

20. Sugie, Y.; Hirai, H.; Kachi-Tonai, H.; Kim, Y.J.; Kojima, Y.; Shiomi, Y.; Sugiura, A.; Sugiura, A.; Suzuki, Y.; Yoshikawa, N.; et al. New pyrrolizidinone antibiotics CJ-16,264 and CJ-16,367. *J. Antibiot.* **2001**, *54*, 917–925, doi:10.7164/antibiotics.54.917.

21. Wyche, T.P.; Alvarenga, R.F.R.; Piotrowski, J.S.; Duster, M.N.; Warrack, S.R.; Cornilescu, G.; De Wolfe, T.J.; Hou, Y.; Braun, D.R.; Ellis, G.A.; et al. Chemical genomics, structure elucidation, and in vivo studies of the marine-derived anticlostridial ecteinamycin. *ACS Chem. Biol.* **2017**, *12*, 2287–2295, doi:10.1021/acschembio.7b00388.

22. Garo, E.; Starks, C.M.; Jensen, P.R.; Fenical, W.; Lobkovsky, E.; Clardy, J. Trichodermamides A and B, cytotoxic modified dipeptides from the marine-derived fungus *Trichoderma virens*. *J. Nat. Prod.* **2003**, *66*, 423–426, doi:10.1021/np0204390.

23. Carver, C.E.; Mallet, A.L.; Vercaemer, B. Biological synopsis of the solitary tunicate *Ciona intestinalis*. *Can. Man. Rep. Fish. Aquat. Sci.* **2006**, *2746*, 1-55.

24. Bouchemousse, S.; Bishop, J.D.; Viard, F. Contrasting global genetic patterns in two biologically similar, widespread and invasive *Ciona* species (Tunicata, Ascidiacea). *Sci. Rep.* **2016**, *6*, 24875, doi:10.1038/srep24875.

25. Caputi, L.; Andreakis, N.; Mastrototaro, F.; Cirino, P.; Vassillo, M.; Sordino, P. Cryptic speciation in a model invertebrate chordate. *Proc. Natl. Acad. Sci. USA.* **2007**, *104*, 9364–9369, doi:10.1073/pnas.0610158104.

26. Zhan, A.; Briski, E.; Bock, D.G.; Ghabooli, S.; MacIsaac, H.J. Ascidians as models for studying invasion success. *Mar. Biol.* **2015**, *162*, 2449–2470, doi:10.1007/s00227-015-2734-5.

27. Satoh, N.; Satou, Y.; Davidson, B.; Levine, M. *Ciona intestinalis*: An emerging model for whole-genome analyses. *Trends Genet.* **2003**, *19*, 376–381, doi:10.1016/S0168-9525(03)00144-6.

28. Aiello, A.; Fattorusso, E.; Imperatore, C.; Menna, M.; Muller, W.E. Iodocionin, a cytotoxic iodinated metabolite from the Mediterranean ascidian *Ciona edwardsii*. *Mar. Drugs* **2010**, *8*, 285–291, doi:10.3390/md8020285.

29. Fedders, H.; Michalek, M.; Grotzinger, J.; Leippe, M. An exceptional salt-tolerant antimicrobial peptide derived from a novel gene family of haemocytes of the marine invertebrate *Ciona intestinalis*. *Biochem. J.* **2008**, *416*, 65–75, doi:10.1042/BJ20080398.

30. Cahill, P.L.; Fidler, A.E.; Hopkins, G.A.; Wood, S.A. Geographically conserved microbiomes of four temperate water tunicates. *Environ. Microbiol. Rep.* **2016**, *8*, 470–478, doi:10.1111/1758-2229.12391.

31. Holmström, C.; James, S.; Neilan, B.A.; White, D.C.; Kjelleberg, S. *Pseudoalteromonas tunicata* sp. nov., a bacterium that produces antifouling agents. *Int. J. Syst. Bacteriol.* **1998**, *48*, 1205–1212, doi:10.1099/00207713-48-4-1205.

32. James, S.G.; Holmstrom, C.; Kjelleberg, S. Purification and characterization of a novel antibacterial protein from the marine bacterium D2. *Appl. Environ. Microbiol.* **1996**, *62*, 2783–2788, doi:10.1128/aem.62.8.2783-2788.1996.

33. Nothias, L.F.; Petras, D.; Schmid, R.; Duhrkop, K.; Rainer, J.; Sarvepalli, A.; Protsyuk, I.; Ernst, M.; Tsugawa, H.; Fleischauer, M.; et al. Feature-based molecular networking in the GNPS analysis environment. *Nat. Methods* **2020**, *17*, 905–908, doi:10.1038/s41592-020-0933-6.

34. Allard, P.M.; Peresse, T.; Bisson, J.; Gindro, K.; Marcourt, L.; Pham, V.C.; Roussi, F.; Litaudon, M.; Wolfender, J.L. Integration of molecular networking and *in-silico* MS/MS fragmentation for natural products dereplication. *Anal. Chem.* **2016**, *88*, 3317–3323, doi:10.1021/acs.analchem.5b04804.

35. Oppong-Danquah, E.; Parrot, D.; Blümel, M.; Labes, A.; Tasdemir, D. Molecular networking-based metabolome and bioactivity analyses of marine-adapted fungi co-cultivated with phytopathogens. *Front. Microbiol.* **2018**, *9*, 1–20, doi:10.3389/fmicb.2018.02072.

36. Silber, J.; Ohlendorf, B.; Labes, A.; Erhard, A.; Imhoff, J.F. Calcarides A-E, antibacterial macrocyclic and linear polyesters from a *Calcarisporium* strain. *Mar. Drugs* **2013**, *11*, 3309–3323, doi:10.3390/md11093309.

37. Utermann, C.; Parrot, D.; Breusing, C.; Stuckas, H.; Staufenberger, T.; Blümel, M.; Labes, A.; Tasdemir, D. Combined genotyping, microbial diversity and metabolite profiling studies on farmed *Mytilus* spp. from Kiel Fjord. *Sci. Rep.* **2018**, *8*, 7983, doi:10.1038/s41598-018-26177-y.

38. Gomes, N.C.; Fagbola, O.; Costa, R.; Rumjanek, N.G.; Buchner, A.; Mendona-Hagler, L.; Smalla, K. Dynamics of fungal communities in bulk and maize rhizosphere soil in the tropics. *Appl. Environ. Microbiol.* **2003**, *69*, 3758–3766, doi:10.1128/aem.69.7.3758-3766.2003.

39. Hopple, J.S., Jr.; Vilgalys, R. Phylogenetic relationships in the mushroom genus *Coprinus* and dark-spored allies based on sequence data from the nuclear gene coding for the large ribosomal subunit RNA: Divergent domains, outgroups, and monophyly. *Mol. Phylogenet. Evol.* **1999**, *13*, 1–19, doi:10.1006/mpev.1999.0634.

40. Sanger, F.; Nicklen, S.; Coulson, A.R. DNA sequencing with chain-terminating inhibitors. *Proc. Natl. Acad. Sci. USA.* **1977**, *74*, 5463–5467, doi:10.1073/pnas.74.12.5463.

41. Altschul, S.F.; Gish, W.; Miller, W.; Myers, E.W.; Lipman, D.J. Basic local alignment search tool. *J. Mol. Biol.* **1990**, *215*, 403–410, doi:10.1016/S0022-2836(05)80360-2.

42. Wang, Q.; Garrity, G.M.; Tiedje, J.M.; Cole, J.R. Naive Bayesian classifier for rapid assignment of rRNA sequences into the new bacterial taxonomy. *Appl. Environ. Microbiol.* **2007**, *73*, 5261–5267, doi:10.1128/AEM.00062-07.

43. Wu, B.; Wiese, J.; Labes, A.; Kramer, A.; Schmaljohann, R.; Imhoff, J.F. Lindgomycin, an unusual antibiotic polyketide from a marine fungus of the Lindgomycetaceae. *Mar. Drugs* **2015**, *13*, 4617–4632, doi:10.3390/md13084617.

44. Stevens, R.B. *Mycology Guidebook*; University of Washington Press: Seattle, WA, USA, 1974; p. 682.

45. Matobole, R.; van Zyl, L.; Parker-Nance, S.; Davies-Coleman, M.; Trindade, M. Antibacterial activities of bacteria isolated from the marine sponges *Isodictya compressa* and *Higginsia bidentifera* collected from Algoa Bay, South Africa. *Mar. Drugs* **2017**, *15*, 47, doi:10.3390/md15020047.

46. Pfeifer Barbosa, A.L.; Wenzel-Storjohann, A.; Barbosa, J.D.; Zidorn, C.; Peifer, C.; Tasdemir, D.; Cicek, S.S. Antimicrobial and cytotoxic effects of the *Copaifera reticulata* oleoresin and its main diterpene acids. *J. Ethnopharmacol.* **2019**, *233*, 94–100, doi:10.1016/j.jep.2018.11.029.

47. Parrot, D.; Blümel, M.; Utermann, C.; Chianese, G.; Krause, S.; Kovalev, A.; Gorb, S.N.; Tasdemir, D. Mapping the surface microbiome and metabolome of brown seaweed *Fucus vesiculosus* by amplicon sequencing, integrated metabolomics and imaging techniques. *Sci. Rep.* **2019**, *9*, 1061, doi:10.1038/s41598-018-37914-8.

48. Chambers, M.C.; Maclean, B.; Burke, R.; Amodei, D.; Ruderman, D.L.; Neumann, S.; Gatto, L.; Fischer, B.; Pratt, B.; Egertson, J.; et al. A cross-platform toolkit for mass spectrometry and proteomics. *Nat. Biotechnol.* **2012**, *30*, 918–920, doi:10.1038/nbt.2377.

49. Pluskal, T.; Castillo, S.; Villar-Briones, A.; Oresic, M. MZmine 2: Modular framework for processing, visualizing, and analyzing mass spectrometry-based molecular profile data. *BMC Bioinform.* **2010**, *11*, 395, doi:10.1186/1471-2105-11-395.

50. Hammer, Ø.; Harper, D.A.T.; Ryan, P.D. PAST: Paleontological statistics software package for education and data analysis. *Palaeontol. Electron.* **2001**, *4*, 1–9.

51. Wang, M.; Carver, J.J.; Phelan, V.V.; Sanchez, L.M.; Garg, N.; Peng, Y.; Nguyen, D.D.; Watrous, J.; Kapono, C.A.; Luzzatto-Knaan, T.; et al. Sharing and community curation of mass spectrometry data with Global Natural Products Social Molecular Networking. *Nat. Biotechnol.* **2016**, *34*, 828–837, doi:10.1038/nbt.3597.

52. Shannon, P.; Markiel, A.; Ozier, O.; Baliga, N.S.; Wang, J.T.; Ramage, D.; Amin, N.; Schwikowski, B.; Ideker, T. Cytoscape: A software environment for integrated models of biomolecular interaction networks. *Genome Res.* **2003**, *13*, 2498–2504, doi:10.1101/gr.1239303.

53. van Santen, J.A.; Jacob, G.; Singh, A.L.; Aniebok, V.; Balunas, M.J.; Bunsko, D.; Neto, F.C.; Castaño-Espriu, L.; Chang, C.; Clark, T.N.; et al. The Natural Products Atlas: An open access knowledge base for microbial natural products discovery. *ACS Cent. Sci.* **2019**, *5*, 1824–1833, doi:10.1021/acscentsci.9b00806.

54. Allen, F.; Pon, A.; Wilson, M.; Greiner, R.; Wishart, D. CFM-ID: A web server for annotation, spectrum prediction and metabolite identification from tandem mass spectra. *Nucleic Acids Res.* **2014**, *42*, 94–99, doi:10.1093/nar/gku436.

55. Stewart, E.J. Growing unculturable bacteria. *J. Bacteriol.* **2012**, *194*, 4151–4160, doi:10.1128/JB.00345-12.

56. Vartoukian, S.R.; Palmer, R.M.; Wade, W.G. Strategies for culture of 'unculturable' bacteria. *FEMS Microbiol. Lett.* **2010**, *309*, 1–7, doi:10.1111/j.1574-6968.2010.02000.x.

57. Da Silva, R.R.; Dorrestein, P.C.; Quinn, R.A. Illuminating the dark matter in metabolomics. *Proc. Natl. Acad. Sci. USA.* **2015**, *112*, 12549–12550, doi:10.1073/pnas.1516878112.

58. Romanenko, L.A.; Kalinovskaya, N.I.; Mikhailov, V.V. Taxonomic composition and biological activity of microorganisms associated with a marine ascidian *Halocynthia aurantium*. *Russ. J. Mar. Biol.* **2001**, *27*, 291–296, doi:10.1023/a:1012548513766.

59. Menezes, C.B.; Bonugli-Santos, R.C.; Miqueletto, P.B.; Passarini, M.R.; Silva, C.H.; Justo, M.R.; Leal, R.R.; Fantinatti-Garboggini, F.; Oliveira, V.M.; Berlinck, R.G.; et al. Microbial diversity associated with algae, ascidians and sponges from the north coast of Sao Paulo state, Brazil. *Microbiol. Res.* **2010**, *165*, 466–482, doi:10.1016/j.micres.2009.09.005.

60. Evans, J.S.; Erwin, P.M.; Shenkar, N.; Lopez-Legentil, S. A comparison of prokaryotic symbiont communities in nonnative and native ascidians from reef and harbor habitats. *FEMS Microbiol. Ecol.* **2018**, *94*, fiy139, doi:10.1093/femsec/fiy139.

61. Ivanova, E.P.; Vysotskii, M.V.; Svetashev, V.I.; Nedashkovskaya, O.I.; Gorshkova, N.M.; Mikhailov, V.V.; Yumoto, N.; Shigeri, Y.; Taguchi, T.; Yoshikawa, S. Characterization of *Bacillus* strains of marine origin. *Int. Microbiol.* **1999**, *2*, 267–271, doi:10.2436/IM.V2I4.9225.

62. Mukherjee, S.; Kearns, D.B. The structure and regulation of flagella in *Bacillus subtilis. Annu. Rev. Genet.* **2014**, *48*, 319–340, doi:10.1146/annurev-genet-120213-092406.

63. Kearns, D.B.; Losick, R. Swarming motility in undomesticated *Bacillus subtilis. Mol. Microbiol.* **2003**, *49*, 581–590, doi:10.1046/j.1365-2958.2003.03584.x.

64. Dror, H.; Novak, L.; Evans, J.S.; Lopez-Legentil, S.; Shenkar, N. Core and dynamic microbial communities of two invasive ascidians: Can host-symbiont dynamics plasticity affect invasion capacity? *Microb. Ecol.* **2019**, *78*, 170–184, doi:10.1007/s00248-018-1276-z.

65. Rangarajan, S.; Saleena, L.M.; Nair, S. Diversity of *Pseudomonas* spp. isolated from rice rhizosphere populations grown along a salinity gradient. *Microb. Ecol.* **2002**, *43*, 280–289, doi:10.1007/s00248-002-2004-1.

66. Hugenholtz, P. Exploring prokaryotic diversity in the genomic era. *Genome Biol.* **2002**, *3*, reviews0003.1, doi:10.1186/gb-2002-3-2-reviews0003.

67. Alain, K.; Querellou, J. Cultivating the uncultured: Limits, advances and future challenges. *Extremophiles* **2009**, *13*, 583–594, doi:10.1007/s00792-009-0261-3.

68. López-Legentil, S.; Erwin, P.M.; Turon, M.; Yarden, O. Diversity of fungi isolated from three temperate ascidians. *Symbiosis* **2015**, *66*, 99–106, doi:10.1007/s13199-015-0339-x.

69. Wiese, J.; Imhoff, J.F. Marine bacteria and fungi as promising source for new antibiotics. *Drug Dev. Res.* **2019**, *80*, 24–27, doi:10.1002/ddr.21482.

70. Chen, L.; Wang, X.-N.; Fu, C.-M.; Wang, G.-Y. Phylogenetic analysis and screening of antimicrobial and antiproliferative activities of culturable bacteria associated with the ascidian *Styela clava* from the Yellow Sea, China. *Biomed. Res. Int.* **2019**, *2019*, 1–14, doi:10.1155/2019/7851251.

71. Pereira, F. Have marine natural product drug discovery efforts been productive and how can we improve their efficiency? *Expert Opin. Drug Discov.* **2019**, *14*, 717–722, doi:10.1080/17460441.2019.1604675.

72. Pages, J.M.; James, C.E.; Winterhalter, M. The porin and the permeating antibiotic: A selective diffusion barrier in Gram-negative bacteria. *Nat. Rev. Microbiol.* **2008**, *6*, 893–903, doi:10.1038/nrmicro1994.

73. Holmström, C.; Rittschof, D.; Kjelleberg, S. Inhibition of settlement by larvae of *Balanus amphitrite* and *Ciona intestinalis* by a surface-colonizing marine bacterium. *Appl. Environ. Microbiol.* **1992**, *58*, 2111–2115, doi:10.1128/aem.58.7.2111-2115.1992.

74. Thompson, T.E. Acidic allomones in marine organisms. *J. Mar. Biol. Assoc. UK* **1988**, *68*, 499–517, doi:10.1017/S0025315400043368.

75. Trivedi, S.; Ueki, T.; Yamaguchi, N.; Michibata, H. Novel vanadium-binding proteins (vanabins) identified in cDNA libraries and the genome of the ascidian *Ciona intestinalis*. *Biochim. Biophys. Acta (BBA) Gene Struct. Expr.* **2003**, *1630*, 64–70, doi:10.1016/j.bbaexp.2003.09.007.

76. Wiese, J.; Ohlendorf, B.; Blümel, M.; Schmaljohann, R.; Imhoff, J.F. Phylogenetic identification of fungi isolated from the marine sponge *Tethya aurantium* and identification of their secondary metabolites. *Mar. Drugs* **2011**, *9*, 561–585, doi:10.3390/md9040561.

77. Duarte, A.W.F.; Barato, M.B.; Nobre, F.S.; Polezel, D.A.; de Oliveira, T.B.; dos Santos, J.A.; Rodrigues, A.; Sette, L.D. Production of cold-adapted enzymes by filamentous fungi from King George Island, Antarctica. *Polar Biol.* **2018**, *41*, 2511–2521, doi:10.1007/s00300-018-2387-1.

78. Danuello, A.; de Castro, R.C.; Pilon, A.C.; Bueno, P.C.P.; Pivatto, M.; Vieira Junior, G.M.; Carvalho, F.A.; Oda, F.B.; Perez, C.J.; Lopes, N.P.; et al. Fragmentation study of clerodane diterpenes from *Casearia* species by tandem mass spectrometry (quadrupole time-of-flight and ion trap). *Rapid Commun. Mass Spectrom.* **2020**, e8781, doi:10.1002/rcm.8781.

79. Carroll, A.R.; Copp, B.R.; Davis, R.A.; Keyzers, R.A.; Prinsep, M.R. Marine natural products. *Nat. Prod. Rep.* **2020**, *37*, 175–223, doi:10.1039/c9np00069k.

80. Yang, K.L.; Wei, M.Y.; Shao, C.L.; Fu, X.M.; Guo, Z.Y.; Xu, R.F.; Zheng, C.J.; She, Z.G.; Lin, Y.C.; Wang, C.Y. Antibacterial anthraquinone derivatives from a sea anemone-derived fungus *Nigrospora* sp. *J. Nat. Prod.* **2012**, *75*, 935–941, doi:10.1021/np300103w.

81. Li, D.H.; Cai, S.X.; Zhu, T.J.; Wang, F.P.; Xiao, X.; Gu, Q.Q. New cytotoxic metabolites from a deep-sea-derived fungus, *Phialocephala* sp., strain FL30r. *Chem. Biodivers.* **2011**, *8*, 895–901, doi:10.1002/cbdv.201000134.

82. Huang, Z.; Shao, C.; Chen, Y.; She, Z.; Lin, Y.; Zhou, S. A new isocoumarin from mangrove endophytic fungus (no. dz17) on the south China Sea coast. *Chem. Nat. Compd.* **2007**, *43*, 655–658, doi:10.1007/s10600-007-0221-z.

83. Xia, X.; Zhang, J.; Zhang, Y.; Wei, F.; Liu, X.; Jia, A.; Liu, C.; Li, W.; She, Z.; Lin, Y. Pimarane diterpenes from the fungus *Epicoccum* sp. HS-1 associated with *Apostichopus japonicus. Bioorg. Med. Chem. Lett.* **2012**, *22*, 3017–3019, doi:10.1016/j.bmcl.2012.01.055.

84. Fenical, W.; Jensen, P.R. Developing a new resource for drug discovery: Marine actinomycete bacteria. *Nat. Chem. Biol.* **2006**, *2*, 666–673, doi:10.1038/nchembio841.

85. Rai, M.; Gade, A.; Zimowska, B.; Ingle, A.P.; Ingle, P. Marine-derived *Phoma*—The gold mine of bioactive compounds. *Appl. Microbiol. Biotechnol.* **2018**, *102*, 9053–9066, doi:10.1007/s00253-018-9329-2.

86. Liu, Z.; Zhao, J.Y.; Sun, S.F.; Li, Y.; Liu, Y.B. Fungi: Outstanding source of novel chemical scaffolds. *J. Asian Nat. Prod. Res.* **2020**, *22*, 99–120, doi:10.1080/10286020.2018.1488833.

87. Jones, E.B.G.; Suetrong, S.; Sakayaroj, J.; Bahkali, A.H.; Abdel-Wahab, M.A.; Boekhout, T.; Pang, K.-L. Classification of marine Ascomycota, Basidiomycota, Blastocladiomycota and Chytridiomycota. *Fungal Divers.* **2015**, *73*, 1–72, doi:10.1007/s13225-015-0339-4.

88. Fan, B.; Parrot, D.; Blümel, M.; Labes, A.; Tasdemir, D. Influence of OSMAC-based cultivation in metabolome and anticancer activity of fungi associated with the brown alga *Fucus vesiculosus. Mar. Drugs* **2019**, *17*, 67, doi:10.3390/md17010067.

89. Petersen, L.E.; Marner, M.; Labes, A.; Tasdemir, D. Rapid metabolome and bioactivity profiling of fungi associated with the leaf and rhizosphere of the Baltic seagrass *Zostera marina. Mar. Drugs* **2019**, *17*, 419, doi:10.3390/md17070419.

90. Jin, L.; Quan, C.; Hou, X.; Fan, S. Potential pharmacological resources: Natural bioactive compounds from marine-derived fungi. *Mar. Drugs* **2016**, *14*, 76, doi:10.3390/md14040076.

91. Nicoletti, R.; Trincone, A. Bioactive compounds produced by strains of *Penicillium* and *Talaromyces* of marine origin. *Mar. Drugs* **2016**, *14*, 37, doi:10.3390/md14020037.

92. Kim, H.Y.; Park, H.M.; Lee, C.H. Mass spectrometry-based chemotaxonomic classification of *Penicillium* species (*P. echinulatum*, *P. expansum*, *P. solitum*, and *P. oxalicum*) and its correlation with antioxidant activity. *J. Microbiol. Methods* **2012**, *90*, 327–335, doi:10.1016/j.mimet.2012.06.006.

93. Oppong-Danquah, E.; Passaretti, C.; Chianese, O.; Blümel, M.; Tasdemir, D. Mining the metabolome and the agricultural and pharmaceutical potential of sea foam-derived fungi. *Mar. Drugs* **2020**, *18*, 128, doi:10.3390/md18020128.

94. Qi, J.; Shao, C.L.; Li, Z.Y.; Gan, L.S.; Fu, X.M.; Bian, W.T.; Zhao, H.Y.; Wang, C.Y. Isocoumarin derivatives and benzofurans from a sponge-derived *Penicillium* sp. fungus. *J. Nat. Prod.* **2013**, *76*, 571–579, doi:10.1021/np3007556.

95. Zheng, C.J.; Shao, C.L.; Wu, L.Y.; Chen, M.; Wang, K.L.; Zhao, D.L.; Sun, X.P.; Chen, G.Y.; Wang, C.Y. Bioactive phenylalanine derivatives and cytochalasins from the soft coral-derived fungus, *Aspergillus elegans. Mar. Drugs* **2013**, *11*, 2054–2068, doi:10.3390/md11062054.

96. Florey, H.W.; Jennings, M.A.; Gilliver, K.; Sanders, A.G. Mycophenolic acid an antibiotic from *Penicillium brevicompactum* Dierckx. *Lancet* **1946**, *247*, 46–49, doi:10.1016/s0140-6736(46)90242-5.

97. Kim, E.L.; Li, J.L.; Dang, H.T.; Hong, J.; Lee, C.O.; Kim, D.K.; Yoon, W.D.; Kim, E.; Liu, Y.; Jung, J.H. Cytotoxic cytochalasins from the endozoic fungus *Phoma* sp. of the giant jellyfish *Nemopilema nomurai. Bioorg. Med. Chem. Lett.* **2012**, *22*, 3126–3129, doi:10.1016/j.bmcl.2012.03.058.

98. Scherlach, K.; Boettger, D.; Remme, N.; Hertweck, C. The chemistry and biology of cytochalasans. *Nat. Prod. Rep.* **2010**, *27*, 869–886, doi:10.1039/b903913a.

99. Kim, E.L.; Wang, H.; Park, J.H.; Hong, J.; Choi, J.S.; Im, D.S.; Chung, H.Y.; Jung, J.H. Cytochalasin derivatives from a jellyfish-derived fungus *Phoma* sp. *Bioorg. Med. Chem. Lett.* **2015**, *25*, 2096–2099, doi:10.1016/j.bmcl.2015.03.080.

100. Zhang, W.; Che, Q.; Tan, H.; Qi, X.; Li, J.; Li, D.; Gu, Q.; Zhu, T.; Liu, M. Marine *Streptomyces* sp. derived antimycin analogues suppress HeLa cells via depletion HPV E6/E7 mediated by ROS-dependent ubiquitin-proteasome system. *Sci. Rep.* **2017**, *7*, 42180, doi:10.1038/srep42180.

Chapter 3

Diversity, bioactivity profiling and untargeted metabolomics of the cultivable gut microbiota of *Ciona intestinalis*

Utermann, C., Echelmeyer, V.A., Oppong-Danquah, E., Blümel, M., and Tasdemir, D. 2021, *Marine Drugs*, 19, 6; DOI: 10.3390/md19010006

Diversity, Bioactivity Profiling and Untargeted Metabolomics of the Cultivable Gut Microbiota of *Ciona intestinalis*

Caroline Utermann [1], Vivien A. Echelmeyer [1], Ernest Oppong-Danquah [1], Martina Blümel [1] and Deniz Tasdemir [1,2]*

[1] GEOMAR Centre for Marine Biotechnology (GEOMAR-Biotech), Research Unit Marine Natural Products Chemistry, GEOMAR Helmholtz Centre for Ocean Research Kiel, Am Kiel-Kanal 44, 24106 Kiel, Germany; cutermann@geomar.de (C.U.); vivienechelmeyer@web.de (V.A.E.); eoppong-danquah@geomar.de (E.O.-D.); mbluemel@geomar.de (M.B.)

[2] Faculty of Mathematics and Natural Sciences, Kiel University, Christian-Albrechts-Platz 4, 24118 Kiel, Germany

* Correspondence: dtasdemir@geomar.de; Tel.: +49-431-600-4430

Abstract: It is widely accepted that the commensal gut microbiota contributes to the health and well-being of its host. The solitary tunicate *Ciona intestinalis* emerges as a model organism for studying host–microbe interactions taking place in the gut, however, the potential of its gut-associated microbiota for marine biodiscovery remains unexploited. In this study, we set out to investigate the diversity, chemical space, and pharmacological potential of the gut-associated microbiota of *C. intestinalis* collected from the Baltic and North Seas. In a culture-based approach, we isolated 61 bacterial and 40 fungal strains affiliated to 33 different microbial genera, indicating a rich and diverse gut microbiota dominated by Gammaproteobacteria. In vitro screening of the crude microbial extracts indicated their antibacterial (64% of extracts), anticancer (22%), and/or antifungal (11%) potential. Nine microbial crude extracts were prioritized for in-depth metabolome mining by a bioactivity- and chemical diversity-based selection procedure. UPLC-MS/MS-based metabolomics combining automated (feature-based molecular networking and in silico dereplication) and manual approaches significantly improved the annotation rates. A high chemical diversity was detected where peptides and polyketides were the predominant classes. Many compounds remained unknown, including two putatively novel lipopeptides produced by a *Trichoderma* sp. strain. This is the first study assessing the chemical and pharmacological profile of the cultivable gut microbiota of *C. intestinalis*.

Keywords: tunicate; *Ciona intestinalis*; gut-associated microbiota; marine natural products; antimicrobial activity; anticancer activity; untargeted metabolomics; feature-based molecular networking; in silico MS/MS-based dereplication

1. Introduction

The animal gut is one of the most densely colonized microbial habitats representing a highly specialized internal ecosystem [1–3]. The commensal gut microbiota is known for contributing to the host's health and homeostasis by assisting, e.g., chemical defense, immunity, metabolic capacity, and digestion [1–3]. For instance, vertebrate-associated gut bacteria provide "colonization resistance" through, e.g., short-chain fatty acids to inhibit proliferation of pathogenic microorganisms such as *Salmonella enterica* [3,4]. Commensal gut bacteria also induce immune reactions by producing antimicrobial peptides or aid nutrient uptake by breaking down complex polysaccharides [3,4]. In the marine world, cultivable gut-associated bacteria of farmed fish, such as *Vibrio* sp., have been reported to inhibit common aquaculture pathogens, e.g., *Vibrio anguillarum* and *Pasteurella piscicida* [5,6]. The current evidence suggests that *Vibrio* spp. residing in the alimentary tract of the alga-feeding sea

urchin *Strongylocentrotus* spp. promote the animal´s digestion by breaking down large algal polysaccharides such as alginates [7].

Marine microorganisms represent unparalleled resources for biodiscovery of compounds with great pharmaceutical application potential [8,9]. The majority of marine natural products (MNPs) discovered between 2014 and 2018 originate from bacteria or fungi [9]. Microorganisms associated with invertebrate hosts such as sponges and tunicates are promising resources for marine biodiscovery [8,10–12]. For example, ascidian-associated bacteria are prolific producers of antibiotics and anticancer drug leads [11,13] including the anticancer drug Yondelis® produced by a gammaproteobacterial symbiont of the colonial sea squirt *Ecteinascidia turbinata* [14]. However, the gut microbiota of marine sessile animals has rarely been studied. The few available examples include the ascomycete fungi *Aspergillus* sp. and *Letendraea* sp., which were isolated from the gut of marine crustaceans [15–17]. They yielded novel cytotoxic aspochalazines [15,16] and the anti-inflammatory polyketide phomopsiketone D [17], rendering the gut-associated microbiota of marine invertebrates as a valuable and underexploited source for MNP biodiscovery.

Host-associated microbial communities can be analyzed by culture-dependent and -independent methods. Culture-based studies capture only a small fraction of the actual microbiota (~ 0.001 to 1%), often select for easily culturable microorganisms, and, therefore, do not adequately reflect the microbial diversity [18,19]. In contrast, culture-independent approaches such as metagenomics and amplicon sequencing allow comprehensive description of the microbiota of interest, although the large majority of the detected microorganisms remains uncultivable [19]. Hence, comparison of the microbial diversity obtained by both methodologies often reveals a huge discrepancy [20], mainly due to the large fraction of uncultured microorganisms and the strong impact of the applied cultivation media on the culture-dependent microbial diversity [18,19]. Despite recent advances enabling, e.g., the access to compounds of yet uncultivable microorganisms via heterologous expression, marine biodiscovery studies still largely apply cultivation-dependent methods, mainly due to their high efficiency for bioactivity screening [21].

For decades, the sea vase *Ciona* spp. (chordate subphylum Tunicata) has served as a model organism for developmental biology, evolution, and chordate immunity [22,23]. Recently, *C. intestinalis* and *C. robusta* were introduced as model organisms for studying host–microbe interactions in animal gastrointestinal tracts, because they feature a compartmentalized gut resembling that of the vertebrates [2,23,24]. The gut of the filter feeder is in constant contact with millions of microbial cells posing a great challenge for the tunicate; on the one hand it must defend against pathogenic microorganisms, but at the same time allow colonization of commensals [2,25]. Initial studies have reported a few gut-associated Gammaproteobacteria (e.g., *Shewanella* sp. and *Vibrio* sp. [23,26,27]) and Ascomycota (e.g., *Penicillium* sp. and *Trichoderma* sp. [28]) from *C. intestinalis* and *C. robusta*. In line with this, amplicon sequencing of the bacterial community associated with *C. intestinalis* and *C. robusta* described a specific and diverse gut community dominated by Gammaproteobacteria [29], while culture-dependent and -independent studies on the tunic-associated microbiota of *Ciona* spp. revealed comparably high abundance of Alphaproteobacteria [30,31]. However, no information exists on chemical composition or biological activities of the gut-associated microbial community of *C. intestinalis*. This fact prompted us to isolate and study cultivable bacteria and fungi associated with the gut of *C. intestinalis* to explore their chemical machinery. Dissected guts of *C. intestinalis* sampled at two sites in Germany (Helgoland, North Sea and Kiel Fjord, Baltic Sea) yielded 61 bacterial and 40 fungal isolates. An initial bioactivity screening (antimicrobial and anticancer) and chemical profiling of the crude extracts of these microorganisms allowed selection of nine microbial extracts for LC-MS/MS-based untargeted metabolomics employing feature-based molecular networking (FBMN) [32], in silico [33] and manual dereplication tools. This study enabled us to prioritize two bacterial and three fungal strains for purification and characterization of their bioactive constituents in future.

2. Results

2.1. Cultivable Fraction of the Gut Microbiota of C. intestinalis

Application of six different cultivation media led to 61 bacterial and 40 fungal isolates from the gut of *C. intestinalis* sampled in Helgoland (H) and Kiel Fjord (K; Figure 1a, Table S1). The number of bacterial isolates was much higher in the Baltic Sea samples than in the North Sea samples (H: 24, K: 37). However, samples from Kiel Fjord (Baltic Sea) and the North Sea island Helgoland yielded similar numbers of fungal isolates (H: 18, K: 22). As expected, the applied isolation media had a remarkable influence on the number of isolated microorganisms (Figure 1b). Isolation on modified Wickerham medium (WSP) yielded the highest number of isolates (32, compared to other media: 7–24 isolates). Bacterial isolates derived mainly from Marine Broth (MB; 26%) and tryptic soy broth (TSB; 31%) media, while gut-associated fungal strains were mainly obtained from WSP medium (20 isolates; other media: 1–7 fungal isolates). Similar to our previous study that reported the tunic-associated microbiota of *C. intestinalis* [31], we used media resembling the natural habitat of the isolates, i.e., media adjusted to Baltic (CB) or North Sea (CN) salinity containing *C. intestinalis* powder. They yielded many microbial strains (*n* = 20), and the microbial genera *Acrostalagmus*, *Arthopyrenia*, *Cordyceps,* and *Sporosarcina* were exclusively isolated from these media. Accordingly, the *C. intestinalis* media CB and CN proved valuable for isolating a diverse tunicate-associated microbiota.
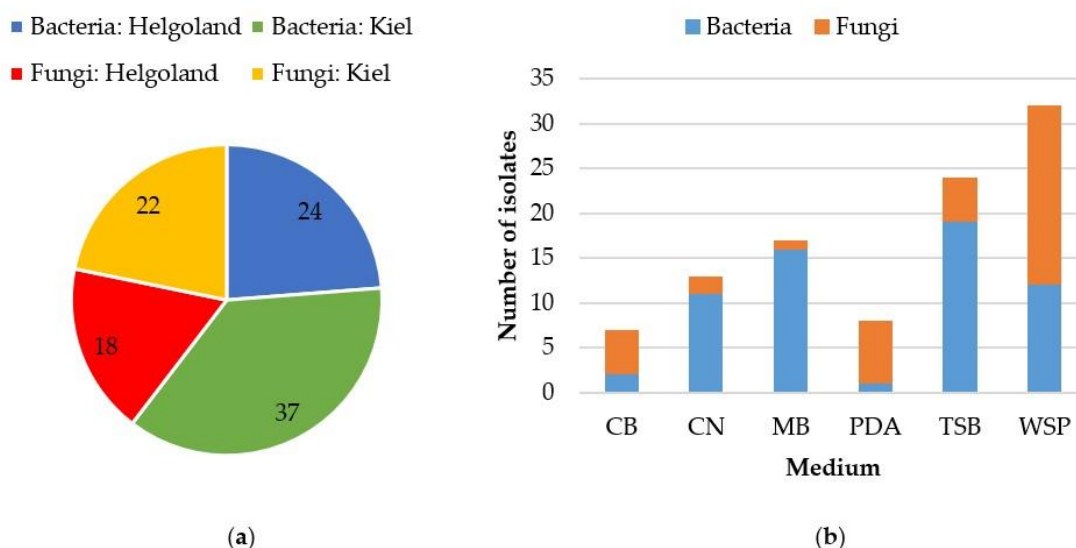
Figure 1. Distribution of bacterial (*n* = 61) and fungal (*n* = 40) isolates deriving from the gut of *Ciona intestinalis* sampled in the North (Helgoland) and Baltic Seas (Kiel Fjord). Numbers of bacterial and fungal isolates are displayed for (**a**) the two different sampling sites and (**b**) with respect to the used isolation media. CB/CN: *C. intestinalis* media adjusted to Baltic (CB) or North Sea (CN) salinity; MB: Marine Broth; PDA: potato dextrose agar; TSB: trypticase soy broth; WSP: modified Wickerham medium.

Compositionally, the cultivable microbiota was affiliated to three bacterial (Actinobacteria, Firmicutes, Proteobacteria) and two fungal phyla (Ascomycota, Mucoromycota; Table S1). Sanger sequencing allowed identification of all but one isolate to species (31 isolates) or genus (69 isolates) level. The gut-associated bacterial community was dominated by *Shewanella* sp. (H: 7 isolates, K: 6 isolates) and *Vibrio* sp. (H: 6 isolates, K: 8 isolates; Figure 2a). Out of 13 bacterial genera, six were exclusively found in Baltic *C. intestinalis* gut samples (*Klebsiella*, *Micromonospora*, *Nocardiopsis*, *Pseudomonas*, *Rhodococcus*, and *Sporosarcina*), while only two were exclusive to Helgoland (*Escherichia* and *Ruegeria*). Moreover, *Bacillus* sp. showed

higher abundance in Kiel (9 isolates) compared to samples from Helgoland (2 isolates). *Penicillium* was the predominant fungal genus with four (from H) or five isolates (from K), respectively (Figure 2b). Out of 20 detected fungal genera, only *Fusarium*, *Galactomyces*, *Penicillium*, and *Trichoderma* were common to both locations indicating a differential fungal diversity of the gut of *C. intestinalis* collected from Helgoland and Kiel Fjord. Helgoland-exclusive fungal genera included, e.g., *Arthrinium* sp. (2 isolates) and *Aspergillus* sp. (3 isolates). The gut of Baltic *C. intestinalis* delivered 10 exclusive fungal genera such as *Mucor* sp. (2 isolates), *Purpureocillium* sp. (3 isolates), and *Sarocladium* sp. (2 isolates).
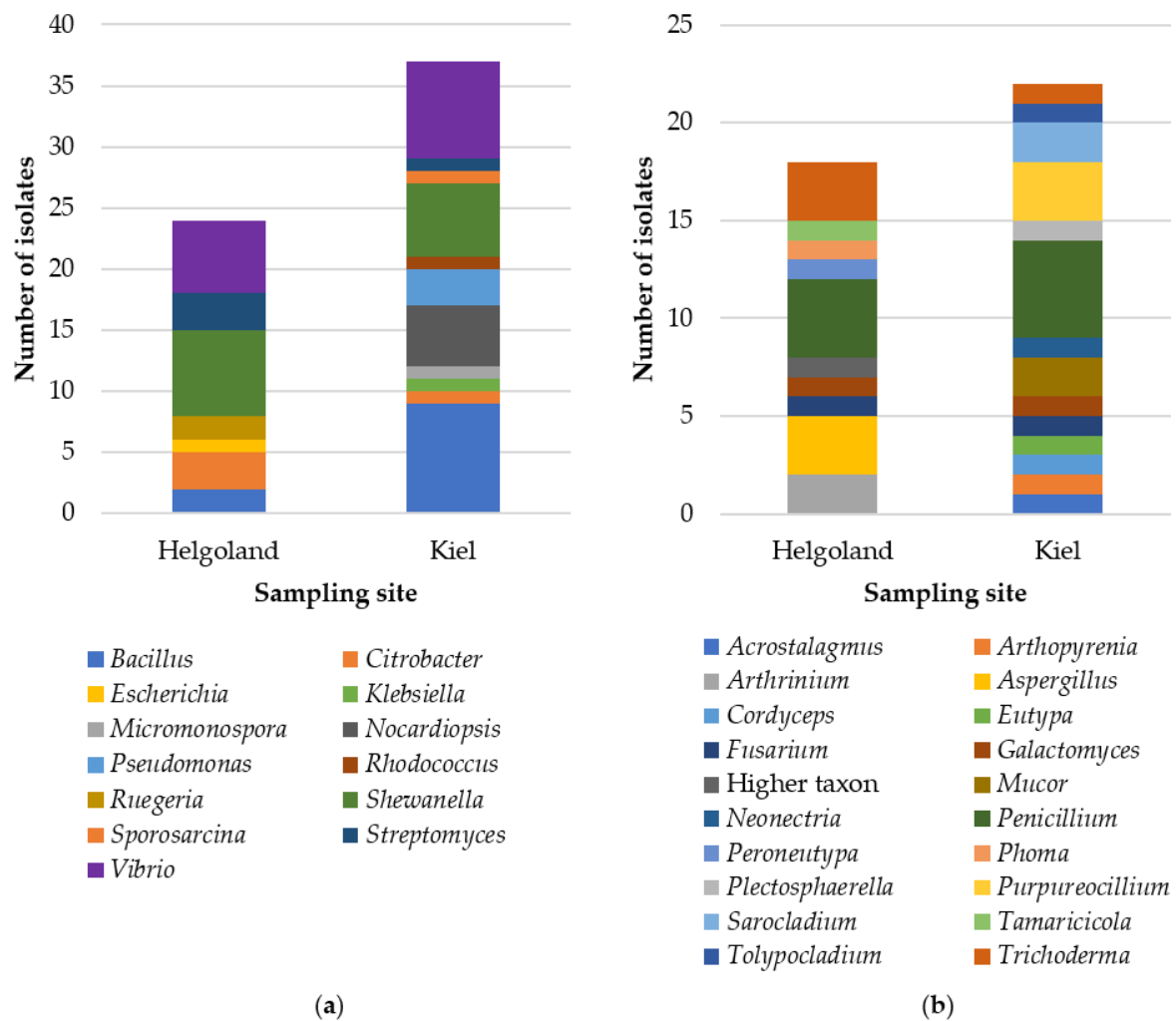
Figure 2. Diversity of (**a**) bacterial and (**b**) fungal isolates associated with the gut of *C. intestinalis* at genus level. The designation "Higher taxon" refers to isolate CHG49 (only identified to family level, Pleosporaceae).

2.2. Biological Activities of Gut-Derived Microbial Extracts

To assess the biotechnological potential of the gut-associated microbiota, bacterial isolates were cultured on the agar media glucose–yeast–malt (GYM) and Marine Broth (MB), while fungi were grown on solid casamino acids–glucose (CAG) and potato dextrose agar (PDA) media. Extracts received identification codes referring to the host organism *C. intestinalis* (C), the sampling site (H or K), the origin of the microbial isolates (gut, G), the respective strain number, and cultivation medium (CAG, GYM, MB or PDA). For example, CHG2-MB is the Marine Broth extract of strain 2 that was isolated from the gut of *C. intestinalis* sampled in Helgoland.

In vitro bioactivities were determined for 103 microbial crude extracts against eight human microbial pathogens including the ESKAPE panel (see Section 4.4.), *Candida albicans,* and *Cryptococcus neoformans,* and against four cancer cell lines. A total of 68 extracts (reflecting 66%) were active at a bioactivity threshold of ≥ 80% inhibition (= highly active, test concentration of 100 µg/mL) in at least one assay (Table S2). Most frequently, activity was observed against the Gram-positive bacterial pathogens methicillin-resistant *Staphylococcus aureus* (MRSA; 62%) and *Enterococcus faecium* (50%; Figure 3, Table S2). Notably, twelve crude extracts derived from the fungi *Acrostalagmus luteoalbus* (CKG66-CAG), *Galactomyces candidum* (CKG25-CAG, -PDA), *Penicillium* sp. (CHG25-CAG, -PDA, CHG35-CAG, -PDA, CKG23-CAG, -PDA, CKG63-PDA), and Pleosporaceae sp. (CHG49-CAG, -PDA) inhibited the growth of at least one Gram-negative test strain. The *Penicillium* sp. extract CHG25-CAG showed 98% to 100% growth inhibitory activity against all four Gram-negative bacterial pathogens (*Acinetobacter baumannii*, *Escherichia coli*, *Klebsiella pneumoniae,* and *Pseudomonas aeruginosa*). Eleven extracts exhibited antifungal activity against *Candida albicans* and/or *Cryptococcus neoformans*. Among them, three extracts, namely, extracts produced by *Streptomyces* sp. (CHG48-GYM) and *Trichoderma* sp. (CHG34-PDA and CKG62-PDA), were active against both fungal pathogens. Anticancer activity was detected in 23 crude extracts. Proliferation of all four cancer cell lines was inhibited by five bacterial (*Micromonospora* sp. CKG20-GYM; *Nocardiopsis prasina* CKG58-GYM; *Streptomyces* sp. CHG40-GYM, CHG48-GYM, CHG64-GYM) as well as ten fungal extracts (*A. luteoalbus* CKG66-CAG; *G. candidum* CKG25-CAG, -PDA; *Penicillium* sp. CHG25-CAG, -PDA, CKG23-CAG; Pleosporaceae CHG49-CAG; and *Trichoderma* sp. CHG34-CAG, -PDA, CKG62-PDA). Five extracts showed somewhat narrow spectrum anticancer activity, for example, *Fusarium* sp. extract CHG38-CAG strongly inhibited the growth of the human melanoma cells (A375, 98%) and colon cancer cells (HCT116, 93%), but was only moderately or poorly active against the lung cancer (A549, 65%) and breast cancer cells (MB231, 40%).
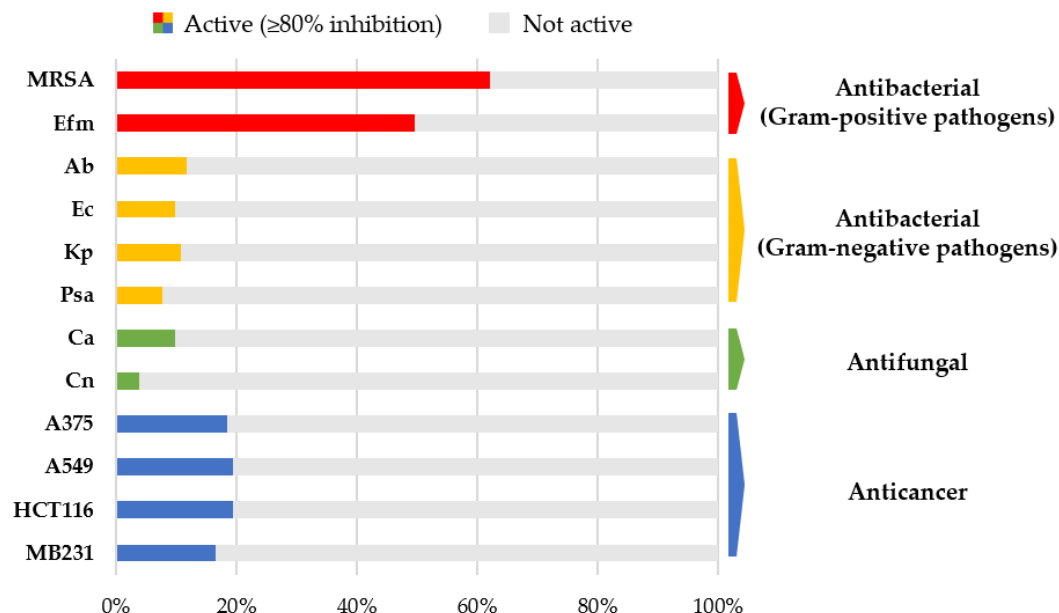
Figure 3. Antimicrobial and anticancer activities of 103 microbial crude extracts. Extracts were classified as active when showing inhibitory activity ≥ 80% at a test concentration of 100 µg/mL. Activities were determined against Gram-positive bacterial pathogens (red; MRSA: methicillin-resistant *Staphylococcus aureus*, Efm: *Enterococcus faecium*), Gram-negative bacterial pathogens (yellow; Ab: *Acinetobacter baumannii*, Ec: *Escherichia coli*, Kp: *Klebsiella pneumoniae*, Psa: *Pseudomonas aeruginosa*), fungal pathogens (green; Ca: *Candida albicans*, Cn: *Cryptococcus neoformans*) and cancer cell lines (blue; A375: malignant melanoma, A549: lung carcinoma, HCT116: colon cancer, MB231: breast cancer).

2.3. Bioactivity- and Metabolome-Based Selection of Microbial Extracts

In order to prioritize the most promising candidates out of 68 active crude extracts, we applied a two-step selection approach. In the first step, all extracts with i) high antimicrobial activity (≥ 80% inhibition) against at least one bacterial and one fungal pathogen, or ii) high anticancer activity (≥ 80% inhibition) against at least one cancer cell line, or iii) both, high antimicrobial and anticancer activity (≥ 80% inhibition), were selected. This approach allowed us to prioritize 26 extracts, including eight bacterial extracts obtained from *Bacillus* sp. (CKG24-GYM), *Micromonospora* sp. (CKG20-GYM), *N. prasina* (CKG58-GYM), *Pseudomonas anguilliseptica* (CKG38-GYM, -MB), and *Streptomyces* sp. (CHG40-GYM, CHG48-GYM, CHG64-GYM), as well as 18 fungal extracts originating from *A. luteoalbus* (CKG66-CAG), *Fusarium* sp. (CHG38-CAG, -PDA, CKG32-CAG), *G. candidum* (CKG25-CAG, -PDA), *Penicillium* sp. (CHG25-CAG, -PDA, CHG35-CAG, -PDA, CKG23-CAG, -PDA, CKG63-PDA), Pleosporaceae (CHG49-CAG, -PDA), and *Trichoderma* sp. (CHG34-CAG, -PDA, CKG62-PDA).

In the second step, metabolite profiling by an untargeted UPLC-MS/MS-based approach was applied to the 26 pre-selected extracts in order to detect those with the richest and most diverse chemistry. Pre-processed MS/MS data were converted into peak lists (*m/z* value, retention time, intensity) to generate PCoA (Principal Coordinates Analysis) plots reflecting the chemical distinctiveness of the bacterial (Figure 4) and fungal extracts (Figure 5).
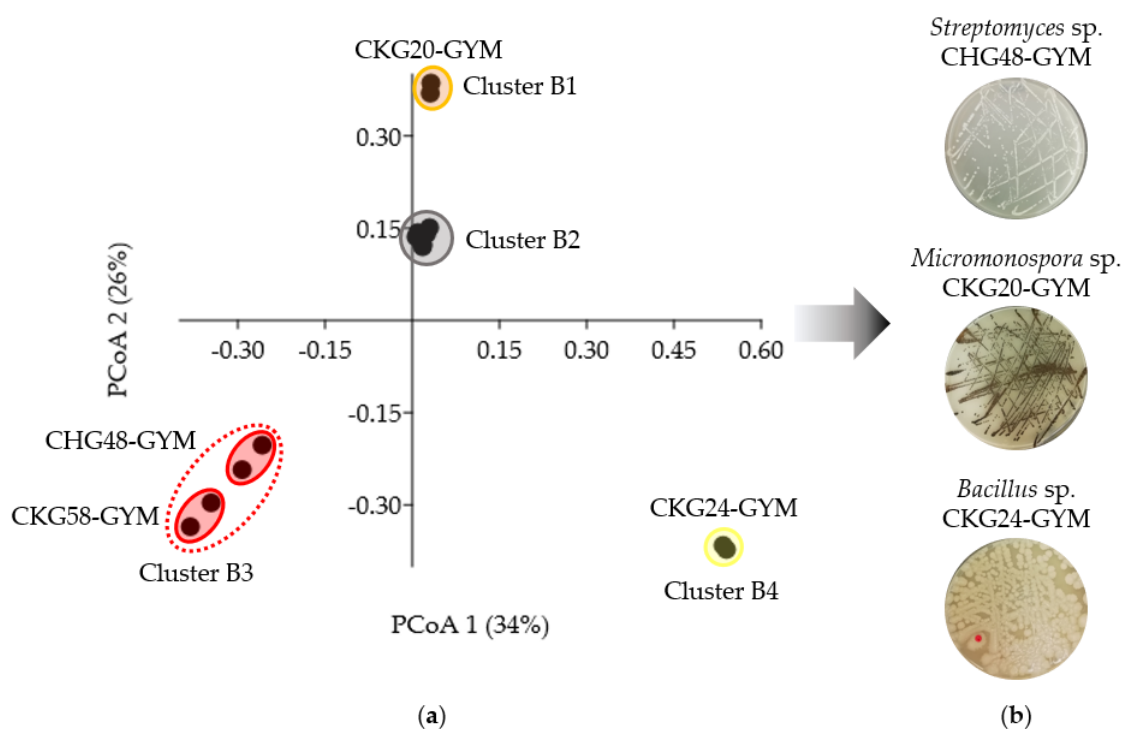
Figure 4. UPLC-MS/MS-based selection of bacterial extracts for in-depth metabolomics. (**a**) PCoA (Principal Coordinates Analysis) plot of eight pre-selected bioactive extracts. Cluster B2 includes extracts produced by *Pseudomonas anguilliseptica* (CKG38-glucose–yeast–malt (GYM) and -MB) and *Streptomyces* sp. (CHG40-GYM and CHG64-GYM). (**b**) Solid cultures of three bacterial extracts prioritized for further chemical investigations.
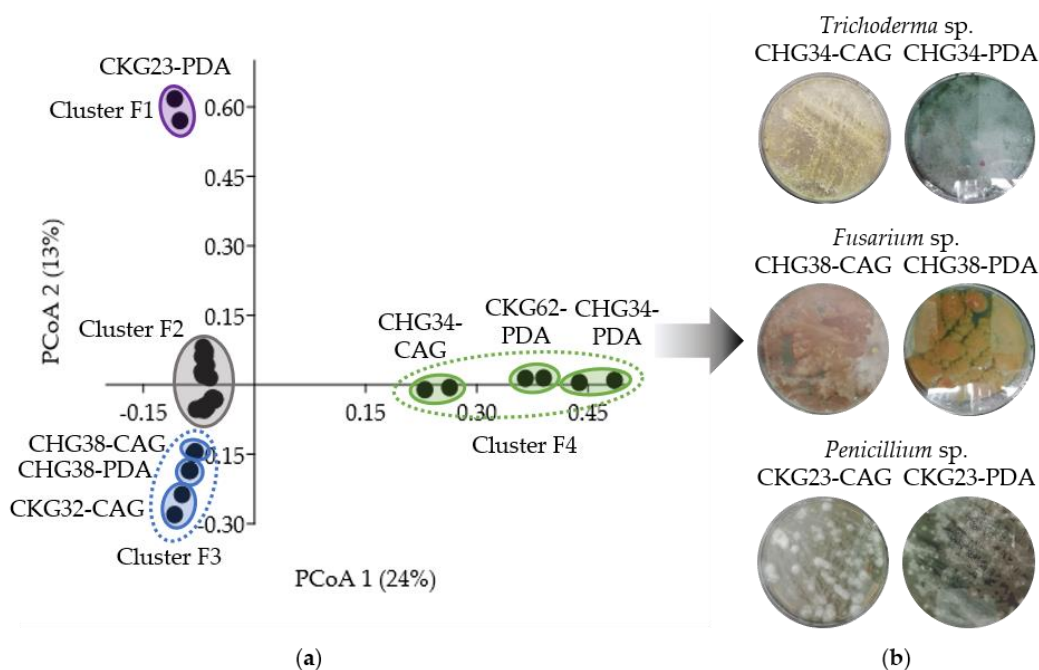
Figure 5. UPLC-MS/MS-based selection of fungal extracts for in-depth metabolomics. (**a**) PCoA plot of 18 pre-selected bioactive extracts. Cluster F2 includes extracts produced by *Acrostalagmus luteoalbus* (CKG66-casamino acids–glucose (CAG)), *Galactomyces candidum* (CKG25-CAG and -PDA), *Penicillium* sp. (CHG25-CAG and -PDA, CHG35-CAG and -PDA, CKG23-CAG, and CKG63-PDA), and Pleosporaceae sp. (CHG49-CAG and -PDA). (**b**) Solid cultures of six fungal extracts prioritized for further chemical investigations.

The PCoA plot of the eight pre-selected bacterial extracts clustered into four groups (B1–B4; Figure 4a). Three clusters, i.e., B1, B3, and B4, showed significant differences in their chemical profiles compared to cluster B2 (R = 1, $p < 0.05$; Table S3). The chemically distinct extracts in clusters B1, B3, and B4 had a higher number of detected peaks (80–110) compared to those clustering as B2 (9–66 peaks). *Micromonospora* sp. extract CKG20-GYM and *Bacillus* sp. extract CKG24-GYM clustered separately as B1 and B4, respectively. Accordingly, both were selected for further analysis. Cluster B3 was formed by two actinobacterial extracts with similar chemistry, namely, *N. prasina* extract CKG58-GYM and *Streptomyces* sp. extract CHG48-GYM. The latter extract was selected from cluster B3, since it showed higher bioactivity against *C. neoformans* (100% inhibition at 100 µg/mL; Table S2), and displayed, with 103 peaks, a more distinct metabolome than the other *Streptomyces* extracts CHG40-GYM (61 peaks) and CHG64-GYM (66 peaks) in cluster B2 (Figure S1). Hence, metabolite profiling aided the prioritization of the three bacterial extracts CHG48-GYM (*Streptomyces* sp.), CKG20-GYM (*Micromonospora* sp.), and CKG24-GYM (*Bacillus* sp.) for subsequent metabolomics studies (Figure 4b).

The same process was applied to 18 bioactive fungal extracts resulting in four different clusters in the PCoA plot (clusters F1–F4; Figure 5a). Extracts of three clusters (F1, F3, and F4) had significantly different metabolite profiles compared to extracts from cluster F2 (R = 0.68–1, $p < 0.01$; Table S4). Cluster F1 contained only one extract (*Penicillium* sp. CKG23-PDA), which was selected due to its strikingly different chemical profile. Cluster F3 consisted of three extracts obtained from two *Fusarium* sp. strains CHG38 (CAG and PDA) and CKG32 (PDA). From those, we selected strain CHG38 (CAG and PDA) because of the additional antifungal and anticancer bioactivities observed for the extract CHG38-CAG (96% inhibition against *C. neoformans,* 98% and 93% inhibition against cancer cell lines A375 and HCT116, respectively; Table S2). Similarly, cluster F4 contained in total three extracts from two *Trichoderma* sp. isolates CHG34 (CAG and PDA) and CKG62 (PDA). Revisiting these extracts´ bioactivities led to the selection of *Trichoderma* sp. strain CHG34 (CAG and PDA),

as its PDA extract showed in addition strong antibacterial (MRSA, 94%) and antifungal (*C. neoformans,* 92%) activities (Table S2). In addition, we added *Penicillium* sp. CKG23-CAG (cluster F2) to the analysis pipeline, although it did not fulfill the chemical distinctiveness criterion. It shared only few metabolites with the PDA extract from the same *Penicillium* sp. strain (CKG23-PDA), which clustered in F1. Therefore, we aimed to analyze, comparatively, these two chemically different extracts (CKG23-CAG and CKG23-PDA) produced by the same *Penicillium* sp. strain. In total, six fungal extracts were prioritized for further chemical analyses, namely CHG34-CAG and -PDA (*Trichoderma* sp.), CHG38-CAG and -PDA (*Fusarium* sp.), and CKG23-CAG and -PDA (*Penicillium* sp.; Figure 5b). This sums up to a total of nine microbial crude extracts for subsequent in-depth metabolomic analyses.

2.4. IC$_{50}$ Determinations of Prioritized Microbial Extracts

All nine prioritized extracts were subjected to IC$_{50}$ determinations (half maximal inhibitory concentration) against bacterial and fungal human pathogens (Table 1) as well as cancer cell lines (Table 2). The lowest IC$_{50}$ values against the Gram-positive test strains MRSA and *E. faecium* were obtained for *Streptomyces* sp. CHG48-GYM, *Micromonospora* sp. CKG20-GYM, *Bacillus* sp. CKG24-GYM, and *Fusarium* sp. CHG38-CAG (Table 1). Notably, the anti-MRSA potency of *Bacillus* sp. extract CKG24-GYM (IC$_{50}$ value 0.4 µg/mL) was about eight times higher than the positive control chloramphenicol (IC$_{50}$ 3.1 µg/mL). Another very potent bacterium was *Micromonospora* sp. grown in GYM medium (CKG20-GYM), which showed superior activity (IC$_{50}$ 0.1 µg/mL) to the reference antibiotic ampicillin (IC$_{50}$ 0.4 µg/mL) against *E. faecium.* Only *Penicillium* sp. extracts CKG23-CAG and -PDA showed inhibitory activity against the four Gram-negative bacterial test strains *A. baumannii*, *E. coli*, *K. pneumoniae*, and *P. aeruginosa.* Notably, IC$_{50}$ values of the CAG extract were more potent (IC$_{50}$ values between 4.9 and 15.8 µg/mL) than those of the PDA extract (IC$_{50}$ values between 31.4 and 42.6 µg/mL). Concerning antifungal activity, the lowest IC$_{50}$ value against *C. albicans* was exerted by the PDA extract of *Trichoderma* sp. isolate CHG34 (IC$_{50}$ value 3.7 µg/mL). With an IC$_{50}$ value of 13.1 µg/mL, *Streptomyces* sp. CHG48-GYM emerged as the most potent extract towards the yeast-like pathogen *C. neoformans*. When tested against cancer cell lines, all extracts showed inhibitory activity against at least one cancer cell line (IC$_{50}$ values between 0.02 and 92.3 µg/mL; Table 2). *Streptomyces* sp. extract CHG48-GYM showed the strongest anticancer activity with an IC$_{50}$ value 0.02 µg/mL against the lung carcinoma cell line A549, which was much lower compared to the positive control (IC$_{50}$ 1.3 µg/mL). *Micromonospora* sp. extract CKG20-GYM showed potent in vitro cytotoxicity against all four cancer cell lines (IC$_{50}$ values between 0.8 and 1.6 µg/mL). Among the fungal extracts, *Penicillium* sp. extract CKG23-CAG exerted the strongest antiproliferative effects (IC$_{50}$ values between 2.0 and 8.5 µg/mL).

Table 1. IC$_{50}$ values (in µg/mL) of selected extracts against eight microbial human pathogens. MRSA: methicillin-resistant *S. aureus*; Efm: *E. faecium*; Ab: *A. baumannii*; Ec: *E. coli*; Kp: *K. pneumoniae*; Psa: *P. aeruginosa*; Ca: *C. albicans*; Cn: *C. neoformans*. Positive controls: chloramphenicol (MRSA, Ec, Kp), ampicillin (Efm), doxycycline (Ab), polymyxin B (Psa), nystatin (Ca), and amphotericin (Cn).

Extract	Identification	MRSA	Efm	Ab	Ec	Kp	Psa	Ca	Cn
CHG48-GYM	*Streptomyces* sp.	5.0	4.5	> 100	> 100	> 100	> 100	12.9	13.1
CKG20-GYM	*Micromonospora* sp.	10.3	0.1	> 100	> 100	> 100	> 100	> 100	> 100
CKG24-GYM	*Bacillus* sp.	0.4	2.0	> 100	> 100	> 100	> 100	> 100	17.1
CHG34-CAG	*Trichoderma* sp.	> 100	> 100	> 100	> 100	> 100	> 100	> 100	> 100
CHG34-PDA	*Trichoderma* sp.	36.8	32.0	> 100	> 100	> 100	> 100	3.7	58.8
CHG38-CAG	*Fusarium* sp.	4.0	3.0	> 100	> 100	> 100	> 100	9.9	20.9
CHG38-PDA	*Fusarium* sp.	10.8	7.6	> 100	> 100	> 100	> 100	11.4	> 100
CKG23-CAG	*Penicillium* sp.	19.8	29.8	4.9	15.6	8.9	15.8	> 100	> 100
CKG23-PDA	*Penicillium* sp.	8.3	18.1	42.5	41.0	31.4	42.6	> 100	> 100
Positive control		3.1	0.4	0.02	1.4	0.4	0.4	1.3	0.1

Table 2. IC$_{50}$ values (µg/mL) of selected extracts against four cancer cell lines. A375: malignant melanoma cell line; A549: lung carcinoma cell line; HCT116: colon cancer cell line; MB231: breast cancer cell line. Positive control: doxorubicin.

Extract	Identification	A375	A549	HCT116	MB231
CHG48-GYM	*Streptomyces* sp.	5.8	0.02	21.4	22.1
CKG20-GYM	*Micromonospora* sp.	0.8	1.6	1.3	1.4
CKG24-GYM	*Bacillus* sp.	70.7	67.9	86.6	> 100
CHG34-CAG	*Trichoderma* sp.	67.9	70.1	71.9	69.7
CHG34-PDA	*Trichoderma* sp.	19.3	31.1	24.1	32.8
CHG38-CAG	*Fusarium* sp.	35.9	70.1	62.1	> 100
CHG38-PDA	*Fusarium* sp.	92.3	> 100	> 100	> 100
CKG23-CAG	*Penicillium* sp.	2.0	4.9	8.5	2.5
CKG23-PDA	*Penicillium* sp.	5.2	17.5	27.6	9.0
Positive control		0.8	1.3	13.3	2.3

2.5. Feature-Based Molecular Networking and Dereplication of Nine Prioritized Microbial Extracts

We comparatively analyzed the metabolome of the nine prioritized extracts by an integrated dereplication strategy combining FBMN, in silico dereplication tools, and manual approaches. Chemical structures of the putatively annotated metabolites, dereplication tables, and generated FBMNs are shown in the Supplementary Figures S2–S8 and Tables S5–S10.

Global metabolome analyses of three selected bacterial extracts, *Streptomyces* sp. CHG48-GYM, *Micromonospora* sp. CKG20-GYM, and *Bacillus* sp. CKG24-GYM, revealed a high metabolite diversity with a total of 220 nodes (ions) organized into 35 molecular clusters (Figure 6). Out of the 35 molecular clusters, 21 were putatively annotated as acetamide derivatives, cyclic peptides (including lipo- and depsipeptides), diterpenoid glycosides, glycerophospholipids, isocoumarin derivatives, nonactic acid polyketides, oxazolidone alkaloids, phenazine alkaloids, and polyketide glycosides. The global FBMN was dominated by several types of cyclic peptides, produced by *Micromonospora* sp. (CKG20-GYM) and *Bacillus* sp. (CKG24G-GYM). The *Bacillus* sp. extract CKG24-GYM exhibited the richest metabolite diversity (89 nodes), followed by *Streptomyces* sp. CHG48-GYM (73 nodes), and *Micromonospora* sp. CKG20-GYM (61 nodes). The chemical diversity of *Bacillus sp.* extract CKG24-GYM was also reflected in the number of exclusive clusters (15 exclusive molecular clusters) compared to CHG48-GYM (11 exclusive molecular clusters) and CKG20-GYM (6

exclusive molecular clusters). Most molecular clusters (91%) in the composite FBMN were exclusive to one bacterial extract. Shared metabolites, only detected in two molecular clusters, remained unannotated.

In-depth chemical investigations of *Streptomyces* sp. extract CHG48-GYM led to the putative annotation of the alkaloids streptazolin (**2**) and streptenol E (**3**), the diterpenoid glycoside platensimycin B4 (**6**), the linear polyketide alpiniamide A (**7**), and four nonactic acid polyketides (**12**,**14**,**18**,**33**; Figure 6 and Figure S3 and Table S5). Nonactic-acid-type polyketides formed the two largest clusters in the molecular network of *Streptomyces* sp., representing protonated ([M + H]$^+$) and sodiated adducts ([M + Na]$^+$) detected from this chemical family (Figure S3). FBMN-based dereplication led to the putative annotation of, e.g., nonactic acid polyketides. MS/MS library spectra of bonactin (**14**) and homononactyl homononactate (**18**) deposited at the Global Natural Products Social Molecular Networking platform (GNPS, [34]) revealed a precise match with the MS/MS spectra detected for *m/z* 401.2540 [M + H]$^+$ (**14**) and *m/z* 415.2702 [M + H]$^+$ (**18**; Figures S9 and S10). This aided manual identification of nonactyl nonactoate (**12**) and nonactin (**33**). Nevertheless, most compounds and clusters could not be linked to any known chemical entity, and, therefore, many compounds (76%) in *Streptomyces* sp. extract CHG48-GYM remained unknown.
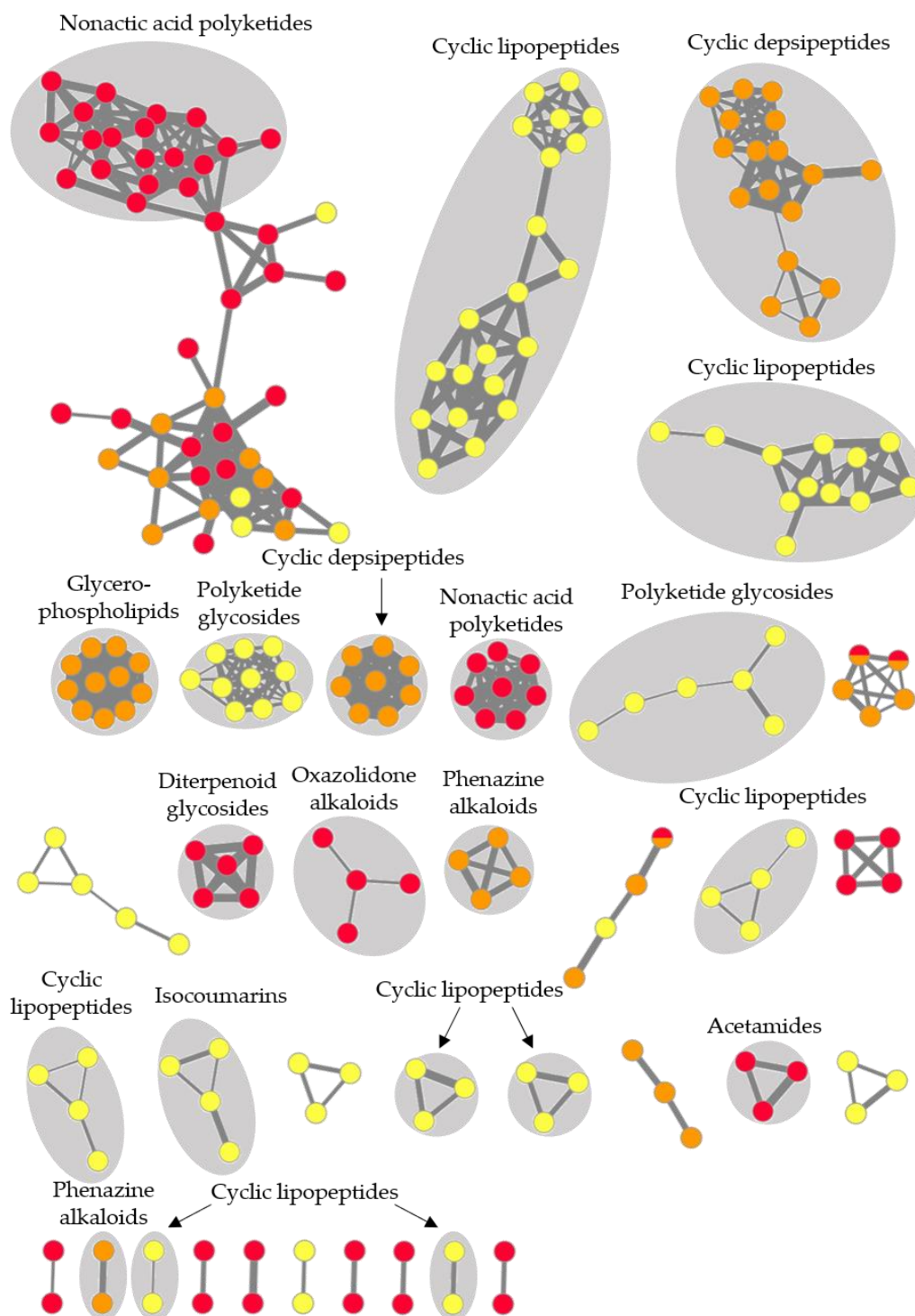
Figure 6. UPLC-MS/MS-based metabolome of three bacterial extracts. The feature-based molecular network (FBMN) displays only clusters containing ≥ 2 nodes. The width of edges represents the cosine similarity between 2 nodes. Nodes are color-coded by the respective extract: red: *Streptomyces* sp. extract CHG48-GYM; orange: *Micromonospora* sp. extract CKG20-GYM; yellow: *Bacillus* sp. extract CKG24-GYM.

The *Micromonospora* sp. isolate CKG20 (GYM medium) showed the lowest chemical diversity of all prioritized bacterial extracts (Figure 6 and Figure S4, Table S6). Putatively identified compounds belonged to phenazine alkaloids (**44**,**48**) and cyclic depsipeptides (**51**–**53**), of which the latter was the dominant chemical family in this extract. Cyclic depsipeptides

95

were represented in three molecular clusters in the FBMN, since MS/MS analysis detected three different adduct types ([M + H]$^+$, [M + Na]$^+$, [M + K]$^+$) that formed their own clusters due to their specific fragmentation patterns. In addition, the GNPS dereplication workflow annotated three compounds to known ubiquitous cell membrane components, i.e., glycerophospholipids (**42**,**45**,**50**). The majority (60%) of the detected metabolites and two molecular clusters did not match with any known compound.

Putatively identified compounds of *Bacillus* sp. extract CKG24-GYM were classified into three different chemical families, namely, isocoumarin derivatives (**55**,**59**,**60**), polyketide glycosides (**64**), and various cyclic lipopeptides (**61**–**63**,**65**,**66**,**68**–**72**,**74**,**76**,**77**,**79**,**81**,**82**,**84**–**87**; Figure 6, Figure S5, Table S7). In the FBMN, the dominance of cyclic lipopeptides was reflected by eight molecular clusters putatively annotated to this NP family. Putatively annotated cyclic lipopeptides can be further classified into bacillomycins (**61**-**63**; *m/z* 1071.5811-1099.6122 [M + H]$^+$), plipistatins (**65**,**66**,**68**–**72**; *m/z* 731.4171–753.4296 [M + 2H]$^{2+}$), and surfactins (**74**,**76**,**77**,**79**,**81**,**82**,**84**–**87**; *m/z* 994.6426–1064.7209 [M + H]$^+$; Figure S5, Table S7). The putative assignment to three different subfamilies (bacillomycins, plipistatins, surfactins) and the detection of different adduct types (e.g., surfactins: [M + H]$^+$ and [M + Na]$^+$ adducts) explain the formation of several distinct lipopeptide clusters. The highest annotation rate in this study (71%) was achieved for this extract, i.e., only 10 compounds (**54**,**56**–**58**,**67**,**73**,**75**,**78**,**80**,**83**) remained unannotated.

FBMN-based analysis also proved the high metabolite diversity (411 ions in total, 52 distinct molecular clusters) of the six selected fungal extracts (Figure 7). Putatively annotated clusters included alkaloids (indole and cytochalasan alkaloids), peptides (e.g., peptaibols), polyketides (e.g., macrolides), steroids (ergosterols), and terpenoids (mero- and sesquiterpenoids). The largest molecular cluster, putatively annotated by GNPS and in silico dereplication workflows, is xanthone and zearalenone type polyketides. It contained metabolites produced by all three fungal strains. With the exception of this shared polyketide cluster, the chemical diversity of the selected strains differed. As an example, *Trichoderma* sp. showed 171–173 nodes and 24 exclusive clusters in the global network and was the most chemically diverse. *Fusarium* sp. and *Penicillium* sp. produced only eight and fifteen exclusive clusters, respectively.

Trichoderma sp. isolate CHG34 produced ergosterols, sorbicillinoid-type polyketides, and peptaibols (Figure 7, Figure S6 and Table S8), of which the latter dominated the metabolome. Various peptaibols such as trichokindins (**125**,**143**,**144**,**147**,**150**,**151**,**154**,**155**,**157**) and neoatroviridins (**149**,**156**,**160**) were putatively annotated. As depicted in the FBMN (Figure S6), peptaibols are often detected as doubly charged (sodiated) ions ([M + 2H]$^{2+}$ and [M + 2Na]$^{2+}$) [35,36]. Accordingly, several distinct peptaibol clusters such as trichokindins and neoatroviridins were annotated. Despite our integrated dereplication efforts, most compounds (73%) in the *Trichoderma* extracts remained unannotated (Table S8). The amino acid sequence of two unannotated compounds, *m/z* 770.5386 [M + H]$^+$ (**103**) and *m/z* 754.5424 [M + H]$^+$ (**105**) (highlighted as "putatively novel lipopeptides" in the global MN; Figure 7 and S6 and Table S8), were putatively predicted based on characteristic MS/MS fragments (Figure 8 and Figure S11). Tandem mass spectrometry (MS/MS) is an essential tool in peptide chemistry since mass differences of produced fragment ions allow the determination of the amino acid sequence of peptides [37]. Analysis of the MS/MS spectra of **103** and **105** revealed that both compounds contained seven amino acid residues. The first observed fragment of **103** (*m/z* value of 184.1341) reflects the fatty acyl moiety Oc (octanoyl) connected to Gly ($C_{10}H_{18}NO_2$) at the N-terminus of the putative peptide. The loss of *m/z* 230.1994 ($C_{12}H_{26}N_2O_2$) positioned Leu/Ile-Leuol/Ileol at the C-terminus of **103**. The full sequence of **103** (*m/z* 770.5386 [M + H]$^+$) determined by MS/MS fragmentation was proposed as N-Oc-Gly-Gly-Leu/Ile-Val-Ser-Leu/Ile-Leuol/Ileol. The second putatively novel linear peptide (**105**, *m/z* 754.5424 [M + H]$^+$) had a similar amino acid sequence as **103** but with Ser replaced by Ala. Accordingly, these two molecular ions may be novel linear seven-residue lipopeptides produced by

Trichoderma sp. strain CHG34. The CAG and PDA extract of *Trichoderma* sp. CHG34 showed a high overlap of their chemical space (82%) with 61 shared metabolites (Table S8).

In *Fusarium* sp. extracts CHG38-CAG and -PDA, the cyclic lipopeptide fusaristatin A (**182**) and chromone (**164**,**165**), isocoumarin (**166**), naphthoquinone (**162**,**163**,**168**), xanthone (**171**,**178**), and zearalenone (**169**,**176**,**179**) polyketides were annotated (Figure 7, Figure S7 and Table S9). According to the cluster analysis, xanthone and zearalenone polyketides dominated the FBMN by forming the two largest clusters. Zearalenone (**176**) was predicted by the GNPS-based MS/MS spectral match and guided us to putatively annotate 2'-hydroxyzearalanol (**169**) and zearalanone (**179**) in the same cluster. The majority of compounds (62%) remained unidentified. Notably, cultivation of *Fusarium* sp. strain CHG38 triggered the production of several metabolites that were exclusive to either CAG (10 compounds) or PDA (16 compounds) medium.
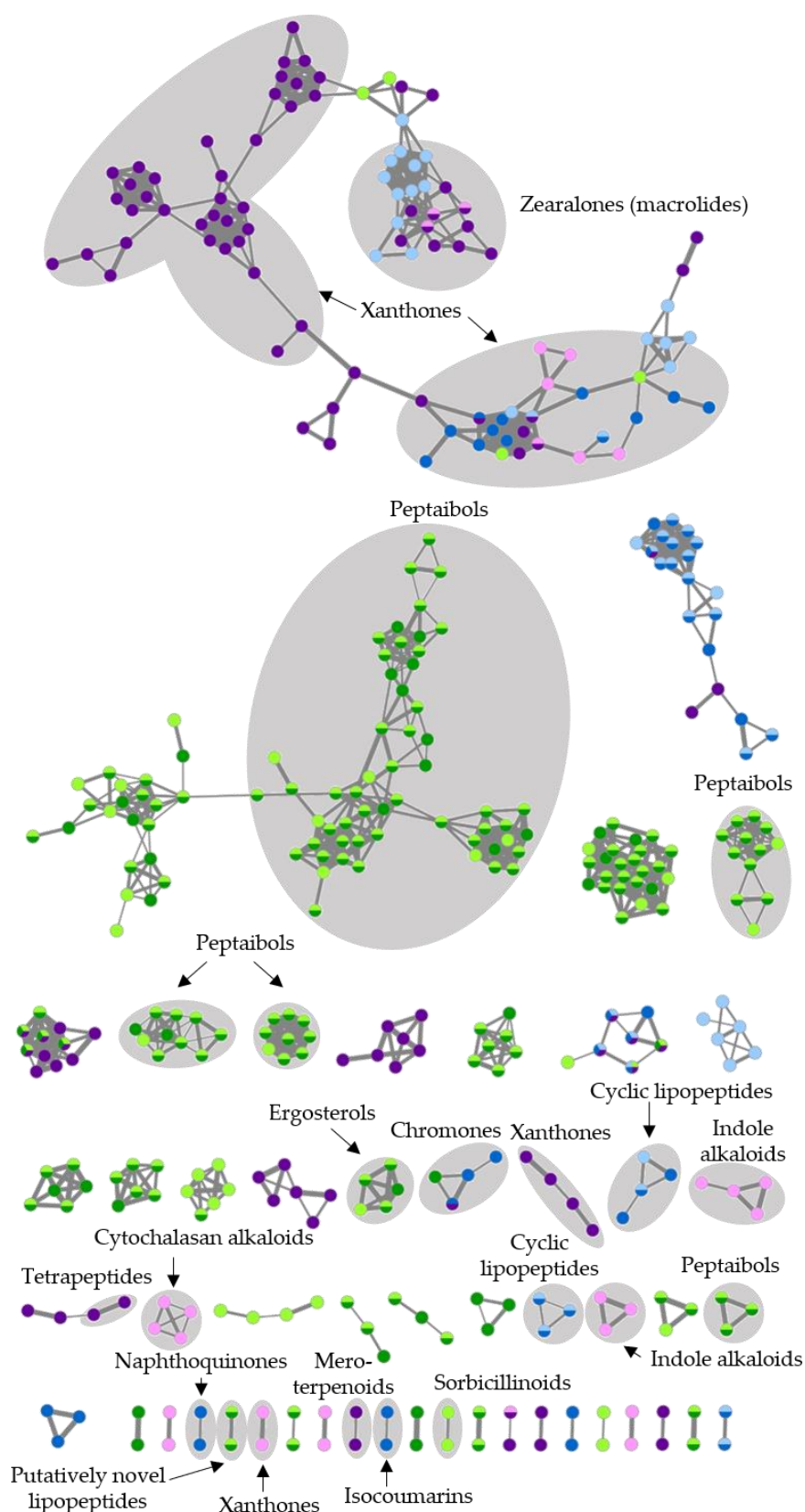
Figure 7. Global UPLC-MS/MS-based metabolome of six fungal extracts. The FBMN displays only molecular clusters containing ≥ 2 nodes. The width of edges represents the cosine similarity between 2 nodes. Nodes are color-coded by the respective extract (CAG: light color; PDA: strong color): green: *Trichoderma* sp. strain CHG34; blue: *Fusarium* sp. strain CHG38; purple: *Penicillium* sp. strain CKG23.

Oc – Gly		Gly	Leu/Ile	Val	Ser	Leu/Ile – Leuol/Ileol

| m/z | 184.1341 | 241.1556 | 354.2390 | 453.3080 | 540.3392 | 770.5386 |

(a)

Oc – Gly		Gly	Leu/Ile	Val	Ala	Leu/Ile – Leuol/Ileol

| m/z | 184.1333 | 241.1559 | 354.2397 | 453.3080 | 524.3521 | 754.5424 |

(b)
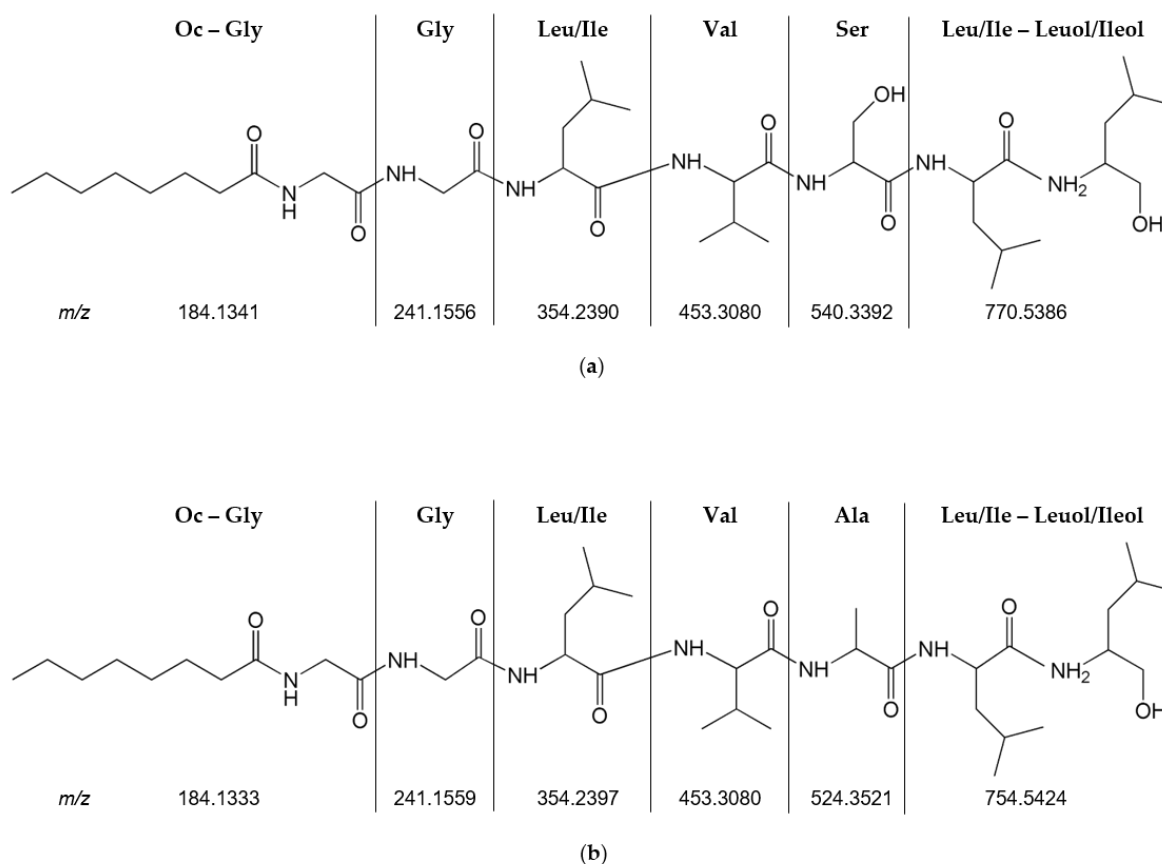
Figure 8. Two putatively novel seven-residue lipopeptides detected in *Trichoderma* sp. extracts CHG34-CAG and CHG34-PDA. Structures were putatively predicted based on the experimentally determined MS/MS fragments for (**a**) compound **103** (m/z 770.5386 [M + H]$^+$) and (**b**) compound **105** (m/z 754.5423 [M + H]$^+$). Ala: alanine; Gly: glycine; Leu/Ile: (iso)leucine (leucine is displayed); Leuol/Ileol: (iso)leucinol (leucinol is displayed); Oc: octanoyl; Ser: serine; Val: valine.

The metabolome of *Penicillium* sp. strain CKG23 contained eight different chemical families, such as cytochalasans (**209,212**), indole alkaloids (**206,219**), meroterpenoids (**222**), sesquiterpenoids (**213**), and various types of polyketides including zearalenone derivatives (**197,199,205,208,224**; Figure 7 and Figure S8, Table S10). The largest cluster in the FBMN belonged to the polyketide family xanthones, which were also detected in *Fusarium* and *Trichoderma* sp. extracts in the global FBMN. Notably, the CAG and PDA extracts of *Penicillium* sp. strain CKG23 shared only seven molecular ions (Figure S12). Moreover, CKG23-PDA showed a strikingly higher chemical diversity with 185 detected peaks compared to CKG23-CAG (51 peaks). For example, most putatively identified compounds in the zearalenone cluster were only detected in the PDA extract of *Penicillium* sp. (**197,199,205,224**), while no compound was exclusive to extract CKG23-CAG.

The untargeted metabolomics approach employed here revealed the huge chemical inventory of nine microbial extracts (Table 3). The metabolomes showed large variations between the different microbial taxa, but also the applied cultivation media impacted the chemical diversity. Compared to low annotation rates of < 2% normally achieved in untargeted metabolomics studies [38], the integrated dereplication effort applied herein significantly improved the putative annotation rates ranging from 24% (*Streptomyces* sp. extract CHG48-GYM) to 71% (*Bacillus* sp. extract CKG24G). Nevertheless, many compounds and molecular

clusters did not match any known compounds, suggesting that they could represent putatively new compounds.

Table 3. Summary of the chemical inventory of nine selected crude extracts explored by untargeted FBMN-based metabolomics. Each extract is given with the number of nodes detected in the global bacterial (Figure 6) or fungal (Figure 7) FBMNs. In addition, putatively identified chemical families and annotation rates are indicated for each strain.

Extract	Identification	Nodes	Putatively annotated chemical families	Annotation rate (%)
CHG48-GYM	*Streptomyces* sp.	73	Acetamides, diterpenoid glycosides, linear polyketides, nonactic acid polyketides, oxazolidone alkaloids	24
CKG20-GYM	*Micromonospora* sp.	61	Cyclic depsipeptides, phenazine alkaloids, glycerophospholipids	40
CKG24-GYM	*Bacillus* sp.	89	Cyclic lipopeptides, isocoumarins, polyketide glycosides	71
CHG34-CAG	*Trichoderma* sp.	173	Ergosterols, peptaibols, sorbicillinoids	27
CHG34-PDA	*Trichoderma* sp.	171		
CHG38-CAG	*Fusarium* sp.	53	Chromones, cyclic lipopeptides, isocoumarins, naphthoquinones, xanthones, zearalenones	38
CHG38-PDA	*Fusarium* sp.	54		
CKG23-CAG	*Penicillium* sp.	29	Cytochalasans, indole alkaloids, mero- and sesquiterpenoids, styrylpyrones, tetrapeptides, xanthones, zearalenones	48
CKG23-PDA	*Penicillium* sp.	108		

3. Discussion

In the present study, the unexplored gut microbiota of the tunicate *C. intestinalis* was investigated for its potential to deliver novel MNPs with pharmaceutical potential. The obtained strain collection represents with 101 gut-associated bacteria and fungi (Figure 1a, Table S1) the most comprehensive strain collection from the tunicate's gut available to date. A diverse microbial community (i.e., 33 different genera) was obtained from six different isolation media, which showed different suitability for growth of a diverse array of microorganisms (Figure 1b). For instance, glucose is a common carbon source for fungi [39], and, accordingly, most fungi were obtained from the glucose-containing media, WSP and PDA. In addition, media containing several carbon sources and other complex compounds often yield the highest microbial diversity [18], and this is in line with our finding that most isolates were obtained from the complex WSP medium (glucose, malt extract, peptone, and yeast extract). This indicates that the selection of isolation media has a huge impact on the isolated microbiota due to specific nutrient requirements of different microorganisms [18,19]. Furthermore, other cultivation conditions such as temperature (22 °C) also significantly influence the cultivable fraction of bacteria and fungi [18,19].

Although highly abundant bacterial genera such *Shewanella* and *Vibrio* and fungal genera such as *Penicillium* and *Trichoderma* (Figure 2) were previously isolated from the gut of *Ciona* spp. [23,26–28], most microbial genera were isolated for the first time from the gut of *C. intestinalis*. The high abundance of Gammaproteobacteria is in accordance with a previous culture-independent study performed on the gut microbiome of *Ciona* spp. [29]. We have recently described the cultivable microbiota of the tunic of *C. intestinalis* [31] that differed strikingly from the gut-associated microbial community isolated herein. Both tissues shared only few microbial genera (e.g., bacteria: *Bacillus* and *Vibrio*; fungi: *Fusarium* and *Penicillium*), which is in accordance with culture-independent microbiome studies on the gut and tunic of *Ciona* spp., indicating tissue-specific microbial communities [29,30]. Moreover, the diversity of culture-dependent fungi was higher in the gut (gut: 40 isolates assigned to 20 genera; tunic: 22 isolates, 15 genera), while bacteria were more prominent in the tunic (89 isolates assigned 37 genera; gut: 61 isolates, 13 genera) [31]. In line with our previous study on the tunic-

associated microbiota [31], the gut-associated microbiota, especially the bacterial community, was more diverse in Kiel than in Helgoland samples (Figures 1 and 2). This may be attributed to different salinity levels (Kiel: brackish, Helgoland: oceanic salinity) and the comparably higher anthropogenic input, i.e., more eutrophic conditions, at the sampling site in Kiel Fjord [31]. Moreover, samples were obtained from different depths (Helgoland: < 1 m depth; Kiel: approx. 3 m depth) and different artificial surfaces (Helgoland: pontoon; Kiel: mussel-cultivation basket), which both may have influenced the obtained microbial diversity. Other parameters not determined in this study, e.g., diet, water temperature, and the age and genetic background of the sampled specimens, may be additional factors shaping the diversity of the cultivable microbiota [18,40,41].

Gut-derived microbial extracts (n = 103) were screened against a panel of cancer cell lines and microbial pathogens, since ascidians and their associated microorganisms are well-known producers of MNPs with antimicrobial and anticancer properties [11,13,42]. The antimicrobial assays included the so-called ESKAPE panel, drug-resistant bacterial pathogens that were categorized by the WHO as priority level 1 and 2 for the discovery of new antimicrobial agents [43]. Most extracts (n = 65) exhibited activity against MRSA and/or *E. faecium*, but also anticancer (n = 23) and antifungal (n = 11) activities were observed (Figure 3, Table S2), exceeding bioactivity levels previously reported for cultivable bacteria associated with solitary ascidians [44,45]. The high rate of bioactivity observed in this study is in line with the excellent biodiscovery potential reported for tunicates and their microbial associates [11,13,42]. As outlined before, an intact gut microbiota has crucial functions for the health and performance of its host [1,3]. Possible functions related to chemical defense and nutrition were already proposed for cultivable bacteria obtained from the intestine of a solitary ascidian and a sea urchin [46,47]. The high proportion of microorganisms with, e.g., antibacterial properties (64%) indicates their potential involvement in the tunicate's chemical defense. However, it was beyond the scope of this study to detect specific functions fulfilled by specific cultivable gut-associated microorganisms in the host–microbiota interplay.

Bioactive crude extracts (n = 68) were subjected to a two-step selection procedure considering the bioactivity profile and chemical diversity of the extracts to prioritize the most promising extracts for in-depth metabolome mining. This strategy aided prioritization of nine microbial extracts affiliated to the bacterial genera *Bacillus*, *Micromonospora*, and *Streptomyces* as well as the fungal genera *Fusarium*, *Penicillium*, and *Trichoderma* (Figures 4 and 5). These microbial genera are known as the most talented producers of MNPs highlighting the strength of the applied prioritization pipeline (e.g., [9,48,49]).

The integrated dereplication approach combining automated and manual dereplication tools allowed the putative identification of 94 metabolites (Tables S5–S10). They belonged to various NP classes such as alkaloids, lipids, peptides, polyketides, steroids, and terpenoids, revealing a huge metabolic capacity of the prioritized microbial strains. Dereplication was substantially supported by the recently released FBMN workflow [32], which, in combination with other tools, led to annotation rates of up to 71%. Increasing annotation rates in untargeted metabolomic experiments is crucial to overcome time-consuming re-isolation of known compounds, which severely hampers biodiscovery efforts [33].

Untargeted metabolomics studies on fungi (e.g., *Fusarium* and *Penicillium* spp. [31,50,51]) and bacteria (e.g., *Streptomyces* and *Salinispora* spp. [52]) cultured on the same medium already revealed huge chemical variations at both species and strain level and are therefore used as chemotaxonomic species discrimination markers ([51] and references therein). Hence, we expected to find distinct chemical profiles of strains from the same genus, e.g., *Penicillium* or *Streptomyces* (Figure 4, Figure 5 and Figure S1, Tables S3–S4). Beyond this, variations in metabolite diversity in different media is also a well-known phenomenon in the OSMAC (one strain–many compounds) approach [53]. In line with this, *Fusarium* sp. strain CHG38 and *Penicillium* sp. strain CKG23 showed differential bioactivities and metabolomes when cultured on two different media (Figure 7, Figure S7–S8 and S12, Table 1, Table 2 and Tables S9–S10). Furthermore, the fungal cultivation media CAG and PDA appeared to trigger

the production of various (bioactive) metabolites, e.g., the metabolomes of *Fusarium* sp. CHG38 and *Penicillium* sp. CKG23 were richer when cultured on PDA medium, while cultivation of *Trichoderma* sp. on CAG yielded more compounds (Figure 7, Tables S8–S10). Both media contain the simple sugar glucose, an ideal carbon source for fungal growth [39], plus an additional mixed carbon source, which seemingly meets requirements for fungal growth and production of secondary metabolites. In contrast, GYM and MB media used for bacterial strains were not equally suitable as only one bacterial extract obtained from cultivation on MB medium met the bioactivity selection criterion (*P. anguilliseptica* extract CKG38-MB), while seven GYM extracts exerted strong antimicrobial and/or anticancer activities (Table S2). While MB medium mimics the major mineral composition of seawater, GYM medium lacks these minerals, but contains glucose and malt extract, which are easily accessible carbon sources. However, eleven bacterial strains, including all *Vibrio* sp. isolates, failed to grow on GYM medium. This may be attributed to the lack of sodium chloride (NaCl) in this medium, since most *Vibrio* spp. require NaCl for growth [54]. Apart from the media composition, other parameters such as the temperature, solid regime (in contrast to liquid cultures) or aeration may have influenced the observed chemical composition [53,55]. Moreover, artificial laboratory conditions often lack important environmental cues such as multispecies interactions, which can lead to, e.g., silencing of important biosynthetic gene clusters [55]. Therefore, the obtained metabolomic compositions may not necessarily reflect the true metabolite repertoire of the organism [55].

The observed anti-MRSA and *E. faecium* activity of *Streptomyces* sp. extract CHG48 (Table 1) might be explained by the diterpenoid glycoside platensimycin B (**6**) and two nonactic acid polyketides (**18**,**33**), all with reported antibacterial activities [56-59]. The putatively annotated polyketide homononactyl homononactate (**18**) shows weak activity against colon cancer cell line HCT116 [60], but not against lung cancer cell line A549 [56]. Hence, this compound cannot explain the detected selective anticancer activities against cell lines A549 and A375 (Table 2). Moreover, none of the dereplicated metabolites can explain the detected antifungal activities of *Streptomyces* sp. extract CHG48-GYM against *C. albicans* and *C. neoformans* (Table 1), and the annotation rate was the lowest detected in this study (24%; Table S5). We therefore consider *Streptomyces* sp. isolate CHG48 as a promising candidate strain for isolation of its chemical constituents.

The antibacterial and anticancer activities (Tables 1 and 2) of *Micromonospora* sp. (CKG20-GYM) may be attributed to the putatively annotated cyclic depsipeptides rakicidins (**51**–**53**) [61-63] and the phenazine alkaloid diazepinomicin (**44**) [49,64] (Figure 6 and Figure S4, Table S6), for which these activities are known. About 60% of the detected compounds remained unannotated, including a putatively novel rakicidin derivative (**49**), which is worth investigating in future studies.

The *Bacillus* sp. extract CKG24-GYM inhibited the growth of microbial pathogens and showed antiproliferative activity against cancer cell lines A375, A549 and HCT116 (Tables 1 and 2). Anti-MRSA activity has been described for the putatively identified isocoumarin derivative amicoumacin-A (**55**) [65] and the polyketide glycoside aurantinin B (**64**) [66]. Inhibitory activities against colon cancer cell line HCT116 are reported for some surfactin-like lipopeptides (**79**,**82**,**84**,**86**) [67]. Bacillomycins (**61**–**63**) [68] and some cyclic lipopeptides (**65**,**66**,**68**–**72**) reportedly show antifungal properties [69] possibly relating to the observed fungicidal activity of CKG24-GYM. In combination with the high annotation rate (71%), these results render *Bacillus* sp. extract CKG24-GYM not favorable for future studies.

Among the fungi, *Trichoderma* spp. are the major source of peptaibols [70,71] and, accordingly, extracts of *Trichoderma* sp. strain CHG34 were dominated by this NP class (Figure 7 and Figure S6, Table S8). Moderate anticancer activities were observed in both *Trichoderma* sp. extracts (CHG34-CAG, -PDA; Table 2), which may originate from the putatively identified peptaibols neoatroviridin B–D (**149**,**156**,**160**) [72]. Antibacterial activity was only detected in the PDA extract of *Trichoderma* sp. strain CHG34 (Table 1), but none of the compounds exclusive to this extract (**90**,**92**,**111**) could be putatively identified as

annotation rates remained low for *Trichoderma* sp. strain CHG34 (27%). Two new lipopeptide structures (**103**,**105**) were proposed based on the predicted amino acid sequences from the product ions. Future efforts will encompass isolation and confirmation of the putative structures and also exploration of this strain for other novel MNPs for the treatment of infectious diseases.

As outlined above, *Fusarium* sp. extracts showed different bioactivities and metabolomes (Figure 7, Figure S7, Table 1, Table 2 and Table S9). The antimicrobial and anticancer properties of *Fusarium* sp. extract CHG38-PDA may originate from the putatively annotated xanthone derivative griseoxanthone C (**178**) [73,74] and the naphthoquinone norjavanicin (**163**) [75]. In addition, the shared metabolite fusaristatin A (**182**) reportedly inhibits the proliferation of lung cancer cells [76]. *Fusarium* spp. are also prominent producers of mycotoxins, including the macrolide zearalenone (**176**) detected in this study [77]. Zearalenone (**176**) shows antifungal but no antibacterial activities [78]. Hence, antibacterial activities of *Fusarium* sp. extract CHG38-CAG remain unresolved, since none of its putatively annotated compounds have been shown to possess antibacterial activities. Accordingly, extract CHG38-CAG is highlighted for future chemical investigations.

Detailed LC-MS/MS analyses of the *Penicillium* sp. isolate CKG23 revealed distinct chemical profiles of its CAG and PDA extracts (Figure 5a, Figure 7, Figures S8 and S12, Table S10). Anticancer activities of CKG23-CAG may be attributed to the putatively identified indole alkaloid communesin B (**219**) and the cytochalasan chaetoglobosin A (**212**) that were shown to inhibit the proliferation of cancer cell lines A549 (**212**,**219**) and HCT116 (**219**) [79,80]. In addition, the meroterpenoid andrastin A (**222**) putatively annotated in CKG23-CAG is a farnesyltransferase inhibitor that prevents correct functioning of, e.g., RAS proteins (common oncogenes), rendering it a promising anticancer lead compound [81]. Antiproliferative activity of CKG23-PDA and observed antibacterial activities (including Gram-negative pathogens) of both *Penicillium* sp. extracts could not be linked to any of the dereplicated compounds. Moreover, extract CKG23-PDA had the most distinct chemistry of all *Penicillium* sp. extracts (Figure 5a), indicating that the PDA extract of *Penicillium* sp. CKG23 is worth pursuing in future studies.

In this study, we showed that the cultivable fraction of the gut-associated microbiota of *C. intestinalis* is diverse and specific. The majority of the yet unexplored gut-associated cultivable microorganisms showed antimicrobial and/or anticancer activities, suggesting a significant potential for discovery of new drug leads. Computationally assisted metabolome mining of nine prioritized bioactive crude extracts led to the putative identification of 94 metabolites assigned to 24 different chemical families. Nevertheless, most compounds and molecular clusters remained unannotated and may therefore be novel MNPs. Several extracts containing putatively novel and bioactive metabolites were highlighted, in particular *Streptomyces* extract CHG48-CAG, *Trichoderma* sp. extracts CHG34-CAG and CHG34-PDA, *Fusarium* sp. extract CHG38-CAG, and *Penicillium* sp. extract CKG23-PDA. This emphasizes the benefit of working with marine microorganisms obtained from previously unexplored sources and is in line with the strongly increasing contribution of microorganisms in MNP discovery [9]. It is widely accepted that MNPs have higher success rates in drug discovery compared to their terrestrial counterparts [82]. Being evolved and prevalidated by natural pressures and adaptation processes for millions of years, NPs represent "privileged scaffolds in drug discovery" [83], whose bioactivity and structural diversity surpass any synthetic compound prepared in the laboratory [84]. To conclude, the obtained cultivable gut-associated microbial community of *C. intestinalis* delivered several promising microorganisms that seem to harbor an unexplored chemical space. Putatively novel compounds and their bioactivities need to be verified in future isolation and structure elucidation studies.

4. Materials and Methods

4.1. Sampling and Isolation of Microorganisms

Ciona intestinalis was sampled in September 2017 at two locations, the German North Sea island Helgoland (Germany, 54.177102, 7.893053) and Kiel Fjord (Kiel, Germany, Baltic Sea, 54.382062, 10.162059). Samples were collected in local harbors from a pontoon (Helgoland, < 1 m depth) or from a mussel cultivation basket (Kiel Fjord, approximately 3 m depth). Dissection and inoculation of microbiological samples were conducted at the same day.

Six solid media (1.8% agar) were used to isolate a diverse bacterial and fungal community from the ascidian's gut: two *C. intestinalis* media adjusted to Baltic (CB) and North Sea salinity (CN; [31]), MB (3.74% Marine Broth 2216), potato dextrose agar (PDA [85]), TSB (0.3% trypticase soy broth, 1% sodium chloride) and modified Wickerham medium (WSP [86]). Agar (bacteriology grade) and sodium chloride were purchased from AppliChem (Darmstadt, Germany), malt extract, Marine Broth, and trypticase soy broth from Becton Dickinson (Sparks, MD, USA), glucose, peptone (from soymeal), and granulated yeast extract from Merck (Darmstadt, Germany), and potato infusion powder was ordered at Sigma Aldrich (Steinheim, Germany).

The gut (*n* = 2 biological replicates per sampling site) was carefully dissected and placed into a sterile 1.5 mL reaction tube. The dissected gut was diluted 1:1 with sterile artificial seawater (1.8% (K) or 3% (H) Instant ocean, Blacksburg, VA, USA) and gently homogenized with a sterile pestle. Agar media were inoculated with 100 µL aliquots and their 1:10 and 1:100 dilutions. Petri dishes were checked for growth of fungi and bacteria after incubation for one and three weeks in the dark at 22 °C. Microbial colonies showing distinct macroscopic phenotypes were transferred to fresh agar plates until pure cultures were obtained. Microbial strains were cryo-conserved at −80 °C using the ready-to-use Microbank™ system (Richmond Hill, ON, Pro Lab Diagnostics, Canada).

4.2. DNA Extraction and Identification of Microbial Isolates

DNA was extracted by applying a freeze and thaw protocol (bacteria) or by mechanical lysis (fungi) as described elsewhere [31,87]. If subsequent PCR amplification of the target fragment failed, DNA extraction was repeated with the DNeasy Plant Mini Kit (Qiagen, Hilden, Germany) according to the manufacturer's instructions. Some modifications of the protocol were applied as previously described [31].

Molecular identification was performed following established protocols for amplification of the 16S rRNA gene (bacteria) or the ITS1-5.8S-ITS2 region (fungi) [87]. The 18S and 28S rRNA gene were additionally amplified for fungal strains with ambiguous identification (for protocols see [88,89]). PCR conditions for amplifying the large ribosomal subunit of the rRNA were modified as previously described [31]. Sanger sequencing [90] of successfully amplified DNA fragments was conducted at LGC Genomics GmbH (Berlin, Germany). FASTA files of quality checked and trimmed DNA sequences were searched against the NCBI (National Center for Biotechnology Information) nucleotide database using BLAST (Basic Local Alignment Search Tool [91]). One bacterial isolate (CKG60) could only be identified at family level. Application of Naive Bayesian rRNA Classifier v2.11 of the Ribosomal Database Project using the 16S rRNA training set at a 95% confidence threshold [92] resulted in identification of this isolate to genus level. Bacterial and fungal DNA sequences were deposited in GenBank under the accession numbers MW065489-549 (gut-associated bacteria), MW064137-74 (gut-associated fungi, ITS), and MW064175-6 (gut-associated fungi, 18S; Table S1).

4.3. Cultivation and Extraction of Gut-Associated Microbial Strains

Out of 101 gut-derived microbial isolates, 29 were excluded from cultivation due to laboratory safety concerns based on the Technical Rules for Biological Agents (TRBA 460, TRBA 466). Fifteen additional strains were excluded, since they were affiliated to the same species as another strain isolated from the same sampling site, which led to the final selection of 27 bacterial and 30 fungal strains for cultivation (*n* = 57; Table S2). Microbial isolates were

cultured in duplicate (i.e., two biological replicates) on two different media. Bacterial isolates were cultured on the solid agar media glucose–yeast–malt (GYM [93]) and MB. Solid casamino acids–glucose (CAG [94]) and PDA media were used for growing fungal strains. Ingredients not listed in Section 4.1. were purchased from Carl Roth (Karlsruhe, Germany). CAG, GYM and PDA were chosen due to their excellent potential to trigger production of novel and bioactive compounds (see [31] and references therein). MB medium was chosen to ensure sufficient growth of all bacterial isolates. For cultivation of precultures, solid media were inoculated with cryo-conservation beads and incubated in the dark at 22 °C until the agar was completely overgrown. Main cultures were inoculated by transferring microbial colonies or an overgrown piece of agar with an inoculation loop to the respective agar medium. Fungi were inoculated on five agar plates and bacteria on ten plates in parallel. As outlined above, each strain was cultivated on two respective media in duplicate yielding 20 (fungi) or 40 (bacteria) petri dishes per strain. Microbial cultures were grown in the dark for seven (bacteria) or 21 (fungi) days at 22 °C. Eleven bacterial strains did not grow on GYM medium, hence were only cultivated on MB medium.

For solvent extractions, the agar was cut with a flat spatula and mixed with 200 mL (fungi) or 400 mL (bacteria) ethyl acetate (EtOAc; VWR International, Leuven, Belgium) in a glass bottle. The mixture was homogenized with a T25 basic Ultra Turrax (IKA-Werke, Staufen, Germany; 30 s at 13,000 rpm), which was followed by maceration overnight (120 rpm, 22 °C). The solvent was decanted and washed with an equal volume of ultra-purified water to remove salts (Arium Lab water systems, Sartorius, Goettingen, Germany) in a liquid–liquid partitioning experiment. The EtOAc phase was transferred to a round bottom flask. The extraction process was repeated in the same manner, with the only exception that the extraction process was reduced to 15 min in an ultrasonic bath. Combined EtOAc extracts were evaporated to dryness and re-solubilized in 4 mL methanol (MeOH; ULC-MS grade, Biosolve Chimie, Dieuze, France). Extracts were filtered through a 0.2 µm PTFE (polytetrafluoroethylene) filter (VWR International, Darmstadt, Germany), dried again in pre-weighed vials to determine their extract weight, and stored at −20 °C. Media blanks were prepared as controls by using the same protocol.

4.4. Biological Assays

Dried crude extracts were dissolved in dimethyl sulfoxide (Carl Roth) at a concentration of 20 mg/mL. Microbial pathogens included the ESKAPE panel (*Enterococcus faecium*, Efm, DSM 20477; methicillin-resistant *Staphylococcus aureus*, MRSA, DSM 18827; *Klebsiella pneumoniae*, Kp, DSM 30104; *Acinetobacter baumannii*, Ab, DSM 30007; *Pseudomonas aeruginosa*, Psa, DSM 1128; *Escherichia coli*, Ec, DSM 1576), as well as the pathogenic fungi *Candida albicans* (Ca, DSM 1386) and *Cryptococcus neoformans* (Ca, DSM 6973). The following four cancer cell lines were selected for anticancer assays: A375 (malignant melanoma cell line), A549 (lung carcinoma cell line), HCT116 (colon cancer cell line), and MDA-MB231 (human breast cancer line). Test organisms and cell lines were purchased from Leibniz Institute DSMZ-German Collection of Microorganisms and Cell Cultures (Braunschweig, Germany) and CLS Cell Lines Service (Eppelheim, Germany). Tests were performed in 96-well plates at a final concentration of 100 µg/mL as previously described [95,96]. For each extract, its two biological replicates were tested in duplicate each (i.e., two technical replicates). The antibiotics amphotericin (Cn), ampicillin (Efm), chloramphenicol (MRSA, Ec, Kp), doxycycline (Ab), nystatin (Ca), polymyxin B (Psa), and the cytostatic agent doxorubicin (cancer cell lines) served as positive controls. Prioritized extracts were additionally subjected to IC_{50} determinations (also two biological and two technical replicates) by applying a previously published protocol [95].

4.5. Metabolomic Analyses

4.5.1. UPLC-QToF-MS/MS Measurements

All solvents used for UPLC-based metabolomic analyses were ordered at Biosolve Chimie or LGC Standards (Wesel, Germany) in ULC-MS grade. Crude extracts (two biological replicates each) re-dissolved in MeOH (final concentration of 1.0 mg/mL) were measured on an Acquity UPLC I-Class System connected to a Xevo G2-XS QToF Mass Spectrometer (Waters, Milford, MA, USA). Crude extracts were injected (0.3 µL) and separated on an Acquity UPLC HSS T3 column (High Strength Silica C18, 1.8 µm, 2.1 × 100 mm, Waters) operating at 40 °C. The binary mobile phase consisted of ultra-purified water (A) and acetonitrile (B), both spiked with 0.1% formic acid. The elution gradient pumped at a flow rate of 0.6 mL/min was as follows (% of A given): initial, 99%; 11.5 min, 1%; 14.5 min, 1%; 14.5–16 min 99%. LC-MS chromatograms and MS/MS fragmentation spectra were recorded as previously described [31]. The same settings were applied to analyze MeOH (solvent control) and media blanks.

4.5.2. Pre-Processing of UPLC-MS/MS Data and Statistics

The ProteoWizard tool msconvert 3.0.20010 was used to transform acquired spectra to mzXML format [97]. Quality filtering and removal of media and contaminant peaks were carried out in MZmine 2.53 [98]. Briefly, mass lists were compiled for compounds with a retention time (R_t) between 1 and 12 min with an intensity above 30,000 (MS) or 50 (MS/MS). Chromatograms were built at a minimum peak height of 60,000 and an m/z tolerance of 0.005 Da or 15 ppm. Deconvolution of chromatograms was performed with the baseline cut-off algorithm using the same noise level and peak height as above. Isotope grouping and alignment of peaks was performed with an m/z tolerance of 0.001 Da or 10 ppm and an R_t tolerance of 0.5 min. The alignment of peaks was conducted with the join aligner method by using an m/z to R_t ratio of 75:25. Finally, peak lists were filtered with an m/z range of 150–1200 Da. Media and solvent control peaks were detected using the same approach (noise level: 1000; peak height: 3000) and subsequently removed from the filtered peak list. Filtered peak lists were subjected to statistical analyses to assess the chemical distinctiveness of the microbial extracts. Therefore, PCoA plots reflecting the metabolomic (dis)similarities of the selected extracts and ANOSIM scores (Euclidean distance) were calculated in Past v3.12 [99].

4.5.3. Feature-Based Molecular Networking and Dereplication

Processed MS/MS data of prioritized extracts (see Section 2.3.) were submitted in MGF format to the FBMN workflow [32] available at the open access platform GNPS [34]. FBMNs were compiled as previously described [31] and visualized with Cytoscape v3.7.1 [100]. Compounds showing distinct peaks in the LC-MS chromatograms above the noise threshold were subjected to a dereplication workflow combining automated and manual dereplication tools. The prediction of putative molecular formulae was performed in MassLynx v4.1 (Waters). Four NP databases, i.e., Dictionary of Natural Products (http://dnp.chemnetbase.com), MarinLit (http://pubs.rsc.org/marinlit/), The Natural Products Atlas (https://www.npatlas.org/joomla/index.php/search/basic-search [101]) and Reaxys (https://www.reaxys.com), were inspected for putative hits for the predicted molecular formulae. In parallel, pre-processed MS/MS data were subjected to the dereplication workflow of GNPS [34]. The same dataset was also automatically dereplicated by applying the in silico MS/MS database of the Universal Natural Product Database [33]. Putatively annotated NPs were verified by comparing the biological sources, R_t, and MS/MS spectra (if detected), of which the latter was aided by the in-silico prediction tool CFM-ID 3.0 [102].

Supplementary Materials: The following are available online at https://www.mdpi.com/1660-3397/19/1/6/s1, Figure S1: Venn diagram of exclusive and shared peaks of *N. prasina* and *Streptomyces* sp. extracts. Figure S2: Structures of putatively identified compounds. Figures S3–S8: FBMNs of prioritized crude extracts. Figures S9–S11: MS/MS spectra of putatively annotated compounds. Figure S12: Comparative metabolome analyses of *Penicillium* sp. isolate CKG23. Table S1: Taxonomic classification of microbial strains isolated from the gut of *C. intestinalis* sampled in Helgoland and Kiel Fjord. Table S2: Antimicrobial and anticancer activities of microbial crude extracts.

Tables S3–S4: Statistical comparison of chemically distinct microbial crude extracts. Tables S5–S10: Putatively identified compounds in prioritized microbial crude extracts.

References

1. Lozupone, C.A.; Stombaugh, J.I.; Gordon, J.I.; Jansson, J.K.; Knight, R. Diversity, stability and resilience of the human gut microbiota. *Nature* **2012**, *489*, 220–230, doi:10.1038/nature11550.
2. Dishaw, L.J.; Cannon, J.P.; Litman, G.W.; Parker, W. Immune-directed support of rich microbial communities in the gut has ancient roots. *Dev. Comp. Immunol.* **2014**, *47*, 36–51, doi:10.1016/j.dci.2014.06.011.
3. Fraune, S.; Anton-Erxleben, F.; Augustin, R.; Franzenburg, S.; Knop, M.; Schröder, K.; Willoweit-Ohl, D.; Bosch, T.C.G. Bacteria–bacteria interactions within the microbiota of the ancestral metazoan *Hydra* contribute to fungal resistance. *ISME J.* **2014**, *9*, 1543–1556, doi:10.1038/ismej.2014.239.
4. Pickard, J.M.; Zeng, M.Y.; Caruso, R.; Nunez, G. Gut microbiota: Role in pathogen colonization, immune responses, and inflammatory disease. *Immunol. Rev.* **2017**, *279*, 70–89, doi:10.1111/imr.12567.
5. Westerdahl, A.; Olsson, J.C.; Kjelleberg, S.; Conway, P.L. Isolation and characterization of turbot (*Scophtalmus maximus*)-associated bacteria with inhibitory effects against *Vibrio anguillarum*. *Appl. Environ. Microbiol.* **1991**, *57*, 2223–2228, doi:10.1128/aem.57.8.2223-2228.1991.
6. Sugita, H.; Matsuo, N.; Hirose, Y.; Iwato, M.; Deguchi, Y. *Vibrio* sp. strain NM 10, isolated from the intestine of a Japanese coastal fish, has an inhibitory effect against *Pasteurella piscicida*. *Appl. Environ. Microbiol.* **1997**, *63*, 4986–4989, doi:10.1128/AEM.63.12.4986-4989.1997.
7. Sawabe, T.; Oda, Y.; Shiomi, Y.; Ezura, Y. Alginate degradation by bacteria isolated from the gut of sea urchins and abalones. *Microb. Ecol.* **1995**, *30*, 193–202, doi:10.1007/BF00172574.
8. Kobayashi, J.; Ishibashi, M. Bioactive metabolites of symbiotic marine microorganisms. *Chem. Rev.* **1993**, *93*, 1753–1769, doi:10.1021/cr00021a005.
9. Carroll, A.R.; Copp, B.R.; Davis, R.A.; Keyzers, R.A.; Prinsep, M.R. Marine natural products. *Nat. Prod. Rep.* **2020**, *37*, 175–223, doi:10.1039/c9np00069k.
10. Martins, A.; Vieira, H.; Gaspar, H.; Santos, S. Marketed marine natural products in the pharmaceutical and cosmeceutical industries: Tips for success. *Mar. Drugs* **2014**, *12*, 1066–1101, doi:10.3390/md12021066.
11. Chen, L.; Hu, J.S.; Xu, J.L.; Shao, C.L.; Wang, G.Y. Biological and chemical diversity of ascidian-associated microorganisms. *Mar. Drugs* **2018**, *16*, 362, doi:10.3390/md16100362.
12. Thomas, T.R.A.; Kavlekar, D.P.; LokaBharathi, P.A. Marine drugs from sponge-microbe association—A review. *Mar. Drugs* **2010**, *8*, 1417–1468, doi:10.3390/md8041417.
13. Casertano, M.; Menna, M.; Imperatore, C. The ascidian-derived metabolites with antimicrobial properties. *Antibiotics* **2020**, *9*, 510, doi:10.3390/antibiotics9080510.
14. Rath, C.M.; Janto, B.; Earl, J.; Ahmed, A.; Hu, F.Z.; Hiller, L.; Dahlgren, M.; Kreft, R.; Yu, F.; Wolff, J.J.; et al. Meta-omic characterization of the marine invertebrate microbial consortium that

produces the chemotherapeutic natural product ET-743. *ACS Chem. Biol.* **2011**, *6*, 1244–1256, doi:10.1021/cb200244t.

15. Liu, Y.; Zhao, S.; Ding, W.; Wang, P.; Yang, X.; Xu, J. Methylthio-aspochalasins from a marine-derived fungus *Aspergillus* sp. *Mar. Drugs* **2014**, *12*, 5124–5131, doi:10.3390/md12105124.
16. Li, X.; Zhao, Z.; Ding, W.; Ye, B.; Wang, P.; Xu, J. Aspochalazine A, a novel polycyclic aspochalasin from the fungus *Aspergillus* sp. Z4. *Tetrahedron Lett.* **2017**, *58*, 2405–2408, doi:10.1016/j.tetlet.2017.04.071.
17. Xu, Y.; Huang, R.; Liu, H.; Yan, T.; Ding, W.; Jiang, Y.; Wang, P.; Zheng, D.; Xu, J. New polyketides from the marine-derived fungus *Letendraea* sp. 5XNZ4-2. *Mar. Drugs* **2019**, *18*, 18, doi:10.3390/md18010018.
18. Alain, K.; Querellou, J. Cultivating the uncultured: Limits, advances and future challenges. *Extremophiles* **2009**, *13*, 583–594, doi:10.1007/s00792-009-0261-3.
19. Garza, D.R.; Dutilh, B.E. From cultured to uncultured genome sequences: Metagenomics and modeling microbial ecosystems. *Cell. Mol. Life Sci.* **2015**, *72*, 4287–4308, doi:10.1007/s00018-015-2004-1.
20. Tamaki, H.; Sekiguchi, Y.; Hanada, S.; Nakamura, K.; Nomura, N.; Matsumura, M.; Kamagata, Y. Comparative analysis of bacterial diversity in freshwater sediment of a shallow eutrophic lake by molecular and improved cultivation-based techniques. *Appl. Environ. Microbiol.* **2005**, *71*, 2162–2169, doi:10.1128/AEM.71.4.2162-2169.2005.
21. Chen, L.; Fu, C.; Wang, G. Microbial diversity associated with ascidians: A review of research methods and application. *Symbiosis* **2017**, *71*, 19–26, doi:10.1007/s13199-016-0398-7.
22. Carver, C.E.; Mallet, A.L.; Vercaemer, B. Biological synopsis of the solitary tunicate *Ciona intestinalis. Can. Man. Rep. Fish. Aquat. Sci.* **2006**, *2746*, 1–55.
23. Dishaw, L.J.; Flores-Torres, J.A.; Mueller, M.G.; Karrer, C.R.; Skapura, D.P.; Melillo, D.; Zucchetti, I.; De Santis, R.; Pinto, M.R.; Litman, G.W. A Basal chordate model for studies of gut microbial immune interactions. *Front. Immunol.* **2012**, *3*, 96, doi:10.3389/fimmu.2012.00096.
24. Leigh, B.A.; Liberti, A.; Dishaw, L.J. Generation of germ-free *Ciona intestinalis* for studies of gut-microbe interactions. *Front. Microbiol.* **2016**, *7*, 2092, doi:10.3389/fmicb.2016.02092.
25. Franchi, N.; Ballarin, L. Immunity in Protochordates: The tunicate perspective. *Front. Immunol.* **2017**, *8*, 674, doi:10.3389/fimmu.2017.00674.
26. Dishaw, L.J.; Leigh, B.; Cannon, J.P.; Liberti, A.; Mueller, M.G.; Skapura, D.P.; Karrer, C.R.; Pinto, M.R.; De Santis, R.; Litman, G.W. Gut immunity in a protochordate involves a secreted immunoglobulin-type mediator binding host chitin and bacteria. *Nat. Commun.* **2016**, *7*, 10617, doi:10.1038/ncomms10617.
27. Leigh, B.; Karrer, C.; Cannon, J.P.; Breitbart, M.; Dishaw, L.J. Isolation and characterization of a *Shewanella* phage-host system from the gut of the tunicate, *Ciona intestinalis. Viruses* **2017**, *9*, 60, doi:10.3390/v9030060.
28. Liberti, A.; Cannon, J.P.; Litman, G.W.; Dishaw, L.J. A soluble immune effector binds both fungi and bacteria via separate functional domains. *Front. Immunol.* **2019**, *10*, 369, doi:10.3389/fimmu.2019.00369.
29. Dishaw, L.J.; Flores-Torres, J.; Lax, S.; Gemayel, K.; Leigh, B.; Melillo, D.; Mueller, M.G.; Natale, L.; Zucchetti, I.; De Santis, R.; et al. The gut of geographically disparate *Ciona intestinalis* harbors a core microbiota. *PLoS ONE* **2014**, *9*, e93386, doi:10.1371/journal.pone.0093386.
30. Blasiak, L.C.; Zinder, S.H.; Buckley, D.H.; Hill, R.T. Bacterial diversity associated with the tunic of the model chordate *Ciona intestinalis. ISME J.* **2014**, *8*, 309–320, doi:10.1038/ismej.2013.156.
31. Utermann, C.; Echelmeyer, V.A.; Blümel, M.; Tasdemir, D. Culture-dependent microbiome of the *Ciona intestinalis* tunic: Isolation, bioactivity profiling and untargeted metabolomics. *Microorganisms* **2020**, *8*, 1732, doi:10.3390/microorganisms8111732.
32. Nothias, L.F.; Petras, D.; Schmid, R.; Duhrkop, K.; Rainer, J.; Sarvepalli, A.; Protsyuk, I.; Ernst, M.; Tsugawa, H.; Fleischauer, M.; et al. Feature-based molecular networking in the GNPS analysis environment. *Nat. Methods* **2020**, *17*, 905–908, doi:10.1038/s41592-020-0933-6.
33. Allard, P.M.; Peresse, T.; Bisson, J.; Gindro, K.; Marcourt, L.; Pham, V.C.; Roussi, F.; Litaudon, M.; Wolfender, J.L. Integration of molecular networking and *in-silico* MS/MS fragmentation for natural products dereplication. *Anal. Chem.* **2016**, *88*, 3317–3323, doi:10.1021/acs.analchem.5b04804.
34. Wang, M.; Carver, J.J.; Phelan, V.V.; Sanchez, L.M.; Garg, N.; Peng, Y.; Nguyen, D.D.; Watrous, J.; Kapono, C.A.; Luzzatto-Knaan, T.; et al. Sharing and community curation of mass spectrometry data with Global Natural Products Social Molecular Networking. *Nat. Biotechnol.* **2016**, *34*, 828–837, doi:10.1038/nbt.3597.
35. Poirier, L.; Montagu, M.; Landreau, A.; Mohamed-Benkada, M.; Grovel, O.; Sallenave-Namont, C.; Biard, J.F.; Amiard-Triquet, C.; Amiard, J.C.; Pouchus, Y.F. Peptaibols: Stable markers of fungal development in the marine environment. *Chem. Biodivers.* **2007**, *4*, 1116–1128, doi:10.1002/cbdv.200790100.

36. Marik, T.; Tyagi, C.; Balazs, D.; Urban, P.; Szepesi, A.; Bakacsy, L.; Endre, G.; Rakk, D.; Szekeres, A.; Andersson, M.A.; et al. Structural diversity and bioactivities of peptaibol compounds from the Longibrachiatum Clade of the filamentous fungal fenus *Trichoderma*. *Front. Microbiol.* **2019**, *10*, 1434, doi:10.3389/fmicb.2019.01434.

37. Paizs, B.; Suhai, S. Fragmentation pathways of protonated peptides. *Mass Spectrom. Rev.* **2005**, *24*, 508–548, doi:10.1002/mas.20024.

38. da Silva, R.R.; Dorrestein, P.C.; Quinn, R.A. Illuminating the dark matter in metabolomics. *Proc. Natl. Acad. Sci. USA* **2015**, *112*, 12549–12550, doi:10.1073/pnas.1516878112.

39. de Oliveira Costa, O.; Nahas, E. Growth and enzymatic responses of phytopathogenic fungi to glucose in culture media and soil. *Braz. J. Microbiol.* **2012**, *43*, 332–340, doi:10.1590/s1517-83822012000100039.

40. Goddard-Dwyer, M.; Lopez-Legentil, S.; Erwin, P.M. Microbiome variability across the native and invasive range of the ascidian *Clavelina oblonga*. *Appl. Environ. Microbiol.* **2020**, AEM.02233-20, doi:10.1128/AEM.02233-20.

41. Giatsis, C.; Sipkema, D.; Smidt, H.; Verreth, J.; Verdegem, M. The colonization dynamics of the gut microbiota in tilapia larvae. *PLoS ONE* **2014**, *9*, e103641, doi:10.1371/journal.pone.0103641.

42. Menna, M. Antitumor potential of natural products from Mediterranean ascidians. *Phytochem. Rev.* **2009**, *8*, 461–472, doi:10.1007/s11101-009-9131-y.

43. Global Priority List of Antibiotic-Resistant Bacteria to Guide Research, Discovery, and Development of New Antibiotics (World Health Organization 2017). Available online: https://www.who.int/medicines/publications/global-priority-list-antibiotic-resistant-bacteria/en/ (accessed on 19 October 2020).

44. Chen, L.; Wang, X.-N.; Fu, C.-M.; Wang, G.-Y. Phylogenetic analysis and screening of antimicrobial and antiproliferative activities of culturable bacteria associated with the ascidian *Styela clava* from the Yellow Sea, China. *Biomed. Res. Int.* **2019**, *2019*, 1–14, doi:10.1155/2019/7851251.

45. Romanenko, L.A.; Kalinovskaya, N.I.; Mikhailov, V.V. Taxonomic composition and biological activity of microorganisms associated with a marine ascidian *Halocynthia aurantium*. *Russ. J. Mar. Biol.* **2001**, *27*, 291–296, doi:10.1023/a:1012548513766.

46. Meziti, A.; Kormas, K.A.; Pancucci-Papadopoulou, M.-A.; Thessalou-Legaki, M. Bacterial phylotypes associated with the digestive tract of the sea urchin *Paracentrotus lividus* and the ascidian *Microcosmus* sp. *Russ. J. Mar. Biol.* **2007**, *33*, 84–91, doi:10.1134/s1063074007020022.

47. Laport, M.S.; Bauwens, M.; Collard, M.; George, I. Phylogeny and antagonistic activities of culturable bacteria associated with the gut microbiota of the sea urchin (*Paracentrotus lividus*). *Curr. Microbiol.* **2018**, *75*, 359–367, doi:10.1007/s00284-017-1389-5.

48. Agrawal, S.; Acharya, D.; Adholeya, A.; Barrow, C.J.; Deshmukh, S.K. Nonribosomal peptides from marine microbes and their antimicrobial and anticancer potential. *Front. Pharmacol.* **2017**, *8*, 828, doi:10.3389/fphar.2017.00828.

49. Hifnawy, M.S.; Fouda, M.M.; Sayed, A.M.; Mohammed, R.; Hassan, H.M.; AbouZid, S.F.; Rateb, M.E.; Keller, A.; Adamek, M.; Ziemert, N.; et al. The genus *Micromonospora* as a model microorganism for bioactive natural product discovery. *RSC Adv.* **2020**, *10*, 20939–20959, doi:10.1039/d0ra04025h.

50. Macia-Vicente, J.G.; Shi, Y.N.; Cheikh-Ali, Z.; Grun, P.; Glynou, K.; Kia, S.H.; Piepenbring, M.; Bode, H.B. Metabolomics-based chemotaxonomy of root endophytic fungi for natural products discovery. *Environ. Microbiol.* **2018**, *20*, 1253–1270, doi:10.1111/1462-2920.14072.

51. Oppong-Danquah, E.; Passaretti, C.; Chianese, O.; Blümel, M.; Tasdemir, D. Mining the metabolome and the agricultural and pharmaceutical potential of sea foam-derived fungi. *Mar. Drugs* **2020**, *18*, 128, doi:10.3390/md18020128.

52. Crüsemann, M.; O'Neill, E.C.; Larson, C.B.; Melnik, A.V.; Floros, D.J.; da Silva, R.R.; Jensen, P.R.; Dorrestein, P.C.; Moore, B.S. Prioritizing natural product diversity in a collection of 146 bacterial strains based on growth and extraction protocols. *J. Nat. Prod.* **2016**, *80*, 588–597, doi:10.1021/acs.jnatprod.6b00722.

53. Bode, H.B.; Bethe, B.; Hofs, R.; Zeeck, A. Big effects from small changes: Possible ways to explore nature's chemical diversity. *Chembiochem* **2002**, *3*, 619–627, doi:10.1002/1439-7633(20020703)3:7<619::AID-CBIC619>3.0.CO;2-9.

54. Tison, D.L.; Kelly, M.T. *Vibrio* species of medical importance. *Diagn. Microbiol. Infect. Dis.* **1984**, *2*, 263–276, doi:10.1016/0732-8893(84)90057-9.

55. Romano, S.; Jackson, S.A.; Patry, S.; Dobson, A.D.W. Extending the "One Strain Many Compounds" (OSMAC) principle to marine microorganisms. *Mar. Drugs* **2018**, *16*, 244, doi:10.3390/md16070244.

56. Huang, H.; Lan, X.; Wang, Y.; Tian, L.; Fang, Y.; Zhang, L.; Zhang, K.; Zheng, X. New bioactive derivatives of nonactic acid from the marine *Streptomyces griseus* derived from the plant *Salicornia* sp. *Phytochem. Lett.* **2015**, *12*, 190–195, doi:10.1016/j.phytol.2015.04.001.

57. Jeong, S.Y.; Shin, H.J.; Kim, T.S.; Lee, H.S.; Park, S.K.; Kim, H.M. Streptokordin, a new cytotoxic compound of the methylpyridine class from a marine-derived *Streptomyces* sp. KORDI-3238. *J. Antibiot.* **2006**, *59*, 234–240, doi:10.1038/ja.2006.33.
58. Kusche, B.R.; Smith, A.E.; McGuirl, M.A.; Priestley, N.D. Alternating pattern of stereochemistry in the nonactin macrocycle is required for antibacterial activity and efficient ion binding. *J. Am. Chem. Soc.* **2009**, *131*, 17155–17165, doi:10.1021/ja9050235.
59. Zhang, C.; Ondeyka, J.; Guan, Z.; Dietrich, L.; Burgess, B.; Wang, J.; Singh, S.B. Isolation, structure and biological activities of platensimycin B4 from *Streptomyces platensis*. *J. Antibiot.* **2009**, *62*, 699–702, doi:10.1038/ja.2009.106.
60. Han, L.; Huo, P.; Chen, H.; Li, S.; Jiang, Y.; Li, L.; Xu, L.; Jiang, C.; Huang, X. New derivatives of nonactic and homononactic acids from *Bacillus pumilus* derived from *Breynia fruticosa*. *Chem. Biodivers.* **2014**, *11*, 1088–1098, doi:10.1002/cbdv.201300350.
61. Oku, N.; Matoba, S.; Yamazaki, Y.M.; Shimasaki, R.; Miyanaga, S.; Igarashi, Y. Complete stereochemistry and preliminary structure-activity relationship of rakicidin A, a hypoxia-selective cytotoxin from *Micromonospora* sp. *J. Nat. Prod.* **2014**, *77*, 2561–2565, doi:10.1021/np500276c.
62. Yamazaki, Y.; Kunimoto, S.; Ikeda, D. Rakicidin A: A hypoxia-selective cytotoxin. *Biol. Pharm. Bull.* **2007**, *30*, 261–265, doi:10.1248/bpb.30.261.
63. Landwehr, W.; Karwehl, S.; Schupp, P.J.; Schumann, P.; Wink, J. Biological active rakicidins A, B and E produced by the marine *Micromonospora* sp. isolate Guam1582. *Adv. Biotechnol. Microbiol.* **2016**, *1*, 1–5, doi:10.19080/aibm.2016.01.555558.
64. Charan, R.D.; Schlingmann, G.; Janso, J.; Bernan, V.; Feng, X.; Carter, G.T. Diazepinomicin, a new antimicrobial alkaloid from a marine *Micromonospora* sp. *J. Nat. Prod.* **2004**, *67*, 1431–1433, doi:10.1021/np040042r.
65. Itoh, J.; Omoto, S.; Shomura, T.; Nishizawa, N.; Miyado, S.; Yuda, Y.; Shibata, U.; Inouye, S. Amicoumacin-A, a new antibiotic with strong antiinflammatory and antiulcer activity. *J. Antibiot.* **1981**, *34*, 611–613, doi:10.7164/antibiotics.34.611.
66. Konda, Y.; Nakagawa, A.; Harigaya, Y.; Onda, M.; Masuma, R.; Omura, S. Aurantinin B, a new antimicrobial antibiotic from bacterial origin. *J. Antibiot.* **1988**, *41*, 268–270, doi:10.7164/antibiotics.41.268.
67. Zhuravleva, O.I.; Afiyatullov, S.S.; Ermakova, S.P.; Nedashkovskaya, O.I.; Dmitrenok, P.S.; Denisenko, V.A.; Kuznetsova, T.A. New C14-surfactin methyl ester from the marine bacterium *Bacillus pumilus* KMM 456. *Russ. Chem. Bull.* **2011**, *59*, 2137–2142, doi:10.1007/s11172-010-0369-8.
68. Mhammedi, A.; Peypoux, F.; Besson, F.; Michel, G. Bacillomycin F, a new antibiotic of iturin group: Isolation and characterization. *J. Antibiot.* **1982**, *35*, 306–311, doi:10.7164/antibiotics.35.306.
69. Kimura, K.; Nakayama, S.; Nakamura, J.; Takada, T.; Yoshihama, M.; Esumi, Y.; Itoh, Y.; Uramoto, M. SNA-60-367, new peptide enzyme inhibitors against aromatase. *J. Antibiot.* **1997**, *50*, 529–531, doi:10.7164/antibiotics.50.529.
70. Mohamed-Benkada, M.; Montagu, M.; Biard, J.F.; Mondeguer, F.; Verite, P.; Dalgalarrondo, M.; Bissett, J.; Pouchus, Y.F. New short peptaibols from a marine *Trichoderma* strain. *Rapid Commun. Mass Spectrom.* **2006**, *20*, 1176–1180, doi:10.1002/rcm.2430.
71. Mukherjee, P.K.; Wiest, A.; Ruiz, N.; Keightley, A.; Moran-Diez, M.E.; McCluskey, K.; Pouchus, Y.F.; Kenerley, C.M. Two classes of new peptaibols are synthesized by a single non-ribosomal peptide synthetase of *Trichoderma virens*. *J. Biol. Chem.* **2011**, *286*, 4544–4554, doi:10.1074/jbc.M110.159723.
72. Oh, S.U.; Yun, B.S.; Lee, S.J.; Kim, J.H.; Yoo, I.D. Atroviridins A-C and neoatroviridins A-D, novel peptaibol antibiotics produced by *Trichoderma atroviride* F80317. I. Taxonomy, fermentation, isolation and biological activities. *J. Antibiot.* **2002**, *55*, 557–564, doi:10.7164/antibiotics.55.557.
73. Hawas, U.W.; Farrag, A.R.H.; Ahmed, E.F.; Abou El-Kassem, L.T. Cytotoxic effect of *Fusarium equiseti* fungus metabolites against N-Nitrosodiethylamine- and CCL4-induced hepatocarcinogenesis in rats. *Pharm. Chem. J.* **2018**, *52*, 326–333, doi:10.1007/s11094-018-1816-3.
74. Wang, Q.X.; Bao, L.; Yang, X.L.; Guo, H.; Yang, R.N.; Ren, B.; Zhang, L.X.; Dai, H.Q.; Guo, L.D.; Liu, H.W. Polyketides with antimicrobial activity from the solid culture of an endolichenic fungus *Ulocladium* sp. *Fitoterapia* **2012**, *83*, 209–214, doi:10.1016/j.fitote.2011.10.013.
75. Holenstein, J.; DÉFago, G. Inheritance of naphthazarin production and pathogenicity to pea in *Nectria haematococca*. *J. Exp. Bot.* **1983**, *34*, 927–935, doi:10.1093/jxb/34.7.927.
76. Shiono, Y.; Tsuchinari, M.; Shimanuki, K.; Miyajima, T.; Murayama, T.; Koseki, T.; Laatsch, H.; Funakoshi, T.; Takanami, K.; Suzuki, K. Fusaristatins A and B, two new cyclic lipopeptides from an endophytic *Fusarium* sp. *J. Antibiot.* **2007**, *60*, 309–316, doi:10.1038/ja.2007.39.
77. Desjardins, A.E. *Fusarium Mycotoxins: Chemistry, Genetics, and Biology*; American Phytopathological Society (APS Press): St. Paul, MN, USA, 2006.

78. Utermark, J.; Karlovsky, P. Role of zearalenone lactonase in protection of *Gliocladium roseum* from fungitoxic effects of the mycotoxin zearalenone. *Appl. Environ. Microbiol.* **2007**, *73*, 637–642, doi:10.1128/AEM.01440-06.

79. Pompeo, M.M.; Cheah, J.H.; Movassaghi, M. Total synthesis and anti-cancer activity of all known communesin alkaloids and related derivatives. *J. Am. Chem. Soc.* **2019**, *141*, 14411–14420, doi:10.1021/jacs.9b07397.

80. Huang, S.; Chen, H.; Li, W.; Zhu, X.; Ding, W.; Li, C. Bioactive chaetoglobosins from the mangrove endophytic fungus *Penicillium chrysogenum*. *Mar. Drugs* **2016**, *14*, 172, doi:10.3390/md14100172.

81. Nielsen, K.F.; Dalsgaard, P.W.; Smedsgaard, J.; Larsen, T.O. Andrastins A-D, *Penicillium roqueforti* metabolites consistently produced in blue-mold-ripened cheese. *J. Agr. Food Chem.* **2005**, *53*, 2908–2913, doi:10.1021/jf047983u.

82. Sigwart, J.D.; Blasiak, R.; Jaspars, M.; Jouffray, J.-B.; Tasdemir, D. Unlocking the potential of marine biodiscovery. *Nat. Prod. Rep.* **2021**, doi:10.1039/d0np00067a.

83. Davison, E.K.; Brimble, M.A. Natural product derived privileged scaffolds in drug discovery. *Curr. Opin. Chem. Biol.* **2019**, *52*, 1–8, doi:10.1016/j.cbpa.2018.12.007.

84. Newman, D.J.; Cragg, G.M. Natural products as sources of new drugs over the nearly four decades from 01/1981 to 09/2019. *J. Nat. Prod.* **2020**, *83*, 770–803, doi:10.1021/acs.jnatprod.9b01285.

85. Oppong-Danquah, E.; Parrot, D.; Blümel, M.; Labes, A.; Tasdemir, D. Molecular networking-based metabolome and bioactivity analyses of marine-adapted fungi co-cultivated with phytopathogens. *Front. Microbiol.* **2018**, *9*, 1–20, doi:10.3389/fmicb.2018.02072.

86. Silber, J.; Ohlendorf, B.; Labes, A.; Erhard, A.; Imhoff, J.F. Calcarides A-E, antibacterial macrocyclic and linear polyesters from a *Calcarisporium* strain. *Mar. Drugs* **2013**, *11*, 3309–3323, doi:10.3390/md11093309.

87. Utermann, C.; Parrot, D.; Breusing, C.; Stuckas, H.; Staufenberger, T.; Blümel, M.; Labes, A.; Tasdemir, D. Combined genotyping, microbial diversity and metabolite profiling studies on farmed *Mytilus* spp. from Kiel Fjord. *Sci. Rep.* **2018**, *8*, 7983, doi:10.1038/s41598-018-26177-y.

88. Gomes, N.C.; Fagbola, O.; Costa, R.; Rumjanek, N.G.; Buchner, A.; Mendona-Hagler, L.; Smalla, K. Dynamics of fungal communities in bulk and maize rhizosphere soil in the tropics. *Appl. Environ. Microbiol.* **2003**, *69*, 3758–3766, doi:10.1128/aem.69.7.3758-3766.2003.

89. Hopple, J.S., Jr.; Vilgalys, R. Phylogenetic relationships in the mushroom genus *Coprinus* and dark-spored allies based on sequence data from the nuclear gene coding for the large ribosomal subunit RNA: Divergent domains, outgroups, and monophyly. *Mol. Phylogenet. Evol.* **1999**, *13*, 1–19, doi:10.1006/mpev.1999.0634.

90. Sanger, F.; Nicklen, S.; Coulson, A.R. DNA sequencing with chain-terminating inhibitors. *Proc. Natl. Acad. Sci. USA* **1977**, *74*, 5463–5467, doi:10.1073/pnas.74.12.5463.

91. Altschul, S.F.; Gish, W.; Miller, W.; Myers, E.W.; Lipman, D.J. Basic local alignment search tool. *J. Mol. Biol.* **1990**, *215*, 403–410, doi:10.1016/S0022-2836(05)80360-2.

92. Wang, Q.; Garrity, G.M.; Tiedje, J.M.; Cole, J.R. Naive Bayesian classifier for rapid assignment of rRNA sequences into the new bacterial taxonomy. *Appl. Environ. Microbiol.* **2007**, *73*, 5261–5267, doi:10.1128/AEM.00062-07.

93. Wu, B.; Wiese, J.; Labes, A.; Kramer, A.; Schmaljohann, R.; Imhoff, J.F. Lindgomycin, an unusual antibiotic polyketide from a marine fungus of the Lindgomycetaceae. *Mar. Drugs* **2015**, *13*, 4617–4632, doi:10.3390/md13084617.

94. Stevens, R.B. *Mycology Guidebook*; University of Washington Press: Seattle, WA, USA, 1974; p. 682.

95. Pfeifer Barbosa, A.L.; Wenzel-Storjohann, A.; Barbosa, J.D.; Zidorn, C.; Peifer, C.; Tasdemir, D.; Cicek, S.S. Antimicrobial and cytotoxic effects of the *Copaifera reticulata* oleoresin and its main diterpene acids. *J. Ethnopharmacol.* **2019**, *233*, 94–100, doi:10.1016/j.jep.2018.11.029.

96. Petersen, L.E.; Marner, M.; Labes, A.; Tasdemir, D. Rapid metabolome and bioactivity profiling of fungi associated with the leaf and rhizosphere of the Baltic seagrass *Zostera marina*. *Mar. Drugs* **2019**, *17*, 419, doi:10.3390/md17070419.

97. Chambers, M.C.; Maclean, B.; Burke, R.; Amodei, D.; Ruderman, D.L.; Neumann, S.; Gatto, L.; Fischer, B.; Pratt, B.; Egertson, J.; et al. A cross-platform toolkit for mass spectrometry and proteomics. *Nat. Biotechnol.* **2012**, *30*, 918–920, doi:10.1038/nbt.2377.

98. Pluskal, T.; Castillo, S.; Villar-Briones, A.; Oresic, M. MZmine 2: Modular framework for processing, visualizing, and analyzing mass spectrometry-based molecular profile data. *BMC Bioinform.* **2010**, *11*, 395, doi:10.1186/1471-2105-11-395.

99. Hammer, Ø.; Harper, D.A.T.; Ryan, P.D. PAST: Paleontological statistics software package for education and data analysis. *Palaeontol. Electron.* **2001**, *4*, 1–9.

100. Shannon, P.; Markiel, A.; Ozier, O.; Baliga, N.S.; Wang, J.T.; Ramage, D.; Amin, N.; Schwikowski, B.; Ideker, T. Cytoscape: A software environment for integrated models of biomolecular interaction networks. *Genome Res.* **2003**, *13*, 2498–2504, doi:10.1101/gr.1239303.

101. van Santen, J.A.; Jacob, G.; Singh, A.L.; Aniebok, V.; Balunas, M.J.; Bunsko, D.; Neto, F.C.; Castaño-Espriu, L.; Chang, C.; Clark, T.N.; et al. The Natural Products Atlas: An open access knowledge base for microbial natural products discovery. *ACS Cent. Sci.* **2019**, *5*, 1824–1833, doi:10.1021/acscentsci.9b00806.

102. Djoumbou-Feunang, Y.; Pon, A.; Karu, N.; Zheng, J.; Li, C.; Arndt, D.; Gautam, M.; Allen, F.; Wishart, D.S. CFM-ID 3.0: Significantly improved ESI-MS/MS prediction and compound identification. *Metabolites* **2019**, *9*, 72, doi:10.3390/metabo9040072.

Discussion

Invasive ascidians represent a global threat for biodiversity, aquaculture, and shipping industries (Lambert 2007, Shenkar and Swalla 2011, Zhan et al. 2015). The spread of *C. intestinalis* along the coast of the Canadian province PEI is a particularly striking example, since massive fouling of the ascidian on cultivated blue mussels causes enormous losses at local mussel farms (Ramsay et al. 2008, Daigle and Herbinger 2009). Despite some general eco-physiological and habitat characteristics potentially promoting *C. intestinalis* during propagation in PEI, research on other aspects contributing to its invasive character is lacking. In order to shed light on additional factors influencing the invasiveness of *C. intestinalis*, the present study aimed to investigate for the first time the potential contribution of metabolites and associated microorganisms (Chapter 1), which have been reported to be involved in the invasion success of other marine species (Svensson et al. 2013, Vilcinskas 2015). Therefore, microbiomes and metabolomes of native (Helgoland, North Sea; Kiel, Baltic Sea) and invasive (PEI) *C. intestinalis* populations were comparatively analyzed. Prior to this, the taxonomic classification of *C. intestinalis* was verified by sequencing the mitochondrial marker gene COX3-ND1. In line with the proposed distribution of *C. intestinalis* and *C. robusta* (Bouchemousse et al. 2016), all samples were clearly assigned to *C. intestinalis*.

16S rRNA gene amplicon sequencing data showed a vast bacterial diversity in the ascidian's tunic. It was comparable to that of the invasive ascidian *Polyandrocarpa* spp. collected in North Carolina (Evans et al. 2017), but higher than previously reported for *C. intestinalis* (Blasiak et al. 2014). Higher bacterial diversity of *C. intestinalis'* tunic detected in this study may be related to the application of different hypervariable regions (this study: V3-V4, Blasiak et al. 2014: V1-V3), sequencing technologies (this study: Illumina MiSeq; Blasiak et al. 2014: 454 pyrosequencing), and databases for taxonomic classification of OTUs (this study: SILVA; Blasiak et al. 2014: Ribosomal Database Project, RDP). Since similar sequencing-based studies for ascidian gut microbiomes are either lacking (Chen et al. 2017) or not reporting alpha diversity measures (Dishaw et al. 2014), a similar comparison was not possible. In addition, microbiome analysis revealed significant differences in the distribution of the 39 bacterial phyla detected in the host (gut, tunic) and seawater references. *Ciona intestinalis'* microbiome did not merely reflect seawater conditions suggesting species-specificity of the associated microbial community as already shown for *Ciona* spp. and various other ascidians (Tianero et al. 2015, Cahill et al. 2016). Beyond this, acquired bacterial profiles also showed taxa specific to one sampling site, exemplified by OTU14 (*Leptolyngbya* sp.), OTU13 (*Bifidobacterium* sp.), and OTU4 (*Pseudomonas* sp.), which exclusively occurred in Canadian, Helgoland and Kiel samples. Location-specificity of bacterial taxa indicates that part of the ascidian microbiome relates to the environmental conditions of the habitat. Moreover, the bacterial consortium of *C. intestinalis* contained a stable fraction. For example, several bacteria specifically associated with the tunic (OTU1, *Kordiimonas* sp.; OTU3 *Arenibacter* sp.) and gut (OTU10 and OTU16, unclassified) were detected across all sampling sites. These OTUs were also detected in the same tissues of *C. intestinalis* and *C. robusta* sampled in different geographical areas (Blasiak et al. 2014, Dishaw et al. 2014, Cahill et al. 2016), further corroborating their stable association with the tunic or the gut of *C. intestinalis*.

The first metabolome study on *C. intestinalis* (Chapter 1) was based on UPLC-MS/MS data analyzed by state-of-the-art automated dereplication tools (FBMN, ISDB) as well as manual comparison to (M)NP databases (DNP, MarinLit, Reaxys). Generated FBMN contained >1000 nodes and dereplication efforts putatively annotated compounds to 19 different chemical families. Hence, this comprehensive analysis of the sea squirt's chemical space showed a huge chemical diversity, confirming that ascidians are prolific producers of MNPs (Schmidt et al. 2012). Previous LC-MS-based studies on solitary (Palanisamy et al.

2017b) and colonial (Buedenbender et al. 2017) ascidians reported lower numbers of detected metabolites. This observation may indicate a comparably rich metabolome of *C. intestinalis* but also methodological differences such as the use of different solvents (this study: MeOH/DCM; Palanisamy et al. 2017b: MeOH/CHCl$_3$; Buedenbender et al. 2017: MeOH) may play a role. Compounds putatively identified in this study were dominated by alkaloids (37%) and lipids (41%). This finding matches literature, since ascidians are an excellent source of alkaloids (Palanisamy et al. 2017a, Dou and Dong 2019) and a previous study on *C. intestinalis* evinced high abundance of lipids such as the omega-3 fatty acids docosahexaenoic and eicosapentaenoic acid (Zhao et al. 2015). Despite the combined automated and manual dereplication strategy, most compounds detected in this study remained unannotated (66%), thus underlining the knowledge gap regarding the chemical composition of *C. intestinalis*. In line with the microbiome analysis, also metabolomics showed location- and tissue-specificity in combination with ubiquitous metabolites detected in all samples. For instance, the FBMN of individual inner body and tunic metabolomes contained 1156 nodes in total, of which most (863) were detected in both tissues, while 98 and 195 nodes were exclusively detected in inner body and tunic tissues, respectively. Overall stable metabolomes with tissue-specific signatures are well-known from other marine invertebrates. For example, the metabolome of *Mytilus galloprovincialis* contained a considerable proportion (30%) of metabolites specifically produced in either digestive glands, gills, or posterior adductor muscles (Cappello et al. 2018). Taken together, these findings are in accordance with a global study investigating the microbiome and metabolome of 32 phylogenetically diverse ascidians. They demonstrated species-specificity and stable core microbes/ubiquitous metabolites in conjunction with location-specific signatures across all samples (Tianero et al. 2015). This pattern indicates high microbial and metabolic flexibility, which may be advantageous for *C. intestinalis* when adapting to changing environmental conditions.

In-depth analyses of microbial and metabolite data obtained from native and invasive *C. intestinalis* populations highlighted bacterial taxa and SMs, which may contribute to the overall fitness of *C. intestinalis* but also to its invasion success in PEI. Its chemical defense may be supported by associated microorganisms producing antifouling and antimicrobial compounds (Schmidt 2015). Such bioactive metabolites are reportedly produced by several bacterial taxa particularly abundant in Canadian tunicates, e.g., the cyanobacteria *Leptolyngbya* (Choi et al. 2010) and *Synechococcus* (Brilisauer et al. 2019) or the alphaproteobacteria *Roseobacter* sp. (Brinkhoff et al. 2004) and *Ruegeria* sp. (Muscholl-Silberhorn et al. 2008, Pujalte et al. 2014). Similarly, the metabolome of Canadian specimens contained two exclusive microbe-derived compounds (antibiotic YM 47525 and rubomycin M) with reported antimicrobial properties (Zbarskiĭ et al. 1991, Sugawara et al. 1997). Furthermore, some putatively annotated metabolites and identified cyanobacteria such as the Canada-specific bacterial genus *Leptolyngbya* show toxicity to invertebrates (Choi et al. 2010). Hence, these compounds may be toxic for (some) native invertebrates, which may enhance the competitiveness of *C. intestinalis* in its new habitat as predicted by the NWH. Further experiments are needed to verify the supposed contribution of bioactive SMs to the invasion success of *C. intestinalis*. These could include, e.g., common garden experiments or feeding assays testing the palatability of *C. intestinalis* and its competitors (e.g., *S. clava* and *M. edulis*) against common generalist predators in PEI (e.g., *C. maenas* and *A. rubens*). Moreover, the Canadian population showed a more diverse microbiota and a richer metabolome compared to both native populations. To the best of our knowledge, no comparable metabolomics studies have been performed on invasive ascidian populations yet, but few microbiome studies are available. Notably, there is no consistency between their

results. Microbial diversity was either increased (*Styela plicata*, Dror et al. 2019) or decreased (*Herdmania momus*, Dror et al. 2019; *Clavelina oblonga*, Goddard-Dwyer et al. 2020) in invasive populations or no clear trend regarding the microbial diversity was detected for native vs. invasive specimens (*Didemnum vexillum*, Casso et al. 2020). This may indicate different microbial community structures and microbial colonization strategies in different invasive ascidian species. Regarding *C. intestinalis*, higher metabolite and microbial diversity may guarantee rapid and flexible adaption to new habitats. Differences between invasive and native specimens were also observed with regard to extract yield, i.e., Canadian populations gave lower extract yields compared to native specimens (Helgoland and Kiel Fjord). In combination with the extraordinarily high biomass production of *C. intestinalis* in PEI, this may provide evidence for a metabolism shift towards biomass accumulation as described for the EICA hypothesis. However, these findings regarding invasive *C. intestinalis* need verification in future studies analyzing several invasive and native populations to exclude that the observed invasion-specific patterns are resulting from different environmental conditions in three habitats.

The combined analysis of microbiome and metabolome data represents a novelty in invasive ascidian research and provided profound knowledge on *C. intestinalis'* chemical repertoire and microbiota as well as first insights into their putative roles for the invasiveness of the sea vase tunicate. Such combined microbiome-metabolome analyses are recommended for future studies due to the intimate alliance of hosts and their microbial colonizers, which significantly contribute to the chemical makeup of the ascidian (Schmidt et al. 2012, Tianero et al. 2015). Our results gave first indications that the NWH and EICA may contribute to the invasion success of *C. intestinalis* in PEI. Hence, in addition to known beneficial eco-physiological traits facilitating the propagation of *C. intestinalis* in new habitats, associated microorganisms and metabolites may promote the invasion success *C. intestinalis*. In line with this, there is increasing evidence that often the interplay of several factors contributes to the invasiveness of an organism (Lau and Schultheis 2015, Murphy et al. 2019).

In contrast to their harmful environmental and economic effects as non-native fouling species, ascidians are an important source for pharmaceutical agents (Blunt et al. 2008, Schmidt et al. 2012, Palanisamy et al. 2017a). This is impressively illustrated by the fact that one third of approved marine-derived anticancer drugs derive from ascidians (Dyshlovoy and Honecker 2020). In line with the ascent of microorganisms as primary source for novel MNPs (Carroll et al. 2020), Proteobacteria were shown to be the actual producers of two approved ascidian-derived anticancer drugs (Rath et al. 2011, Xu et al. 2012). One major advantage of microbial biotechnology is the sustainable supply, since microorganisms isolated from any source can be unlimitedly cultured in the laboratory and require no exploitation of marine habitats (Romano et al. 2017). Accordingly, the second part of this doctoral research project set out to explore the MNP discovery potential of the cultivable microbial consortium associated with the tunic (Chapter 2) and gut (Chapter 3) of *C. intestinalis*. Although *Ciona* spp. are widely used model organisms in biology (Satoh et al. 2003, Carver et al. 2006, Dishaw et al. 2012), the biotechnological potential of their associated microbiota remained largely unknown, with only one tunic-derived bacterium studied so far (Holmström et al. 2002 and references therein).

The cultivation of microorganisms from tunic and seawater reference samples (Chapter 2) and gut tissues (Chapter 3) yielded in total 313 microbial isolates (242 bacteria and 71 fungi). Obtained isolates received identification codes referring to the host organism *C. intestinalis* (C), sampling site (Helgoland = H or Kiel = K), sample type (tunic = T, seawater = W, gut = G), and strain number, e.g., CKT60 relates to isolate 60 isolated from the tunic of

C. intestinalis sampled in Kiel. Two '*C. intestinalis* media' adjusted to Baltic Sea (CB) and North Sea salinity (CN) were designed to mimic the natural habitat of the microorganisms. They proved as suitable isolation media, since they yielded 27% of all obtained isolates and several bacterial and fungal taxa were exclusively isolated from these cultivation media. The isolation of strain CKT60 highlights the added value of these media. Isolate CKT60 showed exactly the same BLAST match (i.e., *Kiloniella laminariae*, accession number NR_042646) as OTU9, which, fittingly, was exclusive to *C. intestinalis* from Kiel Fjord and particularly abundant in its tunic (Chapter 1, Table S9). Hence, as mentioned in a recent review (Romano et al. 2017), imitation of natural growth conditions is a valuable tool for decreasing the proportion of unculturables. In line with the culture-independent microbiome analysis (Chapter 1), the isolation-based approach detected tissue- and location-specific bacterial communities. For instance, bacterial richness as well as abundance of Alphaproteobacteria were higher in *C. intestinalis'* tunic (89 bacterial isolates, 22% assigned to Alphaproteobacteria) compared to the ascidian's gut (61 bacterial isolates, 3% assigned to Alphaproteobacteria). Both approaches also revealed higher microbial richness in specimens from Kiel Fjord compared to samples from Helgoland, which may be attributed to, e.g., higher nutrient levels in the strongly anthropogenically influenced Kiel Fjord (Hans and Elmgren 1990, Nikulina et al. 2008). Another overarching result is the clear differentiation of the ascidian microbiota from its surrounding seawater, e.g., 79% of culturable microbial genera detected in tunic and gut samples were absent in seawater references. Nevertheless, cultivation studies usually represent only a minute fraction of the actual microbial diversity and often target easily culturable microorganisms (Alain and Querellou 2009). This so-called "great plate count anomaly" (Staley and Konopka 1985) also applies in this study to, e.g., the lack of several bacterial phyla such as Epsilonbacteraeota, Tenericutes, and Verrucomicrobia, which were abundant in the gut and tunic of *C. intestinalis* according to the amplicon sequencing data (Chapter 1, Figure 1).

The cultivable fraction of fungi was larger in the ascidian samples (gut: 40 isolates, tunic: 22 isolates) compared to the ambient seawater (9 isolates). Higher fungal diversity in marine hosts compared to surface seawater is common. Due to their osmotrophic feeding style, fungi preferably grow on nutrient-rich substrates such as animal hosts and sediments (Richards et al. 2012). Interestingly, saprotrophic fungi have been reported to decompose major constituents of the ascidians' tunic (tunicin) and gut mucus (chitin; Kohlmeyer and Kohlmeyer 1979, Hartl et al. 2012), which may also attribute to the comparably high abundance of cultivable fungi in the ascidian's gut and tunic. Hence, this study showed for the first time that *C. intestinalis* hosts a diverse culturable fungal community in its gut and tunic.

Microbial crude extracts (*n* = 208) produced by tunic- (Chapter 2) and gut-derived microbial strains (Chapter 3) were tested in a series of *in vitro* antibacterial, antifungal, and anticancer assays. Since an enormous amount of crude extracts showed activity in at least one assay, we decided to set a high bioactivity threshold (≥ 80% inhibition at a test concentration of 100 µg/mL in at least one bioassay), which was fulfilled by 45% of tunic- and 66% of gut-derived extracts. Gut- and tunic-associated microorganisms delivered 21 crude extracts in total (i.e., 10%) with activity against *C. albicans* and/or *C. neoformans*, which range among the most harmful fungal pathogens (Karkowska-Kuleta et al. 2009). While generally lesser susceptible Gram-negative human pathogens (Pages et al. 2008, Zgurskaya et al. 2015) were only inhibited by few gut-derived fungal extracts, antibacterial activity was ubiquitously observed and mainly detected against MRSA (tunic: 42% of microbial extracts, gut: 62%), one of the most threatening drug-resistant pathogens (Liu et al. 2019). Notably, antibacterial activities were more prevalent than anticancer activities (gut: 22%, tunic: 6%),

contradicting a recent review on ascidian-associated microorganisms that identified more MNPs with anticancer (47%) than with antimicrobial properties (31%; Casertano et al. 2020). According to Newman and Cragg 2016, the overall low number of antimicrobial MNPs and the lack of approved marine-derived antibiotics may partly be related to the well supported funding schemes on anticancer MNP discovery, while antibiotic research is only scarcely supported (Newman and Cragg 2016). Hence, lacking funds for antimicrobial MNP discovery may have led to a discrepancy between the actual and the reported proportion of antimicrobial and anticancer MNPs.

The overwhelming amount of 115 highly bioactive microbial crude extracts guided us to apply further prioritization steps for selecting the most promising microbial extracts for in-depth chemical studies. A 2-step selection procedure was developed that considered bioactivity profiles and chemical diversity of each extract. This approach prioritized seven microbial extracts produced by the tunic-associated microbiota (Chapter 2) and nine crude extracts obtained from the gut microflora of *C. intestinalis* (Chapter 3). Except for one extract, the applied prioritization strategy selected only actinobacterial ($n = 4$) and fungal extracts ($n = 11$). This predominance of Actinobacteria and fungi as most diverse and promising MNPs producers is in line with a recent review stating that these two taxa delivered 72.3% of MNPs isolated from ascidian-associated microorganisms (Casertano et al. 2020).

Prioritized microbial extracts were subjected to in-depth chemical investigations based on the sophisticated methods already used for the analysis of the ascidian metabolome (Chapter 1). Putatively annotated compounds ($n = 170$) revealed a vast chemical diversity as they were assigned to nearly 50 different chemical families. In line with literature, polyketides were highly abundant among putatively identified fungal secondary metabolites (Keller et al. 2005) and peptides dominated annotated bacterial chemical profiles (Gulder and Moore 2009). Many detected compounds could not be assigned to known chemical scaffolds and putatively annotated metabolites did often not (fully) explain the observed biological activities. The gut-derived *Penicillium* sp. strain CKG23 (Chapter 3) showed strikingly different chemistry on different cultivation media (CAG, PDA) and altogether, eight different chemical families were putatively annotated. Therefore, *Penicillium* sp. strain CKG23 is the most versatile metabolite producer discovered in this study. Its CAG extract is particularly attractive because anticancer and antibacterial activities could not be linked to putatively identified compounds. The observed activity against Gram-negative bacteria is of high interest due to the urgent need of effective treatments against Gram-negatives. Multidrug-resistance is widespread in Gram-negative nosocomial pathogens raising mortality rates to up to 50% (Pages et al. 2008, Zgurskaya et al. 2015). Several additional fungal extracts and one *Streptomyces* sp. strain (CKT43-GYM) showed antibacterial and/or antifungal activities, which could not be related to any of the putatively annotated metabolites. Three additional microbial extracts (*P. destructans* CHT56-CAG; *Streptomyces* sp. CHG48-GYM and CKT43-GYM) are particularly favorable for isolation of putatively novel anticancer lead compounds. *Streptomyces* spp. are the most rewarding source for natural pharmaceuticals (Anandan et al. 2016). Moreover, actinomycetes are the major source for clinically used antibiotics (Culp et al. 2019, van Bergeijk et al. 2020). Thus, the selection of *Streptomyces* sp. strains CHG48 and CKT43 for purification of novel bioactive compounds is particularly favorable. In addition, it is recommended to purify unidentified compound **49** of *Micromonospora* sp. extract CKG20-GYM (Chapter 3). According to FBMN, this metabolite is a putatively novel rakicidin derivative. Rakicidins reportedly exhibit broad-spectrum antibacterial activities (Landwehr et al. 2016) and are also promising anticancer lead compounds due to their hypoxia-selective cytotoxicity (Oku et al. 2014) rendering compound **49** a promising candidate for isolation and structure

elucidation. MS/MS-based prediction of the linear structure of two putatively novel lipopeptides (m/z values of 754.5424 and 770.5386 [M + H]$^+$) detected in *Trichoderma* sp. CHG34 (Chapter 3) should be confirmed in a prospective study. Bioactive fungal-derived linear lipopeptides were already described in the literature. For example, *Penicillium fellutanum* isolated from the intestine of a marine fish yielded fellutamide A and B, which exhibited potent cytotoxicity against three cancer cell lines (Shigemori et al. 1991). Structurally related linear lipopeptides were also isolated from terrestrial ascomycetes *Metulocladosporiella* sp. (fellutamide C and D) and *Colispora cavincola* (cavinafungin A and B), both showing broad-spectrum antifungal activity against six different *Candida* species and *Aspergillus fumigatus* (Xu et al. 2011, Ortiz-Lopez et al. 2015). Thus, putatively novel lipopeptides produced by *Trichoderma* sp. strain CHG34 are valuable targets for compound purification and structure elucidation, also due to the unresolved antimicrobial activities of its PDA extract. Based on the variety of promising microbial crude extracts for the discovery of novel anticancer and antimicrobial lead compounds, it can be concluded that the applied 2-step selection strategy performed well and allowed time- and resource-efficient screening of crude extracts. Moreover, this study clearly evinced that so far unstudied culturable fungi associated with *C. intestinalis* harbor a huge potential for marine biodiscovery and are the most precious source for bioactive and novel MNPs. This exceeded expectations, since so far Actinobacteria were reported as primary source for MNPs from microbial associates of ascidians (Casertano et al. 2020).

Several compounds putatively annotated in bacterial and fungal extracts have other relevant bioactivities, indicating that the pharmaceutical potential of tunic- and gut-associated microorganisms may go beyond anticancer and antimicrobial activities. For instance, anti-inflammatory (e.g., amicoumacin-A in *Bacillus* sp. extract CKG24-GYM, Itoh et al. 1981) and anti-viral (e.g., mycophenolic acid in *Penicillium* sp. extract CKG35-PDA, Williams et al. 1968) activities are reported from putatively identified compounds. Moreover, *Bacillus* sp. strain CKG24 produced nine surfactin-like lipopeptides. These *Bacillus*-specific NPs show multiple bioactivities (e.g., anticancer and antiviral) and are excellent biosurfactants with high industrial application potential due to their amphiphilic character (Peypoux et al. 1999, Abdel-Mawgoud et al. 2008).

Phylogenetic analysis excluded 23 tunic- and 15 gut-derived strains from the initial bioactivity screening, i.e., only one representative strain was selected if strains isolated from the same sampling site and tissue were affiliated to the same species. Since the metabolic repertoire is often phylogenetically conserved, the taxonomy-based selection of representative strains is well justified (Macia-Vicente et al. 2018). However, a MN-based study detected between 8 and 288 nodes in the crude extracts of several *Salinispora arenicola* strains evincing strikingly different chemistry of strains affiliated to the same species (Crüsemann et al. 2016). Hence, these so far untouched strains may still represent an additional valuable reservoir for discovery of bioactive MNPs worth to examine in future studies.

The integrated dereplication workflow applied in this study (Chapters 1-3) proved very successful to increase annotation rates to up to 73%, which is a significant improvement compared to annotation scores usually ≤10% (da Silva et al. 2015, Oppong-Danquah et al. 2020). The key advantage of the applied FBMN is the clustering of closely related compounds based on their isotopic patterns and retention times. At the same time redundant and contaminant peaks are automatically removed, which significantly improves compound annotation. The present study delivered many examples of successful FBMN-aided dereplication, such as the putative identification of tetrapyrroles in the ascidian's crude extracts (Chapter 1) as well as of cyclic octapeptides (surugamides; Chapter 2) and nonactic acids (Chapter 3) in *Streptomyces* sp. extracts. The ISDB workflow delivered additional hits, such

as the putative identification of indole alkaloids and polyunsaturated amino alcohols (crucigasterins) in the metabolome of *C. intestinalis* (Chapter 1). Including additional computational dereplication tools may not further enhance annotation rates, since the underlying algorithms highly depend on data deposition by database curators and users and this is particularly problematic for rarely studied taxa and unusual chemical families (Dührkop et al. 2020). For instance, the GNPS workflow DEREPLICATOR+ (Mohimani et al. 2018) did not generate any additional putative hits for *P. destructans* strain CHT56 (data not shown), indicating that the applied dereplication strategy is reaching the limits of successful compound annotation. Nevertheless, the brand-new tool CANOPUS (published end of 2020) may allow the chemical classification of further compounds or molecular clusters. CANOPUS uses a combination of two machine learning techniques that allow prediction of compound classes independent from deposited MS/MS spectra (Dührkop et al. 2020).

To conclude, the applied sequencing- and LC-MS/MS-based technologies proved successful to study the microbiome and chemical inventory of native and invasive *C. intestinalis* populations (Chapter 1). Our study showed an interplay of stable core microbes and tissue- and location-specific bacteria and metabolites, indicating a large capacity to rapidly adapt to changing environmental conditions. Moreover, bacterial and chemical diversity was highest in invasive specimens, although this needs verification in future studies probing *C. intestinalis* at a global scale. This study showed, also for the first time, that the associated microbiota of *C. intestinalis* and its (microbial) metabolites may provide beneficial functions, such as antimicrobial activity, promoting the overall fitness of the sea vase tunicate and its proliferation in new habitats. In a culture-based approach (Chapters 2 and 3), most of the 150 bacteria and 62 fungi isolated from the tunic and gut of native *C. intestinalis* specimens exhibited antimicrobial or anticancer activities. In-depth metabolome mining of selected microorganisms showed a rich chemistry, while many compounds represent putatively novel metabolites. Several promising candidate strains were highlighted for future studies to isolate novel antibiotic or anticancer leads. Fungi, which have been isolated for the first time from *C. intestinalis,* proved as particularly rich source of diverse and bioactive MNPs. Hence, the conducted MNP screening of tunic- and gut-derived microbiota of *C. intestinalis* demonstrated an excellent potential for discovery of therapeutic agents against cancer and infectious diseases, also emphasizing the developed prioritization and applied dereplication strategy as a powerful workflow for MNP discovery.

Outlook

The presented doctoral thesis delivered intriguing comparative insights into the microbial and metabolite composition of native and invasive *C. intestinalis* populations and determined the potential of the tunic- and gut-associated microbiota of native *C. intestinalis* in marine biodiscovery. This study delivered the first results on so far unexplored research fields and thereby lays the foundation for future research projects on this model organism that go beyond the specific aims of this study. Prospective studies could include but may not be limited to:

- **Global sampling campaign of native and invasive *C. intestinalis* populations with an extended experimental design**

   Expanding the sampling campaign to additional invasive and native populations will allow to verify observed differences in their microbiome and metabolome profiles and their potential contribution to the invasiveness of *C. intestinalis*. Several invasive populations along the Canadian (e.g., Nova Scotia, Newfoundland) and US Atlantic coast (e.g., Massachusetts, New Hampshire) as well as the Chinese coastline (e.g., Yellow and/or

Bohai Sea) should be included and compared to additional native populations (e.g., Swedish Baltic Sea, European North Atlantic). Furthermore, it is advised to acquire metagenomic datasets. This would (1) provide valuable information regarding the metabolic capacity of the associated microbiota and (2) inform about potentially associated fungi. The mycobiome has not been studied on NGS basis for any ascidian species so far, but the re-occurring isolation of fungi from *Ciona* spp. (this study and Liberti et al. 2019) and other ascidians (López-Legentil et al. 2015) suggests their specific association. Metatranscriptomic analysis would further complement this dataset by elucidating activated genes and thereby, allow to identify active metabolic pathways (Bashiardes et al. 2016). Manual comparison of, e.g., metagenomic and metabolomic data would allow an ultimate link between produced metabolites and their potential microbial producers. This assessment of so-called "product–producer pairs" will provide deep insights into the microbial contribution to *C. intestinalis'* metabolome (van der Hooft et al. 2020) and therefore, allow further conclusions regarding its potential support during colonization of new habitats. Integration of these omics datasets is still a challenge and automated tools are missing; hence, it remains a future challenge to generate and optimize chemical and bioinformatic workflows allowing a fully automated and comprehensive metagenome-metatranscriptome-metabolome comparison (Aguiar-Pulido et al. 2016).

- **Isolation, structure elucidation, and bioactivity studies of novel anticancer and antimicrobial lead compounds**
  The most promising gut- and tunic-derived microbial strains should be subjected to large-scale cultivation to produce enough microbial biomass for compound purification, structure elucidation and bioactivity assessments of pure compounds. It is advisable to probe the production of target compounds in liquid cultures, since this facilitates upscaling of promising lead compounds at an industrial scale. Isolation of novel and bioactive compounds would further validate the applied prioritization pipeline and may also allow optimization of the applied selection and dereplication strategies. To verify the MS/MS-based prediction, purification of the putatively novel linear lipopeptides produced by *Trichoderma* sp. CHG34 should be targeted as well. Pure compounds should also be tested for general cytotoxicity, a common obstacle for development of anticancer drugs (Remesh 2012), by including normal cells such as human skin keratinocytes to the bioassay panel. Beyond this, anticancer/antimicrobial bioactivities of pure compounds would need verification in *in vivo* studies and studies determining the mechanism of action should be conducted as well.

- **Explore hidden metabolite repertoire**

  Several techniques, such as OSMAC and co-cultivation, to enhance the chemical space of an organism are successfully established in our laboratory (Oppong-Danquah et al. 2018, Fan et al. 2019). Such manipulation strategies may trigger the activation of so far silent BGCs, and thereby, the production of additional novel and bioactive metabolites. Hence, promising microbial producer strains could be subjected to additional cultivation experiments to further explore their chemical repertoire. To fully exhaust the biotechnological potential of the gut and tunic microbiota of *C. intestinalis*, previously excluded strains (see above) should be subjected to the same MNP discovery pipeline. This would allow a comparison of their bioactivities and chemistry to that of the tested representative strains.

References

Abdel-Mawgoud, A.M.; Aboulwafa, M.M.; Hassouna, N.A. Optimization of surfactin production by *Bacillus subtilis* isolate BS5. *Appl. Biochem. Biotechnol.* 2008, 150, 305-325, doi:10.1007/s12010-008-8155-x.

Aguiar-Pulido, V.; Huang, W.; Suarez-Ulloa, V.; Cickovski, T.; Mathee, K.; Narasimhan, G. Metagenomics, metatranscriptomics, and metabolomics approaches for microbiome analysis. *Evol. Bioinform.* 2016, 12, 5-16, doi:10.4137/EBO.S36436.

Alain, K.; Querellou, J. Cultivating the uncultured: Limits, advances and future challenges. *Extremophiles* 2009, 13, 583-594, doi:10.1007/s00792-009-0261-3.

Anandan, R.; Dharumadurai, D.; Manogaran, G.P. An introduction to actinobacteria. In *Actinobacteria-Basics and Biotechnological Applications*, Dhanasekaran, D.; Jiang, Y., Eds. Intechopen: 2016; p. 3-37.

Bashiardes, S.; Zilberman-Schapira, G.; Elinav, E. Use of metatranscriptomics in microbiome research. *Bioinform. Biol. Insights* 2016, 10, 19-25, doi:10.4137/BBI.S34610.

Blasiak, L.C.; Zinder, S.H.; Buckley, D.H.; Hill, R.T. Bacterial diversity associated with the tunic of the model chordate *Ciona intestinalis. ISME J.* 2014, 8, 309-320, doi:10.1038/ismej.2013.156.

Blunt, J.W.; Copp, B.R.; Hu, W.P.; Munro, M.H.; Northcote, P.T.; Prinsep, M.R. Marine natural products. *Nat. Prod. Rep.* 2008, 25, 35-94, doi:10.1039/b701534h.

Bouchemousse, S.; Bishop, J.D.; Viard, F. Contrasting global genetic patterns in two biologically similar, widespread and invasive *Ciona* species (Tunicata, Ascidiacea). *Sci. Rep.* 2016, 6, 24875, doi:10.1038/srep24875.

Brilisauer, K.; Rapp, J.; Rath, P.; Schollhorn, A.; Bleul, L.; Weiss, E.; Stahl, M.; Grond, S.; Forchhammer, K. Cyanobacterial antimetabolite 7-deoxy-sedoheptulose blocks the shikimate pathway to inhibit the growth of prototrophic organisms. *Nat. Commun.* 2019, 10, 545, doi:10.1038/s41467-019-08476-8.

Brinkhoff, T.; Bach, G.; Heidorn, T.; Liang, L.; Schlingloff, A.; Simon, M. Antibiotic production by a *Roseobacter* clade-affiliated species from the German Wadden Sea and its antagonistic effects on indigenous isolates. *Appl. Environ. Microbiol.* 2004, 70, 2560-2565, doi:10.1128/aem.70.4.2560-2565.2003.

Buedenbender, L.; Carroll, A.; Ekins, M.; Kurtböke, D. Taxonomic and metabolite diversity of Actinomycetes associated with three Australian ascidians. *Diversity* 2017, 9, 53, doi:10.3390/d9040053.

Cahill, P.L.; Fidler, A.E.; Hopkins, G.A.; Wood, S.A. Geographically conserved microbiomes of four temperate water tunicates. *Environ. Microbiol. Rep.* 2016, 8, 470-478, doi:10.1111/1758-2229.12391.

Cappello, T.; Giannetto, A.; Parrino, V.; Maisano, M.; Oliva, S.; De Marco, G.; Guerriero, G.; Mauceri, A.; Fasulo, S. Baseline levels of metabolites in different tissues of mussel *Mytilus galloprovincialis* (Bivalvia: Mytilidae). *Comp. Biochem. Physiol. Part D Genomics Proteomics* 2018, 26, 32-39, doi:10.1016/j.cbd.2018.03.005.

Carroll, A.R.; Copp, B.R.; Davis, R.A.; Keyzers, R.A.; Prinsep, M.R. Marine natural products. *Nat. Prod. Rep.* 2020, 37, 175-223, doi:10.1039/c9np00069k.

Carver, C.E.; Mallet, A.L.; Vercaemer, B. Biological synopsis of the solitary tunicate *Ciona intestinalis. Can. Man. Rep. Fish. Aquat. Sci.* 2006, 2746, 1-55.

Casertano, M.; Menna, M.; Imperatore, C. The ascidian-derived metabolites with antimicrobial properties. *Antibiotics* 2020, 9, 510, doi:10.3390/antibiotics9080510.

Casso, M.; Turon, M.; Marco, N.; Pascual, M.; Turon, X. The microbiome of the worldwide invasive ascidian *Didemnum vexillum. Front. Mar. Sci.* 2020, 7, 201, doi:10.3389/fmars.2020.00201.

Chen, L.; Fu, C.; Wang, G. Microbial diversity associated with ascidians: A review of research methods and application. *Symbiosis* 2017, 71, 19-26, doi:10.1007/s13199-016-0398-7.

Choi, H.; Engene, N.; Smith, J.E.; Preskitt, L.B.; Gerwick, W.H. Crossbyanols A−D, toxic brominated polyphenyl ethers from the Hawai'ian bloom-forming cyanobacterium *Leptolyngbya crossbyana. J. Nat. Prod.* 2010, 73, 517-522, doi:10.1021/np900661g.

Crüsemann, M.; O'Neill, E.C.; Larson, C.B.; Melnik, A.V.; Floros, D.J.; da Silva, R.R.; Jensen, P.R.; Dorrestein, P.C.; Moore, B.S. Prioritizing natural product diversity in a collection of 146 bacterial strains based on growth and extraction protocols. *J. Nat. Prod.* 2016, 80, 588-597, doi:10.1021/acs.jnatprod.6b00722.

Culp, E.J.; Yim, G.; Waglechner, N.; Wang, W.; Pawlowski, A.C.; Wright, G.D. Hidden antibiotics in actinomycetes can be identified by inactivation of gene clusters for common antibiotics. *Nat. Biotechnol.* 2019, 37, 1149–1154, doi:10.1038/s41587-019-0241-9.

da Silva, R.R.; Dorrestein, P.C.; Quinn, R.A. Illuminating the dark matter in metabolomics. *Proc. Natl. Acad. Sci. USA* 2015, 112, 12549-12550, doi:10.1073/pnas.1516878112.

Daigle, R.M.; Herbinger, C.M. Ecological interactions between the vase tunicate (*Ciona intestinalis*) and the farmed blue mussel (*Mytilus edulis*) in Nova Scotia, Canada. *Aquat. Invasions* 2009, 4, 177-187, doi:10.3391/ai.2009.4.1.18.

Dishaw, L.J.; Flores-Torres, J.; Lax, S.; Gemayel, K.; Leigh, B.; Melillo, D.; Mueller, M.G.; Natale, L.; Zucchetti, I.; De Santis, R.; et al. The gut of geographically disparate *Ciona intestinalis* harbors a core microbiota. *PLoS ONE* 2014, 9, e93386, doi:10.1371/journal.pone.0093386.

Dishaw, L.J.; Flores-Torres, J.A.; Mueller, M.G.; Karrer, C.R.; Skapura, D.P.; Melillo, D.; Zucchetti, I.; De Santis, R.; Pinto, M.R.; Litman, G.W. A Basal chordate model for studies of gut microbial immune interactions. *Front. Immunol.* 2012, 3, 96, doi:10.3389/fimmu.2012.00096.

Dou, X.; Dong, B. Origins and bioactivities of natural compounds derived from marine ascidians and their symbionts. *Mar. Drugs* 2019, 17, 670, doi:10.3390/md17120670.

Dror, H.; Novak, L.; Evans, J.S.; Lopez-Legentil, S.; Shenkar, N. Core and dynamic microbial communities of two invasive ascidians: Can host-symbiont dynamics plasticity affect invasion capacity? *Microb. Ecol.* 2019, 78, 170-184, doi:10.1007/s00248-018-1276-z.

Dührkop, K.; Nothias, L.F.; Fleischauer, M.; Reher, R.; Ludwig, M.; Hoffmann, M.A.; Petras, D.; Gerwick, W.H.; Rousu, J.; Dorrestein, P.C.; et al. Systematic classification of unknown metabolites using high-resolution fragmentation mass spectra. *Nat. Biotechnol.* 2020, doi:10.1038/s41587-020-0740-8.

Dyshlovoy, S.A.; Honecker, F. Marine compounds and cancer: Updates 2020. *Mar. Drugs* 2020, 18, 643, doi:10.3390/md18120643.

Evans, J.S.; Erwin, P.M.; Shenkar, N.; Lopez-Legentil, S. Introduced ascidians harbor highly diverse and host-specific symbiotic microbial assemblages. *Sci. Rep.* 2017, 7, 11033, doi:10.1038/s41598-017-11441-4.

Fan, B.; Parrot, D.; Blümel, M.; Labes, A.; Tasdemir, D. Influence of OSMAC-based cultivation in metabolome and anticancer activity of fungi associated with the brown alga *Fucus vesiculosus*. *Mar. Drugs* 2019, 17, 67, doi:10.3390/md17010067.

Goddard-Dwyer, M.; Lopez-Legentil, S.; Erwin, P.M. Microbiome variability across the native and invasive range of the ascidian *Clavelina oblonga*. *Appl. Environ. Microbiol.* 2020, 87, e02233-02220, doi:10.1128/AEM.02233-20.

Gulder, T.A.; Moore, B.S. Chasing the treasures of the sea - bacterial marine natural products. *Curr. Opin. Microbiol.* 2009, 12, 252-260, doi:10.1016/j.mib.2009.05.002.

Hans, C.; Elmgren, R. Biological effects of eutrophication in the Baltic Sea, particularly the coastal zone. *Ambio* 1990, 19, 109-112.

Hartl, L.; Zach, S.; Seidl-Seiboth, V. Fungal chitinases: Diversity, mechanistic properties and biotechnological potential. *Appl. Microbiol. Biotechnol.* 2012, 93, 533-543, doi:10.1007/s00253-011-3723-3.

Holmström, C.; Egan, S.; Franks, A.; McCloy, S.; Kjelleberg, S. Antifouling activities expressed by marine surface associated *Pseudoalteromonas* species. *FEMS Microbiol. Ecol.* 2002, 41, 47-58, doi:10.1111/j.1574-6941.2002.tb00965.x.

Itoh, J.; Omoto, S.; Shomura, T.; Nishizawa, N.; Miyado, S.; Yuda, Y.; Shibata, U.; Inouye, S. Amicoumacin-A, a new antibiotic with strong antiinflammatory and antiulcer activity. *J. Antibiot.* 1981, 34, 611-613, doi:10.7164/antibiotics.34.611.

Karkowska-Kuleta, J.; Rapala-Kozik, M.; Kozik, A. Fungi pathogenic to humans: Molecular bases of virulence of *Candida albicans*, *Cryptococcus neoformans* and *Aspergillus fumigatus*. *Acta Biochim. Pol.* 2009, 56, 211–224, doi:10.18388/abp.2009_2452.

Keller, N.P.; Turner, G.; Bennett, J.W. Fungal secondary metabolism - from biochemistry to genomics. *Nat. Rev. Microbiol.* 2005, 3, 937-947, doi:10.1038/nrmicro1286.

Kohlmeyer, J.; Kohlmeyer, E. Fungi in animal substrates. In *Marine Mycology. The Higher Fungi*, Kohlmeyer, J.; Kohlmeyer, E., Eds. Academic Press: London, UK, 1979; p. 137-142.

Lambert, G. Invasive sea squirts: A growing global problem. *J. Exp. Mar. Biol. Ecol.* 2007, 342, 3-4, doi:10.1016/j.jembe.2006.10.009.

Landwehr, W.; Karwehl, S.; Schupp, P.J.; Schumann, P.; Wink, J. Biological active rakicidins A, B and E produced by the marine *Micromonospora* sp. isolate Guam1582. *Adv. Biotechnol. Microbiol.* 2016, 1, 1-5, doi:10.19080/aibm.2016.01.555558.

Lau, J.A.; Schultheis, E.H. When two invasion hypotheses are better than one. *New Phytol.* 2015, 205, 958-960, doi:10.1111/nph.13260.

Liberti, A.; Cannon, J.P.; Litman, G.W.; Dishaw, L.J. A soluble immune effector binds both fungi and bacteria via separate functional domains. *Front. Immunol.* 2019, 10, 369, doi:10.3389/fimmu.2019.00369.

Liu, M.; El-Hossary, E.M.; Oelschlaeger, T.A.; Donia, M.S.; Quinn, R.J.; Abdelmohsen, U.R. Potential of marine natural products against drug-resistant bacterial infections. *Lancet Infect. Dis.* 2019, 19, e237-e245, doi:10.1016/s1473-3099(18)30711-4.

López-Legentil, S.; Erwin, P.M.; Turon, M.; Yarden, O. Diversity of fungi isolated from three temperate ascidians. *Symbiosis* 2015, 66, 99-106, doi:10.1007/s13199-015-0339-x.

Macia-Vicente, J.G.; Shi, Y.N.; Cheikh-Ali, Z.; Grun, P.; Glynou, K.; Kia, S.H.; Piepenbring, M.; Bode, H.B. Metabolomics-based chemotaxonomy of root endophytic fungi for natural products discovery. *Environ. Microbiol.* 2018, 20, 1253-1270, doi:10.1111/1462-2920.14072.

Mohimani, H.; Gurevich, A.; Shlemov, A.; Mikheenko, A.; Korobeynikov, A.; Cao, L.; Shcherbin, E.; Nothias, L.F.; Dorrestein, P.C.; Pevzner, P.A. Dereplication of microbial metabolites through database search of mass spectra. *Nat. Commun.* 2018, 9, 4035, doi:10.1038/s41467-018-06082-8.

Murphy, K.J.; Sephton, D.; Klein, K.; Bishop, C.D.; Wyeth, R.C. Abiotic conditions are not sufficient to predict spatial and interannual variation in abundance of *Ciona intestinalis* in Nova Scotia, Canada. *Mar. Ecol. Prog. Ser.* 2019, 628, 105-123, doi:10.3354/meps13076.

Muscholl-Silberhorn, A.; Thiel, V.; Imhoff, J.F. Abundance and bioactivity of cultured sponge-associated bacteria from the Mediterranean Sea. *Microb. Ecol.* 2008, 55, 94-106, doi:10.1007/s00248-007-9255-9.

Newman, D.J.; Cragg, G.M. Drugs and drug candidates from marine sources: An assessment of the current "state of play". *Planta Med.* 2016, 82, 775-789, doi:10.1055/s-0042-101353.

Nikulina, A.; Polovodova, I.; Schönfeld, J. Foraminiferal response to environmental changes in Kiel Fjord, SW Baltic Sea. *eEarth* 2008, 3, 37-49, doi:10.5194/ee-3-37-2008.

Oku, N.; Matoba, S.; Yamazaki, Y.M.; Shimasaki, R.; Miyanaga, S.; Igarashi, Y. Complete stereochemistry and preliminary structure-activity relationship of rakicidin A, a hypoxia-selective cytotoxin from *Micromonospora* sp. *J. Nat. Prod.* 2014, 77, 2561-2565, doi:10.1021/np500276c.

Oppong-Danquah, E.; Parrot, D.; Blümel, M.; Labes, A.; Tasdemir, D. Molecular networking-based metabolome and bioactivity analyses of marine-adapted fungi co-cultivated with phytopathogens. *Front. Microbiol.* 2018, 9, 1-20, doi:10.3389/fmicb.2018.02072.

Oppong-Danquah, E.; Passaretti, C.; Chianese, O.; Blümel, M.; Tasdemir, D. Mining the metabolome and the agricultural and pharmaceutical potential of sea foam-derived fungi. *Mar. Drugs* 2020, 18, 128, doi:10.3390/md18020128.

Ortiz-Lopez, F.J.; Monteiro, M.C.; Gonzalez-Menendez, V.; Tormo, J.R.; Genilloud, O.; Bills, G.F.; Vicente, F.; Zhang, C.; Roemer, T.; Singh, S.B.; et al. Cyclic colisporifungin and linear cavinafungins, antifungal lipopeptides isolated from *Colispora cavincola. J. Nat. Prod.* 2015, 78, 468-475, doi:10.1021/np500854j.

Pages, J.M.; James, C.E.; Winterhalter, M. The porin and the permeating antibiotic: A selective diffusion barrier in Gram-negative bacteria. *Nat. Rev. Microbiol.* 2008, 6, 893-903, doi:10.1038/nrmicro1994.

Palanisamy, S.K.; Rajendran, N.M.; Marino, A. Natural products diversity of marine ascidians (tunicates; Ascidiacea) and successful drugs in clinical development. *Nat. Prod. Bioprospect.* 2017a, 7, 1-111, doi:10.1007/s13659-016-0115-5.

Palanisamy, S.K.; Trisciuoglio, D.; Zwergel, C.; Del Bufalo, D.; Mai, A. Metabolite profiling of ascidian *Styela plicata* using LC-MS with multivariate statistical analysis and their antitumor activity. *J. Enzyme Inhib. Med. Chem.* 2017b, 32, 614-623, doi:10.1080/14756366.2016.1266344.

Peypoux, F.; Bonmatin, J.M.; Wallach, J. Recent trends in the biochemistry of surfactin. *Appl. Microbiol. Biotechnol.* 1999, 51, 553-563, doi:10.1007/s002530051432.

Pujalte, M.J.; Lucena, T.; Ruvira, M.A.; Arahal, D.R.; Macián, M.C. The family Rhodobacteraceae. In *The Prokaryotes*, Rosenberg E., DeLong E.F., Lory S., Stackebrandt E., Thompson F., Eds. Springer: Berlin/Heidelberg, Germany, 2014; p. 439-512.

Ramsay, A.; Davidson, J.; Landry, T.; Arsenault, G. Process of invasiveness among exotic tunicates in Prince Edward Island, Canada. *Biol. Invasions* 2008, 10, 1311-1316, doi:10.1007/s10530-007-9205-y.

Rath, C.M.; Janto, B.; Earl, J.; Ahmed, A.; Hu, F.Z.; Hiller, L.; Dahlgren, M.; Kreft, R.; Yu, F.; Wolff, J.J.; et al. Meta-omic characterization of the marine invertebrate microbial consortium that produces

the chemotherapeutic natural product ET-743. *ACS Chem. Biol.* 2011, 6, 1244-1256, doi:10.1021/cb200244t.

Remesh, A. Toxicities of anticancer drugs and its management. *Int. J. Basic Clin. Pharmacol.* 2012, 1, 2-12, doi:10.5455/2319-2003.ijbcp000812.

Richards, T.A.; Jones, M.D.; Leonard, G.; Bass, D. Marine fungi: Their ecology and molecular diversity. *Ann. Rev. Mar. Sci.* 2012, 4, 495-522, doi:10.1146/annurev-marine-120710-100802.

Romano, G.; Costantini, M.; Sansone, C.; Lauritano, C.; Ruocco, N.; Ianora, A. Marine microorganisms as a promising and sustainable source of bioactive molecules. *Mar. Environ. Res.* 2017, 128, 58-69, doi:10.1016/j.marenvres.2016.05.002.

Satoh, N.; Satou, Y.; Davidson, B.; Levine, M. *Ciona intestinalis*: An emerging model for whole-genome analyses. *Trends Genet.* 2003, 19, 376-381, doi:10.1016/S0168-9525(03)00144-6.

Schmidt, E.W. The secret to a successful relationship: Lasting chemistry between ascidians and their symbiotic bacteria. *Invertebr. Biol.* 2015, 134, 88-102, doi:10.1111/ivb.12071.

Schmidt, E.W.; Donia, M.S.; McIntosh, J.A.; Fricke, W.F.; Ravel, J. Origin and variation of tunicate secondary metabolites. *J. Nat. Prod.* 2012, 75, 295-304, doi:10.1021/np200665k.

Shenkar, N.; Swalla, B.J. Global diversity of Ascidiacea. *PLoS ONE* 2011, 6, e20657, doi:10.1371/journal.pone.0020657.

Shigemori, H.; Wakuri, S.; Yazawa, K.; Nakamura, T.; Sasaki, T.; Kobayashi, J.i. Fellutamides A and B, cytotoxic peptides from a marine fish-possessing fungus *Penicillium fellutanum*. *Tetrahedron* 1991, 47, 8529-8534, doi:10.1016/s0040-4020(01)82396-6.

Staley, J.T.; Konopka, A. Measurement of in situ activities of nonphotosynthetic microorganisms in aquatic and terrestrial habitats. *Annu. Rev. Microbiol.* 1985, 39, 321-346, doi:10.1146/annurev.mi.39.100185.001541.

Sugawara, T.; Tanaka, A.; Nagai, K.; Suzuki, K.; Okada, G. New members of the trichothecene family. *J. Antibiot.* 1997, 50, 778-780, doi:10.7164/antibiotics.50.778.

Svensson, J.R.; Nylund, G.M.; Cervin, G.; Toth, G.B.; Pavia, H.; Callaway, R. Novel chemical weapon of an exotic macroalga inhibits recruitment of native competitors in the invaded range. *J. Ecol.* 2013, 101, 140-148, doi:10.1111/1365-2745.12028.

Tianero, M.D.; Kwan, J.C.; Wyche, T.P.; Presson, A.P.; Koch, M.; Barrows, L.R.; Bugni, T.S.; Schmidt, E.W. Species specificity of symbiosis and secondary metabolism in ascidians. *ISME J.* 2015, 9, 615-628, doi:10.1038/ismej.2014.152.

van Bergeijk, D.A.; Terlouw, B.R.; Medema, M.H.; van Wezel, G.P. Ecology and genomics of Actinobacteria: New concepts for natural product discovery. *Nat. Rev. Microbiol.* 2020, 18, 546–558, doi:10.1038/s41579-020-0379-y.

van der Hooft, J.J.J.; Mohimani, H.; Bauermeister, A.; Dorrestein, P.C.; Duncan, K.R.; Medema, M.H. Linking genomics and metabolomics to chart specialized metabolic diversity. *Chem. Soc. Rev.* 2020, 49, 3297-3314, doi:10.1039/d0cs00162g.

Vilcinskas, A. Pathogens as biological weapons of invasive species. *PLoS Pathog.* 2015, 11, e1004714, doi:10.1371/journal.ppat.1004714.

Williams, R.H.; Lively, D.H.; DeLong, D.C.; Cline, J.C.; Sweeny, M.J. Mycophenolic acid: Antiviral and antitumor properties. *J. Antibiot.* 1968, 21, 463-464, doi:10.7164/antibiotics.21.463.

Xu, D.; Ondeyka, J.; Harris, G.H.; Zink, D.; Kahn, J.N.; Wang, H.; Bills, G.; Platas, G.; Wang, W.; Szewczak, A.A.; et al. Isolation, structure, and biological activities of fellutamides C and D from an undescribed *Metulocladosporiella* (Chaetothyriales) using the genome-wide *Candida albicans* fitness test. *J. Nat. Prod.* 2011, 74, 1721-1730, doi:10.1021/np2001573.

Xu, Y.; Kersten, R.D.; Nam, S.J.; Lu, L.; Al-Suwailem, A.M.; Zheng, H.; Fenical, W.; Dorrestein, P.C.; Moore, B.S.; Qian, P.Y. Bacterial biosynthesis and maturation of the didemnin anti-cancer agents. *J. Am. Chem. Soc.* 2012, 134, 8625-8632, doi:10.1021/ja301735a.

Zbarskiĭ, V.B.; Lazhko, E.I.; Pomanova, N.P.; Fomicheva, E.V.; Saburova, T.P. Rubomycins M and N-new anthracycline antibiotics. *Russ. J. Bioorg. Chem.* 1991, 17, 1698-1701.

Zgurskaya, H.I.; Lopez, C.A.; Gnanakaran, S. Permeability barrier of Gram-negative cell envelopes and approaches to bypass it. *ACS Infect. Dis.* 2015, 1, 512-522, doi:10.1021/acsinfecdis.5b00097.

Zhan, A.; Briski, E.; Bock, D.G.; Ghabooli, S.; MacIsaac, H.J. Ascidians as models for studying invasion success. *Mar. Biol.* 2015, 162, 2449-2470, doi:10.1007/s00227-015-2734-5.

Zhao, Y.; Wang, M.; Lindstrom, M.E.; Li, J. Fatty acid and lipid profiles with emphasis on n-3 fatty acids and phospholipids from *Ciona intestinalis*. *Lipids* 2015, 50, 1009-1027, doi:10.1007/s11745-015-4049-1.

Appendix

Supplementary Information accompanying Chapter 1

Supplementary Figures S1-S11

Figure S1. Genotyping of *C. intestinalis* with the mitochondrial marker gene COX3-ND1.

Figure S2. Influence of the quality filtering steps on the total number of observed read pairs from amplicon sequencing.

Figure S3. Rarefaction curves of OTU abundances for *C. intestinalis* and seawater samples.

Figure S4. Multivariate ordination plots of the bacterial community associated with *C. intestinalis*.

Figure S5. Across sample type and geographic origin comparison of the *C. intestinalis* associated microbiome.

Figure S6. Extraction yields of crude extracts from population level extractions.

Figure S7. Chemical structures of putatively identified compounds in crude extracts of *C. intestinalis* by UPLC-MS/MS analysis.

Figure S8. Molecular network (MN) of individual *C. intestinalis* metabolomes.

Figure S9. Multivariate ordination plots of UPLC-MS profiles of *C. intestinalis* extracts.

Figure S10. Statistical correlation of individual tunic microbiomes and metabolomes.

Figure S11. Solvent extracts of different *C. intestinalis* samples.

Supplementary Tables S1-S12

Table S1. Metadata for microbiome samples analyzed in this study.

Table S2. Metadata for metabolome samples analyzed in this study.

Table S3. Parameters of the individual extractions.

Table S4. Alpha diversity measures of amplicon sequences.

Table S5. Tukey's HSD test comparing observed (OTU count), estimated (Chao1) OTUs, and phylogenetic diversity (PD) detected in ascidian samples at three different sampling sites.

Table S6. ANOSIM comparison of amplicon sequencing results.

Table S7. Significantly different abundant bacterial phyla.

Table S8. Significantly different abundant bacterial classes, families and genera.

Table S9. Significantly different abundant OTUs.

Table S10. Classification of abundant OTUs detected in this study.

Table S11. Putative annotation of metabolites detected in *C. intestinalis* bulk extracts (population level).

Table S12. ANOSIM comparison of UPLC-MS/MS profiles of *C. intestinalis* extracts.

Supplementary References 1-38
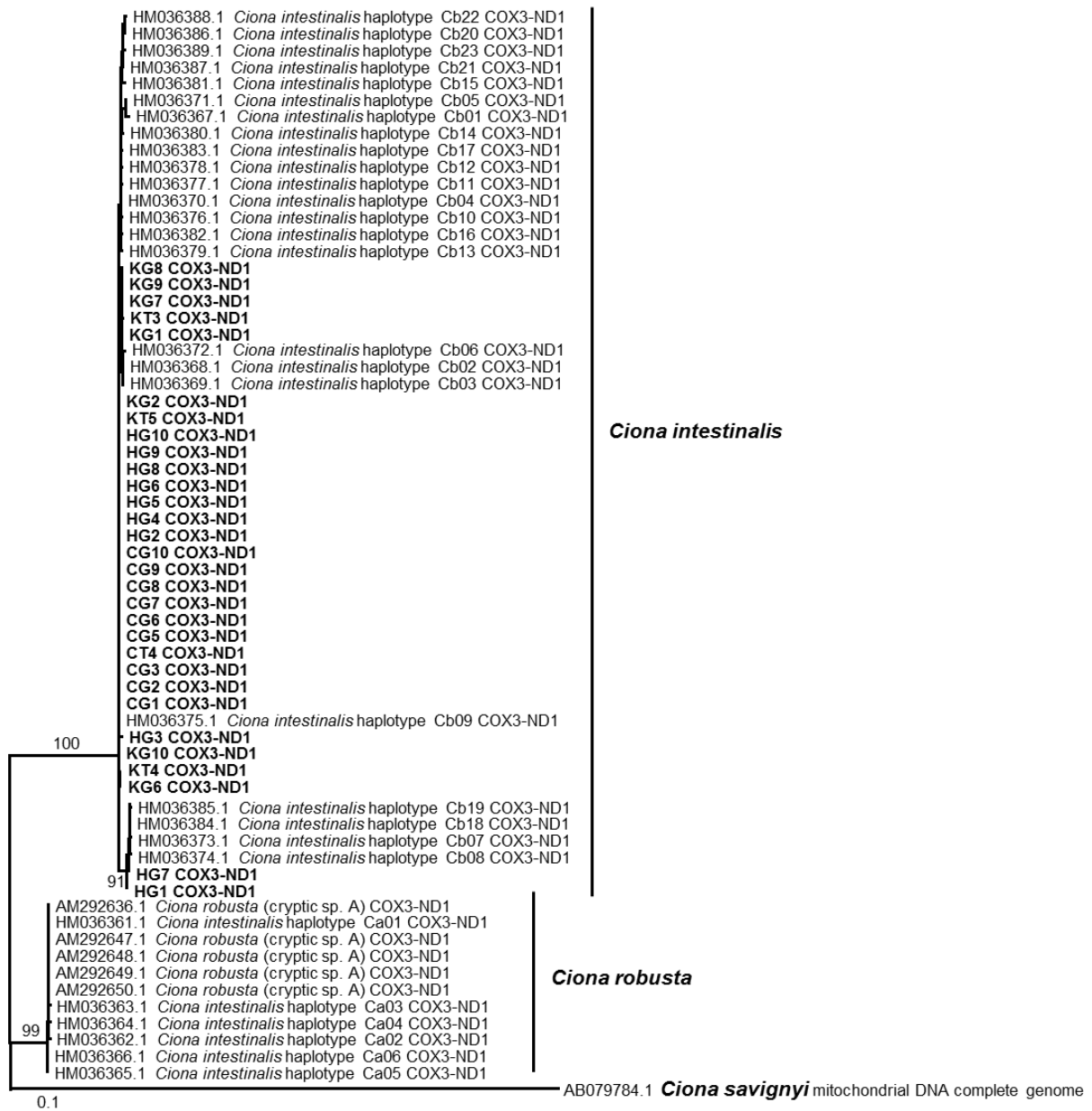
Figure S1. Genotyping of _C. intestinalis_ with the mitochondrial marker gene COX3-ND1. A maximum likelihood tree was constructed in MEGA7. Genotyped individuals (n = 30) are in bold. Sampling sites and types are abbreviated as follows: C = Canada, H = Helgoland, K = Kiel; G = gut, T = tunic.
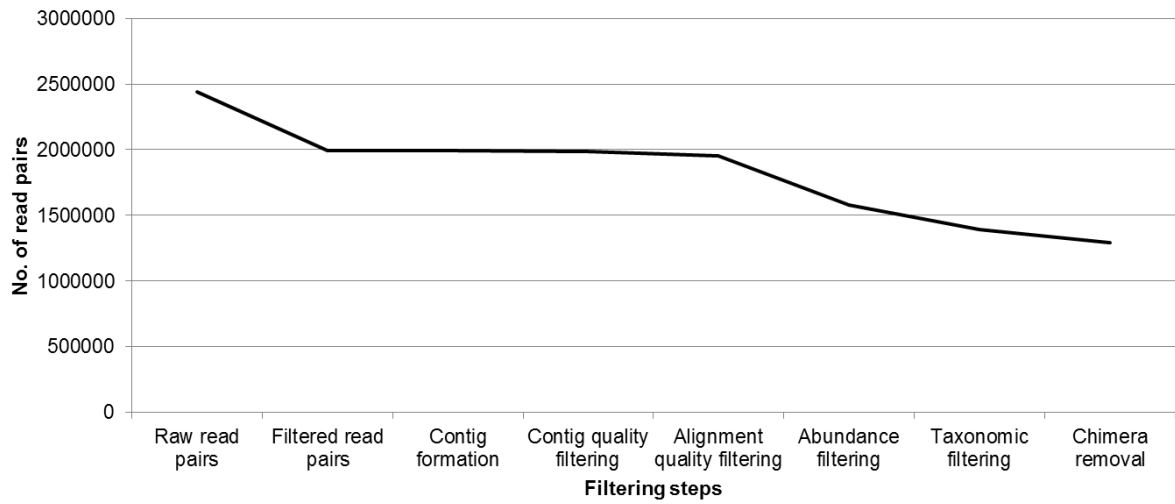
Figure S2. Influence of the quality filtering steps on the total number of observed read pairs from amplicon sequencing. Amplicon sequences were quality filtered in seven steps. The corresponding number of read pairs remaining after each filtering step is shown.
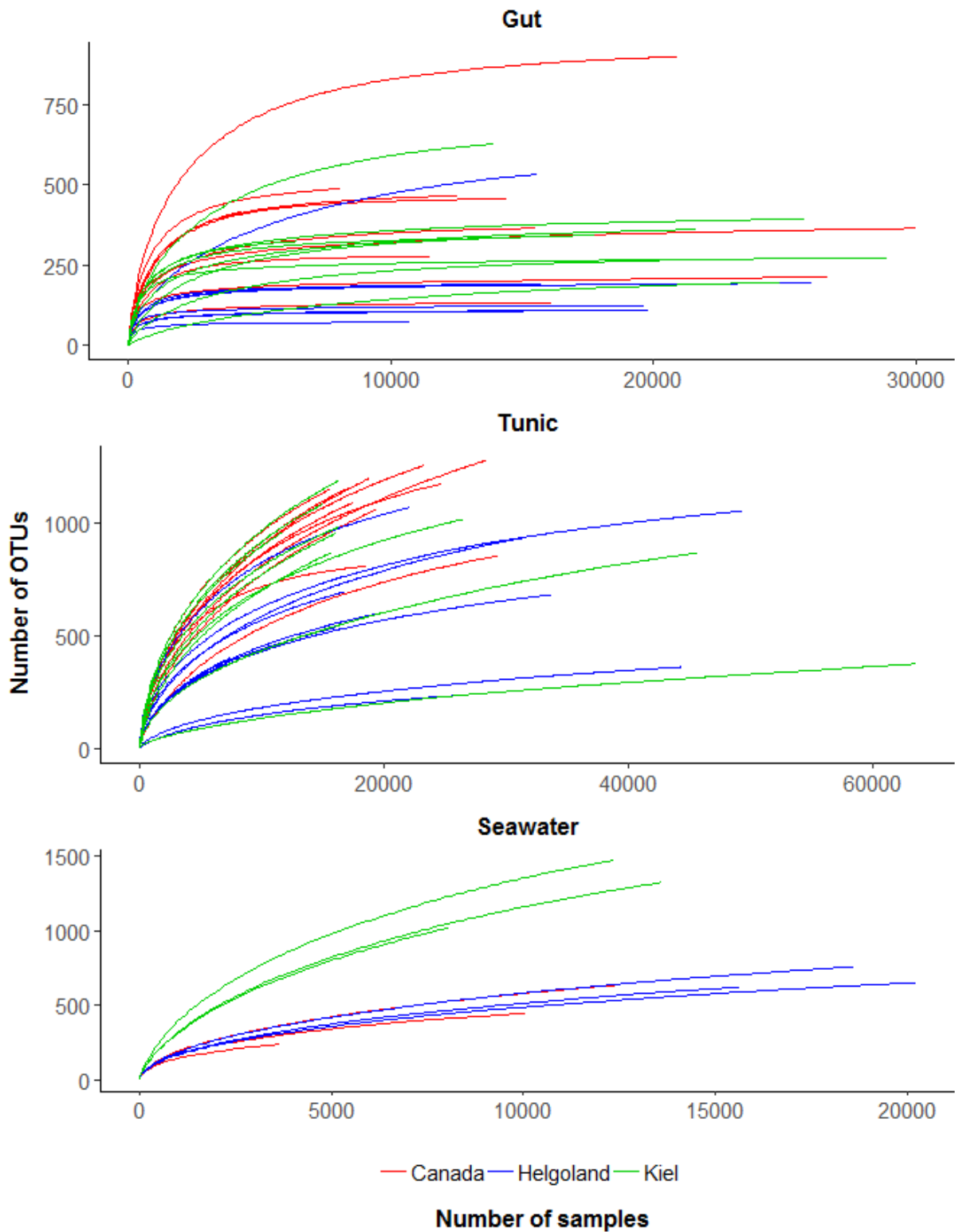
Figure S3. Rarefaction curves of OTU abundances for *C. intestinalis* and seawater samples. The number of sequences is plotted against the number of detected OTUs. Sampling sites are color coded: red = Canada, blue = Helgoland, green = Kiel Fjord. Top: gut, middle: tunic, bottom: seawater reference samples.
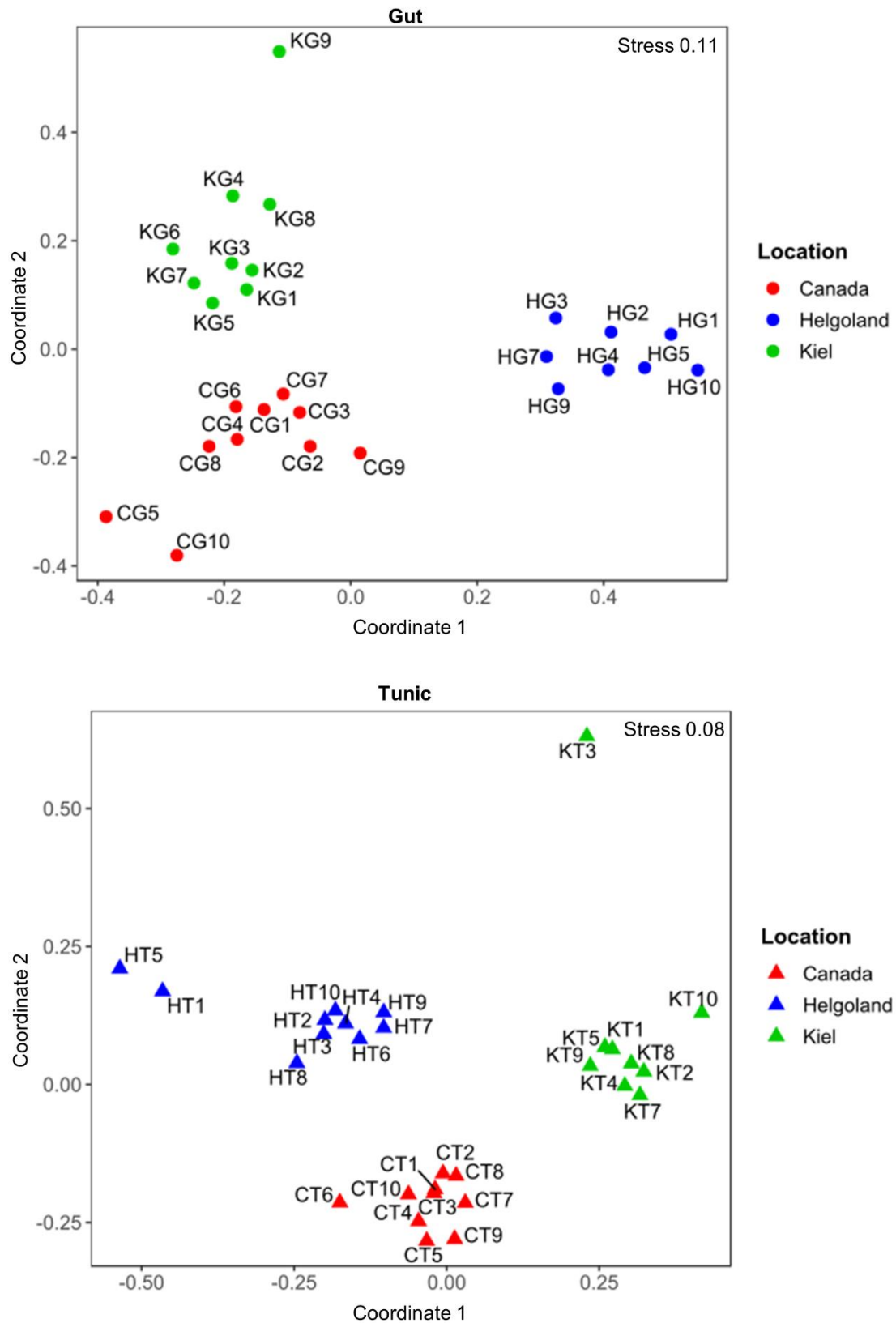
Figure S4. Multivariate ordination plots of the bacterial community associated with *C. intestinalis***.** NMDS plots are based on Bray-Curtis similarity. Sampling sites and types are abbreviated as follows: C = Canada, H = Helgoland, K = Kiel; G = gut, T = tunic.
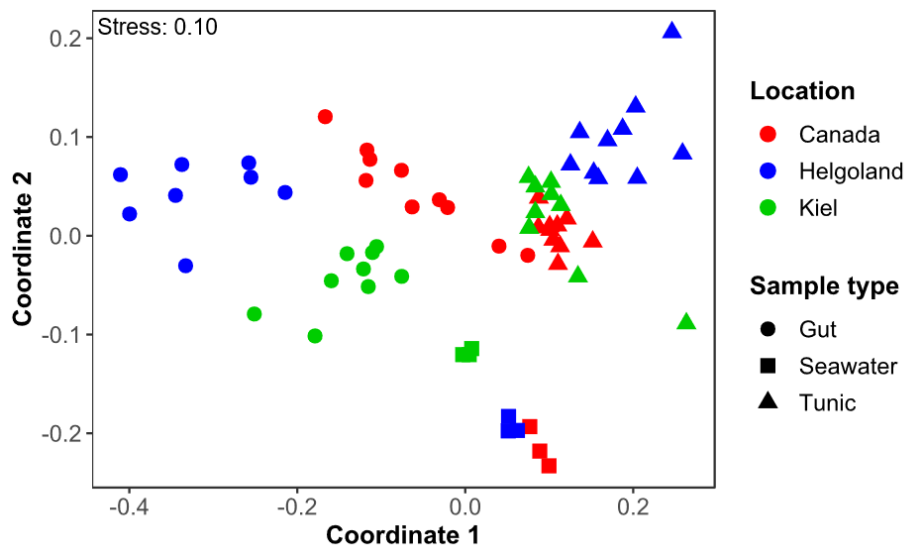
Figure S5. Across sample type and geographic origin comparison of the *C. intestinalis* associated microbiome. The 2D nMDS plot was calculated using the full set of detected OTUs (5211) and is based on weighted UniFrac distances.
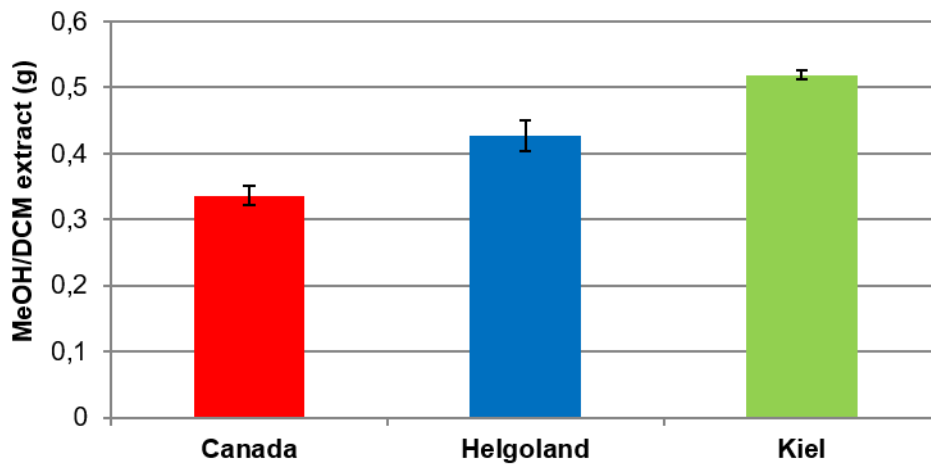
Figure S6. Extraction yields of crude extracts from population level extractions. Whole body bulk samples consisting of each 13 g of dry powder were extracted (n = 3 for each sampling site). Yields are given as average values with standard deviation in g.
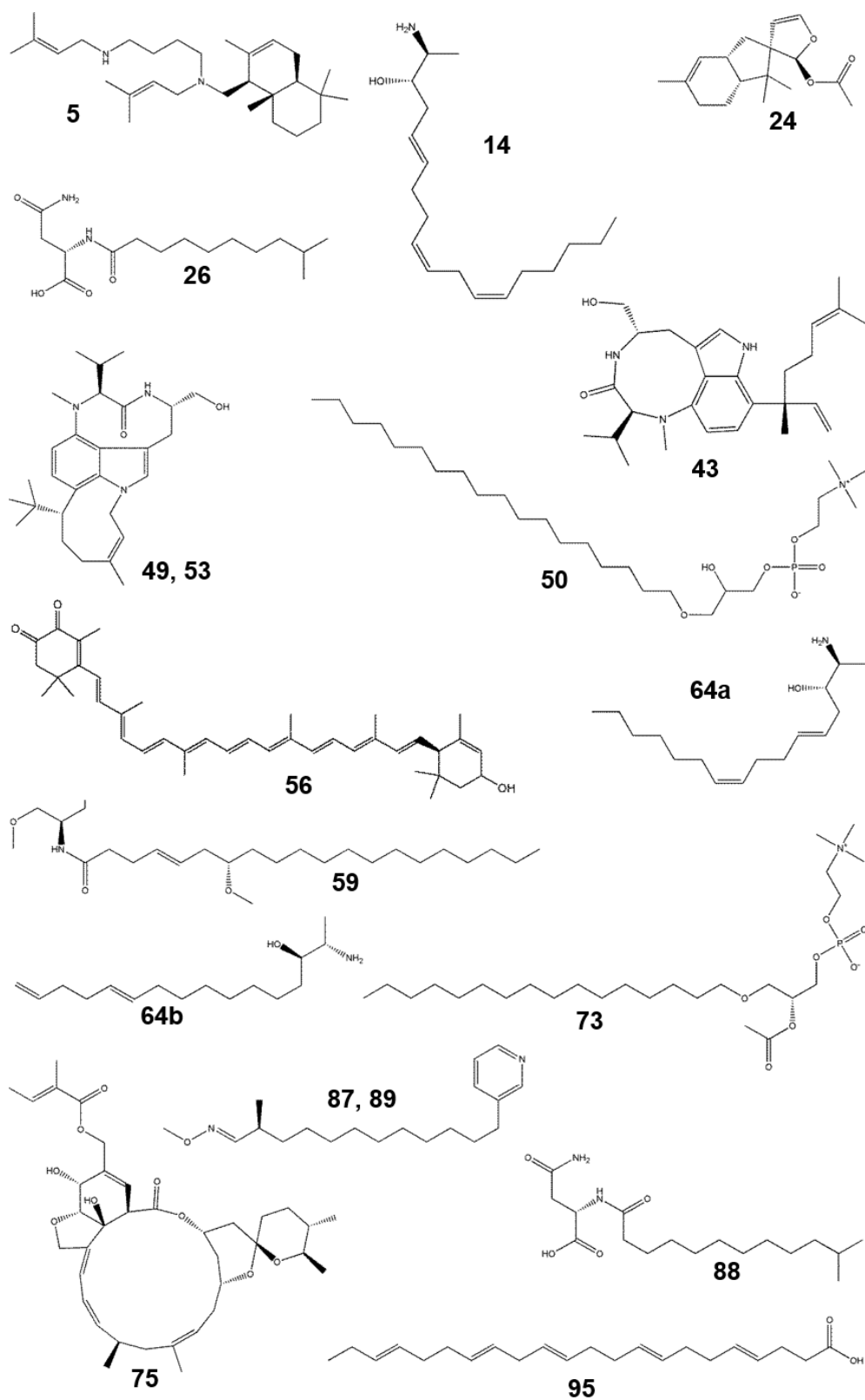
Figure S7. Chemical structures of putatively identified compounds in crude extracts of *C. intestinalis* by UPLC-MS/MS analysis. Structures are given with their respective peak number (see Table S11). The following compounds are shown in Figure 6 in the original publication: **12**, **15**, **55**, **60**, **69**, **79**, **90**, **96**, **99**, **100**, **103**.

104a

104b

105

108

111

107

117

120
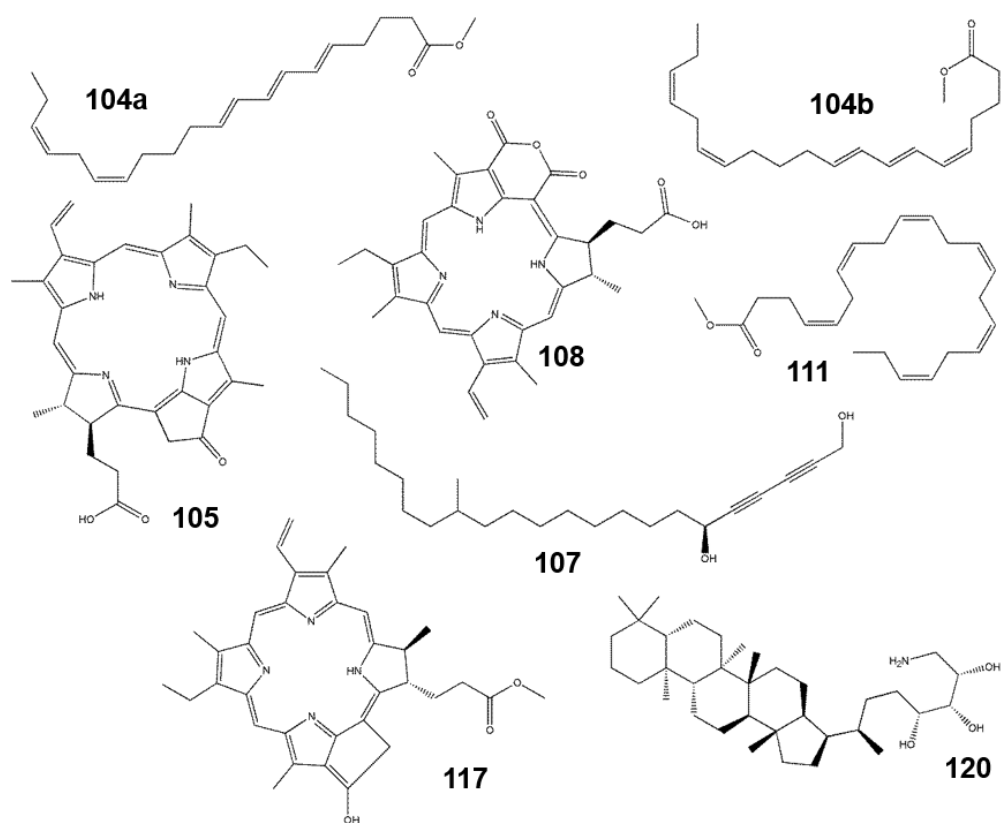
Figure S7. (continued)
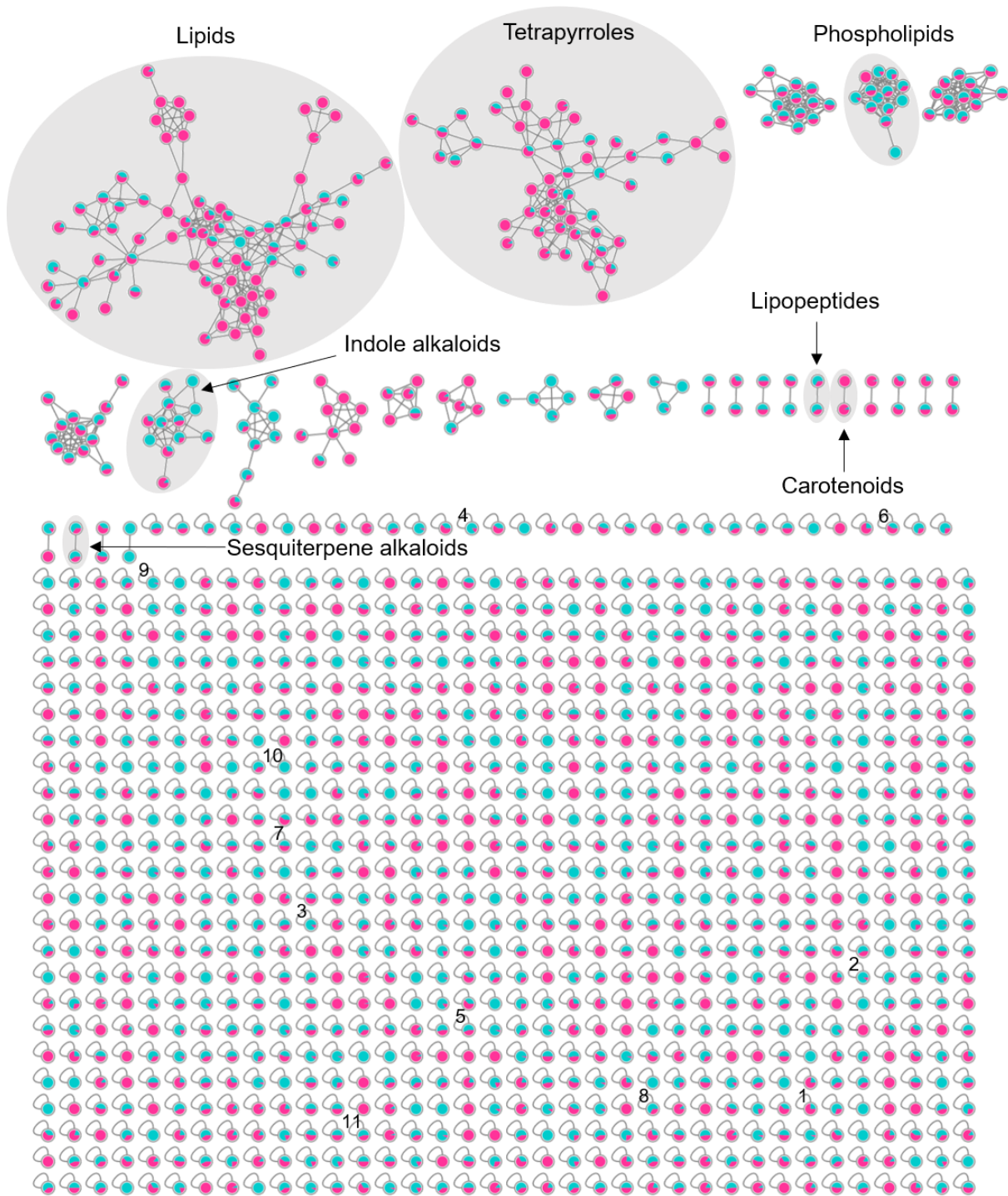
Figure S8. Molecular network (MN) of individual *C. intestinalis* metabolomes. The MN was constructed via the online platform GNPS [1] by using pre-filtered MS/MS-data of individual level extracts from inner body and tunic (ions must occur in ≥5 replicates). Nodes are color-coded and reflect the respective tissue: pink = tunic, cyan = inner body. Proportions are given by the number of replicates containing a respective node. Single nodes are numbered and were putatively annotated to the following chemical families: 1, 3, 4 = polyunsaturated amino alcohols; 2 = sesquiterpenoid; 5 = lipoamide; 6 = alkylpyridine; 7 = unsaturated fatty acid; 8 = acetylenic alcohol; 9 = hopanoid; 10 = tetrapyrrole; 11 = linear peptide. Putative annotations are in accordance with population metabolomes (Table S11).
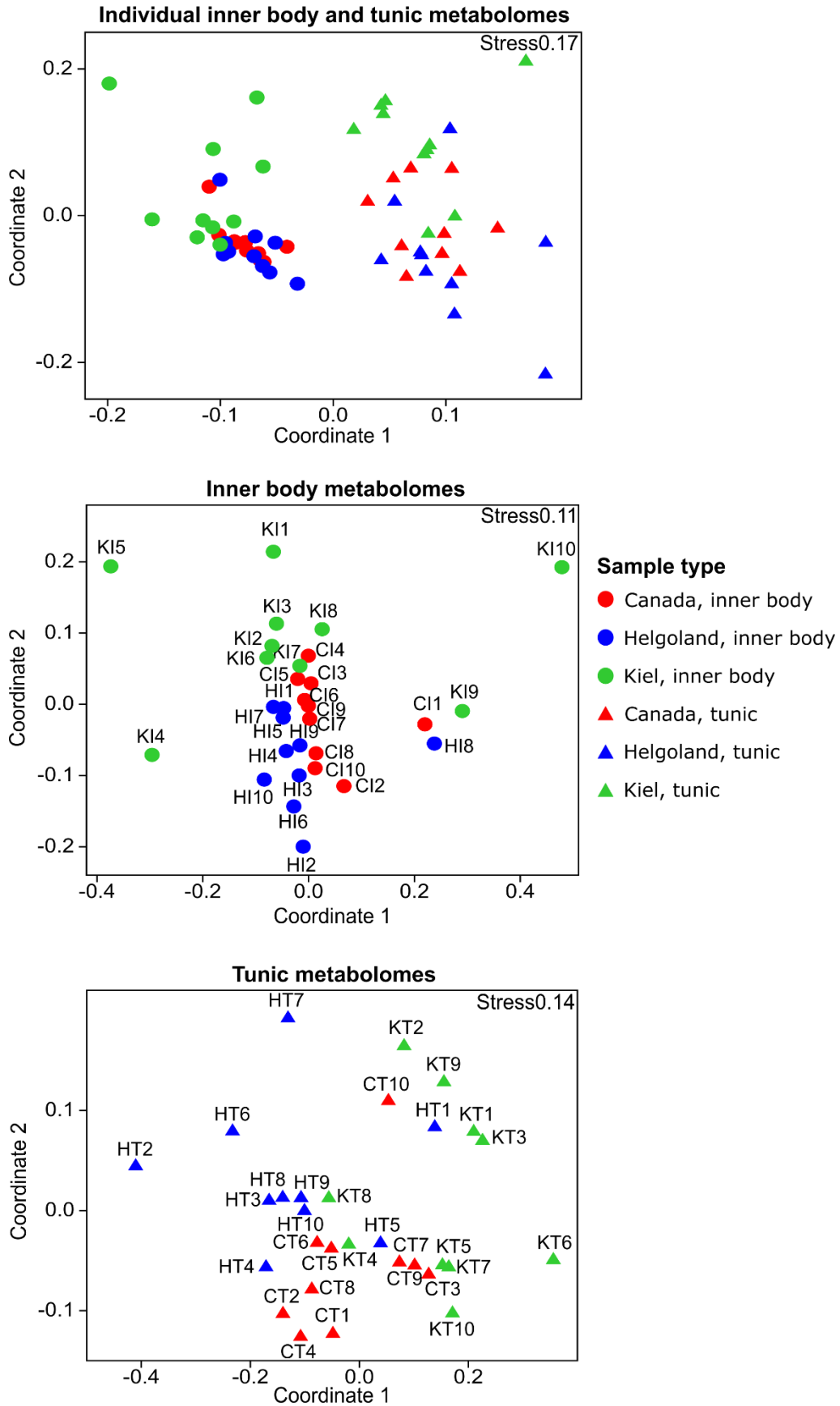
Figure S9. Multivariate ordination plots of UPLC-MS profiles of *C. intestinalis* extracts. NMDS plots are based on a Bray-Curtis similarity matrix. Sampling sites and types are abbreviated as follows: C = Canada, H = Helgoland, K = Kiel; I = inner body, T = tunic.
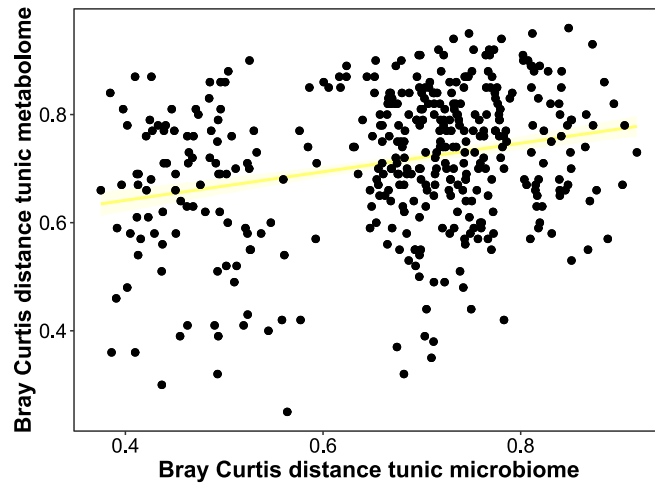
Figure S10. Statistical correlation of individual tunic microbiomes and metabolomes. The regression plot is based on the respective Bray-Curtis similarity matrices of both datasets and the regression line is given with its confidence interval (95%).
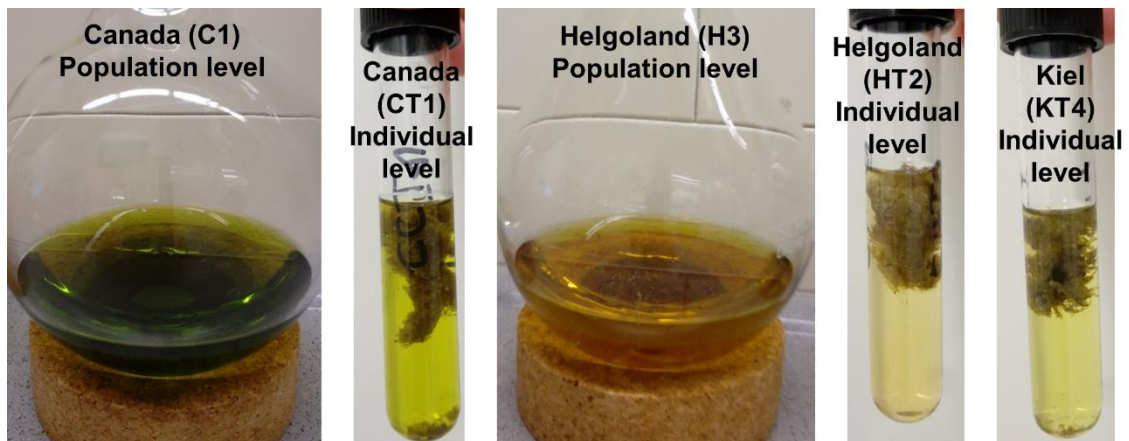
Figure S11. Solvent extracts of different *C. intestinalis* samples. Crude methanol extracts from population and individual level ascidian samples are shown. Sampling sites and types are abbreviated as follows: C = Canada, H = Helgoland, K = Kiel; T = tunic. Pictures by Caroline Utermann.

Table S1. Metadata for microbiome samples analyzed in this study. Sample labels are a combination of the sampling site (C: Canada, H: Helgoland, K: Kiel Fjord) and the respective sample type (G: gut, T: tunic, W: seawater).

Sampling site	Sample type	Replicates (n)	Sample labels
Canada		10	CG1-10
Helgoland	Ascidian, gut	8	HG1-5, HG7, HG9-10
Kiel		9	KG1-9
Canada		10	CT1-10
Helgoland	Ascidian, tunic	10	HT1-10
Kiel		9	KT1-5, KT7-10
Canada		3	CW1-3
Helgoland	Seawater	3	HW1-3
Kiel		3	KW1-3

Table S2. Metadata for metabolome samples analyzed in this study. Sample labels are a combination of the sampling site (C: Canada, H: Helgoland, K: Kiel) and the respective sample type (I: inner body, T: tunic).

Sampling site	Extraction series	Sample type	Replicates (n)	Sample labels
Canada			3	C1-3
Helgoland	Population level	Whole animal	3	H1-3
Kiel			3	K1-3
Canada			10	CT1-10
Helgoland		Ascidian, tunic	10	HT1-10
Kiel			10	KT1-10
Canada	Individual level		10	CI1-10
Helgoland		Ascidian, inner body	10	HI1-10
Kiel			10	KI1-10

Table S3. Parameters of the individual extractions. Samples are given with their dry weight prior extraction and the respective extract weight. Sampling sites and types are abbreviated as follows: C = Canada, H = Helgoland, K = Kiel; I = inner body, T = tunic.

Sample	Dry weight (mg)	Extract (mg)
CI1	33	3.0
CI2	43.6	3.1
CI3	14.8	2.6
CI4	14.5	1.5
CI5	16.2	2.1
CI6	15.3	2.4
CI7	21.4	2.6
CI8	32.8	3.2
CI9	23.3	3.0
CI10	31.1	2.0
CT1	74.2	1.7
CT2	73.1	1.7
CT3	23.7	0.5
CT4	27.9	0.7
CT5	60.5	1.2
CT6	72.4	3.1
CT7	32.8	1.0
CT8	63	2.9
CT9	30.7	0.5
CT10	47.2	1.2
HI1	26.1	5.4
HI2	67.8	12.0
HI3	46.5	14.0
HI4	27.2	5.3
HI5	45.6	6.9
HI6	55.6	11.1
HI7	26.2	9.1
HI8	56.7	8.5
HI9	53	8.4
HI10	46.9	8.5
HT1	14.1	1.4
HT2	137	14.8
HT3	68.4	6.9
HT4	70.6	4.8

Sample	Dry weight (mg)	Extract (mg)
HT5	28.8	0.8
HT6	99.1	8.8
HT7	70.9	8.7
HT8	60.6	4.4
HT9	60.3	4.0
HT10	57.3	4.2
KI1	6.4	0.8
KI2	22.5	2.3
KI3	17.8	0.9
KI4	26.4	2.8
KI5	24.9	1.4
KI6	12.7	0.5
KI7	13.8	1.4
KI8	20.3	1.2
KI9	45.5	2.0
KI10	16.6	1.2
KT1	18.7	0.6
KT2	36.2	1.2
KT3	21.3	0.4
KT4	38.5	1.6
KT5	21.3	0.5
KT6	3.1	0.8
KT7	24.4	0.5
KT8	31.8	1.7
KT9	26.5	1.2
KT10	26.8	0.6

Table S4. Alpha diversity measures of amplicon sequences. The five different indices are given as average values with standard deviation (SD). Sampling sites and types are abbreviated as follows: C = Canada, H = Helgoland, K = Kiel; G = gut, T = tunic, W = seawater.

Group	OTU count (Count)	SD (Count)	Chao1	SD (Chao1)	Faith's Phylogenetic Diversity (PD)	SD (PD)	Shannon (H')	SD (H')	Simpson (D)	SD (D)
CG	337	145	387	181	18.7	6.7	4.5	0.7	0.96	0.03
HG	148	74	181	134	9.7	3.9	3.6	0.4	0.93	0.04
KG	256	89	317	111	14.8	4.6	3.5	1.5	0.79	0.29
CT	506	88	961	183	25.2	3.5	4.1	0.6	0.91	0.07
HT	289	125	535	210	14.1	5.5	3.2	1.0	0.86	0.10
KT	445	168	850	325	22.3	8.0	3.9	1.1	0.88	0.12
CW	308	55	522	127	15.6	2.9	4.1	0.3	0.95	0.02
HW	334	16	601	34	18.4	0.7	4.2	0.1	0.96	0.00
KW	722	52	1381	73	35.7	2.5	5.2	0.3	0.97	0.01
G (all)	247	134	295	169	14.7	6.5	3.9	1.1	0.89	0.19
T (all)	413	159	782	305	20.5	7.6	3.7	1.0	0.88	0.10
W (all)	455	194	835	397	23.3	9.2	4.5	0.5	0.96	0.02
C (G, T)	421	147	674	339	21.9	6.3	4.3	0.7	0.93	0.06
H (G, T)	219	126	358	251	12.1	5.3	3.4	0.8	0.90	0.09
K (G, T)	350	164	583	360	18.6	7.6	3.7	1.4	0.84	0.23

Table S5. Tukey's HSD test comparing observed (OTU count), estimated (Chao1) OTUs, and phylogenetic diversity (PD) detected in ascidian samples at three different sampling sites. Sampling sites and types are abbreviated as follows: C = Canada, H = Helgoland, K = Kiel; G = gut, T = tunic.

Compared groups	p (OTU count)	p (Chao1)	p (PD)
CG x HG	0.045	0.477	0.039
CG x HT	0.993	0.802	0.673
CG x KG	0.869	0.998	0.857
CG x KT	0.607	<0.001	0.901
CT x HG	<0.001	<0.001	<0.001
CT x HT	0.006	0.001	0.002
CT x KG	0.001	<0.001	0.006
CT x KT	0.973	0.959	0.974
HG x KG	0.675	0.911	0.660
HG x KT	<0.001	<0.001	0.001
HT x KG	1.000	0.357	1.000
HT x KT	0.147	0.038	0.061

Table S6. ANOSIM comparison of amplicon sequencing results. ANOSIM was computed based on the Bray-Curtis similarity index in order to statistically compare the different sample groups. Results are given with the respective R and p value.

Test		Compared groups	R	p
Sample type		Gut x Seawater	0.7280	0.0001
		Gut x Tunic	0.7035	0.0001
		Tunic x Seawater	0.9592	0.0001
Sampling site	Gut	Canada x Helgoland	0.9716	0.0001
		Canada x Kiel	0.7331	0.0001
		Helgoland x Kiel	0.9839	0.0001
	Tunic	Canada x Helgoland	0.8362	0.0001
		Canada x Kiel	0.8337	0.0001
		Helgoland x Kiel	0.8038	0.0001

Table S7. Significantly different abundant bacterial phyla. Significance testing was performed with the Kruskal-Wallis-Test. Significant phyla with a relative abundance >0.05% are shown. Sampling sites and types are abbreviated as follows: C = Canada, H = Helgoland, K = Kiel; G = gut, T = tunic, W = seawater.

| Phylum	Statistics	p	Relative abundance (%)									
			All	CG	CT	CW	HG	HT	HW	KG	KT	KW
Acidobacteria	24.8	1.7E-03	0.3	0.6	0.4	0.0	0.3	0.1	0.0	0.2	0.5	0.2
Actinobacteria	52.8	1.2E-08	5.4	5.2	0.9	3.5	19.4	0.3	5.1	8.3	1.2	7.7
Bacteroidetes	43.0	8.9E-07	16.6	9.6	21.0	30.8	3.8	19.8	46.3	3.7	21.6	28.3
Chloroflexi	21.5	5.9E-03	1.2	2.7	0.7	0.0	0.5	2.2	0.2	1.1	0.5	0.4
Cyanobacteria	49.0	6.5E-08	8.5	19.0	11.6	1.3	13.9	0.1	1.6	11.0	0.1	8.1
Epsilonbacteraeota	42.9	9.1E-07	3.2	1.5	0.4	0.5	0.7	0.0	0.5	5.8	12.9	3.4
Firmicutes	52.3	1.5E-08	3.9	1.5	0.0	0.1	26.9	0.0	0.3	1.8	0.2	1.0
Patescibacteria	18.4	1.9E-02	0.6	0.8	0.2	0.0	1.0	0.6	0.1	0.6	1.3	0.3
Planctomycetes	29.9	2.2E-04	0.3	0.2	0.3	0.0	0.0	0.4	0.2	0.2	0.4	0.1
Proteobacteria	36.1	1.7E-05	53.8	50.1	60.7	62.4	19.5	74.3	42.0	56.1	58.7	47.6
Spirochaetes	21.8	5.4E-03	0.1	0.1	0.1	0.0	0.0	0.2	0.0	0.1	0.0	0.1
Tenericutes	47.5	1.3E-07	2.3	4.7	0.0	0.0	8.1	0.1	0.0	4.2	0.1	0.3
Verrucomicrobia	25.8	1.2E-03	1.6	1.5	3.2	1.1	0.7	1.6	2.9	0.6	1.8	0.6

Table S8. Significantly different abundant bacterial classes, families and genera. Significance testing was performed with the Kruskal-Wallis-Test. Significant phyla with a relative abundance ≥1% are shown. Sampling sites and types are abbreviated as follows: C = Canada, H = Helgoland, K = Kiel; G = gut, T = tunic, W = seawater.

Taxonomic identification	Statistics	p	Relative abundance (%)									
			All	CG	CT	CW	HG	HT	HW	KG	KT	KW
Class												
Acidimicrobiia	42.2	1.27E-06	1.6	2.8	0.8	0.8	0.5	0.2	3.9	2.7	1.0	3.5
Actinobacteria	54.6	5.19E-09	3.6	2.2	0.0	2.8	17.5	0.1	1.1	4.9	0.1	3.9
Alphaproteobacteria	48.0	9.95E-08	39.2	35.2	51.7	43.7	15.2	67.6	26.5	18.5	46.4	29.2
Anaerolineae	28.7	3.57E-04	1.1	2.5	0.7	0.0	0.3	2.2	0.0	0.8	0.5	0.3
Bacteroidia	43.2	8.03E-07	16.5	9.5	20.9	30.1	3.8	19.8	46.1	3.7	21.5	28.0
Campylobacteria	40.7	2.38E-06	3.2	1.5	0.4	0.5	0.7	0.0	0.5	5.8	12.9	3.4
Clostridia	52.7	1.25E-08	3.4	1.2	0.0	0.1	23.4	0.0	0.2	1.5	0.2	1.0
Deltaproteobacteria	28.5	3.85E-04	1.9	3.6	1.8	0.2	1.0	1.2	2.2	2.8	1.3	2.4
Gammaproteobacteria	40.3	2.82E-06	12.6	11.2	7.1	18.5	3.2	5.4	13.3	34.7	10.9	16.0
Mollicutes	42.3	1.20E-06	2.3	4.7	0.0	0.0	8.1	0.1	0.0	4.2	0.1	0.3
Oxyphotobacteria	49.3	5.61E-08	8.5	18.9	11.6	1.2	13.8	0.1	1.6	11.0	0.1	8.1
Verrucomicrobiae	26.9	7.41E-04	1.6	1.5	3.2	1.1	0.7	1.6	2.9	0.6	1.8	0.6
Family												
Alphaproteobacteria (unclassified)	46.4	2.03E-07	6.0	2.0	12.5	0.0	0.8	17.4	0.4	0.3	6.5	0.1
Arcobacteraceae	37.9	7.88E-06	2.4	0.5	0.4	0.2	0.0	0.0	0.2	3.3	12.6	0.7
Bifidobacteriaceae	50.7	2.96E-08	1.4	0.0	0.0	0.0	11.5	0.0	0.0	0.0	0.0	0.0
Cyanobiaceae	52.9	1.14E-08	5.8	16.7	0.1	1.1	10.7	0.1	1.6	10.5	0.1	7.3
Entomoplasmatales *incertae sedis*	48.0	9.90E-08	2.2	4.5	0.0	0.0	7.9	0.0	0.0	4.1	0.0	0.0
Flavobacteriaceae	43.6	6.78E-07	13.0	7.3	18.2	19.1	2.0	19.2	30.2	2.4	20.0	10.4
Gammaproteobacteria (unclassified)	30.7	1.57E-04	1.0	1.2	2.1	0.1	0.1	0.9	0.4	0.4	1.4	0.5
Halieaceae	36.1	1.70E-05	1.4	1.9	0.9	1.5	0.6	0.3	2.6	2.7	0.7	2.9
Kiloniellaceae	26.1	9.98E-04	1.1	0.1	0.0	0.0	1.8	0.0	0.0	0.0	6.1	0.0
Kordiimonadaceae	53.6	8.11E-09	5.4	0.1	19.5	0.0	0.0	13.0	0.0	0.0	2.6	0.0
Lachnospiraceae	38.4	6.22E-06	1.1	0.1	0.0	0.0	8.6	0.0	0.1	0.1	0.0	0.1
Oxyphotobacteria (unclassified)	55.3	3.94E-09	1.1	0.9	3.0	0.1	3.0	0.0	0.1	0.4	0.0	0.6
Phormidesmiaceae	48.4	8.14E-08	1.1	0.4	7.0	0.0	0.0	0.0	0.0	0.0	0.0	0.1
Pseudomonadaceae	44.9	3.89E-07	2.9	0.0	0.0	0.0	0.0	0.0	0.0	20.6	0.3	0.8
Rhizobiaceae	32.3	8.11E-05	2.9	2.9	2.9	0.1	1.3	4.2	0.0	1.2	6.9	0.3
Rhizobiales (unclassified)	50.0	4.09E-08	1.3	0.0	1.2	0.0	0.0	6.9	0.0	0.1	0.6	0.0
Rhodobacteraceae	41.9	1.42E-06	13.5	24.6	5.4	33.4	8.2	7.3	21.4	9.2	13.7	23.8
S25_593 (Rickettsiales)	47.9	1.03E-07	1.6	0.1	2.2	0.0	0.3	7.4	0.0	0.1	0.7	0.0
Sphingomonadaceae	40.0	3.26E-06	1.4	1.2	1.7	0.0	0.1	3.8	0.0	0.5	2.3	0.3
Terasakiellaceae	26.1	1.02E-03	1.1	0.1	0.9	0.2	0.8	4.0	0.0	0.2	1.1	0.2
Genus												
Acrophormium (PCC_7375)	51.1	2.48E-08	1.1	0.3	6.6	0.0	0.0	0.0	0.0	0.0	0.0	0.0
Alphaproteobacteria (unclassified)	46.4	2.03E-07	6.0	2.0	12.5	0.0	0.8	17.4	0.4	0.3	6.5	0.1
Arcobacter	37.9	7.88E-06	2.4	0.5	0.4	0.2	0.0	0.0	0.2	3.3	12.6	0.7
Bifidobacterium	50.7	2.96E-08	1.4	0.0	0.0	0.0	11.5	0.0	0.0	0.0	0.0	0.0
Candidatus Hepatoplasma	48.0	9.90E-08	2.2	4.5	0.0	0.0	7.9	0.0	0.0	4.1	0.0	0.0

Taxonomic identification	Statistics	p	Relative abundance (%)									
			All	CG	CT	CW	HG	HT	HW	KG	KT	KW
Flavobacteriaceae (unclassified)	41.8	1.50E-06	3.2	2.3	6.4	1.2	0.2	6.0	4.4	0.3	3.4	2.3
Gammaproteobacteria (unclassified)	30.7	1.57E-04	1.0	1.2	2.1	0.1	0.1	0.9	0.4	0.4	1.4	0.5
Kiloniella	27.0	7.02E-04	1.1	0.0	0.0	0.0	1.7	0.0	0.0	0.0	6.1	0.0
Kordiimonas	53.6	8.11E-09	5.4	0.1	19.5	0.0	0.0	13.0	0.0	0.0	2.6	0.0
Lentibacter	34.8	2.89E-05	1.3	0.5	0.1	3.6	0.1	0.2	0.1	1.2	4.7	3.8
Oxyphotobacteria (unclassified)	55.3	3.94E-09	1.1	0.9	3.0	0.1	3.0	0.0	0.1	0.4	0.0	0.6
Planktomarina	44.3	5.08E-07	2.1	0.0	0.0	19.0	0.0	0.0	12.7	0.0	0.0	13.2
Pricia	41.6	1.58E-06	4.7	2.0	5.8	0.0	0.0	9.4	0.0	1.0	14.0	0.0
Pseudahrensia	27.2	6.53E-04	1.2	0.6	1.1	0.0	1.2	2.5	0.0	0.3	3.0	0.1
Pseudomonas	44.9	3.89E-07	2.9	0.0	0.0	0.0	0.0	0.0	0.0	20.6	0.3	0.8
Rhizobiales (unclassified)	50.0	4.09E-08	1.3	0.0	1.2	0.0	0.0	6.9	0.0	0.1	0.6	0.0
Rhodobacteraceae (unclassified)	28.2	4.32E-04	4.6	9.1	3.0	1.0	3.2	4.3	1.1	5.3	5.1	2.6
Roseobacter	35.0	2.70E-05	1.6	9.0	0.2	0.1	0.6	0.1	0.0	0.3	0.0	0.1
Rickettsiales group S25_593	47.9	1.03E-07	1.6	0.1	2.2	0.0	0.3	7.4	0.0	0.1	0.7	0.0
Synechococcus (CC9902)	52.7	1.21E-08	5.4	15.8	0.0	1.1	10.6	0.1	1.6	8.9	0.1	6.8

Table S9. Significantly different abundant OTUs. Significance testing across all sample groups was performed with the Kruskal-Wallis-Test for abundant OTUs (≥0.15%). Sampling sites and types are abbreviated as follows: C = Canada, H = Helgoland, K = Kiel; G = gut, T = tunic, W = seawater.

OTU	Phylum	Lowest taxonomic classification	Statistics	p	Relative abundance (%)									
					All	CG	CT	CW	HG	HT	HW	KG	KT	KW
OTU1	Proteobacteria	*Kordiimonas* sp.	53.7	8E-09	5.28	0.13	19.33	0.00	0.00	12.61	0.00	0.01	2.50	0.00
OTU2	Proteobacteria	Alphaproteobacteria	46.5	2E-07	5.60	1.43	11.82	0.00	0.80	16.94	0.00	0.09	6.12	0.02
OTU3	Bacteroidetes	*Pricia* sp.	41.6	2E-06	4.65	2.02	5.65	0.00	0.00	9.27	0.00	1.01	13.78	0.02
OTU4	Proteobacteria	*Pseudomonas* sp.	47.8	1E-07	2.93	0.00	0.00	0.00	0.00	0.00	0.00	20.54	0.31	0.84
OTU5	Epsilonbacteraeota	*Arcobacter* sp.	40.4	3E-06	0.98	0.00	0.00	0.04	0.00	0.00	0.03	0.14	6.89	0.09
OTU6	Cyanobacteria	*Synechococcus* sp. (CC9902)	55.9	3E-09	2.90	9.72	0.03	0.64	8.44	0.05	1.28	1.54	0.03	1.08
OTU7	Proteobacteria	Rickettsiales group S25_593	47.9	1E-07	1.64	0.08	2.25	0.00	0.34	7.39	0.00	0.05	0.69	0.00
OTU8	Cyanobacteria	*Synechococcus* sp. (CC9902)	51.7	2E-08	2.52	6.09	0.02	0.38	2.20	0.01	0.25	7.39	0.05	5.36
OTU9	Proteobacteria	*Kiloniella* sp.	33.3	5E-05	0.83	0.00	0.00	0.00	0.00	0.00	0.00	0.03	5.94	0.00
OTU10	Bacteria (unclassified)	Bacteria (unclassified)	25.9	1E-03	1.48	1.54	0.00	0.00	4.98	0.00	0.00	4.55	0.00	0.00
OTU11	Proteobacteria	*Planktomarina* sp.	44.3	5E-07	1.94	0.03	0.00	17.96	0.00	0.00	11.63	0.00	0.00	12.34
OTU12	Proteobacteria	Terasakiellaceae	43.6	7E-07	0.78	0.03	0.90	0.01	0.04	3.88	0.00	0.00	0.24	0.00
OTU13	Actinobacteria	*Bifidobacterium* sp.	52.3	1E-08	1.13	0.00	0.00	0.00	9.16	0.02	0.01	0.00	0.00	0.00
OTU14	Cyanobacteria	*Acrophormium* sp. (PCC-7375)	53.3	1E-08	0.86	0.27	5.35	0.00	0.00	0.00	0.00	0.00	0.00	0.00
OTU15	Proteobacteria	*Roseobacter* sp.	56.9	2E-09	1.32	8.51	0.02	0.08	0.00	0.01	0.00	0.00	0.00	0.00
OTU16	Tenericutes	*Candidatus* Hepatoplasma	43.0	9E-07	1.22	4.44	0.00	0.00	1.75	0.00	0.00	2.31	0.00	0.00
OTU17	Proteobacteria	*Lentibacter* sp.	35.8	2E-05	1.24	0.46	0.04	3.50	0.07	0.16	0.06	1.17	4.57	3.77
OTU18	Bacteroidetes	Flavobacteriaceae	63.4	1E-10	0.70	0.00	0.00	0.00	0.00	4.55	0.00	0.00	0.00	0.00
OTU19	Proteobacteria	Rhizobiales	46.8	2E-07	0.85	0.00	0.10	0.00	0.00	5.36	0.00	0.00	0.04	0.00
OTU20	Epsilonbacteraeota	*Arcobacter* sp.	53.0	1E-08	0.36	0.00	0.00	0.00	0.00	0.00	0.00	0.64	1.92	0.08
OTU21	Actinobacteria	PeM15	47.2	1E-07	0.70	0.50	0.00	0.05	3.24	0.07	0.93	0.92	0.02	0.88
OTU22	Proteobacteria	*Candidatus* Gigarickettsia	26.1	1E-03	0.51	0.00	0.00	0.00	0.00	0.00	0.00	3.67	0.00	0.00

OTU	Phylum	Lowest taxonomic classification	Statistics	p	Relative abundance (%)									
					All	CG	CT	CW	HG	HT	HW	KG	KT	KW
OTU23	Bacteroidetes	*Formosa* sp.	56.6	2E-09	0.57	0.00	0.00	0.39	0.00	0.00	11.94	0.00	0.00	0.00
OTU24	Epsilonbacteraeota	*Arcobacter* sp.	41.5	2E-06	0.54	0.00	0.00	0.00	0.00	0.00	0.00	1.44	2.44	0.14
OTU25	Tenericutes	*Candidatus* Hepatoplasma	63.6	9E-11	0.75	0.00	0.00	0.00	6.12	0.00	0.00	0.00	0.00	0.00
OTU26	Proteobacteria	Rhizobiales	55.7	3E-09	0.34	0.01	0.98	0.00	0.00	1.26	0.00	0.00	0.00	0.00
OTU27	Proteobacteria	*Pseudahrensia* sp.	41.5	2E-06	0.46	0.16	0.79	0.01	0.00	1.10	0.00	0.06	0.94	0.02
OTU28	Bacteroidetes	*Maritimimonas* sp.	49.4	5E-08	0.44	0.18	2.50	0.00	0.00	0.18	0.00	0.00	0.01	0.00
OTU29	Proteobacteria	*Filomicrobium* sp.	32.9	6E-05	0.39	0.44	0.50	0.00	0.06	0.53	0.01	0.21	0.94	0.03
OTU30	Proteobacteria	*Neptunomonas* sp.	44.9	4E-07	0.40	0.02	0.01	0.00	0.00	0.00	0.00	1.44	1.36	0.07
OTU31	Cyanobacteria	Oxyphotobacteria	56.9	2E-09	0.46	0.50	0.00	0.00	3.04	0.00	0.05	0.00	0.00	0.05
OTU32	Chloroflexi	Ardenticatenaceae	58.9	8E-10	0.28	0.00	0.00	0.00	0.00	1.83	0.00	0.00	0.00	0.00
OTU33	Proteobacteria	*Tateyamaria* sp.	47.3	1E-07	0.42	0.43	0.00	0.03	1.34	0.01	0.12	1.15	0.01	0.40
OTU34	Proteobacteria	*Litoreibacter* sp.	46.2	2E-07	0.35	0.41	0.62	0.00	0.07	1.09	0.00	0.00	0.09	0.00
OTU35	Proteobacteria	Devosiaceae	35.8	2E-05	0.32	0.10	0.71	0.00	0.00	0.66	0.00	0.07	0.58	0.00
OTU36	Firmicutes	*Anaerostipes* sp.	55.0	4E-09	0.37	0.00	0.00	0.00	2.99	0.00	0.03	0.00	0.00	0.00
OTU38	Bacteroidetes	Flavobacteriaceae	44.1	5E-07	0.34	0.15	1.26	0.00	0.00	0.70	0.00	0.01	0.12	0.00
OTU39	Firmicutes	*Romboutsia* sp.	43.5	7E-07	0.42	0.03	0.00	0.00	3.20	0.01	0.00	0.17	0.00	0.01
OTU40	Epsilonbacteraeota	*Sulfurovum* sp.	42.0	1E-06	0.44	0.70	0.01	0.05	0.21	0.00	0.13	1.63	0.08	1.25
OTU41	Proteobacteria	*Sphingorhabdus* sp.	42.9	9E-07	0.30	0.21	0.25	0.00	0.00	1.29	0.00	0.02	0.18	0.00
OTU42	Proteobacteria	*Amylibacter* sp.	40.1	3E-06	0.55	0.01	0.01	7.97	0.01	0.04	2.68	0.00	0.01	0.98
OTU43	Proteobacteria	Rhizobiaceae	28.0	5E-04	0.24	0.18	0.14	0.00	0.00	0.31	0.00	0.06	1.00	0.00
OTU44	Proteobacteria	*Ahrensia* sp.	33.5	5E-05	0.28	0.52	0.55	0.00	0.00	0.36	0.01	0.01	0.42	0.00
OTU45	Bacteroidetes	Flavobacteriaceae	54.0	7E-09	0.29	0.00	0.00	0.00	0.00	0.00	0.00	0.08	2.00	0.03
OTU46	Proteobacteria	*Candidatus* Tenderia	36.6	1E-05	0.25	0.19	0.35	0.02	0.00	0.71	0.00	0.04	0.38	0.03
OTU47	Firmicutes	*Clostridium sensu stricto 1*	49.1	6E-08	0.34	0.00	0.00	0.00	2.77	0.00	0.00	0.00	0.00	0.00
OTU48	Proteobacteria	HOC36	43.1	9E-07	0.34	1.24	0.02	0.01	0.35	0.00	0.00	0.69	0.02	0.09
OTU49	Proteobacteria	*Pseudahrensia* sp.	26.6	8E-04	0.26	0.06	0.09	0.00	0.79	0.79	0.00	0.15	0.01	0.01
OTU50	Firmicutes	*Intestinibacter* sp.	59.5	6E-10	0.30	0.00	0.00	0.00	2.45	0.00	0.00	0.00	0.00	0.00
OTU51	Proteobacteria	*Sphingorhabdus* sp.	40.1	3E-06	0.25	0.05	0.21	0.00	0.00	0.04	0.00	0.19	1.26	0.03
OTU52	Actinobacteria	*Bifidobacterium* sp.	54.1	7E-09	0.27	0.00	0.00	0.00	2.17	0.01	0.00	0.00	0.00	0.00
OTU53	Proteobacteria	Rhodobacteraceae	44.8	4E-07	0.25	0.58	0.13	0.00	0.00	0.01	0.00	0.93	0.08	0.09
OTU54	Proteobacteria	Rhizobiaceae	35.4	2E-05	0.25	0.05	0.04	0.00	0.00	0.00	0.00	0.31	1.36	0.04
OTU55	Proteobacteria	*Ruegeria* sp.	41.7	2E-06	0.28	0.61	0.10	0.00	1.18	0.15	0.00	0.01	0.00	0.00
OTU56	Bacteroidetes	Cryomorphaceae	33.7	5E-05	0.25	0.00	0.00	0.05	0.01	0.00	5.26	0.00	0.00	0.00
OTU57	Proteobacteria	*Pseudahrensia* sp.	22.2	4E-03	0.24	0.02	0.01	0.00	0.00	0.01	0.00	0.10	1.59	0.05
OTU58	Verrucomicrobia	*Rubritalea* sp.	26.1	1E-03	0.20	0.12	1.02	0.00	0.05	0.00	0.02	0.02	0.13	0.00
OTU59	Proteobacteria	Rhodobacteraceae	38.4	6E-06	0.34	2.06	0.07	0.05	0.05	0.01	0.00	0.00	0.00	0.00
OTU61	Proteobacteria	Gammaproteobacteria	48.3	9E-08	0.24	0.27	0.87	0.00	0.00	0.03	0.00	0.01	0.40	0.01
OTU62	Proteobacteria	SAR86 clade	54.7	5E-09	0.33	0.01	0.00	3.93	0.00	0.00	2.99	0.00	0.00	0.22
OTU63	Proteobacteria	Rhodobacteraceae	27.0	7E-04	0.18	0.14	0.23	0.02	0.03	0.67	0.00	0.05	0.06	0.06
OTU64	Proteobacteria	*Ascidiaceihabitans* sp.	58.9	8E-10	0.27	0.00	0.00	0.64	0.00	0.00	4.14	0.00	0.00	1.04
OTU66	Proteobacteria	*Pseudorhodobacter* sp.	39.9	3E-06	0.20	0.19	0.01	0.00	0.00	0.00	0.00	0.19	0.99	0.12
OTU67	Bacteroidetes	Flavobacteriaceae	41.7	2E-06	0.18	0.34	0.80	0.00	0.00	0.02	0.00	0.00	0.00	0.00
OTU68	Firmicutes	*Lachnospiraceae* sp.	58.0	1E-09	0.24	0.00	0.00	0.00	1.97	0.00	0.00	0.00	0.00	0.00
OTU69	Proteobacteria	Rhodobacteraceae	51.5	2E-08	0.20	0.00	0.00	0.00	0.00	0.00	0.00	0.08	1.35	0.05

OTU	Phylum	Lowest taxonomic classification	Statistics	p	Relative abundance (%)									
					All	CG	CT	CW	HG	HT	HW	KG	KT	KW
OTU70	Proteobacteria	PS1 clade	36.9	1E-05	0.15	0.04	0.15	0.00	0.00	0.64	0.00	0.03	0.11	0.00
OTU71	Bacteroidetes	*Psychroserpens* sp.	41.0	2E-06	0.17	0.21	0.37	0.03	0.00	0.32	0.00	0.00	0.17	0.03
OTU72	Proteobacteria	Beijerinckiaceae	37.2	1E-05	0.19	0.11	0.17	0.01	0.00	0.02	0.00	0.05	0.97	0.00
OTU73	Proteobacteria	Rhizobiaceae	32.4	8E-05	0.18	0.17	0.47	0.01	0.01	0.26	0.00	0.07	0.21	0.03
OTU74	Proteobacteria	Rhodobacteraceae	54.0	7E-09	0.31	1.95	0.00	0.07	0.00	0.00	0.00	0.03	0.00	0.00
OTU75	Actinobacteria	*Ilumatobacter* sp.	39.0	5E-06	0.23	0.66	0.07	0.00	0.02	0.01	0.00	0.55	0.06	0.55
OTU76	Bacteroidetes	Flavobacteriaceae	49.2	6E-08	0.19	0.33	0.89	0.01	0.00	0.00	0.00	0.00	0.01	0.00
OTU77	Proteobacteria	*Filomicrobium* sp.	19.0	1E-02	0.17	0.26	0.15	0.00	0.22	0.39	0.00	0.09	0.09	0.00
OTU78	Proteobacteria	Hyphomonadaceae	47.3	1E-07	0.16	0.10	0.75	0.01	0.00	0.18	0.00	0.00	0.02	0.00
OTU79	Proteobacteria	*Kiloniella* sp.	31.2	1E-04	0.21	0.00	0.00	0.00	1.65	0.04	0.00	0.00	0.00	0.00
OTU80	Cyanobacteria	Oxyphotobacteria	43.8	6E-07	0.18	0.01	1.19	0.00	0.00	0.00	0.00	0.00	0.00	0.00
OTU81	Proteobacteria	Rhodobacteraceae	37.7	8E-06	0.15	0.06	0.21	0.00	0.02	0.49	0.00	0.09	0.10	0.00
OTU82	Proteobacteria	Rhizobiaceae	33.3	5E-05	0.16	0.41	0.24	0.02	0.08	0.29	0.00	0.00	0.02	0.00
OTU83	Bacteroidetes	Cryomorphaceae	58.6	9E-10	0.27	0.00	0.00	1.98	0.00	0.00	1.95	0.00	0.00	1.90
OTU85	Proteobacteria	*Anderseniella* sp.	33.9	4E-05	0.18	0.28	0.29	0.00	0.00	0.05	0.00	0.18	0.40	0.11
OTU86	Epsilonbacteraeota	*Arcobacter* sp.	35.4	2E-05	0.19	0.00	0.00	0.00	0.00	0.00	0.00	0.76	0.59	0.04
OTU87	Proteobacteria	Rhizobiaceae	31.3	1E-04	0.15	0.24	0.27	0.00	0.00	0.21	0.00	0.09	0.19	0.04
OTU88	Actinobacteria	*Ilumatobacter* sp.	40.3	3E-06	0.16	0.36	0.05	0.00	0.11	0.01	0.49	0.37	0.02	0.18
OTU89	Bacteroidetes	*Formosa* sp.	64.0	8E-11	0.19	0.00	0.00	0.41	0.00	0.00	3.73	0.00	0.00	0.00
OTU90	Bacteroidetes	NS3a marine group	59.0	7E-10	0.33	0.00	0.00	4.91	0.00	0.00	0.16	0.00	0.00	2.09
OTU91	Bacteroidetes	*Ulvibacter* sp.	44.3	5E-07	0.15	0.18	0.27	0.00	0.00	0.00	0.00	0.11	0.43	0.03
OTU92	Proteobacteria	SUP05 cluster	46.0	2E-07	0.19	0.00	0.00	0.00	0.00	0.00	0.00	1.10	0.23	0.01
OTU93	Proteobacteria	*Altererythrobacter* sp.	32.7	7E-05	0.15	0.03	0.07	0.00	0.00	0.63	0.00	0.01	0.22	0.05
OTU94	Proteobacteria	Sphingomonadaceae	35.8	2E-05	0.15	0.06	0.17	0.00	0.00	0.30	0.00	0.20	0.26	0.00
OTU95	Proteobacteria	Rhodobacteraceae	24.8	2E-03	0.15	0.18	0.06	0.00	0.12	0.00	0.00	0.62	0.10	0.05
OTU96	Bacteroidetes	*Tenacibaculum* sp.	31.4	1E-04	0.16	0.17	0.17	0.00	0.77	0.06	0.02	0.00	0.00	0.00
OTU98	Actinobacteria	*Mycobacterium* sp.	49.5	5E-08	0.18	0.27	0.01	0.02	0.00	0.00	0.00	0.75	0.02	0.58
OTU99	Proteobacteria	Rhodobacteraceae	34.6	3E-05	0.15	0.14	0.25	0.01	0.00	0.23	0.00	0.02	0.33	0.07
OTU100	Bacteroidetes	Bacteroidia	37.2	1E-05	0.15	0.00	0.00	0.00	1.14	0.07	0.00	0.00	0.00	0.00
OTU103	Proteobacteria	*Candidatus* Puniceispirillum	64.0	8E-11	0.24	0.00	0.00	2.99	0.00	0.00	0.84	0.00	0.00	1.40
OTU104	Firmicutes	*Terrisporobacter* sp.	63.6	9E-11	0.15	0.00	0.00	0.00	1.17	0.00	0.01	0.00	0.00	0.00
OTU105	Proteobacteria	*Halioglobus* sp.	33.3	5E-05	0.15	0.11	0.01	0.00	0.12	0.01	0.00	0.71	0.03	0.23
OTU106	Proteobacteria	*Ruegeria* sp.	36.9	1E-05	0.16	0.76	0.11	0.00	0.16	0.04	0.00	0.00	0.00	0.00
OTU114	Firmicutes	*Dorea* sp.	37.4	1E-05	0.17	0.00	0.00	0.00	1.36	0.01	0.01	0.00	0.00	0.00
OTU123	Proteobacteria	Rhodobacteraceae	30.9	1E-04	0.15	0.34	0.01	0.00	0.31	0.00	0.00	0.37	0.02	0.05
OTU161	Bacteroidetes	NS5 marine group	63.9	8E-11	0.17	0.00	0.01	2.71	0.00	0.00	0.49	0.00	0.00	0.45

Table S10. Classification of abundant OTUs detected in this study. Abundant OTUs: ≥1% of overall relative abundance. Rel. abund. = Relative abundance, Id. = Identity, Ubc = uncultured bacterium clone, Uncult. = Uncultured.

OTU	Rel. abund. (%)	Silva classification (lowest taxonomic rank; class, genus)	Next related hit according to BLAST				Lowest taxonomic classification according to BLAST			
			Classification	Accession no.	Id. (%)	Source	Classification	Accession no.	Id. (%)	Source
OTU1	5.3	Alphaproteobacteria, *Kordiimonas*	Ubc SanDiego_a6487	KF799727.1	98.76	Ascidian (*Ciona intestinalis*; gut)	*Kordiimonas* sp.	KF494349.1	98.76	Ascidian (*Ciona intestinalis*; tunic)
OTU2	5.6	Alphaproteobacteria, unclassified	Ubc Woods-Hole_a4133	KF799375.1	98.75	Ascidian (*Ciona intestinalis*; gut)	Rhizobiales	e.g. MN006421.1	93.27	Various
OTU3	4.7	Bacteroidia, *Pricia*	Ubc Woods-Hole_a5311	KF799010.1	98.57	Ascidian (*Ciona intestinalis*; gut)	*Arenibacter* sp.	KF494352.1	98.57	Ascidian (*Ciona intestinalis*; tunic)
OTU4	2.9	Gammaproteobacteria, *Pseudomonas*	*Pseudomonas* sp.	MH244157.1	99.30	Sediment				
OTU6	2.9	Oxyphotobacteria, *Synechococcus*_CC9902	Ubc DNA47	MG011059.1	99.75	Krill (*Euphausia mucronata*; stomach)	*Synechococcus* sp.	MH358353.1	99.75	Marine environment
OTU7	1.6	Alphaproteobacteria, unclassified (S25-593 group)	Ubc SanDiego_a6337	KF799711.1	99.01	Ascidian (*Ciona intestinalis*; gut)	Uncult. alphaproteo-bacterium_1-21	FJ659126.1	95.04	Ascidian (*Aplidium conicum*; tunic)
OTU8	2.5	Oxyphotobacteria, *Synechococcus*_CC9902	Ubc HAMb1_059	JX983984.1	98.77	Marine biofilm	*Synechococcus* sp.	KU867940.1	98.52	Seawater
OTU10	1.5	Unclassified (Bacteria)	Ubc Woods-Hole_a5143	KF798938.1	99.51	Ascidian (*Ciona intestinalis*; gut)	n.a. (only 76% identity)			
OTU11	1.9	Alphaproteobacteria, *Planktomarina*	Uncult. alphaproteobacterium clone PI_4d12b	AY580449.1	99.26	Seawater	Rhodo-bacteraceae	KU173743.1 or NR_125550.1	99.01	Seawater
OTU13	1.1	Actinobacteria, *Bifidobacterium*	*Bifidobacterium dentium*	LR134349.1	100	Human (Dental Caries)				
OTU15	1.3	Alphaproteobacteria, *Roseobacter*	Marine bacterium BPY-W9	AB562975.1	98.01	Red algae (*Porphyra yezoensis*, Japan)	*Roseobacter* sp.	MK224709.1	97.27	Red algae (*Neogoniolithon brassica-florida*)
OTU16	1.2	Mollicutes, *Candidatus_Hepatoplasma*	Ubc Woods-Hole_a5449	KF799049.1	91.08	Ascidian (*Ciona intestinalis*; gut)	n.a. (only 82% identity)			
OTU17	1.2	Alphaproteobacteria, *Lentibacter*	Uncult. marine bacterium, clone 85PALMAR09	HE981604.1	99.50	Seawater	*Litoreibacter* sp.	KJ513684.1	99.26	Seawater

Table S11. Putative annotation of metabolites detected in *C. intestinalis* bulk extracts (population level). Each detected compound is given with the experimentally determined *m/z* value. Putative molecular formulae were calculated by the elemental composition tool in the MassLynx software. The dereplication tool(s) (Derep. tool(s)) used to annotate the compounds are DNP (Dictionary of Natural Products [2]), GNPS (Dereplication workflow available at Global Natural Product Social Molecular Networking [1]), ISDB-UNPD (*in silico* MS/MS database of the Universal Natural Product Database [3]), ML (MarinLit [4]) and MN (molecular networking [1]). Occurrence of abundant peaks (detected in ≥5 replicates) in individual extracts is given with the respective number of replicates for inner body (IB) and tunic (T) extracts separately. R_t: Retention time. IC: Identification confidence level after Sumner et al. 2007 [5]. Nf: No fragmentation pattern detected. ↑: Metabolite production was specifically enhanced (at least 10-fold larger peak area) in the respective sampling location (sampling locations are abbreviated: C = Canada, H = Helgoland, K = Kiel). Underlined occurrence: enhancement/specificity was manually detected from MS chromatograms (peak intensity), since compound was not in automatic peak list. Refs: references.

Peak no.	*m/z* [M+H]$^+$	R_t (min)	Putative molecular formula	IC	Fragmentation pattern	Putative identification	Derep. tool(s)	Chemical family	Biological origin	Occurrence	IB	T	Refs
1	248.161	3.04	$C_{10}H_{21}N_3O_4$	4	124.0692					H3, K1	5	6	
2	466.2826	3.10	$C_{26}H_{35}N_5O_3$	4	Nf					K↑			
3	386.3221	3.10	$C_{13}H_{39}N_9O_4$	4	Nf					K↑			
4	361.3556	3.10	$C_{19}H_{44}N_4O_2$	4	140.1747, 157.2030, 290.3256					not C	13	9	
5	429.4159	3.10	$C_{29}H_{52}N_2$	2	72.1032, 140.1747, 155.1360, 220.0516, 228.2256, 340.2377, 351.1815	Halichonine B	ISDB-UNPD	Sesquiterpene alkaloid	Sponge: *Halichondria okadai*	not C	13	7	[6]
6	517.2661	3.12	$C_{31}H_{48}O_6$	3	345.2962, 363.3029, 439.3996		DNP, ML	Sterol	Various marine invertebrates, e.g. sponge (*Dysidea herbacea*), coral (*Nephthea bayeri*)	H3, K1			[7], [8]
7	211.0554	3.28	$C_5H_{10}N_2O_7$	4	193.0851					H3, K1	5	8	
8	667.4767	3.31	$C_{35}H_{58}N_{10}O_3$	4	Nf								
9	335.1791	3.45	$C_{26}H_{22}$	4	Nf						7	1	
10	480.3527	3.46	$C_{33}H_{41}N_3$	4	318.3422					C↑	21	18	
11	480.3527	3.52	$C_{33}H_{41}N_3$	4	318.3422						4	6	
12	278.2424	3.69	$C_{18}H_{31}NO$	2	250.2857, 262.3000	Crucigasterin 277	ISDB-UNPD	Polyunsaturated amino alcohol	Ascidian: *Pseudodistoma crucigaster*	H↑	16	2	[9]
13	545.296	3.77	$C_{27}H_{44}O_{11}$	4	373.3291, 391.3394					H3, K1	3	7	
14	280.2590	3.74	$C_{18}H_{33}NO$	2	Nf	Crucigasterin E	ISDB-UNPD	Polyunsaturated amino alcohol	Ascidian: *Pseudodistoma crucigaster*		18	3	[10]
15	310.2712	3.92	$C_{19}H_{35}NO_2$	2	81.0943, 86.0830, 95.1129, 135.1490, 145.1371, 257.2605, 274.2864	D-erythro-4,8,10-sphingatrienine	ISDB-UNPD	Glycosphingolipid	Sea cucumber: *Stichopus variegates*	H only			[11]
16	413.3359	3.97	$C_{19}H_{40}N_8O_2$	4	Nf					H3, K1	1	6	
17	554.5435	4.20	$C_{37}H_{67}N_3$	4	72.1018, 137.1615, 197.2366, 276.3089, 279.3187, 333.3840					H only	7	3	
18	340.2194	4.42	$C_{12}H_{29}N_5O_6$	4	Nf					C↑			

147

Peak no.	m/z [M+H]$^+$	R$_t$ (min)	Putative molecular formula	IC	Fragmentation pattern	Putative identification	Derep. tool(s)	Chemical family	Biological origin	Occurrence	IB	T	Refs
19	468.3076	4.41	$C_{24}H_{41}N_3O_6$	4	Nf						26	4	
20	349.1927	4.57	$C_{10}H_{28}N_4O_9$	4	Nf						18	13	
21	454.3291	4.73	$C_{25}H_{39}N_7O$	4	104.1345					not K	24	3	
22	317.1698	4.81	$C_{10}H_{20}N_8O_4$	4	Nf								
23	349.1927	4.84	$C_{10}H_{28}N_4O_9$	4	Nf					H3, K1	3	4	
24	277.2130	4.86	$C_{17}H_{24}O_3$	2	107.1138, 121.1301, 135.1430, 149.1648, 195.9527	Spirodysin	ISDB-UNPD	Sesquiterpenoid	Sponge: *Dysidea* sp.		17	2	[12]
25	599.4107	4.92	$C_{37}H_{58}O_4S$	3	221.1886, 507.3958		MN	Alkyl sulfate		H3, K1	0	8	
26	301.2123	4.98	$C_{15}H_{28}N_2O_4$	2	187.1823, 265.2364, 283.2443	Lipoamide A	DNP, ML	Lipoamide	Bacterium: *Bacillus pumilus*		27	21	[13]
27	568.3410	5.20	$C_{20}H_{49}N_5O_{13}$	4	Nf						24	13	
28	520.3409	5.20	$C_{33}H_{45}NO_4$	4	Nf					C only	10	11	
29	488.2342	5.20	$C_{20}H_{33}N_5O_9$	4	Nf						22	23	
30	453.2224	5.20	$C_{18}H_{28}N_8O_6$	4	Nf					H3	21	23	
31	468.3430	5.27	$C_{25}H_{45}N_3O_5$	4	104.1349, 427.2712, 363.9669						29	21	
32	842.5110	5.35	$C_{38}H_{63}N_{15}O_7$	4	Nf					C only	3	8	
33	480.3438	5.36	$C_{26}H_{45}N_3O_5$	4	Nf					not H	18	26	
34	454.2899	5.47	$C_{19}H_{35}N_9O_4$	4	313.3146					not K	18	0	
35	376.2775	5.47	$C_{14}H_{33}N_9O_3$	3	Nf		MN	Tetrapyrrole		C only			
36	506.4057	5.54	$C_{27}H_{55}NO_7$	4	104.1349					H↑	11	8	
37	235.1639	5.57	$C_6H_{18}N_8O_2$	4	Nf					C↑			
38	542.3815	5.57	$C_{29}H_{47}N_7O_3$	4	Nf					C only	9	0	
39	512.3700	5.61	$C_{27}H_{49}N_3O_6$	4	104.135						10	19	
40	321.2397	5.67	$C_{15}H_{32}N_2O_5$	4	151.1442					H↑	2	7	
41	270.3127	5.69	$C_{18}H_{39}N$	3	Nf		MN	Tetrapyrrole		H only			
42	496.3393	5.72	$C_{27}H_{41}N_7O_2$	4	104.1346, 184.1077, 478.3760						27	21	
43	438.2986	5.88	$C_{27}H_{39}N_3O_2$	2	266.3131, 284.3345, 420.3313	Lyngbyatoxin A	ISDB-UNPD	Indole alkaloid	E.g. Cyanobacterium: *Moorea producens*		15	8	[14]
44	276.2263	5.94	$C_9H_{25}N_9O$	4	Nf					C↑	4	2	
45	494.3591	5.94	$C_{27}H_{47}N_3O_5$	4	104.1345, 184.1088						23	18	
46	522.3537	6.08	$C_{28}H_{47}N_3O_6$	4	104.1343, 184.1078, 504.3933						27	22	
47	480.3438	6.14	$C_{21}H_{46}N_7O_3Cl$	4	Nf					not H	20	27	
48	985.7030	6.18	$C_{64}H_{92}N_2O_6$	4	Nf					H only			
49	452.3128	6.46	$C_{28}H_{41}N_3O_2$	2	280.3400, 298.3514, 434.3490	Blastmycetin E	ISDB-UNPD	Indole alkaloid	Bacterium: *Streptoverticillium blastmyceticum*		28	22	[15]
50	510.3580	6.49	$C_{26}H_{56}NO_6P$	2	104.1346, 184.1077, 327.3210	Lyso-platelet-activating factor (C18)	GNPS	Phospholipid	Sponge: *Spirastrella purpurea*		19	6	[16]
51	506.3597	6.50	$C_{23}H_{48}N_7O_3Cl$	4	Nf					not H	13	17	
52	508.3776	6.55	$C_{29}H_{45}N_7O$	4	104.1350, 184.1079					H↑	13	11	

148

Peak no.	m/z [M+H]+	Rt (min)	Putative molecular formula	IC	Fragmentation pattern	Putative identification	Derep. tool(s)	Chemical family	Biological origin	Occurrence	IB	T	Refs
53	452.3128	6.63	$C_{28}H_{41}N_3O_2$	2	280.3400, 298.3514, 434.3490	Blastmycetin E	ISDB-UNPD	Indole alkaloid	Bacterium: *Streptoverticillium blastmyceticum*		27	14	[15]
54	302.2427	6.70	$C_{11}H_{27}N_9O$	4	Nf					C only	5	2	
55	588.3503	6.70	$C_{29}H_{45}N_7O_6$	2	Nf	MIP-A3	DMNP	Linear peptide	Snail: *Achatina fulica*	C only	9	7	[17]
56	581.4004	6.75	$C_{40}H_{52}O_3$	2	221.1906, 489.3869	α-Doradecin	DNP	Carotenoid	Crab: *Chiromantes haematocheir*	H3, K1	0	6	[18]
57	494.3591	6.77	$C_{27}H_{47}N_3O_5$	4	Nf						20	23	
58	452.3128	6.77	$C_{28}H_{41}N_3O_2$	4	Nf	Blastmycetin E	ISDB-UNPD	Indole alkaloid	Bacterium: *Streptoverticillium blastmyceticum*				[15]
59	428.3738	6.77	$C_{25}H_{49}NO_4$	2	Nf	(4E)-N-[(2R)-1-hydroxy-3-methoxypropan-2-yl]-7-methoxyicos-4-enamide	DNP, ML	Lipopeptide	Cyanobacterium (not identified)		12	6	[19]
60	619.3134	6.77	$C_{33}H_{46}O_{11}$	2	Nf	Antibiotic YM 47525	DNP	Sesquiterpenoid	Fungus (not identified)	C only			[20]
61	344.3479	6.91	$C_{17}H_{41}N_7$	4	Nf						28	27	
62	508.3776	6.91	$C_{29}H_{45}N_7O$	4	104.1351					not H	18	25	
63	482.3227	6.91	$C_{25}H_{43}N_3O_6$	4	Nf						26	3	
64	254.2425	6.99	$C_{16}H_{31}NO$	3	184.2121, 219.2468, 237.2642	a: Crucigasterin D, b: Obscuraminol C	DNP	Polyunsaturated amino alcohol	Ascidian: *Pseudodistoma crucigaster* (a) or *Pseudodistoma obscurum* (b)		2	6	(a) [10], (b) [21]
65	377.2661	7.03	$C_{19}H_{32}N_6O_2$	4	201.2046, 285.2580					H↑	13	1	
66	349.2691	7.03	$C_{17}H_{36}N_2O_5$	4	Nf					H↑	3	10	
67	494.3591	7.03	$C_{27}H_{47}N_3O_5$	4	Nf					C↑	16	13	
68	639.4067	7.12	$C_{30}H_{58}N_2O_{12}$	4	Nf					C only	1	13	
69	599.4107	7.12	$C_{40}H_{54}O_4$	2	109.1296, 185.1529, 233.1781, 341.3246, 544.3911	a: Crassostreaxanthin A, b: Crassostreaxanthin B	DNP, ML	Carotenoid	Bivalve: *Crassostrea gigas*	<u>C↑</u>			[22]
70	466.3312	7.12	$C_{30}H_{43}NO_3$	4	448.3555, 312.3705, 294.3555								
71	370.3654	7.12	$C_{19}H_{43}N_7$	4	Nf						14	10	
72	277.2130	7.21	$C_{13}H_{28}N_2O_4$	4	Nf						26	19	
73	524.3705	7.32	$C_{26}H_{54}NO_7P$	2	104.1354, 184.1063, 341.3518, 506.4213	Platelet-activating factor (PAF)	GNPS	Phospholipid	Various types of cells and animals		27	17	[23]
74	466.3268	7.41	$C_{25}H_{43}N_3O_5$	4	294.3566, 312.3678, 448.3652						29	23	
75	627.3563	7.57	$C_{36}H_{50}O_9$	2	469.3168, 367.3693, 283.0604	Milbemycin α20	DNP	Macrolide	Bacterium: *Streptomyces hygroscopicus* subsp. *aureolacrimosus*				[24]
76	550.3897	7.63	$C_{35}H_{51}NO_4$	4	104.1348, 184.1081, 532.4282						27	21	
77	597.2744	7.63	$C_{23}H_{36}N_{10}O_9$	4	Nf						4	2	
78	376.3172	7.63	$C_{19}H_{41}N_3O_4$	4	Nf					C↑	1	12	

149

Peak no.	m/z [M+H]$^+$	R$_t$ (min)	Putative molecular formula	IC	Fragmentation pattern	Putative identification	Derep. tool(s)	Chemical family	Biological origin	Occurrence	IB	T	Refs
79	403.2805	7.76	C$_{19}$H$_{39}$NaO$_5$S	2	293.2614, 311.2804	Sodium 10-(hydroxymethyl)-2,6,14-trimethylpentadecyl sulfate	ML	Alkyl sulfate	Ascidian: *Ciona edwardsii*	H↑	13	2	[25]
80	552.4021	7.76	C$_{31}$H$_{49}$N$_7$O$_2$	4	Nf					C only	1	6	
81	441.2969	7.76	C$_{23}$H$_{40}$N$_2$O$_6$	4	Nf					H↑	8	5	
82	508.3776	7.83	C$_{29}$H$_{45}$N$_7$O	4	104.1351					not H	12	27	
83	303.2285	7.91	C$_{15}$H$_{30}$N$_2$O$_4$	4	Nf						29	30	
84	320.2177	8.14	C$_{14}$H$_{29}$N$_3$O$_5$	3	140.1022, 166.0831, 302.2524					H3, K1	4	7	
85	451.2999	8.51	C$_{33}$H$_{38}$O	4	Nf					H3	8	1	
86	317.2417	8.51	C$_{12}$H$_{28}$N$_8$O$_2$	4	235.3066						15	11	
87	305.2441	8.55	C$_{19}$H$_{32}$N$_2$O	2	163.1834	Ikimine A	ISDB-UNPD	Alkylpyridine	Sponge (not identified)		4	6	[26]
88	329.2441	8.60	C$_{17}$H$_{32}$N$_2$O$_4$	2	175.1824, 215.2166, 311.2789	Lipoamide C	DNP, ML	Lipoamide	Bacterium: *Bacillus pumilus*		17	22	[13]
89	305.2441	8.79	C$_{19}$H$_{32}$N$_2$O	2	163.1834	Ikimine A	ISDB-UNPD	Alkylpyridine	Sponge (not identified)				[26]
90	609.2709	8.87	C$_{35}$H$_{36}$N$_4$O$_6$	2	531.2986, 559.2847, 591.3218	10-hydroxyphaeophorbide a	DNP	Tetrapyrroles	E.g. ascidian: *Trididemnum solidum*	C↑	7	15	[27]
91	289.2116	9.00	C$_{14}$H$_{28}$N$_2$O$_4$	4	215.2158, 229.2335, 239.2176, 257.2284					H only			
92	625.2678	9.02	C$_{36}$H$_{33}$N$_8$O$_3$	4	538.3119, 566.3060, 581.3383, 608.3168					C only	2	15	
93	400.4145	9.09	C$_{25}$H$_{53}$NO$_2$	4	Nf						27	30	
94	603.2276	9.09	C$_{27}$H$_{43}$N$_2$O$_8$Br	4	501.2975, 527.2592, 529.2766					not K			
95	331.2587	9.10	C$_{22}$H$_{34}$O$_2$	2	Nf	Clupanodonic acid	ISDB-UNPD	Unsaturated fatty acid	Fish oil	not K	12	13	[28]
96	609.2709	9.28	C$_{35}$H$_{36}$N$_4$O$_6$	2	531.2986, 559.2847, 591.3218	10-hydroxyphaeophorbide a	DNP	Tetrapyrrole	E.g. ascidian: *Trididemnum solidum*	C↑, not K	10	16	[27]
97	641.4202	9.36	C$_{26}$H$_{56}$N$_8$O$_{10}$	4	Nf					C only	1	12	
98	681.4148	9.36	C$_{28}$H$_{56}$N$_8$O$_{11}$	4	Nf					C only	0	10	
99	581.4004	9.36	C$_{40}$H$_{52}$O$_3$	2	109.1293, 147.1132, 149.1319, 157.1320, 185.1702, 197.1720, 237.1925, 355.2922	Trikentriorhodin	DNP	Carotenoid	Sponge: *Trikentrion helium*	<u>C only</u>	0	11	[29]
100	658.4239	9.37	C$_{33}$H$_{39}$NO$_{13}$	2	109.1300, 127.130, 223.1872	Rubomycin M	DNP	Anthracycline glycoside	Bacterium: *Streptomyces coeruleorubidus*	C only	1	12	[30]
101	291.2291	9.60	C$_{19}$H$_{30}$O$_2$	3	121.1306, 135.1477, 149.1646, 163.1814, 241.2334, 259.2451		DNP, ML	Unsaturated fatty acid	Various marine origins, e.g. sponge (e.g. *Stelletta* sp.) and alga (e.g. *Lobophora variegata*)	H3, K1	4	11	[31], [32]

Peak no.	m/z [M+H]⁺	R_t (min)	Putative molecular formula	IC	Fragmentation pattern	Putative identification	Derep. tool(s)	Chemical family	Biological origin	Occurrence	IB	T	Refs
102	348.2455	9.68	$C_{23}H_{29}N_3$	2	140.1022, 166.0836, 330.2850						5	13	
103	593.2771	9.69	$C_{35}H_{36}N_4O_5$	2	533.3050	Pheophorbide A	DNP	Tetrapyrrole	E.g. ascidian: *Trididemnum solidum*	C↑	26	11	[27]
104	317.2454	10.18	$C_{21}H_{32}O_2$	2	267.2503, 285.2617	a: 5E,7E,9E,14Z,17Z-eicosapentaenoic acid, b: 5Z,7E,9E,14Z,17Z-eicosapentaenoic acid	ISDB-UNPD	Unsaturated fatty acid	Alga: *Ptilota filicina*		2	15	[33]
105	535.2693	10.25	$C_{33}H_{34}N_4O_3$	2	507.3204	Pyropheophorbide A	DNP, ML	Tetrapyrrole	E.g. bivalve: *Ruditapes philippinarum*		28	29	[34]
106	293.2431	10.44	$C_{14}H_{32}N_2O_4$	4	81.0950, 95.1122, 109.1295, 123.1465, 137.1631, 243.2490, 261.2608						2	3	
107	363.2984	10.46	$C_{24}H_{42}O_2$	2	Nf	Strongylodiol G	ISDB-UNPD	Acetylenic alcohol	Sponge: *Petrosia* sp.		22	11	[35]
108	565.2440	10.48	$C_{33}H_{32}N_4O_5$	2	Nf	Purpurin 18	DNP	Tetrapyrrole	E.g. bivalve: *Ruditapes philippinarum*		18	0	[34]
109	681.4148	10.48	$C_{44}H_{56}O_6$	4	Nf					C only	4	12	
110	639.3239	10.64	$C_{43}H_{38}N_6$	4	566.3386. 579.3464					H3, K1	1	6	
111	343.2594	10.71	$C_{23}H_{34}O_2$	2	269.2657, 293.2670, 311.2781	Docosahexaenoic acid methyl ester	ISDB-UNPD	Unsaturated fatty acid	Ascidian: *Pseudodistoma aureum*		7	13	[36]
112	647.5734	10.89	$C_{43}H_{76}O_2$	4	Nf					H only			
113	732.5054	10.99	$C_{42}H_{63}N_9O$	4	Nf						11	25	
114	518.4949	11.30	$C_{34}H_{63}NO_2$	4	250.2922, 262.2921, 280.3038					H↑	15	2	
115	793.4943	11.60	$C_{53}H_{64}N_2O_4$	4	Nf					C only	1	9	
116	564.3982	11.79	$C_{27}H_{49}N_9O_4$	4	Nf					C only	0	14	
117	549.2866	11.91	$C_{34}H_{36}N_4O_3$	2	461.2792, 436.2999	Methyl pyropheophorbide a	DNP	Tetrapyrrole	E.g. cyanobacterium: *Spirulina maxima*	H3, K1	1	13	[37]
118	748.5408	11.99	$C_{35}H_{75}N_5O_{10}$	4	Nf						28	10	
119	573.1493	11.99	$C_{24}H_{29}N_2O_{12}Cl$	4	135.1505, 554.5661					C↑			
120	546.4907	11.99	$C_{35}H_{63}NO_3$	2	Nf	Bacteriohopane-aminotriol	DNP	Hopanoid	Bacterium: e.g. *Rhodopseudomonas acidophila*		19	1	[38]
121	543.1011	12.10	$C_{21}H_{21}N_6O_8Cl$	4	Nf					C only			

151

Table S12. ANOSIM comparison of UPLC-MS/MS profiles of *C. intestinalis* extracts. ANOSIM calculations were based on the Bray-Curtis similarity index and results are given with the respective R score and p value.

Test	Extraction procedure	Tissue(s)	Compared groups	R	p
Sampling sites (all metabolites)	Population level	Whole body	Canada x Helgoland	0.6667	0.1
			Canada x Kiel	0.5556	0.09
			Helgoland x Kiel	0.8889	0.1
Sampling sites (core metabolites only)			Canada x Helgoland	1	0.1
			Canada x Kiel	1	0.1
			Helgoland x Kiel	1	0.1
Tissue	Individual level	Inner body & tunic	Inner body x tunic	0.6768	0.0001
Sampling sites		Inner body	Canada x Helgoland	0.2502	0.0025
			Canada x Kiel	0.2342	0.0011
			Helgoland x Kiel	0.3184	0.0003
		Tunic	Canada x Helgoland	0.2484	0.0049
			Canada x Kiel	0.3562	0.0027
			Helgoland x Kiel	0.4518	0.0012

Supplementary References

1. Wang, M.; Carver, J.J.; Phelan, V.V.; Sanchez, L.M.; Garg, N.; Peng, Y.; Nguyen, D.D.; Watrous, J.; Kapono, C.A.; Luzzatto-Knaan, T.; et al. Sharing and community curation of mass spectrometry data with Global Natural Products Social Molecular Networking. *Nat. Biotechnol.* **2016**, *34*, 828-837, doi:10.1038/nbt.3597.
2. Blunt, J.W.; Munro, M.H. *Dictionary of marine natural products with CD-ROM*. CRC Press: 2007.
3. Allard, P.M.; Peresse, T.; Bisson, J.; Gindro, K.; Marcourt, L.; Pham, V.C.; Roussi, F.; Litaudon, M.; Wolfender, J.L. Integration of molecular networking and *in-silico* MS/MS fragmentation for natural products dereplication. *Anal. Chem.* **2016**, *88*, 3317-3323, doi:10.1021/acs.analchem.5b04804.
4. Blunt, J.W.; Copp, B.R.; Keyzers, R.A.; Munro, M.H.G.; Prinsep, M.R. Marine natural products. *Nat. Prod. Rep.* **2017**, *34*, 235-294, doi:10.1039/c6np00124f.
5. Sumner, L.W.; Amberg, A.; Barrett, D.; Beale, M.H.; Beger, R.; Daykin, C.A.; Fan, T.W.; Fiehn, O.; Goodacre, R.; Griffin, J.L.; et al. Proposed minimum reporting standards for chemical analysis Chemical Analysis Working Group (CAWG) Metabolomics Standards Initiative (MSI). *Metabolomics* **2007**, *3*, 211-221, doi:10.1007/s11306-007-0082-2.
6. Ohno, O.; Chiba, T.; Todoroki, S.; Yoshimura, H.; Maru, N.; Maekawa, K.; Imagawa, H.; Yamada, K.; Wakamiya, A.; Suenaga, K.; et al. Halichonines A, B, and C, novel sesquiterpene alkaloids from the marine sponge *Halichondria okadai* Kadota. *Chem. Commun.* **2011**, *47*, 12453-12455, doi:10.1039/c1cc15557a.
7. Kashman, Y.; Zviely, M. New alkylated scalarins from the sponge *Dysidea herbacea*. *Tetrahedron Lett.* **1979**, *20*, 3879-3882, doi:10.1016/S0040-4039(01)95551-0.
8. Shao, Z.Y.; Zhu, D.Y.; Guo, Y.W. Nanjiols A-C, new steroids from the Chinese soft coral *Nephthea bayeri*. *J. Nat. Prod.* **2002**, *65*, 1675-1677, doi:10.1021/np020087x.
9. Jares-Erijman, E.A.; Bapat, C.P.; Lithgow-Bertelloni, A.; Rinehart, K.L.; Sakai, R. Crucigasterins, new polyunsaturated amino alcohols from the Mediterranean tunicate *Pseudodistoma crucigaster*. *J. Org. Chem.* **1993**, *58*, 5732-5737, doi:10.1021/jo00073a036.
10. Ciavatta, M.L.; Manzo, E.; Nuzzo, G.; Villani, G.; Varcamonti, M.; Gavagnin, M. Crucigasterins A–E, antimicrobial amino alcohols from the Mediterranean colonial ascidian *Pseudodistoma crucigaster*. *Tetrahedron* **2010**, *66*, 7533-7538, doi:10.1016/j.tet.2010.07.056.
11. Sugawara, T.; Zaima, N.; Yamamoto, A.; Sakai, S.; Noguchi, R.; Hirata, T. Isolation of sphingoid bases of sea cucumber cerebrosides and their cytotoxicity against human colon cancer cells. *Biosci. Biotechnol. Biochem.* **2006**, *70*, 2906-2912, doi:10.1271/bbb.60318.
12. Cameron, G.M.; Stapleton, B.L.; Simonsen, S.M.; Brecknell, D.J.; Garson, M.J. New sesquiterpene and brominated metabolites from the tropical marine sponge *Dysidea* sp. *Tetrahedron* **2000**, *56*, 5247-5252, doi:10.1016/S0040-4020(00)00434-8.
13. Berrue, F.; Ibrahim, A.; Boland, P.; Kerr, R.G. Newly isolated marine *Bacillus pumilus* (SP21): A source of novel lipoamides and other antimicrobial agents. *Pure Appl. Chem.* **2009**, *81*, 1027-1031, doi:10.1351/pac-con-08-09-25.
14. Jiang, W.; Zhou, W.; Uchida, H.; Kikumori, M.; Irie, K.; Watanabe, R.; Suzuki, T.; Sakamoto, B.; Kamio, M.; Nagai, H. A new lyngbyatoxin from the Hawaiian cyanobacterium *Moorea producens*. *Mar. Drugs* **2014**, *12*, 2748-2759, doi:10.3390/md12052748.
15. Irie, K.; Funaki, A.; Koshimizu, K.; Hayashi, H.; Arai, M. Structure of blastmycetin E, a new teleocidin-related compound, from *Streptoverticillium blastmyceticum*. *Tetrahedron Lett.* **1989**, *30*, 2113-2116, doi:10.1016/S0040-4039(01)93726-8.
16. Lin, K.; Yang, P.; Yang, H.; Liu, A.H.; Yao, L.G.; Guo, Y.W.; Mao, S.C. Lysophospholipids from the Guangxi sponge *Spirastrella purpurea*. *Lipids* **2015**, *50*, 697-703, doi:10.1007/s11745-015-4028-6.
17. Ikeda, T.; Yasuda-Kamatani, Y.; Minakata, H.; Kenny, P.T.M.; Nomoto, K.; Muneoka, Y. *Mytilus*-inhibitory peptide analogues isolated from the ganglia of a pulmonate mollusc, *Achatina fulica*. *Comp. Biochem. Physiol.* **1992**, *101*, 245-249, doi:10.1016/0742-8413(92)90268-C.
18. Matsuno, T.; Ookubo, M. The first isolation and identification of fritschiellaxanthin from a crab *Sesarma haematocheir* (Akategani in Japanese). *Bull. Jpn. Soc. Sci. Fish.* **1982**, *48*, 653-659, doi:10.2331/suisan.48.653.
19. Wan, F.; Erickson, K.L. Serinol-derived malyngamides from an Australian cyanobacterium. *J. Nat. Prod.* **1999**, *62*, 1698-1699, doi:10.1021/np990291t.
20. Sugawara, T.; Tanaka, A.; Nagai, K.; Suzuki, K.; Okada, G. New members of the trichothecene family. *J. Antibiot.* **1997**, *50*, 778-780, doi:10.7164/antibiotics.50.778.

21. Garrido, L.; Zubia, E.; Ortega, M.J.; Naranjo, S.; Salva, J. Obscuraminols, new unsaturated amino alcohols from the tunicate *Pseudodistoma obscurum*: Structure and absolute configuration. *Tetrahedron* **2001**, *57*, 4579-4588, doi:10.1016/S0040-4020(01)00372-6.
22. Fujiwara, Y.; Maoka, T.; Ookubo, M.; Matsuno, T. Crassostreaxanthins A and B, novel marine carotenoids from the oyster *Crassostrea gigas*. *Tetrahedron Lett.* **1922**, *33*, 4941-4944, doi:10.1016/S0040-4039(00)61240-6.
23. Benveniste, J.; Henson, P.M.; Cochrane, C.G. Leukocyte-dependent histamine release from rabbit platelets. The role of IgE, basophils, and a platelet-activating factor. *J. Exp. Med.* **1972**, *136*, 1356-1377, doi:10.1084/jem.136.6.1356.
24. Nonaka, K.; Tsukiyama, T.; Okamoto, Y.; Sato, K.; Kumasaka, C.; Yamamoto, T.; Maruyma, F.; Yoshikawa, H. New milbemycins from *Streptomyces hygroscopicus* subsp. *aureolacrimosus*: Fermentation, isolation and structure elucidation. *J. Antibiot.* **2000**, *53*, 694-704, doi:10.7164/antibiotics.53.694.
25. Imperatore, C.; Aiello, A.; D'Aniello, F.; Luciano, P.; Vitalone, R.; Meli, R.; Raso, G.M.; Menna, M. New bioactive alkyl sulfates from Mediterranean tunicates. *Molecules* **2012**, *17*, 12642-12650, doi:10.3390/molecules171112642.
26. Carroll, A.R.; Scheuer, P.J. Four beta-alkylpyridines from a sponge. *Tetrahedron* **1990**, *46*, 6637-6644, doi:10.1016/S0040-4020(01)87855-8.
27. Rinehart, K.L.; Kishore, V.; Bible, K.C.; Sakai, R.; Sullins, D.W.; Li, K.M. Didemnins and tunichlorin: Novel natural products from the marine tunicate *Trididemnum solidum*. *J. Nat. Prod.* **1988**, *51*, 1-21, doi:10.1021/np50055a001.
28. Tomiyama, T. The chemical composition of tunny liver oil. *Bull. Chem. Soc. Jpn.* **2014**, *9*, 141-147, doi:10.1080/03758397.1933.10857049.
29. Aguilar-Martinez, M.; Liaaen-Jensen, S. Animal carotenoids. 9. Trikentriorhodin. *Acta Chem. Scand. B* **1974**, *10*, 1247-1248, doi:10.3891/acta.chem.scand.28b-1247.
30. Zbarskiĭ, V.B.; Lazhko, E.I.; Pomanova, N.P.; Fomicheva, E.V.; Saburova, T.P. Rubomycins M and N-new anthracycline antibiotics. *Russ. J. Bioorg. Chem.* **1991**, *17*, 1698-1701.
31. Zhao, Q.; Lee, S.Y.; Hong, J.; Lee, C.O.; Im, K.S.; Sim, C.J.; Lee, D.S.; Jung, J.H. New acetylenic acids from the marine sponge *Stelletta* species. *J. Nat. Prod.* **2003**, *66*, 408-411, doi:10.1021/np020440z.
32. Gutierrez-Cepeda, A.; Fernandez, J.J.; Norte, M.; Montalvao, S.; Tammela, P.; Souto, M.L. Acetate-derived metabolites from the brown alga *Lobophora variegata*. *J. Nat. Prod.* **2015**, *78*, 1716-1722, doi:10.1021/acs.jnatprod.5b00415.
33. Lopez, A.; Gerwick, W.H. Two new icosapentaenoic acids from the temperate red seaweed *Ptilota filicina* J. Agardh. *Lipids* **1987**, *22*, 190-194, doi:10.1007/BF02537301.
34. Watanabe, N.; Yamamoto, K.I.; Ihshikawa, H.; Yagi, A.; Sakata, K.; Brinen, L.S.; Clardy, J. New chlorophyll-a-related compounds isolated as antioxidants from marine bivalves. *J. Nat. Prod.* **1993**, *56*, 305-317, doi:10.1021/np50093a001.
35. Watanabe, K.; Tsuda, Y.; Hamada, M.; Omori, M.; Mori, G.; Iguchi, K.; Naoki, H.; Fujita, T.; Van Soest, R.W. Acetylenic strongylodiols from a *Petrosia* (*Strongylophora*) Okinawan marine sponge. *J. Nat. Prod.* **2005**, *68*, 1001-1005, doi:10.1021/np040233u.
36. Pearce, A.N.; Appleton, D.R.; Babcock, R.C.; Copp, B.R. Distomadines A and B, novel 6-hydroxyquinoline alkaloids from the New Zealand ascidian, *Pseudodistoma aureum*. *Tetrahedron Lett.* **2003**, *44*, 3897-3899, doi:10.1016/s0040-4039(03)00831-1.
37. Osuka, A.; Wada, Y.; Shinoda, S. Covalently linked pyropheophorbide dimers as models of the special pair in the photosynthetic reaction center. *Tetrahedron* **1996**, *52*, 4311-4326, doi:10.1016/0040-4020(96)00131-7.
38. Neunlist, S.; Rohmer, M. A novel hopanoid, 30-(5'-adenosyl)hopane, from the purple non-sulphur bacterium *Rhodopseudomonas acidophila*, with possible DNA interactions. *Biochem. J.* **1985**, *228*, 769-771, doi:10.1042/bj2280769.

Supplementary Information accompanying Chapter 2

Supplementary Figures S1-S8

Figure S1. Number of microbial strains isolated from the tunic of *C. intestinalis* and seawater reference.

Figure S2. Distribution of bacterial orders across the sample types and their geographic locations.

Figure S3. Distribution of fungal orders across the sample types and their geographic locations.

Figure S4. Chemical structures of putatively identified compounds in the crude extracts of five selected microbial strains isolated from the tunic of *C. intestinalis*.

Figure S5. FBMN of the crude extract of *Pyrenochaeta* sp. strain CHT58 cultivated on PDA medium.

Figure S6. FBMN of the crude extract of *Pseudogymnoascus destructans* strain CHT56 cultivated on CAG medium.

Figure S7. FBMN of the crude extract of *Penicillium* sp. strain CKT35 cultivated on medium PDA.

Figure S8. FBMN of the crude extract of *Boeremia exigua* strain CKT91 cultivated on CAG (blue nodes) and PDA (red nodes) media.

Supplementary Tables S1-S10

Table S1. Parameters for MZmine-processing of UPLC-MS/MS data.

Table S2. Identification of microbial strains isolated from *C. intestinalis* and seawater reference in Helgoland and Kiel Fjord.

Table S3. Bioactivity (%) of crude extracts derived from tunic-associated microbial strains at a test concentration of 100 µg/mL.

Table S4. Bioactivity-based selection criterion for the prioritization of extracts for in-depth chemical analyses.

Table S5. ANOSIM comparison of chemically different extracts.

Table S6. Putative annotation of metabolites detected in the crude extract of *Pyrenochaeta* sp. strain CHT58 cultivated on PDA medium.

Table S7. Putative annotation of metabolites detected in the crude extract of *Pseudogymnoascus destructans* strain CHT56 cultivated on CAG medium.

Table S8. Putative annotation of metabolites detected in the crude extract of *Penicillium* sp. strain CKT35 cultivated on PDA medium.

Table S9. Putative annotation of metabolites detected in the crude extracts of *Boeremia exigua* strain CKT91 cultivated on CAG and PDA media.

Table S10. Putative annotation of metabolites detected in the crude extracts of *Streptomyces* sp. strain CKT43 cultivated on GYM and MB media.

Supplementary References 1-45
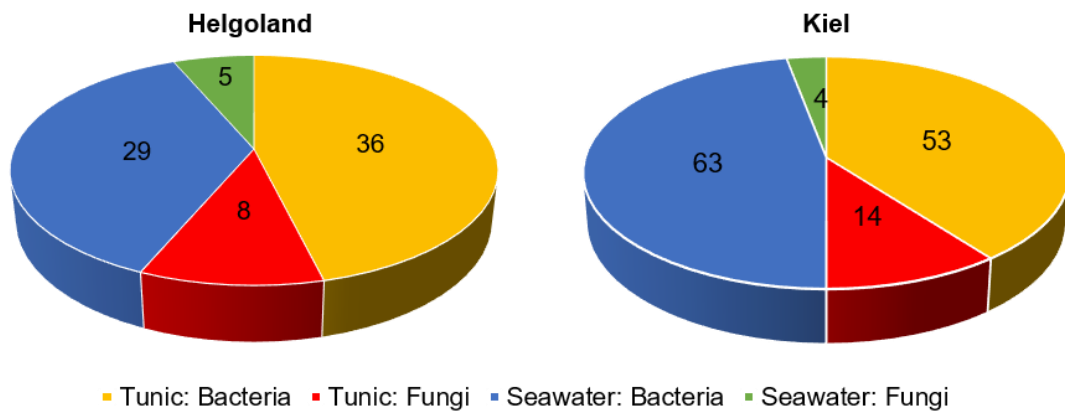
Figure S1. Number of microbial strains isolated from the tunic of *C. intestinalis* **and seawater reference.** Left: number of the isolates from Helgoland samples, right: number of the isolates from Kiel samples.
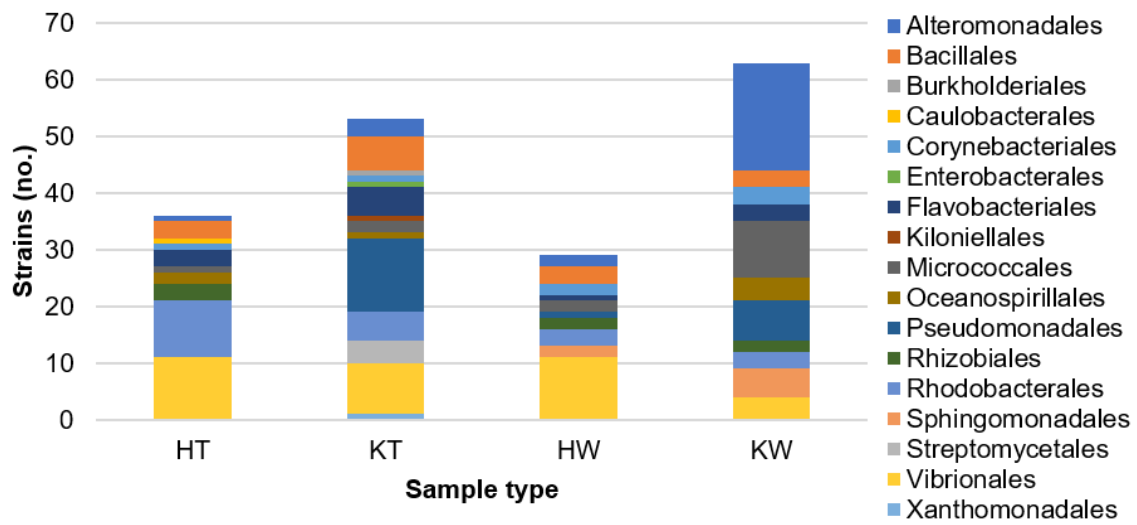
Figure S2. Distribution of bacterial orders across the sample types and their geographic locations. Sample types are abbreviated as: HT: Helgoland, tunic; KT: Kiel, tunic; HW: Helgoland, seawater; KW: Kiel, seawater.
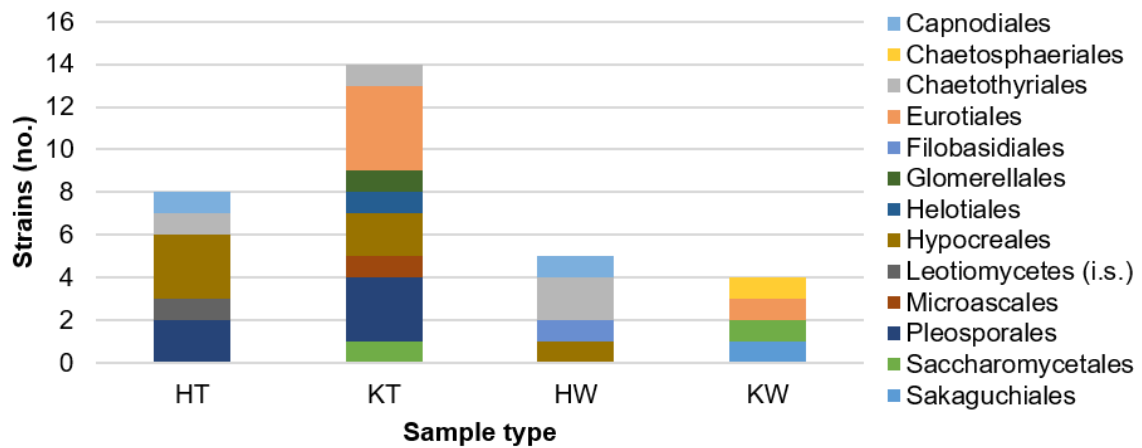
Figure S3. Distribution of fungal orders across the sample types and their geographic locations. Sample types are abbreviated as: HT: Helgoland, tunic; KT: Kiel, tunic; HW: Helgoland, seawater; KW: Kiel, seawater. i.s. = *incertae sedis* (taxonomic placement of order uncertain).
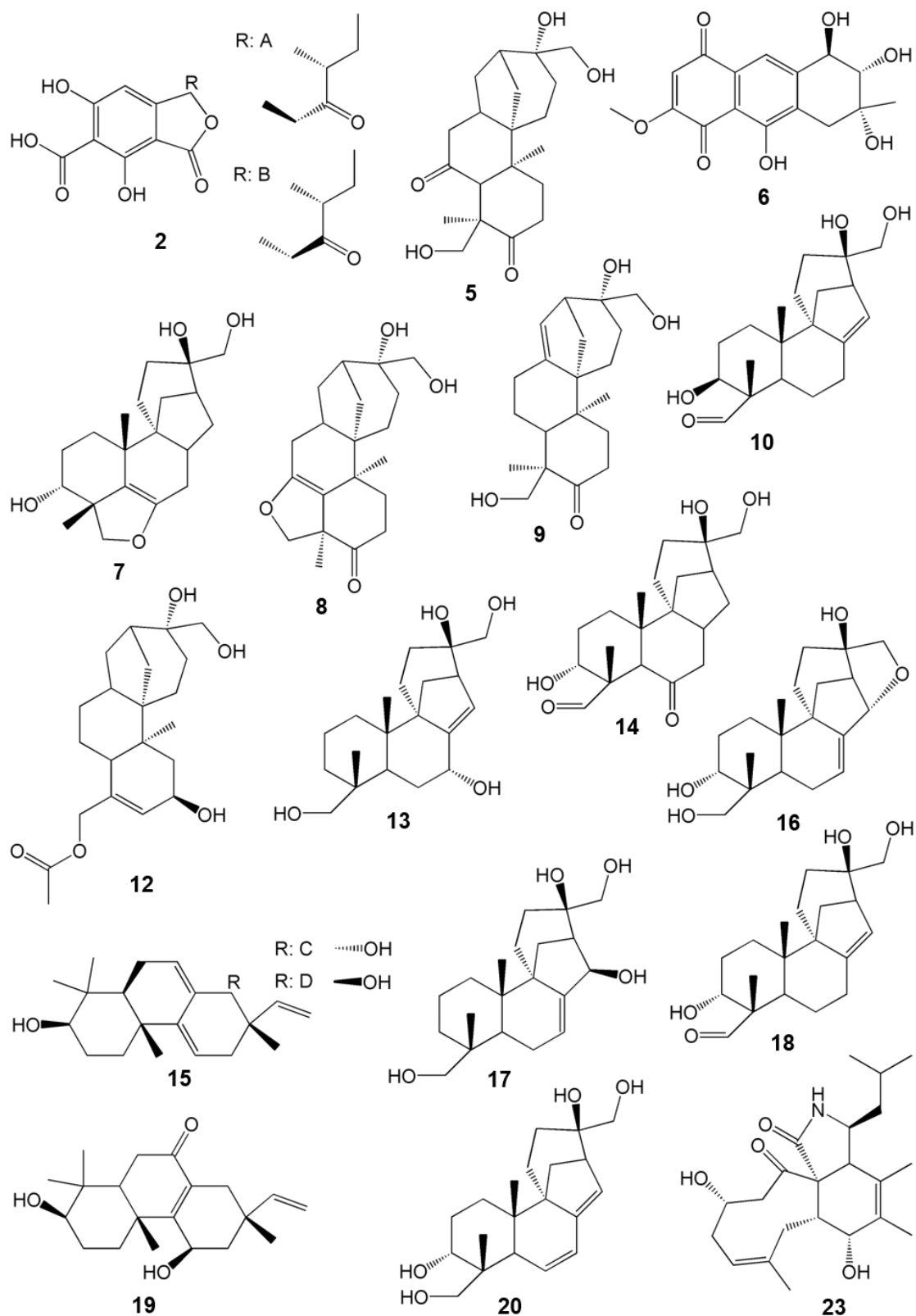
157

Figure S4. Chemical structures of putatively identified compounds in the crude extracts of five selected microbial strains isolated from the tunic of *C. intestinalis*. Structures are given with their respective peak number (see Tables S6-S10). The following compounds are shown in Figure 7 in the original publication: **123**, **126**, **129**, **141** and **145**.

158
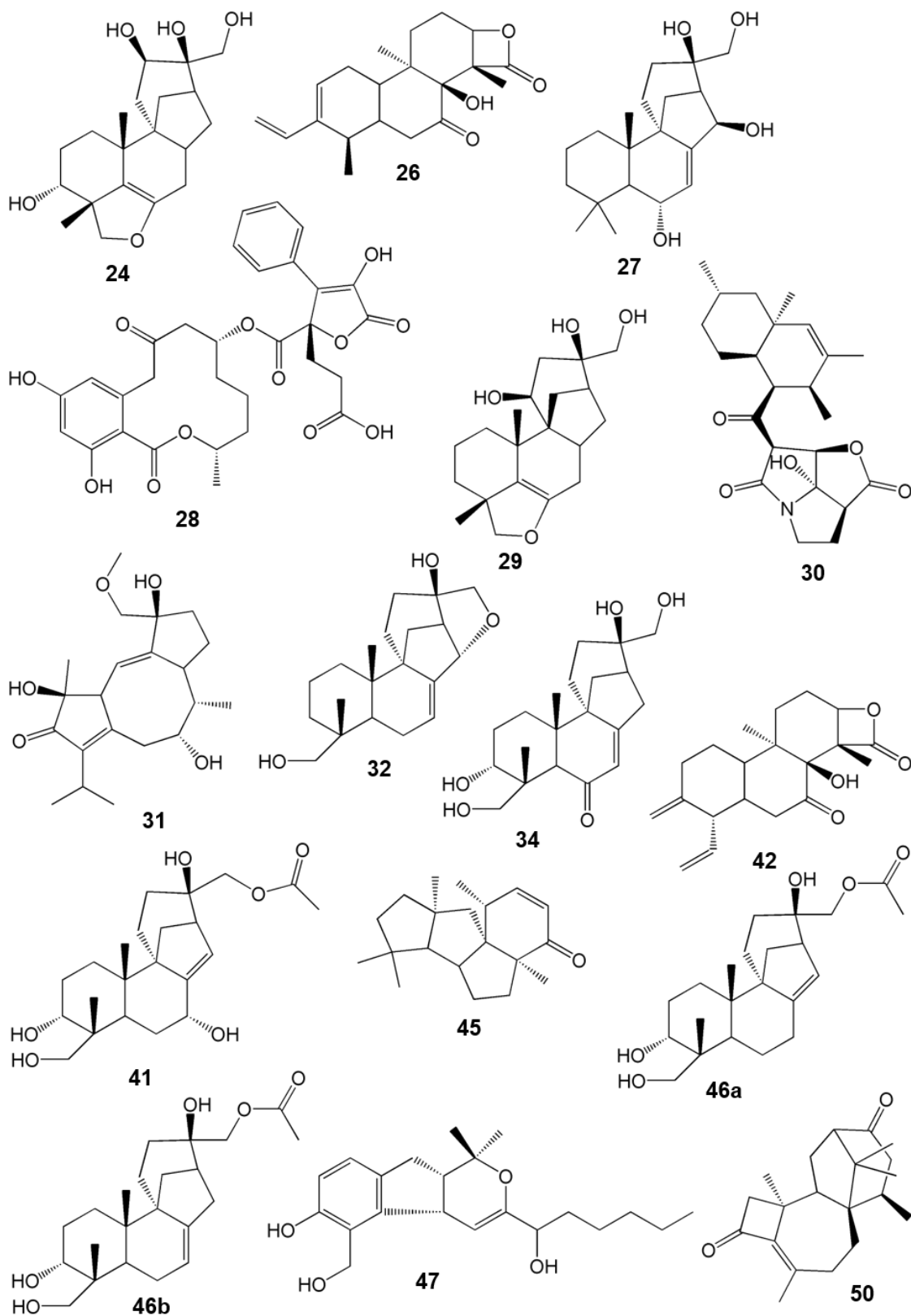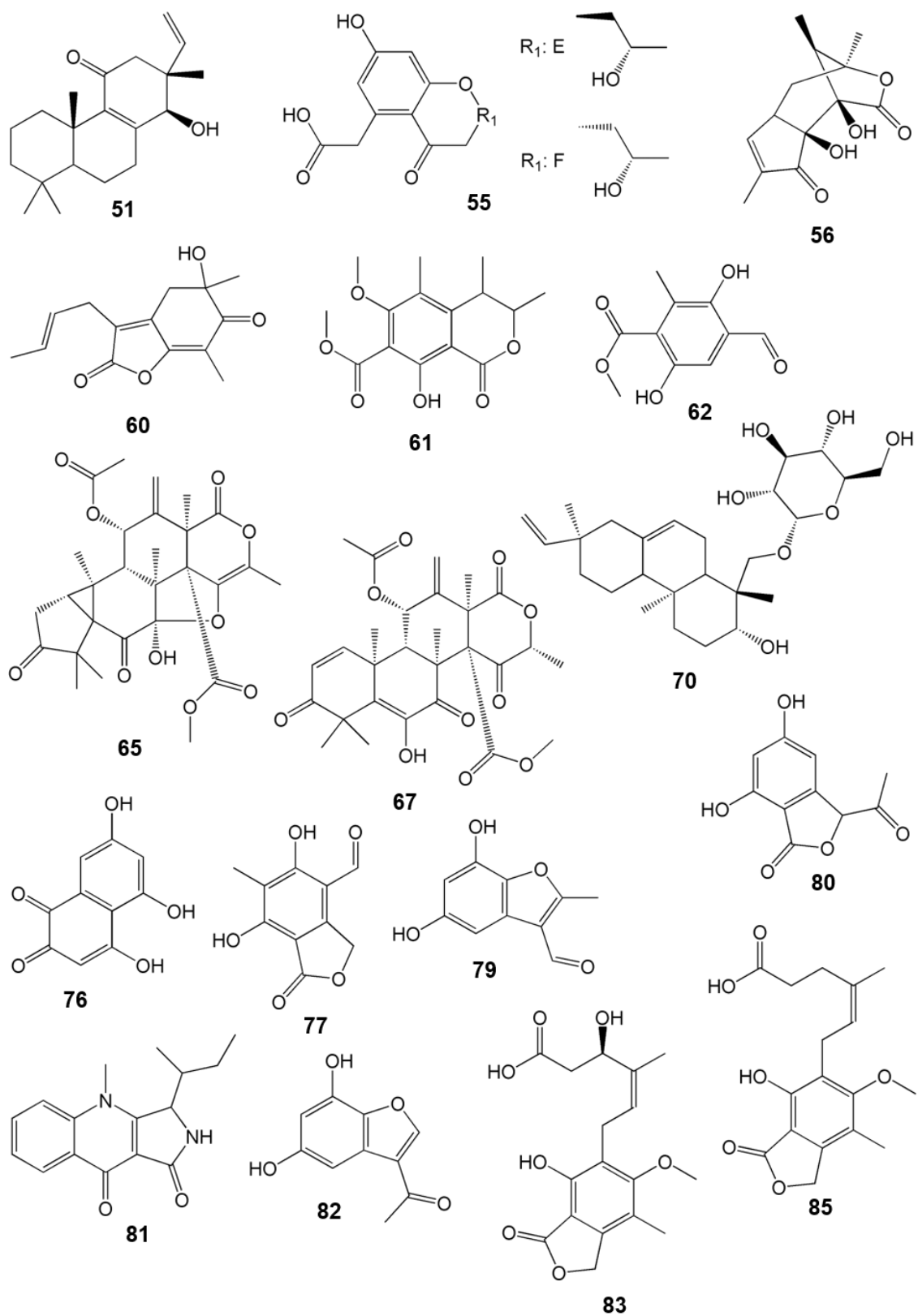
Figure S4. (continued)

Figure S4. (continued)
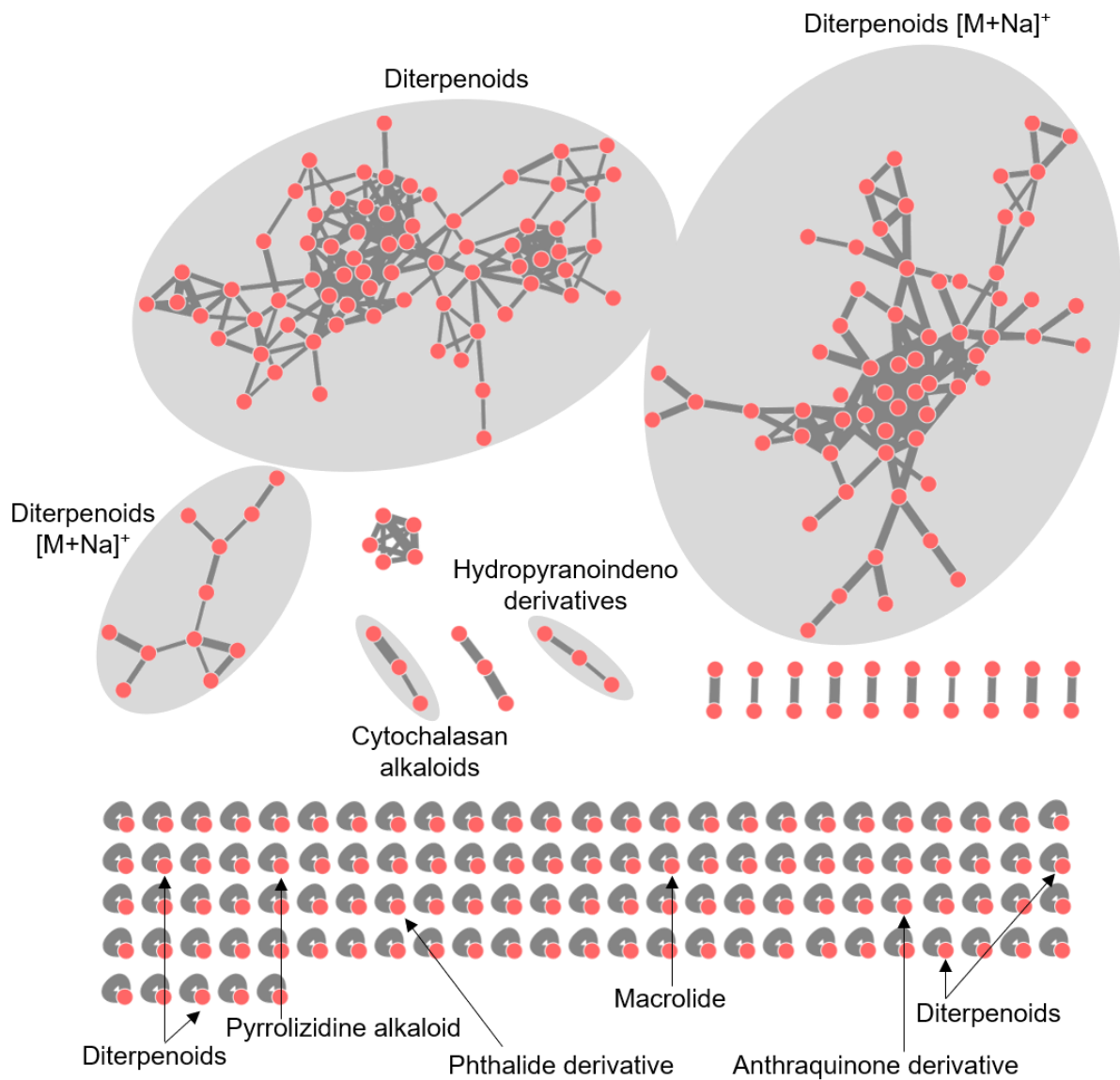
84

86

87

89

90

92

93

96

100

101

102

Figure S4. (continued)

103

104

105

106

107

109

110

124

127

128

146

Figure S4. (continued)

162

Figure S5. FBMN of the crude extract of *Pyrenochaeta* sp. strain CHT58 cultivated on PDA medium. Putatively annotated clusters are highlighted in grey (see Table S6 for putatively annotated compounds).
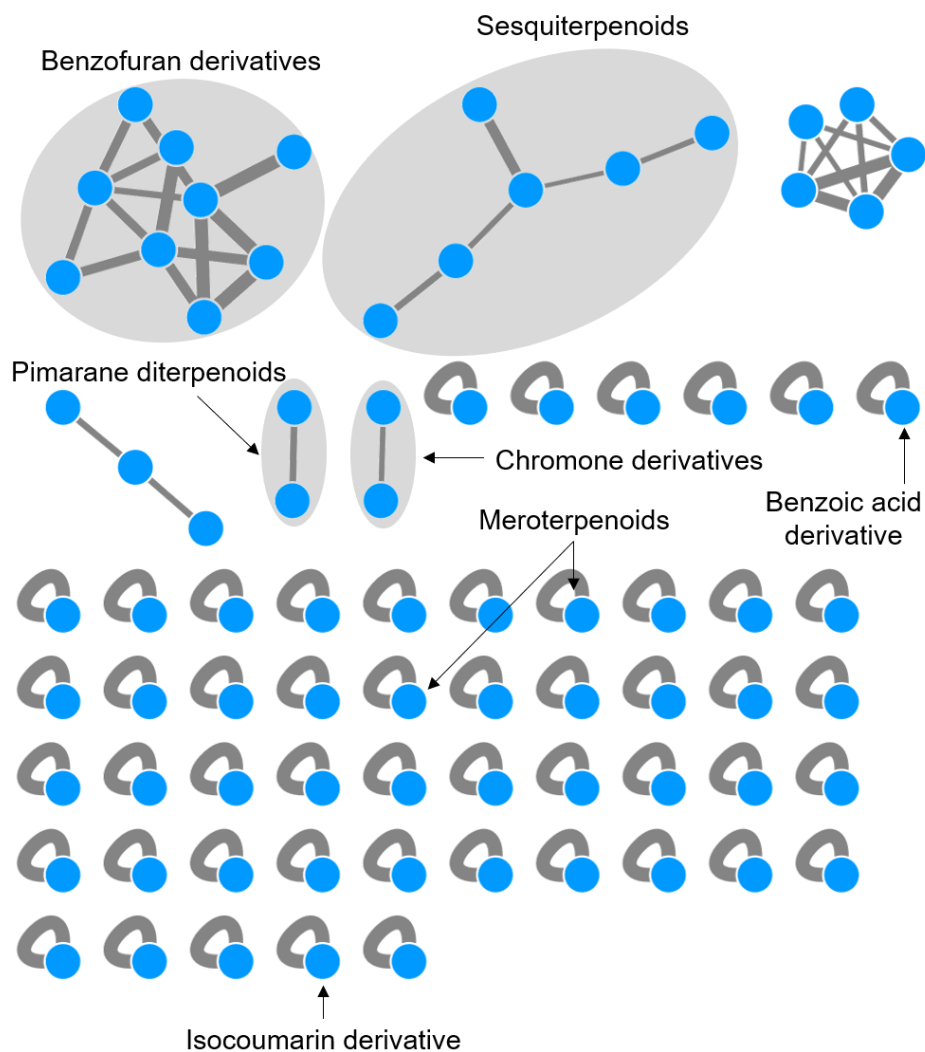
Figure S6. FBMN of the crude extract of *Pseudogymnoascus destructans* strain CHT56 cultivated on CAG medium. Putatively annotated clusters are highlighted in grey (see Table S7 for putatively annotated compounds).
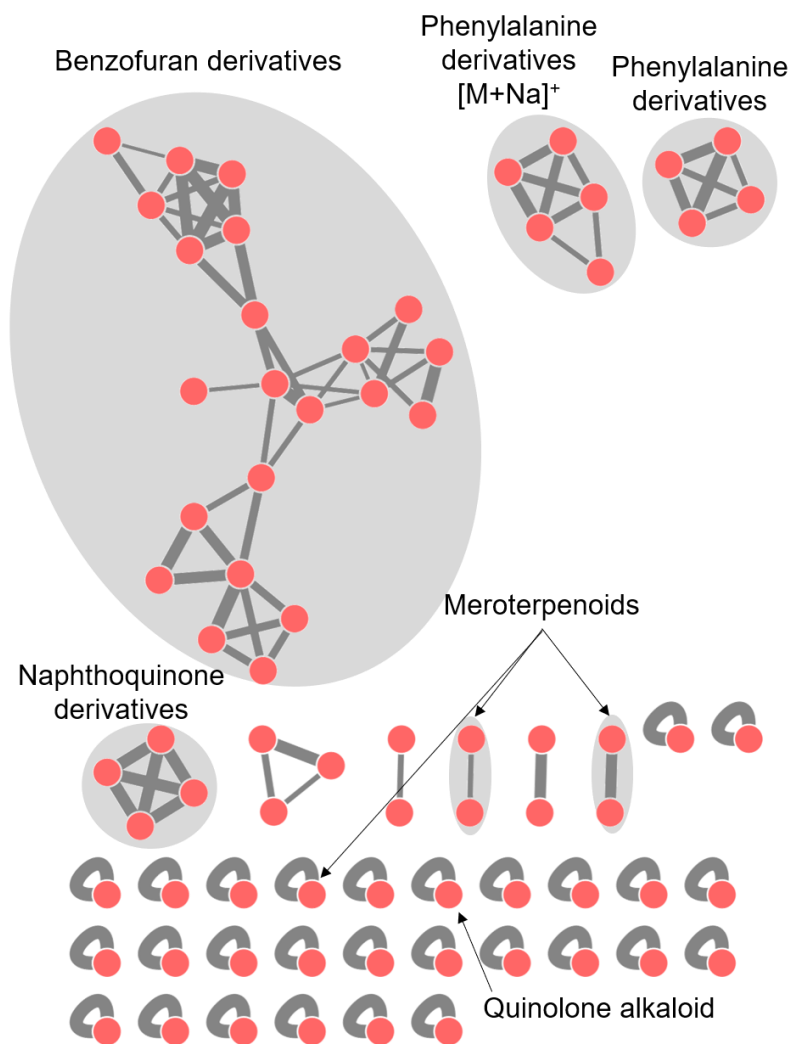
Figure S7. FBMN of the crude extract of *Penicillium* sp. strain CKT35 cultivated on PDA medium. Putatively annotated clusters are highlighted in grey (see Table S8 for putatively annotated compounds).
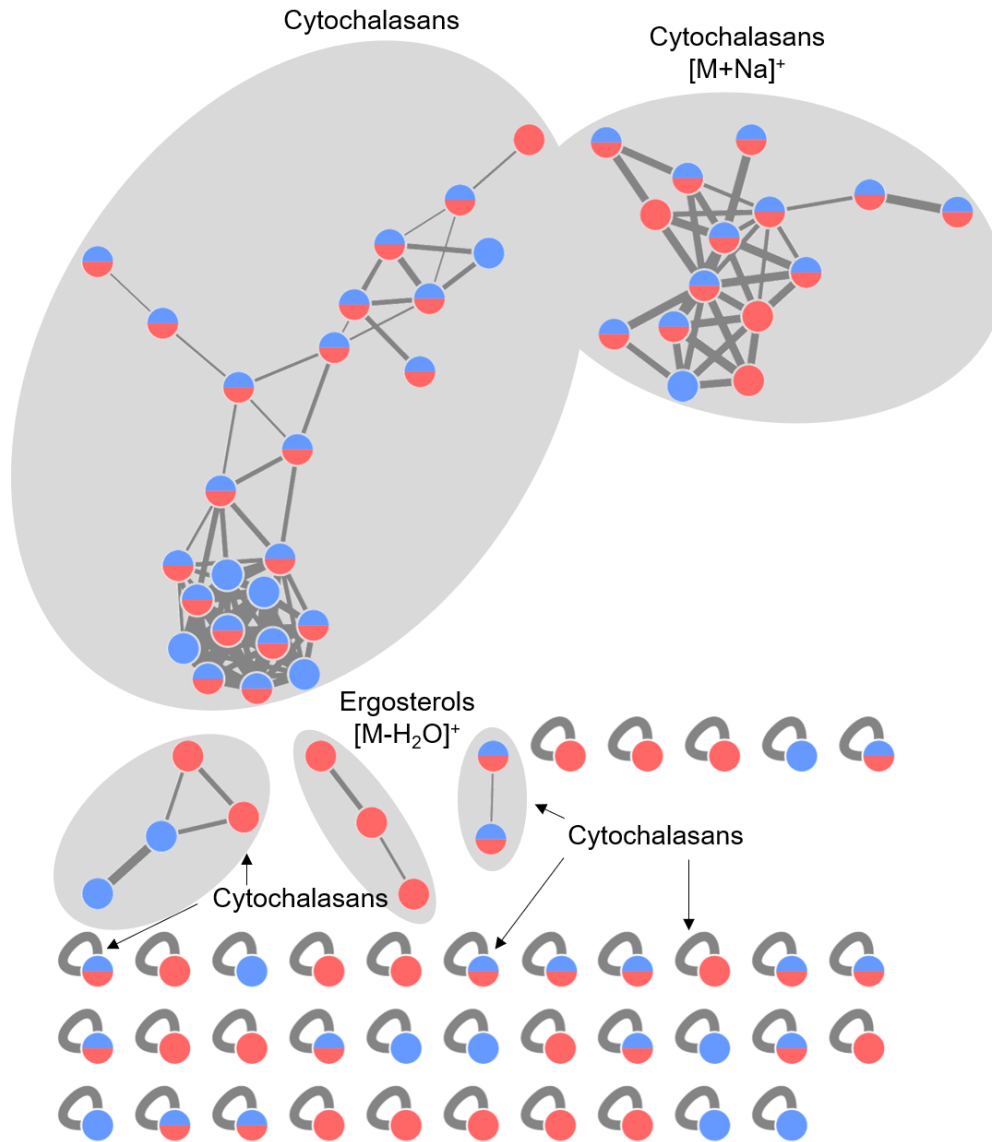
**Figure S8. FBMN of the crude extracts of *Boeremia exigua* strain CKT91 cultivated on CAG (blue nodes) and PDA (red nodes) media.** Putatively annotated clusters are highlighted in grey (see Table S9 for putatively annotated compounds).

Table S1. Parameters for MZmine-processing of UPLC-MS/MS data. The applied parameters are given for the global MN (four selected fungal strains) and for the selected seven crude extracts separately for each processing step. R_t = retention time in minutes.

Processing step	Parameter	Four selected fungal strains	CHT56-CAG (*Pseudogymnoascus destructans*)	CHT58-PDA (*Pyrenochaeta* sp.)	CKT35-PDA (*Penicillium* sp.)	CKT43-GYM, CKT43-MB (*Streptomyces* sp.)	CKT91-CAG, CKT91-PDA (*Boeremia exigua*)
Mass list	MS1 noise level	1.00E+04	1.00E+04	3.00E+04	3.00E+04	3.00E+04	3.00E+04
	MS2 noise level	5.00E+01					
	R_t	2-12	3-11	3-10	2-12	1-11	2-12
Chromatogram building	Min. peak height	3.00E+04	3.00E+04	6.00E+04	6.00E+04	6.00E+04	6.00E+04
	m/z tolerance	0.05 Da or 15 ppm					
Deconvolution	Min. peak height	3.00E+04	3.00E+04	6.00E+04	6.00E+04	6.00E+04	6.00E+04
	Peak duration	0.0-0.5 min					
	Baseline level	1.00E+04	1.00E+04	3.00E+04	3.00E+04	3.00E+04	3.00E+04
Isotope grouping	*m/z* tolerance	0.01 Da or 10 ppm					
	R_t tolerance	0.5 min					
	Maximum charge	3					
Alignment	Algorithm	Join aligner					
	m/z tolerance	0.01 Da or 10 ppm					
	R_t tolerance	0.5 min					
	Weight *m/z*:R_t	75/25					
	Detected peaks	817	78	284	74	187	86

Table S2. Identification of microbial strains isolated from *C. intestinalis* and seawater reference in Helgoland and Kiel Fjord. Strains were named after their respective sample type and sampling location (CHT = *C. intestinalis* from Helgoland, tunic; CKT = *C. intestinalis* from Kiel, tunic; HW = Helgoland, seawater; KW = Kiel, seawater) and are given with their isolation medium as well as Genbank accession number (acc. no.). Closest three related strains are given according to BLAST [1] and the resulting lowest possible taxonomic classification. RG = risk group (according to TRBA 460 and TRBA 466), uncult. = uncultured, * = identification to genus by Ribosomal Database Project (RDP; [2]).

Strain	Medium	Acc. no.	Amplicon	Closest related species (Blast)	Acc. no. closest related species	Lowest taxonomic classification (order)	RG
CHT2	CMN	MW012283	16S	*Vibrio* sp. *Vibrio* sp. *Vibrio splendidus*	MG309537.1 MG309367.1 LS483022.1	*Vibrio* sp. (Vibrionales)	2
CHT3	MA	MW012284	16S	*Leisingera aquimarina* *Leisingera aquimarina* Marine alpha proteobacterium BBAT3	KX218295.1 KX218294.1 AF365994.1	*Leisingera aquimarina* (Rhodobacterales)	1
CHT5	MA	MW012285	16S	*Shewanella pneumatophori* Uncult. bacterium 6-36A Uncult. bacterium 5-20A	MH169286.1 MG952522.1 MG952508.1	*Shewanella* sp. (Alteromonadales)	1
CHT6	MA	MW012286	16S	*Vibrio* sp. *Vibrio* sp. *Vibrio gigantis*	KF188534.1 KF188493.1 GU194170.1	*Vibrio gigantis* (Vibrionales)	1
CHT7	MA	MW012287	16S	*Ruegeria* sp. Uncult. bacterium Woods-Hole_a4093 *Ruegeria faecimaris*	KY513434.1 KF799356.1 NR_104546.1	*Ruegeria faecimaris* (Rhodobacterales)	1
CHT8	MA	MW012288	16S	*Ruegeria* sp. *Ruegeria* sp. *Ruegeria atlantica*	KY363633.1 KX833139.1 JN128252.1	*Ruegeria atlantica* (Rhodobacterales)	1
CHT9	CMN	MW012289	16S	*Vibrio hemicentroti* *Vibrio* sp. *Vibrio* sp.	LS482994.1 LC416556.1 LC416555.1	*Vibrio* sp. (Vibrionales)	1
CHT10	CMN	MW012290	16S	*Kangiella* sp. *Kangiella* sp. *Kangiella sediminilitoris*	MG889588.2 KP795388.1 CP012418.1	*Kangiella* sp. (Oceanospirillales)	1
CHT13	WSP30	MW012291	16S	*Aurantimonas coralicida* *Aurantimonas litoralis* *Aurantimonas manganoxydans*	MH725320.1 KR140222.1 LC066380.1	*Aurantimonas* sp. (Rhizobiales)	1

Strain	Medium	Acc. no.	Amplicon	Closest related species (Blast)	Acc. no. closest related species	Lowest taxonomic classification (order)	RG
CHT14	WSP30	MW012292	16S	*Photobacterium damselae* *Photobacterium damselae* *Photobacterium damselae*	MG386399.1 MH368432.1 CP018297.1	*Photobacterium damselae* (Vibrionales)	2
CHT15	TSB3+10	MW012293	16S	*Bacillus* sp. *Bacillus* sp. *Bacillus altitudinis*	MG970354.1 MG970353.1 MG970351.1	*Bacillus* sp. (Bacillales)	1
CHT16	MA	MW012294	16S	Uncult. *Vibrio* sp. Uncult. *Vibrio* sp. *Vibrio anguillarum*	MG554532.1 MG554529.1 CP022468.1	*Vibrio* sp. (Vibrionales)	2
CHT17	MA	MW012295	16S	Uncult. bacterium JS10_F09 *Vibrio chagasii* *Vibrio chagasii*	KT318724.1 LN832958.1 LN832949.1	*Vibrio* sp. (Vibrionales)	1
CHT18	TSB3+10	MW012296	16S	*Brevundimonas vesiculari* *Brevundimonas vesiculari* *Brevundimonas nasdae*	MG819328.1 MG685726.1 MG322225.1	*Brevundimonas* sp. (Caulobacterales)	2
CHT22a	CMN	MW012297	16S	*Marixanthomonas ophiurae* Uncult. bacterium denovo39636 Uncult. bacterium denovo37181	MK215855.1 KU635267.1 KU633651.1	*Marixanthomonas ophiurae* (Flavobacteriales)	1
CHT22b	MA	MW012298	16S	Marine bacterium I4017 Uncult. *Vibrio* sp. MUM_Aug34 *Vibrio pectenicida*	KJ469389.1 KC108888.1 NR_118241.1	*Vibrio* sp. (Vibrionales)	1
CHT23	MA	MW012299	16S	*Amphritea* sp. Bacterium GAA07 *Amphritea spongicola*	KP843673.1 KP684316.1 NR_135881.1	*Amphritea spongicola* (Oceanospirillales)	1
CHT25	TSB3+10	MW012300	16S	*Pseudorhodobacter aquimaris* *Rhodobacter* sp. *Rhodobacter* sp.	NR_108680.1 EU979476.1 EU979477.1	*Pseudorhodobacter aquimaris* (Rhodobacterales)	1
CHT27	WSP30	MW012301	16S	*Bacillus velezensis* *Bacillus velezensis* *Bacillus velezensis*	MG970354.1 MG970353.1 MG970351.1	*Bacillus* sp. (Bacillales)	1
CHT28	WSP30	MW012302	16S	*Leisingera aquimarina* *Leisingera aquimarina* Marine alpha proteobacterium BBAT3	KX218295.1 KX218294.1 AF365994.1	*Leisingera aquimarina* (Rhodobacterales)	1

Strain	Medium	Acc. no.	Amplicon	Closest related species (Blast)	Acc. no. closest related species	Lowest taxonomic classification (order)	RG
CHT29	TSB3+10	MW012303	16S	*Arenibacter* sp. *Arenibacter* sp. *Arenibacter troitsensis*	KY810503.1 HG529986.1 JQ898112.1	*Arenibacter* sp. (Flavobacteriales)	1
CHT30	WSP30	MW012304	16S	*Micrococcus yunnanensis* *Micrococcus aloeverae* *Micrococcus aloeverae*	MG649988.1 MG028596.1 MG561895.1	*Micrococcus* sp. (Micrococcales)	1
CHT32	PDA	MW017476	ITS	*Fusarium venenatum* *Fusarium venenatum* *Fusarium venenatum*	MH681155.1 MH681152.1 NR_156290.1	*Fusarium* sp. (Hypocreales)	2
CHT33	PDA	MW017477	ITS	*Fusarium venenatum* *Fusarium venenatum* *Fusarium venenatum*	MH681155.1 MH681152.1 NR_156290.1	*Fusarium* sp. (Hypocreales)	2
CHT34	WSP30	MW012305	16S	*Vibrio* sp. *Vibrio* sp. *Vibrio parahaemolyticus*	MK167378.1 MH997741.1 MK053885.1	*Vibrio* sp. (Vibrionales)	2
CHT35	WSP30	MW017478	ITS	*Cladosporium* sp. *Cladosporium cf. cladosporioides* *Cladosporium cf. cladosporioides*	MF510502.1 MH399546.1 MH399542.1	*Cladosporium* sp. (Capnodiales)	1
CHT37	WSP30	MW017479, MW012374, MW017496	ITS, 18S, 28S	*Emericellopsis maritima* *Acremonium breve* *Acremonium persicinum,* *Emericellopsis pallida* *Emericellopsis pallida* *Emericellopsis maritima,* *Acremonium* sp. *Emericellopsis alkalina* *Emericellopsis alkalina* *Emericellopsis alkalina*	MH871998.1 MH859569.1 MG813195.1, MH443384.1 NG_062927.1 NG_062926.1, KC987248.1 KC987247.1 KC987234.1	*Emericellopsis maritima* (Hypocreales)	1
CHT39	MA	MW012306	16S	*Vibrio* sp. *Vibrio anguillarum* *Vibrio anguillarum*	MG788349.1 CP023433.1 CP023293.1	*Vibrio* sp. (Vibrionales)	2
CHT40	WSP30	MW012375	18S	*Pseudochaetosphaeronema larense* *Pseudochaetosphaeronema martinelli* *Didymosphaeria variabile*	NG_061147.1 NG_062412.1 NG_064914.1	*Pseudochaetosphaeronema larense* (Pleosporales)	1

Strain	Medium	Acc. no.	Amplicon	Closest related species (Blast)	Acc. no. closest related species	Lowest taxonomic classification (order)	RG
CHT41	WSP30	MW012307	16S	*Mycolicibacterium monacense* *Mycolicibacterium doricum* *Mycolicibacterium aichiense*	AP022617.1 AP022605.1 AP022561.1	*Mycolicibacterium* sp. (Corynebacteriales)	1
CHT42	WSP30	MW012308	16S	*Ruegeria lacuscaerulensis* *Ruegeria* sp. *Ruegeria* sp.	MH283809.1 MG819700.1 MG996714.1	*Ruegeria* sp. (Rhodobacterales)	1
CHT43	WSP30	MW012309	16S	*Primorskyibacter* sp. *Thalassococcus* sp. *Thalassococcus lentus*	KY086433.2 MG889583.2 NR_109663.1	*Primorskyibacter* sp. (Rhodobacterales)	1
CHT46	MA	MW012310	16S	*Litoreibacter albidus* *Litoreibacter* sp. *Litoreibacter ascidiaceicola*	KX961718.1 KJ786461.1 NR_134068.1	*Litoreibacter* sp. (Rhodobacterales)	1
CHT47	MA	MW012311	16S	*Roseovarius arcticus* *Roseovarius arcticus* *Sulfitobacter* sp.	MK617616.1 NR_169499.1 FJ889642.1	*Roseovarius arcticus* (Rhodobacterales)	1
CHT48	MA	MW012312	16S	*Vibrio rumoiensis* *Vibrio* sp. *Vibrio* sp.	AP018685.1 MF537054.1 MF537053.1	*Vibrio* sp. (Vibrionales)	1
CHT49	CMN	MW012313	16S	*Ruegeria atlantica* *Ruegeria* sp. Bacterium CSR-55	HE584803.1 LC053425.1 KJ018058.1	*Ruegeria atlantica* (Rhodobacterales)	1
CHT50	TSB3+10	MW017480, MW012376, MW017497	ITS, 18S, 28S	Uncult. fungus C2_EH11 Melanized limestone ascomycete CR-2004 *Cladophialophora chaetospira,* *Cladophialophora boppii* *Cladophialophora boppii* *Fonsecaea nubica,* *Phialophora verrucosa* *Phialophora verrucosa* *Phialophora verrucosa*	JX042985.1 AY559331.1 EU035403.1, NG_062637.1 AJ232946.1 GU197483.1, AB550778.1 AB550777.1 AB550776.1	Herpotrichiellaceae unclassified (Chaetothyriales)	2
CHT51	CMN	MW012314	16S	*Vibrio alginolyticus* *Vibrio* sp. *Vibrio* sp.	CP017916.1 KX453258.1 KX453256.1	*Vibrio* sp. (Vibrionales)	2

Strain	Medium	Acc. no.	Amplicon	Closest related species (Blast)	Acc. no. closest related species	Lowest taxonomic classification (order)	RG
CHT52	TSB3+10	MW012315	16S	*Arenibacter* sp. *Arenibacter* sp. *Arenibacter latericius*	KY810503.1 HG529986.1 NR_024893.1	*Arenibacter* sp. (Flavobacteriales)	2
CHT53	WSP30	MW012316	16S	*Ochrobactrum* sp. *Ochrobactrum* sp. *Ochrobactrum pseudogrignonense*	KX822681.1 KJ777141.1 GU991856.1	*Ochrobactrum pseudogrignonense* (Rhizobiales)	1
CHT54	WSP30	MW012317	16S	*Bacillus amyloliquefaciens* *Bacillus amyloliquefaciens* *Bacillus* sp.	MH910761.1 MH910713.1 MG309364.1	*Bacillus* sp. (Bacillales)	1
CHT55	WSP30	MW012318	16S	*Ochrobactrum* sp. *Ochrobactrum* sp. *Ochrobactrum grignonense*	KX822681.1 KJ777141.1 FJ950543.1	*Ochrobactrum grignonense* (Rhizobiales)	1
CHT56	PDA	MW012377	18S	*Pseudogymnoascus destructans* *Geomyces destructans* *Geomyces destructans*	KF866376.1 GU350433.1 GQ489025.1	*Pseudogymnoascus destructans* (Leotiomycetes *incertae sedis*)	1
CHT58	PDA	MW017481	ITS	*Pyrenochaeta unguis-hominis* *Pyrenochaeta unguis-hominis* *Pyrenochaeta unguis-hominis*	KP794081.1 KP132548.1 KP132547.1	*Pyrenochaeta* sp. (Pleosporales)	1
CKT1	MA	MW012319	16S	*Pseudomonas* sp. *Pseudomonas* sp. *Pseudomonas anguilliseptica*	NR_042607.1 NR_042451.1 NR_044569.1	*Pseudomonas* sp. (Pseudomonadales)	1
CKT2*	MA	MW012320	16S	*Litoreibacter janthinus* *Thalassobacter* sp. *Roseovarius* sp.	NR_112983.1 FR821226.1 FJ425225.1	*Litoreibacter* sp. (Rhodobacterales)	1
CKT3*	MA	MW012321	16S	*Pelagicola litoralis* *Roseobacter* sp. Uncult. bacterium SF-Oct-32	NR_044158.1 EU195951.1 HQ225294.1	*Pelagicola* sp. (Rhodobacterales)	1
CKT4	MA	MW012322	16S	*Neptunomonas concharum* Uncult. bacterium Q31008 Uncult. bacterium Stn3_Sep_26	NR_118152.1 JX193435.1 KX014554.1	*Neptunomonas concharum* (Oceanospirillales)	1
CKT5	MA	MW012323	16S	*Pseudomonas peli* *Pseudomonas* sp. *Pseudomonas* sp.	MF077147.1 MG786374.1 MG758017.1	*Pseudomonas* sp. (Pseudomonadales)	1

Strain	Medium	Acc. no.	Amplicon	Closest related species (Blast)	Acc. no. closest related species	Lowest taxonomic classification (order)	RG
CKT6	MA	MW012324	16S	*Flaviramulus* sp. *Flaviramulus* sp. *Flaviramulus ichthyoenteri*	KC756867.1 JX431889.1 NR_118464.1	*Flaviramulus ichthyoenteri* (Flavobacteriales)	1
CKT7	MA	MW012325	16S	*Vibrio aestuarianus* *Vibrio aestuarianus* *Vibrio aestuarianus*	AJ845015.1 AJ845014.1 AJ845012.1	*Vibrio aestuarianus* (Vibrionales)	1
CKT8	CMB	MW012326	16S	*Pseudomonas peli* *Pseudomonas* sp. *Pseudomonas* sp.	MF077147.1 MG786374.1 MG758017.1	*Pseudomonas* sp. (Pseudomonadales)	1
CKT10	CMB	MW012327	16S	*Pseudomonas guineae* *Pseudomonas peli* *Pseudomonas cuatrocienegasensis*	MH392634.1 KJ643969.1 MF077147.1	*Pseudomonas* sp. (Pseudomonadales)	1
CKT11	CMB	MW012328	16S	*Vibrio aestuarianus* *Vibrio* sp. *Vibrio* sp.	NR_113780.1 HQ449463.1 HM012774.1	*Vibrio aestuarianus* (Vibrionales)	1
CKT12	CMB	MW012329	16S	*Pseudomonas peli* *Pseudomonas* sp. *Pseudomonas* sp.	MF077147.1 MG786374.1 MG758017.1	*Pseudomonas* sp. (Pseudomonadales)	1
CKT14	CMN	MW012330	16S	*Pseudomonas* sp. Uncult. bacterium HJ-38 *Pseudomonas peli*	MH392634.1 KJ643969.1 MF077147.1	*Pseudomonas* sp. (Pseudomonadales)	1
CKT15	TSB3+10	MW012331	16S	*Pseudomonas* sp. Uncult. bacterium HJ-38 *Pseudomonas peli*	MH392634.1 KJ643969.1 MF077147.1	*Pseudomonas* sp. (Pseudomonadales)	1
CKT16	TSB3+10	MW012332	16S	*Hydrogenophaga* sp. *Hydrogenophaga crassostreae* Uncult. *Hydrogenophaga* sp. TST2N32	KU198320.2 CP017476.1 KX119551.1	*Hydrogenophaga crassostreae* (Burkholderiales)	1
CKT17	TSB3+10	MW012333	16S	Bacterium BW3PhG33 *Lysobacter* sp. *Lysobacter spongiicola*	KC012871.1 GU217698.1 NR_041587.1	*Lysobacter spongiicola* (Xanthomonadales)	1
CKT18	TSB3+10	MW012334	16S	*Vibrio aestuarianus* *Vibrio* sp. *Vibrio* sp.	NR_113780.1 HQ449463.1 HM012774.1	*Vibrio aestuarianus* (Vibrionales)	1

Strain	Medium	Acc. no.	Amplicon	Closest related species (Blast)	Acc. no. closest related species	Lowest taxonomic classification (order)	RG
CKT19	TSB3+10	MW012335	16S	*Vibrio anguillarum* *Vibrio anguillarum* *Vibrio anguillarum*	MG264177.1 CP023310.1 CP023054.1	Vibrio *anguillarum* (Vibrionales)	2
CKT20	WSP30	MW012336	16S	*Bacillus pumilus* *Bacillus pumilus* *Bacillus pumilus*	MF077157.1 MH045994.1 MH045860.1	*Bacillus* sp. (Bacillales)	1
CKT21	CMN	MW012337	16S	*Pseudomonas guineae* *Pseudomonas peli* *Pseudomonas glareae*	NR_042607.1 NR_042451.1 NR_145562.1	*Pseudomonas* sp. (Pseudomonadales)	1
CKT22	CMN	MW012338	16S	Uncult. *Roseobacter* sp. C139300178 Uncult. *Roseobacter* sp. C139300006 *Phaeobacter arcticus*	JX528567.1 JX528395.1 NR_043888.1	*Phaeobacter arcticus* (Rhodobacterales)	1
CKT23	CMN	MW012339	16S	*Shewanella* sp. *Shewanella* sp. *Shewanella colwelliana*	MF045124.1 MF045122.1 KX756553.1	*Shewanella* sp. (Alteromonadales)	1
CKT24	CMN	MW012340	16S	*Arenibacter* sp. *Arenibacter* sp. *Arenibacter echinorum*	KU948154.1 KF273918.1 KF911336.1	*Arenibacter echinorum* (Flavobacteriales)	1
CKT25	TSB3+10	MW012341	16S	*Vibrio aestuarianus* *Vibrio* sp. *Vibrio* sp.	NR_113780.1 HQ449463.1 HM012774.1	*Vibrio aestuarianus* (Vibrionales)	1
CKT28	WSP30	MW017482	ITS	*Cyphellophora reptans* *Cyphellophora reptans* *Phialophora reptans*	NR_121346.1 EU514699.1 AB190380.1	*Cyphellophora reptans* (Chaetothyriales)	1
CKT29	MA	MW012342	16S	*Marinobacter* sp. Uncult. bacterium AB-4 *Marinobacter litoralis*	KY770365.1 KX651417.1 KY926903.1	*Marinobacter litoralis* (Alteromonadales)	1
CKT30*	MA	MW012343	16S	Uncult. Bacteroidetes bacterium D *Salegentibacter* sp. *Salinimicrobium marinum*	KC169760.1 AY576719.1 GQ866113.1	*Salinimicrobium* sp. (Flavobacteriales)	1
CKT32	TSB3+10	MW012344	16S	*Pseudomonas* sp. *Pseudomonas* sp. *Pseudomonas peli*	MH815093.1 MH814721.1 MG581693.1	*Pseudomonas* sp. (Pseudomonadales)	1

Strain	Medium	Acc. no.	Amplicon	Closest related species (Blast)	Acc. no. closest related species	Lowest taxonomic classification (order)	RG
CKT33	CMN	MW012345	16S	*Vibrio splendidus* *Vibrio* sp. *Vibrio anguillarum*	MH010050.1 MG788349.1 CP023433.1	*Vibrio* sp. (Vibrionales)	2
CKT34	CMN	MW012346	16S	*Arthrobacter* sp. *Arthrobacter* sp. *Arthrobacter citreus*	MH018914.1 JN006271.1 GQ149484.1	*Arthrobacter* sp. (Micrococcales)	1
CKT35	WSP30	MW017483	ITS	*Penicillium bialowiezense* *Penicillium brevicompactum* *Penicillium biourgeianum*	MH854996.1 MH481701.1 KX067821.1	*Penicillium* sp. (Eurotiales)	1
CKT36	WSP30	MW012347	16S	*Bacillus pumilus* *Bacillus pumilus* *Bacillus pumilus*	MF077157.1 MH045994.1 MH045860.1	*Bacillus* sp. (Bacillales)	1
CKT37	TSB3+10	MW012348	16S	*Vibrio aestuarianus* *Vibrio aestuarianus* *Vibrio aestuarianus*	AJ845015.1 AJ845014.1 AJ845012.1	*Vibrio aestuarianus* (Vibrionales)	1
CKT38	TSB3+10	MW012349	16S	*Bacillus mycoides* *Bacillus* sp. *Bacillus* sp.	MH169305.1 MF948894.1 MH096031.1	*Bacillus* sp. (Bacillales)	1
CKT39	CMN	MW012350	16S	*Streptomyces* sp. *Streptomyces* sp. *Streptomyces badius*	MK292047.1 MK271721.1 MK156399.1	*Streptomyces* sp. (Streptomycetales)	1
CKT41	WSP30	MW012351	16S	*Bacillus amyloliquefaciens* *Bacillus halotolerans* *Bacillus amyloliquefaciens*	MH236415.1 MH236414.1 MH236413.1	*Bacillus* sp. (Bacillales)	1
CKT43	WSP30	MW012352	16S	*Streptomyces sampsonii* *Streptomyces* sp. *Streptomyces* sp.	MK878388.1 MK129408.1 MK129407.1	*Streptomyces* sp. (Streptomycetales)	1
CKT48	WSP30	MW012353	16S	*Bacillus pumilus* *Bacillus pumilus* *Bacillus pumilus*	MF077157.1 MH045994.1 MH045860.1	*Bacillus* sp. (Bacillales)	1
CKT49	WSP30	MW017484	ITS	*Penicillium brasilianum* *Penicillium brasilianum* *Penicillium brasilianum*	KY469061.1 KY469042.1 LT558939.1	*Penicillium brasilianum* (Eurotiales)	1
CKT50	WSP30	MW012354	16S	Uncult. bacterium f6h4 Uncult. bacterium f4s2 *Yokenella regensburgei*	DQ068814.1 DQ068792.1 KJ397957.1	Enterobacteriaceae unclassified (Enterobacterales)	2

Strain	Medium	Acc. no.	Amplicon	Closest related species (Blast)	Acc. no. closest related species	Lowest taxonomic classification (order)	RG
CKT51-I	WSP30	MW012355	16S	*Shewanella putrefaciens* *Shewanella hafniensis* *Shewanella putrefaciens*	CP028435.1 MF612155.1 KX271690.1	*Shewanella* sp. (Alteromonadales)	2
CKT51-II	WSP30	MW012356	16S	*Bacillus* sp. *Bacillus* sp. *Bacillus megaterium*	MF418041.1 MF418038.1 MH179091.1	*Bacillus* sp. (Bacillales)	1
CKT52	MA	MW012357	16S	*Bizionia* sp. *Bizionia* sp. *Bizionia fulviae*	KX066849.1 HF912806.2 NR_137258.1	*Bizionia fulviae* (Flavobacteriales)	1
CKT54	TSB3+10	MW017485	ITS	*Fusarium* sp. *Fusarium oxysporum* *Fusarium oxysporum*	KU556574.1 HQ603748.1 KY949601.1	*Fusarium* sp. (Hypocreales)	2
CKT55	WSP30	MW017486	ITS	*Boeremia exigua* *Boeremia exigua* *Boeremia exigua*	KY949620.1 KY419536.1 MF925487.1	*Boeremia exigua* (Pleosporales)	1
CKT56	MA	MW012358	16S	*Ruegeria* sp. Uncult. bacterium APY15 *Ruegeria atlantica*	MH023307.1 JQ347396.1 HE584803.1	*Ruegeria atlantica* (Rhodobacterales)	1
CKT57	MA	MW012359	16S	*Pseudomonas* sp. Uncult. bacterium HJ-38 *Pseudomonas peli*	MH392634.1 KJ643969.1 MF077147.1	*Pseudomonas* sp. (Pseudomonadales)	1
CKT58	CMN	MW017487	ITS	*Penicillium bialowiezense* Fungal sp. PdlM07-12 *Penicillium biourgeianum*	MH854996.1 MG923832.1 KX067821.1	*Penicillium* sp. (Eurotiales)	1
CKT59	CMN	MW012360	16S	*Pseudomonas* sp. Uncult. bacterium HJ-38 *Pseudomonas peli*	MH392634.1 KJ643969.1 MF077147.1	*Pseudomonas* sp. (Pseudomonadales)	1
CKT60	CMN	MW012361	16S	*Kiloniella laminariae* *Kiloniella* sp. Uncult. alpha proteobacterium MERTZ_0CM_263	NR_042646.1 KM101108.2 AF425762.1	*Kiloniella laminariae* (Kiloniellales)	1
CKT61	CMB	MW012362	16S	*Pseudomonas guineae* *Pseudomonas peli* *Pseudomonas glareae*	NR_042607.1 NR_042451.1 NR_145562.1	*Pseudomonas* sp. (Pseudomonadales)	1

Strain	Medium	Acc. no.	Amplicon	Closest related species (Blast)	Acc. no. closest related species	Lowest taxonomic classification (order)	RG
CKT62	CMB	MW012363	16S	*Vibrio aestuarianus* *Vibrio* sp. *Vibrio* sp.	NR_113780.1 HQ449463.1 HM012774.1	*Vibrio aestuarianus* (Vibrionales)	1
CKT65	MA	MW012364	16S	*Salegentibacter* sp. Uncult. bacterium BF2009_Sep_21m_E5 *Salegentibacter salarius*	FR772274.1 JX864700.1 NR_044244.1	*Salegentibacter* sp. (Flavobacteriales)	1
CKT67	TSB3+10	MW012365	16S	*Serinicoccus* sp. *Serinicoccus* sp. *Serinicoccus chungangensis*	CP014989.1 DQ985074.1 NR_117788.1	*Serinicoccus* sp. (Micrococcales)	1
CKT68	WSP30	MW012366	16S	*Paracoccus aquimaris* *Paracoccus sp.* *Paracoccus aquimaris*	NR_148324.1 LC094992.1 KP716798.1	*Paracoccus* sp. (Rhodobacterales)	2
CKT74	CMB	MW012367	16S	*Pseudomonas* sp. Uncult. bacterium HJ-38 *Pseudomonas peli*	MH392634.1 KJ643969.1 MF077147.1	*Pseudomonas* sp. (Pseudomonadales)	1
CKT75	CMN	MW012368	16S	*Mycobacterium* sp. *Mycobacterium* sp. *Mycobacterium lutetiense*	MG835594.1 MG835593.1 NR_151953.1	*Mycobacterium* sp. (Corynebacteriales)	2
CKT76	TSB3+10	MW012369	16S	*Vibrio aestuarianus* *Vibrio* sp. *Vibrio* sp.	NR_113780.1 HQ449463.1 HM012774.1	*Vibrio* sp. (Vibrionales)	1
CKT77	CMN	MW012370	16S	*Streptomyces* sp. *Streptomyces* sp. *Streptomyces badius*	MK292047.1 MK271721.1 MK156399.1	*Streptomyces* sp. (Streptomycetales)	1
CKT78	CMB	MW017488	ITS	*Penicillium crustosum* *Penicillium crustosum* *Penicillium crustosum*	MG975627.1 MG596635.1 KT876714.1	*Penicillium crustosum* (Eurotiales)	1
CKT79	CMB	MW012378	18S	*Pseudallescheria ellipsoidea* *Pseudallescheria ellipsoidea* *Pseudallescheria boydii*	NG_063099.1 U43911.1 U43915.1	*Pseudallescheria* sp. (Microascales)	2
CKT80	MA	MW012371	16S	*Streptomyces* sp. *Streptomyces* sp. *Streptomyces badius*	MK292047.1 MK271721.1 MK156399.1	*Streptomyces* sp. (Streptomycetales)	1

Strain	Medium	Acc. no.	Amplicon	Closest related species (Blast)	Acc. no. closest related species	Lowest taxonomic classification (order)	RG
CKT81	CMB	MW017489	ITS	*Pithomyces chartarum* Fungal sp. strain A210A *Pithomyces chartarum*	MH860227.1 KU837820.1 KX664331.1	*Pithomyces chartarum* (Pleosporales)	1
CKT84	CMN	MW017490	ITS	*Fusarium graminearum* *Fusarium graminearum* *Fusarium graminearum*	MK212898.1 MK212894.1 MK212893.1	*Fusarium* sp. (Hypocreales)	1
CKT85	PDA	MW017491	ITS	*Cadophora luteo-olivacea* *Cadophora luteo-olivacea* *Cadophora luteo-olivacea*	MH859460.1 MG944391.1 MG944390.1	*Cadophora luteo-olivacea* (Helotiales)	1
CKT86	TSB3+10	MW017492	ITS	*Plectosphaerella cucumerina* *Plectosphaerella cucumerina* *Plectosphaerella cucumerina*	KT596812.1 KU204705.1 MH791266.1	*Plectosphaerella cucumerina* (Glomerellales)	1
CKT90	PDA	MW017493	ITS	*Pichia* sp. Uncult. ascomycete BF-OTU252 *Wickerhamomyces onychis*	EU877913.1 AM901934.1 KT207216.1	*Wickerhamomyces* sp. (Saccharomycetales)	1
CKT91	WSP30	MW017494	ITS	*Phoma* sp. *Phoma* sp. *Boeremia exigua*	MH550515.1 MH550514.1 MH859059.1	*Boeremia exigua* (Pleosporales)	1
HW2	MA	MW013337	16S	*Vibrio owensii* *Vibrio owensii* *Vibrio owensii*	LC369696.1 MG896198.1 MG896189.1	*Vibrio* sp. (Vibrionales)	1
HW3	MA	MW013338	16S	*Vibrio splendidus* *Vibrio* sp. *Vibrio anguillarum*	MH010050.1 MG788349.1 CP023433.1	*Vibrio* sp. (Vibrionales)	2
HW4	MA	MW013339	16S	*Vibrio comitans* *Vibrio comitans* *Vibrio comitans*	KR347260.1 AB681692.1 DQ922917.1	*Vibrio comitans* (Vibrionales)	1
HW5	MA	MW013340	16S	*Pseudoalteromonas carrageenovora* *Pseudoalteromonas carrageenovora* *Pseudoalteromonas arctica*	LT965929.1 LT965928.1 MG681184.1	*Pseudoalteromonas* sp. (Alteromonadales)	1
HW6	MA	MW013341	16S	*Vibrio alginolyticus* *Vibrio* sp. *Vibrio* sp.	CP017916.1 KX453212.1 KX453210.1	*Vibrio* sp. (Vibrionales)	2

Strain	Medium	Acc. no.	Amplicon	Closest related species (Blast)	Acc. no. closest related species	Lowest taxonomic classification (order)	RG
HW8	MA	MW013342	16S	*Vibrio* sp. *Vibrio breoganii* *Vibrio* sp.	MH807583.1 CP016177.1 KX197382.1	*Vibrio* sp. (Vibrionales)	1
HW9	MA	MW013343	16S	Marine bacterium I4017 *Vibrio pectenicida* *Vibrio pectenicida*	KJ469389.1 NR_118241.1 NR_029344.1	*Vibrio pectenicida* (Vibrionales)	1
HW10	TSB3+10	MW013344	16S	*Kocuria* sp. *Kocuria palustris* *Kocuria palustris*	KY296995.1 MF319775.1 KY933468.1	*Kocuria palustris* (Micrococcales)	1
HW11	TSB3+10	MW013345	16S	*Knoellia* sp. *Knoellia subterranea* *Knoellia* sp.	DQ812538.1 NR_028932.1 KP191088.1	*Knoellia subterranea* (Micrococcales)	1
HW12	TSB3+10	MW013346	16S	*Paracoccus* sp. Uncult. bacterium isolate RA2-73 *Paracoccus alkenifer*	KU163256.1 KT834758.1 LT221244.1	*Paracoccus alkenifer* (Rhodobacterales)	1
HW13	TSB3+10	MW013347	16S	Uncult. *Vibrio* Uncult. *Vibrio* *Vibrio owensii*	MG554543.1 MG554505.1 CP025797.1	*Vibrio* sp. (Vibrionales)	1
HW14	CMN	MW013348	16S	*Vibrio splendidus* *Cellulophaga* sp. *Cellulophaga* sp.	CP031055.1 JX435328.1 JX435323.1	*Vibrio* sp. (Vibrionales)	2
HW15	CMN	MW013349	16S	*Chryseomicrobium imtechense* *Chryseomicrobium palamuruense* *Chryseomicrobium* sp.	MH643668.1 MG461542.1 KX889925.1	*Chryseomicrobium* sp. (Bacillales)	1
HW16	CMN	MW013350	16S	Uncult. bacterium Shelves_A_113 Uncult. bacterium Shelves_A_62 *Corynebacterium casei*	MF092438.1 MF092420.1 KP790025.1	*Corynebacterium casei* (Corynebacteriales)	1
HW18	CMN	MW013351	16S	*Cellulophaga fucicola* *Cellulophaga fucicola* *Cellulophaga* sp.	KX453201.1 KX453191.1 LN881203.1	*Cellulophaga fucicola* (Flavobacteriales)	1
HW23	WSP30	MW013352	16S	*Idiomarina* sp. *Idiomarina* sp. *Idiomarina loihiensis*	EF409425.1 EF409424.1 KM407721.1	*Idiomarina loihiensis* (Alteromonadales)	1

Strain	Medium	Acc. no.	Amplicon	Closest related species (Blast)	Acc. no. closest related species	Lowest taxonomic classification (order)	RG
HW25	TSB3+10	MW013353	16S	*Staphylococcus pasteuri* *Staphylococcus pasteuri* *Staphylococcus pasteuri*	MG815139.1 MG757632.1 MG680735.1	*Staphylococcus pasteuri* (Bacillales)	2
HW27	MA	MW013354	16S	*Vibrio ostreicida* *Vibrio ostreicida* *Vibrio ostreicida*	NR_133887.1 EU652412.2 KX130913.1	*Vibrio* sp. (Vibrionales)	1
HW28	WSP30	MW013355	16S	*Epibacterium mobile* *Epibacterium mobile* Bacterium strain InAD-034	MK493584.1 MK493561.1 MF401241.1	Rhodobacteraceae unclassified (Rhodobacterales)	1
HW30	TSB3+10	MW012380	ITS	*Cryptococcus magnus* *Cryptococcus* sp. *Cryptococcus magnus*	JQ425367.1 HQ426594.1 EU871517.1	*Cryptococcus magnus* (Filobasidiales)	1
HW32	TSB3+10	MW013356	16S	*Sphingomonas* sp. Uncult. bacterium YD200-16 *Sphingomonas aquatilis*	KJ606800.1 JX441481.1 NR_024997.1	*Sphingomonas* sp. (Sphingomonadales)	1
HW33	TSB3+10	MW013357	16S	*Staphylococcus capitis* *Staphylococcus capitis* Uncult. bacterium 16s_M.Zamir	MF033474.1 MG557816.1 MG461572.1	*Staphylococcus* sp. (Bacillales)	1
HW35	CMN	MW013358	16S	*Palleronia abyssalis* *Palleronia abyssalis* *Palleronia abyssalis*	KJ638255.1 MG383388.1 KJ638254.1	*Palleronia abyssalis* (Rhodobacterales)	1
HW36	CMN	MW013359	16S	*Erythrobacter* sp. *Erythrobacter citreus* *Erythrobacter citreus*	KT185356.1 AB012062.1 LN846110.1	*Erythrobacter* sp. (Sphingomonadales)	1
HW37	TSB3+10	MW013360	16S	*Vibrio aestuarianus* *Vibrio* sp. *Vibrio* sp.	NR_113780.1 HQ449463.1 HM012774.1	*Vibrio aestuarianus* (Vibrionales)	1
HW38	PDA	MW012381, MW014884	ITS, 18S	Uncult. fungus C2_EH11 Melanized limestone ascomycete CR-2004 *Cladophialophora chaetospira,* *Cladophialophora boppii* *Exophiala lecanii-corni* *Fonsecaea nubica*	JX042985.1 HM239803.1 EU035403.1, NG_062637.1 CP034379.1 GU197483.1	Herpotrichiellaceae unclassified (Chaetothyriales)	2

Strain	Medium	Acc. no.	Amplicon	Closest related species (Blast)	Acc. no. closest related species	Lowest taxonomic classification (order)	RG
HW40	WSP30	MW012382, MW014885, MW017498	ITS, 18S, 28S	*Capnodiales* sp. *Capnodiales* sp. *Extremus antarcticus*, *Capnodiales* sp. CCFEE 5271 *Capnodiales* sp. CCFEE 5389 *Extremus antarcticus* CCFEE 451, *Saxophila tyrrhenica* *Saxophila tyrrhenica* *Capnodiales* sp. CCFEE 5551	KC315866.1 GU250338.1 NG_064939.1, KC315866.1 GU250338.1 NG_064939.1, NG_059571.1 KR781051.1 KC315879.1	Capnodiales unclassified	1
HW41	TSB3+10	MW013361	16S	*Methylobacterium* sp. *Methylobacterium* sp. *Methylobacterium oryzae*	FN868948.1 MG807376.1 MF692767.1	*Methylobacterium* sp. (Rhizobiales)	1
HW42	TSB3+10	MW013362	16S	*Vibrio owensii* *Vibrio campbellii* *Vibrio* sp.	MG896198.1 CP026321.1 KY655411.1	*Vibrio* sp. (Vibrionales)	1
HW43	TSB3+10	MW013363	16S	*Rhodococcus cerastii* Unidentified microorganism edSeq16_20-D3 Unidentified microorganism edSeq14_4-D1	MG645219.1 MG271100.1 MG270621.1	*Rhodococcus* sp. (Corynebacteriales)	1
HW44	PDA	MW012383, MW014886, MW017499	ITS, 18S, 28S	Uncult. fungus C2_EH11 Melanized limestone ascomycete CR-2004 *Cladophialophora chaetospira*, *Cladophialophora boppii* *Cladophialophora boppii* *Fonsecaea nubica*, *Phialophora verrucosa* *Phialophora verrucosa* *Phialophora verrucosa*	JX042985.1 AY559331.1 EU035403.1, NG_062637.1 AJ232946.1 GU197483.1, AB550778.1 AB550777.1 AB550776.1	Herpotrichiellaceae unclassified (Chaetothyriales)	2
HW45	PDA	MW013364	16S	*Methylobacterium* sp. *Methylobacterium* sp. *Methylobacterium oryzae*	KP128697.1 KF441619.1 MF692767.1	*Methylobacterium* sp. (Rhizobiales)	1

181

Strain	Medium	Acc. no.	Amplicon	Closest related species (Blast)	Acc. no. closest related species	Lowest taxonomic classification (order)	RG
HW47	CMN	MW012384	ITS	*Purpureocillium lilacinum* *Purpureocillium lilacinum* *Purpureocillium lilacinum*	MH865347.1 MH865301.1 MH865154.1	*Purpureocillium lilacinum* (Hypocreales)	2
HW48	CMN	MW013365	16S	Uncult. bacterium A1_27 Uncult. bacterium A1_27 *Psychrobacter glacincola*	HG795730.1 HG795728.1 KU579265.1	*Psychrobacter* sp. (Pseudomonadales)	1
KW1	MA	MW013366	16S	*Psychrobacter* sp. *Psychrobacter* sp. *Psychrobacter maritimus*	MF537176.1 MF537175.1 MH368410.1	*Psychrobacter* sp. (Pseudomonadales)	1
KW2	MA	MW013367	16S	*Pseudoalteromonas tunicata* *Pseudoalteromonas tunicata* *Pseudoalteromonas* sp.	KY319053.1 CP011032.1 KX755364.1	*Pseudoalteromonas tunicata* (Alteromonadales)	1
KW3	MA	MW013368	16S	*Shewanella* sp. *Shewanella* sp. *Shewanella colwelliana*	MF594130.1 MF045123.1 KX756553.1	*Shewanella colwelliana* (Alteromonadales)	1
KW4	MA	MW013369	16S	*Pseudoalteromonas tunicata* *Pseudoalteromonas tunicata* *Pseudoalteromonas* sp.	KY319053.1 CP011032.1 KX755364.1	*Pseudoalteromonas tunicata* (Alteromonadales)	1
KW5	MA	MW013370	16S	*Pseudoalteromonas* sp. *Pseudoalteromonas* sp. *Pseudoalteromonas ulvae*	KU647930.1 MK743964.1 KF472191.1	*Pseudoalteromonas* sp. (Alteromonadales)	1
KW6	MA	MW013371	16S	*Lentibacter* sp. strain HYO3 Uncult. bacterium SEM1C041 *Lentibacter algarum*	KX755376.1 KJ094194.1 NR_108333.1	*Lentibacter algarum* (Rhodobacterales)	1
KW7	MA	MW013372	16S	*Pseudoalteromonas carrageenovora* *Pseudoalteromonas* sp. *Pseudoalteromonas* sp.	MH362718.1 MH333259.1 MF401566.1	*Pseudoalteromonas* sp. (Alteromonadales)	1
KW8	MA	MW013373	16S	*Psychrobacter glaciei* *Psychrobacter fjordensis* *Psychrobacter cryohalolentis*	NR_148850.1 NR_148330.1 NR_075055.1	*Psychrobacter* sp. (Pseudomonadales)	2
KW9*	MA	MW013374	16S	Uncult. Flavobacteriaceae bacterium C114Chl024 *Mesonia algae* *Mesonia algae*	JX525404.1 LT601221.2 LT601219.2	*Mesonia* sp. (Flavobacteriales)	1

Strain	Medium	Acc. no.	Amplicon	Closest related species (Blast)	Acc. no. closest related species	Lowest taxonomic classification (order)	RG
KW10	MA	MW013375	16S	*Vibrio anguillarum* Uncult. bacterium 2010ECS-StA#54 Uncult. bacterium SanDiego_a6617	CP011460.1 KM471344.1 KF799860.1	Vibrio *anguillarum* (Vibrionales)	2
KW11*	CMB	MW013376	16S	*Cobetia marina* *Halomonas* sp. *Cobetia amphilecti*	MH169273.1 CP028367.1 KX418494.1	*Cobetia* sp. (Oceanospirillales)	1
KW12	CMB	MW013377	16S	*Pseudoalteromonas tunicata* *Pseudoalteromonas tunicata* *Pseudoalteromonas* sp.	KY319053.1 CP011032.1 KX755364.1	*Pseudoalteromonas tunicata* (Alteromonadales)	1
KW13	CMB	MW013378	16S	*Erythrobacter* sp. *Erythrobacter* sp. *Erythrobacter vulgaris*	MG953322.1 MG833278.1 LK391640.1	*Erythrobacter* sp. (Sphingomonadales)	1
KW14	CMB	MW013379	16S	*Arthrobacter* sp. *Glutamicibacter protophormiae* *Arthrobacter protophormiae*	MF801344.1 KX768287.1 KT261110.1	*Glutamicibacter protophormiae* (Micrococcales)	1
KW15	CMB	MW013380	16S	*Paracoccus* sp. Uncult. bacterium ncd2046h03c1 *Paracoccus zhejiangensis*	FJ267566.1 JF168258.1 CP025430.1	*Paracoccus* sp. (Rhodobacterales)	1
KW16	CMB	MW013381	16S	*Erythrobacter* sp. *Erythrobacter citreus* *Erythrobacter citreus*	MN435731.1 MK254653.1 MK254652.1	*Erythrobacter* sp. (Sphingomonadales)	1
KW18	CMB	MW013382	16S	*Pseudoalteromonas* sp. *Pseudoalteromonas* sp. *Pseudoalteromonas undina*	MG388120.1 MF289546.1 KU588389.1	*Pseudoalteromonas* sp. (Alteromonadales)	1
KW19	CMB	MW013383	16S	*Psychrobacter nivimaris* *Psychrobacter sp.* *Psychrobacter proteolyticus*	MH978646.1 MG309426.1 LS483016.1	*Psychrobacter* sp. (Pseudomonadales)	1
KW21	CMN	MW013384	16S	*Olleya marilimosa* *Olleya marilimosa* *Olleya algicola*	JN175350.2 NR_104945.2 KY341922.1	*Olleya marilimosa* (Flavobacteriales)	1
KW22	CMN	MW013385	16S	*Aurantimonas coralicida* *Aurantimonas manganoxydans* *Aurantimonas coralicida*	NR_042319.1 NR_114936.1 NR_115134.1	*Aurantimonas* sp. (Rhizobiales)	1

Strain	Medium	Acc. no.	Amplicon	Closest related species (Blast)	Acc. no. closest related species	Lowest taxonomic classification (order)	RG
KW23	CMN	MW013386	16S	*Pseudoalteromonas carrageenovora* *Pseudoalteromonas* sp. *Pseudoalteromonas* sp.	MH362718.1 MH333259.1 MF401566.1	*Pseudoalteromonas* sp. (Alteromonadales)	1
KW24	CMN	MW013387	16S	*Pseudomonas* sp. *Pseudomonas* sp. *Pseudomonas stutzeri*	KR012328.1 KR012234.1 AJ270454.1	*Pseudomonas stutzeri* (Pseudomonadales)	1
KW25*	CMN	MW013388	16S	*Mesonia algae* *Mesonia algae* *Mesonia algae*	LT601221.2 LT601219.2 LT601217.2	*Mesonia* sp. (Flavobacteriales)	1
KW26	CMN	MW013389	16S	*Bacillus* sp. *Bacillus* sp. *Bacillus pumilus*	MH411221.1 MH411112.1 MF079375.1	*Bacillus* sp. (Bacillales)	1
KW27	CMN	MW013390	16S	*Pseudoalteromonas* sp. *Pseudoalteromonas marina* *Pseudoalteromonas marina*	MF537048.1 MH362719.1 MH362716.1	*Pseudoalteromonas* sp. (Alteromonadales)	1
KW28	CMN	MW013391	16S	*Agrococcus* sp. *Agrococcus* sp. *Agrococcus baldri*	KM362887.1 KY476554.1 HF913436.1	*Agrococcus baldri* (Micrococcales)	1
KW29	CMN	MW013392	16S	Uncult. alpha proteobacterium SGSH999 *Sphingopyxis baekryungensis* Uncult. bacterium CFL_Lb37	GQ347702.1 NR_043014.1 KJ365389.1	*Sphingopyxis baekryungensis* (Sphingomonadales)	1
KW30	WSP30	MW013393	16S	Uncult. bacterium Shelves_A_110 *Psychrobacter* sp. *Psychrobacter nivimaris*	MF092435.1 KY382827.1 MH478336.1	*Psychrobacter nivimaris* (Pseudomonadales)	1
KW31	TSB3+10	MW013394	16S	*Serinicoccus* sp. *Serinicoccus* sp. *Serinicoccus chungangensis*	DQ985074.1 KM886154.1 NR_117788.1	*Serinicoccus* sp. (Micrococcales)	1
KW33	TSB3+10	MW013395	16S	*Shewanella algicola* *Shewanella gelidii* *Shewanella arctica*	NR_149298.1 NR_151921.1 NR_117528.1	*Shewanella* sp. (Alteromonadales)	2
KW34	TSB3+10	MW013396	16S	*Pseudomonas* sp. *Pseudomonas* sp. *Pseudomonas peli*	MH109498.1 MH109497.1 MF077147.1	*Pseudomonas* sp. (Pseudomonadales)	1

184

Strain	Medium	Acc. no.	Amplicon	Closest related species (Blast)	Acc. no. closest related species	Lowest taxonomic classification (order)	RG
KW36	TSB3+10	MW013397	16S	*Shewanella putrefaciens* *Shewanella hafniensis* *Shewanella hafniensis*	MH304320.1 KX271693.1 KX271692.1	*Shewanella* sp. (Alteromonadales)	2
KW37	TSB3+10	MW013398	16S	*Pseudoalteromonas ulvae* *Pseudoalteromonas tunicata* *Pseudoalteromonas piscicida*	NR_025032.1 NR_029365.1 NR_114583.1	*Pseudoalteromonas* sp. (Alteromonadales)	1
KW38	TSB3+10	MW013399	16S	*Arthrobacter echini* *Arthrobacter echini* *Arthrobacter* sp.	NR_148833.1 KJ789956.1 FR693359.1	*Arthrobacter echini* (Micrococcales)	2
KW39*	WSP30	MW013400	16S	*Cobetia* sp. *Cobetia* sp. *Cobetia litoralis*	LN881270.1 LN881234.1 AB646235.1	*Cobetia* sp. (Oceanospirillales)	1
KW40	MA	MW013401	16S	*Vibrio* sp. *Vibrio* sp. *Vibrio anguillarum*	MF537054.1 MF537053.1 CP022468.1	*Vibrio* sp. (Vibrionales)	2
KW41	MA	MW013402	16S	*Pseudoalteromonas agarivorans* *Pseudoalteromonas prydzensis* *Pseudoalteromonas carrageenovora*	MH362723.1 MH362721.1 MH362718.1	*Pseudoalteromonas* sp. (Alteromonadales)	1
KW42	TSB3+10	MW013403	16S	*Planococcus* sp. *Planococcus maritimus* *Planococcus maritimus*	KX645673.1 MF405217.1 MF276799.1	*Planococcus* sp. (Bacillales)	1
KW43	WSP30	MW013404	16S	*Arthrobacter echini* *Arthrobacter echini* *Arthrobacter* sp.	NR_148833.1 KJ789956.1 FR693359.1	*Arthrobacter echini* (Micrococcales)	2
KW44	WSP30	MW013405	16S	*Exiguobacterium* sp. *Exiguobacterium* sp. *Exiguobacterium aurantiacum*	MF537096.1 MF537083.1 KY196514.1	*Exiguobacterium* sp. (Bacillales)	1
KW45	WSP30	MW013406	16S	*Sulfitobacter dubius* *Sulfitobacter dubius* *Sulfitobacter* sp.	MH725548.1 MH725547.1 MG210570.1	*Sulfitobacter dubius* (Rhodobacterales)	1
KW46	WSP30	MW013407	16S	*Rhodococcus* sp. *Rhodococcus* sp. *Rhodococcus cerastii*	MH173295.1 KY405925.2 MG645219.1	*Rhodococcus* sp. (Corynebacteriales)	1

Strain	Medium	Acc. no.	Amplicon	Closest related species (Blast)	Acc. no. closest related species	Lowest taxonomic classification (order)	RG
KW47	WSP30	MW013408	16S	*Shewanella baltica* *Shewanella baltica* *Shewanella putrefaciens*	MH304331.1 MH304326.1 MH304324.1	*Shewanella* sp. (Alteromonadales)	2
KW48	CMN	MW013409	16S	*Pseudoalteromonas tunicata* *Pseudoalteromonas tunicata* *Pseudoalteromonas* sp.	CP031961.1 KY319053.1 CP011032.1	*Pseudoalteromonas tunicata* (Alteromonadales)	1
KW49	WSP30	MW012385	ITS	*Candida sequanensis* *Candida sequanensis* *Candida sequanensis*	FM178365.1 NR_111302.1 KM435341.1	*Candida sequanensis* (Saccharomycetales)	2
KW50*	WSP30	MW013410	16S	*Cobetia* sp. *Cobetia* sp. *Cobetia litoralis*	LN881270.1 LN881234.1 AB646235.1	*Cobetia* sp. (Oceanospirillales)	1
KW51	WSP30	MW013411	16S	*Rhodococcus* sp. *Rhodococcus* sp. *Rhodococcus cerastii*	MH236179.1 KY405925.2 MG645219.1	*Rhodococcus* sp. (Corynebacteriales)	1
KW52	WSP30	MW013412	16S	*Halomonas sulfidaeris* *Halomonas titanicae* *Halomonas titanicae*	NR_027185.1 NR_116997.1 NR_117300.1	*Halomonas sulfidaeris* (Oceanospirillales)	1
KW53	WSP30	MW013413	16S	*Vibrio porteresiae* *Vibrio porteresiae* Uncult. *Vibrio* sp. 12L_112	HM749744.1 NR_044248.1 KP183078.1	*Vibrio porteresiae* (Vibrionales)	1
KW54	WSP30	MW013414	16S	*Alteromonas* sp. Uncult. bacterium SS-23C02 *Alteromonas stellipolaris*	MF443678.1 KX177874.1 CP015345.1	*Alteromonas* sp. (Alteromonadales)	1
KW55	CMB	MW013415	16S	*Pseudoalteromonas tunicata* *Pseudoalteromonas tunicata* *Pseudoalteromonas* sp.	KY319053.1 CP011032.1 KX755364.1	*Pseudoalteromonas tunicata* (Alteromonadales)	1
KW56	CMN	MW013416	16S	Uncult. bacterium CFL_Lb37 *Sphingopyxis baekryungensis* *Sphingopyxis baekryungensis*	KJ365389.1 HF913434.1 HE800827.1	*Sphingopyxis baekryungensis* (Sphingomonadales)	1
KW57	TSB3+10	MW013417	16S	*Okibacterium* sp. *Okibacterium* sp. *Mycetocola zhadangensis*	KU507611.1 HM224472.1 NR_109597.1	Microbacteriaceae unclassified (Micrococcales)	1
KW58	TSB3+10	MW013418	16S	*Microbacterium phyllosphaerae* *Microbacterium foliorum* *Microbacterium* sp.	MF541529.1 MG195155.1 MF458881.1	*Microbacterium* sp. (Micrococcales)	1

Strain	Medium	Acc. no.	Amplicon	Closest related species (Blast)	Acc. no. closest related species	Lowest taxonomic classification (order)	RG
KW60	CMN	MW013419	16S	*Vibrio cortegadensis* *Vibrio cyclitrophicus* *Vibrio cyclitrophicus*	NR_148247.1 NR_115806.1 NR_042467.1	*Vibrio* sp. (Vibrionales)	1
KW61	WSP30	MW012386	ITS	*Penicillium* sp. *Penicillium* sp. *Penicillium chrysogenum*	MK268129.1 MK267794.1 MH048884.1	*Penicillium* sp. (Eurotiales)	1
KW63	MA	MW013420	16S	*Shewanella* sp. *Shewanella* sp. *Shewanella colwelliana*	MF045122.1 MF045121.1 KX756553.1	*Shewanella colwelliana* (Alteromonadales)	1
KW65	CMN	MW013421	16S	*Serinicoccus* sp. *Serinicoccus* sp. *Serinicoccus chungangensis*	KP872112.1 KM886155.1 NR_117788.1	*Serinicoccus* sp. (Micrococcales)	1
KW66	CMN	MW013422	16S	*Erythrobacter* sp. *Erythrobacter* sp. *Erythrobacter litoralis*	KX989363.1 KX989361.1 KY047411.1	*Erythrobacter* sp. (Sphingomonadales)	1
KW67	CMN	MW013423	16S	*Arthrobacter agilis* *Arthrobacter agilis* *Arthrobacter* sp.	LT984721.1 CP024915.1 MG860335.1	*Arthrobacter* sp. (Micrococcales)	1
KW68	CMN	MW013424	16S	*Psychrobacter* sp. *Psychrobacter* sp. *Psychrobacter nivimaris*	MG309426.1 MH707184.1 MH478336.1	*Psychrobacter nivimaris* (Pseudomonadales)	1
KW69	TSB3+10	MW013425	16S	*Arthrobacter echini* *Arthrobacter echini* *Arthrobacter* sp.	NR_148833.1 KJ789956.1 FR693359.1	*Arthrobacter echini* (Micrococcales)	2
KW71	TSB3+10	MW013426	16S	*Rhodococcus* sp. *Rhodococcus* sp. *Rhodococcus cerastii*	MH236179.1 KY405925.2 MG645219.1	*Rhodococcus* sp. (Corynebacteriales)	1
KW72	WSP30	MW013427	16S	*Aurantimonas coralicida* *Aurantimonas litoralis* *Aurantimonas manganoxydans*	MH725320.1 KR140222.1 LC066380.1	*Aurantimonas* sp. (Rhizobiales)	1
KW74	WSP30	MW012387	ITS	*Dendrophoma cytisporoides* *Dendrophoma cytisporoides* Uncult. fungus OTU_F382_R420	NR_153978.1 JQ889273.1 MF976669.1	*Dendrophoma cytisporoides* (Chaetosphaeriales)	1
KW75	WSP30	MW014887	18S	*Sakaguchia lamellibrachiae* *Sakaguchia lamellibrachiae* *Symmetrospora marina*	AB126646.1 AB263120.1 KJ806313.1	*Sakaguchia lamellibrachiae* (Sakaguchiales)	2

Strain	Medium	Acc. no.	Amplicon	Closest related species (Blast)	Acc. no. closest related species	Lowest taxonomic classification (order)	RG
KW76	WSP30	MW013428	16S	*Pseudoalteromonas agarivorans* *Pseudoalteromonas carrageenovora* *Pseudoalteromonas* sp.	MH362723.1 MH362718.1 MH333259.1	*Pseudoalteromonas* sp. (Alteromonadales)	1

Table S3. Bioactivity (%) of crude extracts derived from tunic-associated microbial strains at a test concentration of 100 µg/mL. Values are given as average values of the two biological replicates, which were tested twice (technical replicate). Test organisms and cell lines are abbreviated as follows: MRSA: Methicillin-resistant *Staphylococcus aureus*, Efm: *Enterococcus faecium*, Ca: *Candida albicans*, Cn: *Cryptococcus neoformans*, A375: Malignant melanoma, A549: Lung carcinoma, HCT116: Colon cancer, MB231: Breast cancer. Several bacterial strains did not grow on GYM medium and hence, were only cultivated on MB medium. "-": Inhibition values ≤ 20%. Bold: Inhibition values ≥ 80%.

Strain	Lowest taxonomic classification	Medium	MRSA	Efm	Ca	Cn	A375	A549	HCT116	MB231
CHT3	*Leisingera aquimarina*	GYM	-	-	-	21	-	-	-	22
		MB	**80**	-	-	-	-	-	-	-
CHT5	*Shewanella* sp.	MB	36	-	-	-	-	-	-	-
CHT6	*Vibrio gigantis*	MB	60	-	-	-	-	-	-	-
CHT7	*Ruegeria faecimaris*	MB	35	-	-	-	-	-	-	-
CHT9	*Vibrio* sp.	MB	-	-	-	-	-	-	-	-
CHT10	*Kangiella* sp.	MB	**100**	**99**	-	-	-	-	-	-
CHT13	*Aurantimonas* sp.	GYM	46	-	-	-	-	-	-	-
		MB	**85**	-	-	-	-	-	-	-
CHT15	*Bacillus* sp.	GYM	54	44	-	48	-	-	-	-
		MB	61	-	-	-	-	-	-	-
CHT17	*Vibrio* sp.	MB	70	-	-	-	-	-	-	-
CHT22a	*Marixanthomonas ophiurae*	MB	52	-	-	-	-	-	-	-
CHT22b	*Vibrio* sp.	MB	**100**	-	-	-	-	-	-	-
CHT23	*Amphritea spongicola*	MB	**91**	**100**	-	-	-	-	-	-
CHT25	*Pseudorhodobacter aquimaris*	MB	74	-	-	-	-	-	-	-
CHT27	*Bacillus* sp.	GYM	42	39	-	37	-	-	-	-
		MB	44	-	-	-	-	-	-	-
CHT29	*Arenibacter* sp.	MB	-	-	-	-	-	-	-	-
CHT30	*Micrococcus* sp.	GYM	**100**	**100**	-	32	-	-	-	-
		MB	42	-	-	37	20	-	-	-
CHT35	*Cladosporium* sp.	CAG	**92**	38	-	-	-	-	-	-
		PDA	**85**	-	-	-	-	-	-	-
CHT37	*Emericellopsis maritima*	CAG	-	-	-	-	28	45	-	-
		PDA	-	-	-	-	56	57	72	**81**
CHT40	*Pseudochaetosphaeronema larense*	CAG	-	-	-	-	-	-	-	-
		PDA	50	-	-	-	63	-	40	59
CHT41	*Mycolicibacterium* sp.	MB	-	-	-	-	-	-	-	-
CHT42	*Ruegeria* sp.	MB	23	-	-	29	59	-	30	-
CHT43	*Primorskyibacter* sp.	MB	66	-	-	-	-	-	-	-
CHT46	*Litoreibacter* sp.	MB	75	-	-	-	-	-	-	-

Strain	Lowest taxonomic classification	Medium	MRSA	Efm	Ca	Cn	A375	A549	HCT116	MB231
CHT47	*Roseovarius arcticus*	MB	66	-	-	-	-	-	-	-
CHT48	*Vibrio* sp.	MB	52	-	-	-	-	-	-	-
CHT49	*Ruegeria atlantica*	MB	60	-	-	-	-	-	-	-
CHT53	*Ochrobactrum pseudogrignonense*	GYM	60	-	-	-	-	-	-	-
		MB	76	-	-	-	-	-	-	-
CHT54	*Bacillus* sp.	GYM	33	67	-	38	-	-	-	-
		MB	61	-	-	-	-	-	-	-
CHT55	*Ochrobactrum grignonense*	GYM	**86**	-	-	-	-	-	-	-
		MB	58	-	-	-	-	-	-	-
CHT56	*Pseudogymnoascus destructans*	CAG	**100**	**100**	-	31	30	-	-	**81**
		PDA	**88**	-	-	-	-	-	-	-
CHT58	*Pyrenochaeta* sp.	CAG	**99**	43	36	44	-	-	48	-
		PDA	**100**	**99**	**99**	**87**	23	33	62	36
CKT1	*Pseudomonas* sp.	MB	49	-	-	-	-	-	-	-
CKT2	*Litoreibacter* sp.	MB	59	-	-	-	-	-	-	-
CKT3	*Pelagicola* sp.	MB	47	-	-	-	-	-	-	-
CKT4	*Neptunomonas concharum*	MB	**85**	72	-	-	-	-	-	-
CKT6	*Flaviramulus ichthyoenteri*	MB	-	-	-	-	-	-	-	-
CKT10	*Pseudomonas* sp.	MB	**99**	**97**	-	-	-	-	-	-
CKT11	*Vibrio aestuarianus*	MB	59	27	-	-	-	-	-	-
CKT12	*Pseudomonas* sp.	GYM	79	-	-	-	-	-	-	-
		MB	48	-	-	-	-	-	-	-
CKT16	*Hydrogenophaga crassostreae*	GYM	**100**	**100**	-	33	-	-	-	-
		MB	**100**	**100**	-	-	-	-	-	-
CKT17	*Lysobacter spongiicola*	GYM	**100**	**100**	-	26	-	-	-	-
		MB	**100**	**100**	-	-	-	-	-	-
CKT20	*Bacillus* sp.	GYM	46	46	-	30	-	-	-	-
		MB	27	-	-	-	-	-	-	-
CKT21	*Pseudomonas* sp.	GYM	74	-	-	-	41	23	34	39
		MB	74	-	-	-	-	-	-	-
CKT22	*Phaeobacter arcticus*	MB	73	-	-	-	-	-	-	-
CKT23	*Shewanella* sp.	MB	**100**	**100**	-	-	-	-	-	-
CKT24	*Arenibacter echinorum*	MB	-	-	-	-	-	-	-	-
CKT28	*Cyphellophora reptans*	CAG	**98**	-	-	-	-	-	-	-
		PDA	70	-	-	-	-	-	-	-
CKT29	*Marinobacter litoralis*	MB	**97**	**100**	-	-	-	-	-	-

Strain	Lowest taxonomic classification	Medium	MRSA	Efm	Ca	Cn	A375	A549	HCT116	MB231
CKT30	*Salinimicrobium* sp.	MB	-	-	-	-	-	-	-	-
CKT34	*Arthrobacter* sp.	GYM	**90**	**100**	-	-	-	-	25	-
		MB	-	-	-	-	-	30	-	-
CKT35	*Penicillium* sp.	CAG	**98**	51	**100**	76	42	-	33	22
		PDA	**99**	**100**	**100**	76	34	-	29	-
CKT38	*Bacillus* sp.	GYM	**88**	**100**	-	70	-	-	-	25
		MB	55	50	-	-	-	-	-	-
CKT39	*Streptomyces* sp.	GYM	**100**	**100**	-	31	-	-	-	-
		MB	**95**	45	-	25	55	-	33	-
CKT41	*Bacillus* sp.	GYM	**100**	35	-	-	-	-	-	-
		MB	**99**	**92**	-	-	-	-	-	-
CKT43	*Streptomyces* sp.	GYM	**100**	**100**	**91**	**100**	**98**	**89**	**97**	**95**
		MB	**100**	**99**	56	**100**	43	51	49	49
CKT49	*Penicillium brasilianum*	CAG	46	-	-	-	55	45	53	50
		PDA	**99**	**100**	**98**	47	41	20	44	36
CKT51-II	*Bacillus* sp.	GYM	-	-	-	41	-	-	-	-
		MB	66	38	-	-	-	-	-	-
CKT52	*Bizionia fulviae*	GYM	71	72	-	-	-	-	25	-
		MB	**95**	**100**	-	-	-	-	-	-
CKT56	*Ruegeria atlantica*	MB	49	-	-	-	-	-	-	-
CKT60	*Kiloniella laminariae*	MB	**85**	86	-	-	-	-	38	-
CKT65	*Salegentibacter* sp.	MB	-	-	22	-	-	-	-	-
CKT67	*Serinicoccus* sp.	GYM	**99**	**97**	-	49	-	-	-	-
		MB	-	-	-	23	20	-	-	-
CKT78	*Penicillium crustosum*	CAG	-	-	-	-	-	-	21	27
		PDA	-	-	-	-	-	-	-	21
CKT81	*Pithomyces chartarum*	CAG	**85**	**93**	**99**	65	23	27	24	49
		PDA	**100**	**97**	**100**	65	43	48	35	73
CKT84	*Fusarium* sp.	CAG	**98**	**97**	**88**	52	45	55	30	35
		PDA	**100**	**98**	**100**	75	51	65	42	47
CKT85	*Cadophora luteo-olivacea*	CAG	-	25	-	-	**90**	78	**87**	**84**
		PDA	-	-	-	-	35	-	21	21
CKT86	*Plectosphaerella cucumerina*	CAG	**100**	**100**	-	-	34	21	32	20
		PDA	70	-	-	-	37	22	-	33
CKT90	*Wickerhamomyces* sp.	CAG	**83**	**98**	-	-	-	-	-	-
		PDA	**100**	44	-	-	-	-	-	-

Strain	Lowest taxonomic classification	Medium	MRSA	Efm	Ca	Cn	A375	A549	HCT116	MB231
CKT91	*Boeremia exigua*	CAG	-	-	-	-	62	**82**	63	78
		PDA	**100**	77	25	22	**85**	**86**	**78**	**86**

Table S4. Bioactivity-based selection criterion for the prioritization of extracts for in-depth chemical analyses. A high bioactivity threshold was applied, i.e. extracts are considered active against a test strain or cancer cell line if ≥ 80% inhibitory activity at a test concentration of 100 µg/mL was observed. For each possible combination of observed bioactivities, it is indicated, whether this combination led to the selection of an extract (yes) or not (no). Activities are defined as follows: antibacterial: activity against MRSA and *E. faecium*; antifungal: activity against at least one pathogenic yeast (*C. albicans* or *C. neoformans*); antimicrobial: antibacterial + antifungal activity (as defined before); anticancer: activity against at least one of the four cancer cell lines (A375, A549, HCT116, MB231).

Observed bioactivities			
Antimicrobial		Anticancer	Selected?
Antibacterial	Antifungal		
Yes	Yes	Yes	Yes (antimicrobial + anticancer)
Yes	Yes	No	Yes (antimicrobial)
Yes	No	No	No
Yes	No	Yes	Yes (anticancer)
No	Yes	Yes	Yes (anticancer)
No	Yes	No	No
No	No	Yes	Yes (anticancer)
No	No	No	No

Table S5. ANOSIM comparison of chemically different extracts. ANOSIM (Euclidean distance) was computed to statistically verify differential clustering of the extracts CHT58-CAG (*Pyrenochaeta* sp.), CKT35-PDA (*Penicillium* sp.), CKT91-CAG and CKT91-PDA (*Boeremia exigua*). Remaining: extracts CHT37-PDA (*Emericellopsis maritima*), CHT56-CAG (*Pseudogymnoascus destructans*), CKT49-PDA (*Penicillium brasilianum*), CKT81-CAG and CKT81-PDA (*Pithomyces chartarum*), CKT84-CAG and CKT84-PDA (*Fusarium* sp.) and CKT85-CAG (*Cadophora luteo-olivacea*).

Compared groups	R value	p value
All	0.7849	0.0001
CHT58-PDA x remaining	0.9824	0.0069
CKT35-PDA x remaining	0.8843	0.0064
CKT91-CAG and CKT91-PDA x remaining	0.5588	0.0071

Table S6. Putative annotation of metabolites detected in the crude extract of *Pyrenochaeta* sp. strain CHT58 cultivated on PDA medium. Each detected compound is given with the experimentally determined *m/z* value and the predicted putative molecular formula. Putative identifications were based on the accurate mass, predicted putative molecular formulae, the retention time (R_t in min), the fragmentation pattern and biological origin. *Only putative molecular formula with best ppm shown (more than 1 molecular formula possible). ᐃDifferent isomers with same *m/z* value and molecular formula, which cannot be differentiated based on MS/MS data. IC: Identification confidence level after Sumner et al. 2007 [3]. Nf: No fragmentation pattern detected or fragmentation below noise threshold of 5e[1]. n.a. = putatively novel compound (known NPs do not match). Ref = reference.

No.	*m/z* value	R_t (min)	Adduct	Putative molecular formula	IC	ppm	Fragmentation pattern	Putative identification	Chemical family	Biological origin	Ref
1	377.1941	3.17	[M+Na]+	$C_{19}H_{30}O_6$	4	0.3	Nf	n.a.			
2	309.0978	3.24	[M+H]+	$C_{15}H_{16}O_7$	3	1.3	291.0882, 273.0760, 255.0653, 245.0816, 227.0710, 221.0426, 181.0141, 93.0706	Ascolactone A or B	Phthalide derivative	*Ascochyta salicorniae* (fungus)	[4]
3	290.1008	3.36	[M+H]+	$C_{11}H_{11}N_7O_3$	4	2.1	272.0908, 245.0808	n.a.			
4	377.1938	3.47	[M+Na]+	$C_{19}H_{30}O_6$	4	-0.5	Nf	n.a.			
5	373.1993	3.62	[M+Na]+	$C_{20}H_{30}O_5$	3	0.6	Nf	Aphidicolin A9	Diterpenoid	*Botryotinia fuckeliana* (fungus)	[5]
6	321.0981	3.85	[M+H]+	$C_{16}H_{16}O_7$	3	2.2	303.0897, 289.0728, 271.0616, 243.0652, 254.0514, 243.0652, 229.0875, 227.0695, 217.0504, 207.0651, 151.0392	10-deoxybostrycin	Anthraquinone derivative	*Nigrospora* sp. (fungus)	[6]
7	335.2215	3.96	[M+H]+	$C_{20}H_{30}O_4$	3	-2.1	Nf	Aphidicolin A58	Diterpenoid	*Botryotinia fuckeliana* (fungus)	[7]
8	333.2066	4.04, 4.46, 5.7, 6.3, 7.78ᐃ	[M+H]+	$C_{20}H_{28}O_4$	3	0	315.2002, 297.1773, 269.1871, 243.1402, 225.1272	Aphidicolin A63	Diterpenoid	*Botryotinia fuckeliana* (fungus)	[8]
9	335.2215	4.23	[M+H]+	$C_{20}H_{30}O_4$	3	-2.1	Nf	Aphidicolin A33	Diterpenoid	*Botryotinia fuckeliana* (fungus)	[5]
10	335.2227	4.31	[M+H]+	$C_{20}H_{30}O_4$	3	1.5	Nf	Aphidicolin A38	Diterpenoid	*Botryotinia fuckeliana* (fungus)	[5]
11	359.1836	4.58	[M+H]+	$C_{17}H_{22}N_6O_3$	4	1.1	317.1724	n.a.			
12	387.2141	4.73	[M+Na]+	$C_{21}H_{32}O_5$	3	-1.5	Nf	Aphidicolin A70	Diterpenoid	*Botryotinia fuckeliana* (fungus)	[5]
13	359.2191	5	[M+Na]+	$C_{20}H_{32}O_4$	3	-1.9	Nf	Aphidicolin A35	Diterpenoid	*Botryotinia fuckeliana* (fungus)	[5]
14	373.1984	5	[M+Na]+	$C_{20}H_{30}O_5$	3	-1.9	Nf	Aphidicolin A11	Diterpenoid	*Botryotinia fuckeliana* (fungus)	[5]
15	303.2327	5.16	[M+H]+	$C_{20}H_{30}O_2$	3	1	285.2225, 267.2115, 173.1342, 161.1338, 159.1189, 149.1324, 145.0996, 133.1012, 121.1028, 119.0856, 109.1018	Wentinoid C or D	Diterpenoid	*Aspergillus wentii* (fungus)	[7]
16	357.2038	5.24	[M+Na]+	$C_{20}H_{30}O_4$	3	-1.1	Nf	Aphidicolin A54	Diterpenoid	*Botryotinia fuckeliana* (fungus)	[5]

No.	*m/z* value	R_t (min)	Adduct	Putative molecular formula	IC	ppm	Fragmentation pattern	Putative identification	Chemical family	Biological origin	Ref
17	359.2196	5.32	[M+Na]+	$C_{20}H_{32}O_4$	3	-0.6	Nf	Aphidicolin A46	Diterpenoid	*Botryotinia fuckeliana* (fungus)	[5]
18	335.222	5.32	[M+H]+	$C_{20}H_{30}O_4$	3	-0.6	299.1965, 289.2251, 271.2039, 257.1883, 253.1990, 229.1680, 227.1432, 219.1374, 213.1630, 205.1536, 203.1424, 199.1478, 189.1649, 185.1324, 175.1089, 173.1331, 171.1170, 167.1059, 161.1303, 159.1160, 157.1013, 149.0942, 147.1154, 145.1038, 139.1182, 137.0944, 135.1199, 133.1020, 131.0872, 123.1195, 121.1002, 119.0865, 111.0840, 109.1014, 107.0857, 93.0710	Aphidicolin A37	Diterpenoid	*Botryotinia fuckeliana* (fungus)	[5]
19	319.2271	5.47	[M+H]+	$C_{20}H_{30}O_3$	3	-0.6	275.0874, 233.0437, 189.1269, 167.0352, 149.0978, 93.0702	Wentinoid F	Diterpenoid	*Aspergillus wentii* (fungus)	[7]
20	335.2227	5.55	[M+H]+	$C_{20}H_{30}O_4$	3	0.6	Nf	Aphidicolin A41	Diterpenoid	*Botryotinia fuckeliana* (fungus)	[5]
21	317.2123	5.62	[M+H]+	$C_{20}H_{28}O_3$	3	1.9	Nf	n.a.			
22	374.2335	5.63	[M+H]+	$C_{22}H_{31}NO_4$*	4	1.1	356.2203, 338.2126, 224.1295, 222.1142, 133.1017	n.a.			
23	376.2492	5.78	[M+H]+	$C_{22}H_{33}NO_4$	2	1.1	358.2390, 340.2285, 314.2489, 253.1965, 241.1965	Periconiasin I	Cytochalasan	*Periconia* sp. (fungus)	[7]
24	373.1996	5.92	[M+Na]+	$C_{20}H_{30}O_5$	3	1.3	358.2399, 340.2212, 314.2465, 260.1649, 241.1958	Aphidicolin A61	Diterpenoid	*Botryotinia fuckeliana* (fungus)	[5]
25	403.2103	6.15	[M+Na]+	$C_{21}H_{32}O_6$	3	1.5	Nf	n.a.			
26	331.1918	6.15	[M+H]+	$C_{20}H_{26}O_4$	3	2.7	285.1854, 271.1707, 255.1385, 253.1597, 246.1269, 243.1754, 227.1445, 191.0710, 185.0972, 175.0763, 163.0763	Hawaiinolide B	Diterpenoid	*Paraconiothyrium hawaiiense* (fungus)	[9]
27	359.2206	6.22	[M+Na]+	$C_{20}H_{32}O_4$	3	2.2	Nf	Aphidicolin A48	Diterpenoid	*Botryotinia fuckeliana* (fungus)	[5]
28	583.1831	6.22	[M+H]+	$C_{30}H_{30}O_{12}$	3	2.6	511.1395, 493.1300, 465.1280, 423.1118, 405.1028, 389.1071, 361.1062, 345.1097, 333.1063, 301.1031, 283.0966, 273.0782, 269.0845, 257.0845, 255.0650, 245.0871, 235.0582, 231.0632, 229.0855, 227.0734, 219.0664, 191.0723, 167.0353, 161.0597, 151.0392, 123.0456	Talarodilactone B	Macrolide	*Talaromyces rugulosus* (fungus)	[10]
29	335.2208	6.54	[M+H]+	$C_{20}H_{30}O_4$	3	-4.2	Nf	Aphidicolin A64	Diterpenoid	*Botryotinia fuckeliana* (fungus)	[5]
30	402.2286	6.54	[M+H]+	$C_{23}H_{31}NO_5$	3	1.5	384.2193, 374.2318, 356.2223, 338.2108, 241.1943	CJ-16,264	Pyrrolizidine alkaloid	Unknown fungus	[11]
31	387.2153	6.69	[M+Na]+	$C_{21}H_{32}O_5$	3	1.5	Nf	Brassicicene F	Diterpenoid	*Alternaria brassicicola* (fungus)	[12]
32	319.2279	6.8	[M+H]+	$C_{20}H_{30}O_3$	3	1.9	301.2173, 291.2337, 283.2069, 273.2217, 255.2120, 211.1494, 193.1600, 189.1641,	Aphidicolin A57	Diterpenoid	*Botryotinia fuckeliana* (fungus)	[5]

195

No.	*m/z* value	R_t (min)	Adduct	Putative molecular formula	IC	ppm	Fragmentation pattern	Putative identification	Chemical family	Biological origin	Ref
							185.1329, 175.1488, 173.1328, 171.1180, 165.0913, 163.1123, 161.1332, 159.1173, 157.1016, 149.1327, 147.1174, 145.1021, 137.1330, 135.1169, 133.1013, 123.1166, 121.1021, 119.0860, 109.1019, 107.0860, 105.0706, 93.0700				
33	317.2125	6.95	[M+H]+	$C_{20}H_{28}O_3$	3	2.5	317.2117, 300.2907, 282.2806, 270.2800, 243.1767, 201.1281, 189.1275, 173.1335, 159.1172, 145.1019, 133.1013, 119.0860, 95.0864	n.a.			
34	351.2173	7.11	[M+H]+	$C_{20}H_{30}O_5$	3	0.6	Nf	Aphidicolin A53	Diterpenoid	*Botryotinia fuckeliana* (fungus)	[5]
35	317.2119	7.17	[M+H]+	$C_{20}H_{28}O_3$	3	0.6	Nf	n.a.			
36	235.1341	7.25	[M+H]+	$C_{14}H_{18}O_3$	3	3	207.1382, 203.1069, 193.1229, 191.1428, 189.1278, 185.0968, 179.1072, 175.1121, 161.0964, 159.1173, 157.1014, 147.1168, 144.0936, 142.0781, 139.0398, 133.1015, 129.0697, 119.0860, 105.0702	n.a.			
37	567.1875	7.32	[M+H]+	$C_{30}H_{30}O_{11}$	3	1.6	531.1674, 513.1566, 495.1455, 485.1612, 467.1511, 391.1179, 389.1031, 373.1081, 371.0923, 363.1235, 275.0925, 273.0772, 267.0664, 259.0970, 257.0821, 241.0869, 229.0868, 217.0868, 167.0346, 153.0550, 151.0397, 123.0446	n.a.			
38	319.2287	7.51	[M+H]+	$C_{20}H_{30}O_3$	3	4.4	Nf	n.a.			
39	317.2125	7.7	[M+H]+	$C_{20}H_{28}O_3$	3	2.5	299.2018, 281.1901, 271.2071, 253.1964, 243.1376, 201.1267, 173.1336, 159.1179, 145.1019, 139.0778, 133.1020, 119.0862, 95.0862	n.a.			
40	317.2125	7.88	[M+H]+	$C_{20}H_{28}O_3$	3	2.5	Nf	n.a.			
41	417.2249	8.16	[M+Na]+	$C_{22}H_{34}O_6$	3	-1	Nf	Aphidicolin A32	Diterpenoid	*Botryotinia fuckeliana* (fungus)	[5]
42	331.1914	8.16	[M+H]+	$C_{20}H_{26}O_4$	3	1.5	285.1862, 271.1705, 255.1378, 253.1606, 246.1281, 243.1753, 227.1440, 191.0714, 185.0970, 175.0758, 163.0769	Hawaiinolide A	Diterpenoid	*Paraconiothyrium hawaiiense* (fungus)	[9]
43	498.3797	8.35	[M+H]+	$C_{28}H_{51}NO_6$•	4	0.4	480.3681, 236.1501, 162.1126, 144.1023	n.a.			
44	498.3795	8.54	[M+H]+	$C_{28}H_{51}NO_6$•	4	0	480.3691, 436.3773, 236.1502, 162.1126, 144.1023	n.a.			
45	287.2377	8.7	[M+H]+	$C_{20}H_{30}O$	3	0.7	269.2265, 241.1960, 227.1789, 215.1799, 213.1643, 199.1494, 185.1323, 175.1504, 173.1328, 171.1169, 161.1331, 159.1170,	Conidiogenone B	Diterpenoid	*Penicillium* sp. (fungus)	[13]

No.	m/z value	R_t (min)	Adduct	Putative molecular formula	IC	ppm	Fragmentation pattern	Putative identification	Chemical family	Biological origin	Ref
							157.1014, 151.1124, 147.1160, 145.1029, 133.1035, 131.0861, 119.0863				
46	401.2299	8.78	[M+Na]$^+$	$C_{22}H_{34}O_5$	3	-1.2	Nf	a: aphidicolin A23, b: aphidicolin A50	Diterpenoid	*Botryotinia fuckeliana* (fungus)	[5]
47	347.222	8.78	[M+H]$^+$	$C_{21}H_{30}O_4$	3	-0.6	329.2059, 269.1911, 251.1773 225.1639,159.1180, 145.1011	Aspergillodiol	Hydropyrano-indeno derivative	*Aspergillus versicolor* (fungus)	[14]
48	500.3948	9.06	[M+H]$^+$	$C_{28}H_{53}NO_{6^\bullet}$	4	-0.6	482.3836, 438.3966, 236.1499, 162.1135, 144.1021	n.a.			
49	551.1915	9.17	[M+H]$^+$	$C_{30}H_{30}O_{10}$	4	-0.4	497.1592, 391.1183, 373.1078, 267.0645, 259.0966, 257.0809, 241.0867, 229.0860, 217.0868, 153.0541, 151.0395	n.a.			
50	301.2168	9.25	[M+H]$^+$	$C_{20}H_{28}O_2$	3	0	283.2092, 255.2111, 227.1792, 185.1351, 175.1486, 173.1334, 171.1149, 159.1779, 157.1020, 147.1188, 145.1016, 133.1026, 121.1039, 119.0863, 107.0864, 105.0708, 95.0862	Harziandione	Diterpenoid	*Trichoderma atroviride* (fungus)	[15]
51	303.2333	9.33	[M+H]$^+$	$C_{20}H_{30}O_2$	3	3	285.2242, 177.1627, 175.1490 151.9207, 149.0956, 147.1167, 139.0779, 123.1156, 121.1021, 109.1024, 107.0853, 105.0681, 95.0868, 93.0696, 81.0703, 79.0540	Botrysphin B	Diterpenoid	*Botryosphaeria laricina* (fungus)	[16]

Table S7. Putative annotation of metabolites detected in the crude extract of *Pseudogymnoascus destructans* strain CHT56 cultivated on CAG medium. Each detected compound is given with the experimentally determined *m/z* value and the predicted putative molecular formula. Putative identifications were based on the accurate mass, predicted putative molecular formulae, the retention time (R_t in min), the fragmentation pattern and biological origin. *Only putative molecular formula with best ppm shown (more than 1 molecular formula possible). ᐃDifferent isomers with same *m/z* value and molecular formula, which cannot be differentiated based on MS/MS data. IC: Identification confidence level after Sumner et al. 2007 [3]. Nf: No fragmentation pattern detected or fragmentation below noise threshold of 5e[1]. n.a. = putatively novel compound (known NPs do not match). Ref = reference.

No.	*m/z* value	R_t (min)	Adduct	Putative molecular formula	IC	ppm	Fragmentation pattern	Putative identification	Chemical family	Biological origin	Ref
52	413.1804	3.91	[M-H$_2$O]$^+$	C$_{17}$H$_{22}$N$_{10}$O$_{4*}$	4	1.5	249.118, 245.1402, 221.1146, 129.0537	n.a.			
53	267.1223	4.84	[M+H]$^+$	C$_{14}$H$_{18}$O$_5$	4	-3.4	249.1100, 221.1175, 151.0368, 123.0437, 99.0797, 71.0863	n.a.			
54	291.1222	4.96	[M+H]$^+$	C$_{16}$H$_{18}$O$_5$	4	-3.4	273.1115, 245.1171, 193.0531, 99.0804	n.a.			
55	281.1017	5.11	[M+H]$^+$	C$_{14}$H$_{16}$O$_6$	3	-2.8	221.0442, 211.0230, 207.1018, 191.0332, 165.0531	Corynechromone E or F	Chromone derivative	*Corynespora cassiicola* (fungus)	[17]
56	253.1067	5.14	[M+H]$^+$	C$_{13}$H$_{16}$O$_5$	3	-3.6	235.0970, 207.1010, 193.0438, 183.0279, 165.0173, 139.0372, 137.0223	Acremostrictin	Sesquiterpenoid	*Acremonium strictum* (fungus)	[18]
57	265.1065	5.34	[M+H]$^+$	C$_{14}$H$_{16}$O$_5$	4	-4.1	247.0953, 237.1100, 219.1009, 209.0434, 201.0900, 177.0532, 165.0532	n.a.			
58	265.1069	5.48	[M+H]$^+$	C$_{14}$H$_{16}$O$_5$	4	-2.6	247.0973, 219.1008, 209.0424, 201.0903, 177.0530, 165.0533	n.a.			
59	291.1227	5.59	[M+H]$^+$	C$_{16}$H$_{18}$O$_5$	4	-1.7	273.1115, 245.1171, 193.0531, 99.0804	n.a.			
60	249.1116	5.82	[M+H]$^+$	C$_{14}$H$_{16}$O$_4$	3	-4.4	221.1166	Phialofurone	Benzofuran derivative	*Phialocephala* sp. (fungus)	[19]
61	295.1172	6.05	[M+H]$^+$	C$_{15}$H$_{18}$O$_6$	3	-3.4	267.1231, 251.1295, 235.0968, 221.0431, 217.0852, 207.1008, 197.0437, 165.0538	3,4-dihydro-6-methoxy-8-hydroxy-3,4,5-trimethyl-isocoumarin-7-carboxylic acid methyl ester	Isocoumarin derivative	Unknown fungus	[20]
62	211.0596	6.28	[M+H]$^+$	C$_{10}$H$_{10}$O$_5$	3	-4.7	179.0332, 151.0377, 128.9502	Hypoxyphenone	Benzoic acid derivative	*Hypoxylon* sp. (fungus)	[21]
63	525.3033	6.46	[M+H]$^+$	C$_{23}$H$_{44}$N$_2$O$_{11}$	4	1.9	Nf	n.a.			
64	467.2999	6.46	[M+H]$^+$	C$_{26}$H$_{42}$O$_7$	4	-2.1	177.1277, 175.1137, 149.1330, 135.1166, 133.1003, 121.0978, 113.0946, 109.1005, 95.0862	n.a.			
65	529.2076	6.61	[M+H]$^+$	C$_{28}$H$_{32}$O$_{10}$	3	0.4	Nf	Aspermeroterpene A	Meroterpenoid	*Aspergillus terreus* (fungus)	[22]
66	357.2034	6.75	[M+H]$^+$	C$_{18}$H$_{24}$N$_6$O$_{2*}$	4	-1.4	Nf	n.a.			
67	529.2073	6.87	[M+H]$^+$	C$_{28}$H$_{32}$O$_{10}$	3	-0.2	Nf	Aspermeroterpene B	Meroterpenoid	*Aspergillus terreus* (fungus)	[22]

No.	*m/z* value	R_t (min)	Adduct	Putative molecular formula	IC	ppm	Fragmentation pattern	Putative identification	Chemical family	Biological origin	Ref
68	789.2764	7.06-7.18	[M+H]$^+$	$C_{42}H_{44}O_{15}$	4	0.8	Nf	n.a.			
69	1053.3766	7.09	[M+H]$^+$	$C_{52}H_{36}N_{28*}$	4	0.9	971.3932, 735.2479, 435.2361, 247.0930	n.a.			
70	317.2102	7.41, 7.9$^\Delta$	[M+H]$^+$	$C_{20}H_{28}O_3$	3	-4.7	299.2006, 281.1910, 263.1822, 237.1586, 237.1611, 197.1319, 151.1088, 137.0890	(9ξ,13α)-6,9-dihydroxypimara-5,8(14),15-trien-7-one	Pimarane diterpenoid	*Epicoccum* sp. (fungus)	[23]
71	789.2755	7.41	[M+H]$^+$	$C_{42}H_{44}O_{15}$	4	-0.4	555.1884, 408.3155	n.a.			
72	393.2422	8.2	[M+H]$^+$	$C_{26}H_{32}O_3$	4	-2	315.1731, 293.2056, 273.1625, 249.1645, 243.1741, 235.1513, 225.1621, 173.1361, 171.1132, 159.1169, 133.0636, 105.0683	n.a.			
73	393.2424	9.07	[M+H]$^+$	$C_{26}H_{32}O_3$	4	-1.5	375.2322, 243.1759, 225.1634, 223.1468, 195.1156, 183.1155, 169.1017, 159.1152, 157.0998, 145.1002. 133.0650, 131.0474	n.a.			
74	263.2363	10.47	[M+H]$^+$	$C_{18}H_{30}O$	4	-4.6	245.2263, 175.1476, 149.1320, 133.1000, 123.1158, 121.1015, 109.0997, 81.0693	n.a.			
75	337.1665	10.47	[M+H]$^+$	$C_{14}H_{21}N_8Cl$	4	2.7	185.0091	n.a.			

Table S8. Putative annotation of metabolites detected in the crude extract of *Penicillium* sp. strain CKT35 cultivated on PDA medium. Each detected compound is given with the experimentally determined *m/z* value and the predicted putative molecular formula. Putative identifications were based on the accurate mass, predicted putative molecular formulae, the retention time (R_t in min), the fragmentation pattern and biological origin. *Only putative molecular formula with best ppm shown (more than 1 molecular formula possible). ΔDifferent isomers with same *m/z* value and molecular formula, which cannot be differentiated based on MS/MS data. IC: Identification confidence level after Sumner et al. 2007 [3]. Nf: No fragmentation pattern detected or fragmentation below noise threshold of 5e[1]. n.a. = putatively novel compound (known NPs do not match). Ref = reference.

No.	*m/z* value	R_t (min)	Adduct	Putative molecular formula	IC	ppm	Fragmentation pattern	Putative identification	Chemical family	Biological origin	Ref
76	207.0302	2.14, 2.64, 4.86Δ	[M+H]+	$C_{10}H_6O_5$	3	4.3	179.0345, 165.0189, 161.0234, 137.0238	Flaviolin	Naphthoquinone derivative	Several fungal taxa, e.g. *Aspergillus niger*	[24]
77	209.0454	2.33	[M+H]+	$C_{10}H_8O_5$	2	1.9	191.0349, 181.0501, 167.0342, 163.0397, 147.0449, 135.0445	Penibenzone C	Phthalide derivative	*Penicillium purpurogenum* (fungus)	[25]
78	195.0299	2.53	[M+H]+	$C_9H_6O_5$	4	3.1	167.0345, 163.0031, 135.0089, 119.0136	n.a.			
79	193.0512	3.07	[M+H]+	$C_{10}H_8O_4$	3	5.7	175.0393	Penicifuran C	Benzofuran	*Penicillium* sp. (fungus)	[26]
80	209.0459	3.23	[M+H]+	$C_{10}H_8O_5$	2	4.3	163.0398	Acetophthalidin	Phthalide derivative	*Penicillium* sp. (fungus)	[27]
81	293.1273	3.77	[M+Na]+	$C_{16}H_{18}N_2O_2$	3	2.4	214.0741	Quinolactacin A	Quinolone alkaloid	*Penicillium* sp. (fungus)	[28]
82	193.0509	4.31	[M+H]+	$C_{10}H_8O_4$	3	4.1	175.0393, 149.0592, 121.0658	Penicifuran D	Benzofuran	*Penicillium* sp. (fungus)	[26]
83	337.1292	4.59	[M+H]+	$C_{17}H_{20}O_7$	2	1.5	Nf	4'-hydroxy-mycophenolic acid	Meroterpenoid	*Penicillium* sp. (fungus)	[29]
84	319.1176	5.1	[M+H]+	$C_{17}H_{18}O_6$	2	-1.9	Nf	4-hydroxy-6-methoxy-γ,7-dimethyl-3-oxo-5-phthalansorbic acid	Meroterpenoid	*Penicillium rugulosum* (fungus)	[30]
85	321.1345	5.76	[M+H]+	$C_{17}H_{20}O_6$	2	2.2	303.1235, 275.12987, 207.0662, 195.0657, 159.0446)	Mycophenolic acid	Meroterpenoid	*Penicillium* sp. (fungus)	[29]
86	441.2284	6.47	[M+H]+	$C_{26}H_{32}O_6$	3	1.6	363.1965, 211.1483, 173.1311, 171.1171, 151.0382	Tropolactone C	Meroterpenoid	*Aspergillus* sp. (fungus)	[31]
87	501.2503	6.47	[M+H]+	$C_{28}H_{36}O_8$	3	0.2	409.2018, 391.1942, 381.2094, 363.1965, 335.2033, 221.1305, 217.1243, 213.1653, 211.1483, 203.1084, 187.1500, 183.1351, 177.0918, 171.1171, 157.1011, 151.0382	Citreohybridonol	Meroterpenoid	*Penicillium atrovenetum* (fungus)	[32]
88	471.2703	6.55	[M+H]+	$C_{23}H_{38}N_2O_{8*}$	4	-0.6	439.2438, 261.1821, 232.0702	n.a.			
89	523.2224	6.91	[M+H]+	$C_{32}H_{30}N_2O_5$	2	-1.7	256.1335, 238.1228, 134.0960, 122.0595, 117.0701, 105.0338	Asperphenamate B	Phenylalanine derivative	*Penicillium* spp. (fungus)	[33]
90	335.1501	7.14	[M+H]+	$C_{18}H_{22}O_6$	2	1.8	303.1234, 285.1124, 275.1286, 207.0660, 195.0656, 159.0443	Mycophenolic acid methyl ester	Meroterpenoid	*Penicillium* sp.	[34]

No.	m/z value	R_t (min)	Adduct	Putative molecular formula	IC	ppm	Fragmentation pattern	Putative identification	Chemical family	Biological origin	Ref
91	629.0908	7.29	[M+H]$^+$	$C_{28}H_{16}N_6O_{12^*}$	4	0.6	593.0682, 552.0537, 534.0625, 335.0278, 253.0173	n.a.			
92	487.27	7.4	[M+H]$^+$	$C_{28}H_{38}O_7$	2	0.8	377.2110, 349.2166, 243.1750, 225.1644, 215.1801, 199.1489, 185.1326, 175.1487, 159.1171, 157.1014, 151.0391, 145.1013	Andrastin A	Meroterpenoid	*Penicillium* sp. (fungus)	[35]
93	473.254	7.52	[M+H]$^+$	$C_{27}H_{36}O_7$	3	0.2	MS2 (many ions, only >200 noted): 353.2104, **343.2300**, **311.1978**, 293.1867, 283.2126, **237.0764**, 217.1185, 209.1330, 197.0464, 191.0735, 187.1497, 185.1344, 183.1164, 177.0534, 173.1350, **171.1151**, **159.1188**, 157.0966, 145.1013, 131.0849	Citreohybridone C	Meroterpenoid	*Penicillium citreo-viride* (fungus)	[36]
94	568.2222	7.76	[M+Na]$^+$	$C_{35}H_{27}N_{7^*}$	4	-0.7	331.1059, 260.1011, 238.1237, 181.0751, 122.0594, 117.0715, 105.0346)	n.a.			
95	581.3674	7.76	[M+H]$^+$	$C_{29}H_{44}N_{10}O_{3^*}$	4	-0.3	367.2092, 237.1466	n.a.			
96	507.2307	8.03	[M+H]$^+$	$C_{33}H_{26}N_6$	2	2	256.1349, 238.1242, 224.1082, 122.0608, 117.0708, 105.0345	Asperphenamate	Phenylalanine derivative	*Penicillium* spp. (fungus)	[33]
97	376.2852	11.62	[M+H]$^+$	$C_{23}H_{37}NO_3$	4	0	138.0554, 120.0449, 92.0501	n.a.			

Table S9. Putative annotation of metabolites detected in the crude extracts of *Boeremia exigua* strain CKT91 cultivated on CAG and PDA media.
Each detected compound is given with the experimentally determined *m/z* value and the predicted putative molecular formula. Putative identifications were based on the accurate mass, predicted putative molecular formulae, the retention time (R_t in min), the fragmentation pattern and biological origin. $^\Delta$Different isomers with same *m/z* value and molecular formula, which cannot be differentiated based on MS/MS data. IC: Identification confidence level after Sumner et al. 2007 [3]. Nf: No fragmentation pattern detected or fragmentation below noise threshold of $5e^1$. n.a. = putatively novel compound (known NPs do not match). Ref = reference.

No.	*m/z* value	R_t (min)	Adduct	Putative molecular formula	IC	ppm	Fragmentation pattern	Putative identification	Chemical family	Biological origin	Medium	Ref
98	303.1199	2.67	$[M+H]^+$	$C_{12}H_{18}N_2O_7$	4	2.3	Nf	n.a.			PDA	
99	600.2635	5.78	$[M+H]^+$	$C_{24}H_{37}N_7O_{11}$	4	1	Nf	n.a.			CAG, PDA	
100	480.2745	5.92	$[M+H]^+$	$C_{29}H_{37}NO_5$	2	-1	462.2639, 444.2558, 426.2426, 416.2584, 398.2487, 378.2067, 278.1534, 264.1393, 252.1384, 240.1393, 209.1315, 187.1104, 172.0756, 159.1155 145.1000, 120.0790, 105.0688, 91.0529	Cytochalasin B2	Cytochalasan	*Phoma* sp. (fungus)	CAG, PDA	[37]
101	464.2794	6.12, 7.6, 8.39, 8.5, 9.45, 9.74$^\Delta$	$[M+H]^+$	$C_{29}H_{37}NO_4$	3	-1.5	447.2738, 446.2693, 429.2610, 428.2582, 418.2767, 410.2479, 400.2635, 281.1872 , 280.1693, 268.1689, 266.1530, 264.1843, 263.1788, 254.1529, 252.1370, 172.0747, 161.0949, 157.1004, 147.1151, 145.1000, 143.0845, 133.0997, 131.0843, 120.0798, 119.0840, 105.0687, 91.0533	Deoxaphomin	Cytochalasan	*Phoma exigua* (fungus)	CAG, PDA	[38]
102	480.2748	6.3	$[M+H]^+$	$C_{29}H_{37}NO_5$	2	-0.4	462.2648, 444.2540, 416.2583, 282.1481, 264.1377, 120.0796	Cytochalasin B	Cytochalasan	*Phoma exigua* (fungus)	CAG, PDA	[38]
103	480.2743	6.41	$[M+H]^+$	$C_{29}H_{37}NO_5$	2	-1.5	462.2609, 444.2491, 240.1376, 212.1434, 195.1154, 120.0796	Cytochalasin B6	Cytochalasan	*Phoma* sp. (fungus)	CAG, PDA	[39]
104	480.2746	7	$[M+H]^+$	$C_{29}H_{37}NO_5$	2	-0.8	462.2639, 444.2563, 398.2440, 278.1548, 264.1373, 240.1374, 226.1206, 200.1076, 186.1276, 159.1150, 145.1015, 133.1019, 120.0789, 91.0525	Cytochalasin B4	Cytochalasan	*Phoma* sp. (fungus)	CAG, PDA	[39]
105	510.2865	7.09	$[M+H]^+$	$C_{30}H_{39}NO_6$	2	1.8	478.2596, 460.2494, 442.2400, 414.2450, 406.2306, 396.2238, 388.2231, 376.1968, 278.1477, 264.1334, 240.1387, 209.1319, 186.0871, 149.0972, 131.0830, 119.0824	Cytochalasin Z11	Cytochalasan	*Endothia gyrosa* (fungus)	PDA	[40]
106	478.2589	7.24	$[M+H]^+$	$C_{29}H_{35}NO_5$	2	-0.8	460.2487, 442.2378, 432.2536, 414.2420, 278.1541, 266.1538, 264.1380, 252.1379, 250.1227, 240.1375, 198.0917, 185.0943, 172.0744, 157.1004, 145.1001, 143.0848, 133.1000, 131.0834, 120.0796, 119.0846, 105.0692, 91.0534	Cytochalasin B3	Cytochalasan	*Phoma* sp. (fungus)	CAG, PDA	[39]
107	448.2843	8.7, 10.98$^\Delta$	$[M+H]^+$	$C_{29}H_{37}NO_3$	3	-2	449.2923, 430.2736, 229.1962, 215.1794, 200.0701, 172.0741, 121.1012, 109.1021, 107.0821, 95.0857	Deoxaphomin C	Cytochalasan	*Phoma* sp. (fungus)	CAG, PDA	[37]

No.	m/z value	R_t (min)	Adduct	Putative molecular formula	IC	ppm	Fragmentation pattern	Putative identification	Chemical family	Biological origin	Medium	Ref
108	355.2838	9.78	$[M+H]^+$	$C_{21}H_{38}O_4$	4	-2.8	337.2741, 263.2357, 245.2267, 213.9730, 175.1456, 163.1457, 149.1315, 135.1169, 123.1169, 121.0997, 116.0520, 109.1000, 97.0990, 81.0698	n.a.			PDA	
109	427.3204	10.2	$[M+H]^+$	$C_{28}H_{42}O_3$	2	-1.9	409.3159, 391.3037, 283.1731, 125.1308, 69.0689	Dankasterone B	Ergosterol	*Gymnascella dankaliensis* (fungus)	PDA	[41]
110	432.2898	10.5	$[M+H]^+$	$C_{29}H_{37}NO_2$	2	-1.2	241.1952, 217.1948, 200.0696, 172.0747, 147.1157, 121.1003, 109.0999	Proxiphomin	Cytochalasan	*Phoma* sp. (fungus)	CAG, PDA	[39]
111	395.3304	11.82	$[M+H]^+$	$C_{28}H_{42}O$	4	-2.5	311.2373, 307.2408, 293.2247, 251.1765, 211.1485, 199.1459, 159.1105, 109.1014, 83.0846, 69.0697	n.a.			PDA	

Table S10. Putative annotation of metabolites detected in the crude extracts of *Streptomyces* sp. strain CKT43 cultivated on GYM and MB media. Each detected compound is given with the experimentally determined *m/z* value and the predicted putative molecular formula. Putative identifications were based on the accurate mass, predicted putative molecular formulae, the retention time (R_t in min), the fragmentation pattern and biological origin. *Only putative molecular formula with best ppm shown (more than 1 molecular formula possible). IC: Identification confidence level after Sumner et al. 2007 [3]. Nf: No fragmentation pattern detected or fragmentation below noise threshold of $5e^1$. n.a. = putatively novel compound (known NPs do not match). Ref = reference.

No.	*m/z* value	R_t (min)	Adduct	Putative molecular formula	IC	ppm	Fragmentation pattern	Putative identification	Chemical family	Biological origin	Medium	Ref
112	160.0767	1.45	[M+H]$^+$	$C_{10}H_9NO$	4	3.1	132.0818	n.a.			MB	
113	265.1423	3.72	[M+H]$^+$	$C_{11}H_{16}N_6O_2$	4	3.8	Nf	n.a.			MB, GYM	
114	263.1251	4.01	[M+H]$^+$	$C_{11}H_{14}N_6O_2$	4	-1.9	Nf	n.a.			MB, GYM	
115	263.1249	4.12	[M+H]$^+$	$C_{11}H_{14}N_6O_2$	4	-2.7	Nf	n.a.			MB, GYM	
116	235.1317	4.51	[M+H]$^+$	$C_{10}H_{14}N_6O$	4	4.3	195.1388, 177.1278	n.a.			MB	
117	235.1319	4.85	[M+H]$^+$	$C_{10}H_{14}N_6O$	4	5.1	195.1378, 177.1292	n.a.			MB	
118	743.4458	4.76	[M+H]$^+$	$C_{37}H_{58}N_8O_8*$	4	0.3	341.2543, 298.2151, 284.1961, 276.1321, 157.0986, 86.0920	n.a.			GYM	
119	233.1158	5.08	[M+H]$^+$	$C_{10}H_{12}N_6O$	4	2.6	157.9664	n.a.			MB	
120	249.1475	5.19	[M+H]$^+$	$C_{11}H_{16}N_6O$	4	4.4	209.1536, 191.1433, 163.1482	n.a.			MB, GYM	
121	249.1472	5.3	[M+H]$^+$	$C_{11}H_{16}N_6O$	4	3.2	209.1569, 191.1430	n.a.			GYM	
122	221.191	5.38	[M+H]$^+$	$C_{15}H_{24}O$	4	2.3	203.1797, 147.1173, 141.9590, 97.9693	n.a.			MB	
123	225.1501	5.52	[M+H]$^+$	$C_{13}H_{20}O_3$	2	4.4	207.1390, 197.1548, 189.1286, 179.1438, 165.1284, 161.1334, 151.0760, 147.1176, 147.0811, 137.0605. 133.0656, 125.0604, 119.0864, 107.0862, 107.0500, 105.0706	MKN-003A	Butenolide	*Streptomyces* sp. (bacterium)	MB, GYM	[42]
124	227.1656	5.75	[M+H]$^+$	$C_{13}H_{22}O_3$	3	4	Nf	MKN-003C	Butenolide	*Streptomyces* sp. (bacterium)	MB	[42]
125	955.5981	5.75	[M+H]$^+$	$C_{48}H_{78}N_{10}O_{10}$ Or $C_{46}H_{66}N_{24}*$	4	0.3	626.3671, 539.3618, 511.3620, 470.2799, 468.3213, 428.2272, 412.2930, 400.2314, 371.2073, 369.2507, 357.1931, 355.2360, 341.2551, 324.2289, 313.2219, 308.2020, 300.1698, 298.2097, 284.1980, 272.1780, 270.1830, 259.1266, 256.1674, 253.1931, 242.1522, 239.1759, 231.1698, 230.1304, 213.1609, 211.1805, 211.1448, 199.447, 197.1678, 187.0869, 185.1291, 171.1505, 171.1134, 159.0932, 157.0972, 143.1185, 86.0971	n.a.			MB	

No.	*m/z* value	R$_t$ (min)	Adduct	Putative molecular formula	IC	ppm	Fragmentation pattern	Putative identification	Chemical family	Biological origin	Medium	Ref
126	898.6118	6.02	[M+H]$^+$	C$_{47}$H$_{79}$N$_9$O$_8$	2	-1.3	785.5298, 615.4265, 445.2813, 412.2908, 397.2446, 332.1974, 298.2133, 284.1965, 261.1606, 253.1929, 233.1674, 228.1719, 213.1601, 199.1820, 197.1653, 185.1291, 157.1363, 155.1204, 129.1028, 86.0971, 84.0820	Surugamide B	Cyclic octapeptide	*Streptomyces* sp. (bacterium)	MB, GYM	[43]
127	898.6117	6.1	[M+H]$^+$	C$_{47}$H$_{79}$N$_9$O$_8$	2	-1.4	686.4632, 615.4197, 554.3472, 397.2428, 369.2845, 298.2137, 284.1965, 261.1610, 233.1666, 227.1764, 213.1611, 197.1669, 185.1291, 171.1122, 129.1036, 86.0971, 84.0809	Surugamide C	Cyclic octapeptide	*Streptomyces* sp. (bacterium)	MB, GYM	[43]
128	898.6121	6.18	[M+H]$^+$	C$_{47}$H$_{79}$N$_9$O$_8$	2	-1	785.5309, 601.4060, 502.3380, 445.2841, 431.2659, 397.2429, 374.2444, 369.2854, 360.2286, 332.1981, 261.1602, 253.1920, 242.1852, 239.1767, 233.1660, 199.1831, 157.1340, 129.1031, 120.0808, 86.0979, 84.0811	Surugamide D	Cyclic octapeptide	*Streptomyces* sp. (bacterium)	MB, GYM	[43]
129	912.6266	6.29	[M+H]$^+$	C$_{48}$H$_{81}$N$_9$O$_8$	2	-2.2	445.2818, 374.2439, 298.2127, 261.1596, 129.1012	Surugamide A	Cyclic octapeptide	*Streptomyces* sp. (bacterium)	MB, GYM	[43]
130	448.3065	6.61	[M+H]$^+$	C$_{26}$H$_{41}$NO$_{5*}$	4	0.4	430.2956, 412.2844, 355.2642, 337.2538, 319.2439, 213.1642	n.a.			MB	
131	389.2693	6.79	[M+H]$^+$	C$_{24}$H$_{36}$O$_4$	4	0.3	371.2574, 353.2473, 335.2369, 325.2511, 317.2269, 239.1788, 229.1589, 177.1292, 109.0649, 97.0651	n.a.			MB	
132	1054.629	6.97	[M+H]$^+$	C$_{51}$H$_{87}$N$_7$O$_{16*}$	4	0.2	Nf	n.a.			MB	
133	669.4541	7.43	[M+H]$^+$	C$_{32}$H$_{64}$N$_2$O$_{12*}$	4	0.4	339.2649, 313.1871, 297.1458, 240.0987, 228.2325, 203.1395, 186.1132	n.a.			MB	
134	600.1503	7.51	[M+H]$^+$	C$_{30}$H$_{13}$N$_{15}$O$_*$	4	-0.3	550.1147, 540.1298, 522.1205	n.a.			GYM	
135	683.4688	7.84	[M+H]$^+$	C$_{31}$H$_{54}$N$_{16}$O$_2$ Or C$_{33}$H$_{66}$N$_2$O$_{12*}$	4	-0.9	353.2797, 313.1877, 297.1457, 242.2488, 240.0988, 203.1399, 186.1134	n.a.			MB	
136	683.4688	7.9	[M+H]$^+$	C$_{31}$H$_{54}$N$_{16}$O$_2$ Or C$_{33}$H$_{66}$N$_2$O$_{12*}$	4	-0.9	353.2797, 313.1878, 297.1456, 242.2488, 240.0988, 203.1399, 186.1132	n.a.			MB	
137	697.4856	8.33	[M+H]$^+$	C$_{34}$H$_{68}$N$_2$O$_{12*}$	4	0.7	313.1876, 297.1454, 256.2643, 240.0979, 203.1400, 186.1130	n.a.			MB	
138	315.2528	8.38	[M+H]$^+$	C$_{18}$H$_{34}$O$_4$	4	-2.2	97.1003, 83.0846, 75.0433	n.a.			MB, GYM	
139	315.2523	8.46	[M+H]$^+$	C$_{18}$H$_{34}$O$_4$	4	-3.8	111.1182, 97.1002, 83.0843, 75.0430	n.a.			MB, GYM	
140	205.1964	8.71	[M+H]$^+$	C$_{15}$H$_{24}$	4	3.9	149.1333, 135.1174, 123.1174, 121.1017, 109.1018, 107.0859, 95.0865	n.a.			MB, GYM	

No.	*m/z* value	R_t (min)	Adduct	Putative molecular formula	IC	ppm	Fragmentation pattern	Putative identification	Chemical family	Biological origin	Medium	Ref
141	219.1741	9.03	[M+H]+	$C_{15}H_{22}O$	3	-3.7	177.1264, 163.1107, 149.0943	Anaephene A	Alkylphenol derivative	*Hormoscilla* sp. (bacterium)	MB, GYM	[44]
142	357.2634	9.32	[M+H]+	$C_{20}H_{36}O_5$	4	-2	117.0534, 83.0846	n.a.			GYM	
143	785.3582	9.32	[M+H]+	$C_{33}H_{36}N_{24}O$*	4	0	Nf	n.a.			MB, GYM	
144	799.3724	9.67	[M+H]+	$C_{33}H_{42}N_{20}O_5$ Or $C_{35}H_{54}N_6O_{15}$*	4	-0.1	711.3188	n.a.			GYM	
145	507.2712	9.79	[M+H]+	$C_{26}H_{38}N_2O_8$	2	1.2	237.0884, 136.0401	Deformylated antimycin A2a	Macrolide	*Streptomyces* sp. (bacterium)	MB	[45]
146	521.2866	10.2	[M+H]+	$C_{27}H_{40}N_2O_8$	2	0.6	237.0881, 136.0396	Deformylated antimycin A1a	Macrolide	*Streptomyces* sp. (bacterium)	MB, GYM	[45]
147	343.2843	10.24	[M+H]+	$C_{20}H_{38}O_4$	4	-1.5	325.2723, 251.2372, 233.2257, 163.1481, 149.1321, 135.1162, 121.1004, 109.1017, 107.0851, 97.0989, 95.0828, 81.0697	n.a.			GYM	
148	331.2845	10.31	[M+H]+	$C_{19}H_{38}O_4$	4	-0.9	Nf	n.a.			GYM	

206

References

1. Altschul, S.F.; Gish, W.; Miller, W.; Myers, E.W.; Lipman, D.J. Basic local alignment search tool. *J. Mol. Biol.* **1990**, *215*, 403-410, doi: 10.1016/S0022-2836(05)80360-2.

2. Wang, Q.; Garrity, G.M.; Tiedje, J.M.; Cole, J.R. Naive Bayesian classifier for rapid assignment of rRNA sequences into the new bacterial taxonomy. *Appl. Environ. Microbiol.* **2007**, *73*, 5261-5267, doi: 10.1128/AEM.00062-07.

3. Sumner, L.W.; Amberg, A.; Barrett, D.; Beale, M.H.; Beger, R.; Daykin, C.A.; Fan, T.W.; Fiehn, O.; Goodacre, R.; Griffin, J.L.*, et al.* Proposed minimum reporting standards for chemical analysis Chemical Analysis Working Group (CAWG) Metabolomics Standards Initiative (MSI). *Metabolomics* **2007**, *3*, 211-221, doi: 10.1007/s11306-007-0082-2.

4. Seibert, S.F.; Eguereva, E.; Krick, A.; Kehraus, S.; Voloshina, E.; Raabe, G.; Fleischhauer, J.; Leistner, E.; Wiese, M.; Prinz, H.*, et al.* Polyketides from the marine-derived fungus *Ascochyta salicorniae* and their potential to inhibit protein phosphatases. *Org. Biomol. Chem.* **2006**, *4*, 2233-2240, doi: 10.1039/b601386d.

5. Niu, S.; Xia, J.M.; Li, Z.; Yang, L.H.; Yi, Z.W.; Xie, C.L.; Peng, G.; Luo, Z.H.; Shao, Z.; Yang, X.W. Aphidicolin chemistry of the deep-sea-derived fungus *Botryotinia fuckeliana* MCCC 3A00494. *J. Nat. Prod.* **2019**, *82*, 2307-2331, doi: 10.1021/acs.jnatprod.9b00705.

6. Yang, K.L.; Wei, M.Y.; Shao, C.L.; Fu, X.M.; Guo, Z.Y.; Xu, R.F.; Zheng, C.J.; She, Z.G.; Lin, Y.C.; Wang, C.Y. Antibacterial anthraquinone derivatives from a sea anemone-derived fungus *Nigrospora* sp. *J. Nat. Prod.* **2012**, *75*, 935-941, doi: 10.1021/np300103w.

7. Li, X.; Li, X.-D.; Li, X.-M.; Xu, G.-M.; Liu, Y.; Wang, B.-G. Wentinoids A–F, six new isopimarane diterpenoids from *Aspergillus wentii* SD-310, a deep-sea sediment derived fungus. *RSC Adv.* **2017**, *7*, 4387-4394, doi: 10.1039/c6ra27209f.

8. Liu, J.; Zhang, D.; Zhang, M.; Liu, X.; Chen, R.; Zhao, J.; Li, L.; Wang, N.; Dai, J. Periconiasins I and J, two new cytochalasans from an endophytic fungus *Periconia* sp. *Tetrahedron Lett.* **2016**, *57*, 5794-5797, doi: 10.1016/j.tetlet.2016.11.038.

9. Chen, S.; Zhang, Y.; Niu, S.; Liu, X.; Che, Y. Cytotoxic cleistanthane and cassane diterpenoids from the entomogenous fungus *Paraconiothyrium hawaiiense*. *J. Nat. Prod.* **2014**, *77*, 1513-1518, doi: 10.1021/np500302e.

10. Kuppers, L.; Ebrahim, W.; El-Neketi, M.; Ozkaya, F.C.; Mandi, A.; Kurtan, T.; Orfali, R.S.; Muller, W.E.G.; Hartmann, R.; Lin, W.*, et al.* Lactones from the sponge-derived fungus *Talaromyces rugulosus*. *Mar. Drugs* **2017**, *15*, 359, doi: 10.3390/md15110359.

11. Sugie, Y.; Hirai, H.; Kachi-Tonai, H.; Kim, Y.J.; Kojima, Y.; Shiomi, Y.; Sugiura, A.; Sugiura, A.; Suzuki, Y.; Yoshikawa, N.*, et al.* New pyrrolizidinone antibiotics CJ-16,264 and CJ-16,367. *J. Antibiot. (Tokyo)* **2001**, *54*, 917-925, doi: 10.7164/antibiotics.54.917.

12. MacKinnon, S. Components from the phytotoxic extract of *Alternaria brassicicola*, a black spot pathogen of canola. *Phytochemistry* **1999**, *51*, 215-221, doi: 10.1016/s0031-9422(98)00732-8.

13. Du, L.; Li, D.; Zhu, T.; Cai, S.; Wang, F.; Xiao, X.; Gu, Q. New alkaloids and diterpenes from a deep ocean sediment derived fungus *Penicillium* sp. *Tetrahedron* **2009**, *65*, 1033-1039, doi: 10.1016/j.tet.2008.11.078.

14. Lin, W.H.; Li, J.; Fu, H.Z.; Proksch, P. Four novel hydropyranoindeno-derivatives from marine fungus *Aspergillus versicolor*. *Chin. Chem. Lett.* **2001**, *12*, 435-438.

15. Ghisalberti, E.L.; Hockless, D.C.; Rowland, C.; White, A.H. Harziandione, a new class of diterpene from *Trichoderma harzianum*. *J. Nat. Prod.* **1992**, *55*, 1690-1694, doi: 10.1021/np50089a023.

16. Zhang, P.-L.; Han, Y.; Zhang, L.-T.; Wang, X.-L.; Shen, T.; Ren, D.; Lou, H.; Wang, X.-N. Botrysphones A–C and botrysphins A–F, triketides and diterpenoids from the fungus *Botrysphaeria laricina*. *J. Nat. Prod.* **2017**, *80*, 1791-1797, doi: 10.1021/acs.jnatprod.6b01196.

17. Zhao, D.L.; Shao, C.L.; Gan, L.S.; Wang, M.; Wang, C.Y. Chromone derivatives from a sponge-derived strain of the fungus *Corynespora cassiicola*. *J. Nat. Prod.* **2015**, *78*, 286-293, doi: 10.1021/np5009152.

18. Julianti, E.; Oh, H.; Jang, K.H.; Lee, J.K.; Lee, S.K.; Oh, D.C.; Oh, K.B.; Shin, J. Acremostrictin, a highly oxygenated metabolite from the marine fungus *Acremonium strictum*. *J. Nat. Prod.* **2011**, *74*, 2592-2594, doi: 10.1021/np200707y.

19. Li, D.H.; Cai, S.X.; Zhu, T.J.; Wang, F.P.; Xiao, X.; Gu, Q.Q. New cytotoxic metabolites from a deep-sea-derived fungus, *Phialocephala* sp., strain FL30r. *Chem. Biodivers.* **2011**, *8*, 895-901, doi: 10.1002/cbdv.201000134.

20. Huang, Z.J.; Shao, C.L.; Chen, Y.G.; She, Z.G.; Lin, Y.C.; Zhou, S.N. A new isocoumarin from mangrove endophytic fungus (No. dz17) on the South China Sea coast. *Chem. Nat. Compd.* **2007**, *43*, 655-658, doi: 10.1007/s10600-007-0221-z.

21. Chen, Y.S.; Cheng, M.J.; Hsiao, Y.; Chan, H.Y.; Hsieh, S.Y.; Chang, C.W.; Liu, T.W.; Chang, H.S.; Chen, I.S. Chemical constituents of the endophytic fungus *Hypoxylon* sp. 12F 0687 isolated from Taiwanese *Ilex formosana*. *Helv. Chim. Acta* **2015**, *98*, 1167-1176, doi: 10.1002/hlca.201500048.

22. Tang, Y.; Liu, Y.; Ruan, Q.; Zhao, M.; Zhao, Z.; Cui, H. Aspermeroterpenes A-C: Three meroterpenoids from the marine-derived fungus *Aspergillus terreus* GZU-31-1. *Org. Lett.* **2020**, *22*, 1336-1339, doi: 10.1021/acs.orglett.9b04648.

23. Xia, X.; Zhang, J.; Zhang, Y.; Wei, F.; Liu, X.; Jia, A.; Liu, C.; Li, W.; She, Z.; Lin, Y. Pimarane diterpenes from the fungus *Epicoccum* sp. HS-1 associated with *Apostichopus japonicus*. *Bioorg. Med. Chem. Lett.* **2012**, *22*, 3017-3019, doi: 10.1016/j.bmcl.2012.01.055.

24. McGovern, E.P.; Bentley, R. Biosynthesis of flaviolin and 5,8-dihydroxy-2,7-dimethoxy-1,4-naphthoquinone. *Biochemistry* **1975**, *14*, 3138-3143, doi: 10.1021/bi00685a016.

25. Xia, G.Y.; Wang, L.Y.; Xia, H.; Wu, Y.Z.; Wang, Y.N.; Lin, P.C.; Lin, S. Three new polyketides from the endophytic fungus *Penicillium purpurogenum*. *J. Asian Nat. Prod. Res.* **2020**, *22*, 233-240, doi: 10.1080/10286020.2019.1699535.

26. Qi, J.; Shao, C.L.; Li, Z.Y.; Gan, L.S.; Fu, X.M.; Bian, W.T.; Zhao, H.Y.; Wang, C.Y. Isocoumarin derivatives and benzofurans from a sponge-derived *Penicillium* sp. fungus. *J. Nat. Prod.* **2013**, *76*, 571-579, doi: 10.1021/np3007556.

27. Cui, C.B.; Ubukata, M.; Kakeya, H.; Onose, R.; Okada, G.; Takahashi, I.; Isono, K.; Osada, H. Acetophthalidin, a novel inhibitor of mammalian cell cycle, produced by a fungus isolated from a sea sediment. *J. Antibiot. (Tokyo)* **1996**, *49*, 216-219, doi: 10.7164/antibiotics.49.216.

28. Kakinuma, N.; Iwai, H.; Takahashi, S.; Hamano, K.; Yanagisawa, T.; Nagai, K.; Tanaka, K.; Suzuki, K.; Kirikae, F.; Kirikae, T.*, et al.* Quinolactacins A, B and C: novel quinolone compounds from *Penicillium* sp. EPF-6. I. Taxonomy, production, isolation and biological properties. *J. Antibiot. (Tokyo)* **2000**, *53*, 1247-1251, doi: 10.7164/antibiotics.53.1247.

29. Chen, Z.; Zheng, Z.; Huang, H.; Song, Y.; Zhang, X.; Ma, J.; Wang, B.; Zhang, C.; Ju, J. Penicacids A-C, three new mycophenolic acid derivatives and immunosuppressive activities from the marine-derived fungus *Penicillium* sp. SOF07. *Bioorg. Med. Chem. Lett.* **2012**, *22*, 3332-3335, doi: 10.1016/j.bmcl.2012.02.106.

30. Pettit, G.R.; Hogan, F.; Xu, J.P.; Tan, R.; Nogawa, T.; Cichacz, Z.; Pettit, R.K.; Du, J.; Ye, Q.H.; Cragg, G.M.*, et al.* Antineoplastic agents. 536. New sources of naturally occurring cancer cell growth inhibitors from marine organisms, terrestrial plants, and microorganisms. *J. Nat. Prod.* **2008**, *71*, 438-444, doi: 10.1021/np700738k.

31. Cueto, M.; MacMillan, J.B.; Jensen, P.R.; Fenical, W. Tropolactones A–D, four meroterpenoids from a marine-derived fungus of the genus *Aspergillus*. *Phytochemistry* **2006**, *67*, 1826-1831, doi: 10.1016/j.phytochem.2006.01.008.

32. Ozkaya, F.C.; Ebrahim, W.; Klopotowski, M.; Liu, Z.; Janiak, C.; Proksch, P. Isolation and X-ray structure analysis of citreohybridonol from marine-derived *Penicillium atrovenetum*. *Nat. Prod. Res.* **2018**, *32*, 840-843, doi: 10.1080/14786419.2017.1311893.

33. Liu, Z.G.; Bao, L.; Liu, H.W.; Ren, J.W.; Wang, W.Z.; Wang, L.; Li, W.; Yin, W.B. Chemical diversity from the Tibetan Plateau fungi *Penicillium kongii* and *P. brasilianum*. *Mycology* **2018**, *9*, 10-19, doi: 10.1080/21501203.2017.1331937.

34. Xu, X.; Zhang, X.; Nong, X.; Wang, J.; Qi, S. Brevianamides and mycophenolic acid derivatives from the deep-sea-derived fungus *Penicillium brevicompactum* DFFSCS025. *Mar. Drugs* **2017**, *15*, 43, doi: 10.3390/md15020043.

35. Cheng, Z.; Xu, W.; Wang, Y.; Bai, S.; Liu, L.; Luo, Z.; Yuan, W.; Li, Q. Two new meroterpenoids and two new monoterpenoids from the deep sea-derived fungus *Penicillium* sp. YPGA11. *Fitoterapia* **2019**, *133*, 120-124, doi: 10.1016/j.fitote.2018.12.022.

36. Kosemura, S. Meroterpenoids from *Penicillium citreo-viride* B. IFO 4692 and 6200 hybrid. *Tetrahedron* **2003**, *59*, 5055-5072, doi: 10.1016/S0040-4020(03)00739-7.

37. Kim, E.L.; Li, J.L.; Dang, H.T.; Hong, J.; Lee, C.O.; Kim, D.K.; Yoon, W.D.; Kim, E.; Liu, Y.; Jung, J.H. Cytotoxic cytochalasins from the endozoic fungus *Phoma* sp. of the giant jellyfish *Nemopilema nomurai*. *Bioorg. Med. Chem. Lett.* **2012**, *22*, 3126-3129, doi: 10.1016/j.bmcl.2012.03.058.

38. Evidente, A.; Andolfi, A.; Vurro, M.; Zonno, M.C.; Motta, A. Cytochalasins Z4, Z5, and Z6, three new 24-Oxa[14]cytochalasans produced by *Phoma exigua* var. *heteromorpha*. *J. Nat. Prod.* **2003**, *66*, 1540-1544, doi: 10.1021/np030252o.

39. Kim, E.L.; Wang, H.; Park, J.H.; Hong, J.; Choi, J.S.; Im, D.S.; Chung, H.Y.; Jung, J.H. Cytochalasin derivatives from a jellyfish-derived fungus *Phoma* sp. *Bioorg. Med. Chem. Lett.* **2015**, *25*, 2096-2099, doi: 10.1016/j.bmcl.2015.03.080.

40. Xu, S.; Ge, H.M.; Song, Y.C.; Shen, Y.; Ding, H.; Tan, R.X. Cytotoxic cytochalasin metabolites of endophytic *Endothia gyrosa*. *Chem. Biodivers.* **2009**, *6*, 739-745, doi: 10.1002/cbdv.200800034.

41. Amagata, T.; Tanaka, M.; Yamada, T.; Doi, M.; Minoura, K.; Ohishi, H.; Yamori, T.; Numata, A. Variation in cytostatic constituents of a sponge-derived *Gymnascella dankaliensis* by manipulating the carbon source. *J. Nat. Prod.* **2007**, *70*, 1731-1740, doi: 10.1021/np070165m.

42. Cho, K.W.; Lee, H.S.; Rho, J.R.; Kim, T.S.; Mo, S.J.; Shin, J. New lactone-containing metabolites from a marine-derived bacterium of the genus *Streptomyces*. *J. Nat. Prod.* **2001**, *64*, 664-667, doi: 10.1021/np000599g.

43. Takada, K.; Ninomiya, A.; Naruse, M.; Sun, Y.; Miyazaki, M.; Nogi, Y.; Okada, S.; Matsunaga, S. Surugamides A-E, cyclic octapeptides with four D-amino acid residues, from a marine *Streptomyces* sp.: LC-MS-aided inspection of partial hydrolysates for the distinction of D- and L-amino acid residues in the sequence. *J. Org. Chem.* **2013**, *78*, 6746-6750, doi: 10.1021/jo400708u.

44. Brumley, D.; Spencer, K.A.; Gunasekera, S.P.; Sauvage, T.; Biggs, J.; Paul, V.J.; Luesch, H. Isolation and characterization of anaephenes A-C, alkylphenols from a filamentous cyanobacterium (*Hormoscilla* sp., Oscillatoriales). *J. Nat. Prod.* **2018**, *81*, 2716-2721, doi: 10.1021/acs.jnatprod.8b00650.

45. Zhang, W.; Che, Q.; Tan, H.; Qi, X.; Li, J.; Li, D.; Gu, Q.; Zhu, T.; Liu, M. Marine *Streptomyces* sp. derived antimycin analogues suppress HeLa cells via depletion HPV E6/E7 mediated by ROS-dependent ubiquitin-proteasome system. *Sci. Rep.* **2017**, *7*, 42180, doi: 10.1038/srep42180.

Supplementary Information accompanying Chapter 3

Supplementary Figures S1-S12

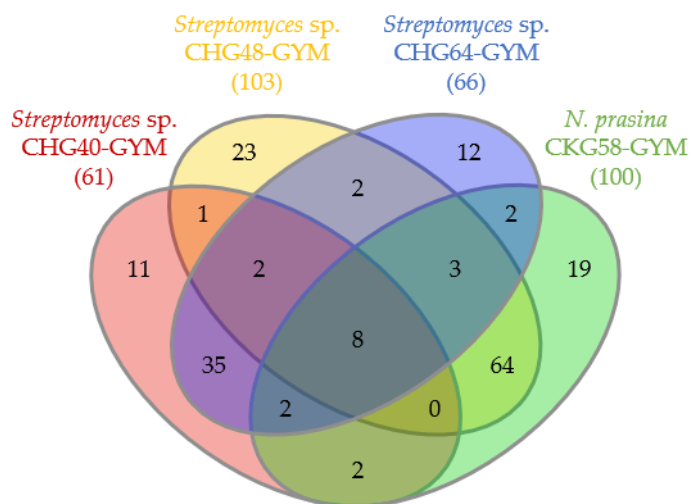## Supplementary Tables S1-S10
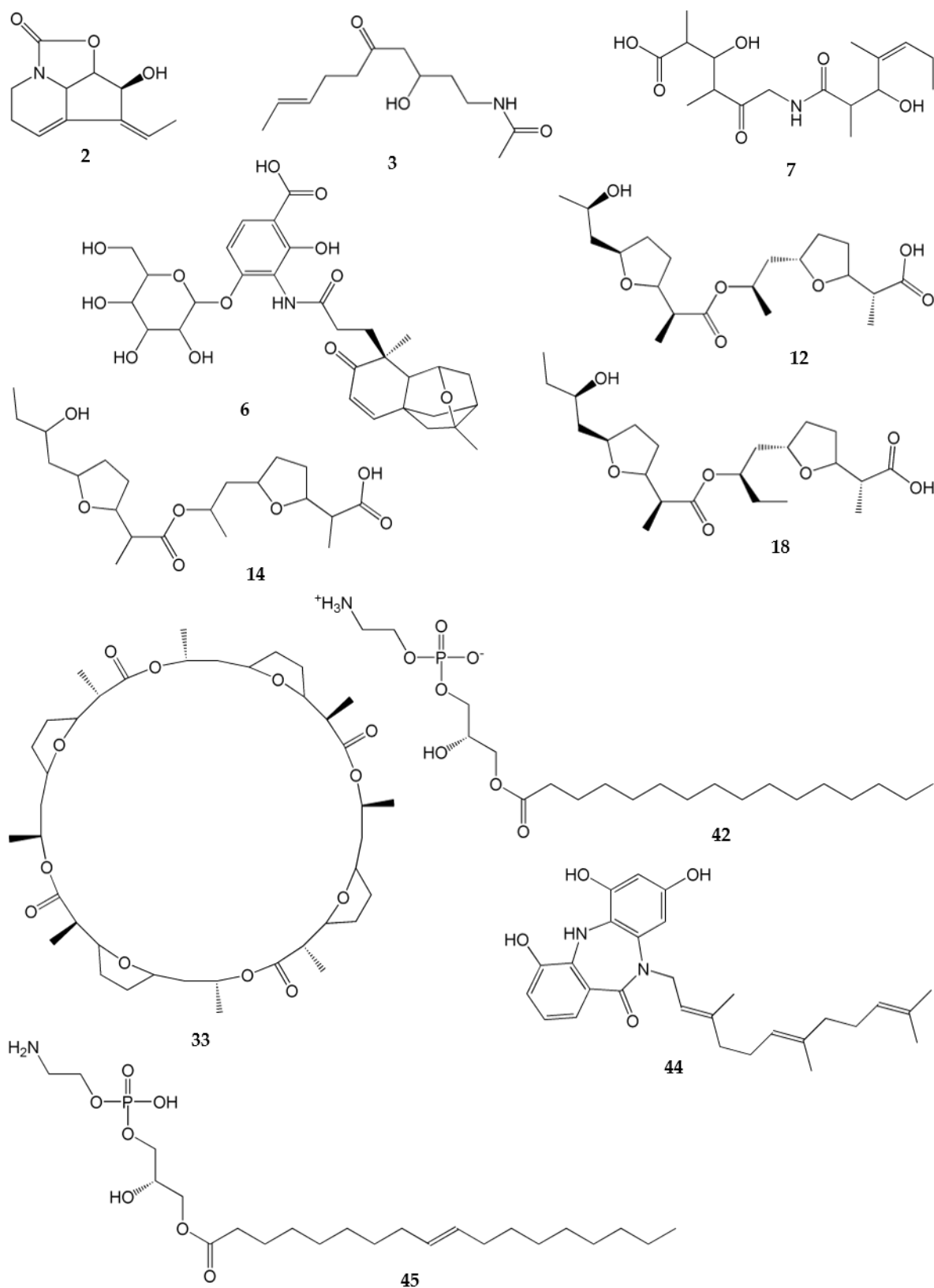
Supplementary References 1-65

Figure S1. Venn diagram of exclusive and shared peaks of three *Streptomyces* sp. extracts (CHG40-GYM, CHG48-GYM, CHG64-GYM) and one *N. prasina* extract (CKG58-GYM).

Figure S2. Putatively identified compounds detected in crude extracts of microorganisms associated with the gut of *C. intestinalis*. Chemical structures are labelled with their respective peak number (see Tables S5-S10).
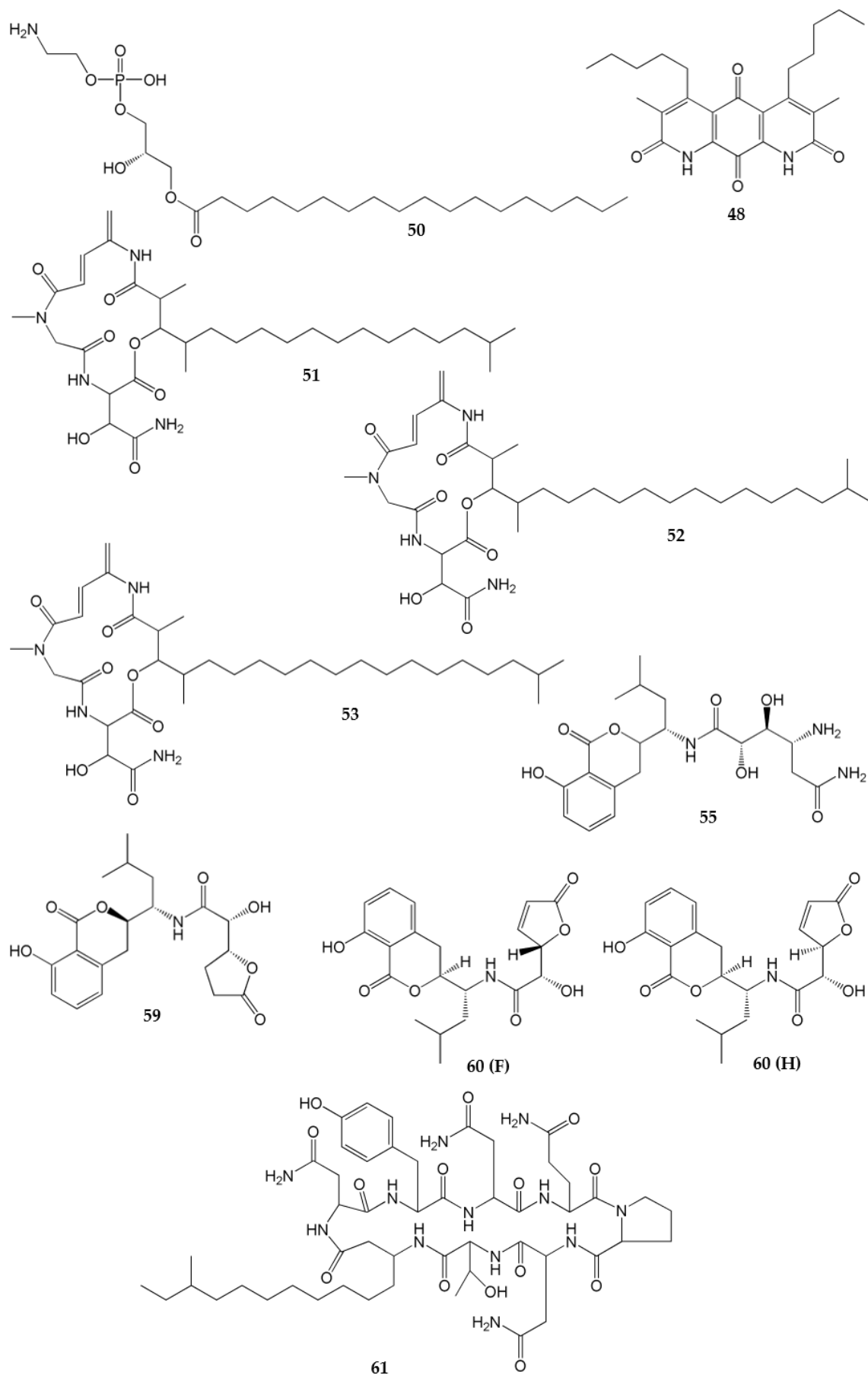
212

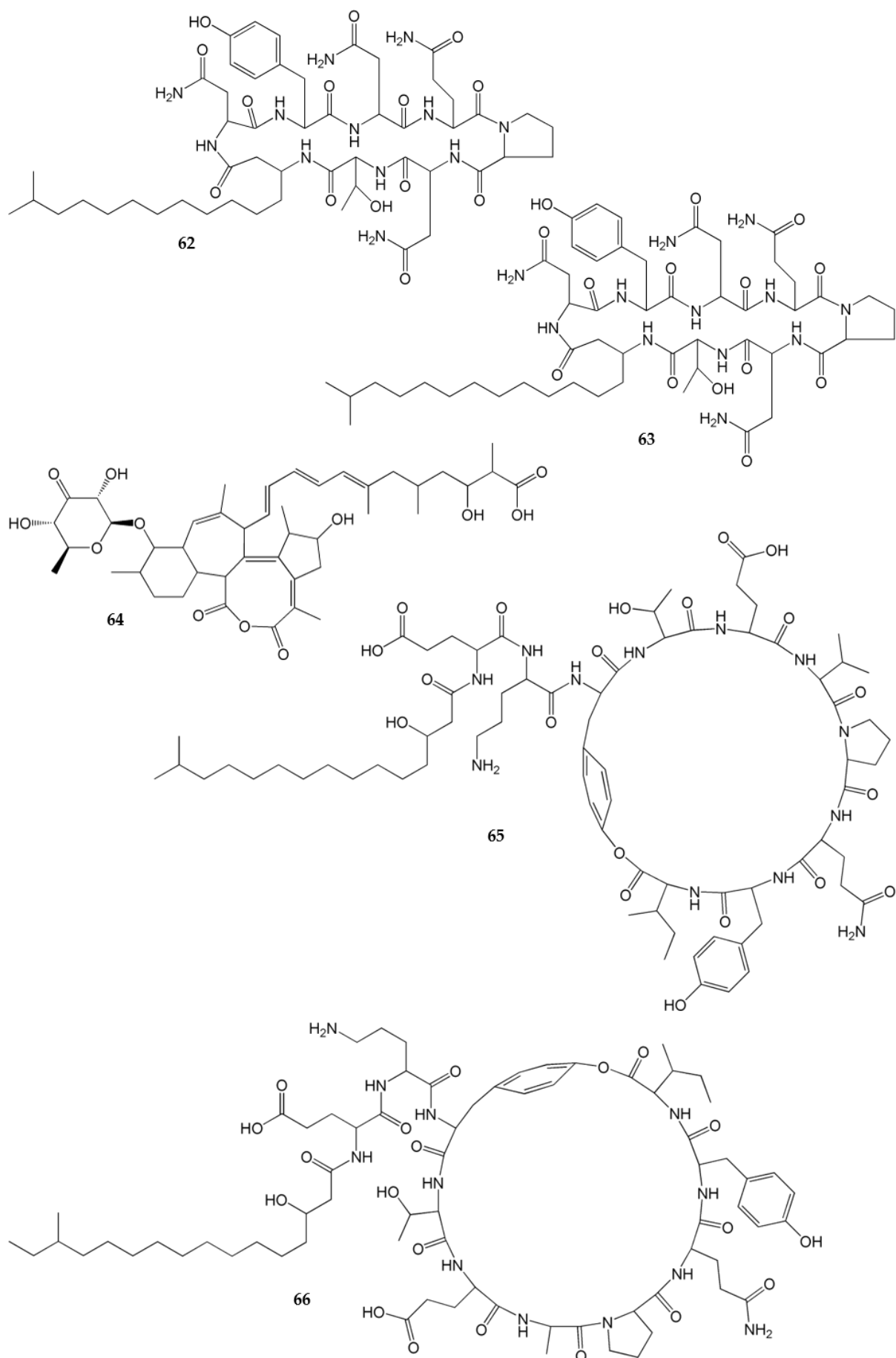**Figure S2. (continued)**

213

Figure S2. (continued)

68a

68b

69

Figure S2. (continued)

215

Figure S2. (continued)

216

Figure S2. (continued)

217

Figure S2. (continued)

110

121

125

Figure S2. (continued)

134

144

143

149

Figure S2. (continued)

220

147

150a

150b

Figure S2. (continued)

151

154a

154b

Figure S2. (continued)

155

157

Figure S2. (continued)

Figure S2. (continued)

224

Figure S2. (continued)

225

219

221

222

224a

224b

232

236

Figure S2. (continued)

226
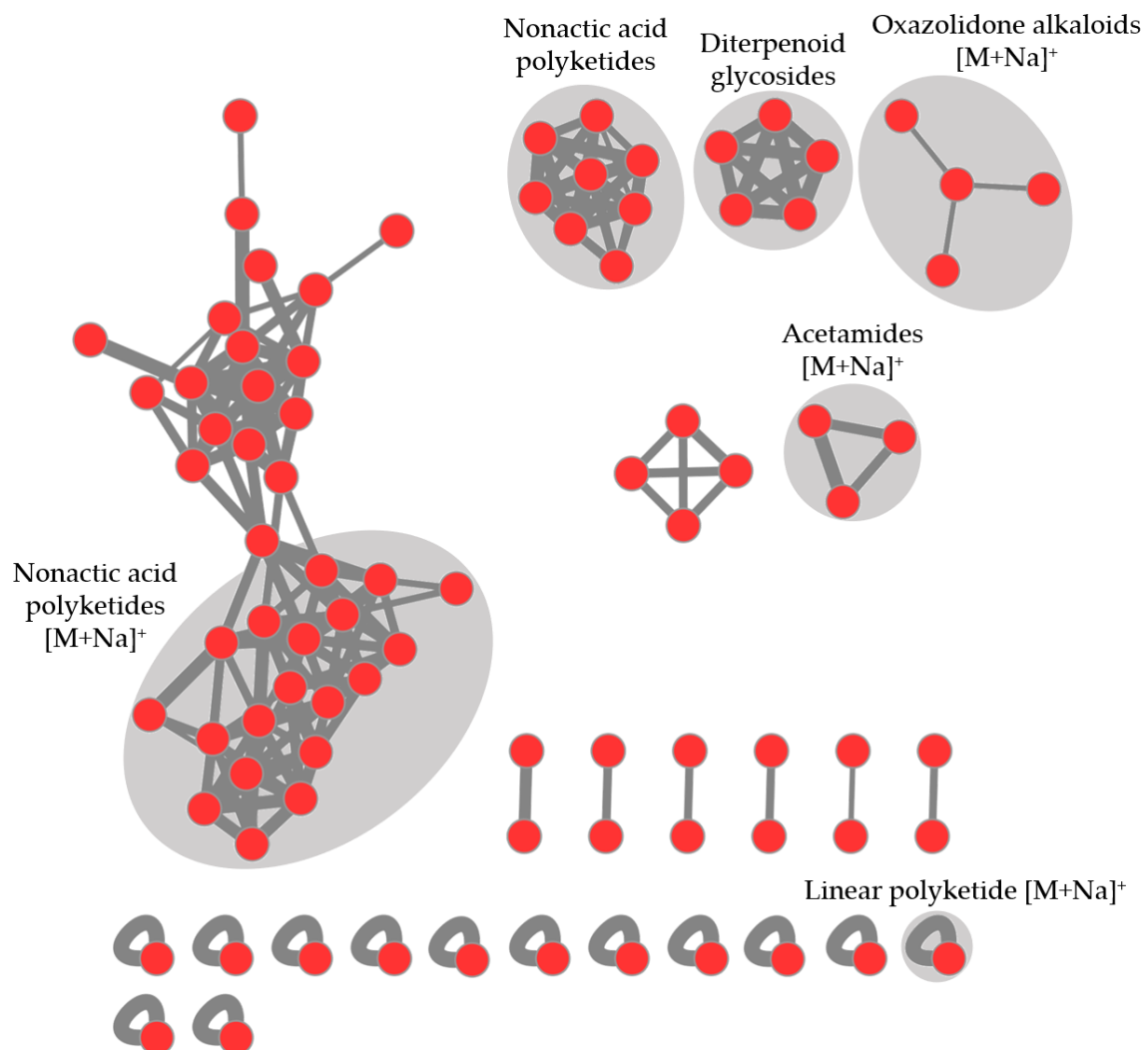
Figure S3. FBMN of *Streptomyces* sp. extract CHG48-GYM. The width of edges represents the cosine similarity between two nodes. See Table S5 for putatively annotated compounds.
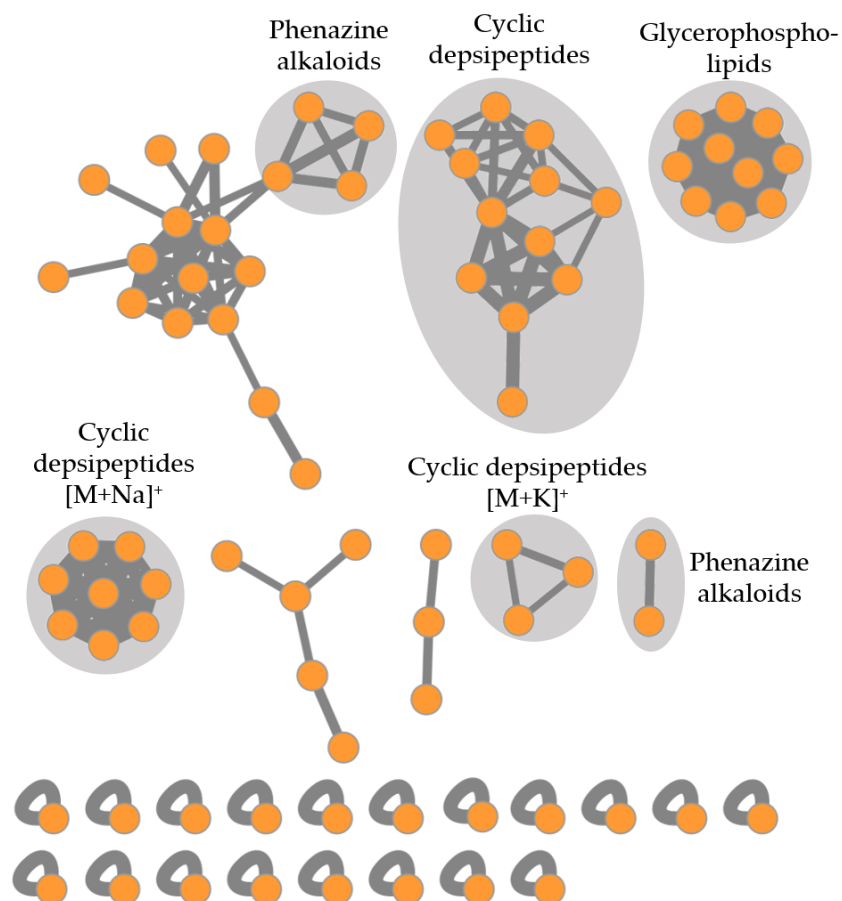
Figure S4. FBMN of *Micromonospora* sp. extract CKG20-GYM. The width of edges represents the cosine similarity between two nodes. The FBMN was generated with edges having cosine score above 0.8. See Table S6 for putatively annotated compounds.
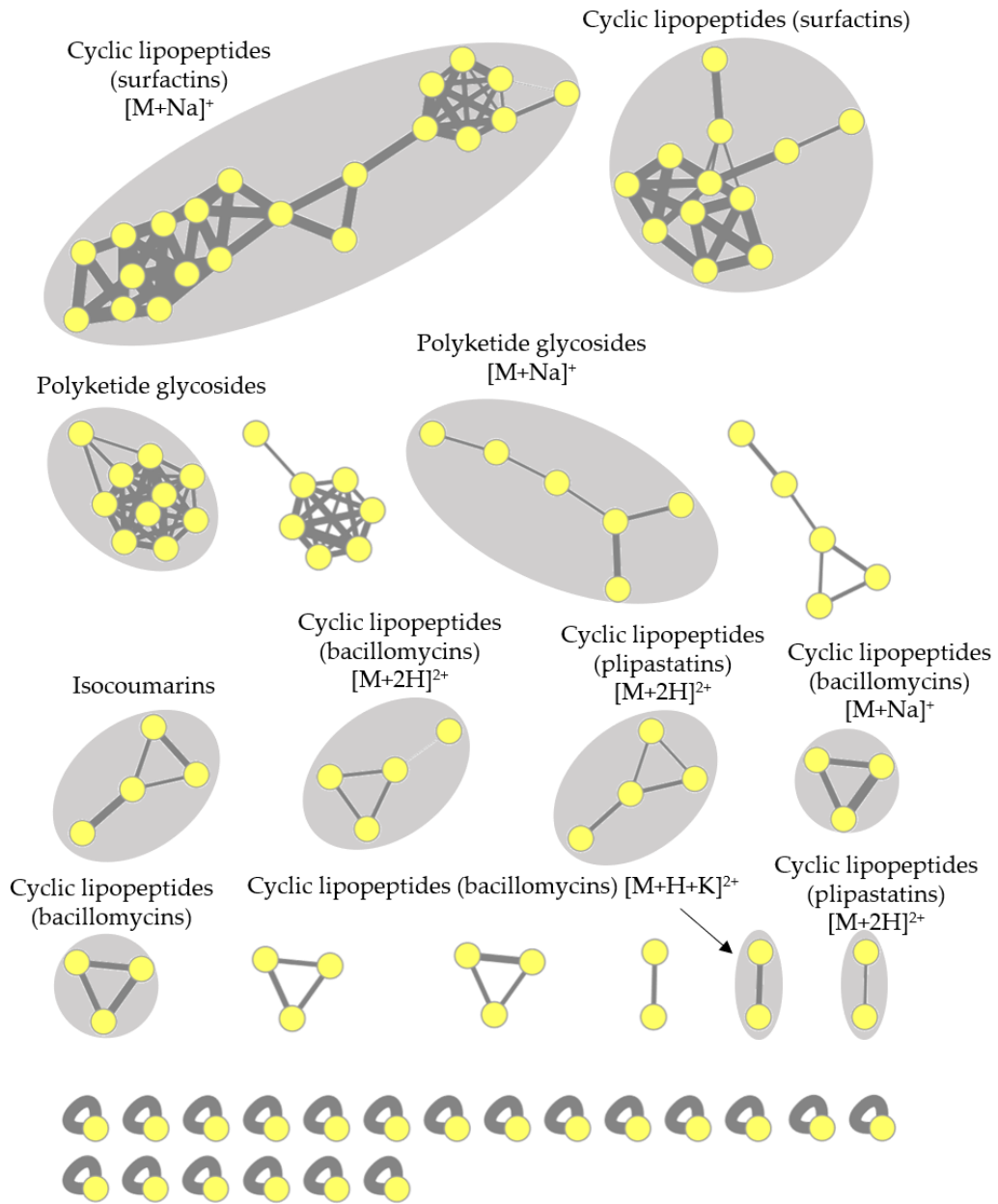
Figure S5. FBMN of *Bacillus* sp. extract CKG24-GYM. The width of edges represents the cosine similarity between two nodes. See Table S7 for putatively annotated compounds.
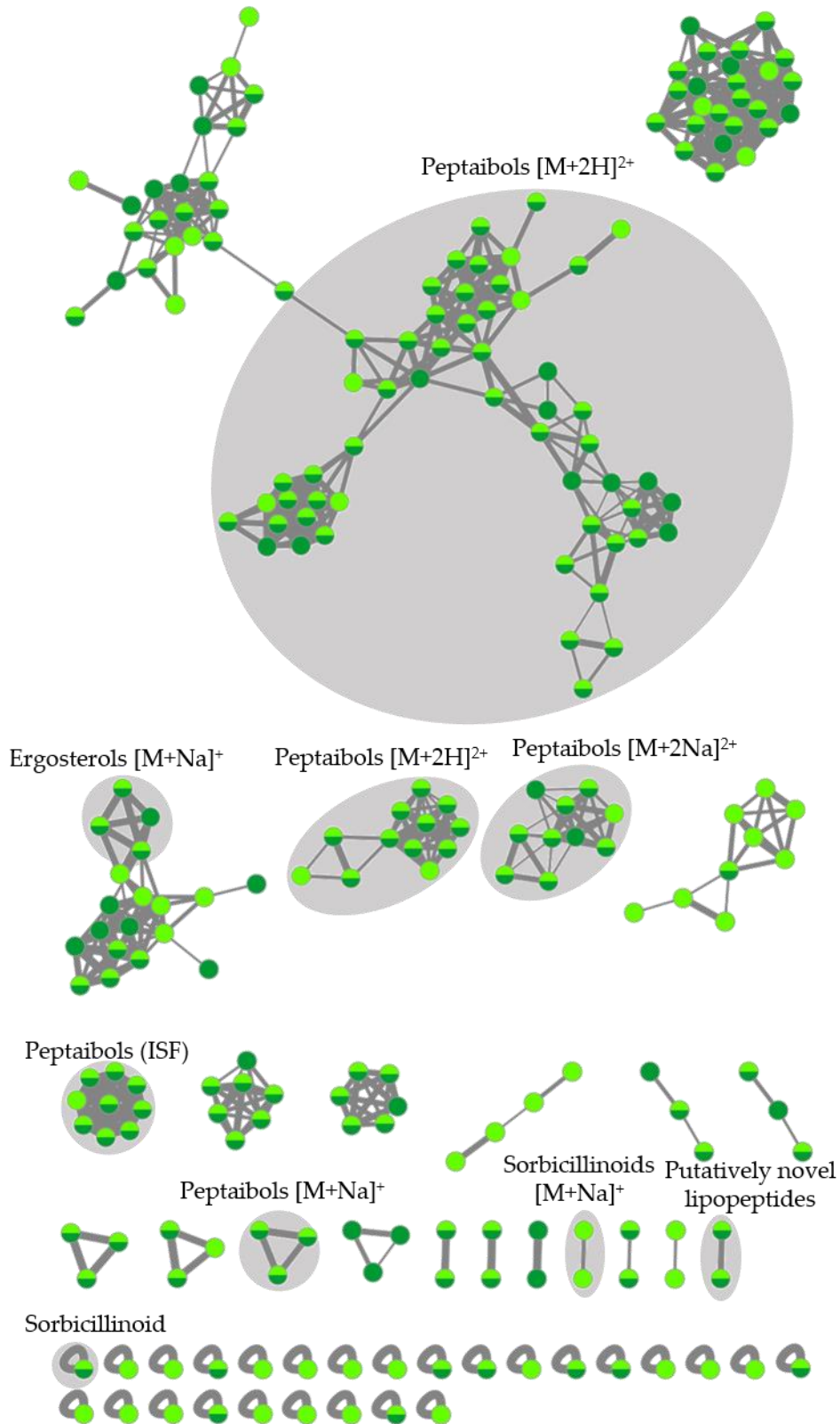
Figure S6. FBMN of *Trichoderma* sp. extracts CHG34-CAG and CHG34-PDA. The width of edges represents the cosine similarity between two nodes. Nodes are color-coded by the respective extracts: light green: CHG34-CAG, dark green: CHG34-PDA. ISF: abundant in source fragments of detected metabolites. See Table S8 for putatively annotated compounds.
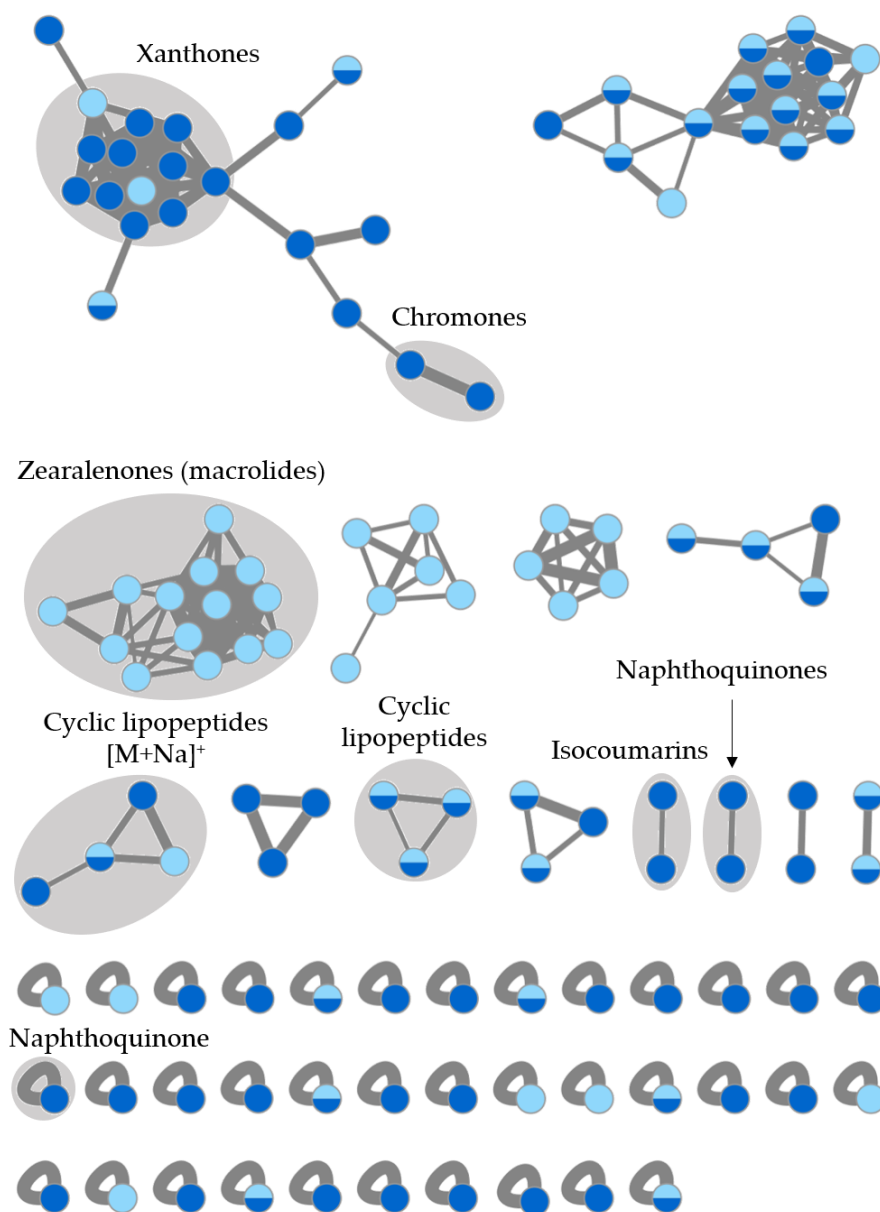
Figure S7. FBMN of *Fusarium* sp. extracts CHG38-CAG and CHG38-PDA. The width of edges represents the cosine similarity between two nodes. Nodes are color-coded by the respective extracts: light blue: CHG38-CAG, dark blue: CHG38-PDA. See Table S9 for putatively annotated compounds.
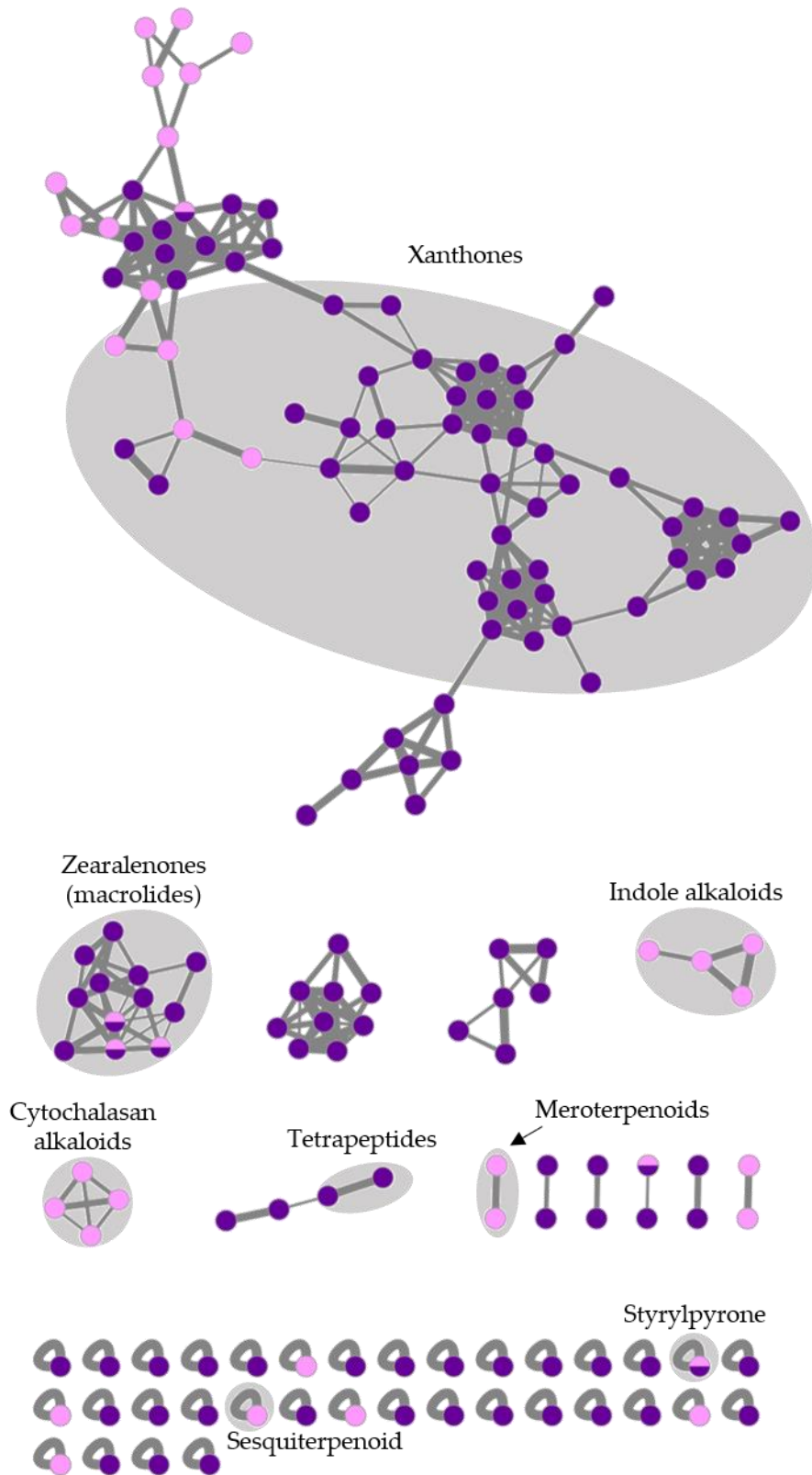
Figure S8. FBMN of *Penicillium* sp. extracts CKG23-CAG and CKG23-PDA. The width of edges represents the cosine similarity between two nodes. Nodes are color-coded by the respective extracts: light purple: CKG23-CAG, dark purple: CKG23-PDA. See Table S10 for putatively annotated compounds.
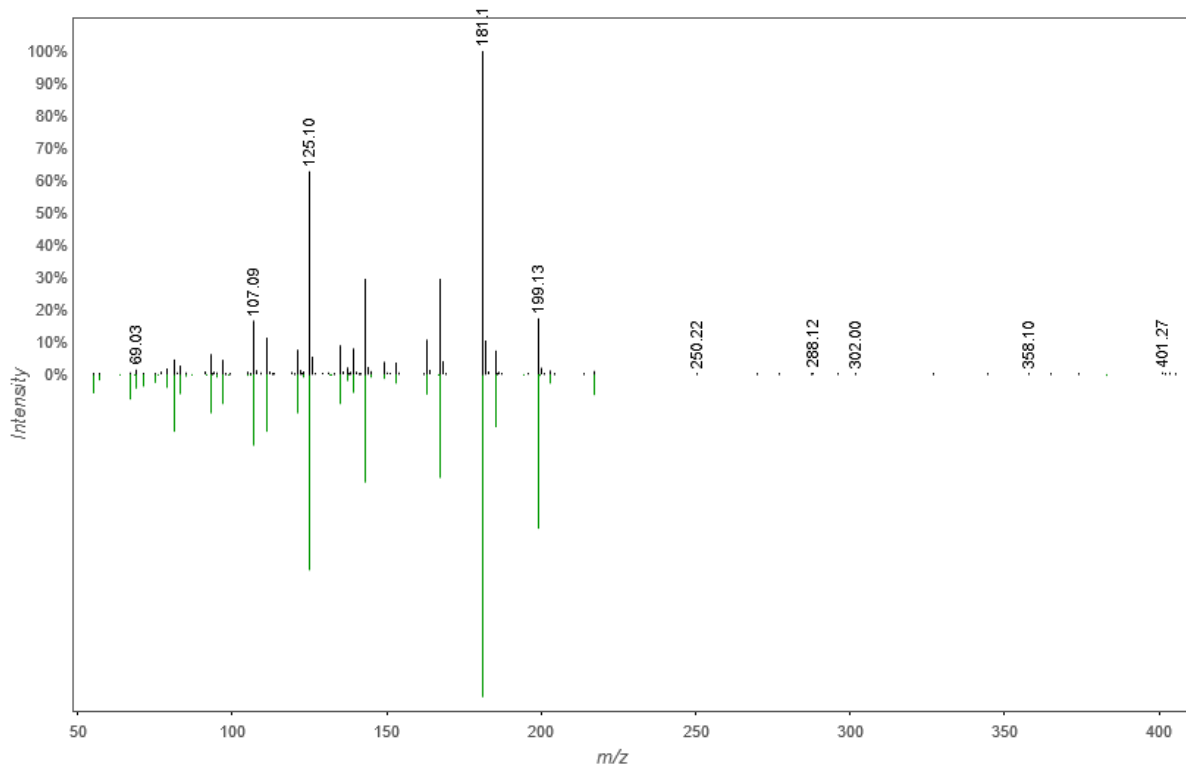
Figure S9. Experimental (black) and library (green) MS/MS spectra of bonactin (14), putatively identified in *Streptomyces* sp. extract CHG48-GYM. The spectral match was generated by the online platform GNPS [1].
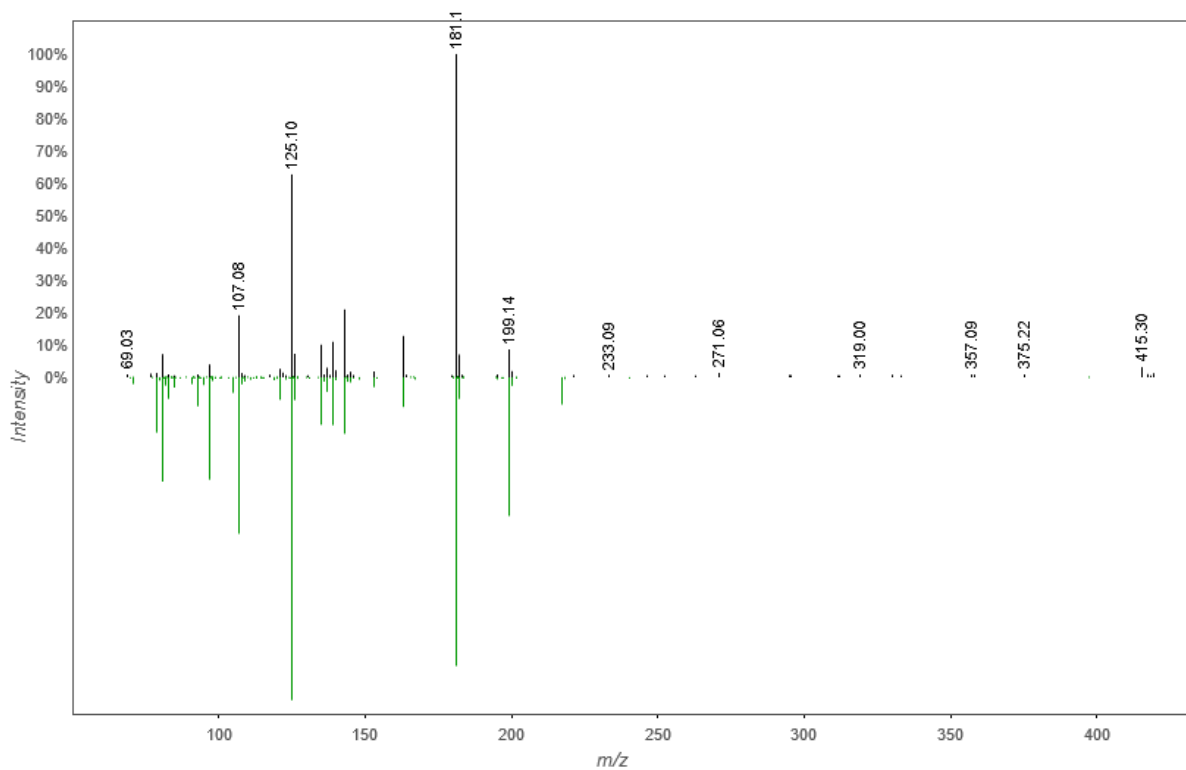
Figure S10. Experimental (black) and library (green) MS/MS spectra of homononactyl homononactate (18), putatively identified in *Streptomyces* sp. extract CHG48-GYM. The spectral match was generated by the online platform GNPS [1].

CHG34-PDA: MS/MS spectrum *m/z* 770.5386 [M+H]⁺ (**103**)
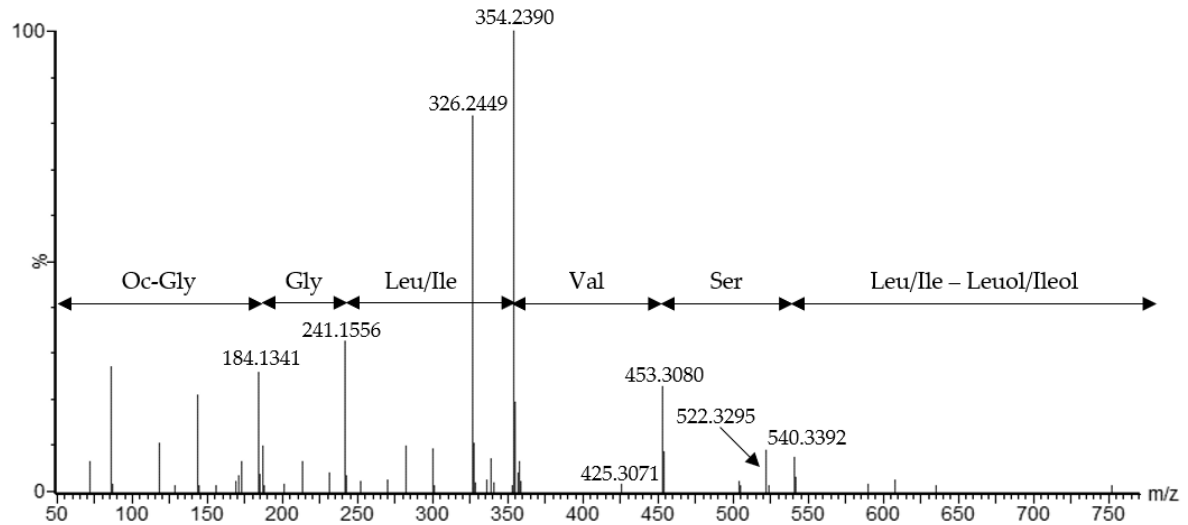
CHG34-PDA: MS/MS spectrum *m/z* 754.5424 [M+H]⁺ (**105**)
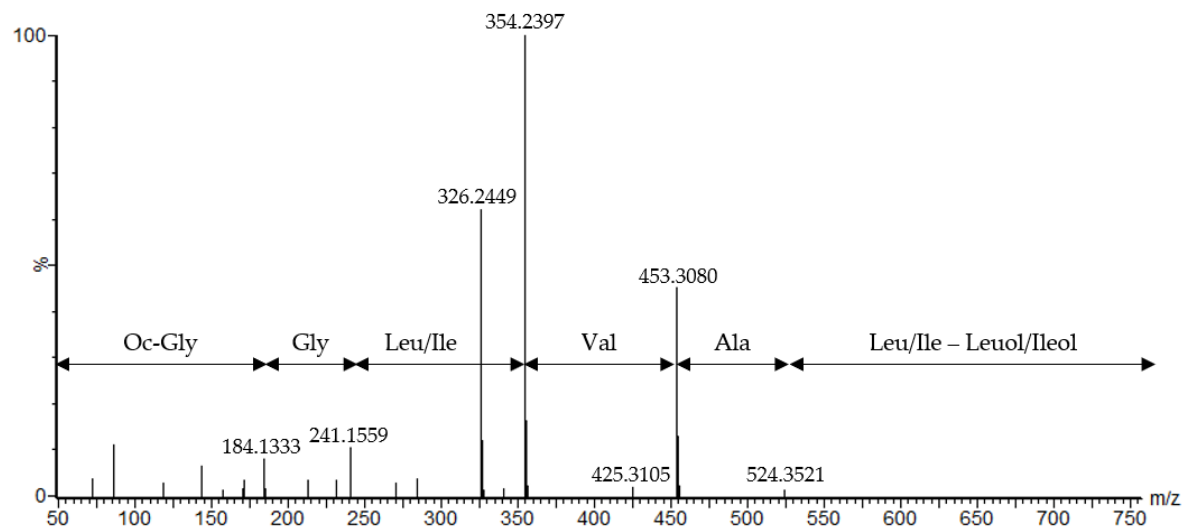
Figure S11. Annotated MS/MS spectra of putatively novel lipopeptides detected in *Trichoderma* sp. extracts CHG34-CAG and CHG34-PDA. The putative amino acid sequences were predicted based on the experimentally determined MS/MS fragmentation pattern of *m/z* 770.5386 [M+H]⁺ (**103**; top) and *m/z* 754.5423 [M+H]⁺ (**105**; bottom; here shown for extract CHG34-PDA). Ala: alanine, Gly: glycine, Leu/Ile: (iso)leucine, Leuol/Ileol: (iso)leucinol, Oc: octanoyl, Ser: serine, Val: valine.
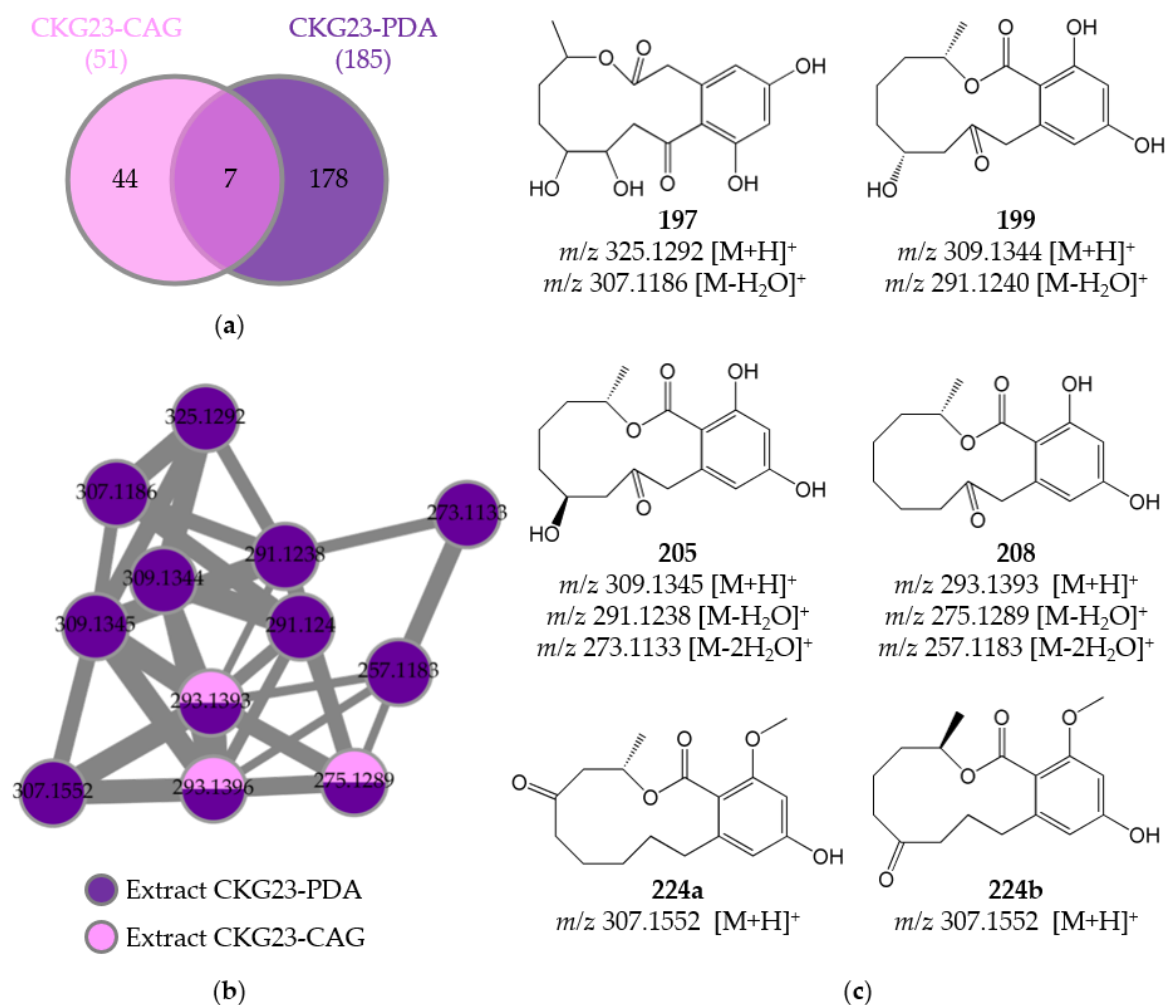
CKG23-CAG (51)   CKG23-PDA (185)

44   7   178

(a)

197
m/z 325.1292 [M+H]⁺
m/z 307.1186 [M-H₂O]⁺

199
m/z 309.1344 [M+H]⁺
m/z 291.1240 [M-H₂O]⁺

205
m/z 309.1345 [M+H]⁺
m/z 291.1238 [M-H₂O]⁺
m/z 273.1133 [M-2H₂O]⁺

208
m/z 293.1393 [M+H]⁺
m/z 275.1289 [M-H₂O]⁺
m/z 257.1183 [M-2H₂O]⁺

224a
m/z 307.1552 [M+H]⁺

224b
m/z 307.1552 [M+H]⁺

325.1292
307.1186
273.1133
291.1238
309.1344
309.1345
291.124
257.1183
293.1393
307.1552
293.1396
275.1289

● Extract CKG23-PDA
○ Extract CKG23-CAG

(b)   (c)

Figure S12. Comparative metabolome analyses of *Penicillium* sp. extracts CKG23-CAG and CKG23-PDA. (**a**) Venn diagram of shared and exclusive peaks detected in extract CKG23-CAG (light purple) and CKG23-PDA (dark purple). (**b**) Zearalenone cluster produced by *Penicillium* sp. isolate CKG23 (see Figure S8 for full FBMN). The width of edges represents the cosine similarity between two nodes. (**c**) Putatively annotated metabolites of the zearalenone cluster are displayed with their *m/z* values and observed adducts. Compound numbers are in accordance with Table S10.

235

Table S1. Taxonomic classification of microbial strains isolated from the gut of *C. intestinalis* sampled in Helgoland and Kiel Fjord. Strain codes are based on the respective sampling location and sampled tissue (CHG = *C. intestinalis* from Helgoland, gut; CKG = *C. intestinalis* from Kiel Fjord, gut). The three closest related strains are given according to the BLAST search [2]. RG = risk group (according to TRBA 460 and TRBA 466). Acc. no.: Accession number.

Strain code	Isolation medium	Acc. no.	Amplicon	Closest related species (BLAST)	Acc. no. closest related species	Lowest taxonomic classification (order)	RG
CHG1	MB	MW065489	16S	Uncultured *Vibrio* sp. Uncultured *Vibrio* sp. *Vibrio owensii*	MG554543.1 MG554505.1 CP025797.1	*Vibrio* sp. (Vibrionales)	1
CHG2	MB	MW065490	16S	*Ruegeria* sp. *Ruegeria* sp. *Ruegeria atlantica*	KY363633.1 KX833139.1 JN128252.1	*Ruegeria atlantica* (Rhodobacterales)	1
CHG3	MB	MW065491	16S	Bacterium b1cb16 *Shewanella* sp. *Shewanella piezotolerans*	EF207071.1 MF975607.1 CP000472.1	*Shewanella* sp. (Alteromonadales)	1
CHG4	MB	MW065492	16S	*Citrobacter amalonaticus* *Citrobacter farmeri* *Citrobacter* sp.	MG238567.1 CP022695.1 LT556085.1	*Citrobacter* sp. (Enterobacterales)	2
CHG5	MB	MW065493	16S	*Shewanella woodyi* *Shewanella woodyi* *Shewanella woodyi*	NR_114412.1 NR_074846.1 CP000961.1	*Shewanella woodyi* (Alteromonadales)	1
CHG6	TSB	MW065494	16S	*Shewanella schlegeliana* *Shewanella sairae* *Shewanella schlegeliana*	MG388302.1 AB274769.1 AB274767.1	*Shewanella* sp. (Alteromonadales)	1
CHG7	TSB	MW065495	16S	*Shewanella putrefaciens* *Shewanella hafniensis* *Shewanella xiamenensis*	MG976650.1 MF612155.1 MF033476.1	*Shewanella* sp. (Alteromonadales)	2
CHG8	TSB	MW065496	16S	*Shewanella* sp. *Shewanella* sp. *Shewanella algae*	KJ748462.1 KJ748460.1 KX218308.1	*Shewanella* sp. (Alteromonadales)	2
CHG9	TSB	MW065497	16S	*Escherichia coli* *Escherichia coli* *Escherichia coli*	CP025753.1 CP025747.1 CP025739.1	*Escherichia coli* (Enterobacterales)	2

Strain code	Isolation medium	Acc. no.	Amplicon	Closest related species (BLAST)	Acc. no. closest related species	Lowest taxonomic classification (order)	RG
CHG10	CMN	MW065498	16S	*Vibrio alginolyticus* *Vibrio alginolyticus* *Vibrio alginolyticus*	KY229785.1 JN188414.1 KY684259.1	*Vibrio* sp. (Vibrionales)	2
CHG11	CMN	MW065499	16S	*Ruegeria* sp. *Ruegeria* sp. *Ruegeria atlantica*	KY363633.1 KX833139.1 HQ908680.1	*Ruegeria atlantica* (Rhodobacterales)	1
CHG12	CMN	MW065500	16S	*Shewanella kaireitica* Uncultured bacterium clone SanDiego_a2585 Uncultured bacterium clone SanDiego_a2547	KX078089.1 KF799676.1 KF799675.1	*Shewanella* sp. (Alteromonadales)	1
CHG16	WSP	MW065501	16S	*Vibrio* sp. *Vibrio* sp. *Vibrio owensii*	MK533523.1 MK533517.1 CP033138.1	*Vibrio* sp. (Vibrionales)	1
CHG19	WSP	MW064137	ITS	Fungal sp. isolate whc1 *Arthrinium arundinis* *Arthrinium sacchari*	MH465392.1 KX778674.1 KX778672.1	*Arthrinium* sp. (Xylariales)	1
CHG20	WSP	MW065502	16S	*Citrobacter freundii* *Citrobacter freundii complex* *Citrobacter freundii*	CP027849.1 CP026231.1 CP011657.1	*Citrobacter freundii* (Enterobacterales)	2
CHG21	WSP	MW065503	16S	*Citrobacter braakii* *Citrobacter* sp. *Citrobacter braakii*	MH368419.1 MH368123.1 CP022049.2	*Citrobacter braakii* (Enterobacterales)	2
CHG22	WSP	MW064138	ITS	Uncultured *Penicillium* clone WPW-OTU-32 *Penicillium hoeksii* *Penicillium hoeksii*	KT581734.1 NR_137913.1 KY305048.1	*Penicillium hoeksii* (Eurotiales)	1
CHG24	WSP	MW064139	ITS	*Aspergillus niger* Fungal sp. SNB-LAP1-7-61 *Aspergillus niger*	MG647867.1 KU977335.1 MH050790.1	*Aspergillus* sp. (Eurotiales)	2

Strain code	Isolation medium	Acc. no.	Amplicon	Closest related species (BLAST)	Acc. no. closest related species	Lowest taxonomic classification (order)	RG
CHG25	WSP	MW064140	ITS	*Penicillium expansum* *Penicillium* sp. *Penicillium ulaiense*	MF303721.1 KP403971.1 LN871568.1	*Penicillium* sp. (Eurotiales)	1
CHG26	WSP	MW064141	ITS	Uncultured *Galactomyces* clone P71B *Geotrichum candidum* *Geotrichum candidum*	MG193553.1 MH680587.1 MF782775.1	*Galactomyces candidum* (Saccharomycetales)	1
CHG28	WSP	MW064142	ITS	*Trichoderma harzianum* *Trichoderma* sp. *Trichoderma harzianum*	MF871539.1 MH285106.1 KY750434.1	*Trichoderma* sp. (Hypocreales)	1
CHG29	PDA	MW064143	ITS	*Phoma* sp. Uncultured *Didymella* clone 191_K9ov *Stagonosporopsis cucurbitacearum*	KF525844.1 KY430454.1 KU168143.1	*Phoma* sp. (Pleosporales)	1
CHG32	TSB	MW065504	16S	*Vibrio rumoiensis* *Vibrio* sp. *Vibrio owensii*	AP018685.1 MG262453.1 MH368433.1	*Vibrio* sp. (Vibrionales)	1
CHG34	WSP	MW064144	ITS	*Trichoderma* sp. *Trichoderma harzianum* *Trichoderma harzianum*	MH285106.1 MF871539.1 KY750434.1	*Trichoderma* sp. (Hypocreales)	1
CHG35	PDA	MW064145	ITS	*Penicillium* sp. *Penicillium antarcticum* *Penicillium atrovenetum*	KY401117.1 KP016829.1 KF679753.1	*Penicillium* sp. (Eurotiales)	1
CHG38	WSP	MW064146	ITS	*Fusarium graminearum* *Fusarium graminearum* *Fusarium graminearum*	MK079896.1 MK079895.1 MK079894.1	*Fusarium* sp. (Hypocreales)	1
CHG39	WSP	MW065505	16S	*Bacillus subtilis* *Bacillus subtilis* *Bacillus velezensis*	MG977677.1 MG976620.1 MG970354.1	*Bacillus* sp. (Bacillales)	1
CHG40	TSB	MW065506	16S	*Streptomyces* sp. *Streptomyces parvus* *Streptomyces lavendulae*	KY613504.1 KY213676.1 KY213666.1	*Streptomyces* sp. (Streptomycetales)	1

Strain code	Isolation medium	Acc. no.	Amplicon	Closest related species (BLAST)	Acc. no. closest related species	Lowest taxonomic classification (order)	RG
CHG41	TSB	MW065507	16S	*Bacillus licheniformis* Uncultured bacterium clone OTU3 *Bacillus licheniformis*	KY886241.1 KP975259.1 KC522129.1	*Bacillus licheniformis* (Bacillales)	1
CHG42	TSB	MW065508	16S	*Shewanella algae* *Shewanella algae* *Shewanella haliotis*	NR_114236.1 NR_117771.1 NR_117770.1	*Shewanella* sp. (Alteromonadales)	2
CHG43	MB	MW065509	16S	*Vibrio splendidus* *Vibrio* sp. *Vibrio anguillarum*	MH010050.1 MG788349.1 CP023433.1	*Vibrio* sp. (Vibrionales)	2
CHG44	MB	MW064147	ITS	*Aspergillus oryzae* *Aspergillus oryzae* *Aspergillus flavus*	MH746006.1 MH625703.1 MH578599.1	*Aspergillus* sp. (Eurotiales)	2
CHG47	WSP	MW064148	ITS	*Arthrinium* sp. *Arthrinium* sp. *Arthrinium arundinis*	MH059547.1 MH059539.1 MK256947.1	*Arthrinium* sp. (Xylariales)	1
CHG48	WSP	MW065510	16S	*Streptomyces* sp. *Streptomyces* sp. *Streptomyces pratensis*	MG637270.1 MG637268.1 MK484235.1	*Streptomyces* sp. (Streptomycetales)	1
CHG49	PDA	MW064175	18S	Uncultured fungus clone nco40d10c1 Uncultured fungus clone nco40a09c1 *Pyrenophora tritici-repentis*	KC670836.1 KC670799.1 U42486.1	Pleosporaceae (Pleosporales)	1
CHG52	WSP	MW064149	ITS	*Penicillium cosmopolitanum* *Penicillium cosmopolitanum* *Penicillium cosmopolitanum*	MH864385.1 MH864384.1 MH864377.1	*Penicillium* sp. (Eurotiales)	1
CHG53	PDA	MW064150	ITS	*Trichoderma* sp. *Trichoderma* sp. *Trichoderma koningii*	MH794211.1 MH284929.1 KX343123.1	*Trichoderma* sp. (Hypocreales)	1
CHG56	TSB	MW064151	ITS	*Aspergillus nidulans* Fungal sp. isolate *Aspergillus quadrilineatus* *Aspergillus nidulans*	MG459155.1 MH041155.1 MG991576.1	*Aspergillus* sp. (Eurotiales)	1

Strain code	Isolation medium	Acc. no.	Amplicon	Closest related species (BLAST)	Acc. no. closest related species	Lowest taxonomic classification (order)	RG
CHG59	PDA	MW064152	ITS	*Tamaricicola* sp. *Tamaricicola* sp. *Comoclathris spartii*	MG977427.1 MG977425.1 KU714703.1	*Tamaricicola* sp. (Pleosporales)	1
CHG60	TSB	MW064153	ITS	*Peroneutypa* sp. *Eutypella scoparia* *Eutypella* sp.	MF359647.1 EU436688.1 JQ922161.1	*Peroneutypa* sp. (Xylariales)	1
CHG61	TSB	MW065511	16S	Uncultured bacterium clone FRA_187_C04_2008-07-09 Uncultured *Vibrio* sp. *Vibrio anguillarum*	FN434816.1 MG554532.1 CP022468.1	*Vibrio* sp. (Vibrionales)	2
CHG64	TSB	MW065512	16S	*Streptomyces microflavus* *Streptomyces* sp. *Streptomyces* sp.	MG855947.1 MH251131.1 MH250821.1	*Streptomyces* sp. (Streptomycetales)	1
CKG1	MB	MW065513	16S	*Pseudomonas* sp. Uncultured marine bacterium isolate TGGE gel band 22TGGE1 *Pseudomonas anguilliseptica*	KX621130.1 KJ814609.1 DQ005209.1	*Pseudomonas* sp. (Pseudomonadales)	1
CKG2	MB	MW065514	16S	*Rhodococcus* sp. *Rhodococcus antrifimi* *Rhodococcus antrifimi*	MG515722.1 LN867321.1 NR_145614.1	*Rhodococcus* sp. (Corynebacteriales)	2
CKG3	MB	MW065515	16S	*Shewanella* sp. *Shewanella* sp. *Shewanella aestuarii*	FR821223.1 FR744880.1 KX271676.1	*Shewanella* sp. (Alteromonadales)	1
CKG4	MB	MW065516	16S	*Vibrio* sp. *Vibrio anguillarum* *Vibrio anguillarum*	MG788349.1 CP023433.1 CP023293.1	*Vibrio* sp. (Vibrionales)	2
CKG5	MB	MW065517	16S	*Nocardiopsis alba* *Nocardiopsis alba* *Nocardiopsis alba*	MH843138.1 MH843137.1 MH843136.1	*Nocardiopsis* sp. (Streptosporangiales)	1

Strain code	Isolation medium	Acc. no.	Amplicon	Closest related species (BLAST)	Acc. no. closest related species	Lowest taxonomic classification (order)	RG
CKG6	MB	MW065518	16S	*Shewanella aestuarii* *Shewanella aestuarii* *Shewanella aestuarii*	KX271676.1 KX271675.1 KX271674.1	*Shewanella aestuarii* (Alteromonadales)	1
CKG7	MB	MW065519	16S	*Vibrio owensii* *Vibrio owensii* *Vibrio owensii*	LC369696.1 MG896198.1 MG896189.1	*Vibrio* sp. (Vibrionales)	1
CKG8	MB	MW065520	16S	*Vibrio* sp. *Vibrio anguillarum* *Vibrio anguillarum*	MG788349.1 CP023433.1 CP023293.1	*Vibrio* sp. (Vibrionales)	2
CKG9	CMN	MW065521	16S	*Vibrio* sp. *Vibrio anguillarum* *Vibrio anguillarum*	MG788349.1 CP023433.1 CP023293.1	*Vibrio* sp. (Vibrionales)	2
CKG10	CMN	MW065522	16S	Uncultured *Vibrio* sp. clone HH101354 Uncultured *Vibrio* sp. clone HH101351 *Vibrio anguillarum*	MG554532.1 MG554529.1 CP022468.1	*Vibrio* sp. (Vibrionales)	2
CKG11	CMN	MW065523	16S	*Shewanella aestuarii* *Shewanella aestuarii* *Shewanella aestuarii*	KX271676.1 KX271675.1 KX271674.1	*Shewanella aestuarii* (Alteromonadales)	1
CKG12	TSB	MW065524	16S	*Vibrio owensii* *Vibrio campbellii* *Vibrio* sp.	MG896198.1 CP026321.1 KY655411.1	*Vibrio* sp. (Vibrionales)	1
CKG13	TSB	MW065525	16S	Uncultured marine bacterium isolate TGGE gel band 22TGGE1 *Pseudomonas* sp. *Pseudomonas peli*	KJ814609.1 JQ012964.1 MG687270.1	*Pseudomonas* sp. (Pseudomonadales)	1
CKG14	TSB	MW065526	16S	*Shewanella* sp. *Shewanella* sp. *Shewanella aestuarii*	FR821223.1 FR744880.1 KX271676.1	*Shewanella* sp. (Alteromonadales)	1
CKG15	TSB	MW065527	16S	*Shewanella* sp. *Shewanella* sp. *Shewanella colwelliana*	MF045123.1 KU647920.1 KC534404.1	*Shewanella colwelliana* (Alteromonadales)	1

Strain code	Isolation medium	Acc. no.	Amplicon	Closest related species (BLAST)	Acc. no. closest related species	Lowest taxonomic classification (order)	RG
CKG16	TSB	MW064154	ITS	*Eutypa lata* *Amphisphaeria umbrina* Uncultured *Eutypella* clone G17312	MF359647.1 KY962999.1 JQ922161.1	*Eutypa lata* (Xylariales)	1
CKG19	TSB	MW065528	16S	*Bacillus pumilus* *Bacillus pumilus* *Bacillus zhangzhouensis*	CP027034.1 KY623354.1 MG937731.1	*Bacillus* sp. (Bacillales)	2
CKG20	TSB	MW065529	16S	*Micromonospora* sp. *Micromonospora* sp. *Micromonospora aurantiaca*	EU437811.1 LC383890.1 MH333275.1	*Micromonospora* sp. (Micromonosporales)	1
CKG21	CMN	MW065530	16S	*Bacillus hwajinpoensis* *Bacillus hwajinpoensis* *Bacillus hwajinpoensis*	MG651497.1 MG651463.1 MG651074.1	*Bacillus hwajinpoensis* (Bacillales)	1
CKG22	PDA	MW064155	ITS	*Penicillium antarcticum* *Penicillium* sp. *Penicillium* sp.	MH828228.1 KY401122.1 KY401117.1	*Penicillium* sp. (Eurotiales)	1
CKG23	WSP	MW064156	ITS	*Penicillium antarcticum* *Penicillium* sp. *Penicillium* sp.	MH828228.1 KY401122.1 KY401117.1	*Penicillium* sp. (Eurotiales)	1
CKG24	WSP	MW065531	16S	*Bacillus subtilis* *Bacillus amyloliquefaciens* *Bacillus subtilis*	KC428745.1 JX517210.1 GQ280056.1	*Bacillus* sp. (Bacillales)	1
CKG25	WSP	MW064157	ITS	*Geotrichum candidum* *Galactomyces candidum* *Geotrichum candidum*	KF713521.1 KF298070.1 KY009607.1	*Galactomyces candidum* (Saccharomycetales)	1
CKG27	WSP	MW065532	16S	*Bacillus muralis* *Bacillus* sp. [*Brevibacterium*] *frigoritolerans*	MF506797.1 MG062899.2 MF467864.1	*Bacillus* sp. (Bacillales)	2
CKG29	WSP	MW065533	16S	*Bacillus amyloliquefaciens* *Bacillus amyloliquefaciens* *Bacillus subtilis*	MG136848.1 MG136846.1 MG977677.1	*Bacillus* sp. (Bacillales)	1

Strain code	Isolation medium	Acc. no.	Amplicon	Closest related species (BLAST)	Acc. no. closest related species	Lowest taxonomic classification (order)	RG
CKG30	WSP	MW065534	16S	*Bacillus pumilus* *Bacillus pumilus* *Bacillus zhangzhouensis*	CP027034.1 KY623354.1 MG937731.1	*Bacillus* sp. (Bacillales)	2
CKG31	PDA	MW065535	16S	*Vibrio* sp. *Shewanella* sp. *Shewanella kaireitica*	LC416561.1 MH333258.1 KX078089.1	*Shewanella kaireitica* (Alteromonadales)	1
CKG32	WSP	MW064158	ITS	*Fusarium graminearum* *Fusarium graminearum* *Fusarium graminearum*	MF800908.1 KY466827.1 KY466825.1	*Fusarium* sp. (Hypocreales)	1
CKG33	WSP	MW064159	ITS	*Mucor hiemalis* *Mucor hiemalis* *Mucor hiemalis*	HQ845045.1 HM037964.1 HM037963.1	*Mucor hiemalis* (Mucorales)	1
CKG36	TSB	MW065536	16S	*Bacillus* sp. *Bacillus cereus* *Bacillus cereus*	CP020437.2 MG977683.1 MG966498.1	*Bacillus* sp. (Bacillales)	2
CKG37	CMN	MW064160	ITS	*Sarocladium strictum* *Sarocladium strictum* *Sarocladium strictum*	MH880255.1 LC314675.1 MF663649.1	*Sarocladium strictum* (Hypocreales)	1
CKG38	CMB	MW065537	16S	*Pseudomonas* sp. *Pseudomonas* sp. *Pseudomonas anguilliseptica*	KT710819.1 KT710818.1 JX177684.1	*Pseudomonas anguilliseptica* (Pseudomonadales)	1
CKG39	TSB	MW065538	16S	*Bacillus licheniformis* *Bacillus licheniformis* *Bacillus licheniformis*	MG980062.1 MG280960.1 MG189544.1	*Bacillus* sp. (Bacillales)	1
CKG40	WSP	MW065539	16S	Uncultured *Klebsiella* sp. clone JXS1-28 *Klebsiella* sp. *Raoultella ornithinolytica*	JN873189.1 KM873628.1 CP010557.1	*Klebsiella* sp. (Enterobacterales)	2
CKG42	WSP	MW064161	ITS	*Elaphocordyceps* sp. *Elaphocordyceps* sp. *Tolypocladium* sp.	KC237381.1 KC237380.1 KX034386.1	*Elaphocordyceps* sp. (Hypocreales)	1

Strain code	Isolation medium	Acc. no.	Amplicon	Closest related species (BLAST)	Acc. no. closest related species	Lowest taxonomic classification (order)	RG
CKG43	WSP	MW065540	16S	*Bacillus subtilis* *Bacillus siamensis* *Bacillus siamensis*	MG928427.1 KY962351.1 KY962340.1	*Bacillus* sp. (Bacillales)	1
CKG44	WSP	MW064162	ITS	*Neonectria coccinea* Uncultured *Neonectria* clone AEW3_110 *Neonectria coccinea*	KJ022022.1 KF823598.1 KC660506.1	*Neonectria coccinea* (Hypocreales)	1
CKG45	WSP	MW064163	ITS	*Purpureocillium lilacinum* *Purpureocillium lilacinum* *Purpureocillium lilacinum*	KY007618.1 MH865347.1 MH865301.1	*Purpureocillium lilacinum* (Hypocreales)	2
CKG46	TSB	MW065541	16S	*Nocardiopsis* sp. *Nocardiopsis prasina* *Nocardiopsis prasina*	MK045298.1 MF594115.1 MF170851.1	*Nocardiopsis prasina* (Streptosporangiales)	1
CKG47	CMN	MW065542	16S	*Vibrio* sp. *Vibrio anguillarum* *Vibrio anguillarum*	MG788349.1 CP023433.1 CP023293.1	*Vibrio* sp. (Vibrionales)	2
CKG49	WSP	MW064164	ITS	*Mucor circinelloides* *Mucor circinelloides* *Mucor circinelloides*	MH911362.1 KC329629.1 JX241658.1	*Mucor circinelloides* (Mucorales)	1
CKG50	CMN	MW065543	16S	*Sporosarcina* sp. *Sporosarcina* sp. *Sporosarcina aquimarina*	KX108967.1 KT368976.1 KF800793.1	*Sporosarcina* sp. (Bacillales)	1
CKG51	CMN	MW064165	ITS	*Penicillium polonicum* *Penicillium polonicum* *Penicillium* sp.	KY978579.1 KY993979.1 KY092668.1	*Penicillium* sp. (Eurotiales)	1
CKG52	CMN	MW065544	16S	*Vibrio* sp. *Vibrio anguillarum* *Vibrio anguillarum*	MG788349.1 CP023433.1 CP023293.1	*Vibrio* sp. (Vibrionales)	2
CKG53	CMN	MW065545	16S	*Streptomyces* sp. *Streptomyces* sp. *Streptomyces lividans*	MK134635.1 MK134629.1 MG856044.1	*Streptomyces* sp. (Streptomycetales)	2

Strain code	Isolation medium	Acc. no.	Amplicon	Closest related species (BLAST)	Acc. no. closest related species	Lowest taxonomic classification (order)	RG
CKG54	CMB	MW064176	18S	*Cordyceps farinosa* Fungal sp. J271 *Isaria farinosa*	MH857775.1 KC242715.1 KC242708.1	*Cordyceps farinosa* (Hypocreales)	1
CKG55	MB	MW065546	16S	*Nocardiopsis alba* *Nocardiopsis alba* *Nocardiopsis alba*	MH333283.1 MF321814.1 MF321809.1	*Nocardiopsis alba* (Streptosporangiales)	1
CKG57	CMB	MW064166	ITS	*Aaosphaeria arxii* *Arthopyrenia* sp. *Massarina igniaria*	MH861193.1 KU747910.1 KR534712.1	*Arthopyrenia* sp. (Pleosporales)	1
CKG58	CMB	MW065547	16S	*Nocardiopsis* sp. *Nocardiopsis prasina* *Nocardiopsis prasina*	MK045298.1 MF594115.1 MF170851.1	*Nocardiopsis prasina* (Streptosporangiales)	1
CKG60	MB	MW065548	16S	*Enterobacter* sp. *Citrobacter gillenii* *Citrobacter gillenii*	MF429589.1 MH392488.1 MG757538.1	*Citrobacter* sp. (Enterobacterales)	2
CKG62	PDA	MW064167	ITS	*Trichoderma* sp. *Trichoderma lixii* *Trichoderma harzianum*	MK290992.1 MK288146.1 MK209008.1	*Trichoderma* sp. (Hypocreales)	1
CKG63	WSP	MW064168	ITS	*Penicillium psychrosexualis* *Penicillium psychrosexualis* *Penicillium psychrosexualis*	MH864839.1 MH864838.1 MH864787.1	*Penicillium* sp. (Eurotiales)	1
CKG64	CMB	MW064169	ITS	*Penicillium polonicum* *Penicillium polonicum* *Penicillium polonicum*	MK271277.1 MK267441.1 MK077720.1	*Penicillium* sp. (Eurotiales)	1
CKG66	CMB	MW064170	ITS	Uncultured fungus clone ZB042802405(86) Fungal sp. strain PS14 *Acrostalagmus luteoalbus*	MF962944.1 MH456880.1 KT824244.1	*Acrostalagmus luteoalbus* (Hypocreales)	1
CKG67_I	CMB	MW064171	ITS	*Purpureocillium lilacinum* *Purpureocillium lilacinum* *Purpureocillium lilacinum*	LC413751.1 MF996819.1 KF706346.1	*Purpureocillium lilacinum* (Hypocreales)	2

Strain code	Isolation medium	Acc. no.	Amplicon	Closest related species (BLAST)	Acc. no. closest related species	Lowest taxonomic classification (order)	RG
CKG67_II	WSP	MW065549	16S	*Nocardiopsis alba* *Nocardiopsis alba* *Nocardiopsis alba*	MH333283.1 MH071379.1 MF321814.1	*Nocardiopsis alba* (Streptosporangiales)	1
CKG68	WSP	MW064172	ITS	*Purpureocillium lilacinum* *Purpureocillium lilacinum* *Purpureocillium lilacinum*	MH865347.1 MH865301.1 MH865154.1	*Purpureocillium lilacinum* (Hypocreales)	2
CKG70	TSB	MW064173	ITS	*Plectosphaerella cucumerina* Fungal sp. strain S255T Fungal sp. strain S255S	MH791266.1 KU839553.1 KU839552.1	*Plectosphaerella cucumerina* (Glomerellales)	1
CKG71	TSB	MW064174	ITS	*Sarocladium strictum* Fungal sp. strain S254T Fungal sp. strain S254S	KY465763.1 KU839539.1 KU839538.1	*Sarocladium strictum* (Hypocreales)	1

Table S2. Antimicrobial and anticancer activities (% inhibition at a test concentration of 100 µg/mL) of microbial crude extracts. Inhibition values are given as average values of the two biological and two technical replicates. Some bacterial isolates were only cultivated on MB medium, since they did not grow on GYM medium. Extracts selected by the bioactivity selection criterion (see Section 2.3.) are highlighted in blue. MRSA: Methicillin-resistant *Staphylococcus aureus*, Efm: *Enterococcus faecium*, Ab: *Acinetobacter baumannii*, Ec: *Escherichia coli*, Kp: *Klebsiella pneumoniae*, Psa: *Pseudomonas aeruginosa*, Ca: *Candida albicans*, Cn: *Cryptococcus neoformans*, A375: Malignant melanoma, A549: Lung carcinoma, HCT116: Colon cancer, MB231: Breast cancer; "-": Inhibition ≤20%; in bold: Inhibition values ≥80%; **AC**: extract was selected based on high anticancer activity (inhibition ≥80%); **AM**: extract was selected based on high antimicrobial activity (inhibition ≥80%).

Strain	Identification	Medium	MRSA	Efm	Ab	Ec	Kp	Psa	Ca	Cn	A375	A549	HCT116	MB231	Selected?
CHG2	*Ruegeria atlantica*	MB	73	-	-	-	-	-	-	-	29	-	-	36	
CHG3	*Shewanella* sp.	MB	**92**	52	-	-	-	-	-	-	-	-	-	-	
CHG5	*Shewanella woodyi*	MB	**95**	78	-	-	-	-	-	-	-	-	-	-	
CHG6	*Shewanella* sp.	GYM	**100**	**92**	-	-	-	-	-	-	-	-	-	-	
		MB	**95**	**80**	-	40	-	-	-	-	-	-	-	-	
CHG12	*Shewanella* sp.	MB	**88**	**100**	-	-	-	-	-	-	-	-	-	26	
CHG16	*Vibrio* sp.	MB	**98**	**100**	-	-	-	-	-	-	-	-	-	-	
CHG19	*Arthrinium* sp.	CAG	-	-	-	-	-	65	-	-	71	78	75	78	
		PDA	-	-	-	-	-	-	-	-	26	53	25	44	
CHG22	*Penicillium hoeksii*	CAG	**85**	-	-	-	-	-	-	-	25	31	25	29	
		PDA	**84**	-	-	-	-	-	-	-	63	48	59	48	
CHG25	*Penicillium* sp.	CAG	**99**	**100**	**98**	**100**	**100**	**100**	-	-	**98**	**93**	**98**	**92**	Yes (AC)
		PDA	**98**	**84**	**97**	**100**	**100**	**99**	-	-	**99**	**98**	**99**	**95**	Yes (AC)
CHG26	*Galactomyces candidum*	CAG	**96**	33	-	-	-	-	-	-	-	-	-	-	
		PDA	54	-	-	-	-	-	-	-	-	-	-	-	
CHG29	*Phoma* sp.	CAG	-	-	-	-	-	-	-	-	-	-	-	-	
		PDA	-	-	-	-	-	-	-	-	-	-	-	-	
CHG32	*Vibrio* sp.	MB	79	-	-	-	-	-	-	-	-	-	-	-	
CHG34	*Trichoderma* sp.	CAG	41	-	-	-	-	-	24	-	**97**	**96**	**95**	**93**	Yes (AC)
		PDA	**94**	**100**	-	-	-	-	**100**	**92**	**98**	**99**	**99**	**98**	Yes (AC & AM)
CHG35	*Penicillium* sp.	CAG	**100**	**100**	**99**	**99**	**100**	**84**	-	21	72	**93**	**95**	64	Yes (AC)
		PDA	**98**	74	**98**	**98**	**100**	77	-	-	**89**	**98**	**98**	72	Yes (AC)
CHG38	*Fusarium* sp.	CAG	**100**	**100**	-	-	-	-	**92**	**96**	**98**	65	**93**	40	Yes (AC & AM)

Strain	Identification	Medium	MRSA	Efm	Ab	Ec	Kp	Psa	Ca	Cn	A375	A549	HCT116	MB231	Selected?
		PDA	**100**	**100**	-	-	-	-	**88**	-	56	-	24	-	Yes (AM)
CHG39	*Bacillus* sp.	GYM	**97**	**100**	-	-	-	-	-	-	69	73	48	69	
		MB	**96**	**94**	-	-	-	-	-	-	30	29	-	31	
CHG40	*Streptomyces* sp.	GYM	**100**	**100**	-	-	-	-	61	37	**98**	**99**	**98**	**99**	Yes (AC)
		MB	**100**	87	-	-	-	-	-	-	51	51	55	61	
CHG41	*Bacillus licheniformis*	GYM	69	-	-	-	-	-	-	-	62	33	38	51	
		MB	66	-	-	-	-	-	-	-	25	33	-	33	
CHG48	*Streptomyces* sp.	GYM	**100**	**100**	-	-	-	-	**100**	97	**98**	**92**	**88**	**93**	Yes (AC & AM)
		MB	**100**	**100**	-	-	-	-	-	72	71	69	71	74	
CHG49	Pleosporaceae	CAG	**99**	84	97	100	100	100	38	53	**99**	95	**98**	94	Yes (AC)
		PDA	98	68	98	100	100	82	28	-	97	97	98	53	Yes (AC)
CHG52	*Penicillium* sp.	CAG	**92**	88	-	-	-	-	-	-	30	-	33	-	
		PDA	**95**	**96**	-	-	-	-	-	-	-	-	20	-	
CHG53	*Trichoderma* sp.	CAG	-	-	-	-	-	-	-	-	-	-	-	-	
		PDA	-	-	-	-	-	-	-	-	-	-	-	-	
CHG56	*Aspergillus* sp.	CAG	67	-	-	-	-	-	-	-	22	26	34	46	
		PDA	70	-	-	-	-	-	-	-	30	37	34	59	
CHG59	*Tamaricicola* sp.	CAG	**92**	-	-	36	-	-	-	-	-	-	-	-	
		PDA	**91**	-	-	37	-	-	-	-	-	-	-	-	
CHG60	*Peroneutypa* sp.	CAG	35	-	-	33	-	-	-	-	-	47	35	46	
		PDA	32	-	-	-	-	-	-	-	-	33	36	25	
CHG64	*Streptomyces* sp.	GYM	**100**	97	-	-	-	-	-	-	**99**	98	**99**	98	Yes (AC)
		MB	**100**	98	-	-	-	-	-	-	-	58	23	50	
CKG5	*Nocardiopsis* sp.	GYM	-	46	-	-	-	-	-	-	29	-	48	-	
		MB	**84**	**94**	-	-	-	-	-	-	22	-	70	-	
CKG6	*Shewanella aestuarii*	MB	**100**	**94**	-	-	-	-	-	-	-	-	-	-	
CKG7	*Vibrio* sp.	MB	34	-	-	-	-	-	-	-	-	-	-	-	
CKG12	*Vibrio* sp.	MB	**100**	74	-	-	-	-	-	-	-	-	-	-	
CKG13	*Pseudomonas* sp.	MB	35	-	-	-	-	-	-	-	-	-	-	-	
CKG15	*Shewanella colwelliana*	MB	**100**	**100**	-	-	-	-	-	-	-	-	-	-	
CKG16	*Eutypa lata*	CAG	46	-	-	31	-	-	-	-	-	26	34	33	

Strain	Identification	Medium	MRSA	Efm	Ab	Ec	Kp	Psa	Ca	Cn	A375	A549	HCT116	MB231	Selected?
		PDA	-	-	-	29	-	-	-	-	-	33	26	32	
CKG20	*Micromonospora* sp.	GYM	**100**	**100**	-	-	-	-	-	-	**98**	**100**	**99**	**100**	Yes (AC)
		MB	53	-	-	-	-	-	-	-	-	-	-	-	
CKG21	*Bacillus hwajinpoensis*	GYM	65	-	-	-	-	-	-	-	-	20	-	-	
		MB	**100**	**100**	-	-	-	-	-	-	-	-	-	-	
CKG23	*Penicillium* sp.	CAG	**100**	**98**	**100**	**100**	**100**	**89**	-	-	**97**	**98**	**98**	**97**	Yes (AC)
		PDA	**100**	**100**	**98**	**100**	**100**	75	-	41	**95**	**98**	77	**92**	Yes (AC)
CKG24	*Bacillus* sp.	GYM	**100**	**100**	-	-	-	-	-	**94**	72	**98**	63	34	Yes (AC & AM)
		MB	**100**	**100**	-	-	-	-	-	-	51	54	43	59	
CKG25	*Galactomyces candidum*	CAG	**100**	**100**	**100**	**100**	**100**	85	-	-	**96**	**99**	**92**	**82**	Yes (AC)
		PDA	**99**	**99**	**100**	**100**	**100**	**93**	-	-	**98**	**99**	**99**	**93**	Yes (AC)
CKG31	*Shewanella kaireitica*	GYM	**100**	**100**	34	-	-	-	-	-	-	27	26	25	
		MB	**100**	**100**	-	-	-	-	-	-	-	20	-	-	
CKG32	*Fusarium* sp.	CAG	**100**	**100**	-	-	-	-	**89**	40	61	20	29	-	Yes (AM)
		PDA	**99**	**86**	-	-	-	-	60	-	21	-	-	-	
CKG33	*Mucor hiemalis*	CAG	62	-	-	-	-	-	-	-	-	27	27	48	
		PDA	77	-	-	-	-	-	-	-	-	-	-	-	
CKG37	*Sarocladium strictum*	CAG	**100**	**94**	-	38	-	-	-	-	-	-	-	-	
		PDA	**95**	47	-	41	-	-	-	-	78	48	58	56	
CKG38	*Pseudomonas anguilliseptica*	GYM	**100**	**100**	-	-	-	-	**85**	49	68	24	**91**	**88**	Yes (AC & AM)
		MB	**100**	**97**	-	-	-	-	**80**	73	-	-	-	-	Yes (AM)
CKG39	*Bacillus* sp.	GYM	-	-	-	-	-	-	-	-	26	-	-	-	
		MB	37	-	-	-	-	-	-	-	31	-	-	-	
CKG42	*Elaphocordyceps* sp.	CAG	76	-	-	-	-	-	-	-	37	-	-	-	
		PDA	**82**	66	-	-	-	-	35	-	38	26	-	-	
CKG43	*Bacillus* sp.	GYM	**92**	**100**	-	-	-	-	-	-	38	-	24	-	
		MB	**94**	**100**	-	-	-	-	-	-	26	-	-	-	
CKG44	*Neonectria coccinea*	CAG	54	-	-	-	-	-	-	-	24	-	-	28	
		PDA	-	-	-	-	-	-	-	-	-	-	-	-	
CKG49	*Mucor circinelloides*	CAG	**89**	**98**	-	-	-	-	-	-	21	35	44	22	

249

Strain	Identification	Medium	MRSA	Efm	Ab	Ec	Kp	Psa	Ca	Cn	A375	A549	HCT116	MB231	Selected?
		PDA	**100**	**100**	-	-	-	-	-	-	66	37	79	43	
CKG50	*Sporosarcina* sp.	GYM	**100**	**96**	-	-	-	-	-	-	-	-	-	-	
		MB	**100**	**98**	-	-	-	-	-	-	-	-	20	-	
CKG54	*Cordyceps farinosa*	CAG	**98**	**95**	-	-	-	-	-	-	56	-	30	-	
		PDA	**99**	**97**	-	-	-	-	-	-	52	24	42	-	
CKG57	*Arthopyrenia* sp.	CAG	66	-	-	-	-	-	-	-	-	-	-	-	
		PDA	52	-	-	-	-	-	-	-	-	-	-	-	
CKG58	*Nocardiopsis prasina*	GYM	**81**	**98**	-	-	-	-	**81**	54	**99**	**99**	**99**	**98**	Yes (AC & AM)
		MB	**100**	**99**	-	-	-	-	26	-	38	-	61	-	
CKG62	*Trichoderma* sp.	CAG	30	-	-	31	-	-	**88**	-	28	-	-	-	
		PDA	70	**100**	-	31	-	-	**93**	74	**98**	**98**	**99**	**98**	Yes (AC & AM)
CKG63	*Penicillium* sp.	CAG	**96**	25	26	-	-	21	36	-	45	50	30	64	
		PDA	76	22	**84**	71	82	59	-	-	51	**80**	49	77	Yes (AC)
CKG64	*Penicillium* sp.	CAG	-	-	-	-	37	-	-	-	-	21	-	37	
		PDA	70	-	-	-	-	-	-	-	-	34	30	45	
CKG66	*Acrostalagmus luteoalbus*	CAG	**100**	**100**	86	28	-	22	-	-	**87**	**89**	**83**	**89**	Yes (AC)
		PDA	**87**	51	-	-	-	-	-	-	25	-	70	-	
CKG70	*Plectosphaerella cucumerina*	CAG	56	-	-	-	-	-	-	-	-	-	-	-	
		PDA	69	-	-	-	-	-	-	-	-	-	-	-	

Table S3. Statistical comparison of chemically distinct bacterial crude extracts. ANOSIM was based on Euclidean distance. Group 1 included the following extracts: *Pseudomonas anguilliseptica* extracts CKG38-GYM and CKG38-MB and *Streptomyces* sp. extracts CHG40-GYM and CHG64-GYM.

Comparison	R value	p value
All	1	0.0001
Group 1 x Group 2 (CHG48-GYM, CKG58-GYM)	1	0.0022
Group 1 x Group 3 (CKG20-GYM)	1	0.0229
Group 1 x Group 4 (CKG24-GYM)	1	0.0232

Table S4. Statistical comparison of chemically distinct fungal crude extracts. ANOSIM was based on Euclidean distance. Group 1 included the following extracts: *Acrostalagmus luteoalbus* extract CKG66-CAG, *Galactomyces candidum* extracts CKG25-CAG and CKG25-PDA, *Penicillium* sp. extracts CHG25-CAG, CHG25-PDA, CHG35-CAG, CHG35-PDA, CKG23-CAG and CKG63-PDA and Pleosporaceae extracts CHG49-CAG and CHG49-PDA.

Comparison	R value	p value
All	0.8363	0.0001
Group 1 x Group 2 (CHG34-CAG, CHG34-PDA, CKG62-PDA)	0.9369	0.0001
Group 1 x Group 3 (CHG38-CAG, CHG38-PDA, CKG32-CAG)	0.6822	0.0001
Group 1 x Group 4 (CKG23-PDA)	0.9996	0.0055

Table S5. Putatively identified compounds produced by Streptomyces sp. extract CHG48-GYM. Putative annotations were based on the accurate mass, the predicted putative molecular formulae (MF), the retention time (R_t), the fragmentation pattern and the biological origin. *MF with best ppm error displayed; IC: Identification confidence level [3]; Nf: No fragmentation detected or below noise threshold ($5e^1$); Ref = reference(s).

No.	*m/z* value	Adduct	R_t (min)	ppm	Putative MF	Fragmentation pattern	IC	Putative identification	Chemical family	Biological origin	Ref
1	225.1104	[M+H]⁺	3.07	1.8	$C_8H_{12}N_6O_2$	181.1201, 164.1114, 141.9593, 97.9700	4	n.a.			
2	208.0976	[M+H]⁺	3.1	1	$C_{11}H_{13}NO_3$	190.0865, 166.0866, 164.1073, 146.0968, 135.0804, 131.0732, 122.0962, 118.0657	3	Streptazolin	Oxazolidone alkaloid	*Streptomyces viridochromogenes*	[4]
3	250.1422	[M+Na]⁺	3.53	1.2	$C_{12}H_{21}NO_3$	138.053	3	Streptenol E	Acetamide	*Streptomyces* sp.	[5]
4	239.1261	[M+H]⁺	3.72	2.1	$C_9H_{14}N_6O_2$	216.0758, 210.1890, 198.0604, 195.1371, 172.0880, 155.0949, 141.9587	4	n.a.			
5	620.235	[M+H]⁺	3.96	1.1	$C_{30}H_{37}NO_{13}$	142.1230, 98.0971	4	n.a.			
6	604.2402	[M+H]⁺	4.04	1.3	$C_{30}H_{37}NO_{12}$	572.0979, 142.1230, 124.1113, 98.0970, 79.0555	3	Platensimycin B4	Diterpenoid glycoside	*Streptomyces platensis*	[6]
7	366.1893	[M+Na]⁺	4.12	0	$C_{17}H_{29}NO_6$	308.1821, 290.1734, 270.1647, 252.1608, 224.1649, 198.0766, 180.0642, 172.0989, 166.1217, 154.1225, 152.0704, 142.0490, 137.0591, 114.0552, 109.1009	3	Alpiniamide A	Linear polyketide	*Streptomyces* sp.	[7]
8	253.1415	[M+H]⁺	4.28	0.8	$C_{10}H_{17}N_6O_2$	228.0977, 209.1505, 205.6684, 186.9429, 182.0986, 165.6180	4	n.a.			
9	253.142	[M+H]⁺	4.44	2.8	$C_{10}H_{17}N_6O_2$	210.0668, 195.9134, 170.9937	4	n.a.			
10	308.1867	[M-H₂O]⁺	4.76	1.6	$C_{17}H_{27}NO_5$	252.1580, 198.0758, 180.0665, 172.0976, 166.1222, 152.0706, 142.0513, 137.0609, 109.1020	4	n.a.			
11	713.2711	[M+H]⁺	5.5	0.1	$C_{39}H_{40}N_2O_{11}$	142.1232, 98.0974	4	n.a.			
12	387.238	[M+H]⁺	5.7	-0.8	$C_{20}H_{34}O_7$	165.1138, 167.1079, 143.0687, 125.0604, 121.1022, 111.0808, 93.0695	2	Nonactyl nonactoate	Nonactic acid polyketide	*Streptomyces* sp.	[8]
13	558.1771	[M+H]⁺	6.01	-1.1	$C_{32}H_{23}N_5O_5$*	174.0918, 162.0919	4	n.a.			
14	401.254	[M+H]⁺	6.24	0.2	$C_{21}H_{36}O_7$	199.1332, 181.1228, 167.1066, 143.0703, 125.0966, 111.0810, 107.0859	2	Bonactin	Nonactic acid polyketide	*Streptomyces* sp.	[9]
15	421.2201	[M+Na]⁺	6.35	0.9	$C_{21}H_{34}O_7$	239.1254, 223.0950	4	n.a.			
16	413.2513	[M+Na]⁺	6.42	-0.5	$C_{20}H_{38}O_7$*	227.1261, 209.1144	4	n.a.			
17	309.1684	[M+H]⁺	6.62	2.9	$C_{13}H_{20}N_6O_3$	265.1174, 221.1151, 207.0990	4	n.a.			
18	415.2705	[M+H]⁺	6.82	2.2	$C_{22}H_{38}O_7$	199.1374, 181.1226, 163.1117, 143.0700, 139.1125, 135.1168, 125.0959, 107.0853, 81.0709	2	Homononactyl homononactate	Nonactic acid polyketide	*Streptomyces griseus*	[10]
19	321.1682	[M+H]⁺	6.89	2.2	$C_{14}H_{20}N_6O_3$	221.1156	4	n.a.			
20	312.1967	[M+H]⁺	7.49	1	$C_{20}H_{25}NO_2$	216.1390, 200.1078, 188.1083, 172.1142, 162.0898, 151.1139	4	n.a.			
21	807.395	[M+H]⁺	7.73	-2.4	$C_{46}H_{54}N_4O_9$	789.3856, 771.2729, 434.1707, 396.1556, 378.1438, 336.1355, 297.1229, 285.1239	4	n.a.			

No.	*m/z* value	Adduct	R_t (min)	ppm	Putative MF	Fragmentation pattern	IC	Putative identification	Chemical family	Biological origin	Ref
22	289.175	[M+Na]$^+$	7.93	-1	$C_{12}H_{22}N_6O$	Nf	4	n.a.			
23	585.3634	[M+H]$^+$	8.12	-0.9	$C_{31}H_{52}O_{10}$	199.1380, 185.1173, 181.1227, 167.1063, 143.0731, 125.0962, 111.0792, 93.0702	4	n.a.			
24	352.1552	[M+H]$^+$	8.4	0.9	$C_{21}H_{21}NO_4$	174.0921, 162.0919	4	n.a.			
25	807.3981	[M+H]$^+$	8.56	1.5	$C_{46}H_{54}N_4O_9$	789.3876, 771.2750, 434.1710, 396.1559, 378.1448, 365.1138, 336.1154, 297.1230, 285.1233	4	n.a.			
26	621.3619	[M+Na]$^+$	8.6	0.6	$C_{32}H_{54}O_{10}$	423.2351, 419.2396, 225.1102, 221.1153	4	n.a.			
27	684.3649	[M+H]$^+$	8.87	0	$C_{40}H_{49}N_3O_7$*	273.1241, 174.0922, 162.0919	4	n.a.			
28	560.4683	[M+H]$^+$	9.06	0.7	$C_{35}H_{61}NO_2$	542.4562, 524.4463	4	n.a.			
29	546.4896	[M+H]$^+$	9.87	1.8	$C_{35}H_{63}NO_3$	528.4788, 510.4700	4	n.a.			
30	783.4903	[M+H]$^+$	10.09	1	$C_{42}H_{70}O_{13}$	199.1337, 185.1174, 181.1226, 167.1068, 143.0703, 125.0961, 111.0809	4	n.a.			
31	797.5042	[M+H]$^+$	10.48	-1.1	$C_{43}H_{72}O_{13}$	199.1342, 181.1236, 167.1073, 143.0718, 125.0973, 107.0860	4	n.a.			
32	811.5203	[M+H]$^+$	10.85	-0.6	$C_{44}H_{74}O_{13}$	Nf	4	n.a.			
33	737.4476	[M+H]$^+$	11.77	0	$C_{40}H_{64}O_{12}$	MS6: 185.1191, 167.1073, 149.0946, 143.0683, 121.1022, 111.0811	2	Nonactin	Nonactic acid polyketide	*Streptomyces* spp.	[11]

Table S6. Putatively identified compounds produced by *Micromonospora* sp. extract CKG20-GYM. Putative annotations were based on the accurate mass, the predicted putative molecular formulae (MF), the retention time (R_t), the fragmentation pattern and the biological origin. $^\Delta$Different isomers with same *m/z* value and molecular formula, which cannot be differentiated based on MS/MS data; IC: Identification confidence level [3]; Ref = reference(s).

No.	*m/z* value	Adduct	R_t (min)	ppm	Putative MF	Fragmentation pattern	IC	Putative identification	Chemical family	Biological origin	Ref
34	243.1348	[M+H]+	2.47	1.2	$C_{11}H_{18}N_2O_4$	201.1239, 165.1032, 154.0877, 137.1081, 100.0399	4	n.a.			
35	218.1417	[M+H]+	3.2	5	$C_{11}H_{15}N_5$	162.9784, 150.0785	4	n.a.			
36	280.124	[M+H]+	4.17	-6.1	$C_8H_{17}N_5O_6$	262.1132, 196.0661	4	n.a.			
37	197.118	[M+H]+	5.67	1	$C_{11}H_{16}O_3$	158.9618, 117.9348, 96.9611	4	n.a.			
38	420.3119	[M-H2O]+	6.8	1.2	$C_{25}H_{43}NO_5$	378.2987, 332.2931, 315.2679, 229.1942, 203.1753, 175.1504, 149.1352, 135.1159, 107.0873	4	n.a.			
39	369.218	[M+H]+	7.48	0.5	$C_{22}H_{28}N_2O_3$	256.0851	4	n.a.			
40	479.2547	[M+H]+	7.72	0.2	$C_{28}H_{34}N_2O_5$	287.0663, 275.0670, 259.0480	4	n.a.			
41	466.2933	[M+H]+	7.85	-0.2	$C_{22}H_{44}NO_7P$	325.2744, 294.2796	4	n.a.			
42	454.2929	[M+H]+	8.08	-1.1	$C_{21}H_{44}NO_7P$	313.2740, 282.2794	2	1-palmitoyl-2-hydroxy-sn-glycero-3-phosphoethanolamine	Glycero-phospholipid	In cell membranes of all organisms	
43	330.2435	[M+H]+	8.11	0.6	$C_{21}H_{31}NO_2$	312.2322	4	n.a.			
44	463.2597	[M+H]+	8.2	0	$C_{28}H_{34}N_2O_4$	271.0725, 259.0725, 243.0536	2	Diazepinomicin	Phenazine alkaloid	*Micromonospora* sp.	[12]
45	480.3098	[M+H]+	8.38, 8.51$^\Delta$	1.7	$C_{23}H_{46}NO_7P$	339.2955, 308.2907	2	1-(9Z-octadecenoyl)-sn-glycero-3-phosphoethanolamine	Glycero-phospholipid	In cell membranes of all organisms	
46	479.2547	[M+H]+	8.62	0.2	$C_{28}H_{34}N_2O_5$	258.0409, 240.0301, 146.0241, 112.0401	4	n.a.			
47	408.0832	[M+H]+	8.78	0	$C_{20}H_{13}N_3O_7$	390.0728, 372.0609, 362.0768, 349.0473, 344.0648, 321.0529, 259.0353, 245.0565, 233.0556, 176.0353	4	n.a.			
48	411.2281	[M+H]+	8.9	-0.7	$C_{24}H_{30}N_2O_4$	393.2157, 383.2320, 285.0869, 271.0714, 259.0710, 243.0767	3	Diazaquinomycin D	Phenazine alkaloid	*Streptomyces* sp.	[13]
49	619.4077	[M+H]+	8.93	1	$C_{33}H_{54}N_4O_7$	427.3684, 400.3203, 376.3233, 305.2831, 297.1194, 280.0945, 279.1076, 262.0820, 252.0987, 224.1024, 220.0929, 208.1091, 202.0814, 193.0606, 167.0832, 149.0701, 123.0920, 121.0773, 109.1015, 96.0452	4	n.a.			
50	482.325	[M+H]+	9.09	0.8	$C_{23}H_{48}NO_7P$	341.3052, 310.3102	2	1-stearoyl-2-hydroxy-sn-glycero-3-phosphoethanolamine	Glycero-phospholipid	In cell membranes of all organisms	

No.	*m/z* value	Adduct	R_t (min)	ppm	Putative MF	Fragmentation pattern	IC	Putative identification	Chemical family	Biological origin	Ref
51	607.4077	[M+H]$^+$	9.27	1	C$_{32}$H$_{54}$N$_4$O$_7$	388.3211, 297.1197, 293.2846, 280.0937, 252.0986, 220.0934, 202.0833, 167.0821, 149.0676, 121.0761	2	Rakicidin A	Cyclic depsipeptide	*Micromonospora* sp.	[14]
52	621.4227	[M+H]$^+$	9.73	0	C$_{33}$H$_{56}$N$_4$O$_7$	402.3372, 350.3409, 307.2997, 297.1193, 280.0944, 252.0985, 220.0929, 167.0816, 149.0691, 121.0767	2	Rakicidin B	Cyclic depsipeptide	*Micromonospora* sp.	
53	635.4383	[M+H]$^+$	10.19	-0.2	C$_{34}$H$_{58}$N$_4$O$_7$	416.3523, 364.3604, 321.3148, 297.1199, 280.0939, 252.0980, 220.0930, 202.0839, 167.0817, 149.0708, 121.0757	2	Rakicidin E	Cyclic depsipeptide	*Micromonospora* sp.	[15]

Table S7. Putatively identified compounds produced by *Bacillus* sp. extract CKG24-GYM. Putative annotations were based on the accurate mass, the predicted putative molecular formulae (MF), the retention time (R_t), the fragmentation pattern and the biological origin. ±Parent mass out of detection limit (>1200 Da) and therefore, the ppm error and fragmentation pattern were not determined; *MF with best ppm error displayed; IC: Identification confidence level [3]; Nf: No fragmentation detected or below noise threshold (5e1); Ref = reference(s).

No.	*m/z* value	Adduct	R_t (min)	ppm	Putative MF	Fragmentation pattern	IC	Putative identification	Chemical family	Biological origin	Ref
54	367.0508	[M+H]+	3.63	-1.4	$C_{12}H_{14}O_{13}$	287.0525, 258.0562, 241.9696, 238.0435, 188.0169, 168.9262, 164.9999, 146.9907	4	n.a.			
55	424.2082	[M+H]+	3.71	-0.5	$C_{20}H_{29}N_3O_7$	407.1817, 390.1540, 330.1343, 274.0708, 250.1446, 232.1337, 215.1069, 159.0442	2	Amicoumacin-A	Isocoumarin	*Bacillus subtilis*	[16]
56	439.2083	[M+H]+	4.12	0.7	$C_{21}H_{30}N_2O_8$	422.1824, 250.1440, 232.1337, 215.1070, 176.0702, 159.0444, 149.0598	4	n.a.			
57	255.1207	[M+H]+	4.25	0.4	$C_9H_{14}N_6O_3$	195.9121	4	n.a.			
58	250.1127	[M+H]+	5.04	-4.4	$C_5H_{14}N_8O_4$	194.0496, 182.0501	4	n.a.			
59	392.1711	[M+H]+	5.43	0.5	$C_{20}H_{25}NO_7$	276.1247, 250.1441, 232.1328, 215.1074, 159.0440, 149.0598, 125.0238	3	Bacillcoumacin D	Isocoumarin	*Bacillus* sp.	[17]
60	390.1556	[M+H]+	5.55	0.8	$C_{20}H_{23}NO_7$	250.1441, 232.1340, 215.1073, 159.0442, 123.0087	3	Antibiotic AI-77-F or -H	Isocoumarin	*Bacillus* spp.	F: [18], H: [19]
61	1071.5811	[M+H]+	6.05	-2.8	$C_{50}H_{78}N_{12}O_{14}$	535.3573, 455.3136, 437.3194, 392.1531, 354.2751, 341.2750, 323.2671, 313.1513, 299.2645, 295.1353, 278.1133, 260.1039, 250.1231, 212.1082, 208.1156, 198.2230, 167.0809, 136.0747	3	Bacillomycin F2	Cyclic lipopeptide	*Bacillus subtilis*	[20], [21]
62	1085.5974	[M+H]+	6.45	-1.9	$C_{51}H_{80}N_{12}O_{14}$	680.4345, 663.4116, 645.3961, 618.3965, 566.3553, 549.3728, 531.3541, 507.3527, 469.3383, 451.3282, 406.1735, 392.1518, 389.1490, 375.1311, 368.2910, 355.2957, 351.2631, 323.1372, 313.2847, 295.1401, 278.1146, 277.1303, 275.1039, 268.2650, 264.0987, 261.0894, 260.1024, 250.1191, 243.1082, 233.0928, 216.0988, 212.2379, 209.0939, 208.1094, 198.0890, 188.1048, 184.1085, 167.0820, 136.0761	3	Bacillomycin F3	Cyclic lipopeptide	*Bacillus subtilis*	[20], [21]
63	1099.6122	[M+H]+	6.88	-2.7	$C_{52}H_{82}N_{12}O_{14}$	694.4479, 677.4232, 660.3998, 632.4120, 580.4044, 563.3820, 545.3659, 483.3513, 465.3430, 406.1723, 392.1563, 389.1466, 382.3062, 375.1307, 369.3107, 365.2799, 351.2995, 337.2898, 327.3002, 323.1351, 313.1502, 309.2888, 295.1408, 278.1149, 275.1031, 264.0986, 261.0858, 250.1187, 233.0918, 226.2534, 212.1035, 209.0947, 188.1048, 184.1090, 167.0815, 136.0763	3	Bacillomycin F5	Cyclic lipopeptide	*Bacillus subtilis*	[20], [21]
64	781.4157	[M+H]+	7.08	-0.8	$C_{44}H_{60}O_{12}$	557.3537, 539.3503, 419.2196, 405.2093, 401.2106, 399.1993, 389.2074, 373.2114, 371.2022, 367.1888, 365.1761, 359.2000, 351.1960, 349.1813, 343.2067, 341.1881, 335.2000, 333.1837, 331.1708, 323.1975, 321.1785, 305.1885, 303.1775, 209.0880, 173.1329,	3	Aurantinin B	Polyketide glycoside	*Bacillus aurantinus*	[22]

No.	*m/z* value	Adduct	R_t (min)	ppm	Putative MF	Fragmentation pattern	IC	Putative identification	Chemical family	Biological origin	Ref
						171.1176, 161.1315, 159.1180, 147.1168, 145.1039, 121.1011, 119.0865					
65	746.4219	[M+2H]$^{2+}$	7.14	n.a.$^±$	$C_{74}H_{114}N_{12}O_{20}$	n.a.$^±$	3	SNA 60-367-5	Cyclic lipopeptide	*Bacillus* sp.	[23]
66	739.4143	[M+2H]$^{2+}$	7.14	n.a.$^±$	$C_{73}H_{112}N_{12}O_{20}$	n.a.$^±$	3	SNA 60-367-6	Cyclic lipopeptide	*Bacillus* sp.	[23]
67	663.3561	[M+H]$^+$	7.24	-0.6	$C_{26}H_{38}N_{20}O_2$ or $C_{28}H_{50}N_6O_{12}$*	501.3020, 421.1306, 365.1053	4	n.a.			
68	753.4296	[M+2H]$^{2+}$	7.37	n.a.$^±$	$C_{75}H_{116}N_{12}O_{20}$	n.a.$^±$	3	a: SNA 60-367-12, b: SNA 60-367-13	Cyclic lipopeptide	*Bacillus* sp.	[23]
69	738.4238	[M+2H]$^{2+}$	7.56	n.a.$^±$	$C_{74}H_{114}N_{12}O_{19}$	n.a.$^±$	3	SNA 60-367-17	Cyclic lipopeptide	*Bacillus* sp.	[23]
70	738.4249	[M+2H]$^{2+}$	7.64	n.a.$^±$	$C_{74}H_{114}N_{12}O_{19}$	n.a.$^±$	3	SNA 60-367-18	Cyclic lipopeptide	*Bacillus* sp.	[23]
71	731.4171	[M+2H]$^{2+}$	7.64	n.a.$^±$	$C_{73}H_{112}N_{12}O_{19}$	n.a.$^±$	3	SNA 60-367-19	Cyclic lipopeptide	*Bacillus* sp.	[23]
72	745.4335	[M+2H]$^{2+}$	7.82	n.a.$^±$	$C_{75}H_{116}N_{12}O_{19}$	n.a.$^±$	3	SNA 60-367-23	Cyclic lipopeptide	*Bacillus* sp.	[23]
73	512.3693	[M+H]$^+$	8.25	-1.4	$C_{27}H_{49}N_3O_6$ or $C_{24}H_{41}N_{13}$*	268.2627, 115.0873, 102.0553, 84.0438	4	n.a.			
74	1008.6603	[M+H]$^+$	10.24	0.6	$C_{51}H_{89}N_7O_{13}$	455.3112, 441.2708, 437.3002, 427.3160, 409.3047, 395.2667, 342.2245, 328.1873, 324.2168, 314.2333, 283.2020, 245.1858, 229.1185, 227.1759, 212.2019, 201.1239, 199.1811, 195.1743, 185.1657, 183.1133, 154.1599, 86.0973	3	Anteiso-C$_{13}$-[Leu7]-surfactin	Cyclic lipopeptide	*Bacillus pumilus*	[24]
75	1064.5789	[M+H]$^+$	10.29	0.4	$C_{48}H_{74}N_{19}O_7Cl$ or $C_{50}H_{86}N_5O_{17}Cl$*	Nf	4	n.a.			
76	994.6426	[M+H]$^+$	10.41	-1.4	$C_{50}H_{87}N_7O_{13}$	455.3094, 441.2723, 437.2990, 342.2255, 328.1864, 324.2165, 314.2322, 296.2226, 285.1454, 283.2004, 269.1878, 231.1687, 229.1176, 227.1760, 215.1026, 212.2016, 201.1236, 199.1812, 195.1743, 185.1639, 86.0975	3	Lipopeptide NO	Cyclic lipopeptide	*Bacillus subtilis*	[25]
77	1022.6801	[M+H]$^+$	10.64	4.7	$C_{52}H_{91}N_7O_{13}$	469.3278, 451.3170, 441.2706, 423.3218, 395.2657, 356.2436, 342.2031, 338.2332, 328.1876, 310.2383, 296.1983, 285.1457, 283.2006, 269.1866, 267.2441, 255.1708, 245.1868, 229.1192, 227.1763, 215.1034, 213.1604, 209.1902, 201.1241, 199.1811, 185.1653, 183.1132, 170.1181, 154.1593, 86.0974	3	Iso-C$_{14}$-[Val7]-surfactin	Cyclic lipopeptide	*Bacillus pumilus*	[24]
78	1078.5947	[M+H]$^+$	10.66	0.5	$C_{51}H_{88}N_5O_{17}Cl$ or $C_{49}H_{76}N_{19}O_7Cl$*	Nf	4	n.a.			
79	1022.6746	[M+H]$^+$	10.76	-0.7	$C_{52}H_{91}N_7O_{13}$	469.3280, 451.3169, 441.2711, 423.3229, 395.2647, 356.2435, 342.2023, 338.2332, 310.2377, 296.1992, 285.1464, 283.2021, 269.1866, 267.2444, 255.1700,	3	n-C$_{14}$-[Val7]-surfactin	Cyclic lipopeptide	*Bacillus pumilus*	[24]

257

No.	*m/z* value	Adduct	R_t (min)	ppm	Putative MF	Fragmentation pattern	IC	Putative identification	Chemical family	Biological origin	Ref
						245.1868, 243.1360, 229.1189, 227.1763, 215.1030, 213.1584, 209.1903, 201.1242, 199.1811, 185.1656, 183.1134, 154.1593, 86.0974					
80	1064.5792	[M+H]$^+$	10.78	0.7	$C_{48}H_{74}N_{19}O_7Cl$ or $C_{50}H_{86}N_5O_{17}Cl^*$	Nf	4	n.a.			
81	1008.6598	[M+H]$^+$	10.8	0.1	$C_{51}H_{89}N_7O_{13}$	469.3280, 451.3174, 441.2707, 427.3165, 395.2650, 356.2438, 342.2028, 338.2325, 328.1869, 310.2381, 296.1968, 285.1455, 283.2013, 269.1865, 255.1698, 253.2272, 243.1342, 231.1708, 229.1192, 227.1756, 213.1611, 201.1238, 199.1807, 185.1652, 86.0971	3	n-C_{13}-[Leu7]-surfactin	Cyclic lipopeptide	*Bacillus pumilus*	[24]
82	1036.692	[M+H]$^+$	10.95	1	$C_{53}H_{93}N_7O_{13}$	483.3431, 465.3328, 455.3480, 441.2714, 437.3377, 395.2664, 370.2592, 352.2489, 342.2029, 328.1875, 324.2541, 311.1967, 296.1978, 285.1458, 283.2004, 269.1868, 267.2441, 255.1712, 253.2282, 245.1872, 240.2331, 229.1195, 227.1764, 215.1037, 213.1607, 201.1243, 199.1815, 185.1657, 183.1137, 170.1186, 154.1597, 86.0977	3	Anteiso-C_{15}-[Leu7]-surfactin	Cyclic lipopeptide	*Bacillus pumilus*	[24]
83	1092.6073	[M+H]$^+$	10.97	0.1	$C_{46}H_{74}N_{25}O_5Cl$ or $C_{48}H_{86}N_{11}O_{15}Cl^*$	Nf	4	n.a.			
84	1022.6751	[M+H]$^+$	11.16	-0.2	$C_{52}H_{91}N_7O_{13}$	483.3442, 465.3320, 441.2701, 395.2653, 370.2591, 356.2491, 342.2023, 328.1870, 324.2528, 296.1963, 285.1446, 283.2008, 269.1873, 255.1707, 240.2331, 231.1708, 229.1192, 227.1765, 215.1028, 213.1597, 201.1245, 199.1814, 185.1651, 183.1138, 86.0979	3	Anteiso-C_{15}-[Val7]-surfactin	Cyclic lipopeptide	*Bacillus pumilus*	[24]
85	1036.6903	[M+H]$^+$	11.18	-1.2	$C_{53}H_{93}N_7O_{13}$	483.3438, 465.3333, 455.3474, 441.2715, 437.3364, 395.2658, 370.2595, 352.2492, 342.2029, 328.1875, 324.2541, 311.1971, 296.1976, 285.1454, 283.2013, 269.1869, 267.2441, 255.1713, 245.1871, 240.2327, 229.1191, 227.1764, 223.2063, 215.1031, 213.1602, 201.1242, 199.1816, 185.1657, 183.1132, 170.1179, 154.1593, 86.0977	3	n-C_{14}-[Leu7]-surfactin	Cyclic lipopeptide	*Bacillus pumilus*	[24]
86	1036.687	[M+H]$^+$	11.48	-3.8	$C_{53}H_{93}N_7O_{13}$	497.3574, 483.3420, 479.3447, 465.3322, 455.3483, 441.2713, 395.2702, 384.2736, 370.2583, 366.2633, 356.2750, 352.2485, 342.2026, 338.2686, 326.2470, 324.2563, 311.1976, 296.1982, 285.1438, 283.2013, 269.1826, 267.2478, 254.2482, 245.1890, 243.1348, 231.1699, 229.1181, 227.1755, 215.1025, 213.1602, 201.1240, 199.1809, 185.1648, 183.1124, 170.1178, 86.0976	3	Anteiso-C_{15}-[Ile7]-surfactin	Cyclic lipopeptide	*Bacillus pumilus*	[24]
87	1064.7209	[M+H]$^+$	11.65	-1.3	$C_{55}H_{97}N_7O_{13}$	511.3743, 493.3648, 483.3786, 441.2816, 398.2912, 395.2643, 380.2790, 352.2855, 342.2029, 328.1868, 296.1967, 285.1422, 283.2024, 268.2642, 255.1717, 245.1867, 233.2294, 229.1197, 227.1754, 215.1038,	3	KMM 1364E	Cyclic lipopeptide	*Bacillus pumilus*	[26]

No.	*m/z* value	Adduct	R$_t$ (min)	ppm	Putative MF	Fragmentation pattern	IC	Putative identification	Chemical family	Biological origin	Ref
						201.1240, 199.1813, 185.1668, 183.1134, 154.1599, 86.0986					

Table S8. Putatively identified compounds produced by *Trichoderma* sp. extracts CHG34-CAG and CHG34-PDA. Putative annotations were based on the accurate mass, the predicted putative molecular formulae (MF), the retention time (R$_t$), the fragmentation pattern and the biological origin. $^{\Delta}$Different isomers with same *m/z* value and molecular formula, which cannot be differentiated based on MS/MS data; $^{\pm}$Parent mass out of detection limit (>1200 Da) and therefore, the ppm error and fragmentation pattern were not determined; *MF with best ppm error displayed; IC: Identification confidence level [3]; Nf: No fragmentation detected or below noise threshold (5e^1); Ref = reference(s).

No.	*m/z* value	Adduct	R$_t$ (min)	ppm	Putative MF	Fragmentation pattern	IC	Putative identification	Chemical family	Biological origin	Medium	Ref
88	237.1132	[M+H]$^+$	4.51	2.1	C$_{13}$H$_{16}$O$_4$	195.9131, 167.4925, 165.0561, 141.9551, 139.0753, 125.0237, 123.0437, 113.0982	3	Trichosorbicillin E	Sorbicillinoid	*Trichoderma reesei*	CAG, PDA	[27]
89	410.218	[M+H]$^+$	5.22	0.2	C$_{21}$H$_{31}$NO$_7$	242.0663, 224.0546, 124.0363	4	n.a.			CAG	
90	562.3585	[M+Na]$^+$	5.23	0.7	C$_{27}$H$_{49}$N$_5$O$_6$*	320.1957	4	n.a.			PDA	
91	473.1602	[M+H]$^+$	5.42	0.4	C$_{28}$H$_{24}$O$_7$	455.1462, 445.1667, 399.1595, 371.1277, 367.1292, 353.1223, 343.1312, 325.1264, 321.1139, 315.1418, 301.1224, 293.1167, 279.0644, 277.1200, 275.0994, 269.0819, 265.1236, 253.0858, 247.1097, 243.1052, 241.0905, 237.0936, 209.0972	4	n.a.			CAG	
92	451.2694	[M+H]$^+$	5.52	-0.4	C$_{25}$H$_{38}$O$_7$	289.2172, 271.2065, 217.1958, 215.1443, 205.1220, 197.1335, 187.1477, 185.1332, 182.1101, 171.1170, 169.1024, 159.1187, 157.1004, 155.0854, 151.1133, 147.1177, 145.1024, 137.0966, 133.1015, 131.0863, 127.0398, 119.0860, 105.0706, 99.0446	4	n.a.			PDA	
93	473.1603	[M+H]$^+$	5.69	0.6	C$_{28}$H$_{24}$O$_7$	455.1467, 445.1640, 427.1577, 399.1595, 381.1467, 371.1253, 353.1160, 343.1339, 325.1219, 321.1107, 303.1033, 293.1172, 279.0655, 275.1062, 269.0769, 265.1217, 253.0830, 247.1122, 243.0975, 241.0873, 209.0973	4	n.a.			CAG	
94	391.2457	[M+Na]$^+$	5.96	-0.8	C$_{21}$H$_{36}$O$_5$	359.219	4	n.a.			CAG	
95	259.1335	[M-H$_2$O]$^+$	6.36	0.4	C$_{16}$H$_{20}$O$_4$	241.1224, 223.1130, 213.1285, 197.1323, 195.1142, 185.1317, 180.0920, 171.1167, 169.1014, 167.0865, 165.0684, 157.1010, 155.0842, 145.1008, 143.0855, 141.0714, 129.0699, 105.0713	4	n.a.			CAG	

No.	*m/z* value	Adduct	R_t (min)	ppm	Putative MF	Fragmentation pattern	IC	Putative identification	Chemical family	Biological origin	Medium	Ref
96	277.144	[M+H]$^+$	6.6	0	$C_{16}H_{20}O_4$	231.1372, 201.0457, 195.9114, 143.0857, 129.0681	4	n.a.			CAG	
97	331.1521	[M+H]$^+$	6.76	0.6	$C_{15}H_{18}N_6O_3$	299.1237, 211.1088, 189.1274, 133.0657	4	n.a.			CAG	
98	588.39	[M+H]$^+$	6.86	0	$C_{34}H_{53}NO_7$*	423.2950, 253.1597, 251.1447, 235.1489, 225.1640, 223.1465, 148.0973, 130.0874, 102.0919	4	n.a.			CAG, PDA	
99	189.1278	[M+H]$^+$	6.87	0.5	$C_{13}H_{16}O$	171.1169, 147.1166, 145.1010, 133.0649, 105.0698	4	n.a.			CAG	
100	439.3324	[M+H]$^+$	7.11	-0.2	$C_{28}H_{42}N_2O_2$	279.2345, 209.1549, 173.1328, 161.1080, 149.1325, 137.1328, 109.1021, 95.0867, 81.0709	4	n.a.			CAG, PDA	
101	344.3164	[M+H]$^+$	7.4	-0.3	$C_{20}H_{41}NO_3$	344.3129, 300.2899, 282.2793, 270.2758, 264.2762, 252.2674, 88.0771	4	n.a.			CAG, PDA	
102	345.1677	[M+Na]$^+$	7.76	-0.3	$C_{18}H_{26}O_5$	Nf	4	n.a.			CAG	
103	770.5386	[M+H]$^+$	7.79	-0.8	$C_{38}H_{71}N_7O_9$	453.3084, 354.2396, 326.2451, 300.2278, 241.1562, 184.1345, 143.1185, 86.0972	4	n.a.			CAG, PDA	
104	1197.756	[M+Na]$^+$	7.93	-2.3	$C_{58}H_{102}N_{12}O_{13}$	983.5846, 955.5931, 897.5527, 870.5408, 843.5667, 757.4554, 730.4795, 645.4308, 547.3153, 489.2869, 462.2697, 403.2706	3	Trichodermide C	Peptaibol	*Trichoderma viride*	CAG, PDA	[28]
105	754.5424	[M+H]$^+$	8.12	-2.4	$C_{38}H_{71}N_7O_8$	453.2956, 354.2416, 326.2400, 241.1605, 184.1328, 86.0979	3	n.a.			CAG, PDA	
106	498.379	[M+H]$^+$	8.29	-1	$C_{28}H_{51}NO_6$*	480.3684, 236.1504	4	n.a.			CAG, PDA	
107	751.9497	[M+2Na]$^{2+}$	8.29	-0.7	$C_{71}H_{123}N_{15}O_{17}$	n.a.$^\pm$	3	Tv29-14S-Vc	Peptaibol	*Trichoderma virens*	CAG, PDA	[29]
108	836.4872	[M+H]$^+$	8.29	0.5	$C_{38}H_{69}N_5O_{15}$ or $C_{36}H_{57}N_{19}O_5$*	369.2141, 256.1304	4	n.a.			CAG, PDA	
109	623.4496	[M+H]$^+$	8.29	0	$C_{32}H_{58}N_6O_6$*	324.2295, 215.1763, 211.1452, 183.1501	4	n.a.			CAG, PDA	
110	1197.7583	[M+Na]$^+$	8.39	-0.3	$C_{58}H_{102}N_{12}O_{13}$	1179.7465, 955.5943, 897.5522, 870.5418, 757.4579, 645.4301, 631.4155, 561.3373, 547.3219	3	Trichorozin-II	Peptaibol	*Trichoderma harzianum*	CAG, PDA	[30]
111	553.3351	[M+H]$^+$	8.41	0.2	$C_{26}H_{44}N_6O_7$*	355.1985, 256.1306, 228.1352, 128.0710, 101.0719	4	n.a.			PDA	
112	623.4495	[M+H]$^+$	8.41	-0.2	$C_{32}H_{58}N_6O_6$*	324.2296, 215.1762, 211.1454, 183.1503	4	n.a.			CAG, PDA	
113	961.6072	[M+H]$^+$	8.41	-0.1	$C_{44}H_{72}N_{20}O_5$ or $C_{46}H_{84}N_6O_{15}$*	355.1985, 256.1304	4	n.a.			CAG, PDA	

No.	*m/z* value	Adduct	R_t (min)	ppm	Putative MF	Fragmentation pattern	IC	Putative identification	Chemical family	Biological origin	Medium	Ref
114	345.168	[M+Na]$^+$	8.45	0.6	$C_{18}H_{26}O_5$	Nf	4	n.a.			CAG	
115	623.4493	[M+H]$^+$	8.45	-0.5	$C_{32}H_{58}N_6O_6$*	324.2290, 215.1765, 211.1449, 183.1499	4	n.a.			CAG, PDA	
116	553.335	[M+H]$^+$	8.45	0	$C_{26}H_{44}N_6O_7$*	355.1923, 256.1304, 228.1354, 128.0707, 101.0713	4	n.a.			CAG, PDA	
117	837.4725	[M+H]$^+$	8.45	0.4	$C_{39}H_{64}N_8O_{12}$ or $C_{37}H_{52}N_{22}O_2$*	370.1981, 257.1146, 128.0712	4	n.a.			CAG, PDA	
118	623.4493	[M+H]$^+$	8.52	-0.5	$C_{32}H_{58}N_6O_6$*	324.2288, 215.1760, 211.1449, 183.1497	4	n.a.			CAG, PDA	
119	758.9578	[M+2Na]$^{2+}$	8.52	-0.4	$C_{72}H_{125}N_{15}O_{17}$	n.a.$^\pm$	3	Tv29-14S-VI	Peptaibol	*Trichoderma virens*	CAG, PDA	[29]
120	850.5023	[M+H]$^+$	8.52	-0.2	$C_{39}H_{71}N_5O_{15}$ or $C_{37}H_{59}N_{19}O_5$*	383.2293, 270.1457, 142.0862	4	n.a.			CAG, PDA	
121	874.5392	[M+2H]$^{2+}$	8.59	1.7	$C_{81}H_{142}N_{20}O_{22}$	n.a.$^\pm$	3	Trichorzin MA-2	Peptaibol	*Trichoderma harzianum*	CAG, PDA	[31]
122	1136.6675	[M+H]$^+$	8.59	-0.4	$C_{52}H_{89}N_{13}O_{15}$ or $C_{50}H_{77}N_{27}O_5$*	Nf	4	n.a.			CAG, PDA	
123	623.4504	[M+H]$^+$	8.67	-0.8	$C_{33}H_{54}N_{10}O_2$*	324.2294, 215.1759, 211.1451, 183.1497	4	n.a.			CAG, PDA	
124	975.6241	[M+H]$^+$	8.67	-0.2	$C_{46}H_{70}N_{24}O$ or $C_{48}H_{82}N_{10}O_{11}$*	369.2148, 270.1460	4	n.a.			CAG, PDA	
125	874.5398	[M+2H]$^{2+}$	8.78	1.7	$C_{81}H_{142}N_{20}O_{22}$	n.a.$^\pm$	3	Trichokindin Ia	Peptaibol	*Trichoderma harzianum*	CAG, PDA	[32]
126	1136.6686	[M+H]$^+$	8.78	0.6	$C_{52}H_{89}N_{13}O_{15}$ or $C_{50}H_{77}N_{27}O_5$*	697.3896, 484.2784, 399.2252, 286.1411, 268.1303 197.0926	4	n.a.			CAG, PDA	
127	623.4493	[M+H]$^+$	8.85	-1	$C_{33}H_{54}N_{10}O_2$*	324.2296, 215.1763, 211.1452, 183.1502	4	n.a.			CAG, PDA	
128	975.6257	[M+H]$^+$	8.85	0.1	$C_{51}H_{90}O_{17}$ or $C_{49}H_{78}N_{14}O_7$*	369.2148, 256.1304	4	n.a.			CAG, PDA	
129	976.6094	[M+H]$^+$	8.96	-0.2	$C_{49}H_{77}N_{13}O_8$*	370.1984, 342.2027, 257.1147	4	n.a.			CAG, PDA	
130	623.4506	[M+H]$^+$	8.98	-0.5	$C_{33}H_{54}N_{10}O_2$*	324.2290, 296.1980, 215.1765, 211.1454, 183.1500	4	n.a.			CAG, PDA	
131	867.5361	[M+2H]$^{2+}$	8.98	n.a.$^\pm$	n.a.$^\pm$	n.a.$^\pm$	4	n.a.			CAG, PDA	
132	892.5373	[M+H+Na]$^{2+}$	8.98	n.a.$^\pm$	n.a.$^\pm$	n.a.$^\pm$	4	n.a.			CAG, PDA	
133	892.5372	[M+H+Na]$^{2+}$	9.04	n.a.$^\pm$	n.a.$^\pm$	n.a.$^\pm$	4	n.a.			CAG, PDA	

No.	*m/z* value	Adduct	R_t (min)	ppm	Putative MF	Fragmentation pattern	IC	Putative identification	Chemical family	Biological origin	Medium	Ref
134	909.527	$[M+2H]^{2+}$	9.04	-0.9	$C_{82}H_{140}N_{22}O_{24}$	n.a.±	3	Trichobrachin B-I	Peptaibol	*Trichoderma longibrachiatum*	CAG, PDA	[33]
135	989.6424	$[M+H]^+$	9.04	1.1	$C_{50}H_{80}N_{14}O_7$ or $C_{52}H_{92}O_{17}$*	383.2299, 270.1472	4	n.a.			CAG, PDA	
136	623.4505	$[M+H]^+$	9.04	-0.6	$C_{33}H_{54}N_{10}O_2$*	324.2296, 211.1455, 183.1503	4	n.a.			CAG, PDA	
137	623.4506	$[M+H]^+$	9.08	-0.3	$C_{33}H_{54}N_{10}O_2$*	324.2294, 211.1452, 183.1503	4	n.a.			CAG, PDA	
138	892.5372	$[M+H+Na]^{2+}$	9.08	n.a.±	n.a.±	n.a.±	4	n.a.			CAG, PDA	
139	989.6392	$[M+H]^+$	9.08	0.6	$C_{48}H_{88}N_6O_{15}$ or $C_{46}H_{76}N_{20}O_5$*	383.2303, 270.1464	4	n.a.			CAG, PDA	
140	892.5383	$[M+H+Na]^{2+}$	9.15	n.a.±	n.a.±	n.a.±	4	n.a.			CAG, PDA	
141	623.4499	$[M+H]^+$	9.21	0.5	$C_{32}H_{58}N_6O_6$*	324.2297, 215.1770, 211.1457, 183.1502	4	n.a.			CAG, PDA	
142	990.6248	$[M+H]^+$	9.21	0.9	$C_{47}H_{71}N_{23}O_2$*	384.2148, 356.2190, 271.1308, 142.0871	4	n.a.			CAG, PDA	
143	874.5402	$[M+2H]^{2+}$	9.25	1.7	$C_{81}H_{142}N_{20}O_{22}$	n.a.±	3	Trichokindin Ib	Peptaibol	*Trichoderma harzianum*	CAG, PDA	[32]
144	874.5392	$[M+2H]^{2+}$	9.38	1.7	$C_{81}H_{142}N_{20}O_{22}$	n.a.±	3	Trichokindin IIa	Peptaibol	*Trichoderma harzianum*	CAG, PDA	[32]
145	1136.6674	$[M+H]^+$	9.38	-0.4	$C_{52}H_{89}N_{13}O_{15}$ or $C_{50}H_{77}N_{27}O_5$*	697.3872, 484.2768, 399.2243, 286.1408, 268.1303, 197.0931	4	n.a.			CAG, PDA	
146	1164.6991	$[M+H]^+$	9.41	-0.1	$C_{52}H_{81}N_{27}O_5$ or $C_{54}H_{93}N_{13}O_{15}$	498.2934, 399.2248, 286.1414, 268.1305, 197.0930	4	n.a.			CAG, PDA	
147	881.5459	$[M+2H]^{2+}$	9.5	0.4	$C_{82}H_{144}N_{20}O_{22}$	n.a.±	3	Trichokindin IIb	Peptaibol	*Trichoderma harzianum*	CAG, PDA	[32]
148	844.5923	$[M+2H]^{2+}$	9.57	n.a.±	n.a.±	n.a.±	4	n.a.			CAG, PDA	
149	873.55	$[M+2H]^{2+}$	9.57	2.2	$C_{82}H_{144}N_{20}O_{21}$	n.a.±	3	Neoatroviridin B	Peptaibol	*Trichoderma atroviride*	CAG, PDA	[34]
150	881.5432	$[M+2H]^{2+}$	9.57	0.4	$C_{82}H_{144}N_{20}O_{22}$	n.a.±	3	Trichokindin IIIa/b	Peptaibol	*Trichoderma harzianum*	CAG, PDA	[32]
151	881.547	$[M+2H]^{2+}$	9.61	0.4	$C_{82}H_{144}N_{20}O_{22}$	n.a.±	3	Trichokindin IV	Peptaibol	*Trichoderma harzianum*	CAG, PDA	[32]
152	902.5486	$[M+2H]^{2+}$	9.61	n.a.±	n.a.±	n.a.±	4	n.a.			CAG, PDA	
153	913.543	$[M+2Na]^{2+}$	9.61	n.a.±	n.a.±	n.a.±	4	n.a.			CAG, PDA	

No.	*m/z* value	Adduct	R_t (min)	ppm	Putative MF	Fragmentation pattern	IC	Putative identification	Chemical family	Biological origin	Medium	Ref
154	881.5477	[M+2H]$^{2+}$	9.74	0.4	$C_{82}H_{144}N_{20}O_{22}$	n.a.$^{\pm}$	3	Trichokindin Va/b	Peptaibol	*Trichoderma harzianum*	CAG, PDA	[32]
155	888.5443	[M+2H]$^{2+}$	9.99	-0.8	$C_{83}H_{146}N_{20}O_{22}$	n.a.$^{\pm}$	3	Trichokindin VI	Peptaibol	*Trichoderma harzianum*	CAG, PDA	[32]
156	891.5471	[M+H+Na]$^{2+}$	9.99	n.a.$^{\pm}$	$C_{83}H_{146}N_{20}O_{21}$	n.a.$^{\pm}$	3	Neoatroviridin D	Peptaibol	*Trichoderma atroviride*	CAG, PDA	[34]
157	888.555	[M+2H]$^{2+}$	10.14	-0.8	$C_{83}H_{146}N_{20}O_{22}$	n.a.$^{\pm}$	3	Trichokindin VII	Peptaibol	*Trichoderma harzianum*	CAG, PDA	[32]
158	916.5155	[M+2H]$^{2+}$	10.14	n.a.$^{\pm}$	n.a.$^{\pm}$	n.a.$^{\pm}$	4	n.a.			CAG, PDA	
159	481.2935	[M+Na]$^{+}$	10.33, 10.39$^{\Delta}$	1	$C_{28}H_{42}O_5$	423.2865, 355.2252	3	Ergokonin B	Ergosterol	*Trichoderma koningii*	CAG, PDA	[35]
160	873.5497	[M+2H]$^{2+}$	10.33	2.2	$C_{82}H_{144}N_{20}O_{21}$	n.a.$^{\pm}$	3	Neoatroviridin C	Peptaibol	*Trichoderma atroviride*	CAG, PDA	[34]
161	895.5413	[M+2H]$^{2+}$	10.39	n.a.$^{\pm}$	n.a.$^{\pm}$	n.a.$^{\pm}$	4	n.a.			CAG, PDA	

264

Table S9. Putatively identified compounds produced by *Fusarium* sp. extracts CHG38-CAG and CHG38-PDA. Putative annotations were based on the accurate mass, predicted putative molecular formulae (MF), the retention time (R_t), the fragmentation pattern and the biological origin. *MF with best ppm error; IC: Identification confidence level [3]; Nf: No fragmentation detected or below noise threshold ($5e^1$); Ref = reference(s).

No.	*m/z* value	Adduct	R_t (min)	ppm	Putative MF	Fragmentation pattern	IC	Putative identification	Chemical family	Biological origin	Medium	Ref
162	235.0614	[M+H]$^+$	2.97	3.4	$C_{12}H_{10}O_5$	217.0504, 193.0493, 189.0548, 175.0385, 161.0598, 151.0394, 149.0594, 125.0603, 111.0084	3	Diploquinone A	Naphthoquinone	*Diplodia mutila*	PDA	[36]
163	277.0715	[M+H]$^+$	3.09	1.1	$C_{14}H_{12}O_6$	259.0608, 235.0603, 231.0657, 217.0498, 193.0496, 191.0697, 123.0438	3	Norjavanicin	Naphthoquinone	*Fusarium* sp.	PDA	[37]
164	235.0977	[M+H]$^+$	3.52	3	$C_{13}H_{14}O_4$	217.0866, 191.0711, 176.0474, 163.0749, 151.0393, 135.0808	2	Aloesol	Chromone	*Fusarium* sp.	PDA	[38]
165	233.0820	[M+H]$^+$	3.63	2.6	$C_{13}H_{12}O_4$	217.0872, 191.0711, 151.0393	2	Macrocarpone C	Chromone	*Fusarium tricinctum*	PDA	[39]
166	279.0881	[M+H]$^+$	3.7	4.3	$C_{14}H_{14}O_6$	261.0784, 243.0665, 219.0664, 201.0530, 191.0708, 177.0186, 173.0605, 163.0770	3	(-)-Citreoisocoumarin	Isocoumarin	*Fusarium tricinctum*	PDA	[39]
167	191.0710	[M+H]$^+$	3.97	1	$C_{11}H_{10}O_3$	176.0488, 151.0390, 149.9310, 135.0444, 110.0086	4	n.a.			PDA	
168	359.1109	[M+Na]$^+$	4.37	0.6	$C_{17}H_{20}O_7$	324.5316, 322.0607, 291.0259, 271.0585, 253.8915, 252.3335	3	3-O-Ethyldihydrofusarubin A or B	Naphthoquinone	*Fusarium solani*	PDA	[40]
169	339.1803	[M+H]$^+$	4.58	-1.5	$C_{18}H_{26}O_6$	303.1549, 285.1486, 267.1371, 259.1721, 257.1524, 229.0869, 217.0846, 215.0682, 189.0564, 177.0592, 175.0392, 167.0347, 161.0622, 149.0613, 135.1176	2	2'-hydroxyzearalanol	Zearalenone (Macrolide)	*Penicillium* sp.	CAG	[41]
170	249.0768	[M+H]$^+$	5.46	2	$C_{13}H_{12}O_5$	217.0504, 192.0427, 153.0183	4	n.a.			PDA	
171	259.0615	[M+H]$^+$	5.66	3.5	$C_{14}H_{10}O_5$	244.0369, 231.0674, 213.0604, 191.0726	3	Huperxanthone B	Xanthone	*Aspergillus versicolor*	PDA	[42]
172	384.3954	[M+H]$^+$	5.96	0	$C_{23}H_{49}N_3O$	367.3683, 296.2959	4	n.a.			PDA	
173	629.3642	[M+Na]$^+$	6.23	0.6	$C_{34}H_{54}O_9$	557.3420, 387.2336	4	n.a.			CAG, PDA	
174	690.2125	[M+H]$^+$	6.56	1.6	$C_{40}H_{23}N_{11}O_2$	373.0741, 355.0630	4	n.a.			CAG	
175	412.4270	[M+H]$^+$	6.59	0.7	$C_{25}H_{53}N_3O$	324.3275	4	n.a.			PDA	
176	319.1553	[M+H]$^+$	6.63	2.5	$C_{18}H_{22}O_5$	301.1441, 283.1342, 265.1237, 255.1386, 241.0873, 231.0662, 229.0860, 227.0712, 217.0859, 215.0706, 213.0561, 205.0868, 203.0716, 189.0562, 187.0764, 185.0606, 175.0762, 169.0662, 157.0653	2	Zearalenone	Zearalenone (Macrolide)	*Fusarium graminearum*	CAG	[43]

No.	*m/z* value	Adduct	R_t (min)	ppm	Putative MF	Fragmentation pattern	IC	Putative identification	Chemical family	Biological origin	Medium	Ref
177	575.1199	[M+H]$^+$	7.32	1.6	$C_{30}H_{22}O_{12}$*	287.0563, 274.0464, 259.0613	4	n.a.			CAG, PDA	
178	273.0771	[M+H]$^+$	7.43	2.9	$C_{15}H_{12}O_5$	258.0524, 255.0665, 230.0581, 227.0702	3	Griseoxanthone C	Xanthone	*Fusarium equiseti*	PDA	[44]
179	303.1605	[M-H$_2$O]$^+$	7.47	3	$C_{18}H_{24}O_5$	285.1493, 229.0855, 215.0695, 205.0511, 191.0348, 163.0399	2	Zearalanone	Zearalenone (Macrolide)	*Fusarium* spp.	CAG	[45]
180	289.1786	[M+Na]$^+$	7.91	2.1	$C_{16}H_{26}O_3$	Nf	4	n.a.			PDA	
181	691.4647	[M+H]$^+$	8.95	0.1	$C_{37}H_{62}N_4O_8$*	659.4388, 428.3079, 377.3063, 359.2942, 331.2998, 313.2980, 303.2622, 263.2337, 235.2063, 232.1362, 220.1098, 181.0634, 172.1087, 164.0696, 155.0792, 147.0751, 130.0498, 121.1051	4	n.a.			CAG	
182	659.4385	[M+H]$^+$	9.07	0.2	$C_{36}H_{58}N_4O_7$	428.3166, 377.3065, 359.2950, 331.2991, 303.2691, 263.2368, 232.1301, 215.1033, 185.0930, 172.1086, 164.0710, 155.0815, 147.0771, 130.0506	3	Fusaristatin A	Cyclic lipopeptide	*Fusarium* sp.	CAG, PDA	[46]
183	695.3956	[M+H]$^+$	9.52	1.2	$C_{44}H_{54}O_7$	379.3360, 309.2571, 295.2407, 253.1958, 239.1786, 213.1648, 201.1647, 199.1482, 187.1492, 185.1322, 173.1342, 171.1174, 161.1311, 159.1167, 157.1026, 149.1328, 147.1171, 145.1016, 143.0850, 133.1014, 131.0849	4	n.a.			PDA	
184	437.3425	[M+H]$^+$	10.67	1.1	$C_{30}H_{44}O_2$	401.3213, 381.2794, 367.2639, 353.2500, 341.2487, 339.2319, 327.2321, 313.2170, 307.2427, 267.2122, 225.1645, 211.1495, 197.1337, 183.1170, 169.1021, 157.1024	4	n.a.			CAG, PDA	
185	737.4779	[M-H$_2$O]$^+$	10.82	-0.3	$C_{48}H_{66}O_7$*	701.4548, 593.3277, 575.3162, 567.3481, 441.2057, 381.2049, 363.1950, 313.1449, 295.1334, 293.1901, 275.1901, 267.1755, 249.1637, 225.1637, 209.1335, 201.0553, 199.0755, 195.1171, 183.1152	4	n.a.			CAG	
186	468.3607	[M+H]$^+$	11.44	0.8	$C_{31}H_{47}O_3$	437.3426, 393.2792, 365.2496, 352.2406, 339.2327, 337.2165, 319.2072, 307.2425, 293.2269, 265.1950, 251.1812, 249.1646, 237.1648, 235.1481, 223.1490, 211.1495, 209.1336, 196.1250, 183.1177, 181.1023, 169.1022	4	n.a.			CAG	

No.	*m/z* value	Adduct	R_t (min)	ppm	Putative MF	Fragmentation pattern	IC	Putative identification	Chemical family	Biological origin	Medium	Ref
187	793.5020	[M+H]$^+$	11.54	0.5	C$_{47}$H$_{64}$N$_6$O$_5$*	761.4775, 743.4667, 651.4027	4	n.a.			CAG	
188	755.4899	[M+H]$^+$	11.54	1.6	C$_{48}$H$_{66}$O$_7$	Nf	4	n.a.			CAG	
189	437.3420	[M+H]$^+$	11.59	0	C$_{30}$H$_{44}$O$_2$	419.3311, 401.3185, 381.2783, 357.1451, 335.2753, 313.2141, 299.2004, 275.1782, 259.1690, 223.1484, 211.1479, 195.1165, 183.1165, 169.1019, 159.1168, 145.0999	4	n.a.			PDA	
190	436.3340	[M+H]$^+$	11.68	-0.2	C$_{30}$H$_{43}$O$_2$	421.3112, 385.2896, 365.2484, 337.2177, 323.2018, 317.2274, 311.2021, 301.1965, 297.1866, 261.1650, 235.1489, 209.1336, 195.1180	4	n.a.			CAG, PDA	
191	437.3424	[M+H]$^+$	11.69	0.9	C$_{30}$H$_{44}$O$_2$	421.3102, 419.3308, 401.3206, 385.2891, 337.2167, 323.2014, 317.2267, 313.2159, 311.2007, 301.1959, 297.1853, 275.1794, 263.1789, 261.1641, 259.1678, 253.1947, 249.1632, 235.1484, 223.1482, 221.1327, 211.1483, 209.1327, 197.1323, 195.1172, 183.1167, 169.1006	4	n.a.			PDA	
192	753.4741	[M+H]$^+$	11.82	-0.4	C$_{49}$H$_{60}$N$_4$O$_3$*	735.4622, 656.3732, 638.3626, 623.3362, 605.3292, 587.3196, 565.3297, 523.2813, 521.2742, 509.2715, 497.2628, 495.2540, 481.2378, 477.2425, 469.2356, 467.2224, 463.2249, 313.1443, 295.1342, 221.1326, 201.0557, 199.0752, 195.1175	4	n.a.			CAG	
193	436.3335	[M+H]$^+$	11.93	-1.3	C$_{30}$H$_{43}$O$_2$	421.3098, 403.2995, 393.2770, 385.2880, 340.2391, 325.2155, 323.2359, 321.2568, 319.2407, 307.2062, 293.2261, 279.2098, 265.1939, 251.1783, 249.1631, 237.1637, 235.1479, 225.1630, 223.1380, 211.1479, 208.1323, 197.1318, 195.1164, 184.1246, 169.1005, 155.0851	4	n.a.			CAG, PDA	

267

Table S10. Putatively identified compounds produced by *Penicillium* sp. extracts CKG23-CAG and CKG23-PDA. Putative annotations were based on the accurate mass, the predicted putative molecular formulae (MF), the retention time (R_t), the fragmentation pattern and the biological origin. $^\Delta$Different isomers with same *m/z* value and molecular formula, which cannot be differentiated based on MS/MS data; *MF with best ppm error displayed; IC: Identification confidence level [3]; Nf: No fragmentation detected or below noise threshold ($5e^1$); Ref = reference(s).

No.	*m/z* value	Adduct	R_t (min)	ppm	Putative MF	Fragmentation pattern	IC	Putative identification	Chemical family	Biological origin	Medium	Ref
194	245.082	[M+H]$^+$	1.24	2.4	C$_{14}$H$_{12}$O$_4$	227.0711, 217.0858, 209.0590, 199.0762, 189.0916, 185.0596, 181.0651, 175.0771, 173.0607, 171.0809, 161.0609, 157.0655, 153.0705, 151.0388, 147.0443, 143.0853, 135.0447, 123.0446, 107.0495	3	3-methylbisnoryangonin	Styrylpyrone	*Penicillium glabrum*	CAG, PDA	[47]
195	157.0059	[M+H]$^+$	2.14	1.9	C$_7$H$_5$O$_2$Cl	129.0107, 121.0266, 101.0160, 94.0412	4	n.a.			CAG	
196	233.082	[M+H]$^+$	2.84	2.6	C$_{13}$H$_{12}$O$_4$	194.9539, 191.0710, 187.0742, 173.0598, 149.0604, 147.0451, 123.0438, 121.0669, 85.0288	4	n.a.			PDA	
197	325.1292	[M+H]$^+$	3.46	1.5	C$_{16}$H$_{20}$O$_7$	289.1072, 247.0972, 233.0819, 231.0664, 227.1076, 213.0559, 191.0341, 189.0549, 183.0296, 165.0552	3	11,12-Dihydroxycurvularin	Zearalenone (Macrolide)	*Penicillium citreo-viride*	PDA	[48]
198	327.1235	[M+H]$^+$	3.9	0.9	C$_{19}$H$_{18}$O$_5$	309.1131, 294.0894, 285.0765	3	1,7-Dihydroxy-2-methoxy-3-prenylxanthone	Xanthone	*Phomopsis* sp.	CAG	[49]
199	309.1345	[M+H]$^+$	4	2.3	C$_{16}$H$_{20}$O$_6$	273.1129, 255.1038, 231.1031, 229.1228, 215.0716, 213.0914, 201.0553, 189.0924, 187.0768, 177.0551, 175.0400, 173.0602, 161.0605, 149.0605	3	(3S,7S)-7-hydroxyresorcylide	Zearalenone (Macrolide)	*Penicillium* sp.	PDA	[50]
200	273.0409	[M+H]$^+$	4.12	3.7	C$_{14}$H$_8$O$_6$	245.0457, 227.0340, 217.0508, 199.0397	3	2,8-dihydroxy-9-oxo-9H-xanthene-6-carboxylic acid	Xanthone	*Arthrinium arundinis*	PDA	[51]
201	399.1813	[M+H]$^+$	4.55, 4.87$^\Delta$	1.3	C$_{23}$H$_{26}$O$_6$	381.1706, 363.1587, 355.1514, 352.1281, 348.1369, 339.1246, 327.1208, 311.0899	3	Seco-penicitrinol A	Xanthone	*Penicillium citrinum*	CAG	[52]
202	289.0717	[M+H]$^+$	4.57	1.7	C$_{15}$H$_{12}$O$_6$	274.0483, 270.0526, 246.0534, 243.0657, 200.0488	3	Drimiopsin I	Xanthone	*Penicillium* sp.	PDA	[53]
203	511.2927	[M+H]$^+$	4.96	1.4	C$_{28}$H$_{38}$N$_4$O$_5$	265.1557, 247.1459, 219.1503, 199.1437, 171.1505, 166.0866, 120.0811, 72.0825	2	Bilaid A	Tetrapeptide	*Penicillium* sp.	PDA	[54]
204	447.2936	[M+Na]$^+$	5.22	0.4	C$_{21}$H$_{44}$O$_8$	Nf	4	n.a.			PDA	
205	309.1343	[M+H]$^+$	5.25	1.6	C$_{16}$H$_{20}$O$_6$	291.1229, 273.1129, 255.1022, 245.1183, 231.0663, 227.1073, 217.0497, 213.0556, 207.0497,	3	(3S,7R)-7-hydroxyresorcylide	Zearalenone (Macrolide)	*Penicillium* sp.	PDA	[50]

No.	*m/z* value	Adduct	R_t (min)	ppm	Putative MF	Fragmentation pattern	IC	Putative identification	Chemical family	Biological origin	Medium	Ref
						195.0292, 193.0501, 191.0343, 183.0292, 181.0136, 177.0192, 167.0341, 165.0184, 159.0445, 99.0812, 81.0706						
206	457.2601	[M+H]⁺	5.47	-0.7	$C_{28}H_{32}N_4O_2$	440.2370, 439.2495, 399.2179, 385.2024, 382.1931, 381.1940, 368.1750, 340.1801, 326.1655, 323.1541, 309.1378, 299.1517, 297.1387, 255.1489, 238.1450, 210.1285, 198.1156, 197.1081, 185.1075, 183.0918, 181.0893, 168.0813, 159.0927	2	Communesin A	Indole alkaloid	*Penicillium* sp.	CAG	[55]
207	427.1757	[M+H]⁺	5.47	0	$C_{24}H_{26}O_7$	381.1703, 363.1595, 354.1459, 348.1355, 339.1234, 326.1150, 321.1122, 311.0921, 308.1045, 297.0759	4	n.a.			CAG	
208	293.1393	[M+H]⁺	5.97	1.4	$C_{16}H_{20}O_5$	275.1283, 257.1166, 239.1059, 231.1375, 229.1238, 215.0709, 205.0494, 201.0546, 189.0547, 187.0414, 179.0341, 177.0546, 175.0388, 173.0599, 163.0749, 161.0593, 151.0390, 149.0599, 99.0811, 81.0702	3	Dihydroresorcylide	Zearalenone (Macrolide)	*Penicillium brocae*	CAG, PDA	[56]
209	529.2708	[M+H]⁺	6	1.1	$C_{32}H_{36}N_2O_5$	331.1811, 200.1068, 185.0722, 130.0658	3	Chaetoglobosin D	Cytochalasan alkaloid	*Penicillium expansum*	CAG	[57]
210	509.2773	[M+H]⁺	6.11	-0.8	$C_{29}H_{32}N_8O$*	311.1388, 283.1449, 263.1399, 247.1446, 235.1447, 219.1502, 199.1440, 171.1498, 136.0762, 120.0815	4	n.a.			PDA	
211	357.1341	[M+H]⁺	6.22	0.8	$C_{20}H_{20}O_6$	342.1103, 327.0872, 315.0868, 313.0717, 301.0714, 286.0481, 257.0454, 229.0506	4	n.a.			PDA	
212	529.27	[M+H]⁺	6.29	-0.4	$C_{32}H_{36}N_2O_5$	200.1071, 198.0916, 185.0718, 174.0925, 157.1017, 130.0657	2	Chaetoglobosin A	Cytochalasan alkaloid	*Penicillium chrysogenum*	CAG	[58]
213	307.1551	[M+H]⁺	6.38	2	$C_{17}H_{22}O_5$	265.1435, 201.1277, 155.0864, 135.0807, 133.1008, 131.0864, 105.0695	3	Expansolide A or B	Sesquiterpenoid	*Penicillium expansum*	CAG	[59]
214	707.2095	[M+H]⁺	6.42	-1	$C_{36}H_{30}N_6O_{10}$ or $C_{34}H_{18}N_{20}$*	668.0617, 602.0138, 584.0034, 573.0614, 365.0998, 296.0298, 275.0551	4	n.a.			PDA	
215	313.1084	[M+H]⁺	6.64	2.6	$C_{18}H_{16}O_5$	297.0768, 271.0612, 257.0456, 229.0503	4				PDA	
216	289.0716	[M+H]⁺	6.72	1.4	$C_{15}H_{12}O_6$	274.0482, 270.0525, 246.0518, 243.0660, 232.0370, 228.0396, 200.0479	3	Drimiopsin H	Xanthone	*Penicillium* sp.	PDA	[53]

No.	*m/z* value	Adduct	R_t (min)	ppm	Putative MF	Fragmentation pattern	IC	Putative identification	Chemical family	Biological origin	Medium	Ref
217	305.1296	[M+H]⁺	6.72	2	$C_{19}H_{16}N_2O_2$	277.1343, 234.1274, 220.1120, 187.0869, 132.0810	4	n.a.			CAG	
218	339.0871	[M+H]⁺	6.85	0.6	$C_{19}H_{14}O_6$	324.0636, 321.0758, 311.0922, 296.0687, 293.0815, 283.0966, 269.0456, 265.0869, 249.0918	4	n.a.			PDA	
219	509.2922	[M+H]⁺	7.04	1	$C_{32}H_{36}N_4O_2$	491.2809, 451.2503, 437.2342, 381.1972, 367.1808, 357.2074, 343.1924, 340.1916, 326.1661, 323.1545, 309.1391, 255.1501, 253.1346, 197.1083, 185.1085, 183.0922, 159.0922, 95.0501	2	Communesin B	Indole alkaloid	*Penicillium* sp.	CAG	[55]
220	357.1341	[M+H]⁺	7.05	0.8	$C_{20}H_{20}O_6$	341.1023, 327.0877, 313.1076, 311.0921, 301.0721, 286.0482, 273.0771, 258.0528, 247.0608, 230.0600	4	n.a.			PDA	
221	359.1135	[M+H]⁺	7.22, 7.71ᐃ	1.1	$C_{19}H_{18}O_7$	341.1030, 326.0796, 323.0922, 313.1078, 302.0749, 271.0614, 257.0455	3	Penixanthone D	Xanthone	*Penicillium* sp.	PDA	[60]
222	487.27	[M+H]⁺	7.22	0.8	$C_{28}H_{38}O_7$	395.2227, 377.2127, 367.2277, 349.2178, 243.1752, 225.1640, 215.1806, 185.1337, 183.1183, 175.1487, 171.1180, 161.1338, 151.0396	2	Andrastin A	Meroterpenoid	*Penicillium* sp.	CAG	[61]
223	319.1455	[M+H]⁺	7.28	2.5	$C_{20}H_{18}N_2O_2$	291.1506, 234.1290, 201.1029, 188.0718, 132.0817, 91.0551	4	n.a.			CAG	
224	307.1552	[M+H]⁺	7.42	2.1	$C_{17}H_{22}O_5$	289.1434, 271.1339, 243.1392, 229.0860, 193.0503, 191.0710, 189.0561, 175.0766, 165.0543, 163.0751	3	a: 5-oxolasiodiplodin, b: 7-oxolasiodiplodin	Zearalenone (Macrolide)	*a: Lasiodiplodia theobromae, b: Lasiodiplodia sp.*	PDA	a: [62], b: [63]
225	355.1188	[M+H]⁺	7.54	1.7	$C_{20}H_{18}O_6$*	339.0874, 325.0719, 311.0926	4	n.a.			PDA	
226	357.1346	[M+H]⁺	8	2.2	$C_{20}H_{20}O_6$	342.1128, 327.0954, 315.0874, 313.0724, 301.0730, 286.0486, 281.0819, 273.0769, 258.0534, 255.0661, 247.0605	4	n.a.			PDA	
227	711.2451	[M+H]⁺	8.12	-0.6	$C_{41}H_{54}N_4O_8$*	679.2186, 636.2005, 356.1266, 341.1040, 327.1239, 232.0929	4	n.a.			PDA	
228	367.2253	[M+Na]⁺	8.13	1.1	$C_{22}H_{32}O_3$	320.1843, 252.0905, 242.1019, 234.1131, 224.0923, 198.1151, 149.0231, 138.0189	4	n.a.			CAG	
229	389.2327	[M+H]⁺	8.39	-0.3	$C_{23}H_{32}O_5$	Nf	4	n.a.			CAG	
230	865.5916	[M+H]⁺	8.8	0.1	$C_{47}H_{76}N_8O_7$*	594.4034, 526.3393, 481.3192, 413.2555, 408.3224, 368.2338, 340.2582, 300.1718, 295.2392,	4	n.a.			CAG	

No.	*m/z* value	Adduct	R$_t$ (min)	ppm	Putative MF	Fragmentation pattern	IC	Putative identification	Chemical family	Biological origin	Medium	Ref
						272.1769, 267.2441, 227.1761, 199.1817, 159.0919						
231	500.3957	[M+H]$^+$	8.95	1.2	C$_{28}$H$_{53}$NO$_6$*	482.3847, 236.1509, 144.1026	4	n.a.			PDA	
232	371.1132	[M+H]$^+$	9.49	0.3	C$_{20}$H$_{18}$O$_7$	339.0872, 329.1029, 311.0927, 296.0686, 287.0559, 283.0973, 273.0402, 269.0455, 265.0868, 255.0296, 241.0500	3	Chaetoxanthone A	Xanthone	*Chaetomium* sp.	PDA	[64]
233	467.0751	[M+H]$^+$	9.49	-0.4	C$_{24}$H$_6$N$_{10}$O$_2$*	426.0487, 423.0406, 421.0434, 412.9966, 405.0294, 403.0327, 390.0050, 388.0096, 385.0206, 371.9950, 369.9992	4	n.a.			PDA	
234	279.233	[M+H]$^+$	9.66	2.1	C$_{18}$H$_{30}$O$_2$	261.2221, 223.1700, 209.1532, 201.0458, 195.1395, 191.1436, 187.1490, 177.1271, 173.1328, 163.1481, 159.1174, 151.1479, 149.1330, 147.1175, 145.1004, 137.1334, 135.1168, 131.0853, 123.1168, 121.1018, 109.1015, 107.0859, 95.0860, 93.0696, 81.0707	4	n.a.			PDA	
235	279.2333	[M+H]$^+$	9.74	3.2	C$_{18}$H$_{30}$O$_2$	261.2222, 209.1537, 201.0462, 195.1386, 191.1434, 187.1488, 177.1286, 173.1329, 163.1490, 159.1176, 151.1487, 149.1335, 147.1167, 145.1022, 137.1336, 135.1173, 133.1024, 131.0863, 123.1177, 121.1020, 109.1017, 107.0863, 95.0861, 93.0698, 81.0708, 79.0556	4	n.a.			PDA	
236	343.1188	[M+H]$^+$	9.82	1.7	C$_{19}$H$_{18}$O$_6$	327.0860, 313.0720, 301.0718, 287.0565, 275.0558, 259.0612, 233.0453, 213.0556	3	Umbilicaxanthone A	Xanthone	*Umbilicaria proboscidea*	PDA	[65]
237	843.3354	[M+H]$^+$	9.82	0	C$_{46}$H$_{46}$N$_6$O$_{10}$ or C$_{44}$H$_{34}$N$_{20}$*	364.0936	4	n.a.			PDA	
238	714.4153	[M+H]$^+$	10.44	-0.7	C$_{47}$H$_{55}$NO$_5$*	696.4050, 571.2720	4	n.a.			PDA	
239	850.4537	[M+H]$^+$	10.93	0.8	C$_{49}$H$_{51}$N$_{15}$ or C$_{51}$H$_{63}$NO$_{10}$*	377.3211, 341.1031, 326.0794, 313.1082	4	n.a.			PDA	

References

1. Wang, M.; Carver, J.J.; Phelan, V.V.; Sanchez, L.M.; Garg, N.; Peng, Y.; Nguyen, D.D.; Watrous, J.; Kapono, C.A.; Luzzatto-Knaan, T.; et al. Sharing and community curation of mass spectrometry data with Global Natural Products Social Molecular Networking. *Nat. Biotechnol.* **2016**, *34*, 828-837, doi:10.1038/nbt.3597.

2. Altschul, S.F.; Gish, W.; Miller, W.; Myers, E.W.; Lipman, D.J. Basic local alignment search tool. *J. Mol. Biol.* **1990**, *215*, 403-410, doi:10.1016/S0022-2836(05)80360-2.

3. Sumner, L.W.; Amberg, A.; Barrett, D.; Beale, M.H.; Beger, R.; Daykin, C.A.; Fan, T.W.; Fiehn, O.; Goodacre, R.; Griffin, J.L.; et al. Proposed minimum reporting standards for chemical analysis Chemical Analysis Working Group (CAWG) Metabolomics Standards Initiative (MSI). *Metabolomics* **2007**, *3*, 211-221, doi:10.1007/s11306-007-0082-2.

4. Drautz, H.; Zähner, H.; Kupfer, E.; Keller-Schierlein, W. 164. Stoffwechselprodukte von Mikroorganismen, 205. Mitteilung. Isolierung und Struktur von Streptazolin. *Helv. Chim. Acta* **1981**, *64*, 1752-1765, doi:10.1002/hlca.19810640605.

5. Puder, C.; Loya, S.; Hizi, A.; Zeeck, A. New co-metabolites of the streptazolin pathway. *J. Nat. Prod.* **2001**, *64*, 42-45, doi:10.1021/np000377i.

6. Zhang, C.; Ondeyka, J.; Guan, Z.; Dietrich, L.; Burgess, B.; Wang, J.; Singh, S.B. Isolation, structure and biological activities of platensimycin B4 from *Streptomyces platensis*. *J. Antibiot.* **2009**, *62*, 699-702, doi:10.1038/ja.2009.106.

7. Paulus, C.; Rebets, Y.; Zapp, J.; Ruckert, C.; Kalinowski, J.; Luzhetskyy, A. New alpiniamides from *Streptomyces* sp. IB2014/011-12 assembled by an unusual hybrid non-ribosomal peptide synthetase Trans-AT polyketide synthase enzyme. *Front. Microbiol.* **2018**, *9*, 1959, doi:10.3389/fmicb.2018.01959.

8. Fleck, W.F.; Ritzau, M.; Heinze, S.; Gräfe, U. Isolation of dimeric nonactic acid from the nonactin-producing *Streptomyces* spec. JA 5909-1. *J. Basic Microbiol.* **1996**, *36*, 235-238, doi:10.1002/jobm.3620360405.

9. Schumacher, R.W.; Talmage, S.C.; Miller, S.A.; Sarris, K.E.; Davidson, B.S.; Goldberg, A. Isolation and structure determination of an antimicrobial ester from a marine sediment-derived bacterium. *J. Nat. Prod.* **2003**, *66*, 1291-1293, doi:10.1021/np020594e.

10. Huang, H.; Lan, X.; Wang, Y.; Tian, L.; Fang, Y.; Zhang, L.; Zhang, K.; Zheng, X. New bioactive derivatives of nonactic acid from the marine *Streptomyces griseus* derived from the plant *Salicornia* sp. *Phytochem. Lett.* **2015**, *12*, 190-195, doi:10.1016/j.phytol.2015.04.001.

11. Jeong, S.Y.; Shin, H.J.; Kim, T.S.; Lee, H.S.; Park, S.K.; Kim, H.M. Streptokordin, a new cytotoxic compound of the methylpyridine class from a marine-derived *Streptomyces* sp. KORDI-3238. *J. Antibiot.* **2006**, *59*, 234-240, doi:10.1038/ja.2006.33.

12. Charan, R.D.; Schlingmann, G.; Janso, J.; Bernan, V.; Feng, X.; Carter, G.T. Diazepinomicin, a new antimicrobial alkaloid from a marine *Micromonospora* sp. *J. Nat. Prod.* **2004**, *67*, 1431-1433, doi:10.1021/np040042r.

13. Maskey, R.P.; Grun-Wollny, I.; Laatsch, H. Isolation and structure elucidation of diazaquinomycin C from a terrestrial *Streptomyces* sp. and confirmation of the akashin structure. *Nat. Prod. Res.* **2005**, *19*, 137-142, doi:10.1080/14786410410001704741.

14. McBrien, K.D.; Berry, R.L.; Lowe, S.E.; Neddermann, K.M.; Bursuker, I.; Huang, S.; Klohr, S.E.; Leet, J.E. Rakicidins, new cytotoxic lipopeptides from *Micromonospora* sp. fermentation, isolation and characterization. *J. Antibiot.* **1995**, *48*, 1446-1452, doi:10.7164/antibiotics.48.1446.

15. Oku, N.; Matoba, S.; Yamazaki, Y.M.; Shimasaki, R.; Miyanaga, S.; Igarashi, Y. Complete stereochemistry and preliminary structure-activity relationship of rakicidin A, a hypoxia-selective cytotoxin from *Micromonospora* sp. *J. Nat. Prod.* **2014**, *77*, 2561-2565, doi:10.1021/np500276c.

16. Itoh, J.; Omoto, S.; Shomura, T.; Nishizawa, N.; Miyado, S.; Yuda, Y.; Shibata, U.; Inouye, S. Amicoumacin-A, a new antibiotic with strong antiinflammatory and antiulcer activity. *J. Antibiot.* **1981**, *34*, 611-613, doi:10.7164/antibiotics.34.611.

17. Bai, J.; Liu, D.; Yu, S.; Proksch, P.; Lin, W. Amicoumacins from the marine-derived bacterium *Bacillus* sp. with the inhibition of NO production. *Tetrahedron Lett.* **2014**, *55*, 6286-6291, doi:10.1016/j.tetlet.2014.09.100.

18. Shimojima, Y.; Hayashi, H.; Ooka, T.; Shibukawa, M. Production, isolation and pharmacological studies of AI-77s. *Agr. Biol. Chem.* **2014**, *46*, 1823-1829, doi:10.1080/00021369.1982.10865335.

19. Xia, M.; Liu, S.W.; Zhou, Z.H.; Tuo, L.; Ling, B.; Guo, L.; Dong, Y.P.; Wang, F.F.; Jiang, Z.K.; Li, X.J.; et al. Studies on amicoumacin group antibiotics produced by *Bacillus* strain XZ7. *Chin. J. Antibiot.* **2014**, *39*, 801-807.

20. Mhammedi, A.; Peypoux, F.; Besson, F.; Michel, G. Bacillomycin F, a new antibiotic of iturin group: isolation and characterization. *J. Antibiot.* **1982**, *35*, 306-311, doi:10.7164/antibiotics.35.306.

21. Peypoux, F.; Marion, D.; Maget-Dana, R.; Ptak, M.; Das, B.C.; Michel, G. Structure of bacillomycin F, a new peptidolipid antibiotic of the iturin group. *Eur. J. Biochem.* **1985**, *153*, 335-340, doi:10.1111/j.1432-1033.1985.tb09307.x.

22. Konda, Y.; Nakagawa, A.; Harigaya, Y.; Onda, M.; Masuma, R.; Omura, S. Aurantinin B, a new antimicrobial antibiotic from bacterial origin. *J. Antibiot.* **1988**, *41*, 268-270, doi:10.7164/antibiotics.41.268.

23. Kimura, K.; Nakayama, S.; Nakamura, J.; Takada, T.; Yoshihama, M.; Esumi, Y.; Itoh, Y.; Uramoto, M. SNA-60-367, new peptide enzyme inhibitors against aromatase. *J. Antibiot.* **1997**, *50*, 529-531, doi:10.7164/antibiotics.50.529.

24. Zhuravleva, O.I.; Afiyatullov, S.S.; Ermakova, S.P.; Nedashkovskaya, O.I.; Dmitrenok, P.S.; Denisenko, V.A.; Kuznetsova, T.A. New C14-surfactin methyl ester from the marine bacterium *Bacillus pumilus* KMM 456. *Russ. Chem. Bull.* **2011**, *59*, 2137-2142, doi:10.1007/s11172-010-0369-8.

25. Liu, X.Y.; Yang, S.Z.; Mu, B.Z. Isolation and characterization of a C12-lipopeptide produced by *Bacillus subtilis* HSO 121. *J. Pept. Sci.* **2008**, *14*, 864-875, doi:10.1002/psc.1017.

26. Kalinovskaya, N.I.; Kuznetsova, T.A.; Ivanova, E.P.; Romanenko, L.A.; Voinov, V.G.; Huth, F.; Laatsch, H. Characterization of surfactin-like cyclic depsipeptides synthesized by *Bacillus pumilus* from ascidian *Halocynthia aurantium*. *Mar. Biotechnol.* **2002**, *4*, 179-188, doi:10.1007/s1012601-0084-4.

27. Zhang, P.; Deng, Y.; Lin, X.; Chen, B.; Li, J.; Liu, H.; Chen, S.; Liu, L. Anti-inflammatory mono- and dimeric sorbicillinoids from the marine-derived fungus *Trichoderma reesei* 4670. *J. Nat. Prod.* **2019**, *82*, 947-957, doi:10.1021/acs.jnatprod.8b01029.

28. Jiao, W.H.; Khalil, Z.; Dewapriya, P.; Salim, A.A.; Lin, H.W.; Capon, R.J. Trichodermides A-E: New peptaibols isolated from the Australian termite nest-ferived fungus *Trichoderma virens* CMB-TN16. *J. Nat. Prod.* **2018**, *81*, 976-984, doi:10.1021/acs.jnatprod.7b01072.

29. Mukherjee, P.K.; Wiest, A.; Ruiz, N.; Keightley, A.; Moran-Diez, M.E.; McCluskey, K.; Pouchus, Y.F.; Kenerley, C.M. Two classes of new peptaibols are synthesized by a single non-ribosomal peptide synthetase of *Trichoderma virens*. *J. Biol. Chem.* **2011**, *286*, 4544-4554, doi:10.1074/jbc.M110.159723.

30. Iida, A.; Sanekata, M.; Wada, S.; Fujita, T.; Tanaka, H.; Enoki, A.; Fuse, G.; Kanai, M.; Asami, K. Fungal metabolites. XVIII. New membrane-modifying peptides, trichorozins I-IV, from the fungus *Trichoderma harzianum*. *Chem. Pharm. Bull.* **1995**, *43*, 392-397, doi:10.1248/cpb.43.392.

31. Goulard, C.; Hlimi, S.; Rebuffat, S.; Bodo, B. Trichorzins HA and MA, antibiotic peptides from *Trichoderma harzianum*. I. Fermentation, isolation and biological properties. *J. Antibiot.* **1995**, *48*, 1248-1253, doi:10.7164/antibiotics.48.1248.

32. Iida, A.; Sanekata, M.; Fujita, T.; Tanaka, H.; Enoki, A.; Fuse, G.; Kanai, M.; Rudewicz, P.J.; Tachikawa, E. Fungal metabolites. XVI. Structures of new peptaibols, trichokindins I-VII, from the fungus *Trichoderma harzianum*. *Chem. Pharm. Bull.* **1994**, *42*, 1070-1075, doi:10.1248/cpb.42.1070.

33. Mohamed-Benkada, M.; Montagu, M.; Biard, J.F.; Mondeguer, F.; Verite, P.; Dalgalarrondo, M.; Bissett, J.; Pouchus, Y.F. New short peptaibols from a marine *Trichoderma* strain. *Rapid Commun. Mass Spectrom.* **2006**, *20*, 1176-1180, doi:10.1002/rcm.2430.

34. Oh, S.U.; Yun, B.S.; Lee, S.J.; Kim, J.H.; Yoo, I.D. Atroviridins A-C and neoatroviridins A-D, novel peptaibol antibiotics produced by *Trichoderma atroviride* F80317. I. Taxonomy, fermentation, isolation and biological activities. *J. Antibiot.* **2002**, *55*, 557-564, doi:10.7164/antibiotics.55.557.

35. Augustiniak, H.; Forche, E.; Reichenbach, H.; Wray, V.; Gräfe, U.; Höfle, G. Isolierung und Strukturaufklarung von Ergokonin A und B; zwei neue antifungische Sterol-Antibiotika aus *Trichoderma koningii*. *Liebigs Ann. Chem.* **1991**, *1991*, 361-366, doi:10.1002/jlac.199119910163.

36. Reveglia, P.; Savocchia, S.; Billones-Baaijens, R.; Masi, M.; Cimmino, A.; Evidente, A. Diploquinones A and B, two new phytotoxic tetrasubstituted 1,4-naphthoquinones from *Diplodia*

273

mutila, a causal agent of grapevine trunk disease. *J. Agr. Food Chem.* **2018**, *66*, 11968-11973, doi:10.1021/acs.jafc.8b05004.

37. Chilton, W.S. Isolation and structure of norjavanicin. *J. Org. Chem.* **1968**, *33*, 4299-4300, doi:10.1021/jo01275a074.

38. Trisuwan, K.; Khamthong, N.; Rukachaisirikul, V.; Phongpaichit, S.; Preedanon, S.; Sakayaroj, J. Anthraquinone, cyclopentanone, and naphthoquinone derivatives from the sea fan-derived fungi *Fusarium* spp. PSU-F14 and PSU-F135. *J. Nat. Prod.* **2010**, *73*, 1507-1511, doi:10.1021/np100282k.

39. Ola, A.R.; Thomy, D.; Lai, D.; Brotz-Oesterhelt, H.; Proksch, P. Inducing secondary metabolite production by the endophytic fungus *Fusarium tricinctum* through coculture with *Bacillus subtilis*. *J. Nat. Prod.* **2013**, *76*, 2094-2099, doi:10.1021/np400589h.

40. Kurobane, I.; Vining, L.C.; McInnes, A.G.; Gerber, N.N. Metabolites of *Fusarium solani* related to dihydrofusarubin. *J. Antibiot.* **1980**, *33*, 1376-1379, doi:10.7164/antibiotics.33.1376.

41. Yang, X.; Khong, T.T.; Chen, L.; Choi, H.D.; Kang, J.S.; Son, B.W. 8'-hydroxyzearalanone and 2'-hydroxyzearalanol: Resorcyclic acid lactone derivatives from the marine-derived fungus *Penicillium* sp. *Chem. Pharm. Bull.* **2008**, *56*, 1355-1356, doi:10.1248/cpb.56.1355.

42. Ma, T.-T.; Shan, W.-G.; Ying, Y.-M.; Ma, L.-F.; Liu, W.-H.; Zhan, Z.-J. Xanthones with α-glucosidase inhibitory activities from *Aspergillus versicolor*, a fungal endophyte of *Huperzia serrata*. *Helv. Chim. Acta* **2015**, *98*, 148-152, doi:10.1002/hlca.201400165.

43. Stob, M.; Baldwin, R.S.; Tuite, J.; Andrews, F.N.; Gillette, K.G. Isolation of an anabolic, uterotrophic compound from corn infected with *Gibberella zeae*. *Nature* **1962**, *196*, 1318, doi:10.1038/1961318a0.

44. Hawas, U.W.; Farrag, A.R.H.; Ahmed, E.F.; Abou El-Kassem, L.T. Cytotoxic effect of *Fusarium equiseti* fungus metabolites against N-Nitrosodiethylamine- and CCL4-induced hepatocarcinogenesis in rats. *Pharm. Chem. J.* **2018**, *52*, 326-333, doi:10.1007/s11094-018-1816-3.

45. Richardson, K.E.; Hagler, W.M.; Mirocha, C.J. Production of zearalenone, α- and β-zearalenol, and α- and β-zearalanol by *Fusarium* spp. in rice culture. *J. Agr. Food Chem.* **1985**, *33*, 862-866, doi:10.1021/jf00065a024.

46. Shiono, Y.; Tsuchinari, M.; Shimanuki, K.; Miyajima, T.; Murayama, T.; Koseki, T.; Laatsch, H.; Funakoshi, T.; Takanami, K.; Suzuki, K. Fusaristatins A and B, two new cyclic lipopeptides from an endophytic *Fusarium* sp. *J. Antibiot.* **2007**, *60*, 309-316, doi:10.1038/ja.2007.39.

47. Hammerschmidt, L.; Wray, V.; Lin, W.; Kamilova, E.; Proksch, P.; Aly, A.H. New styrylpyrones from the fungal endophyte *Penicillium glabrum* isolated from *Punica granatum*. *Phytochem. Lett.* **2012**, *5*, 600-603, doi:10.1016/j.phytol.2012.06.003.

48. Lai, S.; Shizuri, Y.; Yamamura, S.; Kawai, K.; Furukawa, H. New curvularin-type metabolites from the hybrid strain ME 0005 derived from *Penicillium citreo-viride* B. IFO 4692 and 6200. *Bull. Chem. Soc. Jpn.* **1991**, *64*, 1048-1050, doi:10.1246/bcsj.64.1048.

49. Huang, Z.; Yang, R.; Yin, X.; She, Z.; Lin, Y. Structure elucidation and NMR assignments for two xanthone derivatives from a mangrove endophytic fungus (No. ZH19). *Magn. Reson. Chem.* **2010**, *48*, 80-82, doi:10.1002/mrc.2539.

50. Li, F.; Sun, W.; Zhang, S.; Gao, W.; Lin, S.; Yang, B.; Chai, C.; Li, H.; Wang, J.; Hu, Z.; et al. New cyclopiane diterpenes with anti-inflammatory activity from the sea sediment-derived fungus *Penicillium* sp. TJ403-2. *Chin. Chem. Lett.* **2020**, *31*, 197-201, doi:10.1016/j.cclet.2019.04.036.

51. Liao, Z.-J.; Tian, W.-J.; Liu, X.-X.; Jiang, X.; Wu, Y.; Lin, T.; Chen, H.-F. A new xanthone from an endophytic fungus of *Anoectochilus roxburghii*. *Chem. Nat. Compd.* **2018**, *54*, 267-269, doi:10.1007/s10600-018-2320-4.

52. Yang, S.-Q.; Li, X.-M.; Li, X.; Li, H.-L.; Meng, L.-H.; Wang, B.-G. New citrinin analogues produced by coculture of the marine algal-derived endophytic fungal strains *Aspergillus sydowii* EN-534 and *Penicillium citrinum* EN-535. *Phytochem. Lett.* **2018**, *25*, 191-195, doi:10.1016/j.phytol.2018.04.023.

53. Zhuang, Y.-B.; Yin, H.; Zhang, X.-W.; Zhou, W.; Liu, T. Three new xanthones from the fungus *Penicillium* sp. NH-7-1. *Helv. Chim. Acta* **2015**, *98*, 699-703, doi:10.1002/hlca.201400296.

54. Dekan, Z.; Sianati, S.; Yousuf, A.; Sutcliffe, K.J.; Gillis, A.; Mallet, C.; Singh, P.; Jin, A.H.; Wang, A.M.; Mohammadi, S.A.; et al. A tetrapeptide class of biased analgesics from an Australian fungus targets the micro-opioid receptor. *Proc. Natl. Acad. Sci. USA* **2019**, *116*, 22353-22358, doi:10.1073/pnas.1908662116.

55. Numata, A.; Takahashi, C.; Ito, Y.; Takada, T.; Kawai, K.; Usami, Y.; Matsumura, E.; Imachi, M.; Ito, T.; Hasegawa, T. Communesins, cytotoxic metabolites of a fungus isolated from a marine alga. *Tetrahedron Lett.* **1993**, *34*, 2355-2358, doi:10.1016/s0040-4039(00)77612-x.

56. Zhang, P.; Meng, L.-H.; Mándi, A.; Li, X.-M.; Kurtán, T.; Wang, B.-G. Structure, absolute configuration, and conformational study of resorcylic acid derivatives and related congeners from the fungus *Penicillium brocae. RSC Adv.* **2015**, *5*, 39870-39877, doi:10.1039/c5ra02203g.

57. Andersen, B.; Smedsgaard, J.; Frisvad, J.C. *Penicillium expansum*: Consistent production of patulin, chaetoglobosins, and other secondary metabolites in culture and their natural occurrence in fruit products. *J. Agr. Food Chem.* **2004**, *52*, 2421-2428, doi:10.1021/jf035406k.

58. Huang, S.; Chen, H.; Li, W.; Zhu, X.; Ding, W.; Li, C. Bioactive chaetoglobosins from the mangrove endophytic fungus *Penicillium chrysogenum. Mar. Drugs* **2016**, *14*, 172, doi:10.3390/md14100172.

59. Massias, M.; Rebuffat, S.; Molho, L.; Chiaroni, A.; Riche, C.; Bodo, B. Expansolides A and B: Tetracyclic sesquiterpene lactones from *Penicillium expansum. J. Am. Chem. Soc.* **1990**, *112*, 8112-8115, doi:10.1021/ja00178a039.

60. Huang, J.; She, J.; Yang, X.; Liu, J.; Zhou, X.; Yang, B. A new macrodiolide and two new polycyclic chromones from the fungus *Penicillium* sp. SCSIO041218. *Molecules* **2019**, *24*, 1686, doi:10.3390/molecules24091686.

61. Cheng, Z.; Xu, W.; Wang, Y.; Bai, S.; Liu, L.; Luo, Z.; Yuan, W.; Li, Q. Two new meroterpenoids and two new monoterpenoids from the deep sea-derived fungus *Penicillium* sp. YPGA11. *Fitoterapia* **2019**, *133*, 120-124, doi:10.1016/j.fitote.2018.12.022.

62. Matsuura, H.; Nakamori, K.; Omer, E.A.; Hatakeyama, C.; Yoshihara, T.; Ichihara, A. Three lasiodiplodins from *Lasiodiplodia theobromae* IFO 31059. *Phytochemistry* **1998**, *49*, 579-584, doi:10.1016/s0031-9422(98)00267-2.

63. Li, J.; Xue, Y.; Yuan, J.; Lu, Y.; Zhu, X.; Lin, Y.; Liu, L. Lasiodiplodins from mangrove endophytic fungus *Lasiodiplodia* sp. 318. *Nat. Prod. Res.* **2016**, *30*, 755-760, doi:10.1080/14786419.2015.1062762.

64. Pontius, A.; Krick, A.; Kehraus, S.; Brun, R.; Konig, G.M. Antiprotozoal activities of heterocyclic-substituted xanthones from the marine-derived fungus *Chaetomium* sp. *J. Nat. Prod.* **2008**, *71*, 1579-1584, doi:10.1021/np800294q.

65. Řezanka, T.; Jáchymová, J.; Dembitsky, V.M. Prenylated xanthone glucosides from Ural's lichen *Umbilicaria proboscidea. Phytochemistry* **2003**, *62*, 607-612, doi:10.1016/s0031-9422(02)00539-3.

Declaration

I, Caroline Utermann, hereby declare that the dissertation entitled "*Ciona intestinalis* in the spotlight of metabolomics and microbiomics: New insights into its invasiveness and the biotechnological potential of its associated microbiota" was written independently by myself. Apart from the supervisor's guidance, the content and design of the thesis is all my own work and only the listed sources were used. The thesis has never been submitted either partially or wholly as part of a doctoral degree to another examining body and is my first and only doctoral procedure. Chapters 1-3 of the thesis have been published in peer reviewed journals. The thesis has been prepared subject to the Rules of Good Scientific Practice of the German Research Foundation. No academic degree has ever been withdrawn.

_____   _____

Place, Date   Signature